HydroPredict'2008

International Interdisciplinary Conference on

Predictions for Hydrology, Ecology, and Water Resources Management:

Using Data and Models to Benefit Society

15–18 September 2008, Prague, Czech Republic

PROCEEDINGS

Edited by Jiří Bruthans, Karel Kovar and Zbyněk Hrkal

The conference was jointly convened by:

- Faculty of Science, Charles University, Prague, Czech Republic
- International Commission on Groundwater (ICGW), of the International Association of Hydrological Sciences (IAHS)
- T. G. Masaryk Water Research Institute (VÚV), Prague, Czech Republic
- US Geological Survey (USGS)
- Universität für Bodenkultur Wien (BOKU), University of Natural Resources and Applied Life Sciences, Vienna

The conference was sponsored and supported by UNESCO / IHP.

The commercial sponsors of the conference were:

The papers included in this volume were reproduced from the manuscript version submitted by the authors. The papers were accepted as they were submitted. Only minor layout re-arrangements were carried out during editing.

The Editors and the Organizing Committee take no responsibility for any error and omission or for the opinions of the authors.

The Editors wish to acknowledge the conference authors for their patience and cooperation during the editing process.

ISBN 978-80-903635-3-3

This is a publication of the Czech Association of Hydrogeologists (Česká asociace hydrogeologů, ČAH), Czech Republic.

The conference was financially sponsored by the following companies:

Royal Haskoning, Consultants Architects Engineers
The Netherlands
(also groundwater and environment)
http://www.royalhaskoning.com

KISTERS AG
Pioneering Technologies
Aachen, Germany
e-mail:info@kisters.eu
http://www.kisters.eu

Scientific Advisory Committee

The following specialists have served as members of the Scientific Advisory Committee:

Okke Batelaan, Belgium
Andrew Binley, United Kingdom
Jan Fleckenstein, Germany
Steven M. Gorelick, USA
Jason W. Kean, USA
Harald Kunstmann, Germany
Henrik Madsen, Denmark
Geoff Parkin, United Kingdom
Dan Rosbjerg, Denmark
Andreas Schumann, Germany
Eric Servat, France
Jaroslav Solc, USA
Ramesh Teegavarapu, USA
Niko Verhoest, Belgium
Marc Bierkens, the Netherlands
António Chambel, Portugal
Graham Fogg, USA
Majid Hassanizadeh, the Netherlands
Toshiharu Kojiri, Japan
Peter Loucks, USA
Hans-Peter Nachtnebel, Austria
Andrea Rinaldo, Italy
John Schaake, USA
Jan Seibert, Sweden
Uri Shamir, Israel
Edward A. Sudicky, Canada
Stefan Uhlenbrook, the Netherlands
Alicia Wilson, USA

Organizing Committee

Zbyněk Hrkal
Institute of Hydrogeology, Engineering Geology and Applied Geophysics
Faculty of Science, Charles University, Prague, Czech Republic

Karel Kovar
Netherlands Environmental Assessment Agency (MNP), Bilthoven, The Netherlands

Mary C. Hill
US Geological Survey (USGS), Boulder, Colorado, USA
(also on behalf of International Commission on Groundwater, IAHS)

Hans-Peter Nachtnebel
Universität für Bodenkultur Wien (BOKU), University of Natural Resources and Applied Life Sciences, Vienna

Nada Rapantová
VSB-Technical University of Ostrava, Ostrava, Czech Republic
(also President of Czech National Chapter of IAH)

András Szöllösi-Nagy
UNESCO, Paris, France

PREFACE

Predictions produced using mathematical models have become a critical part of water resources management as hydrological and ecological systems have been increasingly affected by human demands. One of the main issues is determining whether discrepancies between data (observations, etc.) and model results occur because of problems with the conceptual models. Another issue is how deficiencies in data and conceptual models affect prediction accuracy and uncertainty. Addressing these issues is made even more difficult when those who develop new methods of data collection and analysis do so without considering the latest theories and models. Data collection that proceeds without the benefit of theory can expend precious resources with little gain. On the other hand, development of theory and conceptual models uninformed by the realities of data collection is unlikely to yield productive results. Either side cannot optimally proceed in isolation.

This interdisciplinary conference brings together scientists and other experts to discuss how to improve predictions by joint use of data and models in the following three fields:
– **hydrology** (groundwater, surface water and catchment, including water quality)
– **ecology** (wetland, riverrine, estuarine, terrestrial)
– **water resources management** (groundwater, vadose zone, and surface water)

The three fields are connected through the central, critical role played by **water**.

The goal of the HydroPredict'2008 conference is to be a forum for presentations on innovative technologies and methods of data collection, analysis, integration (combined use) of data and modelling, new techniques and tools for assessment of model performance, and case studies of both successful and problematic applications for the topics related to problems in hydrology, ecology, and water resources management. To address the resulting issues, the HydroPredict2008 conference brings together scientists, engineers (consultants, practitioners), water resources planners and managers, and policy makers.

The conference includes keynote speakers on diverse topics, and contributed oral and poster presentations.

This (prepublished) proceedings volume contains 85 papers grouped into 13 topics (labelled A through Y3). The papers included in this volume were reproduced from the manuscript version submitted by the authors. The papers were accepted as they were submitted. Only minor layout re-arrangements were carried out during editing. Since a presentation at the conference is not conditioned by submitting a paper for the proceedings, some of the work presented at the conference (orally or by means of a poster) is not contained in this volume.

We wish you a fruitful and enjoyable stay in Prague and in the Czech Republic.

The Hydropredict2008 Organizing Committee
Zbyněk Hrkal, Karel Kovar, Mary C. Hill, Hans-Peter Nachtnebel, Nada Rapantová and András Szöllösi-Nagy

TABLE OF CONTENTS

Topic F: Surface water quality, thermal load and sediments

Topic G: Coastal groundwater systems and groundwater quality

Topic H: Interaction between surface and groundwater systems; Groundwater modelling

<u>**Topic X1:** Predictions: Flood forecasting</u>

<u>**Topic X2:** Predictions: Runoff forecasting</u>

<u>**Topic Y1:** Climate change impacts</u>

Topic Y2: Impacts of land use on water resources

Topic Y3: Management of groundwater and surface water

Hydrological modelling of polar basin river runoff for Indigirka river as an example

IRINA N. BELDIMAN
Saint Petersburg State University, Faculty of Geography and Geoecology, Dept.of Hydrology,31/33,10-ay liniya V.O., 199178, Saint Petersburg, Russia
irinabeldiman@yandex.ru

Abstract The deterministic distributed hydrologic model "Hydrograph" (State Hydrological Institute, St.Petersburg, Russia) was applied for runoff formation process modelling in Indigirka river basin. The unique observational data of highland meteorological station Suntar-Hayata were used for model parameters evaluation and adjustment. The research considers problems and obstacles of runoff formation process modelling for remote unexplored polar territories.

Keywords runoff formation processes modelling; permafrost; mountainous areas; deterministic hydrologic model "Hydrograph"; Indigirka river basin; water balances elements

INTRODUCTION

The relevance of this study is stipulated by the increasing interest in Arctic territories and processes in the zone of permafrost. This is related to global climate and anthropogenic changes, which have an intense impact on circumpolar regions (Su *et al.*, 2005; Georgiyevsky & Shiklomanov, 2003). Indigirka river (basin area at Vorontsovo is equal 305000 km^2) has been chosen for runoff formation process modelling. It is located in the Eastern Siberia in a zone of continuous permafrost and extremely harsh climate. More than 50% of the basin territory is a mountainous area. The object of research presents typical remote and poorly explored territory which can be investigated mainly by means of mathematical modelling.

METHODS

The deterministic distributed hydrologic model "Hydrograph" developed in the State Hydrological Institute (Saint Petersburg, Russia) was applied (Vinogradov, 1988, 1995, 2003). It is a universal modelling system which combines all flow types and is applicable to simulate runoff formation process in the basins of any size and located in any geographical areas. The regional peculiarities of the territory are taken into consideration parametrically. The model allows getting information on the elements of water balance (precipitation, runoff, evaporation) and on the state variables of snow and soil in different points of the basin.

The model input information for Indigirka river consisted of daily series of average air temperatures and moisture deficites, as well as daily rainfall amounts over the period 1966-1984 for 20 meteorological stations. The values of daily water discharges over the same period in the basin outlet were used for results verification.

The allocation of homogeneous types of runoff forming complexes (RFCs) over the basin territory preceded model parameters evaluation. The main criteria used for dividing the basin into typical hydrological landscapes were the type of vegetation and soil. According to the analysis of such data as different kinds of maps, cadastre and reference literature, special studies and observations, the basin area was represented by five RFCs, differing over a range of natural factors. The main types of landscapes of the region depending on elevation are the mountainous tundra and taiga. Parameters of soil profile, vegetation and surface slopes were evaluated for each RFC.

The data of observations at mountain meteorological station Suntar-Hayata (absolute elevation 2068 m) enabled us to adjust soil and vegetation parameters more reliably. This unique station was working at the heads of Indigirka river during the period of 1957-1964 within the framework of international geophysical year. Special observations of water balance components, soil and vegetation characteristics, snow cover and other characteristics were carried out. Results of runoff formation modelling which was conducted for small mountainous watershed (Suntar river, mouth of Saharynia river, basin area is equal 7680 km^2) situated near Suntar-Hayata meteorological station are shown at Fig. 1.

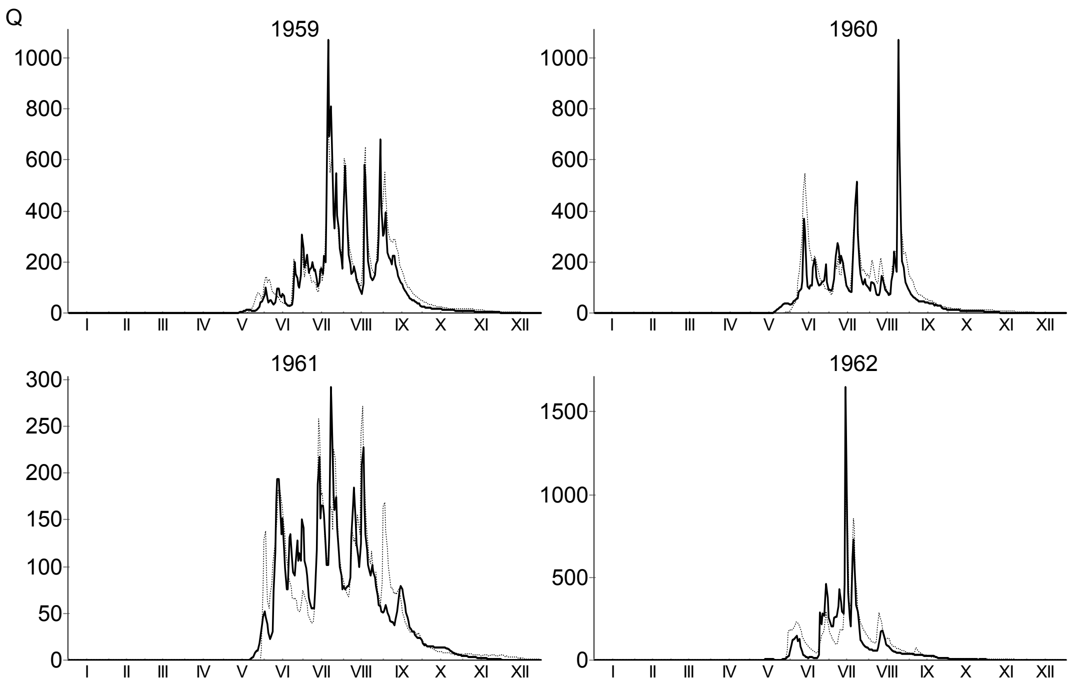

Fig. 1 Observed (solid) and simulated (dotted line) hydrographs (m^3 s^{-1}), Suntar river at Saharynia river mouth, 1959-1962.

The simulation results in the Suntar river basin were considered satisfactory, and thus the same parameters values were used for the runoff process simulation in Indigirka river basin.

RESULTS

The runoff formation processes modelling was conducted in Indigirka river basin for the period of 1966-1984. The obtained results included simulated daily hydrographs at basin outlet, layer values of annual water balances elements averaged for the whole basin (precipitation, evaporation, precipitation interception by vegetal cover, calculated runoff, including its surface, soil and underground components).

Graphic comparison of observed and calculated hydrographs for 1976-1979 is shown in Fig. 1, layer values of water balance components for the same period are presented in Table 1.

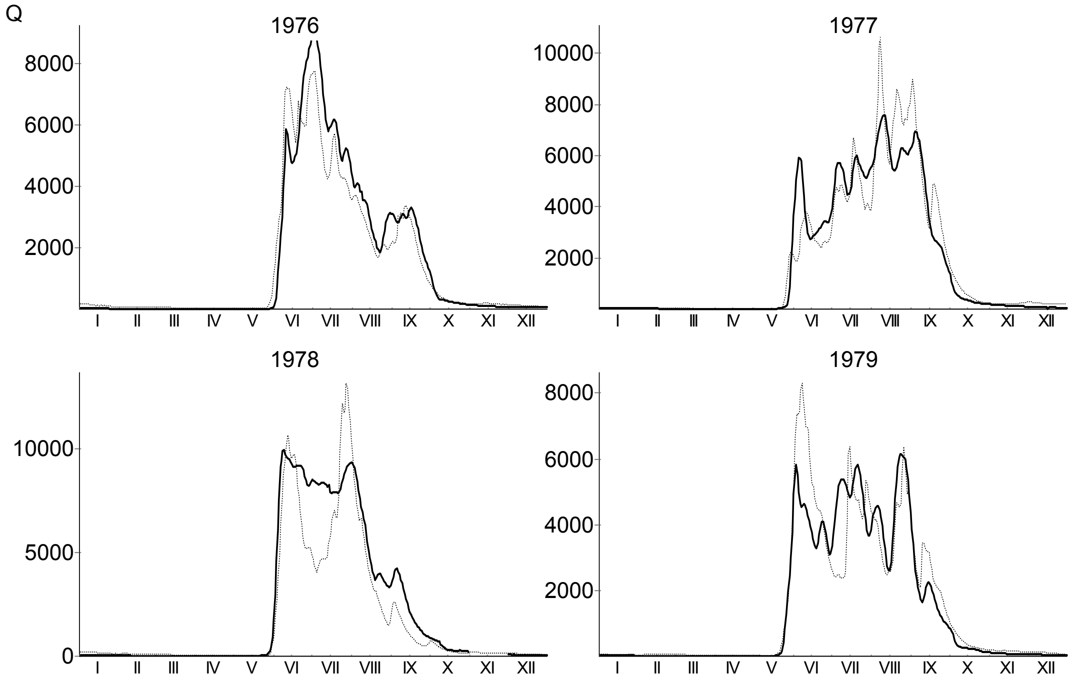

Fig. 2 Observed (solid) and simulated (dotted line) hydrographs (m^3 s^{-1}), Indigirka river at Vorontsovo, 1976-1979.

Table 1 Observed and observed values of water balance elements for the period of 1976-1979 in Indigirka river (mm).

	1976	1977	1978	1979
Calculated runoff	143	184	181	151
Observed runoff	154	176	218	142
Precipitation	309	415	315	312
Evapotranspiration	186	188	170	168
Soil evaporation	124	128	112	113
Snow evaporation	12	11	13	12
Evaporation from vegetal interception capacity	50	49	45	43
Surface flow	0	0	0	0
Subsurface flow	13	9	15	11
Underground flow	130	175	166	140

The value of daily calculated runoff layer amounts to 0.46 while observed layer averages 0.40 millimeters. Root mean square deviation for daily runoff amounts to 0.25 millimeters, Nash-Sutcliffe efficiency (Nash & Sutcliffe, 1970) determined for daily runoff exceeds 0.86, correlation coefficient was 0.93.

The conditions of runoff formation in the studied basin are extremely heterogeneous, that is primarily explained by complex orographic structure of the territory. Many mismatches between observation and calculation values are mainly due to the undercount of precipitation in conditions of highland.

CONCLUSIONS

The deterministic distributed hydrologic model "Hydrograph" showed satisfactory efficiency in runoff formation process simulations for the specific features of continuous permafrost zone and is perspective for further development and use for polar basins.

The main problems and obstacles of runoff formation process modelling for Indigirka river basin and similar areas are considered to be the following:

1. Inadequacy of meteorological data, especially precipitation and temperature, for mountainous parts of the basins. Various kinds of interpolation methods partially improved the situation, but the dependence of the simulation results on insufficient quantity and quality of the data revealed quite clearly.
2. Deficit of information about hydro-physical and thermal parameters of soils and rocks which limit the simulation accuracy in the conditions of continuous permafrost.
3. The lack of information about underground flow in researched territory.

Further evolution of hydrological processes conceptions for polar territories is needed for improvement of modelling results. Primarily it refers to understanding and adequate algorithmic presentation of soil thawing and freezing processes in the permafrost conditions. The additional analysis of all available materials about special and expedition observations is required for more reliable parameters adjustment and systematization.

In spite of all problems, the conducted research can be considered successful for preliminary stage and expects continuation. The obtained materials can be used directly and also for carrying out numeric experiments for modelling of water exchange and runoff forecast under the conditions of anthropogenic changes of landscapes and climate in polar region.

REFERENCES

Georgiyevsky, V. Yu.& Shiklomanov, I. A.. (2003) Climate change and water resources. In: *World Water Resources at the Beginning of the 21 st Century*. Cambridge Univ. Press, 390-413.

Nash J. E., Sutcliffe J. V. (1970) River flow forecasting through conceptual models: 1 A discussion of principles. *J. Hydrol.* **10**(3), 282–290

Su, F., Adam, J. C., Bowling, L. C. & Lettenmaier, D. P. (2005) Streamflow simulations of the terrestrial Arctic domain. J. *Geophys. Res.* **110**, D08112, doi:10.1029/2004JD005518.

Vinogradov, Yu. B. (1988) Mathematical modelling of runoff formation. A critical analysis. *Gidrometeoizdat, Leningrad*, 312 pp. (in Russian)

Vinogradov, Yu. B. (1995) Hydrological modelling of Arctic river runoff. In *Proceedings of the workshop on the ACSYS solid precipitation climatology project* (Reston, VA, USA, 12-15 September 1995), WMO/TD No.739, 144-158

Vinogradov, Yu. B. (2003) River Runoff Modelling. In *Hydrological Cycle*, edited by Shiklomanov I.A., in *Encyclopedia of Life Support Systems (EOLSS)*, Developed under the auspices of the UNESCO, Eolss Publishers, Oxford, UK, [http://www.eolss.net]

Vinogradov, Yu. B. (2003) Runoff Generation and Storage in Watershed. In *Hydrological Cycle*, edited by I.A. Shiklomanov, in *Encyclopedia of Life Support Systems (EOLSS)*, Developed under the auspices of the UNESCO, Eolss Publishers, Oxford, UK, [http://www.eolss.net]

Estimating ungauged stream flows based on model regionalization – Examples from the mountainous, semi-arid Karkheh river basin, Iran

I. MASIH[1, 3], S. UHLENBROOK[1, 2], S. MASKEY[1], M. D. AHMAD[3] & MD. A. ISLAM[3]

1 *UNESCO-IHE Institute for Water Education, PO Box 3015, 2601 DA Delft, The Netherlands*

2 *Delft University of Technology, Section of Water Resources, PO Box 5048, 2600 GA Delft, The Netherlands*

3 *International Water Management Institute (IWMI), Global Research Division, PO Box 2075, Colombo, Sri Lanka*

s.uhlenbrook@unesco-ihe.org

Abstract The study examines the possibility of simulating time series of stream flows for ungauged catchments based on hydrological similarity. As an example the mountainous, semi-arid Karkheh river basin (50,764 km^2) of Iran is presented. The frequently applied HBV model was applied to simulate daily stream flow with parameters transferred from gauged catchment counterparts. Hydrological similarity is defined based on three similarity measures: geographical area, spatial proximity and shape of the flow duration curve (FDC). FDCs for the ungauged catchments were predicted using logarithmic relationship derived from physiographic characteristics of eleven gauged catchments. The study shows that transferring HBV model parameters based on the FDC similarity criterion produces better runoff simulation compared to the similarity criteria based on catchment area and geographical proximity. The validation of the catchment similarity analysis using the FDC on monthly and daily flow simulation resulted in mean Nash-Sutcliffe model efficiency, R_{eff}, of 0.70 and 0.57, respectively. The study concludes that the methods of utilizing FDCs could be applied for estimating ungauged stream flows in the mountainous parts of the Karkheh river basin and source area of other major rivers in that region (e.g. Dez, Karun and Zayandeh Rud).

Keywords ungauged catchments; regionalization; catchment similarity; flow duration curve (FDC)

INTRODUCTION

Stream flow data are a prerequisite for planning and management of water resources and environment, but many river basins world-wide are ungauged or poorly gauged. In particular in water-limited environments, i.e. about half of the global land area, stream flow predictions are essential as these areas are highly sensitive to global and local changes. Hydrologists have responded to this challenge by developing various predictive tools, which are commonly referred to as regionalization methods. However, despite considerable progress in hydrology, the prediction of stream flow for ungauged catchments still remains a major challenge. This paper examines the possibility of simulating time series of stream flows for ungauged catchments based on hydrological similarity. As an example the mountainous, semi-arid Karkheh river basin of Iran is presented (Fig. 1), which drains an area of about 50,764 km^2, of which 80 % is a part of the Zagros mountain ranges of Iran. Details on the study area and overview over the surface water hydrology and water allocations can be found in Masih *et al*. (2008). For this study eleven gauged and two ungauged catchments located in the Zagros mountain ranges in upper Karkheh, ranging in size from 475 to 2572 km^2, were selected.

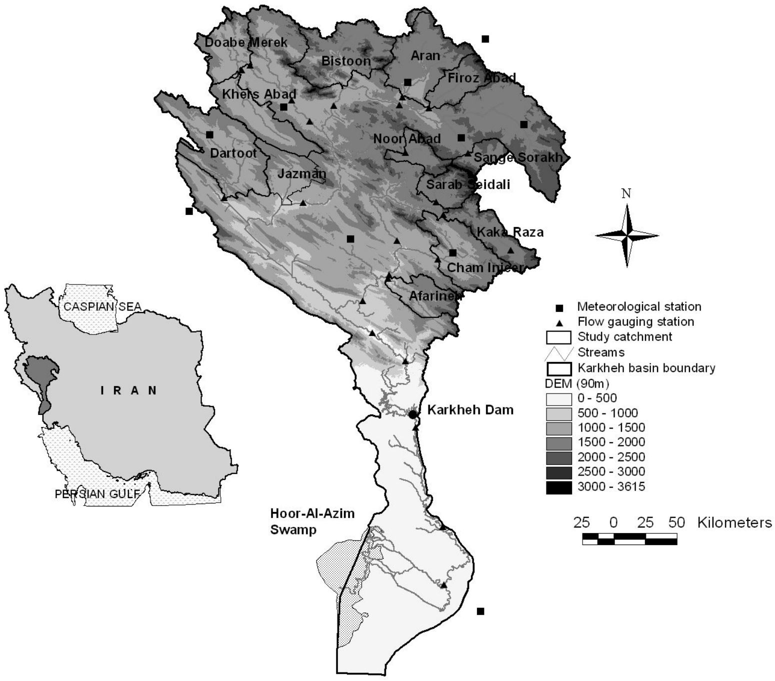

Fig. 1 Location of the Karkheh basin, study catchments and instrumentation network.

METHODOLOGY

The HBV model (Bergström, 1992; Seibert, 2002) was calibrated and validated using the daily climatic and (naturalized) stream flow data for the period of October 1, 1989 to September 30, 1997. The hydrological similarity is defined based on the three similarity measures: geographical area, spatial proximity and shape of the flow duration curve (FDC). FDCs for the ungauged catchments were predicted using logarithmic relationship of the form $Q = a - b\ln D$; where Q is the discharge (m^3/sec), D is the corresponding percentage time of exceedance varying as 5, 10, 15…..95 % and a and b are positive model parameters which were estimated using the developed regression equations (1 & 2) using the catchment characteristics pertaining to precipitation (P, mm/a), catchment slope (S, %), standard deviation of catchment elevation ($SDce$, m), geology type 3, metamorphic rocks, ($G3$, %) and shape, ratio of perimeter over drainage area, (Sh, km^{-1}) of the catchment. The similarity in the FDCs was defined based on the visual comparison of their shapes as well as the estimation of Root Mean Square Error (RMSE). Once the similarity between the catchments was established the whole parameter set of one catchment is transferred to another catchment for stream flow simulations. The results were evaluated using Nash-Sutcliffe efficiency criteria, R_{eff}, at monthly and daily time scales and the mean annual volume balance.

$$a = 81.318 + 7.645S - 0.846G3 - 0.264SDce - 149.890Sh - 0.106P \quad (1)$$

$$b = 18.557 + 1.716S - 0.184G3 - 0.0612SDce - 31.429Sh - 0.0253P \quad (2)$$

RESULTS AND DISCUSSION

The calibration results indicate that the mean monthly and daily R_{eff} values were 0.76 and 0.71, respectively. The validation of estimated parameters, for four of the 11 gauged catchments, further affirmed the suitability of calibrated parameters as indicated by the R_{eff} values averaging at 0.78 and 0.64 at monthly and daily time steps, respectively. The differences in the mean annual volume balance are within reasonable limit: less than 20%, except in two out of 11 catchments during calibration and 1 out of 4 during validation. The reported performance measures for Karkheh basin are generally in agreement with those of other modeling studies (e.g., Merz & Blöschl, 2004).

The results of transposing model parameters based on similarity in area and spatial proximity show that in most cases the simulations were far away from the observed values in most cases both in terms of R_{eff} and the volume balance. The regionalization results, based on FDCs similarities, indicate that the simulated stream flows match well with the observed stream flows in most cases (Table 1). The mean R_{eff} at monthly and daily time steps were 0.70 and 0.57, respectively, and the mean annual volume balance was 13 %. This suggest that this method shows quite higher probability of success for application to ungauged catchments as 8 out of 10 cases results in R_{eff} of more than 0.50 at monthly and daily time scales. The results are in acceptable ranges as in general R_{eff}-values of more than 0.50 are considered as acceptable for flow simulations in ungauged catchments (e.g., Goswami *et al*., 2007).

Table 1 Streamflow simulations by transposing the parameter set of one catchment to another based on similarity of their corresponding FDCs.

Catchment Name	Area (Km^2)	Catchment whose Parameters are used	R_{eff} (-), monthly	R_{eff} (-), daily	Annual Volume Balance (%)
Aran	1938	Firoz Abad	0.82	0.71	31
Firoz Abad	844	Aran	0.66	0.45	-8
Kaka Raza	1137	Doabe Merek	0.82	0.70	28
Doabe Merek	1238	Kaka Raza	0.40	0.34	-39
Sarab Seidali	772	Chaminjeer	0.73	0.53	10
		Noor Abad	0.70	0.60	3
Cham Injeer	1637	Sarab Seidali	0.80	0.64	3
		Noor abad	0.73	0.59	2
Noor abad	600	Cham Injeer	0.64	0.53	18
		Sarab Seidali	0.69	0.59	12

The comparison among the tested methods has clearly shown that the FDC is the best similarity measure and this method was applied to two ungauged catchments named as Bistoon (2065 km^2) and Jazman (956 km^2). These two catchments were selected because of the availability of observed streamflow records during the 1970s. Using these observed streamflows, the FDCs for these catchments were compared with the 11 gauged catchments. The FDC of Bistoon gave best match with the FDC of Aran both in terms of visual comparison as well as RMSE values. The FDC of Jazman was found similar to that of Khers Abad. We also used the developed regional FDC model and estimated selected flow percentiles. Based on these calculations the FDC of these ungauged catchments were estimated and compared with those of gauged catchments. The similarity comparison was in agreement with the one done by using the observed data. Then the time series of stream flows for Bistoon and Jazman were simulated using the parameter set of Aran and Khers Abad, respectively. The results indicate that observed and simulated FDCs match quite well (Fig. 2). The shape of the hydrographs is also concomitant to the other catchments in the basin depicting similar rising and falling patterns in the hydrograph.

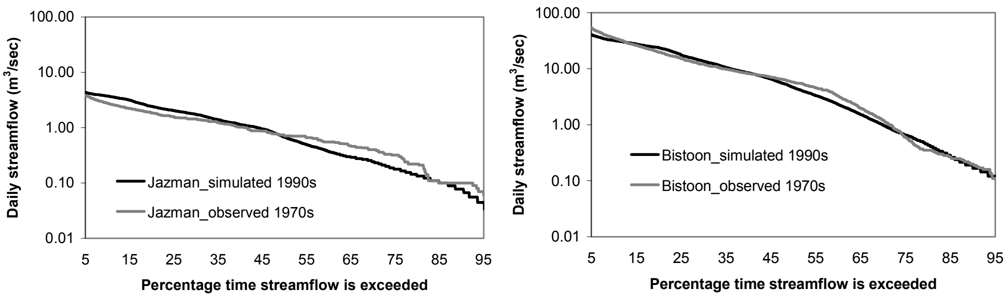

Fig. 2 Comparison of observed and simulated FDCs of Bistoon and Jazman.

CONCLUSIONS

The study has shown that catchment similarity analysis based on FDCs provide sound basis for transposing model parameters from gauged catchments to ungauged catchments in the Karkheh basin and the simulated stream flow would represent the actual hydrological response of ungauged catchments in most cases. The study concludes that the methods of utilizing FDCs could be applied for estimating ungauged stream flows in the mountainous parts of the Karkheh river basin and source area of other major rivers in that region (e.g. Dez, Karun and Zayandeh Rud). The proposed method can be widely replicated worldwide because it can capitalize on the existing knowledge of FDCs regionalization and limited data.

ACKNOWLEDGEMENTS

We are thankful to Ministry of Energy, Meteorological Organization and Agricultural Research and Extension Organization (AREO) of Iran for their cooperation and provision of data. Funds were provided through the Challenge Program on Water and Food (CPWF) and from the International Water Management Institute (IWMI) for which CPWF, IWMI and their donors are highly acknowledged.

REFERENCES

Bergström, S. (1992) The HBV model—its structure and applications. *SMHI, no. 4, Norrköping, Sweden*.

Goswami, M., O'Connor, K. M. & Bhattarai, K. P. (2006) Development of regionalization procedures using a multi-model approach for flow simulation in an ungauged catchment. *J. Hydrol.* **333**, 517-531.

Masih, I., Ahmad, M. D., Turral, H., Uhlenbrook, S. & Karimi, P. (2008) Understanding hydrologic variability for better surface water allocations in Karkheh Basin Iran. In: *Proceedings of the XIIIth IWRA World Water Congress, Montpellier*, France, 1-4 September 2008.

Merz, B. & Blöschl, G. (2004) Regionalization of catchment model parameters. *J. Hydrol.* ***287***, 95–123.

Seibert, J., 2002. HBV light version 2, User's manual. *Oregon State University Department of Forest Engineering Corvallis, Oregon, USA. Uppsala University, Dept. of Earth Science, Hydrology, Uppsala*.

Runoff prediction at different modelling scales

H. P. NACHTNEBEL

Inst. of Water Management, Hydrology and Hydraulic Engineering, University of Natural Resources and Applied Life Sciences, Vienna. Muthg. 18, A-1190 Vienna, Austria

hans_peter.nachtnebel@boku.ac.at

Abstract In this paper an attempt is made to summarise the recent state of hydrological catchment modelling and to evaluate the prediction capability of distributed hydrologic models. The predictability of hydrological processes is still limited due to unknown initial conditions, unobserved state variables, nonlinearities in the fundamental hydrological processes and major uncertainties in the spatio-temporal features of input variables. In real time forecasting major progress has been achieved in the last years by integrating radar data for now casting and by applying non-linear filtering techniques and inverse approaches for improved state estimation and output prediction. The reliable description of the heterogeneity in land related information and in the meteorological input to hydrological models requires substantial improvement.

Keywords distributed hydrological models; scaling; parameter estimation; data assimilation

INTRODUCTION AND BACKGROUND

In the last decades numerous hydrological models were developed to understand hydrological processes at different scales, to describe the reaction of the catchment to human interventions, and to forecasts the runoff behaviour. Obviously, dependent on the spatio-temporal resolution different hydrological processes emerge and their respective model parameters have to estimated, either from land related information or by calibration which is usually achieved by fitting the model output to observed runoff data.

The spatially distributed hydrological models are mostly conceptual, sometimes with a few physically based components while others are described by a simplification of hydraulic processes. Most of the models can be described in a state space formulation including several linear submodels transforming the spatially averaged input into the output, such as the HBV-model (Bergström, 1992), Prevah (Viviroli *et al*., 2007), Lisflood (de Roo *et al*., 2000) and many others (Singh, 1995). The separation into runoff components, mostly defined as surface runoff, interflow and base flow is triggered by thresholds representing a certain storage capacity and release function of subsoil layers. Some of the processes, such as infiltration, require a non-linear description (van Genuchten, 1980, Brutsaert, 2000) and at the plot scale when macropores (Weiler, 2005; Botschek, J *et al*., 2002) are relevant additional thresholds are introduced.

Several aspects will be discussed which limit the predictive capability of hydrological models: the uncertainty in initial conditions, the imprecise information about model input, the non-linearity of the system, the structural heterogeneity and unobservability of the system states and parameters, and the temporal change of system parameters.

INITIAL CONDITIONS AND HYDROLOGICAL DATA BASE

The hydrological model is formulated by a set of differential equations which require initial and boundary conditions for obtaining a solution. The initial conditions are defined by the amount of water stored in the various layers of the model. Snow cover data are available for several time slices but the information about the snow water equivalent is rare, and if available it refers to snow gages at a few locations. Soil moisture data are quite limited, especially in forested regions. In valley floors or in basins with larger flat land areas some groundwater data might be useful to learn about initial conditions in the groundwater system. In alpine catchments this information is in general not available or not useful for regionalisation. Summarising, the estimation of the initial catchment conditions is subjected to major uncertainties.

In general, the hydrological model input refers to spatio-temporal fields of precipitation and temperature while the output is described by time series of the outflow components. The respective data base refers to point observations of rainfall and temperature while the output is only measured as the sum of its components. With the help of a few rain gages the spatial features of the rainfall field have to be interpolated. Comparing the area directly controlled by the rainfall observation network with the catchment area a typical ratio of $1:10^{10}$ is found. The direct measurement error ranges from a few percent up to 30 % when precipitation in a mountainous environment is measured (Sevruk, 1989, 2005). Wood *et al.* (2000) report that the measurement error of precipitation within a 2 km side square grid was about 33 % in a low relief and about 45 % observed at a high relief grid square. Radar data provide some additional information about the spatial characteristics of the rainfall field but this additional information is critical in a mountainous environment.

Discharge measurements are often classified as highly reliable with a measurement error of about 3-5 % during regular runoff conditions. During floods the measurement error may go up to 30 % and in some cases even higher.

NONLINEARITY AND HETEROGENEITY

Nonlinearity in hydrological models has several origins. Either the model equations are non-linear or the parameters in the equation are state dependent which results in a non-linear model or thresholds trigger the behaviour of the processes. Typical threshold parameters characterise preferential flow, the separation of runoff into its components and the storage capacity of different surface and subsurface layers. Altogether, this implies that the overall system is definitely nonlinear and the predictability decreases.

The heterogeneity of the driving parameters, such as slopes, surface roughness, infiltration capacity, storage capacity etc., is extremely high and it is handled in land parametrisation by defining homogeneous subunits, either by gridding or by overlaying and intersection of different land information layers.

The most reliable information in catchment modelling refers to the digital terrain data, river network and land use. Soil maps are available but their quality is often questionable and therefore pedo-transfer functions are difficult to apply. The estimation of catchment model parameters from land information is an attractive task, although not always successful (Sorooshian & Gupta, 1995; Seibert, 1999; Xia *et al*., 2002; Parajka *et al*., 2005; Blöschl, 2005; Ao *et al*., 2006). Frequently regression type procedures are applied in which physiographic catchment features are related with model parameters which were obtained by fitting the model output to observed runoff. Utilizing the established relationship and estimating the model parameters for ungauged catchments the simulation are often not satisfactory in the sense that the fitting is poor and a subsequent recalibration with runoff data yields quite different modelling parameters. Kling and Nachtnebel (2008) related the base flow properties to the regional estimation of runoff separation parameters, which are represented in the model by thresholds, utilizing spatial information contained in soil maps. The method proved to be successful in identifying threshold parameters of an HBV type model.

Due to the large uncertainties in the input the task of parameter estimation from output information is an ill posed problem. A large number of different parameter sets result therefore in similar modelling efficiency (Beven & Freer, 2001). Due to the fact that in most of the applications the model state, e.g. soil moisture content, is not observed an inverse approach (Vrugt *et al*., 2001; Mertens *et al*., 2006; Schmalz *et al*., 2003) is necessary to identify local to regional soil parameters from runoff data, dependent on the spatial resolution of the modelling approach. In the last years numerous estimation procedures based on inverse modelling and data assimilation techniques (Crisan *et al*., 1999; Vrugt *et al*., 2002; Moradkhani *et al*, 2005; Carpenter *et al*., 1999; Troch *et al*., 2003; Evensen, 2007) have been applied to overcome this problem. But as long as there is so much uncertainty in the meteorological input and in spatial information these tools cannot really overcome the problem.

Of course, these tools are helpful in forecasting systems because they may yield better forecast and additionally they provide some information about uncertainty in the forecasts, and this is considered as highly valuable information. Improved flood forecasting could be also achieved by an adaptive neural network giving a higher weight to the most recent observations while the younger past is as well considered as relevant for the actual output but with a lower weighting factor. This only means that recent information is better utilised and therefore the model performance is improved. This does not imply that the understanding of the system has been deepened or that model parameters are estimated more reliably.

OBSERVABILITY OF STATES

The states of the model, mostly representing the volumes of stored water in the snow layer, interception layer, soil and subsoil layers, are not observable at all. Sometimes, a few point data characterizing soil moisture content snow water equivalent may be available and this could theoretically assist in monitoring the state locally. Considering the spatial resolution of the distributed hydrological models the number of the unknown states and thus the dimensionality in the state estimation procedure is increased tremendously. Hidden Markov models may assist in estimating unknown model parameters (Cappe *et al*., 2005; Zucchini & Guttorp, 1991).

In this context it should be considered that hydrological model parameters are not only dependent on the system state but they are seasonally varying and they can be subjected to long term changes. It is evident that surface runoff formation is directly dependent on the development of vegetation layers which are obviously subjected to seasonality and growing stages. In several field experiments the herb layer proofed to be relevant in runoff formation processes at the plot scale (Markart *et al*., 2000; Nachtnebel *et al*., 2005) and this information is typically not included in land use maps.

CONCLUSIONS AND RECOMMENDATIONS

In this paper an attempt was made to summarise the recent state of hydrological catchment modelling and to evaluate their predictive capability. Although land related information is increasingly available major restrictions for predicting ungaged basins still exists. The reasons are seen in the nonlinear features of hydrological processes, in the extremely high dimensionality of states and parameters in distributed models, in the uncertainty in the initial conditions and in the sampling uncertainty of the input variables, especially in the spatio-temporal distribution of rainfall. Further, the assumption of time independent model parameters is critically seen due to (seasonally) varying impacts of the vegetation on land cover and soil properties.

Improvement of hydrological predictability and parameter estimation requires an increased density of observation networks, improved accuracy of measurements and long term observations to cover the broad range of possible hydrological states. Further this may help in improving the knowledge about the long term memory of basins. Another interesting approach is in coupling directly meteorological and hydrological models. Based on the long term analysis of the water balance of about 1500 Austrian catchments the precipitation data had to be regionally substantially modified to achieve sound water balances (Kling *et al*., 2005). Recent flood forecasting projects in Austria (Kahl & Nachtnebel, 2007) led to a modified re-analysis procedure of precipitation data to improve the hydrological modelling output. Until now, meteorologists operate their atmospheric models independently from hydrological models although both models simulate actual evapo-transpiration and simultaneously they are coupled by precipitation.

Remotely sensed spatial information, either from ground based radar systems, airborne information or satellite data require further improvement and integration in modelling and forecasting practise.In real time forecasting major progress has been achieved in the last years by integrating radar data for now casting and by applying non-linear filtering techniques for improved state estimation and output prediction.

The reliable description of the heterogeneity in land related information and in the meteorological input to hydrological models requires substantial improvement.

REFERENCES

Ao, T., Ishidaira, H., Takeuchi K., Kiem, A. S., Yoshitari, J., Fukami, K. & Magome, J. (2006) Relating BTOPMC model paramateres to physical features of Mopex basins. *J. of Hydrology* **320**, 84-102.

Bergström, S. (1992) The HBV-model; its structure and applications. *SHMI Report RH #4,* Norrköpping, Sweden.

Beven, K. J. & Freer, J. (2001) Equifinality, data assimilation, and uncertainty estimation in mechanistic modelling of complex environmental systems. *J. of Hydrology* **249**, 11–29.

Blöschl, G. (2005) Rainfall-runoff modelling of ungauged catchments. *Encyclopedia of Hydrological Sciences,* J. Wiley Sons.

Botschek, J., Krause, S., Abel, T. & Skowronek, A. (2002) Hydrological parameterization of piping in loess-rich soils in the Bergisches Land, Nordrhein-Westfalen, Germany. *J. Plant Nutr. Sci*. **165**, 506-510.

Brutsaert, W. (2000) A concise parameterization of the hydraulic conductivity of unsaturated soils. *Adv. in Water Resources* **23**, 811:815.

Cappé, O., Moulines, E. & Rydén, T. (2005) Inference in Hidden Markov Models. *Springer, ISBN 0-387-40264-0*.

Carpenter, J., Clifford, P. & Fearnhead, P. (1999) Improved particle filter for nonlinear problems, *IEE Proc. Radar Sonar Navig.* **145**,1,2-7.

Crisan, D., del Moral, P. & Loans, T. J. (1999) Nonlinear filtering using branching and interacting particle systems. *Markov Processes Related Fields*. **5**(3),293-319.

De Roo, A., Wesseling, P. C. & Van Deursen, W. P. A. (2000) Physically based river basin modelling with a GIS: The LISFLOOD model. *Hydrological Processes* **14**, 1981-1992.

Evensen, G. (2007) Data Assimilation*. Springer, Berlin, Germany*.

Kahl, B. & Nachtnebel, H. P. (2008) Online updating procedures for a real time hydrological forecasting system. *Proc. of the XXIVth Conference of the Danubian Countries,* Bled, Slovenija.

Kling, H. & Nachtnebel, H. P. (2008) Regional estimation of runoff seperation parameters. Submitted *J. of Hydrology*.

Kling, H., Nachtnebel, H. P. & Fürst, J. (2005) Seasonal Water Balance of Austria. Austrian Federal Ministry of Agriculture, Forestry, Water and Environment (ed.) *The Hydrological Atlas of Austria.*

Markart, G., Pirkl, H., Kohl, B. & Sortier, B. (2000) From point data and cartography to the analysis of runoff and mass-movement processes in torrent catchment areas. In: *Proceedings of the Workshop on Advanced Techniques for the Assessment of Natural Hazards in Mountain Areas.* 5 – 7 June 2000, Igls, Austria. 72–73.

Mertens J., Stenger, R. & Barkle, G. F. (2006) Multiobjective inverse modelling for soil parameter estimation and model verification. *Vadose Zone J.* **5**, 917-933.

Moradkhani, H. & Hsu, K. L. (2005) Uncertainty assessment of hydrological model state and parameters : Sequenitial data assimilation using particle filter. *Water Resour. Res.* **41**,doi :10.1029/2004WR003604.

Nachtnebel, H. P., Leroch, K., Fürst, J., Holzmann, H., Markart, G., Kohl, B., Kirnbauer, R., Pirkl H. & Ramspacher, P. (2005) Abflussverhalten von Einzugsgebieten verschiedener Größe bei Dauerregen. *GZ 58110-VC7/2000, BMfLFUW, Vienna, Austria.*

Parajka J., Merz, R. & Blöschl, G. (2005) A comparison of regionalisation methods for catchment model parameters. *Hydrology and Earth Systems,* **9**, 157-171.

Schmalz, B., Lennartz, B. & van Genuchten, M. Th. (2003) Analysis of unsaturated flow in a large sand tank. *Soil Sci. Vol.* **168**, 3-14.

Seibert, J. (1999) Regionalisation of parameters of a conceptual rainfall runoff model. *Agr. For. Met*., 98-99, 279-293.

Sevruk, B (1989) Wind induced measurement error for high intensity rains. In: (ed. B. Sevruk), *Precipitation measurements. WMO/IAHS/ETH Workshop on precipitation measurement.* Zuerich, Switzerland.

Sevruk, B & Chvíla, B. (2005) Precipitation in Urban Areas. *Atmospheric Research* **77**(1-4), 39-47.

Sorooshian, S. & Gupta, V. K. (1995) Model calibration. In: (ed. V.P. Singh), *Computer Models of Watershed Hydrology.* Water Resources Press, CO, USA.

Troch, P., Paniconi, C. & McLaughlin, D. (2003) Catchment scale hydrological modelling and data assimilation. *Adv. Water Resour.* **26**, 131-135.

Van Genuchten, M. Th. (1980) A closed form equation for predicting the hydraulic conductivity of unsaturated soils. *Soil Sci. Am. J.* **44**, 892-898.

Viviroli, D., Gurtz, J. & Zappa, M. (2007): The Hydrological Modelling System PREVAH. *Geographica Bernensia P40.* Berne: Institute of Geography, University of Berne, ISBN 978-3-905835-01-0

Vrugt, J. A., Pouten, W. & Weerts, A. H. (2001) Information content of data for identifying soil hydraulic parameters from ouflow experiments. *Soil Sci. Soc. J.* **65**, 19-27.

Vrugt, J. A., Gupta, H. V., Bouten, W.& Sorooshian, S. (2002) A shuffled complex evolution Metropolis algorithm for optimisation and uncertainty assessment of hydrologic model parameters. *Water Resour. Res.* **39**(8), 1201.

Weiler, M. (2005). An infiltration model based on flow variability in macropores: development, sensitivity analysis and applications. *J. of Hydrology* **310**(1-4), 294-315.

Wood, S. J., Jones, D. A. & Moore, R. J. (2000) Accuracy of rainfall measurement for scales of hydrological interest. *HESS* **4**(4), 531-543.

Xia, Y, Gupta, H. V., Leplastrier, M., Henderson-Sellers, A. & Bastidas, L. A. (2002) Calibrating land surface model of varying complexity using multi-criteria methods and the Cabauw data set. *J. Hydrometeorlogy* **3**(2), 181-194.

Zucchini, W. & Guttorp, P. (1991) A hidden Markov model for space-time precipitation. *Water Resour. Res.* **27**, 1917-1923.

Use of complex deterministic model of runoff formation processes at basins of any scale

OLGA M. SEMENOVA[1] & TATYANA A. VINOGRADOVA[2]

1 *Department of Experimental Hydrology and Mathematical Modelling of Hydrological Processes, State Hydrological Institute, 2-ya liniya V.O. 23, 199053, Saint-Petersburg, Russia*
omakarieva@gmail.com

2 *Department of Geography and Geoecology, Saint-Petersburg State University, 31/33 10-ya liniya V.O.,199178, Saint-Petersburg, Russia*

Abstract One of the main problems of contemporary mathematical modelling of hydrological processes is considered to be the scaling problem. This report intents to demonstrate that the scaling problem could be solved by using appropriate algorithms of runoff modelling. The problem solution is illustrated by modelling results for watersheds of different sizes dominated by various landscape characteristics within the Lena river basin. The deterministic distributed hydrologic model "Hydrograph" (State Hydrological Institute, Saint-Petersburg, Russia) is applied.

Keywords deterministic distributed modelling; the scaling problem; universal hydrologic model "Hydrograph"; the Lena river basin

INTRODUCTION

At present, the approach oriented to description and modelling of specific river basins and/or single runoff formation processes is prevailing. The value of such models is refuted by defects in their structure and necessity of parameter calibration for any new objects. Scaling problem is considered to be fundamental as this is the main source of uncertainties introduced by hydrologic modelling (Wood, 1995; Kundzewicz, 1993; Beven, 1996; Refsgaard *et al*., 1996). In general it could be summarized in the following main statements: parameters of macro scale models are generalized parameters at the micro scale; relationships and equations are different for different scales; equation parameters are different at different scales; a universal scaling methodology, allowing transition from one set of scale parameters to any other, is highly desired and still undeveloped; data are to be collected at the scale required by modelling (Vinogradov, 2003).

The scaling problem calls for a conflict with essential fundamentals of physics suggesting that the process of runoff formation must be the same in any point of space. The latter implies that mathematical theory and parameters must be the same for all scales if the model is adequate to the natural processes.

The research main objective is to display a solution of the scaling problem in hydrologic modelling using an example of river Lena watersheds of different scales. The study area of river Lena was chosen because this basin is least investigated and represented by sub-watersheds with very different landscapes, geomorphology and climate characteristics. Modelling part of the research employed a deterministic distributed hydrologic model "Hydrograph" (Vinogradov, 1988, 1995, 1998).

METHODS

The deterministic distributed model of runoff formation processes "Hydrograph" is a universal hydrologic modeling system that covers all types of runoff and can be applied for all geographical regions and river basins of any size. Parameters are supposed to be distributed across the basin area (system of representative points) and vertically within soil-vegetation column. Local variations of snow coverage are taken into account. The model is oriented to the simplest meteorological network information with the simultaneous application of methods enhancing it (air temperature and moisture deficit, precipitation layer). The model output consists in continuous runoff hydrograph and distributed variable states reflecting temperature, water, and phase regimes of soil and snow cover for the specified time intervals (24 hours or lower). Model parameters represent water and physical characteristics of soil and vegetable cover, features of hydrographic network, nature of slope and channel runoff transformation. The conceptions used as a basis of the model, its algorithms and features are rather detailed discussed in (Vinogradov, 1988).

The essential and algorithmic content of the model "Hydrograph" differs greatly from other known models. The main differences are related to such problems as water dynamics and changes of phase in soil, formation of surface, subsurface and underground runoff, slope and channel runoff transformation.

The structure of runoff formation model is mainly determined by the accepted approaches describing water dynamics within the river basin. The use of partial differential equations such as equations of Saint-Venant or kinematic wave for surface and channel flow and Boussinesq equation for underground waters, is prevailing in modern deterministic hydrologic models. Here it is assumed that water movement is represented by thin continuous water layer, that is not corresponding with natural process of water motion over the real surface and underground slopes. The incomplete physical validity of these models, lack of reliable information on the real conditions of water movement, requirement of large amount of information about inclinations, morphology, "roughness" coefficients for solving these equations make large-scale basins modelling impossible using these approaches.

The model "Hydrograph" uses integral approach for describing water movement within the basin – the concept of runoff elements (Vinogradov, 1988, 2003). The basin is constituted by the set of elementary slopes or watersheds, which, in their turn, consist of runoff elements system. Runoff element is a part of surface or underground elementary slope or watershed limited by micro-divides which is directed with its open part to the slope non-channel or underground drainage system. The size of runoff elements depends on inclination; the underground runoff elements are larger than surface ones. The equation for water flux Q from all runoff elements of the given level to channel system is:

$$Q = \frac{S+b}{1+[(S-Q_0)/(Q_0+b)]\exp[-a\Delta t(S+b)]} - b \tag{1}$$

Here Q_0 is initial value of runoff Q and S is runoff formation intensity (m^3 s^{-1}); Δt is computation time interval (sec) during which S is constant; $a=a^*\times F^{1}$ and $b=b^*\times F^{1}$, where a^*, b^* - normalized hydraulic coefficients with dimension m^{-1} and m s^{-1}; F – basin area (m). The total water flux to the channel system is described by an equation system such as (1) when values S, Q, a and b are different for the multitude of surface, soil and underground runoff elements of different levels that form a river basin. The types and features of runoff elements determine the transformation character of runoff formation hydrographs in the point of its origin into water flux to the channel system. The derivation of equation (1), runoff elements system and related flow types description, values range of a^* and b^* parameters are represented in (Vinogradov, 1988, 2003).

The concept of runoff elements not only considerably simplifies computations in comparison with numerical solution of the differential equations of movement and continuity, but also allows us to carry out simulations for basins of any size, since the used parameters do not depend on scale.

RESULTS AND CONCLUSIONS

The research included runoff modelling for ten watersheds of different sizes ranging from less than 100 km^2 to greater than 10^6 km^2 with daily computation interval for the period of 1975-1984. The model parameters estimated for small watersheds were sequentially used for large-scale ones.

Observed *vs* simulated hydrographs for four watersheds including Lena at Kusur (2.4 million km^2) for one year (1983) are shown in Fig. 1. Table 1 illustrates the values of statistical characteristics for observed *vs* simulated daily and annual flow layers for five typical basins (simulation period of ten years). Nash-Sutcliffe efficiencies *Ef* (Nash & Sutcliffe, 1970) which is shown in Table 1 below zero indicate that the variance of the observed hydrograph is smaller than the error variance; while an efficiency of one corresponds to a perfect model prediction. For all basins *Ef* exceeds 0.60, and for 3 it exceeds 0.8.

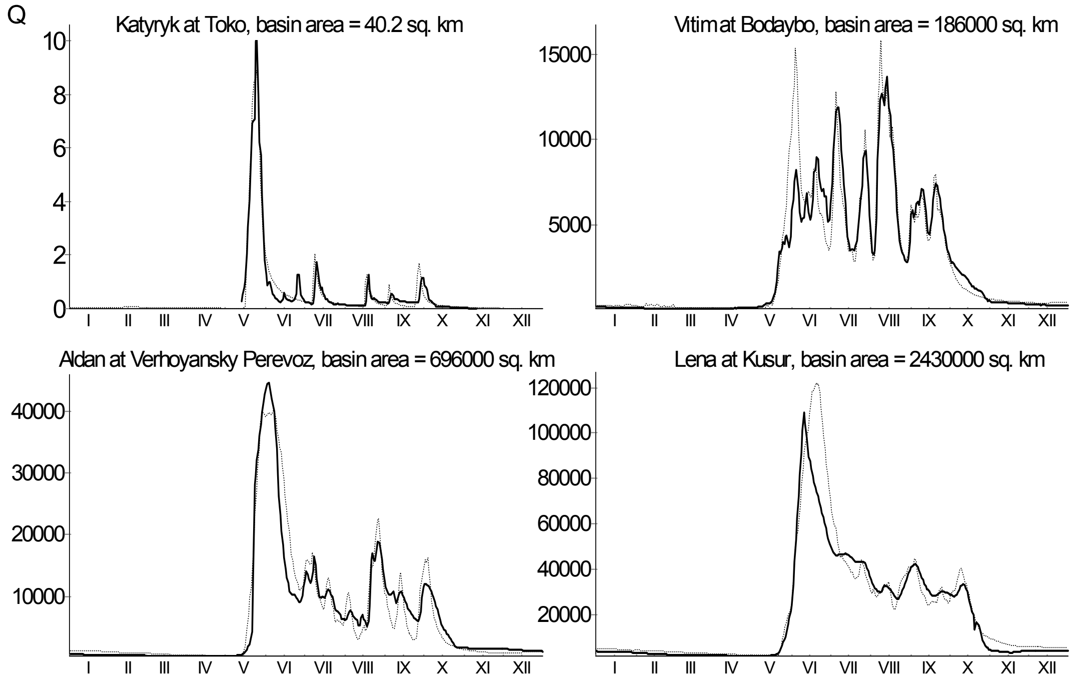

Fig. 1 Observed (solid line) and simulated (dotted line) hydrographs (m^3 s^{-1}) for several watersheds of different scale within the Lena river basin, 1983.

Although results of runoff formation processes for different scale watersheds of the Lena river basin can be considered wholly satisfactory (Fig. 1, Table 1), there was still a large discrepancy between simulations and the real flow. Like all hydrologic models, “Hydrograph” is very sensitive to the meteorological forcing data, particular precipitation. Runoff simulations were most significantly limited by input meteorological data which was nonrepresentative for mountainous territories that makes difficulties for its interpolation from meteorological stations to representative points.

Table 1 Statistical characteristics of observed *vs* simulated daily (numerator) and annual (denominator) flow layer values for different scale watersheds within the Lena river basin.

Basin	Basin area, 10^3 km^2	H_{obs}	H_{calc}	Δ	*RMSD*	*Ef*	*r*	*Er,%*		
								Mean	*Min*	*Max*
Lena at Kusur	2400	0.68 / 248	0.67 / 243	0.01 / 5	0.02 / 6.1	0.89 / 0.88	0.94 / 0.99	0.21 / 0.02	0.17 / 0.02	0.25 / 0.03
Aldan at Verhoyansky Perevoz	696	0.70 / 255	0.81 / 294	-0.11 / -39	0.02 / 14.6	0.85 / 0.56	0.95 / 0.89	0.24 / 0.14	0.20 / 0.04	0.28 / 0.26
Vitim at Bodaybo	186	0.78 / 285	0.78 / 286	0 / -1	0.02 / 18.0	0.84 / 0.89	0.93 / 0.96	0.29 / 0.06	0.20 / 0.02	0.35 / 0.18
Uchur at Ch’ulbyu	108	1.0 / 365	1.04 / 378	-0.4 / -13	0.03 / 18.3	0.84 / 0.38	0.92 / 0.74	0.34 / 0.08	0.27 / 0.05	0.39 / 0.15
Timpton at Nagorny	0.600	1.39 / 507	1.41 / 516	-0.02 / -9	0.05 / 22.3	0.61 / 0.52	0.83 / 0.84	0.58 / 0.10	0.51 / 0.06	0.65 / 0.26
Katyryk at Toko	0.040	1.07 / 392	1.12 / 407	-0.05 / -15	0.05 / 28.3	0.72 / 0.65	0.87 / 0.93	0.40 / 0.07	0.27 / 0.02	0.52 / 0.23

H_{obs} = observed value; H_{calc} = calculated value; Δ = mean deviation; *RMSD* = root mean square deviation; *Ef* = Nash-Sutcliffe Efficiency; *r* = correlation coefficient; *Er* = relative error.

Obtained research results suggest further development of algorithms proposed in model “Hydrograph” which describe runoff formation processes free from the scaling problem.

REFERENCES

Beven, K. J. (1996) A discussion of distributed hydrological modelling. In *Distributed Hydrological Modelling* (ed. by M. B. Abbot & J. C. Refsgaard). *Water Science and Technology Library* **22,** 255-278, Kluwer Academic Publishers.

Kundzewicz, Z. (1993) Where shall we go from? Hydrological research towards the 21st century. *International Conference on Hydrology. Towards the 21st century: Research and operational needs.* 22-26 March 1993, Paris, France, 63-71.

Nash J. E. & Sutcliffe, J. V. (1970) River flow forecasting through conceptual models: 1 A discussion of principles *J. Hydrol.* **10**(3), 282–290.

Refsgaard, J. C., Storm, B. & Abbot M. B. (1996) Comment on “a discussion of distributed hydrological modelling” by K. Beven. In Distributed Hydrological Modelling (ed. by M. B. Abbot, & J. C. Refsgaard). *Water Science and Technology Library* **22**, 279-295, Kluwer Academic Publishers.

Vinogradov, Yu. B. (1988) Mathematical modelling of runoff formation. A critical analysis. *Gidrometeoizdat,* Leningrad, 312 pp. (in Russian)

Vinogradov, Yu. B. (1995) Hydrological modelling of Arctic river runoff. In Proceedings *of the workshop on the ACSYS solid precipitation climatology project* (Reston, VA, USA, 12-15 September 1995), WMO/TD No.739, 144-158.

Vinogradov, Yu. B. (1998) Mathematical Runoff-Erosion-Contamination Model. *Meteorology and Hydrology* **5**, 87-96 (in Russian)

Vinogradov, Yu. B. (2003) River Runoff Modelling. In *Hydrological Cycle*, edited by I.A. Shiklomanov, in *Encyclopedia of Life Support Systems (EOLSS)*, Developed under the auspices of the UNESCO, Eolss Publishers, Oxford, UK, [http://www.eolss.net].

Vinogradov, Yu. B. (2003) Runoff Generation and Storage in Watershed. In *Hydrological Cycle*, edited by I.A. Shiklomanov, in *Encyclopedia of Life Support Systems (EOLSS)*, Developed under the auspices of the UNESCO, Eolss Publishers, Oxford, UK, [http://www.eolss.net].

Wood, E. F. (1995) Scaling behaviour of hydrological fluxes and variables: empirical studies using a hydrological model and remote sensing data. In *Scale Issues in Hydrological Modelling* (ed. by J. D. Kalma & M. Silavapan). Chichester, England, Advanstar Communications, 89-104.

Can parameters of lumped rainfall runoff models be identified within regions with high rainfall spatial variability?

C. N. ALMEIDA, A. M. B. PASSERAT DE SILANS & R. Q. PORTO

Laboratory of Water Resources and Environmental Engineering – LARHENA, Center of Tecnology – University Federal of Paraíba, 58059-900, João Pessoa – Brazil

c.almeida@.pq.cnpq.br

Abstract Discussions about parameters identification have been focused in the international scene mainly with the PUB Project (Predictions in Ungauged Basins). As a contribution, this paper presents a study carried out in the Coastal Northeast Region of Brazil. The Gramame river basin is characterized by a high spatial rainfall variability and a lack of discharge monitoring. Because of this, the planning and management of water resources for this watershed have to be based on synthetic discharge data, whose values depend on rainfall data. It means that, in order to quantify water resources, the use of mathematical techniques are needed. The study uses a brazilian well-know hydrologic rainfall runoff lumped model, SMAP (Lopes *et al.*, 1982), with the Genetic Algorithm (GA) (Duan *et al.*, 1992) optimization technique, in order to find the optimal set of parameters. The aim is to assess the parameters variability when rainfall gauges density are diminished. The GA technique finds the global solution of a mathematical function. In the studied basin, eleven rainfall gauges data were operated from 1972 to 1989, and one discharge gauge with data from 1972 to 1978. These data were used to get the referential set of parameters by the automatic calibration process with GA technique. The methodology was used to discuss and the identifying of optimum model parameters in case of high rainfall spatial variability consists of modification on the spatial rainfall field by sequential subtractions of one to seven rainfall gauges to calculate the average monthly rainfall in the basin. Each subtraction set is compound of N random rain gauges combinations for which the average rainfall was calculated and then the SMAP model was run and calibrated with GA technique. For each subtraction set, statistical analysis were performed on the monthly rainfall average and also on the parameters set. Then, it could be observed how the average monthly rainfall and, consequently, the parameters were affected by different rainfall location for a given rainfall gauges density and also for the variation of rainfall gauges density. Results showed that although there were a wide variation in relation to the spatial distribution of rainfall gauges, little interference occurs in the values found for the automatically calibrated parameters, and to the values of discharges.

Keywords parameter uncertainty; hydrologic conceptual model; automatic calibration

INTRODUCTION

In order to move forward and improve the knowledge of the hydrological cycle and its uncertainties, a program named PUB (Predictions in Ungauged Basins) was created at the beginning of this decade. This program aims to estimate the uncertainty and its consequent minimization in hydrological forecasting (Sivaplan *et al.*, 2003).

With regard to the uncertainties in hydrological forecasts, this can occur at two levels, one that comes from the imperfection of the hydrological model framework, and one that is generated by the data entry of the model. Depending on the model adopted, these uncertainties propagate themselves through it and contribute to the uncertainty of the results. The higher the number of parameters that must be estimated, the more uncertainty in the results.

It is in this context that fits this study, seeking assess and quantify the uncertainties related to the parameters calibrated automatically. To optimize the parameters of the model was used the technique of Genetic Algorithms (Duan *et al.*, 1992). For the analysis of these uncertainties, the SMAP (Lopes *et al.*, 1982), a lumped rainfall runoff model was applied in a basin located on the coast of northeastern Brazil.

For this study, the influence of the spatial distribution of rainfall on the calibrated parameters was investigated, observing his influence on the synthetic discharge data generated by the model.

METHODOLOGY

To assess the uncertainties on the parameters of the calibrated model and the consequent response of this relationship with the discharge, it was carried out changes in spatial distribution of rainfall network located in the studied basin.

Such modifications was the elimination of 1 to 7 Rainfall Gauges (RG's) of the total, it means 11 RG's. The elimination was carried out considering randomic arrangements of rainfall gauges, where average rainfall is calculated by the Thiessen method. Then, simulations were made with possible arrangements. In Table 1, the amount of arrangements drawn for each combination of RG's are shown, which are used to run the simulations.

Table 1 Number of random combinations rainfall gauges (RG's) for each rainfall exclusions gauges.

Combination of RG's eliminated:	Number of arrangements, Ni
	10
2 RG	20
3 RG	91
4 RG	283
5 RG	460
6 RG	460
7 RG	283

After the simulations, a statistical analysis on the automatically calibrated parameters and the synthetic discharge are done.

In the study, the adopted model was the lumped rainfall runoff model SMAP, which is based on 3 reservoirs and is made up of four parameters, Str, Pes, Crec and kk. The input data are potential evapotranspiration and the average monthly rainfall.

In the automatic calibration of the parameters of the model, it was used to the Genetic Algorithms technique, the SCE-UA (Shuffled Complex Evolution), seeking to minimize a mathematical function that relates the calculated and observed discharge. The used objective function prioritizes neither minimum or maximum discharge.

The study was carried out for the river Gramame basin, located in northeastern Brazil (Fig. 1), with input data from 1972 to 1974. This watershed is characterized by a gradient in rainfall rates of 30 mm/km.

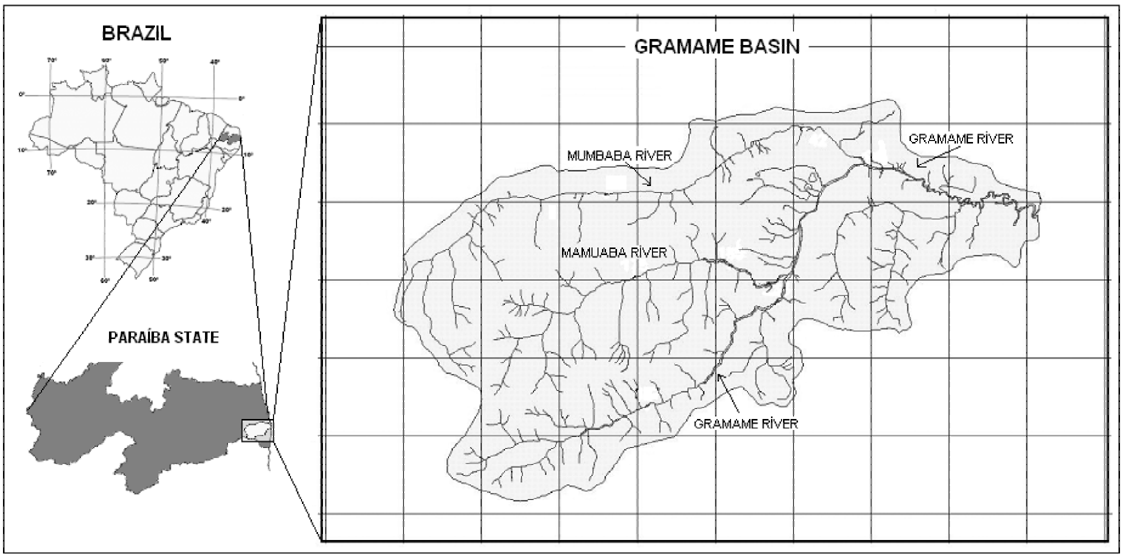

Fig. 1 Location of the study area – river Gramame basin.

RESULTS

As described in the methodology, a series of N simulations was performed with the model SMAP, with N exclusions of RG's. In each simulation the optimal parameters was found. For each set of N withdrawn the average of each parameter was calculated. Then, the average of the parameters versus the number of exclusions were plotted. Fig. 2 shows the variation of parameters and Crec and Pes.

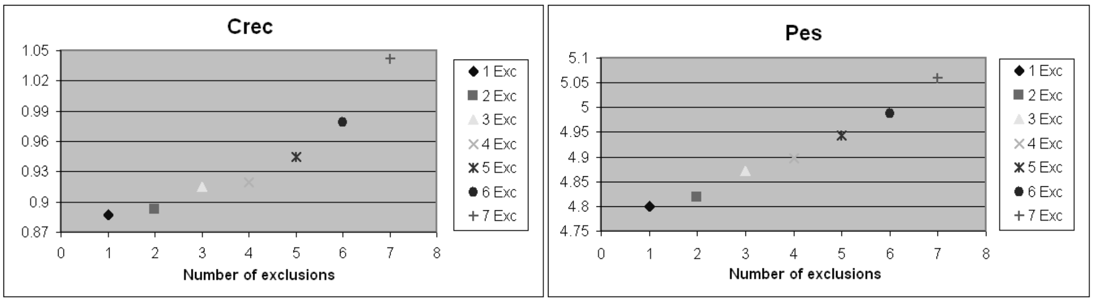

Fig. 2 Variation of parameters Crec and Pes, with 1 to 7 exclusions of RG’s.

It is observed in Fig. 2 that there was a tendency of growth of both parameters (Crec and Pes) as they the number of RG’s exclusion increases. With respect to the parameters Str and Kk, the change was minimal.

It was also determined the average monthly flow rates for the number of withdrawals. Fig. 3 shows the hidrograma with the values of the flow of reference and the average monthly flow rates of the simulations with the number of exclusions ranging from 1 to 7.

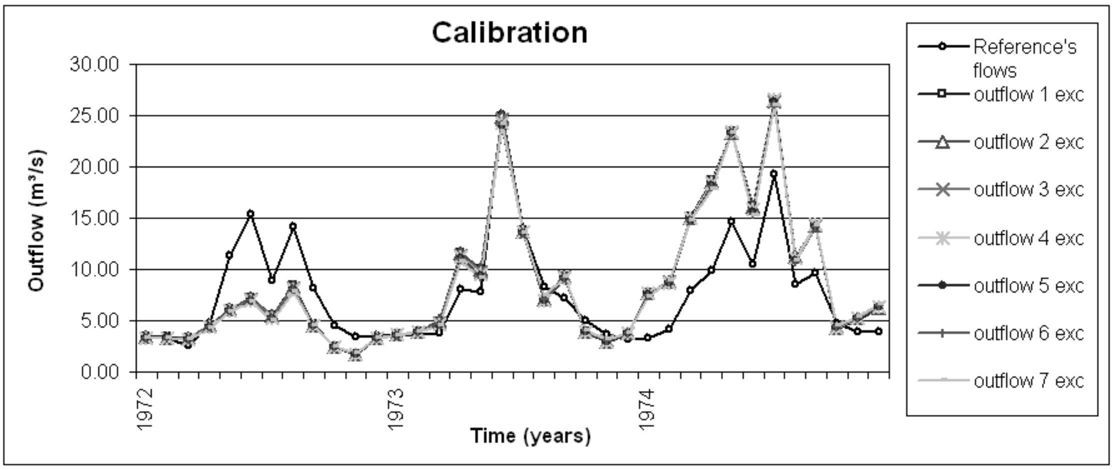

Fig. 3 Range of variation of parameters Crec and Pes, with 1 to 7 exclusions of RG's.

CONCLUSIONS

As was observed in the results, the values of two of the four parameters of the model increase as the number of RG's exclusions increase. However, the range of variation was only 0.15, Crec parameter, and 0.26, Pes parameter, from 1 to 7 exclusions. The parameters Crec and Pes can vary from 1 to 10 and from 0 to 100, respectively. So, it can be verified that the variation is very small. Thus, there was a little interference in the monthly discharge, which was observed by hydrographs. There are not significant differences between the average discharge of N exclusions. However, the results differ from the reference simulation.

So, although there will be a wide variation of the spatial distribution of rainfall gauges, little interference occurred on the results for the automatically calibrated parameters, and on the values of discharges. This indicates that the use of regionalization techniques in watersheds with high variability of rainfall is reliable.

Acknowledgements FINEP and CNPq are acknowledged for the financial support of this research.

REFERENCES

Duan, Q., Sorooshian, S. & Gupta, V. (1992) Effective and efficient global optimization for conceptual rainfall-runoff models. *Water Resources Research* **28**(4), 1015-1031.

Gan, T. Y. & Biftu, G. F. (1996) Automatic calibration of conceptual rainfall – runoff models: optimization algorithms, catchment conditions and model structure. *Water Resources Research* **32**(12), 3513-3524.

Lopes, J. E. G., Braga Jr, B. P. F. & Conejo, J. G. L. (1982) SMAP, A Simplified Hydrologic Model. *Symposium on Rainfall Runoff Modeling. MississiRGi.*

Sivaplan, M., Takeuchi, k., Franks, S. W., Gupta, V. K., Lakshmi, V., Liang, X., McDonnell, J. J., Mediondo, E. M., O'Cornnell, P. E., Pomeroy, J. W., Shrtzer, D., Uhlenbrook, S. & Zehe, E. (2003) IAHS decade on Predictions Ungauged Basins (PUB), 2003-2012: Shaping an Exciting Future for the Hydrological Sciences. *Hydrological Sciences Journal.*

Kuczera, G. & Parente, E. (1992) Effect of Rainfall Errors on Accuracy of Design Flood Estimates. *Water Resources Research* **28**(4), 1145-1153.

Feyen, L., Vrugt, J. A., Nuallain, B. O., Knijff, J. & Roo, A. D. (2007) Parameter optimization and uncertainty assessment for large-scale streamflow simulation with the LISFLOOD model. *Journal of Hydrology* **332**, 276-289.

Uncertainty on reference flows for the award of rights to the use of water in the coastal northeast region of Brazil

A. M. B. PASSERAT DE SILANS, C. N. ALMEIDA & R. Q. PORTO
Laboratório de Recursos Hídricos e Engenharia Ambiental – LARHENA. Centro de Tecnologia – Universidade Federal da Paraíba, Campus Universitário 58059-900 João Pessoa – Brazil
alainsilans@yahoo.com.br

Abstract In the coastal region of the Northeast area of Brazil, daily rainfall shows a high spatial variability with a very strong gradient in the East – West direction. Major cities of the region are concentrated in the coastal region, so the demand for water use has been increasing strongly. The award of rights to the use of water is given by a state agency authority, as a fraction of the Maximum Awardable Water (MAW) in points of calculus spatially distributed in the basin. The MAW is a reference flow calculated from the point of the flow duration curve for mean monthly flows with a ninety percent probability to be exceeded. As the number of streamflow gauges is very little or null in the basins of this region, thus it is necessary the use of hydrological models to generate monthly flows series from daily rainfall data series and then draw the flow duration curve. The purpose of this paper is to analyze the uncertainty associated to the MAW due to a weak representation of the daily rainfall field. The monthly flows series are generated in several points of the Gramame basin in the coastal area of Paraíba state – Brazil, using the hydrologic distributed conceptual model AÇUMOD (Silans *et al.*, 2000). Data inputs of the model are the daily rainfall measured in eleven rain gauges from 1972 to 1989. As in the others basins of the region, the rain gauges density is always smaller than in the Gramame basin, the methodology used to access the uncertainty on MAW is based on sequential subtractions of one to seven rain gauges to describe the daily rainfall field in the basin. Each subtraction set is compound of N random rain gauges combinations for which the AÇUMOD model is run. Statistical analysis of the generated flow series in each subtraction set, shows that the model sensitivity to the rainfall field representation is high, mainly in the upper reaches of the drainage basin. Flow duration curves are generated for each simulation of the subtraction sets, using pseudo-historical series generated by a Thomas-Fiering stochastic model. In each point of calculus, the mean flow duration curve is calculated by the mean monthly flows with a 90% confidence interval. It is shown that the confidence interval for each set of combinations is quite narrow and that uncertainty increases when more than two rain gauges are subtracted. Sensitivity of the model varies in space. The uncertainty on the MAW varies very much in space and show a different behavior than the errors associated to the mean flows.

Keywords hydrologic distributed model AÇUMOD; uncertainty, rainfall spatial variability; rights of use of water

INTRODUCTION

In the coastal region of the Northeast area of Brazil, daily rainfall shows a high spatial variability with a very strong gradient in the East – West direction. Major cities of the region are concentrated in the coastal region, so the demand for water use has been increasing strongly. The award of rights to the use of water is given by the state agency authority, as a fraction of the Maximum Awardable Water (MAW) in points of calculus spatially distributed in the basin. The MAW is a reference flow calculated from the point of the flow duration curve for mean monthly flows with a ninety percent probability to be exceeded. In this region, there is only a very little number of streamflow gauges, so one uses hydrological models to generate monthly flows series from daily rainfall data series and then draw the flow duration curve.

Uncertainty on the generation of run-off due to the spatial sampling of rainfall has been studied by several authors (Faures *et al.*, 1995, Goodrich *et al.*, 1990, Lopes, 1996, Medeiros *et al.*, 2007). All of them showed that the sensitivity of the output of the run-off model is higher as the rainfall gauge density is lower in small semi-arid basins. These authors were interested mainly on the run-off generation process, and not on the use of monthly flows series for water management.

The purpose of this paper is to analyze the uncertainty associated to the MAW due to a weak representation of the daily rainfall field. The monthly flows series are generated in several points of the Gramame basin in the coastal area of Paraíba state – Brazil, using the hydrologic distributed conceptual model AÇUMOD (Passerat de Silans *et al*., 2000).

METHODOLOGY

The study is based on the assumption**:** *"They do exist regional parameters of the model for this region and they do not depend on rainfall gauge density or locations"*. So it is accepted that the model with these parameters is able to represent the "hydrologic truth". As the Gramame basin (Fig. 1) is the only one of the region where a quite good rainfall density gauges network has been operated for a period of seventeen years and streamflow gauges have existed for seven years, it is used the simulation and the duration curves carried out by Paiva (2001) in this basin as references. The spatial representation of the rainfall field is modified sequentially by subtracting from one to seven rainfall gauges (RG) from the original data set (11 rainfall gauges). A set of several (namely seven) rainfall gauges density (RGD) have generated. For each RGD, N simulations are run considering N random combinations of the location of the rainfall gauges as indicated in Table 1.

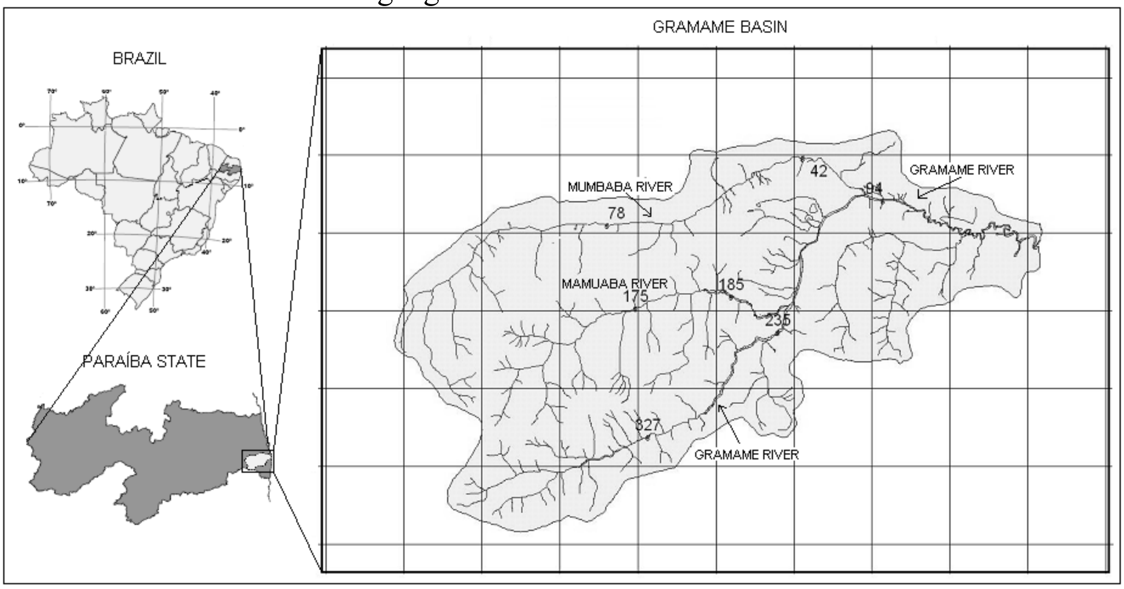

Fig. 1 Location of the Gramame river basin.

Table 1 Number of random combinations rainfall gauges (RG)for each rainfall gauges density.

RGD, subtracting:	Number of possible combinations of rainfall gauges (RG).	Number of random combinations rainfall gauges (RG).
1 RG	11	10
2 RG	55	20
3 RG	165	91
4 RG	330	199
5 RG	462	232
6 RG	462	258

For each seventeen years time series of monthly flows yield by the AÇUMOD model, monthly flow duration curves were generated in seven calculus points (CP´s) spatially distributed in the basin (Fig. 1), by a Thomas Fiering stochastic model. The assessment of the simulations results is based on three different complementary analysis: i) the analysis of the AÇUMOD sensitivity to the RGD; ii) The analysis of the AÇUMOD model output to the intra - rainfall density gauges spatial variability, and iii) the analysis of the Q90 monthly flow of the duration curve (Q90 is the value of the monthly flow with a 90% probability to be exceeded) which we call the Maximum Awardable Water, MAW.

RESULTS

With the first analysis, in which the hydrologic model sensitivity to the rainfall gauges density was assessed it is shown that the monthly flow hydrographs of the simulations move away from the reference hydrograph as the rainfall gauge density diminishes. The average distance between the monthly flow hydrographs of the simulations and the reference hydrograph increases in an exponential way when the density diminishes from three RG´s area subtracted. This distance is not uniform into the space. The sub-basin of Mumbaba river is much more sensitive to the representation of the rainfall field than the others. Diminishing the rainfall gauge density overestimates the mean monthly flow when compared to the mean reference flow. In the Gramame basin portion located uppward the confluence with Mamauba river, the average distance between the monthly flow hydrographs of the simulations and the reference hydrograph is small, however in the sub-basin of the Mamuaba river, the mean monthly flow is underestimated in comparison to the mean reference flow.

In the second analysis, in which the intra-density sensitivity due to the spatial variability of the rainfall gauge field wants assessed. In order to carry out that, three parameters were observed for each RGD used in the simulations. They are the duration curve of: the variation coefficient; the maximum relative error compared to the mean and the minimum (negative) relative error in comparison to the spatial mean. Observing the duration curve of the variation coefficient, it is shown that the sensitivity varies from mean to high, increasing as the rainfall gauges density diminishes. However this sensitivity varies in the space. It is shown that it is higher for the Gramame river and the mean course of the Mamuaba river. Analysing the maximum and minimum errors duration curve, it is shown that in the mean course of the Mumbaba, Gramame and Mamuaba rivers, the greatest errors account for approximately 40% for the RGD, which corresponds to the subtraction of three RG's and 60% for the RGD which corresponds to the subtraction of seven RG's. These maximum errors occur mainly at the peaks of discharge or at the lower flows. But the analysis of the Pearson correlation coefficients shows that the shape of the hydrographs of the random simulations are similar to the shape of the reference simulation. It means, peaks of monthly flows occur at the same time.

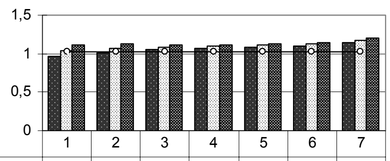

	1	2	3	4	5	6	7
Average-CI ($m^3.s^{-1}$)	0,9637	1,0026	1,0471	1,0719	1,0852	1,1028	1,1425
Average ($m^3.s^{-1}$)	1,0354	1,0622	1,0786	1,0931	1,1068	1,1248	1,1707
Average +CI ($m^3.s^{-1}$)	1,1071	1,1218	1,1101	1,1143	1,1284	1,1468	1,1989
Ref. Simul.($m^3.s^{-1}$)	1,0276	1,0276	1,0276	1,0276	1,0276	1,0276	1,0276

MAW in the lower course of Mumbaba river

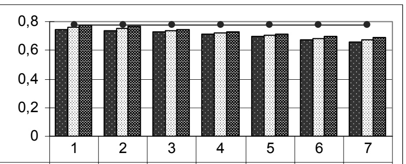

	1	2	3	4	5	6	7
Average - CI (m^3s^{-1})	0,7459	0,7361	0,7301	0,7112	0,6957	0,6697	0,6545
Average (m^3s^{-1})	0,7609	0,7525	0,7388	0,7201	0,7059	0,6829	0,6731
Average + CI (m^3s^{-1})	0,7759	0,7689	0,7475	0,729	0,7161	0,6961	0,6917
Ref. Simul.(m^3s^{-1})	0,7755	0,7755	0,7755	0,7755	0,7755	0,7755	0,7755

MAW for the lower course of Mamuaba river

Fig. 2 MAW with the Confidence Interval (CI)

The third analysis made is to detect the sensitivity of the MAW to the spatial repartition of the rainfall gauge network. The MAW is defined as the 90% probability of exceeding the mean monthly flow. A confidence interval with 90% of significance level is drawn for each rainfall gauges density and the MAW obtained for the reference simulation is located in regard to this confidence interval as shown in the Fig. 2 for two point of calculus as an example.

As it was predictable, the sensitivity of the MAW to the RGD increases as the density diminishes. Generally, the MAW of the simulation reference appears to state away from the confidence interval when the RGD is lower than the one which corresponds to the subtraction of two RG's. It means, from the threshold level of one rainfall gauge for 65 km², the sensitivity of MAW to the rainfall gauge density is higher as the density is lower. It has been observed also that the MAW was underestimated in the Mamuaba river and overestimated in the Gramame river and in the low course of the Mumbaba river, when compared to the MAW estimated by the reference simulation. The percent relative errors were calculated in regard to the MAW estimated by the reference simulation. It was observed small errors in the Mamuaba river (<10%), mean region, but acceptable. There are also errors in the Mumbaba river and very high errors in the Gramame river portion located uppward the confluence with Mamauba river, in this case unacceptable. So the uncertainty on the MAW estimation, due to the spatial repartition of rainfall gauges, is much higher in the Gramame basin than in the others. In that sense, it is noted a difference of behaviour of the sensitivity to the spatial rainfall repartition, when analysed both at the mean hydrographs yielded by the AÇUMOD hydrologic model and at the MAW. This difference might be due to the small flows, because differences in the small flows values can affect drastically the duration curve in the portion corresponding to the higher probabilities to be exceeded.

CONCLUSIONS

The distributed hydrologic model AÇUMOD has been applied to the Gramame basin in the coastal region of Northeast of Brazil, in order to generate time series of mean monthly flows. In this paper it was analysed: i) the sensitivity of the model to the RGD; ii) The sensitivity of the model output to the intra - rainfall gauges density spatial variability, and iii) the uncertainty on the Maximum Awardable Water, MAW. Results show that the model outputs and the MAW are sensitive to the RGD, mainly when the density is lower than one rainfall gauge for 65 km². The results also show great differences of the model sensitivity in the space. Generally, the sensitivity is higher in the upper reaches of the basin. However, the errors related to the reference simulation can be either positives or negatives. The uncertainty on the MAW can be acceptable or unacceptable. The spatial distribution of this uncertainty differs from the spatial errors distribution on the mean flows. Thus, recommendation is made to optimize a rainfall gauge network in this coastal region, looking also at the uncertainties on the references flow for the award of rights to the use of water.

Acknowledgements FINEP is acknowledged for the financial support of this research.

REFERENCES

Faures, J. M., Goodrich, D. C., Woolhiser, D. A. & Sorooshian, S. (1995) Impact of small-scale rainfall variability on runoff modeling. *Journal of Hydrology* **173**, 309-326.

Goodrich, D. C., Whoolhiser, D. A. & Unkrich, C. L. (1990) Rainfall-Sampling Impact on Runoff. *Proceedings of Hydraulics/Hydrology of arid lands Int. Symposium*. San Diego California, July 30-Aug 2, 519-524.

Lopes, V. L. (1996) On the effect of uncertainty in spatial distribution of rainfall on catchment modeling. *Catena* **28**, 107-119.

Medeiros, V. M. A., Moreira, L. F .F. & Righetto, A. M. (2007) Analysis of the Effect of Spatial Variability of Rain-fall in Modeling Runoff in an Experimental Basin in The Northeaster Semi-Arid (in Portuguese). *Revista. Brasileira de Recursos Hídricos* **12**(3), 129-139.

Paiva, A. E. D. B. (2001) Simulações hidrológicas na bacia do rio Gramame com subsídio ao processo de Outorga. Máster Tesis. *University of Paraíba Campina-Grande Brazil*. 132p.

Passerat de Silans, A. M. B., Almeida, C. N., Albuquerque, D. J. & Paiva, A. E. D. B. (2000) An Application of the Hydrologic Distributed Model AÇUMOD at the Peixe Basin – Paraíba State (in Portuguese). *Revista. Brasileira de Recursos Hídricos* **7**(4), 5-20.

Analysis and prediction of time varying tidal components using Kalman filtering

J. H. SUMIHAR, M. VERLAAN & A. W. HEEMINK
Delft Institute of Applied Mathematics, TU Delft, Mekelweg 4, 2628CD, Delft, The Netherlands
j.h.sumihar@ewi.tudelft.nl

Abstract This paper describes a method to improve tidal predictions by estimating time varying tidal components from the difference between the total water level and the astronomical tides predicted using harmonic analysis. The approach is motivated by the fact that the frequency spectrum of harmonic analysis residual always contains some spikes centered on the tidal frequencies. In this work, we model each spike as a narrow-band process, which can be represented as a harmonic oscillation with a certain tidal frequency and with slowly varying harmonic parameters. Our approach is to decompose the residual into several narrow-band processes and to model the slowly varying parameters by a set of stochastic differential equations. To estimate the harmonic parameters of each tidal frequency, analysis is done by combining the residual with the model results by using a Kalman filter. The prediction of the tidal components is performed by running the model using the estimated harmonic parameters. We have applied this scheme to field data taken in the year 1999 at several observing stations in the coastal area around the Netherlands. The experiments with a 24-hour forecast horizon has successfully predicted the tidal components of the harmonic analysis residual and resulted in 20% to 60% variance reduction during the calm period of May-October. However, the scheme does not perform well during stormy periods. This may suggest that the nonlinear interaction between surge and tide should be explored for the success of the prediction under these conditions. Another possible cause is the cross-over between the tidal as well as the surge components. An experiment using generated signals indicates that cross-over occurs between the harmonic components and that the spectrum of the surge component extends over the tidal frequencies. This suggests that although the method is capable of extracting the tidal components from the harmonic analysis residual, the tidal components actually contain other components as well. This in turn hampers the approach from generating accurate prediction during stormy periods.
Keywords harmonic analysis; stochastic; Kalman filter

INTRODUCTION

A number of practical applications motivate the attempt to improve the accuracy of water level prediction. In the Netherlands, for example, accurate water level predictions with several hours forecast horizon is required for proper closure of the storm surge barriers in Eastern Schelde and New Waterway. Furthermore, with the increase in the size of ships using the Euro Channel and the Meuse Channel to Rotterdam harbour, this port has become inaccessible to some ships except during a short period of high water. Therefore, there is also a demand for accurate tidal prediction to allow safe passage.

The operational water level prediction in the Netherlands is based on water level decomposition into astronomical and meteorological components. The astronomical components are analysed and predicted using harmonic analysis. However, the harmonic analysis can not predict completely the astronomical components from the total water level. This is indicated by the fact that the frequency spectrum of the harmonic analysis residual contains a number of spikes centred at astronomical constituent frequencies (see, for example, Fig.1).

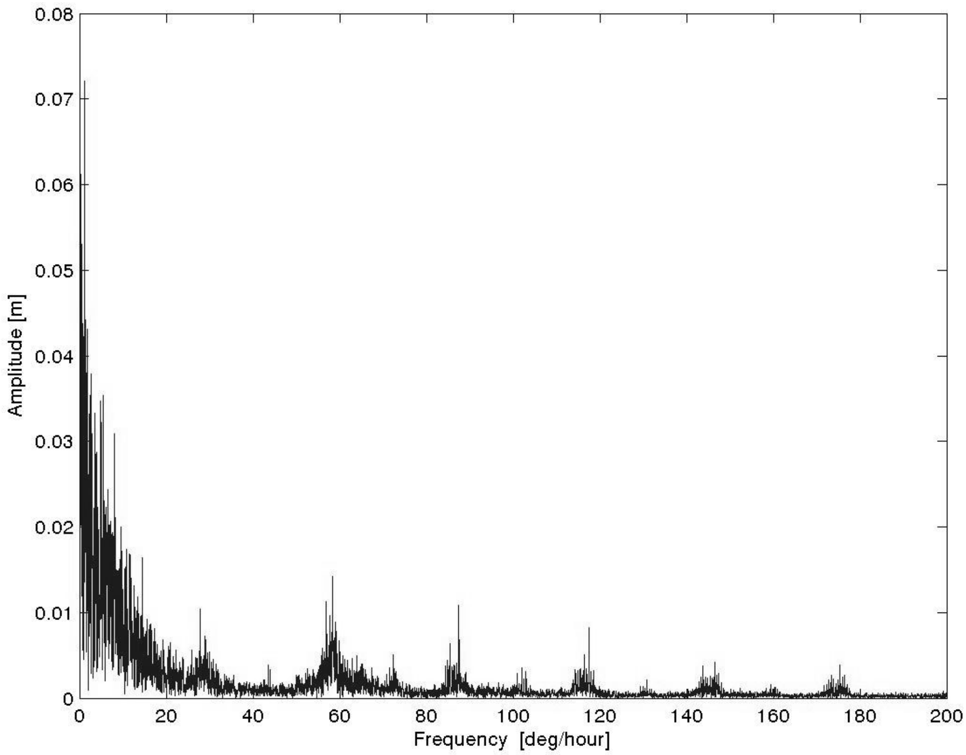

Fig. 1 Frequency spectrum of harmonic analysis residual at Vlissingen, 1 January 1999 – 31 December 1999.

The objective of the study presented in this paper is to improve the accuracy of the astronomical tides predictions by extracting the remaining astronomical tidal components from the harmonic analysis residual. In doing so a Kalman filter is used to estimate the time-varying tidal components. Kalman filtering has been used in tidal analysis (Meyer, 1984) and short-term tidal prediction (Yen *et al.*, 1996). In this paper, we follow the work of Heemink *et al.* (1991).

APPROACH

Following Heemink *et al.* (1991), our approach is to consider each spike in the frequency spectrum of the harmonic analysis residual as a narrow band process. A narrow band process can be shown as a harmonic oscillation with slowly varying harmonic parameters. The frequency spectrum (Fig. 1) suggests that we can approximate the residual $y(t_k)$ by the sum of a number of narrow band processes:

$$y(t_k) \cong \sum_i A_i(t_k)\cos(\omega_i t_k) + B_i(t_k)\sin(\omega_i t_k) \tag{1}$$

where the slowly varying harmonic parameters $A_i(t_k)$ and $B_i(t_k)$ are modelled by stochastic differential equations (Heemink *et al.*, 1991; Jazwinski, 1970) which discrete version reads:

$$\begin{aligned} A_i(t_{k+1}) &= (1 - \Delta t a_i)A_i(t_k) + \sigma_i \Delta\alpha(t_k) \\ B_i(t_{k+1}) &= (1 - \Delta t a_i)B_i(t_k) + \sigma_i \Delta\beta(t_k) \end{aligned}, \tag{2}$$

where Δt is the time step, $\Delta\alpha_i(t_k)$ and $\Delta\beta_i(t_k)$ are mutually independent white noise process with variance Δt. In the state-space form, the overall system of equations can be written as

$$X(t_{k+1}) = \Phi X(t_k) + GW(t_k) \tag{3}$$

where Φ and G are diagonal matrices containing the terms ($1\text{-}\Delta t a_i$) and σ_i respectively, while the state vector $X(t_k)$ is defined as $X(t_k) \equiv [A_1(t_k)B_1(t_k)\cdots A_i(t_k)B_i(t_k)\cdots]^T$, and the noise vector $W(t_k)$ as $W(t_k) \equiv [\Delta\alpha_1(t_k)\Delta\beta_1(t_k)\cdots\Delta\alpha_i(t_k)\Delta\beta_i(t_k)\cdots]^T$.

Moreover, the measurement, $Z(t_k)$ of the water level, $y(t_k)$ can be modelled by the relation:

$$Z(t_k) = M(t_k)X(t_k) + V(t_k) \tag{4}$$

where $V(t_k)$ is the measurement noise with variance R and $M(t_k)$ is the measurement vector defined as $M(t_k) \equiv [\cos(\omega_1 t_k)\sin(\omega_1 t_k)\cdots\cos(\omega_i t_k)\sin(\omega_i t_k)\cdots]^T$.

Now that we have both system and measurement models in stochastic environment, it is possible to use a Kalman filter to estimate the harmonic parameters, $X(t_k)$ contained in the harmonic analysis residual, $Z(t_k)$. A thorough discussion about Kalman filter can be found for example in Jazwinski (1970) and Maybeck (1970). In short, the recursive equations of the Kalman filter implemented to this system read:

- Forecast step:

$$\begin{aligned} X^f(t_{k+1}) &= \Phi X^a(t_k) \\ P^f(t_{k+1}) &= \Phi P^a(t_k)\Phi^T + GQG^T \end{aligned} \tag{5}$$

- Analysis step:

$$\begin{aligned} X^a(t_k) &= X^f(t_k) + K(k)\big(Z(t_k) - M(t_k)X^f(t_k)\big) \\ P^a(t_k) &= (I - K(k)M(t_k))P^f(t_k) \\ K(k) &= P^f(t_k)M(t_k)^T\left(M(t_k)P^f(t_k)M(t_k)^T + R\right)^{-1} \end{aligned} \tag{6}$$

where Q is the covariance of the noise vector $W(t_k)$, which is assumed to be time-invariant, K is the Kalman gain, $X^f(t_{k+1})$ and $P^f(t_{k+1})$ are the forecast mean and covariance of the state vector $X(t_k)$ based on the assimilation of measurements up to time t_k, while $X^a(t_{k+1})$ and $P^a(t_{k+1})$ the analysis mean and covariance. The Kalman filter is used to estimate the harmonic parameters before making predictions. The prediction of water-level $Z(t_k)$ is done subsequently by running (3) and (4) using the estimated harmonic parameters as initial values of $X(t_k)$ and setting the noise terms $W(t_k)$ and $V(t_k)$ to zero.

RESULTS AND DISCUSSION

To evaluate the performance of the proposed approach, some experiments were performed by using real data from several observing stations in the North Sea. Using the model and Kalman filter set-up described previously, we estimated the harmonic parameters of the tidal components within harmonic analysis residual. The estimated harmonic parameters were then used for making predictions. The experiments were performed with four different forecast horizons, namely 10 minutes, 1 h, 6 h, 12 h, and 24 h ahead. In this paper, we present the experiment results obtained using the following tidal constituents: A0, O1, K1, MU2, M2, S2, 2SM2, 3MS4, M4, MS4, M6, 2MS6, M8, 3MS8, and 4MS10. The parameters are a_i=2.3 x 10^{-5}, which is equivalent with a correlation-time of one month, and σ_i=0.02 m for all tidal constituents. For the initial condition we set $X^a(t_o)$=[0…0] and $P^a(t_o)$=$diag([0.05^2…0.05^2])$. Note that the effect of the initial condition vanishes after several time steps due to stability of the Kalman filter setup. The prediction performance is evaluated in term of the fraction of variance reduction, *r*: $r \equiv \left(1 - \frac{\mathrm{var}(S-C)}{\mathrm{var}(S)}\right)$, where S is the harmonic analysis residual, while C the prediction of tidal components in S. The variance reduction is computed by first filtering out the lower frequency components of the signal before propagating it to the Kalman filter. This is done because we are interested only in the astronomical components. The results for location Vlissingen and Europlatform are presented in Fig. 2.

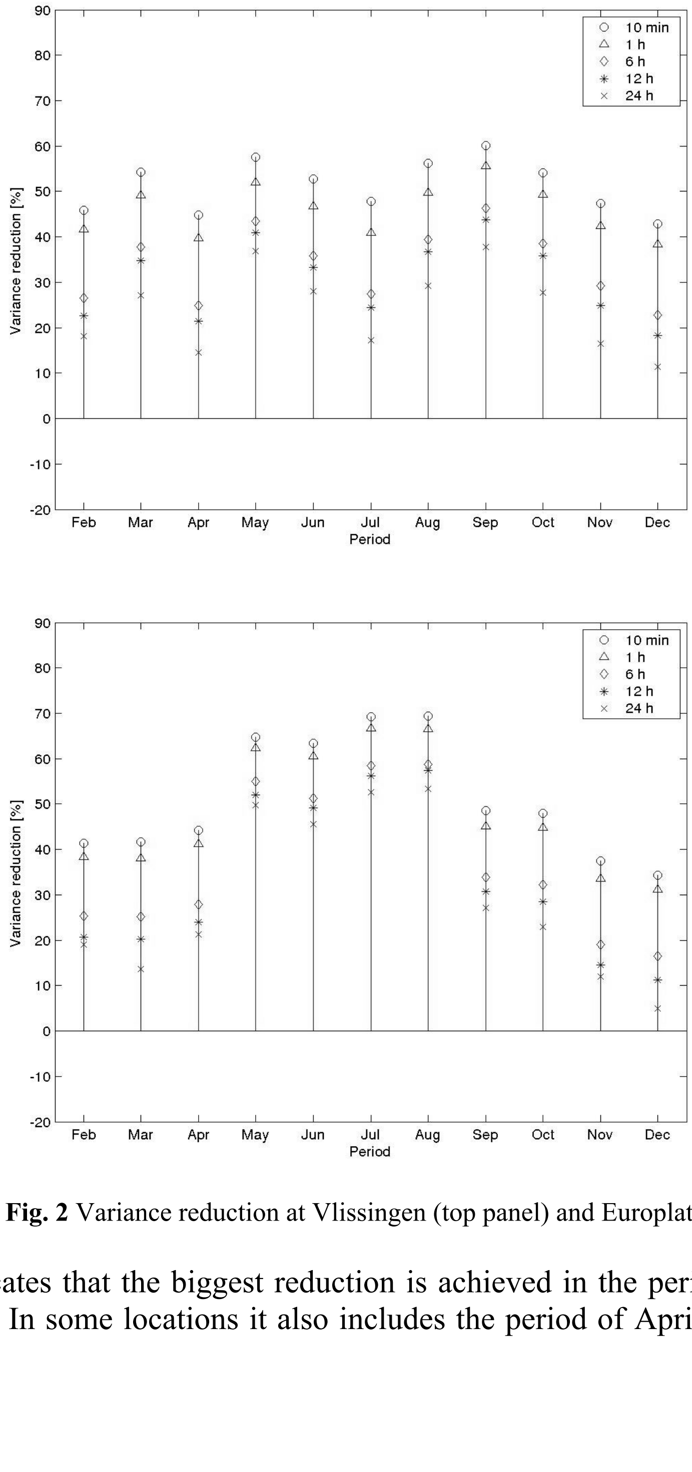

Fig. 2 Variance reduction at Vlissingen (top panel) and Europlatform (bottom panel).

Fig. 2 indicates that the biggest reduction is achieved in the period between May and September. In some locations it also includes the period of April and October. In this period the weather was relatively calm. The variance reduction is ranging from 20% to 60% depending on the location. The results indicate also that the harmonic parameters of the tides are more stationary at stations located further into the sea. This gives rise to a more successful prediction.

However, in the other period, the prediction performance is worse and it degrades quickly for longer forecast horizons. In some locations it yields negative reduction (not shown). This unsatisfactory performance is likely to be due to the nonlinear tide-surge interaction, which is still not yet well understood. Visual inspection on the time series of harmonic analysis residual reveals that in this period the meteorological component has big amplitude. Another possible cause is the cross-over of the meteorological component into the astronomical frequency bands. An experiment using generated signal (not shown), where the meteorological component is modelled by using an AR(1) process with a one-day correlation-time, confirms this. Since the meteorological component usually lasts within a short period like one day, its energy at tidal frequencies also lasts very shortly. This means that during this period the harmonic parameters will vary relatively quickly. Therefore, the assumption that the harmonic parameters are constant during prediction is no longer valid.

It should be noted here that our method has been successful in extracting the tidal components from the harmonic analysis residual. However, using this method there is no way we can separate different components with the same frequency. On the other hand, due to cross-over between frequency components, the energy within the tidal bands may be contributed from several different phenomena. This in turn may cause the respective harmonic parameters to vary quickly in time. This hampers the approach from generating accurate predictions, especially during stormy periods.

CONCLUSION

This paper presents a method for analysis and prediction of the time varying tidal components from a harmonic analysis residual. The method is based on modelling the residual as the sum of some tidal oscillations with slowly varying harmonic parameters. The slowly varying parameters are modelled by using stochastic difference equations and estimated by using a Kalman filter. This method has been implemented by using real data taken from several locations in the North Sea. For the calm period May-October 1999, it yields improvement ranging from 20% to 60% depending on the location. However, it does not perform well during the other period. This may be due to the nonlinear interaction between meteorological and astronomical components. Another possible cause is the cross-over between different components, which can not be separated without any additional independent information. This hampers our approach from producing accurate prediction during stormy periods.

REFERENCES

Heemink, A. W., de Jong, B. & Prins, H. (1991) Adaptive harmonic analysis. *Deutsche Hydrographische Zeitschrift* **44**(2), 91-106

Jazwinski, A. H. (1970) Stochastic processes and filtering theory. *Academic Press*, New York

Maybeck, P.S. (1970) Stochastic models, estimation, and control. *Academic Press* **1**.

Meyer, F. de (1984) Time-variant tidal analysis and the Kalman filter, *Annales Geophysicae*, Vol. 2, No. 5, p. 513-528

Yen, P. H., Jan, C. D., Lee Y. P. & Lee, H. F. (1996) Application of Kalman filter to short-term tide level prediction. *Journal of Waterway, Port, Coastal. and Ocean Engineering* **122**(5), 226-231

Construction, structure, and functionality of a wetland system built in Romania

GH. BREZEANU[1] & OLIVIA CIOBOIU[2]

1 *The Biology Institute of the Romanian Academy Bucharest, str. Splaiul Independenței nr. 246*

2 *The Oltenia Museum Craiova, str. Popa Şapcă nr. 8, 200416 Craiova, Romania*
cioboiuolivia@yahoo.com

Abstract The wetland systems are worldwide known as complementary means for sewage treatment. The functioning of these systems is base don the capacity of the biocoenoses to degrade, transform, and accumulate the polluting substances from the sewage water.
Keyword wetland systems; water treatment

INTRODUCTION

The wetland systems are presently known as complementary means for sewage, domestic, agricultural, and industrial water treatment (Scholes *et al*., 1995, Sobolevski 1997). They proved to be extremely efficient as they do not need electric power and do not require large amounts of money maintenance and functioning (Brezeanu *et al*., 1982).

The wetlands are defined as shallow aquatic ecosystems (40-50 cm deep), covered by vegetation and crossed by a slow water current (Seidel, 1976). The wetland systems can be natural or man-made. Such a man-made system was first built in Europe (1982) within a petrochemical plant.

THE FUNCTIONING OF THE SYSTEM

The functioning of the built system is the result of the structural organization where the essential factor is the biocoenosis, which may trigger the cleaning process of the sewage water due to its diversity and inter-specific relations (Brezeanu *et al*., 2006).

The structures involved in the cleaning process are the bacteria populations made up of petrol-oxidants, phenolic, heterotrophic germs from the carbon, nitrogen, and sulphur cycles. They reduce the polluting substances at the level of mineral salts, which are then used by primary producers and transformed into their own organic matter.

The components of the primary producers – macrophytes, planktonic algae, periphytic algae, are then used by consumers represented by numerous groups of invertebrates such as macrophytes eaters, bacteria eaters, animal eaters, and detritus eaters.

During the cleaning process, there can be notice two essential stages: the first one of degradation and transformation of the polluting substances into elementary substances and then the stage of transformation and accumulation of the resulting substances at the consumers' level (Fig. 1).

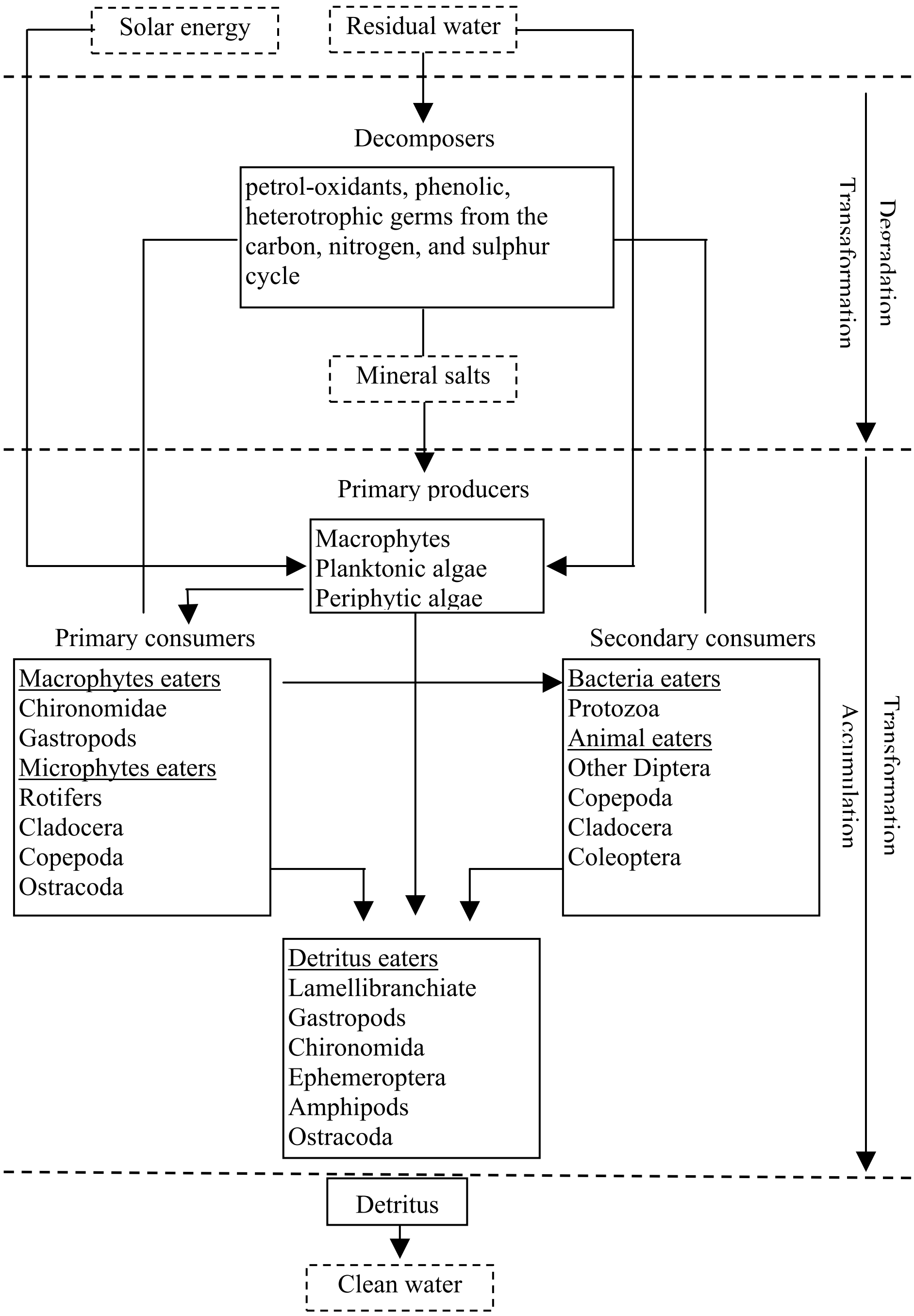

Fig. 1. The chains of the trophic chain that contribute to the energy and matter transfer in the cleaning process of residual water.

THE COMPARTMENTS OF THE SYSTEM

This includes the following parts:

- the settling basin with a surface of 10 hectares and without vegetation;
- the compartment of the reed plantation with a surface of 40 hectares;
- the final compartment for water quality testing with a surface of 5 hectares (Fig. 2).

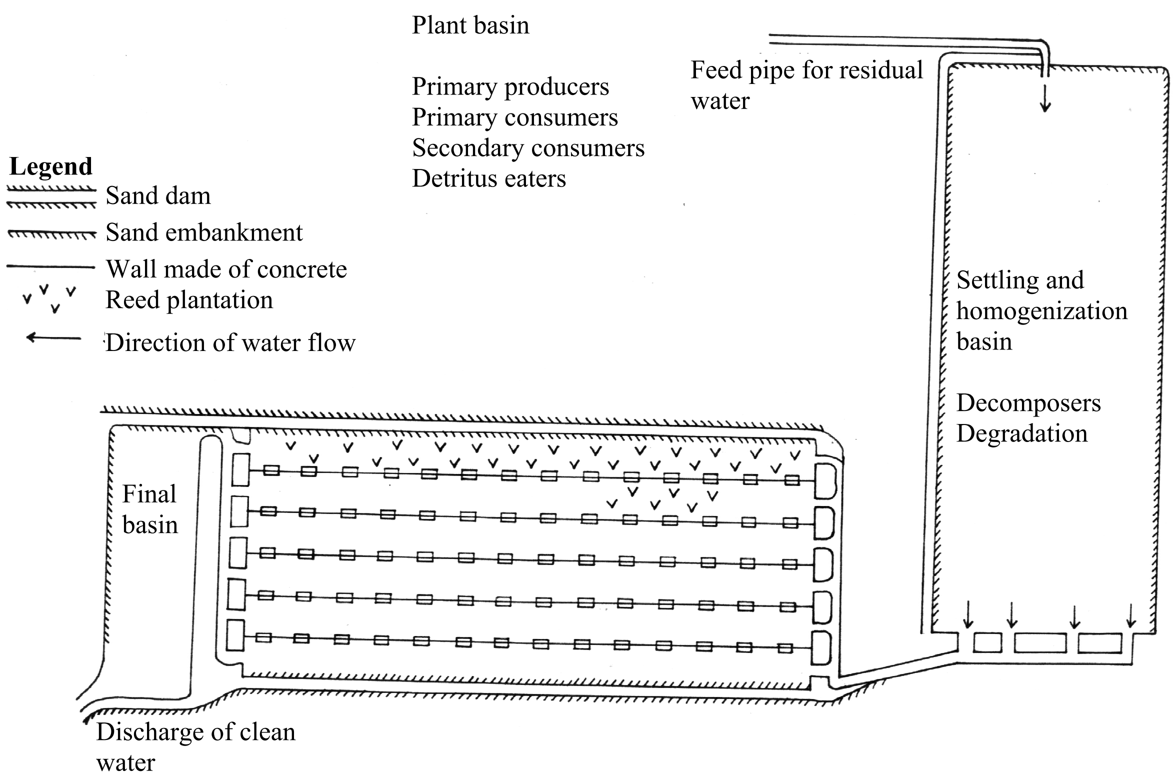

Fig. 2 Plan of the wetland system for residual water cleaning.

Within the compartment for water settling, where polluted water is directly discharged, the cleaning process develops under the action of the physical, chemical, and bacteriologic factors.

The chemical-physical factors are the following ones – the direct contact between air and water and the water oxygenation process.

The bacteriologic factors are the action of the petrol-oxidants, phenolic, heterotrophic germs from the carbon, nitrogen, and sulphur cycles (Fig. 3).

Fig. 3 Apertures for residual water of the wetland system.

Within the reed plantation compartment, the cleaning process started in the first compartment continues under the direct action of all the components from the biocoenoses structure: bacteria, the population of macrophytes producers where the dominant species are *Phragmites communis, Typha latifolia*, and *Scirpus palustris*, of macrophytes planktonic, and periphytic producers, and the populations of primary and secondary consumers.

Within the final compartment where water quality is tested, the cleaning process is mainly induced by the planktonic populations – phytoplankton and zooplankton, as this compartment do not have macrophytes (Brezeanu *et al*., 1993).

The cleaning efficiency of this system is of 80 – 90 percent. Built 20 years ago, the system underwent many stages, such as the construction of the basins and canals and the planting of the aquatic macrophytes (*Scirpus palustris* and *Typha latifolia*). The period necessary for the growing of the plants and for the development of the specific biocoenoses was of about 3 years. After this period, the polluted water was gradually introduced in order to ensure the adaptation of the biocoenotic structures (Brezeanu *et al*., 1982).

CONCLUSIONS

The cleaning function of the system is based on specific structures known as wetlands in the literature in the field: aquatic macrophytes, phytoplankton, periphyton, zooplankton, zoobenthos, and bacteria populations.

In order to clean the water, the wetland has to be crossed by a slow water current carrying a moderate quantity of residues that is to be cleaned within this circuit through the system.

REFERENCES

Brezeanu, Gh., Munteanu, M., Dacin, E. & Gruia, L. (1982) Sistem biologic de epurare avansată de la Combinatul Petrochimic Midia – Năvodari (principiu, proiectul, modalităţi de realizare). *C.N.A. Folosirea raţională şi protecţia apelor II*, 75 – 78.

Brezeanu, Gh. & et al. (1993) Consecinţe ecologice ale poluării cu ape reziduale petroliere. In *Lucrările Sesiunii Ştiinţifice a Inst. de Biol. al Acad. Rom*. Buc., 103 – 106.

Brezeanu, Gh., Ionică, D., Parpală, L. & Cioboiu, O. (2006) Mecanismele de funcţionare ale structurilor biocenotice din sistemele wetland de epurare a apelor uzate (Studiu de caz). In *Lucrările Institutului de Biologie al Acad. Rom.*, Bucureşti.

Scholes, L. N. L., Shutes, R. B. E., Revit, D. M., Forshaw, M., & Purchase, D. (1995) Constructed wetland and sustainable management in the UK. *Internat. Assoc. on Water Quality, Macrophyte Specialist Group, Newsletter* **13**, 11 – 13.

Seidel, K. (1967) Macrophytes and water purification, In *Biological control of water pollution*, (ed. J. Tourbier & R. W. Pierson), *Univ. of Pennsylvania Press, Philadelphia*, 109 – 120

Sobolevski, A. (1997), The capacity of natural wetlands to ameliorate water quality: A review of case studies, In *Fourth. Internat. Conference on acid rock drainage – Proceedings* **4**, 1551 – 1563, Vancouver, B. C. Canada, May 3 – June 6.

Effects of flood duration and vegetation zonation on C and N dynamics of floodplain and riparian vegetation in the Okavango Delta

KELEBOGILE B. MFUNDISI
Harry Oppenheimer Okavango Research Centre, P/Bag 285, Maun, Botswana
kmfundisi@orc.ub.bw/ kmfundisi@daad-alumni.de

Abstract The Okavango Delta is a hydrologically complex and dynamic ecosystem that changes within seasonal, yearly, and decadal time intervals. The amount of water reaching the Okavango River from highlands of Angola has a direct impact on spatio-temporal variation in inundation levels over the Delta. This results in a mosaic of ecologically defined landscape components such as permanent swamps, islands, floodplains and drylands. The objective of this study was to determine the effects of flood duration and vegetation zonation on organic C and total N in the Okavango Delta. Samples were collected along vegetation gradient from island centres across riparian vegetation into floodplains, which relates to inundation duration with floodplains being flooded for a longest period. The highest amounts of organic C and total N was found in riparian forest. The results from ANOVA showed that there were significant differences in the organic C and total N among the different vegetation zones in islands of the Okavango Delta, with $F>6$ and $P< 0.05$. If the temporary swamps of the Okavango Delta could become dry due to climate change, riparian forests in islands will die and grasses typical of those on island centres will take over resulting in reduced soil organic C and total N. On the other extreme if there is too much flooding in the Delta, all the vegetation zones will be flooded and there will be a big lake with less dissolved organic C and total N. Typical dissolved organic C in the Okavango River is 1.9 mg CL^{-1}, whereas that in the temporary swamps is 22.3. Increased duration of inundation will result with DOC typical of the Okavango River, which is permanently inundated. Therefore, the different vegetation zones in the Okavango Delta, particularly riparian forests in temporary swamps influence the carbon and nitrogen biogeochemical cycles. It is important to maintain riparian forests as important components of this system.
Keywords Okavango Delta; Biogeochemical cycles; climate change; riparian forests; floodplains; islands

INTRODUCTION

The Okavango Delta is an inland freshwater wetland found in Northwestern Botswana (Fig. 1). It is contained within a graben at the southern extremity of the East African Rift Valley system (Ellery *et al.*, 1990, 1993). Floodwaters of the Delta mainly originate from rainfall events in highlands of Angola (Ellery *et al.*, 1990, Gieske 1997). The Okavango Delta is annually inundated by water from the Angolan highlands amounting 10km^3 per annum, augmented by direct local rainfall at 5km^3 per annum The area of inundation varies between 4000 and 13 000km^2, depending on the seasonal and annual variation in incoming water flow and local precipitation.

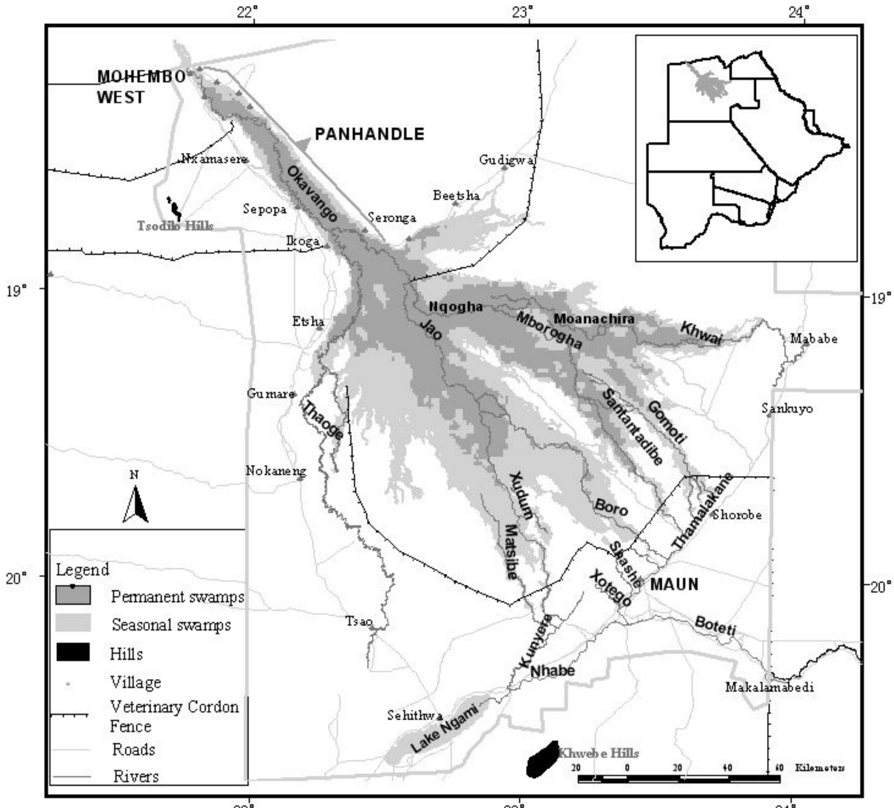

Fig. 1 Map of the Okavango Delta ecosystem.

The Delta is a mosaic of corridors (channels) and patches of islands embedded in a matrix of swamps and floodplains (Mfundisi, 1999). The size of islands varies from anthill, covering some square meters to forest covered islands of several hundred square kilometres. The extent of tree cover is variable with some islands having a complete tree cover and others only narrow fringe close to the island edge with the centre of island either colonized by herbaceous species or devoid of any vegetation (Ellery *et al.*, 1993). Islands selected for this study were those with a fringe of riparian vegetation adjacent to floodplains; island interior community dominated by *Acacia nigrescens*, *Croton megalobotrys* and *Hyphaene ventricosa;* central regions characterized either by short, sparse grassland dominated by *Sporobolus spicatus* or completely devoid of vegetation with sodium carbonate encrusted soil surrounding a central pan of extremely high conductivity.

METHODS

Soil sampling procedures followed were those explained in Brower *et al.* (1990). A belt transect method was used to sample two islands and adjacent floodplains for this study. Samples were collected along vegetation gradient from island centres across riparian vegetation into floodplains, which relates to inundation duration with floodplains being flooded for a longest period. Sampling was done in each vegetation zone at 5m intervals along a 30m transect at 0-20cm depths using a soil corer. The samples were sun dried then oven dried at 110 °C, passed through a 2mm sieve, packaged inside paper bags and send for chemical analysis in the laboratory. All soil samples were analyzed for organic Carbon and total Nitrogen using CNHS analyzer at Harry Oppenheimer Okavango Research Centre.

RESULTS

Organic C and total N along vegetation and flood duration gradient

The results from chemical analysis were plotted in excel to find out if there is any trend in organic C and total N from the island centre across riparian forest into floodplains. It was found that the highest amount of organic C and total N occurred in riparian forests. Figs 2 and 3 depict variations in organic C and total N among the different vegetation zones.

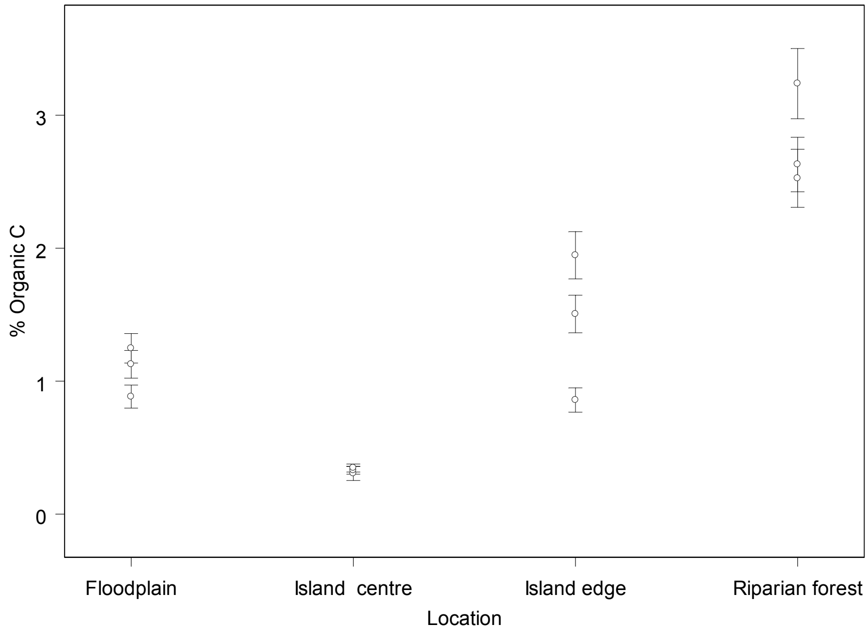

Fig. 2 Percentage organic C in vegetation zones of the Okavango Delta.

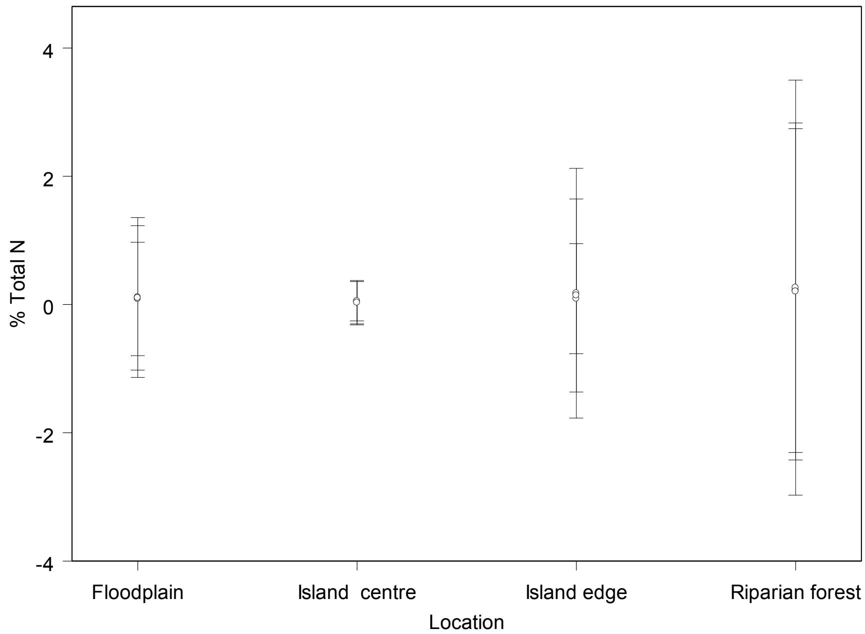

Fig. 3 Percentage total N in vegetation zones of the Okavango Delta.

The results from ANOVA showed that there were significant differences in the organic C and total nitrogen among the different vegetation zones in each transect with $F>6$ and $P< 0.05$. Riparian zones typically act as sinks for nutrients in solution moving along surface hydrologic flow paths. Various processes result in nutrient sequestration or loss in riparian zones, including vegetation uptake, soil adsorption, volatilization, and microbial immobilization (Tufekcioglu *et al.*, 2003, Yeakley *et al.*, 2003). The removal of forest vegetation generally causes transient increases in nutrient exports across the landscape. Understanding nutrient dynamics in riparian zones is essential for their proper management. In the worst scenario, if the temporary swamps of the Okavango Delta dry up, the riparian forests in islands will die and grasses typical of those on island centres will take over resulting in reduced soil organic C and total N. On the other hand if there is too much flooding in the Delta, all the vegetation zones will be flooded and there will be a big lake with less dissolved organic C and total N. Typical dissolved organic C in the Okavango River is 1.9 mg CL^{-1}, whereas that in the floodplains is 22.3 mg/L (Mladenov *et al*., 2005.)

CONCLUSION

The presence of riparian zones in the Okavango Delta adds to its dynamism in organic C and total N. A reduction of the riparian zone due to probable climate change events could lead to a release of organic C and total N. Drying of temporary swamps will result in a shift in vegetation cover, with grasses becoming dominant. This will result in reduced organic C and total N. Increased duration of inundation will result with DOC typical of the Okavango River, which is permanently inundated. The vegetation zonation and flood duration in temporary swamps of the Okavango Delta are important for maintenance of the C and N biogeochemical cycles.

REFERENCES

Brower, J. F., Za,r J. H. & von Ende, C. N. (1990) Field and laboratory methods for general ecology. Third Edition. *Wm C. Brown Publishers.* IA, USA.

Ellery, W. N., Ellery, K. & McCarthy, T. S. (1993) Plant distribution in islands of the Okavango Delta, Botswana: determinants and feedback interactions. *Journal of Ecology* **31**(2), 118–134.

Elllery, W. N., Ellery, K., Roger,s K. H., McCarthy, T. S. & Walker, B. H. (1990) Vegetation of channels of the northeastern Okavango Delta, Botswana. *African Journal of Ecology* **28**, 276–290.

Gieske, A. (1997) Modelling outflow from Jao/Boro River system in the Okavango Delta, Botswana. *Journal of Hydrology* **28**, 227–290.

Mfundisi, K. B. (1999) Sustainable Environmental planning for the Okavango Delta, Botswana: A landscape approach. MS Thesis. *University of New Haven,* West Haven CT, U.S.A.

Mladenov, N., McKnight, D. M., Wolski, P. & Ramberg, L. (2005) Effects of annual flooding on dissolved organic carbon dynamics within a pristine wetland, the Okavango Delta, Botswana. *Wetlands* **25**(3), 622–638.

Tufekcioglu, A., Raich, J. W., Isenhart, T. M. & Schultz, R. C. (2003) Biomass, carbon and nitrogen dynamics of multi-species buffer within agricultural watershed in Iowa, USA. *Agroforestry Systems* **57**, 187–198.

Yeakley, J. A., Coleman, D. C., Haines, B. L., Kloeppel, B. D., Meyer, J. L., Swank, W. T., Argo, B. W., Deal, J. M. & Taylor, S. F. (2003) Hillslope nutrient dynamics following upland vegetation disturbance. *Ecosystems* **6**, 154–167.

Tuning hydrological models for ecological modelling – improving simulations of low flow critical to stream ecology

MARTIN OLSEN[1], LARS TROLDBORG[2], EVA BOEGH[1] & JENS CHRISTIAN REFSGAARD[2]

1 *Department of Environmental, Social and Spatial Change, Roskilde University, P.O. Box 260, DK-4000 Roskilde, Denmark*
maol@ruc.dk

2 *Department of Hydrology, Geological Survey of Denmark and Greenland, Oester Voldgade10, DK-1350 Copenhagen K, Denmark*

Abstract The consequences of using simulated discharge from a conventional hydrological model as input in stream physical habitat modelling was investigated using output from the Danish national hydrological model and a physical habitat model of three small streams. It was found that low flow simulation errors could have large impact on simulation of physical habitat conditions. If these two models are to be used to assess groundwater abstraction impact on physical habitat conditions the hydrological model should be tuned to the purpose.
Keywords physical habitat model; hydrological model; low flow simulation; groundwater abstraction

INTRODUCTION

Most Danish streams are groundwater feed and affected by abstraction of groundwater which is the main source of drinking water in Denmark (Henriksen *et al*., 2008). The majority of Danish streams are small (75% has a width <2.5 m) and physical habitat conditions in smaller streams are often more vulnerable to low flows than larger streams since they need larger proportions of average discharge to maintain good physical conditions (Orth & Leonard 1990).

With the European Water Framework Directive there is an increasing demand for use of more sophisticated integrated models in order to study integrated groundwater, surface water and ecological aspects of water management. The national hydrological model (DK-model) is a physically based integrated groundwater-surface water hydrological model covering almost the whole country (43.000 km^2) (Henriksen *et al*., 2008). A new approach suggests coupling the DK-model with stream specific physical habitat models to bridge the gap between groundwater management and stream ecology e.g. linking discharge reduction to physical conditions in streams.

One of the main problems of combining hydrological models with models of physical habitat in streams is that the two models originate from different disciplines with emphasis on different parts of the flow regime – flow extremes are often the focus in physical habitat modelling whereas hydrological modelling often focus on water balance and average flow conditions.

This paper gives examples of problems experienced when combining a conventional hydrological model with a physical habitat model and finally suggests one possible approach to handle this “focus problem” of hydrological and physical habitat modelling. These examples should work as a motivation for the overall goal of this project - to setup and test a calibration and validation procedure for hydrological models that improves discharge simulations in relation to ecological relevant discharges. The purpose is to make the output from hydrological models directly relevant for the overall purpose e.g. combining a hydrological model with a physical habitat model and assessment of groundwater abstraction impact on stream habitats.

STUDY AREA & METHOD

As case-study for the approach, we use the Langvad Catchment which is located in the capital region at Zealand (Denmark). The area is heavily impacted by groundwater abstraction and is considered an important spawning and rearing area for sea-run brown trout.

Average relative error (*e*) between the DK-model's simulated discharge (Q_{sim}) and observed discharge (Q_{obs}) for each fifth flow percentile (Q_{95} to Q_5) was assessed using flow data from 49 catchments in the DK-model covering the period 1995-2004.

Physical habitat conditions were simulated using the RHYHABSIM (River HYdraulics and HABitat SIMulation) (Jowett, 2004) physical habitat model which was setup for three sections in the Langvad Catchment to represent physical conditions in the three streams; Stream Langvad, Stream Tokkerup and Stream Ledreborg. Physical habitat conditions expressed as *Weighted Usable Area* (WUA) were simulated for three life stages of brown trout (*Salmo trutta*); fry, juvenile and spawner, as a function of discharge. This results in so-called WUA-Q relationships. These three life stages were chosen because the studied sections were classified as "*Potential salmonid spawning and nursery areas"* by the local water authorities. The modelling therefore focused on physical habitat conditions for these specific bioindicators.

Site specific discharge statistics were calculated using data from discharge gauging stations (1998-2002) located close to each of the three stream sections. Discharge statistics were compared to WUA-Q relations to assess which flow percentiles could be considered "critical" to physical habitat conditions. The flow percentiles being critical for physical habitat conditions were then compared with model performance of DK-model in the same flow interval.

For each of the three sections Q_{sim} was assessed for each fifth flow percentile by multiplying the corresponding site specific Q_{obs} percentile with 1-*e*. Site specific Q_{sim} and Q_{obs} flow percentiles were then combined with the site specific WUA-Q relations to assess WUA duration curves for each of the three streams.

RESULTS & DISCUSSION

On average flows lower than Q_{80} are overestimated by more than 100% by the DK-model (Fig. 1). The high hydrological model errors and uncertainties of low flow predictions (i.e. 80-100 percentile flows) must be considered for use if simulations from the DK-model are used in physical habitat modelling.

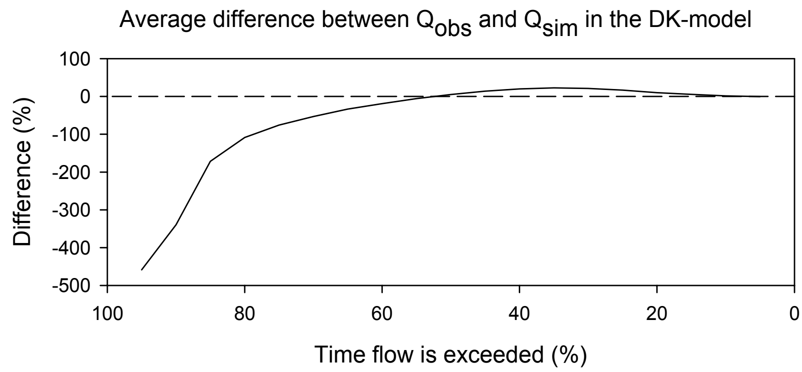

Fig. 1 Average difference between observed discharge (Q_{obs}) and discharge simulated by the DK-model (Q_{sim}) based on flow data from 49 catchments on Zealand, 1995-2004.

Since these smaller streams on Zealand often are spawning and nursery area for trout, focus should be on physical habitat conditions of young life stages (fry and juvenile) and spawning life stage of brown trout. When we compare the flow interval lower than Q_{80} (grey area in Fig. 2) with the physical habitat conditions (WUA) for the three life stages in the three streams we find that the largest changes in WUA for the young life stages happens just in the flow interval lower than Q_{80} in all three streams (Fig. 2). This suggests that assessment of groundwater abstraction impact on physical habitat conditions for young life stages of brown trout is very likely to be influenced by uncertainties related to simulation of low flows.

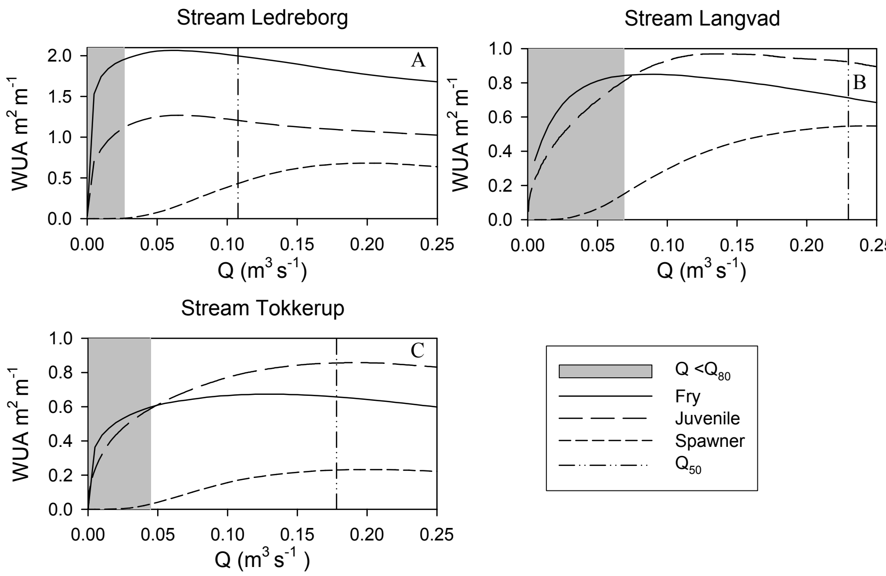

Fig. 2 Physical habitat conditions expressed as Weighted Usable Area (WUA) as a function of discharge (Q) for three life stages of brown trout (fry, juvenile and spawner) in three streams of similar size. The grey area (flows lower than Q_{80}) indicates the interval where the Danish national hydrological models most often have problems simulating observed flows.

Since prediction of WUA for young life stages of trout is most likely to be influenced by errors in low flow simulation we have simulated flow specific WUA for juvenile trout in the three streams. The Q simulation errors from the DK-model result in an overestimation of WUA in all three streams (Fig. 3). So although low flow simulation errors do not have a large impact on water balance they are likely to have a large impact on simulation of physical habitat conditions.

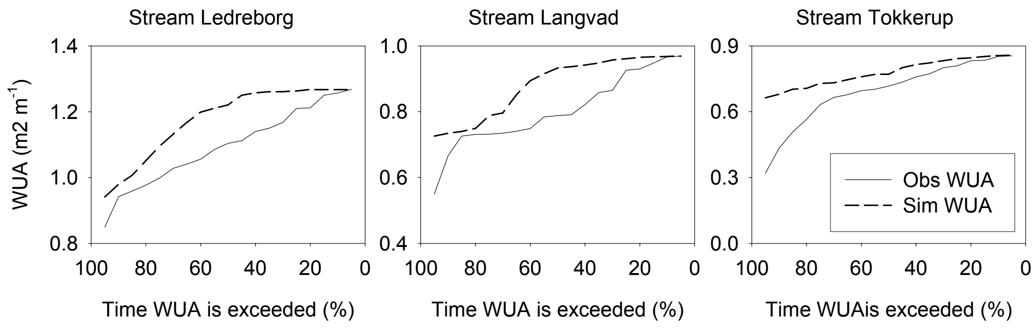

Fig. 3 Duration curves of physical habitat conditions (WUA) for juvenile brown trout in three streams of similar size. Each plot contains WUA based on observed (Obs WUA) and simulated (Sim WUA) discharge.

When the DK-model is used to test abstraction scenarios we are likely to underestimate the effect of groundwater abstraction on physical habitat conditions in streams due to the uncertainties related to low flow simulation. If the DK-model should be used for physical habitat modelling it should be tuned for the purpose.

One way of improving flow simulations is to have different calibration and validation measures for winter and summer period which is relevant to the bioindicator requirements in the different seasons. This could be done using site or region specific Expert Opinion on the relevant bioindicators and critical flow types e.g. a local fish biologist constructing a calendar that shows when high or low flows are most often considered critical for each brown trout life stage. This calendar could then be passed on to the hydrologist that would fine tune the DK-model to fit the flow types considered most important by the biologist. This way we get closer to an integrated approach which considers both the knowledge from biologist and hydrologist.

We expect that this approach is relevant for combination with all kinds of stream ecology models related to discharge especially in relation to predicting reference condition discharge and habitat conditions in streams impacted by groundwater abstraction.

REFERENCES

Orth, D. J. & Leonard, P. M. (1990) Comparison of discharge methods and habitat optimization for recommending instream flows to protect fish habitat. *Regulated rivers: research and management* **5**, 129-138.

Henriksen, H. J., Troldborg, L., Hojberg, A. L. & Refsgaard, J. C. (2008) Assessment of exploitable groundwater resources of Denmark by use of ensemble resource indicators and a numerical groundwater-surface water model. *Journal of Hydrology* **348**(1-2), 224-240.

Jowett, I. G. (2004) RHYHABSIM - River Hydraulics and Habitat Simulation. *User Manual for RHYHABSIM 3.2.*

Interactions between hydrology and biogeochemical cycles of native vegetated mountain watersheds under different management, southern Chile

C. E. OYARZUN[1], R. GODOY[2] & N. E. C. VERHOEST[3]

1 *Instituto de Geociencias, Facultad de Ciencias, Universidad Austral de Chile, Casilla 567, Valdivia, Chile*
coyarzun@uach.cl

2 *Instituto de Botánica, Facultad de Ciencias, Universidad Austral de Chile, Casilla 567, Valdivia, Chile*

3 *Laboratory of Water Management, University of Ghent. Coupure 653, Ghent, Belgium.*

Abstract Forests regulate quality as well as quantity of water, being the base for an integrated management of hydrological resources in forested watersheds. In the Andean range of southern Chile (39º 35' S, 72º 07' W, 600 - 925 m a.s.l.) we selected seven experimental watersheds with evergreen old-growth and deciduous secondary forests for to study the effects of management practices on water quantity and quality. The analysis of runoff changes between a watershed a thinned (35% of basal area removal) and a control paired watershed, both dominated by secondary growth *Nothofagus* forests during four years (2003-2007), showed that the former had a 12.7% increase in annual streamflow and 40% rise during the dry summer season. The runoff chemistry from two control watersheds showed a large seasonal and monthly variation related to phenological conditions of forests.

Keywords field measurements; data collection; evergreen old-growth forests; deciduous secondary forests; small watersheds; southern Chile

INTRODUCTION

Hydrology and biogeochemical information in combination with the watershed approach offers hope in producing integrated knowledge and understanding that can be used to better manage changing landscapes and thereby help sustain their critical ecosystem services into the future (Likens, 2001). The watershed approach to biogeochemistry has been particularly useful in quantifying air-land-water exchanges (Likens & Bormann, 1995). Recently, the watershed-ecosystem approach has been expanded to explore basic ecological mechanisms in relatively unpolluted sites (Perakis & Hedin, 2001). Natural and human-accelerated disturbance (e.g. acid rain, nitrogen saturation, and salinization) also can be addressed by an integrated watershed approach (Likens, 2001).

The native temperate rainforests of southern Chile represent an important reserve of temperate forests of the world, with a high genetic, phytogeographic and ecological significance, covering a total area of 10.5 million ha (CONAF *et al*., 1999). These forests support fundamental ecosystem services such as soil protection, biodiversity conservation, climate regulation, and water quantity and quality control. Under a scenario of global climate change, water quality and water supply becomes one of the main ecosystem functions of forests. Forests regulate quality as well as quantity of water, being the base for an integrated management of hydrological resources in forested watersheds.

Studies about interactions between hydrology and biogeochemical cycles on undisturbed old-growth and secondary managed and unmanaged forests could provide (a) base level information on pristine conditions, and (b) the influence of the management on both water quality and water supply.

STUDY SITE AND FIELD MEASUREMENTS

In the Andean range of southern Chile (39º 35' S, 72º 07' W, 600 - 925 m a.s.l.) we selected seven experimental watersheds with native old-growth and secondary forests: (a) two evergreen pristine old-growth forests, (b) two evergreen disturbed old-growth forests, (c) two deciduous unmanaged secondary forests, and (d) a deciduous managed secondary forest. We started in 2002 a long-term research in hydrology and biogeochemical cycles. The experimental design was the watershed-ecosystem approach following the Hubbard Brook Ecosystem Study model (Likens & Bormann, 1995).

The main tree species of the canopy cover in both the pristine and altered watersheds with evergreen old-growth forests are *Nothofagus dombeyi* (Mirb.) Oerst., *Saxegothae conspicua* Lindl., *Laureliopsis philippiana* Looser and *Dasyphyllum diacanthoides* (Less) Cabr. The deciduous secondary forests consisted of *Nothofagus obliqua* (Mirb.) Oerst and *Nothofagus alpina* (Poepp. et Endl.) Oerst.

Precipitation (P) was recorded with HOBO® tipping bucket rain gauges connected to a data logger and placed in a nearby meadow with no trees within a 40-m radius. We recorded a mean precipitation of 3,926 mm yr^{-1} for the period April 2003- March 2007, with 66% concentrated in autumn and winter and 7% in summer. Runoff (Q) was measured by pressure transducers DIVER and recorded hourly by data loggers in V-notch weirs (90°) installed in the lower part of each watershed. The interception loss (INT) was calculated following: INT = P – (Th + St), where P = rainfall, Th = throughfall and St = stemflow. Twenty fixed throughfall and ten stemflow collectors were installed in each watershed. Evapotranspiration (EVPT) was estimated according EVPT = P – (Q + INT).

The experimental design and collection of water samples for chemical analysis were according to Kleemola & Soderman (1993).

MANAGEMENT PRACTICES

From October 2002, one watershed covered with secondary growth forests was thinned extracting 35% of the total basal area and removing the logs whereas the other one remained unthinned as a control. Both watersheds are adjacent and are located at 600 – 650 m of elevation on deep loam textured volcanic soils (100 - 120 cm) laying over a 90-cm deep pumice layer and a volcanic fossil soil (80 – 100 cm).

In November 2006, one watershed covered with evergreen disturbed old-growth forests was thinned extracting 40% of the total basal area (from 75.9 m^2 ha^{-1} to 45.9 m^2 ha^{-1}) and the other one remained unthinned as a control. Both watershed are adjacent and are located at 725 – 910 m a.s.l.

WATER YIELD AND FOREST MANAGEMENT

Overall, the thinned watershed yielded higher stream discharge values compared to the control catchment for the four years observation period (April 2003 – March 2007), with greater absolute differences during fall and winter, when 67% of the precipitations are concentrated (Fig. 1). In the managed watershed with deciduous *Nothofagus* secondary forests water yield was increased from 2642 to 2975 mm yr^{-1} compared to a control unthinned watershed.

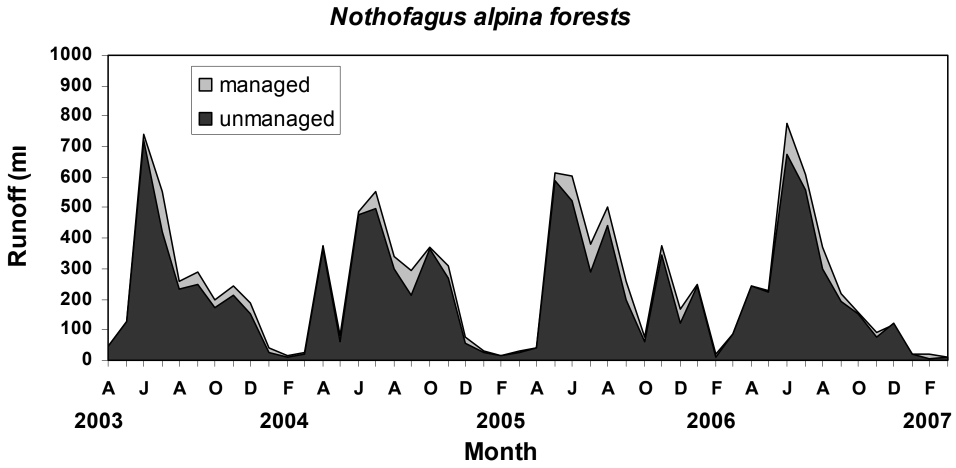

Fig. 1 Monthly streamflow in the thinned and control watersheds during four hydrologic years (April 2003 – March 2007).

TEMPORAL VARIATIONS IN RUNOFF CHEMISTRY

The control watersheds were used to document the natural variability of the runoff chemistry in the deciduous (Fig. 2) and evergreen forests (Fig. 3).

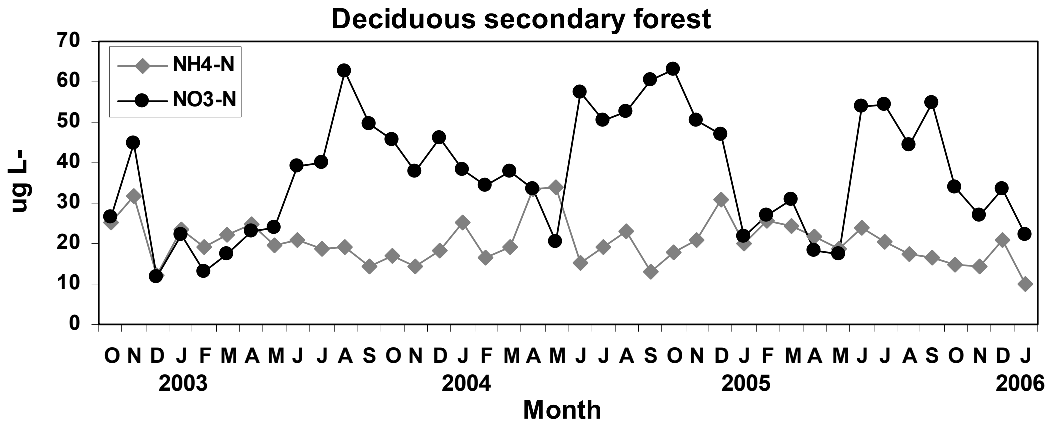

Fig. 2 Monthly variation in runoff concentrations of N species (NH_4-N and NO_3-N) from the control watershed with deciduous secondary forests.

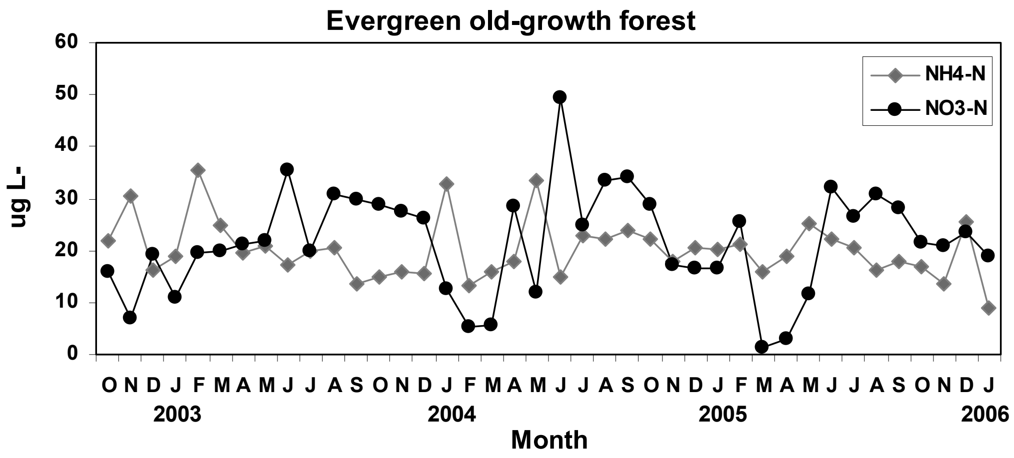

Fig. 3 Monthly variation in runoff concentrations of N species (NH_4-N and NO_3-N) from the control watershed with evergreen old-growth forests.

The runoff chemistry from two control watersheds showed a large seasonal and monthly variation. In general, NO_3-N showed a typical pattern with large concentrations in winter and spring and decreasing concentrations as plant growth and nutrient uptake during summer.

CONCLUSIONS

This study reported the effects of the management of deciduous secondary forests for increasing streamflow. For the period April 2003 – March 2007, the mean value of this increase in total annual streamflow was 12.7%, ranging from 10.9% to 14.6%. For the control watersheds, nitrate concentrations are directly related to the runoff and are relatively small in the growing season and greatest in the winter-spring. Further monitoring and field experiments are planned to investigate for to estimate relationships between soil properties, runoff concentrations and fluxes, litter decomposition in streams and management practices.

Acknowledgements This research was supported by Fondecyt Project 1050313, Bilateral Project Chile-Flanders, Millenium Project PO1-057-F and DIDUACH S-2008-15.

REFERENCES

CONAF, CONAMA, BIRF. (1999) Catastro y Evaluación de los Recursos Vegetacionales Nativos de Chile*. Universidad Austral de Chile and Pontificia Universidad Católica de Chile*, Santiago, Chile.

Kleemola, S. & Soderman, G. (1998) Manual for integrated monitoring. *International Co-operative programme on integrated monitoring on air pollution effects*. Environmental Report 5. Environment Data Centre, National Board of Waters and the Environment. Helsinki.

Likens, G. E. (2001) Biogeochemistry, the watershed approach: Some uses and limitations. *Marine and Freshwater Research* **52**, 5–12.

Likens, G. E. & Bormann, F. H. (1995) Biogeochemistry of a Forested Ecosystem. Springer-Verlag, New York, Berlin.

Perakis, S. S. & Hedin, L. O. (2001) Fluxes and fates of nitrogen in soil of an unpolluted old-growth temperate forest, southern Chile. *Ecology* **82,** 2245-2260.

Prediction of vegetation change on sand bars in a river channel

S. SUGIO & Y. OGAWA

Department of Civil and Environmental Engineering, University of Miyazaki, Gakuenkibanadai-Nishi, Miyazaki 889-2192, Japan

sugio@civil.miyazaki-u.ac.jp

Abstract The change in vegetation on sand bars in a river channel was investigated by quantitative analysis. A vegetation index was proposed to express the state of vegetation on the sand bars and a numerical model was proposed to simulate the change in vegetation. The calculated results clarify the history of vegetation destruction and restoration on the sand bars over the past 41 years. The function was then applied to predict the change in vegetation after ten years on the two sand bars excavated in river improvement work in 1999. The predicted results indicate the future change in vegetation strongly depends on the maintenance of the excavated ground surface elevation of the sand bars.

Keywords vegetation index; dimensionless tractive force; field site; destruction and restoration of vegetation

INTRODUCTION AND BACKGROUND INFORMATION

The existence of vegetation on sand bars in a river channel greatly influences not only the flow of floods but also the formation of the river ecosystems. Therefore, it is important for river management to predict growth of vegetation and expansion of the vegetated zone on sand bar.

Vegetation on the sand bars is composed of woody plants and herbaceous plants. The vegetation grows naturally, but is often destroyed by floods. We have analyzed the process of vegetation destruction through numerical simulation (Sugio & Watanabe, 2004a). However, it was difficult to physically analyze the cycle of restoration and destruction because our determination of the growth of vegetation was somewhat qualitative. Therefore, quantitative analysis by means of a conceptual model might be suitable for predicting the change in vegetation on sand bars.

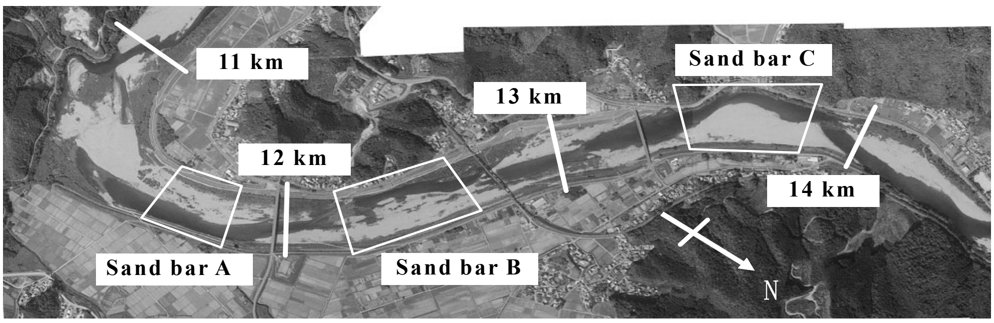

Fig. 1 Location of the study areas along the Kita River.

GENERAL REMARKS

The Kita River flows in the northern part of Miyazaki Prefecture, Japan. The study areas were three sand bars located in the 11 km to 14 km section as shown in Fig.1. Sand bars B and C were excavated in 1999 to lower the ground surface by about two meters for flood control. The slope of channel bed is about 1/1100, and the average width is 210 m in this region. The bed material is gravel with a median diameter of about 40 mm. The annual maximum discharge fluctuated between 300 $m^3 s^{-1}$ and 5,000 $m^3 s^{-1}$ from 1967 to 2007, with an average value of 1860 $m^3 s^{-1}$.

NUMERICAL MODEL OF VEGETATION CHANGE

Vegetation index

To analyze quantitatively changes in vegetation, a vegetation index has been introduced to express both the growth of vegetation and the expansion of the vegetated zone on sand bar A (Sugio & Watanabe, 2004b). A value of zero suggests the entire study area is almost barren ground while a value of 5 suggests thick coverage of woody plants and also that the entire study area is almost completely covered by herbaceous plants. The standard values of the vegetation index were defined as shown in Table 1.

Table 1 Standard values of the vegetation index.

Vegetation situation	Vegetation index	Area ratio (%)		
		Barren ground	Herbaceous	Woody
Thick wooded areas and complete herbaceous coverage	5	5	70	25
Wood colonies and 50% herbaceous coverage	3	35	50	15
50% barren ground and herbaceous coverage	2	50	40	10
Barren ground	0	80	20	0

Vegetation equation

According to the monitoring of vegetation change, vegetation was destroyed by large floods yet the vegetated zone expanded in years for which there were only small floods (Sugio *et al*., 2003). These results suggest the annual maximum discharge deeply affected the vegetation change on the sand bars. In the analysis for the vegetation change on sand bar A, the vegetation index was initially assumed to be a function of the annual maximum discharge. However, the deduced equation could not be applied to the other sand bars in different physical conditions. To analyze the vegetation change on all three sand bars, the equation was modified to improve applicability. Because most vegetation was destroyed by the transportation of bed material, a non-dimensional tractive force was selected as the variable of function (Fujita *et al*., 2003).

Changes in the vegetation index each year were assumed as

$$VF_{i+1} = VF_i + \Delta VF_i \qquad (1)$$

where VF_i is the vegetation index in year i, and ΔVF_i is the variation after flooding with the annual maximum discharge during year i.

The variation was assumed to be calculated by a series of linear functions of the non-dimensional tractive force as shown in Fig. 2. However, because the growth rates and destruction mechanisms were different for woody and herbaceous plants, each series of linear functions was calculated separately. The non-dimensional tractive force τ was calculated as

$$\tau = hI_e / sd_{50} \qquad (2)$$

where h and I_e are the energy gradient and the water depth at the centre of the study area, respectively, and s and d_{50} are the submerged specific gravity and the median diameter of bed material, respectively. The values of h and I_e were calculated from the simulated result of flow in the annual maximum discharge. Parameter values for the calculations were identified by trial and error as the calculated values of the vegetation index coincided with the observed values.

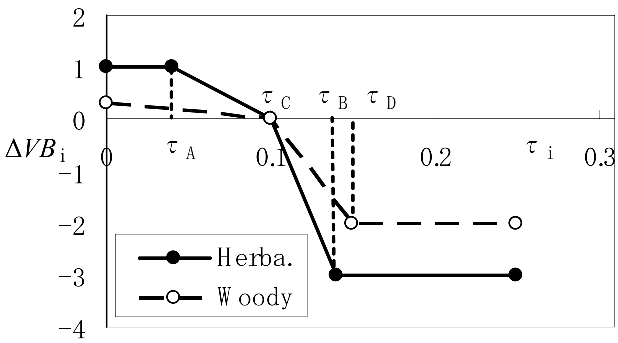

Fig. 2 Equation of vegetation variation.

CALCULATION OF VEGETATION INDEX

The calculation was verified by a comparison of the observed vegetation indices for the three sand bars and those calculated from the equation (Fig.3). From the calculated results, vegetation changes over the past 41 years on the three sand bars were clarified. The barren ground of sand bar A in 1982 resulted from the construction of right levee. High values of the vegetation index just before the excavation on sand bar B and C were caused by a period of small floods between 1983 and 1989. The vegetation destruction due to the excavation on sand bar B and C were large impacts that never occurred in natural conditions.

The equation was then applied to predict vegetation on the excavated sand bars after ten years (Fig. 4). The annual maximum discharges between 1971 and 1980 were used, and the river bed condition in 2007 was applied in the prediction. From the prediction, the value of the vegetation index for sand bar B where the river bed elevation was kept in the excavated state only recovered to half the value of the index for before the excavation. In contrast, the index value near the levee for sand bar C where the river bed rose after the excavation recovered to the almost same value as before the excavation, even though the index value near the waterside did not change.

CONCLUSIONS

The vegetation change on three sand bars was investigated by quantitative analysis. The proposed model clarified the history of vegetation destruction and restoration on three sand bars over the past 41 years, and predicted the state of vegetation on the excavated sand bars after ten years.

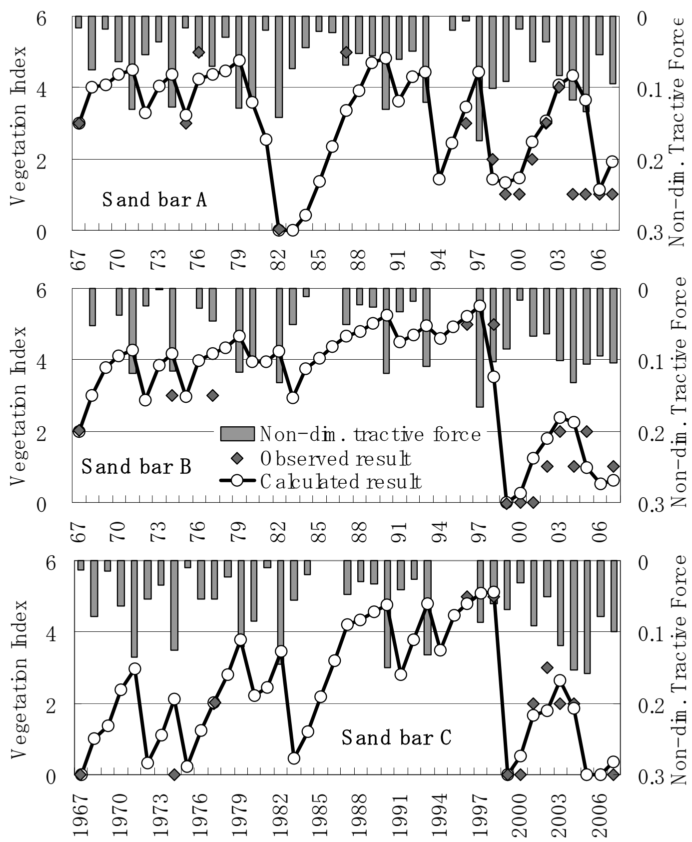

Fig. 3 Comparison of the annual vegetation index.

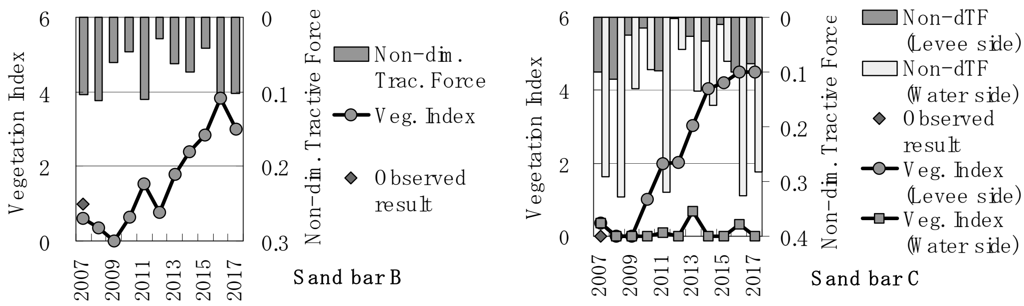

Fig. 4 Prediction of the annual vegetation index.

Acknowledgements This work was supported by research funds from the River Research Group, Japan. The assistance of the River Environment Division of the National Institute for Land and Infrastructure Management, Japan is acknowledged.

REFERENCES

Fujita, K. *et al.* (2003) Mechanism and simulation of the expansion and extinction of stable vegetation areas in a gravel-bed alluvial fan river. *Journal of Hydraulic*, *Coastal and Environmental Eng*., *JSCE* **747,** 41–60.

Sugio, S., Watanabe, K. & Tanoue, A. (2003) Research on the destruction of herbaceous vegetation by flood flow on sand bar in recovering process. *Annual Journal of Hydraulic Eng., JSCE* **47**, 1002–1008.

Sugio, S. & Watanabe, K. (2004a) Destruction of herbaceous vegetation by flood flow on a floodplain in a recovering process. *River Flow 2004*, 1315–1323.

Sugio, S. & Watanabe, K. (2004b) Research on change of topographical features and vegetation on a sand bar due to floods. *Proc. 31th IAHR Congress*, 6254-6264.

The effect of various forest disturbances on water discharge duration curve

K. TAMAI
Forestry & Forest Products Research Institute, 1 Matsunosato, Tsukuba, Ibaraki 305-8687, Japan
a123@ffpri.affrc.go.jp

Abstract The effects of forest disturbance on the discharge duration curve were compared among various disturbances in Sarukawa Experimental forest, located in a “warm and high precipitation region,” and Tatsunokuchi-yama Experimental forest, located in a “warm and low precipitation region.” Increases in discharge volume and the increase ratio caused by forest disturbance were greater and smaller, respectively, in Sarukawa than in Tatsunokuchi-yama. These findings were presumed to be related to the greater water discharge volume and higher level of precipitation in Sarukawa than in Tatsunokuchi-yama. In addition, smaller areas of disturbance may produce smaller increases in the discharge volume and increase ratio.
Keywords paired watershed experiment; long-term observation, warm high precipitation, warm low precipitation

INTRODUCTION

The forest affects water discharge *via* evapotranspiration by vegetation and infiltration through the forest soil. The magnitude of the disturbance effect on water discharge is thought to depend on many factors, such as climate conditions, vegetation activities, disturbance magnitude, and forest treatment after the disturbance. Accordingly, it is very important to compare various types of disturbance under different climate or disturbance conditions. In the present study, the effects of disturbance on water discharge were compared between cases of disturbance in contrasting temperate regions of Japan with high and low precipitation.

SITE DESCRIPTION

The experimental watersheds studied were in Sarukawa Experimental Forest and Tatsunokuchi-yama Experimental Forest. Sarukawa Experimental Forest is located on Kyushu Island, Japan (31°54'N, 131°12'E). This study was performed using data from catchments No. 1 and No. 2 covering areas of 6.57 ha and 9.17 ha, respectively.

Tatsunokuchi-yama Experimental Forest is located on western Honshu Island, Japan (34°42'N, 133°58'E). The experimental forest consists of the Kita-tani and Minami-tani catchments with areas of 17.27 and 22.61 ha, respectively.

Table 1 Disturbed cases in Sarukawa and Tatsunokuchi-yama experimental forests.

Experimental Forest	Case ID	Standard Catchment	Disturbed Catchment	Disturbe Factor	Standard Period	Disturbed Period	Averaged annual precipitation (mm) in Disturbed period	Disturbed area (ha)	Percentage of disturbed area in total catchment area (%)	Treatment after disturbance
Sarukawa	A	No.2	No.1	Clear cut	1977 - 1981	1967 - 1976	2781.6	6.6	100	Planting
	B	No.1	No.2	Partial clear cut		1982- 1986	2999.4	3.8	43	Natural regrowth
Tatsunokuchi - yama	C	Kita- tani	Minami- tani	Forest fire	1937- 1959	1960- 1966	1275.0	22.3	100	Planting
	D	Kita- tani	Minami- tani	Wilt diseace	1968- 1979 1998- 2002	1981- 1992	1123.6	18.8	84	Natural regrowth

The warm indexes in Sarukawa and Tatsunokuchi-yama were reported to be 144 and 130, respectively. On the other hand, the average annual precipitation levels in

Sarukawa (1967–1986) and Tatsunokuchi-yama (1937–2002) were about 2850 mm and 1200 mm, respectively. Thus, the Sarukawa and Tatsunokuchi-yama forests were judged to be located in the “warm, high precipitation region” and the “warm, low precipitation region,” respectively.

ANALYTICAL METHODS

Discharge durationcurve and data

The water discharge observation data were collected from Sarukawa catchments No. 1 and No. 2 in 1967–1986 and from Tatsunokuchi-yama Kita-tani and Minami-tani catchments in 1937–2002.

A paired-catchment experiment comparing discharge duration curves was performed in this study. The discharge duration curve was defined as the line with larger order of daily discharge volume for the 365 values in a year. The left and right sides of the discharge duration curve showed the daily discharge volume at times of high water and drought, respectively. The 95th, 185th, 275th, and 355th largest volumes were referred to as “plentiful water discharge,” “ordinary water discharge,” “low water discharge,” and “drought discharge,” respectively. The ith largest volume within the discharge duration curve in any year was written as $Q_*(yr, i)$ in this study, where the subscript $*$ indicates the control (c) and the disturbed (d) catchment, and yr indicates the year of observation. The regression line in Eq. (1) was calculated for each i between the control and disturbed catchments for the control period:

$$Q_d(yr,i) = a_i Q_c(yr,i) + b_i \tag{1}$$

Here, a_i and b_i are the correlation coefficient and the correlation constant, respectively. Disturbance cases are shown in Table 1 dealt with in this study.

Estimation of increased discharge volume and increased ratio

The potential discharge volume from the disturbed catchment ($Q_{dcal}(yr,i)$) during the disturbed period, the discharge volume to be observed if the forest is not disturbed, was estimated using Eq. (2), which substitutes the observed discharge volume from the control catchment ($Q_{cobs}(yr,i)$) during the disturbed period into Eq. (1):

$$Q_{dcal}(yr,i) = a_i Q_{cobs}(yr,i) + b_i \tag{2}$$

The estimated increase in volume ($\Delta Q_d(yr,i)$) caused by disturbance was calculated using Eq. (3):

$$\Delta Q_d(yr,i) = Q_{dobs}(yr,i) - Q_{dcal}(yr,i) \tag{3}$$

where $Q_{dobs}(yr,i)$ is the observed discharge volume from the disturbed catchment. Each disturbance case included data for a period of 5–12 years.

RESULTS AND DISCUSSION

Regression lines during the control period

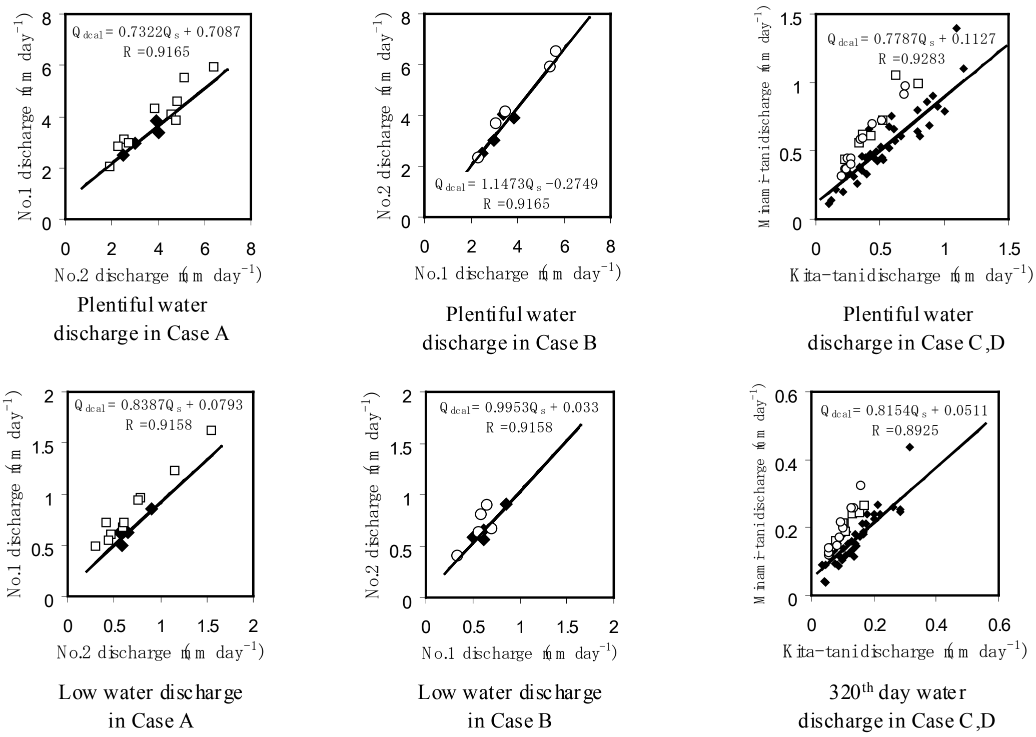

Fig. 1 Discharge volume from control and disturbed catchments; X-axis:Discharge volume from control catchment; Y-axis:Discaharge from disturbed catchment; Left: Case A (Black:Control period, White Disturbed period); Center: Case B (Black:Control period, White Disturbed period); Right: Case C and D (Black:Control period; White square:Disturbed period of Case C, White circle: Disturbed period of Case D); Thick line: Regression line.

Eq. (1) was calculated for "plentiful water discharge (i=95)," "ordinary water discharge (i=175)," "low water discharge (i=265)," and "drought discharge (i=355)". However, Eq. (1) for i=320 was shown instead of i=355 in Cases A and B. As the correlation coefficient for i=355 between catchments No. 1 and No. 2, Sarukawa was much lower than 0.7. The x- and y-axes show the discharge volume from control and disturbed catchments, respectively, in Fig. 1. The majority of white points showing the values in disturbed periods were located to the upper left of the regression lines indicating that the discharge volume increased in disturbed periods on most days.

Estimated increased discharge volume and increased ratio

$\Delta Q_d(yr,i)$ was calculated for each year in disturbed periods. Table 2 shows the averaged $\Delta Q_d(yr,i)$ during each disturbance case. For example, average $\Delta Q_d(yr,95)$ at 5 years during the disturbed period in Case B were 0.207 mm day^{-1}.

Table 2 Increased discharge volume and increased ratio caused by forest disturbances.

	i number in discharge duration curve	Increaswed discharge volume (mm day^{-1})			Increased ratio (%)		
		Case A	Case B	B/A (%)	Case A	Case B	B/A (%
Sarukawa	95th	0.345	0.207	60	9	5	56
	185th	0.238	0.205	86	14	12	86
	275th	0.173	0.110	64	20	16	80
	320th	0.131	0.073	56	22	16	73
	i number in discharge duration curve	Increaswed discharge volume (mm day^{-1})			Increased ratio (%)		
		Case C	Case D	C/D (%)	Case C	Case D	C/D (%)
Tatsunokuchi-yama	95th	0.227	0.158	70	32	28	88
	185th	0.108	0.098	91	33	35	106
	275th	0.066	0.059	89	30	32	107
	355th	0.048	0.056	117	33	43	130

Generally, $\Delta Q_d(yr,i)$ and its standard deviation in Sarukara (Cases A and B) were greater than in Tatsunokuchi-yama (Cases C and D). The average $\Delta Q_d(yr,175)$,$\Delta Q_d(yr,265)$, and $\Delta Q_d(yr,320)$ values in Sarukawa were much greater than in Tatsunokuchi-yama. However, there were no clear differences in average $\Delta Q_d(yr,95)$ value between Sarukawa and Tatsunokuchi-yama because $\Delta Q_d(yr,95)$ included some negative values in Sarukawa. Such values of $\Delta Q_d(yr,95)$ were 0 among 19 values and 4 among 20 values in Tatsunokuchi-yama and Sarukawa, respectively. However, $\Delta Q_d(yr,i)$ was judged to be larger in Sarukawa than in Tatsunokuchi-yama because precipitation was greater in the former than in the latter.

Table 2 also shows the increase ratio calculated by dividing the average $\Delta Q_d(yr,i)$ by the average $Q_{dobs}(yr,i)$. In contrast to the average $\Delta Q_d(yr,i)$, the increase ratio was greater in Tatsunokuchi-yama than in Sarukawa, presumably because the discharge volume in the latter is much greater (fivefold) than that in the former. Thus, the difference in precipitation conditions may also be responsible for the observed difference in the increase ratio between Sarukawa and Tatsunokuchi-yama.

Finally, average $\Delta Q_d(yr,i)$ and increase ratio values were compared between cases in the same forest. There was no clear difference between Cases C and D in Tatsunokuchi-yama. The amounts of disturbed area in the catchments were 100% and 84% in Cases C and D, respectively. On the other hand, in Sarukawa, average $\Delta Q_d(yr,i)$ and increase ratio values in Case B were 56–86% of those in Case A. The amounts of disturbed area in the catchments were 100% and 43% in Cases A and B, respectively. Tamai (2005) reported that clear-cutting of a small area (less than 1.0 ha) had no effect on the discharge duration curve in Minami-tani catchment at Tatsunokuchi-yama. Thus, the small clear-cut area may have resulted in low values of average $\Delta Q_d(yr,i)$ and the increase ratio in Case B compared with Case A. However, it should be noted that the standard deviation of the increase ratio was large and the significance of this result must be examined further in future studies.

The influence of floodplain characteristics on longitudinal dispersion in a natural channel

S. G. WALLIS[1]& J. R. MANSON[2]

1 *School of the Built Environment, Heriot-Watt University, Riccarton, Edinburgh, EH14 4AS*
s.g.wallis@hw.ac.uk

2 *School of Natural Sciences and Mathematics, The Richard Stockton College of New Jersey, PO Box 195, Pomona, NJ 08240, USA.*

Abstract Dispersion coefficients need to be estimated in many river water quality modelling studies. However, even after several decades of scientific investigation this cannot be accomplished with much confidence, particularly for natural channel cross-section shapes. This paper presents theoretical dispersion coefficient computations that highlight some of the issues. The results show that the behaviour of the dispersion coefficient is rather complex once river stage exceeds the bank-full condition. Also, floodplain roughness and uncertainty in floodplain topography are found to have a significant effect on the dispersion coefficient.
Keywords dispersion coefficient; velocity profile; numerical integration; floodplain

INTRODUCTION

The practical application of water quality and pollution incident models to rivers usually requires the estimation of one or more mixing coefficients in order to correctly represent the physical transport processes. When modelling long river reaches it is usual to take a one-dimensional approach, in which the appropriate mixing coefficient is that describing longitudinal dispersion. However, the task of predicting dispersion coefficients for natural rivers is not one that can be accomplished with any great confidence, even after many years of scientific investigation. The main reason for this is that dispersion occurs as the result of the interaction of several different physical processes. Although the individual processes are well understood, and their interaction can be modelled quite successfully for ideal channels, attempts to derive predictive equations for dispersion coefficients in natural channels have met with mixed success (Wallis & Manson, 2004). For example meanders, transient storage and geomorphologically induced secondary currents pose significant problems. Probably the best options for predicting dispersion coefficients in real channels currently lie with theoretically based (Deng *et al.*, 2002), and with neural network based (Rowinski *et al.*, 2005; Wallis *et al.*, 2007), approaches both of which help to establish empirical equations for predicting the coefficient. As might be surmised by the foregoing, however, the success of such empirical equations deteriorates as channels become more complex. In this regard, an interesting but little studied issue is the behaviour of the dispersion coefficient during high flows, particularly as floodplains start to become inundated. The authors have previously reported some theoretical results for such conditions in an idealised channel (Manson & Wallis, 2004), which suggest that very large dispersion coefficients can occur when floodplains contain large areas of slowly moving, shallow water. Since such conditions are not well catered for by existing empirical equations, there are severe problems in predicting dispersion in these circumstances. The aims of the current paper are to apply the approach mentioned above to a natural river cross-section and to explore the influence of floodplain roughness and floodplain topography on the predicted dispersion coefficient.

DATA ANALYSIS AND RESULTS

Dispersion coefficients were calculated using the following flow structure integration:

$$D = -\frac{1}{A}\int_0^w hu \int_0^y \frac{1}{\varepsilon h}\int_0^y hu \; dy\, dy\, dy \tag{1}$$

where D is the dispersion coefficient, A is the cross-sectional area of the flow, h is the local flow depth, u is the difference between the local longitudinal velocity and the cross-sectional averaged velocity, ε is the local transverse mixing coefficient, W is the top flow width and y is the transverse co-ordinate direction. This equation (Fischer, 1967) assumes that dispersion is caused by the interaction of transverse gradients of depth-averaged longitudinal velocity with transverse mixing caused by turbulent diffusion. Hence h, u and ε are depth-averaged quantities that vary with transverse position. Clearly, D can be found if the transverse profiles of h, u and ε are known.

Manson & Wallis (2004) describe the computation of transverse profiles of u and ε, for a given channel cross-section. This uses a numerical solution of the SKM approach (Shiono & Knight, 1991), expressing the local longitudinal bed shear stress using Manning's resistance equation and the local longitudinal shear stress due to transverse momentum exchange using the Boussinesq eddy-viscosity concept, and assumes an equivalence between the mixing of momentum and mass (both being proportional to the product of local depth and local shear velocity). Here a simplified version of this approach was used that ignored the transverse momentum exchange.

Computations were carried out for the channel cross-section shown in Fig. 1, which is based on a natural cross-section of the River Severn, UK, described in Carling *et al.* (2002). Results were obtained for stages between 8 and 14m in order to investigate conditions close to and above the bank-full case. Four cases were examined: Case 1, uniform roughness (Manning's n = 0.03 everywhere); Case 2, rough floodplain (Manning's n = 0.03 for the main channel and = 0.06 for the floodplain); Cases 3 and 4, as Case 1 except errors of +0.5m and -0.5m, respectively, were introduced into the floodplain topography at location P (see Fig. 1). In all cases the channel slope and the non-dimensional transverse mixing coefficient were taken as 0.001 and 0.6, respectively. Results showing the variation of predicted dispersion coefficient with stage for the four cases are shown in Figs. 2 and 4. Some transverse velocity profiles are shown in Fig. 3.

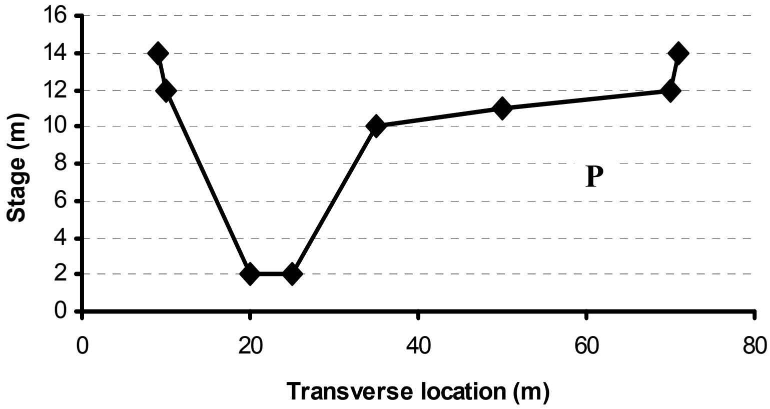

Fig. 1 River cross-section (simplified from Carling *et al.* (2002)).

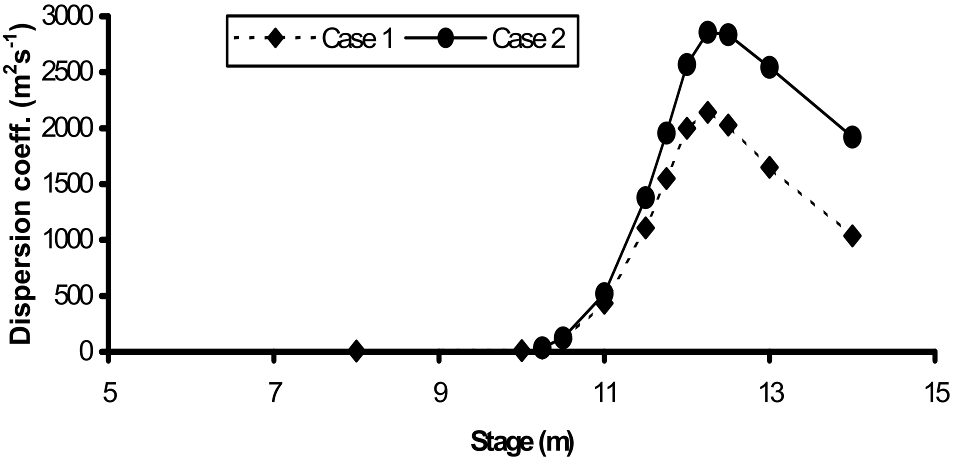

Fig. 2 Dispersion coefficient – stage relationship, showing the influence of floodplain roughness.

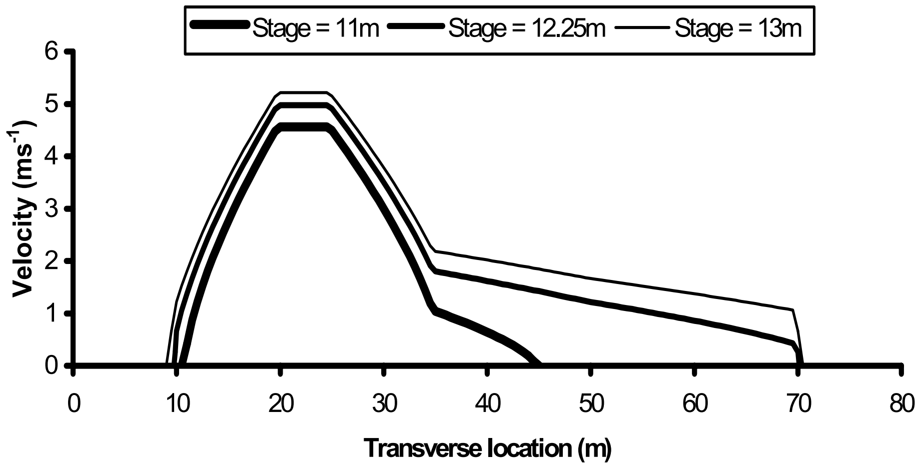

Fig. 3 Transverse velocity profiles for Case 1 for three stages.

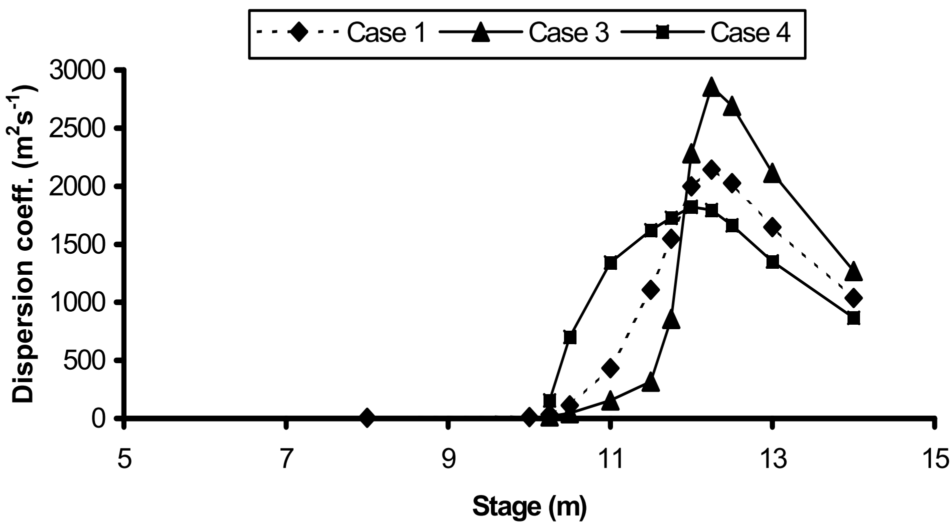

Fig. 4 Dispersion coefficient – stage relationship, showing the influence of floodplain topography.

DISCUSSION

Fig. 2 shows that the dispersion coefficient remains very small at stages less than and equal to the bank-full condition (stage = 10m), with values being of the order of $10m^2s^1$. For Case 1, once the flow begins to occupy the floodplain the dispersion coefficient increases rapidly with values peaking at about $2150m^2s^{-1}$ at a stage a little over 12m. There is then a more gradual reduction for further increases of stage. This behaviour is consistent with dispersion being caused by transverse velocity shear. It is not only the magnitude of the velocity gradients that are important but also the distance over which they exist, as illustrated by the computed transverse velocity profiles shown in Fig. 3. The effect of doubling the floodplain roughness (Case 2) is to increase the maximum dispersion coefficient to about $2850m^2s^{-1}$ (again at a stage a little over 12m), and the increase persists at higher stages.

Fig. 4 shows the effect on the computed dispersion coefficient of uncertainty in the floodplain topography. In comparison to Case 1, some overestimation of the floodplain elevation leads to reductions in dispersion for 11m<stage<12m but to increases for stages>12m. In contrast, some underestimation of the floodplain elevation leads to increases in dispersion for 11m<stage<12m but to decreases for stages>12m. This behaviour can be attributed to the loss and gain, respectively, of flow area on the floodplain caused by the topographic errors. It is interesting to note that in both Figs. 2 and 4, a stage close to the elevation of the far edge of the floodplain (12m) divides the plots into zones of different behaviour.

CONCLUSIONS

Computations for a natural river cross-section have shown that once water spills from the main channel on to the floodplain dispersion coefficients may increase by two orders of magnitude. This is consistent with previous results for an idealised, double trapezoidal channel (Manson & Wallis, 2004). Maximum values occur when the floodplain inundation reaches the far edge of the floodplain, i.e. when the floodplain is covered by a large extent of slowly moving, shallow water. Floodplain roughness appears to have a significant effect, with increased roughness causing increased dispersion. Errors in the elevation data of floodplains appear also to have significant, and complex, effects on the dispersion coefficient. Such knowledge should be helpful in designing data collection exercises for the calibration of water quality models.

REFERENCES

Carling, P. A., Cao, Z. X., Holland, M. J., Ervine, D. A. & Babaeyan-Koopaei, K. (2002) Turbulent flow across a natural compound channel, *Water Resources Research* **38**(12), doi: 10.1029/2001WR000902.

Deng, Z.-Q., Bengtsson, L., Singh, V. P. & Adrian, D. D. (2002) Longitudinal dispersion coefficient in single-channel streams. *Journal of Hydraulic Engineering, ASCE* **128**(10), 901-916.

Fischer, H. B. (1967) The mechanics of dispersion in natural streams. *Journal of the Hydraulics Division, ASCE* **93**(HY6), 187-215.

Manson, J. R. & Wallis, S. G. (2004) Fluvial mixing during floods. *Geophysical Research Letters* **31**(14), L14502, 4 pp.

Rowinski, P. M., Piotrowski, A. & Napiorkowski, J. J. (2005) Are artificial neural network techniques relevant for the estimation of longitudinal dispersion coefficient in rivers? *Hydrological Sciences Journal* **50**(1), 175-187.

Shiono, K. & Knight, D. W. (1991) Turbulent open-channel flows with variable depth across the channel. *Journal of Fluid Mechanics* **222**, 617-646.

Wallis, S. G. & Manson, J. R. (2004) Methods for predicting dispersion coefficients in rivers. *Proceedings of the Institution of Civil Engineers, Water Management* **157**(WM3), 131-141.

Wallis, S. G., Piotrowski, A. Rowinski, P. M. & Napiorkowski, J. J. (2007) Prediction of dispersion coefficients in a small stream using Artificial Neural Networks. *Proceedings of the 32nd IAHR Congress*, Venice, paper B2b-083-O.

Modelling the impact of land-use change on recharge and nitrate loading to the Sherwood Sandstone Aquifer, Nottinghamshire, UK

H. ZHANG & K. M. HISCOCK

School of Environmental Sciences, University of East Anglia, Norwich NR4 7 TJ, UK

h.zhang@uea.ac.uk; k.hiscock@uea.ac.uk

Abstract A change in land-use from arable agriculture to woodland is encouraged in many European countries to reduce leaching of diffuse agricultural pollutants (nitrate) to aquifers. In some cases, however, a reduction of recharge beneath woodland could aggravate water supply shortages. No integrated evaluation of the impact of woodland on groundwater has been undertaken in Britain. Hence, the aim of this study is to evaluate the effect of increasing woodland on groundwater, both quantity and quality, on the Sherwood Sandstone Aquifer, Nottinghamshire, UK, using a modelling approach. After calibration of a groundwater flow and mass transport model, a range of percentages of woodland or grassland shifted from arable land were tested by the model to estimate the minimum percentage cover of woodland or grassland needed to reduce the nitrate concentration below the EU potable water standard (50 mg/litre). The results show that soil nitrogen losses of 9250 kg N/ha/yr, compared with a baseline value of 11935 kg N/ha/yr, could result in a nitrate concentration in a borehole capture zone achieving the EU target. To narrow the gap of nitrogen loss (2685 kg N/ha/yr), the minimum percentage cover of woodland estimated by the model simulations is 40% at a site, compared with a minimum percentage cover of 30% for grassland. As a result of land-use change, a reduction in recharge of 17% occurs when the woodland area is increased by 17% and groundwater levels are predicted to fall by less than 0.5 m. In conclusion, this study demonstrates that a modelling approach is a useful tool to quantify the effect of land use change on nitrate mitigation as well as groundwater resource potential.

Keywords recharge; nitrate pollution; land use change; mass transport modelling; water resources

INTRODUCTION

Nitrate concentrations in UK groundwater have been steadily rising over the past 20 years as a result of nitrate leaching losses from intensive agriculture since the 1940s. Significantly lower woodland cover in England (8.5%) than other European countries (35%) (Swales, 2006) encourages conversion from arable land to woodland (Defra, 2007) and this is a sustainable way to mitigate the issue of high nitrate in the UK based on the preventative ethos of the EU Nitrates Directive. Meanwhile, the impact on groundwater quantity should also be assessed since land-use change to woodland with associated great water demand of trees may reduce groundwater recharge and ultimately stress future water shortages. Therefore, with land-use conversion from arable land to woodland, the benefit of protecting groundwater supplies from nitrate pollution needs to be balanced against a reduction in water yield. However, no previous study has measured directly the effect on water yield of changing short vegetation to woodland given the long timescales involved (Calder, 2008). In this study, a modelling approach is used to estimate the amount of land-use change needed to meet groundwater standards, and assess the impact of such land-use change on groundwater quantity by developing a reliable groundwater flow and mass transport model.

METHODOLOGY

The main methods used in the development of the groundwater model are summarised in Fig. 1. The groundwater recharge calculation developed by the Environment Agency-FAO (FAO, 2006) was used to estimate groundwater recharge by incorporating soil and land use data. Then, an export coefficient model was adopted to estimate nitrogen losses for each 2×2 km grid cell by combination of land use information and agriculture census data. The resulting estimates of groundwater recharge and soil nitrogen losses were spatially analysed in ArcGIS and used as input data in the application of the groundwater transient-state model Visual MODFLOW (Waterloo Hydrogeologic, 2005) and mass transport model MT3DMS (Zheng, 1999). The groundwater model domain covered a total area of 1500 km^2 with a uniformly spaced grid of 500×500 m. Two geological layers were simulated: Triassic Mercia Mudstone and Sherwood Sandstone. Calibration was achieved by amending parameters related to groundwater movement and mass transport and by evaluating convergence between simulated and observed historical data for the year 1986 to 2006. After model calibration (year 1986-2000) and validation (year 2001-2006) with a monthly step, the modelling framework was then capable of predicting different land use scenarios for the next 20 years.

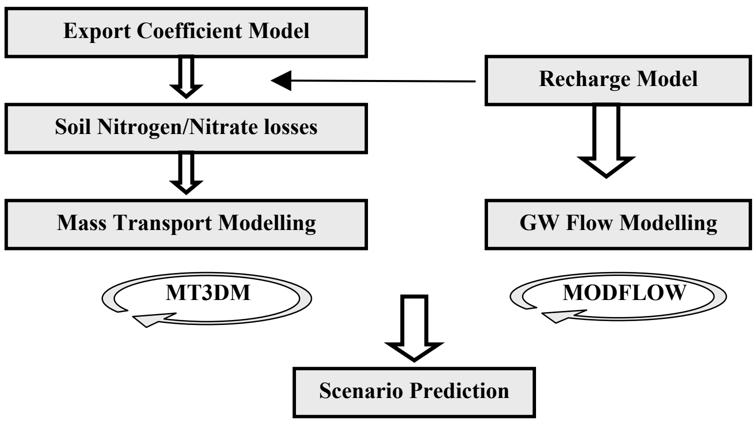

Fig. 1 Steps involved in the groundwater modelling of land-use change scenarios.

RESULTS AND DICUSSION

The transient groundwater flow model was calibrated against groundwater level in 27 observation boreholes and river flow at 10 river gauging stations. The mass transport model was calibrated against nitrate concentration at 24 groundwater monitoring points and groundwater abstraction boreholes. The general model performance after calibration is presented in Table 1.

Table 1 The overall performance for the groundwater flow model and mass transport model.

	RM	ARM	RMS	NRMS
Groundwater flow model	-0.53 m	1.85 m	2.86 m	1.9 %
Mass transport model	-1.86 mg/l	6.54 mg/l	8.11 mg/l	8.2 %

RM = residual mean; ARM = absolute residual mean;
RMS = root mean squared; NRMS = normalized root mean squared.

Apart from the statistical analysis of the model performance given above, a good match of the observed time series data also indicated that the model is able to predict the impact of land-use change on groundwater nitrate concentration and groundwater quantity under different land-use scenarios.

The current nitrate concentrations in most abstraction boreholes in the Sherwood Sandstone Aquifer at outcrop exceed the limit of 50 mg/l. A nitrate concentration of 62.2 mg/l was observed in one selected abstraction borehole. The soil nitrogen loss from a relevant 2×2 km grid cell is 11,935 kg N/yr according to the export coefficient model. The linear regression equation (1) derived from observed data at monitoring sites presents the relationship between groundwater nitrate concentration and soil leachate nitrate concentration,

$$NO_3{}^-{}_{(g)} = 0.521\ NO_3{}^-{}_{(s)} + 3.405 \qquad (1)$$

where $NO_3{}^-{}_{(g)}$ is the nitrate concentration in groundwater (mg/l), $NO_3{}^-{}_{(s)}$ is the nitrate concentration in soil leachate. According to the equation (1), then to reach a groundwater nitrate concentration limit of 50 mg/l, worked backwards to estimate the associated soil leachate nitrogen losses, a limit of 9250 kg N/yr is required under a recharge rate of 115 mm/yr. In this calculation, nitrogen losses from woodland and arable land were set at 9 kg N/ha and 41.4 kg N/ha, respectively, on the sandstone outcrop. Accordingly, the minimum percentage of woodland in a relevant cell is 37.8%, enough to narrow the gap in nitrogen losses (2685 kg N/yr) between the baseline and critical nitrogen losses. In practice, for woodland scenarios, a range of woodland percentages were tested by running the calibrated mass transport model to identify the amount of land needed to shift from arable land to woodland to meet the groundwater nitrate standard. Modelling results show that to achieve a limit of 50 mg/l nitrate in a borehole by the year 2025, the percentage of woodland in a relevant cell is approximately 40% at least, comparable with the estimation of 37.8% calculated using equation (1).

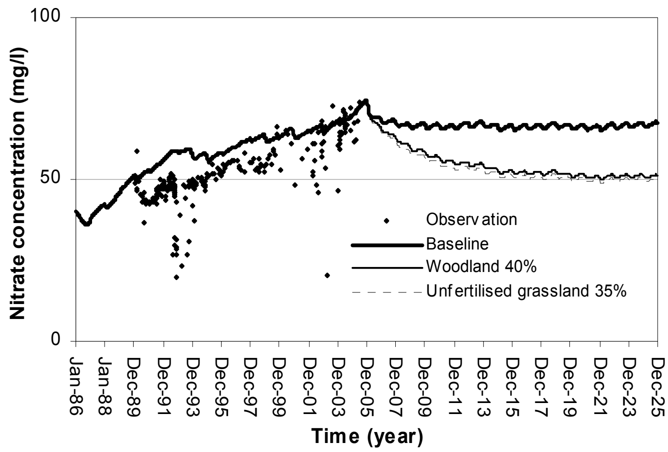

Fig. 2 Modelled groundwater nitrate concentration under different land-use change scenarios for an unconfined borehole abstracting 3285Ml/yr from the unconfined Sherwood Sandstone Aquifer.

With the above approach, a minimum percentage of grassland in a cell determined by mass transport model simulation is 35% comparable with a value of 33.6% calculated using equation (1). The effect of land-use change on groundwater nitrate concentration is presented in Fig. 2. The upper line in Fig. 2 shows the modelled nitrate value against the historical data during the past twenty years from 1986 to 2006 and also shows the nitrate trend for the next two decades under average monthly recharge conditions and without any land-use change. The middle line displays the nitrate trend of a woodland scenario in which woodland cover increases by up to 40% of the total cell area. The lower line indicates the simulation result for a 35% grassland cover scenario.

To assess the impact of each land-use scenario on groundwater level, this study applied different recharge rates to the calibrated model based on different water uptake associated with different vegetation types. For the purpose of this study, the recharge input for the grassland scenario is the same as the baseline recharge due to the similar water use of short-rooted arable crops and grass. On the other hand, the recharge rate is assumed to be reduced by 70% and 45%, respectively, under conifer trees and broadleaf trees compared with grassland (Calder, 2003). Consequently, a woodland area increasing from the baseline value of 23% to a future scenario value of 40% results in a 17% reduction in recharge. The consequent change of groundwater level simulated by the groundwater flow model with reduced recharge is, however, not distinguishable in the predicted period. The results show a maximum decline in head of 0.35 m and mean decrease of 0.12 m. This small change in groundwater level is due to the good aquifer storage properties of the Sherwood Sandstone Aquifer.

CONCLUSIONS

This study has shown that groundwater flow and nitrate transport modelling is a useful tool for forecasting the effects of land-use change on groundwater nitrate concentration and groundwater resource potential. It is concluded that conversion from arable land to woodland provides an effective way to control diffuse nitrate pollution from agriculture as long as the change does not produce a marked decrease in groundwater level and reduction of water yield. By adopting a model simulation approach, it is possible to guide decisions on the least amount of agricultural land-use change required to meet groundwater standards.

Acknowledgements Funding for this study has been supported by the Chinese Scholarship Council and the University of East Anglia.

REFERENCES

Calder, I. R. (2003) Assessing the water use of short vegetation and forests: development of the Hydrological Land Use Change (HYLUC) model. *Water Resources Research* **39**(11), p1318.

Calder, I. R., Harrison, J., Nisbet, T. R. & Smithers, R. J. (2008) Woodland actions for biodiversity and their role in water management. *Woodland Trust Report.*

Defra (2007) A Strategy for England's Trees, Woods and Forests. *Defra, London.*

Swales, V., Farmer, M., Keenleyside, C., Slee, R. W. & Dwyer, J. (2006). The Environmental Contribution of LEADER+ in the UK. Land Use Policy Group. *A report for the Land Use Policy Group SNH, Inverness. IEEP: London.*

FAO (2006) Crop evapotranspiration guidelines for computing crop water requirements. *FAO Irrigation and Drainage Paper No.56.*

Waterloo Hydrogeologic (2005) Visual MODFLOW v.4.1 *User's Manual, Waterloo Hydrogeologic, Ontario, Canada.*

Zheng, C. & Wang, P. (1999) MT3DMS: A modular three-dimensional multispecies transport model for simulation of advection, dispersion, and chemical reactions of contaminants in groundwater systems. *Documentation and User's Guide, U.S. Army Crops of Engineers, Washington DC, USA.*

Identification and quantification of the soil moisture response to the atmospheric forcing

I. EL-BAROUDY & A. ELSHORBAGY

Centre for Advanced Numerical Simulation (CANSIM), Department of Civil & Geological Engineering, University of Saskatchewan, Saskatoon, SK S7N 5A9 Canada

ibe140@mail.usask.ca

Abstract The mutual influence between the soil moisture and the near surface atmospheric conditions adds to the spatial and temporal variability of the soil moisture, which affects the reliability of its direct measurements. The utility of two data-driven techniques; (i) Evolutionary Polynomial Regression, and (ii) Genetic Programming (using Discipulus^{TM}), is investigated in modelling the soil moisture response to the net radiation, precipitation, and air and soil temperatures. The utility of the proposed models is demonstrated through the understanding of the (daily) soil moisture response of three experimental soil covers, D1 (50cm), D2 (35cm), and D3 (100cm), used for the reclamation of watersheds that are disturbed by the oil sands industry. This study demonstrates the effect of both the spatial heterogeneity and temporal variability on the soil moisture response to various atmospheric conditions, shedding some light on the mutual land-atmosphere interaction. The modelling process provides an insight into the soil storage effect on the phase-lag of the soil moisture with respect to the different atmospheric conditions.

Keywords data-driven techniques; genetic programming; evolutionary polynomial regression; oil sands; soil storage effect; soil moisture response

INTRODUCTION AND BACKGROUND INFORMATION

In hydrology-related studies, GP has been applied to model the rainfall–runoff process (Whigham & Crapper, 2001), runoff forecasting (Khu *et al.*, 2001), temperature downscaling (Coulibaly, 2004), and the rainfall–recharge process (Hong *et al.*, 2005). Giustolisi & Savic (2006) developed the evolutionary polynomial regression (EPR) technique and user-friendly tool, which can be considered a restricted version of GP. EPR is a data-driven technique that incorporates the main features of numerical regression together with symbolic regression. EPR was designed so that it avoids producing functions that grow in length over time (Savic *et al.*, 1999). In this paper, the authors aim at challenging both the GP and the EPR techniques using one of the most complicated hydrological processes to predict; that is the soil moisture content.

Soil moisture has a crucial role in both the global energy and hydrological cycles. It controls the partitioning of the available surface energy into sensible and latent heat fluxes; it, also, affects the amounts of evapotranspiration, runoff, infiltration, and deep percolation. Soil system heterogeneity is the main source of the spatial variability of the soil system properties and its flow parameters (Warrick, 2003). This spatial variability affects the local atmospheric dynamics to the extent that it can cause significant changes in the precipitation intensity and temperature fields (Entekhabi *et al.*, 1996).

Soil surface temperature and the near surface atmospheric conditions are directly controlled by the soil moisture (D'Odorico *et al.*, 2000). This control is realized through the effect of the soil moisture on the evapotranspiration process, especially in arid and semi arid regions, and consequently dissipation of land surface energy into sensible heat flux causing the soil surface temperature to rise. The spatial variability of the surface soil moisture (neighboring dry and wet soil patches) induces local circulations, which improves the transport of heat from the soil surface to the near surface layer and affects the temperature fields, (Brutsaert, 1982). Therefore, soil moisture is becoming the focus of many climate studies; recognizing the effect of the soil moisture on the boundary layer and consequently global climate fluctuations. The influence of the soil moisture on the global energy cycle is mutual, i.e. the surface soil moisture responds to the changes in the global energy cycle. The mutual influence between the soil moisture and the near surface atmospheric conditions adds to the soil moisture complex and nonlinear behavior caused by the spatial and temporal variability, (Munro *et al*., 1998).

CASE STUDY

The soil moisture response of an experimental reclamation site, named, the South Bison Hill (SBH), is used as a case study. This research site is one of the six experimental fields of the oil sands reclamation sites located at Syncrude Canada Ltd.'s Mildred Lake mine site north of Fort McMurray, AB, Canada. The SBH is constructed with waste-rock material from oil sands mining in the period from 1980 till 1996 (Parasuraman *et al*., 2007). The area of SBH is 2 km^2; and rises 60 m above the surrounding landscape and has a large flat top several hundred meters in diameter. The underlying shale is covered by a 20 cm layer of peat mineral mix on top of an 80 cm layer of glacial till to reclaim the overburden soil surface. This area was then fertilized and seeded to agronomic barley and planted to white spruce and aspen in the summer of 1999.

This study focuses on three inclined experimental soil covers, D1, D2, and D3, which were constructed in 1999 as part of the SBH site. The thicknesses of the three covers are 50 cm, 35 cm, and 100 cm, respectively. D1 cover is comprised of a peat mineral mix layer of 20 cm thickness overlying a 30 cm of glacial till layer. The thinnest cover, D2, consists of a 15 cm peat layer overlying a 20 cm till layer, while the thickest cover, D3, consists of a 20 cm peat layer overlying an 80 cm till layer. Each soil cover has an area of 1 ha, covering a sloping sub-watershed with a 20 % slope, where each sub-watershed is practically independent from the adjacent sub-watersheds.

The current research uses the daily averaged soil temperature, for each layer, together with the daily averaged air temperature (AT), precipitation (P), net radiation (NR) to predict the corresponding daily soil moisture content, for all covers. The records cover the years 2000 till 2005, considering time periods from May-October, to avoid winter periods when the soil is frozen. The total number of available records amounts to 792 instances, divided equally into two sets for training and testing, respectively. The training and testing data sets include alternating records (every other instance) to allow the data-driven tools to properly capture the evolving hydrological change of the reclaimed (reconstructed) watersheds. The performance of the modeling tools was evaluated based on three error measures: (i) the Root Mean Squared Error (RMSE), (ii) the Mean Absolute Relative Error (MARE), and (iii) Correlation Coefficient (R).

Table 1 provides the average values (training and testing) of the various error measures for both techniques, for the till layer of cover D3. Discipulus™ produced better models than EPR, which is evident by the average value of R. The R-values range from 0.71-0.72 and 0.53-0.70 in training and testing phases, respectively. This is higher than average R values of the EPR models; ranging from 0.51-0.56 and 0.46-0.57 in training and testing phases, respectively. In both techniques, EPR and Discipulus™, the summed-input models produced better performance than time-lag ones. This indicates that the storage effect of the soil moisture response can be quantified using cumulative inputs better than time-lag inputs, which can be attributed to the effect of the soil layer moisture holding capacity

Table 1 Average results of training and testing phases of the EPR and Discipulus™ models for the time-lag and cumulative input experiments (till layer of cover D3).

Tool (*experiment*)	R		MARE		RMSE	
	Training	*Testing*	*Training*	*Testing*	*Training*	*Testing*
EPR (*Time-Lag*)	0.51	0.46	0.02	0.02	0.01	0.01
EPR (*Summation*)	0.56	0.57	0.02	0.03	0.01	0.01
Discipulus (*Time-Lag*)	0.72	0.53	0.02	0.02	0.01	0.01
Discipulus (*Summation*)	0.71	0.70	0.02	0.02	0.01	0.01

The scatter plots, shown in Fig. 1, are the results of the Discipulus™ models of the upper peat for the soil covers D2 and D3, using cumulative inputs. Inclusion of the preceding days' effect as cumulative values, in relatively thick cover, produced efficient models, e.g. linear trend in the scatter plot between the predicted and observed values of the volumetric soil moisture content. The storage effect of the thick cover (100 cm) controlled its moisture response, by including previous days' inputs. As a result the 100 cm cover model performed better than the 35 cm cover.

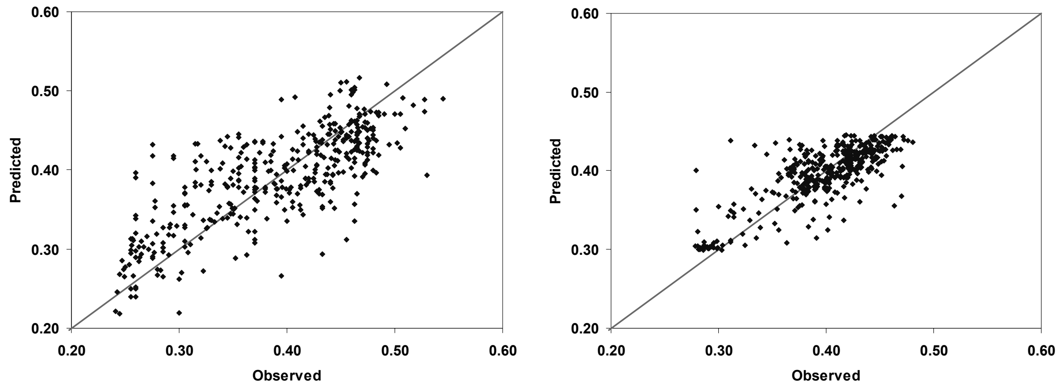

Fig. 1 GP models of the peat D2 cover (left) and D3 cover (right) layers' soil moisture content (testing phase) using cumulative inputs for the two soil covers.

Although the models provided by the EPR technique did not match the performance of the Discipulus™ models (Table 1), the formulae produced by the EPR tool can be a useful tool in giving more insights into the direct effect of each input variable to the explicit characterization of the soil moisture response. The EPR-evolved models have been simplified in a way that results in less than ± 5% deterioration in the prediction accuracy. The following are the best two models produced by the EPR tool for the thinnest soil cover D2, where SM_p and SM_t are the predicted peat and till moisture contents, respectively

$$SM_p = -1.01\times10^{-8}\frac{(\Sigma AT_{20})^2(\Sigma NR_{15})ST_p}{(\Sigma AT_{10})} + 1.31\times10^{-12}\,AT(\Sigma NR_{10})^2(\Sigma NR_{20}) + 0.41 \tag{1}$$

and

$$SM_t = -4.10\times10^{-12}\frac{(\Sigma P_{20})(\Sigma AT_{15})(\Sigma AT_{20})^3 ST_t^3}{(\Sigma AT_{10})(\Sigma NR_{15})} + 2.37\times10^{-5}\frac{(\Sigma P_{20})AT(\Sigma AT_5)(\Sigma AT_{15})}{(\Sigma NR_{15})ST_t} + 0.28 \tag{2}$$

Where the Σ symbol indicates a summed inputs and the subscript figure indicates the previous days' summation period. The constant term (bias) was found to have the highest contribution percentage in both equations, with average values of 72.3 and 92.0%, for the peat and till layers of soil cover D2, respectively. This term reflects the effect of the soil layer holding capacity on its response. The difference in the contribution of the bias between the two layers indicates the effect of the overlying peat layer in trimming the atmospheric forcing on the till layer. As a result, the peat layer is more responsive to the near surface atmospheric conditions, which minimizes the storage effect in this layer. In the mean time, the till layer is not as responsive, and the storage (stabilizing) effect dominates its moisture response.

CONCLUSIONS

The results showed that the storage effect of the soil moisture response can be quantified using summation of inputs better than time-lag inputs, which can be attributed to the effect of the soil layer moisture holding capacity. This effect increases with the increase in the soil cover thickness. The discrepancies that exist in the sub-layers of the soil cover results from the buffering effect of the overlaying surface layer, which trims the effect of the near surface atmospheric forcing. In the mean time, the surface layer exhibits relatively high sensitivity to the atmospheric forcing. The insignificant differences in behavior between the two soil layers indicate the importance of the combined effect of the two layers, as a whole, to characterize the soil moisture response. The adopted data-driven techniques were able to quantify and characterize the above-mentioned dynamics. The overall soil thickness plays a dominant role in determining the controlling process over the soil moisture response. Finally, there is no single data-driven technique/tool that is capable of capturing the inherent variability of the complex soil moisture response processes at all times. This can be mitigated through the incorporation of more than one technique/tool for the same problem.

REFERENCES

Brutsaert, W. (1982) Evaporation into the Atmosphere. *D. Reidel, Dordrecht*, Holland.

Coulibaly, P. (2004) Downscaling daily extreme temperatures with genetic programming. *Geophys. Res. Lett.* **31**, L16203, doi:10.1029/2004GL020075.

D'Odorico, P., Ridolfi, L., Porporato, A. & Rodriguez-Iturbe, I. (2000) "Preferential state of seasonal soil moisture: the impact of climate fluctuations." *Water Resources Research* **36**(8), 2209-2219.

Entekhabi, D., Rodriguez-Iturbe, I. & Castelli, F. (1996) "Mutual interaction of soil moisture state and atmospheric processes." *J. Hydrology* **184**, 3-17.

Giustolisi, O. & Savic, D. A. (2006) "A symbolic data-driven technique based on evolutionary polynomial regression." *J. Hydroinformatics* **8**(3), 207 - 222. doi: 10.2166/hydro.2006.020

Hong, Y. S. T., White, P. A. & Scott, D. M. (2005) Automatic rainfall recharge model induction by evolutionary computational intelligence. *Water Resour. Res.* **41**, W08422, doi:10.1029/2004WR003577.

Khu, S. T., Liong, S. Y., Babovic, V., Madsen, H. & Muttil, N. (2001) Genetic programming and its application in realtime runoff forecasting. *J. Am. Water Resour. Assoc. ASCE* **8**(2), 201–220.

Munro, R. K., Lyons, W. F., Shao, Y., Wood, M. S., Hood, L. M. & Leslie, L. M. (1998) "Modelling land surface-atmosphere interactions over the australian continent with and emphasis on the role of soil moisture." *Environmental Modelling and Software* **13**, 333-339.

Parasuraman, K., Elshorbagy, A.. & Carey, S. K. (2007) "Modelling dynamics of the evapotranspiration process using genetic programming." *Hydrological Science J.* **53**(3), 563-578.

Savic, D. A., Walters, G. A. & Davidson, J. (1999) "A Genetic programming approach to rainfall-runoff modelling.' *Water Resources Management* **13**, 219–231.

Warrick, A..W. (2003) "Soil water dynamics." *Oxford University Press*, New York, NY.

Whigham, P. A. & Crapper, P. F. (2001) Modelling rainfall–runoff using genetic programming. *Math. Comput. Modell.* **33**, 707–721.

Williams, C. A. & Albertson, J. D. (2004) "Soil moisture controls on canopy-scale water and carbon fluxes in an african savanna." *Water Resources Research* **40**, doi:10.1029/2004WR003208.

Evidences about the soil evaporation control by temperature gradients in a semi-arid region

ALAIN M. B. PASSERAT DE SILANS & LOVANIA MARIA WERLANG

Laboratório de Recursos Hídricos e Engenharia Ambiental – LARHENA. Centro de Tecnologia – Universidade Federal da Paraíba, Campus Universitário 58059-900 João Pessoa – Brazil

alainsilans@yahoo.com.br

Abstract The semi-arid region of Brazil with 800.000 km² extension is dominated by the *CAATINGA* vegetation type, with an alternation of small thorny shrubs with bare soil. The soil is narrow and well structured. In other paper we have shown that the soil, the vegetation, and the atmosphere compose a complex and specific arrangement of the climatology of the *CAATINGA*. Then the elaboration of appropriate SVATs models is of great importance to understand the mechanisms of this climatology. In the CARIRI project, an experimental study, in the municipality of São João do Cariri was carried on from March 2001 to October 2003. This is the driest region of Brazil. A mosaic SVAT model has been built from coupled heat and mass transfer theory and the experimental data. It is composed of two vertical columns: one is a soil - sparse vegetation – atmosphere column and the other is a bare soil - atmosphere column. In this paper, we analyze the role of the thermodynamic properties of the soil on the soil moisture dynamics of the bare soil. Then we show how, during the drying of soil, few days after a rain, the evaporation rate of the soil is reduced during daytime by the existence of strong temperatures gradients in the upper soil layer. The strong temperature gradient is due to the low soil thermal diffusivity. In the analysis, we separate the moisture fluxes due to matrix potential gradients from the fluxes due to temperature gradients. Both fluxes are in opposite direction during daytime. Fluxes due to matrix potential gradients are upward, then contributing to soil evaporation, whereas fluxes due to temperature gradients are downward. However, in absolute value, they are of the same order. So the temperature gradients control the soil evaporation rate. Drawing the evolution of the evaporation rate with time, we suggest that four phases of evaporation models have to be considered in such semi-arid region, instead of the classical three phases. The one more phase, occurs at the beginning of the second classical phase, exactly when fluxes due to temperature gradients are opposite but of the same order than fluxes due to the matrix potential.

Keywords Caatinga; soil heat and mass transfer; evaporation control; soil moisture dynamics; semi-arid region; soil temperatures gradients

INTRODUCTION

Heat and mass transfer models in the unsaturated soil have got particular attention along time from the pioneering work of Philip & de Vries (1957) As a fact, water and energy exchange at the land surface play an essential role in hydrology. The soil moisture in the upper soil layer, mainly in the case of a bare soil, governs the partition of rain into run-off and infiltration as well as the partition of available energy into sensible, latent and ground heat fluxes. In semi-arid regions studies about soil heat and mass transfer in the vadoze zone are necessaries due to the high proportion of bare soil in the ecosystems of the region and the role of evaporation in the water budget.

The semi-arid region of Brazil with 800.000 km² extension is dominated by the *CAATINGA* vegetation type, with an alternation of small thorny shrubs with bare soil. The soil is narrow and well structured. Passerat de Silans *et al.* (2004) have shown that the soil, the vegetation, and the atmosphere compose a complex and specific arrangement of the climatology of the *CAATINGA*. Then the elaboration of appropriate SVATs models is of great importance to understand the mechanisms of this climatology. In the CARIRI project, an experimental study was carried on from March 2001 to October 2003. A mosaic SVAT model has been built from coupled heat and mass transfer theory and the observed experimental data. It is composed of two vertical columns: one is a soil - sparse vegetation – atmosphere column and the other is a bare soil - atmosphere column (Goldfarb, 2006; Werlang, 2006).

In this paper, we analyze the role of the thermodynamic properties of the soil on the soil moisture dynamics of the bare soil. So, only the second column of the Cariri mosaic SVAT model is considered in this paper.

EXPERIMENTAL STUDIES

The experiment is located in the Cariri micro-region, the driest area of Brazil, which land is dominated by Caatinga vegetation. Vegetation patches alternate with bare soil. Into the bare soil, temperature gauges were horizontally buried in a vertical profile, at 0, 0,02, 0,05, 0,15 e 0,50 m depths. At 0,05m depth, one heat flux plate gauge and one soil moisture TDR gauge were also buried.

Physical soil properties were measured from 90 core samples around the experiment in several depths and show that the soil is sandy lime with a depth of 0,55 m. The soil shows two layers differing by the bulk soil specific density. The retention curve was determined in laboratory and adjusted to the Van Genuchten´s model. Hydraulic conductivity at saturation was measured in laboratory from undisturbed soil cores, and the conductivity curve K(θ) was determined by Mualem model (1976) for the both soil layers. Thermal diffusivity was calculated by the CLTM method (Passerat de Silans *et al.*, 1996) from the soil temperatures profiles, and then the heat soil conductivity has been deduced and modelled by a modified Johansen model (Werlang, 2006). To do this, organic matter, quartz, other minerals and water soil components were determined from the soil cores.

THEORETICAL BACKGROUND

Heat and mass transfer equations derive from the Philip & de Vries (1957) model with the modifications introduced by Milly (1982) and Passerat de Silans (1986). Basically they are combination of conservation and transport equations for the mass and the heat. The model, described in Werlang (2006), results in a system of two non linear coupled equations:

$$A_1 \frac{\partial h}{\partial t} + B_1 \frac{\partial T}{\partial t} = \frac{\partial}{\partial z}\left(C_1 \frac{\partial h}{\partial z} + D_1 \frac{\partial T}{\partial z} + E_1 \right) \quad (1)$$

$$e\, A_2 \frac{\partial h}{\partial t} + B_2 \frac{\partial T}{\partial t} = \frac{\partial}{\partial z}\left(C_2 \frac{\partial h}{\partial z} + D_2 \frac{\partial T}{\partial z} + E_2 \right) \quad (2)$$

where, C1 (ms^{-1}) and D1 ($m^2s^{-1}\ K^{-1}$) are soil moisture diffusion coefficients associated to the matrix potential and the temperature gradients, respectively:

$$C_1 = D_h = K + \frac{1}{\rho_1} D_{vh} \quad (3)$$

$$\text{e } D_l = D_T = D_{lT} + \frac{1}{\rho_l} D_{vT} \tag{4}$$

where: D_h is the isothermal diffusivity of water into the soil (m.s^{-1}); K is the unsaturated hydraulic conductivity (m.s^{-1}); D_{vh} is the vapour diffusivity due to matrix potential gradient (kg.m^{-1}s^{-1}); D_T the equipotential water diffusivity due to temperature gradient; D_{lT} is the liquid water diffusivity due to temperature gradient (m^{2}s^{-1}K^{-1}) and D_{vT} is the vapour diffusivity due to temperature gradient (kg.m^{-1}s^{-1}K^{-1}).

RESULTS

A simulation was run, from January 2002 12th to 25th, with the model developed by Werlang (2006), with 120 finite volumes describing the vertical space and a time step of 2s. In Fig. 1 (a, b), the value of D_h and D_T were drawn as a function of volumetric soil moisture, θ. It is important to observe the values of the diffusivities. Basically D_h varies from 10^{-4} ms^{-1}, when the soil is moist, to 10^{-15} ms^{-1}, when the soil is dry, and D_T varies from 10^{-7} m^{2}s^{-1}K^{-1}, when the soil is moist, to 10^{-11} m^{2}s^{-1}K^{-1}, when the soil is dry. Then, the soil moisture diffusivity due to the matrix potential (isothermal) is much higher than the diffusivity due to temperature gradient when the soil is moist, the opposite occurring when the soil is dry. In the figure are located the field capacity, CC and the wilting, PM, points, respectively.

In the Caatinga region, strong temperature gradients are observed in the upper soil layer due to the low soil thermal diffusivity. Results are shown for two days of the simulation run, namely the 13th and 15th of January 2002. Fluxes are positive downward and negative upward.

One can observe in the Fig. 2 (a, b) that between 11:20 and 21:00 O'clock, the soil moisture fluxes due to the temperature gradients are in opposite direction than the fluxes due to matrix potential, however they are of the same order. Then one perceives that the temperature gradients are able to strongly control the soil evaporation rates in the Caatinga. In Fig. 3, the soil moisture evolution at 0,05m depth is drawn along the experiment. Four phases of the drying process can be observed. This suggests that the evaporation rate can also be modelled by a four stages process indeed of the classical three stages process. The second stage would be divided in two parts, the first one corresponding to the temperature gradient control.

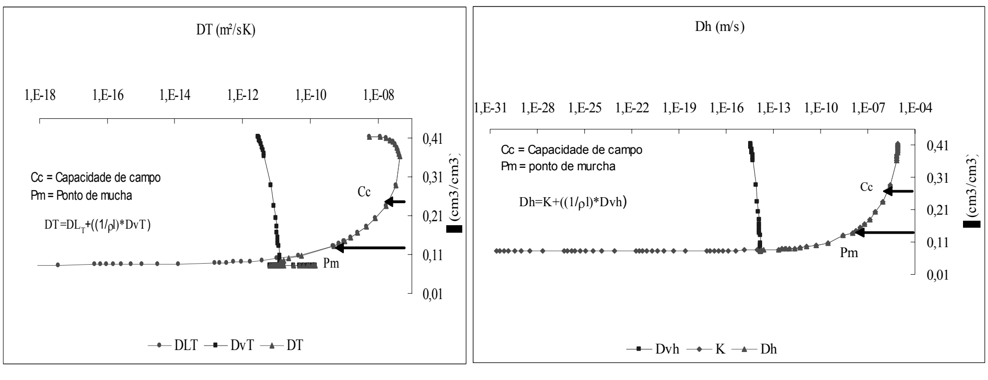

(a) (b)

Fig. 1 Water diffusivity due to the matrix potential gradients (a) to the temperature gradients (b).

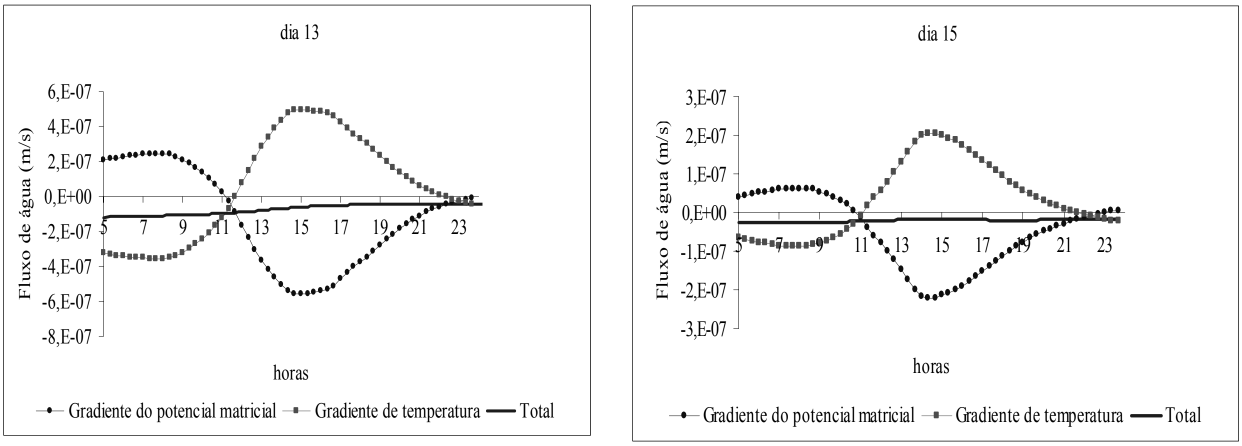

Fig. 2 Soil moisture fluxes due to the matrix potential gradients (-●-); to the temperature gradients (-▪-) and total (—) for the days 13 and 15 of January 2002.

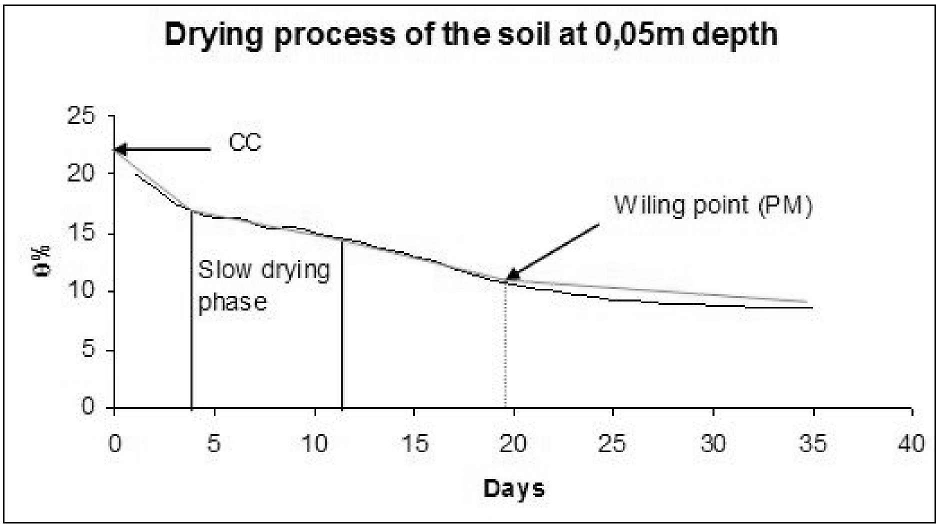

Fig. 3 Four stage drying process (observe the slow drying phase)

CONCLUSIONS

By modelling heat and mass transfer in the soil, using the second column of the Werlang SVAT model for the Caatinga region, we explain the observed low rate of soil evaporation by the role of the upper soil layer temperature gradients in controlling evaporation. They are due to the low soil thermal diffusivity. Then we suggest to model the evaporation rate by a four stages model indeed of the classical three stage model.

REFERENCES

Milly, P. C. D. (1982) Moisture and heat transport in hysteretic, inhomogeneous porous media: a matric head-based formulation and a numerical model. *Water Resour. Res*. **18**, 489-498.

Passerat de Silans, A. M. B, Silva, F. M., Werlang, L. M. & Goldfarb, M. C. (2004) The role of Soil and vegetation in the hydrology of a semi-arid basin: an experimental study in the north-east of Brazil. In: *Hydrology: Science and Practice for the 21st Century*. Londres, **2,** 139-145.

Philip, J. R. & de Vries, D. A. (1957) Moisture movement in porous materials under temperatura gradients. *Trans. Am. Geophys. Union*. **38**, 222-232.

Werlang, L. M. (2006) Transferência de massa e calor no complexo solo-vegetação-atmosfera: sensibilidade do modelo à variabilidade espacial da condutividade térmica do solo. *Tese de doutorado em Engenharia mecânica. Universidade Federal da Paraíba*, João Pessoa, 145p.

Innovative spatial interpolation methods for estimation of missing precipitation records: concepts and applications

R. S. V. TEEGAVARAPU
Department of civil engineering, Florida Atlantic University, Boca Raton, Florida, USA
ramesh@civil.fau.edu

Abstract Deterministic and stochastic weighting methods are the most frequently used methods for estimating missing rainfall values at a gauge based on values recorded at all other available recording gauges. Several innovative spatial interpolation methods using the concepts of correlation, patterns, optimal weighting and spatial clusters, and data driven functional approximation, optimal functional forms were proposed, developed and investigated for estimation of missing precipitation records. Variants of ordinary Kriging are also proposed and tested. These methods use data driven models, universal functional approximation methods and mathematical programming models with non-linear formulations with binary variables and genetic algorithms. Daily precipitation data obtained from rain gauging stations from a temperate climatic region are used to test and derive conclusions about the efficacy these new methods. Results suggest that these innovative spatial interpolation methods are superior to those obtained from traditional spatial interpolation methods.
Keywords missing precipitation records; spatial interpolation; weighting methods; kriging; emerging techniques

INTRODUCTION

Deterministic weighting and stochastic interpolation methods have been used for the spatial construction of rainfall fields or estimating missing rainfall data at points in space. Traditional weighting and data-driven methods generally are used for estimating missing precipitation. Weighting methods belong to a class of spatial interpolation techniques such as inverse-distance (Simanton & Osborn, 1980; Wei & McGuinness, 1973), non-linear deterministic, and stochastic interpolation methods (e.g., kriging). Regression and time series analysis methods belong to data-driven approaches. Variance dependent stochastic interpolation techniques based on geostatistical approaches are also often used for estimation of missing precipitation records. Global interpolation methods that use trend surface analysis and regression (Chang, 2006) provide several advantages compared to deterministic weighting techniques. Trend surface analysis uses a polynomial equation of spatial coordinates to approximate points with known values. These methods and their several variants are discussed in the next few sections.

DETERMINISTIC AND STOCHASTIC ESTIMATION METHODS

The inverse distance weighting method (IDWM) is the most commonly used approach for estimating missing data in the hydrological and geographical sciences. In the U.S., especially in the operational hydrology literature, IDWM is often referred to as the National Weather Service (NWS) method. The IDWM is routinely used for estimating missing rainfall data (ASCE, 1996). In the field of quantitative geography, IDWM is used for spatial interpolation (Sullivan & Unwin, 2003). Several variants of IDWM have been developed. Hodgson (1989) modified IDWM to include a learned search approach that reduces the number of distance calculations. To incorporate topographical aspects, Shepard (1968) proposed a modified IDWM that is referred to as a barrier method.

Variance dependent surface interpolation methods, belonging to the general family of kriging, have been applied to hydrological interpolation problems (Vieux, 2001; Grayson & Gunter, 2001). These interpolation schemes are based on the principle of minimizing the estimate of variance at points where measurements are unavailable. Kriging in various forms has been used to estimate missing precipitation data at stations as well as to interpolate precipitation from point measurements (Dingman, 2002; Vieux, 2001). Ashraf *et al*. (1997) compared interpolation methods (kriging, inverse distance, and co-kriging) to estimate missing precipitation values. They indicated that kriging provided the smallest root mean square error (RMSE). Co-kriging of radar and rain gauge data has been employed Krajewski (1987) to estimate mean areal precipitation. Seo *et al*. (1990a, 1990b) and Seo (1996) described the use of co-kriging and indicator kriging for interpolating rainfall data.

LIMITATIONS OF ESTIMATION METHODS

Teegavarapu & Chandramouli (2005) reported several limitations and advantages of using deterministic and stochastic spatial interpolation techniques to estimate missing precipitation data at a base station using data at all other stations. They indicated that all interpolation techniques will fail to provide accurate estimates of missing precipitation data in two situations: 1) when precipitation is measured at all or a few other stations but no precipitation actually occurred at the base station, and 2) when precipitation is measured at the base station but no precipitation is measured or occurred at all other stations. In case 1, all spatial interpolation techniques will produce a positive estimate whereas in reality zero precipitation is recorded at the base station. It is impossible to estimate missing precipitation data in the second case since point observations are used to estimate the missing value at the base station using spatial interpolation algorithms alone. All interpolation techniques produce a zero estimate for situations encountered in case 2). Data from other sources (e.g., radar based estimates) can be used in these situations to estimate the missing values. However, the reliability of radar-based precipitation measurements is a contentious issue (Teegavarapu, 2008).

Limitations of spatial interpolation methods have been reported in recent studies. Veiux (2001) pointed out several limitations of the inverse distance weighting method (IDWM), with a major one being the “tent pole effect” that leads to greater estimates closer to the point of interest. Grayson & Bloschl (2000) list several limitations of Thiessen polygons and inverse distance methods. They suggested that these methods should not be recommended for spatial interpolation considering their limitations. However, they recommend thin-splines and kriging for interpolating hydrologic variables. The Thiessen polygon approach has the major limitation of not providing a continuous field of estimates when used for spatial interpolation (Unwin & Sullivan, 2003). Brimicombe (2003) indicated that the main point of contention in applying IDWM to spatial interpolation is selecting the number of relevant observation points used for the spatial interpolation.

Correlation weighting techniques and artificial neural network methods are proved conceptually to be superior deterministic approaches compared to traditional inverse distance weighting method and its variants. The Kriging estimation method (KEM) is considered a reliable interpolation technique (Sullivan & Unwin, 2003), but is plagued by several limitations. These include selecting the appropriate semi-variogram, assignment of arbitrary values to sill and nugget parameters and distance intervals, observation value-insensitive variance estimates, and the computational burden to interpolate the surfaces.

INNOVATIVE METHODS FOR ESTIMATION

Distance weighting methods often used for estimating missing rainfall records are re-visited by Teegavarapu & Chandramouli (2005). Conceptual revisions are incorporated into the method and the revised methods are tested for estimation of missing rainfall values. The revisions addressed two main issues relating to the definition of distance used in the calculations and selection process of the nearby gaguges. Artificial neural networks and kriging approach are used to illustrate the advantages of deterministic and stochastic data-driven and interpolation methods compared to traditional distance-based weighting schemes in estimating the missing values. The study recommended three methods, namely coefficient of correlation weighing method (CCWM), artificial neural network estimation method (ANNEM) and kriging estimation method (KEM) for estimation of missing precipitation data, as they are conceptually superior to traditional approaches. All the three methods are data sensitive, with kriging estimation method being computationally most intensive of all the methods. Use of conceptually acceptable surrogate measures for distances and improvised weighting factors improved the estimates from the revised methods.

Universal functional approximators such as artificial neural networks (ANN) are used for fitting a semivariogram model using the raw data in ordinary kriging to estimate missing precipitation data by Teegavarapu (2007a). The use of ANN eliminates the need for the pre-defined authorized semivariogram models to capture the spatial variation of data, and the trial and error process involved in estimation of semivariogram parameters. Utility of universal function approximation-based kriging is assessed and demonstrated through an application to a case study in which missing daily precipitation data at a rain gauge station are estimated. Association rule mining (ARM) based spatial interpolation approach is recently discussed by Teegavarapu (2007b). The innovative approach was used to improve the precipitation estimates provided by traditional and improved deterministic and stochastic spatial interpolation techniques. The ARM methodology besides offering insights into the spatio-temporal precipitation data patterns and the associations among observations, it also helps in addressing one major ubiquitous limitation of all spatial interpolation techniques in accurately estimating missing precipitation records. The use of ARM is not equivalent to the use of correlation analysis to revise estimated precipitation values obtained from deterministic and stochastic interpolation techniques. Considerable improvements in the estimates were achieved when ARM is used in conjunction with the interpolation techniques.

Range and Cluster based optimization methods in space and time were developed by Teegavarapu & Bajaj (2008). Optimization models using mixed integer linear and non-linear programming formulations are developed for estimation of missing precipitation data at gauge. The formulations use binary variables for selection of rain gauges that participate in the spatial interpolation process and also in the process of selection of optimum cluster of rain gauges for estimation of missing data. Several variants of these mathematical programming formulations are proposed to improve the estimates of missing precipitation data. The variants investigated in their study provided improved estimates of precipitation data compared to those obtained from traditional distance-based weighting methods.

A non-linear mathematical programming model using binary variables is proposed and investigated by Teegavarapu & Pathak (2008) to in-fill missing precipitation record using radar (NEXRAD) based rainfall estimates. The model identifies the cluster of NEXRAD data values that can used for infilling the rain gauge records. Results from the application of model suggest that missing rainfall values can be estimated using radar data. The application also revealed several interesting insights, which suggest that optimal selection of NEXRAD values using weights in the grid surrounding rain gaguge is essential for in-filling process. Spatial and temporal variability of weights for different clusters are evident.

CONCLUSIONS

Innovative spatial interpolation methods for estimation of missing precipitation data that were proposed and investigated recently are discussed in this paper. These methods rely on improvised variants of traditional methods that define new weighting schemes and reflect true spatial correlation structure. Universal function approximators as estimators and replacements for semi-variograms in kriging methods are also investigated. Positive kriging that uses optimization for re-analysis of weights are tested. Association rule mining (ARM) is used to develop spatio-temporal rules to improve traditional estimation methods are also briefly discussed in this paper. Optimal spatial weighting methods that rely on range and space clusters using mathematical programming formulations with binary variables are discussed. Results based on several studies suggest that all these innovative and improvised spatial interpolation methods have improved the estimation of missing precipitation records.

REFERENCES

ASCE, Hydrology Handbook (1996) *second edition, American Society of Civil Engineers* ASCE, New York.

Ashraf, M., Loftis, J. C. & Hubbard, K. G. (1997) Application of geostatisticals to evaluate partial weather station network. *Agricultural Forest Meteorology* **84**, 255-271.

Chang, K-T., (2006) Introduction to Geographic Information Systems. *McGraw Hill*, New York.

Dingman, S. L., (2002) Physical Hydrology. *Prentice Hall, NJ.*

Grayson, R. & Gunter, B. (2001) Spatial Patterns in Catchment Hydrology: Observations and Modeling. *Cambridge University Press.*

Hodgson, M. E. (1989) Searching Methods for Rapid Grid Interpolation. *Professional Geographer* **411,** 51-61.

Krajewski, W. F. (1987) Co-kriging of Radar and Rain Gauge Data. *Journal of Geophysics Research* 92D8, 9571-9580.

Salas, J. D. J. (1993) Analysis and Modeling of Hydrological Time Series. *Handbook of Hydrology*, D. R. Maidment, ed, Mc-Graw-Hill, NY

Seo, D. J., Krajewski, W. F. & Bowles, D. S. (1990a) Stochastic Interpolation of Rainfall Data from Rain Gauges and Radar Using Cokriging - 1. Design of Experiments. *Water Resources Research* **26**(3), 469-477.

Seo, D. J., Krajewski, W. F. & Bowles, D. S. (1990b) Stochastic Interpolation of Rainfall Data from Rain Gauges and Radar Using Cokriging - 2. Results. *Water Resources Research* **26**(5), 915-924.

Seo, D. J. (1996) Nonlinear Estimation of Spatial Distribution of Rainfall - An Indicator Cokriging Approach. *Stochastic Hydrology and Hydraulics* **10**,127-150.

Simanton, J. R. & Osborn, H. B. (1980) Reciprocal-Distance Estimate of Point Rainfall. *Journal of Hydraulic Engineering Division* **10**6HY7.

Shepard, D. (1968) A Two-dimensional Interpolation Function for Irregularly Spaced Data. Proceedings of the *Twenty-Third National Conference of the Association for Computing Machinery*, 517-524.

Sullivan, D. O. & Unwin, D. J. (2003) Geographical Information Analysis. *John Wiley & Sons, Inc, NJ.*

Teegavarapu, R. S. V. & Chandramouli, V. (2005) Improved weighting methods, deterministic and stochastic data-driven models for estimation of missing precipitation records. *Journal of Hydrology* **312**, 191-206.

Teegavarapu, R. S. V. (2007a) Use of universal function approximation in variance dependent surface interpolation technique: An application in Hydrology. *Journal of Hydrology* **332**, 16-29.

Teegavarapu, R. S. V. (2007b) Estimation of Missing Precipitation Data using Soft Computing based Spatial Interpolation Techniques. *AGU Fall Meeting.*

Teegavarapu, R. S. V. & Pathak, C. (2008) Infilling of Rain Gaguge Records using Radar (NEXRAD) Data: Influence of spatial and temporal variability of rainfall processes. ASCE, *World Environmental and Water Resources Congress*.

Teegavarapu, R. S. V. & Bajaj (2008) Optimal Spatial Weighting Methods for Estimation of Missing Rain Gaguge Records, ASCE. *World Environmental and Water Resources Congress*.

Vieux, B. E. (2001) Distributed Hydrologic Modeling using GIS. *Water Science and Technology Library, Kluwer Academic Publishers.*

Wei, T. C. & McGuinness, J. L. (1973) Reciprocal Distance Squared Method, a Computer Technique for Estimating Area Precipitation, Technical Report ARS-Nc-8. *U.S. Agricultural Research Service, North Central Region, Ohio.*

Precipitation changes and his influences on the discharge regime of Navrood River

MEHRDAD RAMEZANIPOUR
Assistant prof. Islamic Azad University of Chaloos
mehr5490@yahoo.com

Abstract In this research, tried by using Mann-Kendall statistics to determine the type and time of changes in discharge regime in relation to the precipitation regime in the Navrood basin of Guilan province. The result show that during 38-year term as from 1966-2003, the parameters of discharge and precipitation has been subjected to non-random changes and trend. The linear trend of graphs ditincts that precipitation parameters has a ascending trend in the autumn, spring and summer seasons, only there is without trend change in the winter season also discharge parameter has a ascending trend in the autumn, winter and spring only has a obvious descending trend in the summer. Again, summer season is sensible in relation other seasons with a descending linear trend the discharge regime against ascending linear trend the precipitation in the Navrood river. Also the degree of relationship between discharge and precipitation parameters is not the same in all seasons such that is observed in autumn the highest and in winter and spring the lowest degree of correlation between discharge and precipitation parameters. As a whole by looking at the prepared graphs it is clear that there is a close correlation between trend of discharge and precipitation parameters which Indicate the high correlation of changes in discharge parameter to the changes in precipitation parameter and the roll of the precipitation regime is proved to be one the most important factors in the fluctuation and changes in the discharge changes of Navrood river.
Keywords Navrood; precipitation; regime; discharge regime; mann-kendall statistics; trend

INTRODUCTION AND BACKGROUND INFORMATION

Regime changes of the rivers is dependent to the natural and human different factors but precipitation factor has a important effect on this changes that it is subject matter in this research into the Navrood basin. This basin stand in the west Guilan province of iran country.

Herein, has been worked by different persons specially with Mann-kendal method as discharge trend analysis of the rivers in the southern America (Marengo, 1995), long term trends analysis of annual and monthly precipitation in Japan (Yue *et al.*, 2003), trend analysis in Turkish Precipitation data and hydrological processes (Turgay *et al.*, 2006), and Modarres (2007) described that there is rainfall increase and decrease trends in arid and semi-arid regions of Iran specially in the spring and summer seasons.

METHOD AND RESULTS

To determine the type and time of changes in discharge regime in relation to the precipitation regime used Mann-Kendall method that it include two method, nongraphic and graphic. Nongraphic equation is:

$$\tau=\frac{4P}{N(N-1)}-1 \tag{1}$$

Where τ is kendall statistics, p is sum n_i that is:

$$P = \sum_{i=1}^{N-1} \text{ni} \tag{2}$$

Then τ_t can use as the basis significant level by comparison with the values

$$\tau_t = 0 \pm tg\sqrt{\frac{4N+10}{9N(N-1)}} \tag{3}$$

Where tg is the desired probability point of the Gaussion normal distribution appropriate to a two-tailed test. The 95 per cent probability point used of tg.thus τ_t calculated *±0/22* that *if + 0/22 >* τ *> - 0/22,* climatilogical series is random ness, *if* τ *< - 0/22,* trend is descent and *if* τ *> + 0/22,* trend is ascendant (Roshani, 2003) that table 1 that get of the nongraphic method shows a ascendant change on the Navrood annual and a value near to change on the summer of the precipitation parameter.

Table 1 statistics (τ) values of mean seasonal and annual.

	autumn	winter	spring	summer	annual
Navrood precipitation	-0.01	0	0.12	0.21	0.26
Navrood discharge	0.02	-0.02	0.06	-0.07	-0.05

The graphs of the graphic method is two-tailed, if graphs to be parallel it express series are random ness and if intersect together it means there is a change and the start a descent or ascendant trend on the mean seasonal and annual.
Therefore (Fig. 1) showed that is increased discharge and precipitation trend of parameters on the autumn and don't observed any special change.

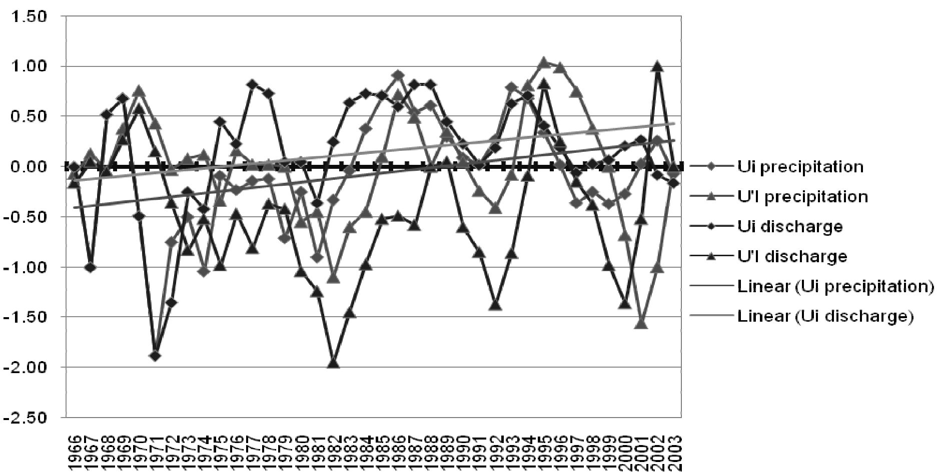

Fig. 1 Autumn mean seasonal linear chart of the discharge and precipitation.

(Fig. 2) showed that there was several probable change during time series but total trend is without special change on the winter.

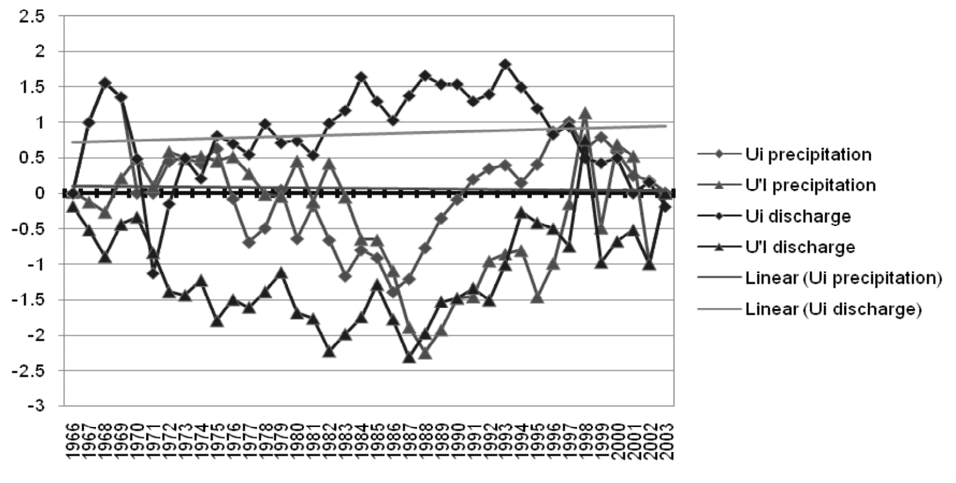

Fig. 2 Winter mean seasonal linear chart of the discharge and precipitation.

(Fig. 3) showed that trend of the discharge increased more than precipitation parameter on the spring,

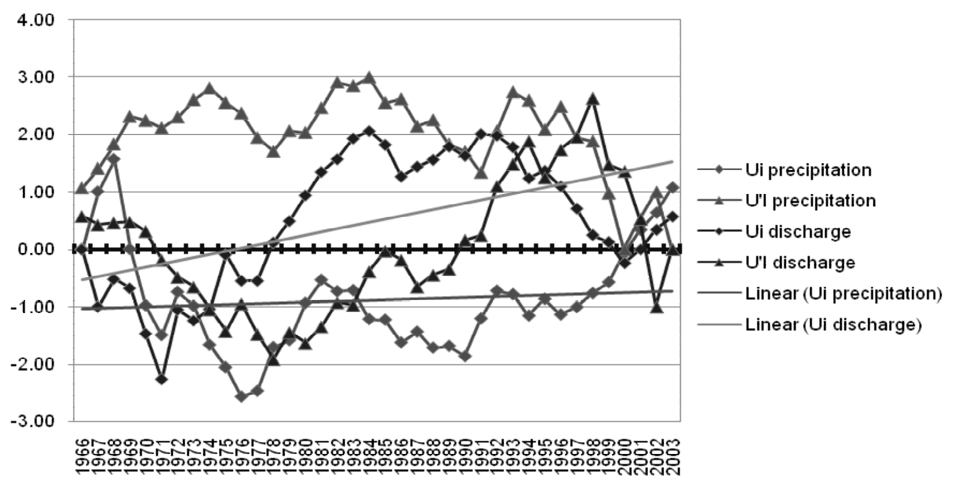

Fig. 3 Spring mean seasonal linear chart of the discharge and precipitation.

(Fig. 4) showed that in middle of time series occured a important and simultaneous change on the discharge and precipitation parameter on the summer,

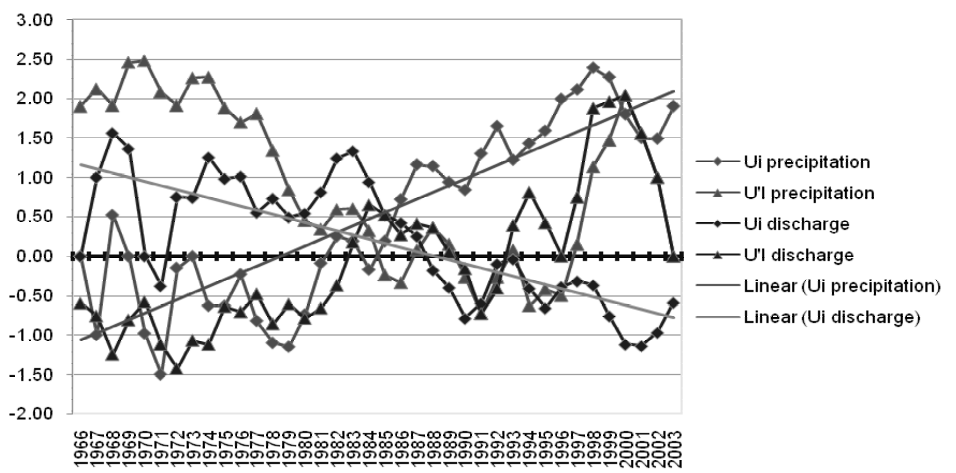

Fig. 4 Summer mean seasonal linear chart of the discharge and precipitation.

(Fig. 5) also upholded a simultaneous change approximately

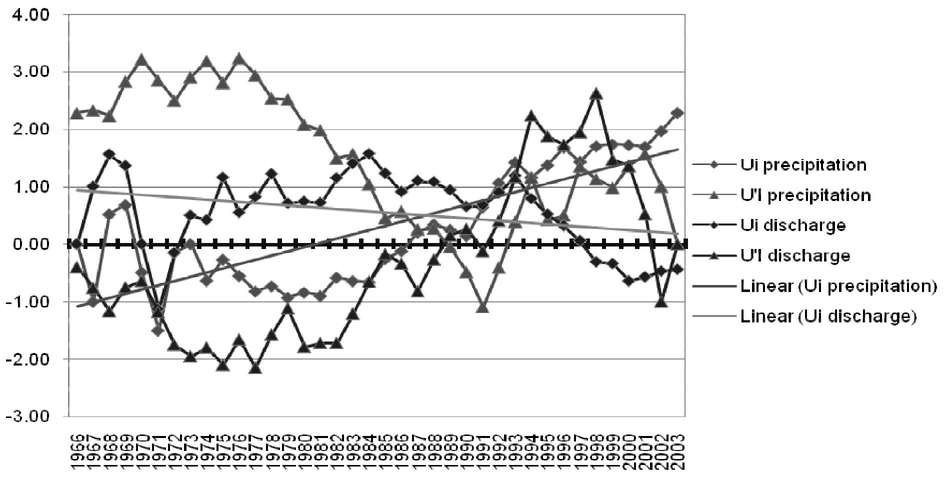

Fig. 5 Mean annual linear chart of the discharge and precipitation.

Generally, trend of the precipitation increased on the autumn,spring,summer and annual seasons that depended to global warming. Again, time Series of the precipitation and discharge on the autumn, winter and spring seasons are pursuant together but on the summer and mean annual trend of the discharge is descent because waster of water increased for agriculture recent decades in this season specially.

REFERENCES

Marengo, J. (1995) Variations and change in south American streamflow. *Climatic Change Journal* **31**(1), 99 -117.

Modarres, R. (2007) Rainfall trends in arid and semi-arid regions of Iran. Journal of Arid Environments **70**(2), 344-355.

Roshani, M. (2003) Research about climate change of the Caspian sea southern coast. *MSC thesis*. 87,108.

Turgay, P. *et al*. (2006) Trend analysis in Turkish precipitation data hydrological processes. **20**(9), 2011-2026.

Yue, S. & Hashino, M. (2003) Long Term trends of annual and monthly precipitation in Japan. *Journal of the American Water Resources Association* **39**(3), 587-596.

High resolution soil moisture from radar instruments: Study area of northeast Austria and southeast Czech Republic

M. DOUBKOVÁ, D. SABEL, C. PATHE, S. HASENAUER, A. BARTSCH & W. WAGNER

Vienna University of Technology, Institute of Photogrammetry and Remote Sensing, Gußhausstraße 27-29, 1040 Vienna, Austria

mdo@ipf.tuwien.ac.at; sh@ipf.tuwien.ac.at; ww@ipf.tuwien.ac.at; ds@ipf.tuwien.ac.at; cp@ipf.tuwien.ac.at; ab@ipf.tuwien.ac.at

Abstract Soil moisture is an important parameter for hydrological modeling and crop yield prediction. The ability of radar sensors to monitor SM has been demonstrated in numerous studies. Yet, only coarse resolution (>25km) SM products are available over the European continent. In this work, the soil moisture product derived from the ERS scatterometer data at 50 km spatial resolution is presented and a downscaling technique is evaluated that provides SM at 1 km scale. The presented downscaling technique stands upon the concept of temporal stability of SM. Despite the high heterogeneity of the study area, additional SM information to that demonstrated by the ERS data could be retrieved from the downscaled product at 1 km spatial resolution. The SM patterns of the downscaled product correlated to the 1 km SM data from the ENVISAT Advanced Synthetic Aperture Radar (ASAR) Global Mode (GM). While these findings are preliminary, they provide promising results for the hydrological and meteorological community operating at spatial scales of 5 km and higher.

Keywords soil moisture; scatterometer; downscaling; ERS; ScanSAR

INTRODUCTION AND BACKGROUND

Soil moisture plays a key role in the Earth energy, water, and carbon cycle (Wagner *et al.* 2007). It can be measured as in-situ point measurements, with use of thermal remote sensing, or with use of active or passive microwave remote sensing instruments. While the in-situ measurements represent conditions at a single point location and their acquisitions are cost and labour intensive, microwave soil moisture products represent values at the regional scale (pixel dimension) and are freely available from a variety of satellites (i.e. ERS, METOP, AMSR-E). A single footprint, however, represents an area of 25 * 25 km or larger. Thus, the finer scale hydrological processes may be entirely omitted with use of coarse resolution microwave products.

In order to fulfill the needs of the hydrological community for finer resolution data development of a high resolution satellite soil moisture product is necessary. A soil moisture product with a 1 km spatial resolution was developed from the ENVISAT Advanced Synthetic Aperture Radar (ASAR) Global Mode (GM) data (Pathe *et al.*, 2008 and Bartsch *et al.*, 2006). Regrettably, the limited ENVISAT ASAR GM coverage does not y*et al*low for data processing over the entire European continent (Pathe *et al.*, 2008).

Recently, a downscaling technique using ASAR Wide Swath (WS) data with 150 m resolution was introduced by Wagner *et al.* (2008). Wagner presents scaling parameters derived from the ENVISAT ASAR WS backscatter as a tool for downscaling of the coarser resolution data (i.e. ERS, METOP, AMSR-E). The study rests upon the concept introduced by Vachaud (Vachaud *et al.,* 1985) that presents spatial patterns of soil moisture as temporally stable. Similarly, the soil moisture at individual locations follows to some extent the mean regional soil moisture value (Pathe *et al.*, 2008).

Considering soil moisture as a critical factor affecting the temporal dynamics of the radar backscatter, also the radar backscatter has a temporally stable component (Wagner *et al.*, 2008). Similarly, for the soil moisture fields (Vischel *et al.,* 2008), a time-invariant linear relationship is found well suited for relating local scale (pixel) and regional scale (50 km) backscatter and soil moisture.

In this paper the downscaling technique introduced by Wagner was applied on 50 km ERS soil moisture data and the downscaled soil moisture product was studied over northeastern Austria and southeastern Czech Republic. The downscaled product was compared to the 1 km ASAR soil moisture product from 13th of March, 2006. Both ERS and ASAR soil moisture products were derived using the change detection approach initially introduced for the ERS scatterometer (Wagner *et al.*, 2003).

The downscaled soil moisture product is of high importance for the selected study area where the complex landscapes cannot be sufficiently described by products with spatial resolution of 25 km or coarser.

METHODS

Northeastern Austria and southeastern Czech Republic (CR) were selected as a study area in order to investigate the performance of the downscaling model in heterogeneous landscape.

83 ASAR GM scenes were preprocessed to a common database. The steps included georeferencing, resampling, incidence angle normalization, generating of scaling information, and finally computing soil moisture (Figs 1c and 1f). The scaling information consists of the coefficient of determination between the soil moisture value at a single pixel (local scale) and soil moisture value averaged over area of 25 * 25 km (regional scale). At areas where high R^2 was achieved, the regional soil moisture estimates from coarse resolution microwave satellites can be used directly at 1 km scale.

Further, the radar backscatter downscaling coefficients and the soil moisture downscaling parameters were computed (Wagner *et al.*, 2008). The downscaling backscatter coefficients are linear parameters representing the relation between the local and the regional backscatter time series and form the base for computation of the downscaling parameters of soil moisture. The final downscaled product is retrieved according to

$$\theta_{dis}(x,y,t) = c(x,y) + d(x,y) * \theta_{ERS}(x,y,t)$$

where θ_{dis} represents the final downscaled soil moisture at time t, θ_{ERS} stands for the coarse resolution ERS data and c and d are the downscaling soil moisture parameters. The soil moisture downscaling parameters c and d govern how much wetter or dryer is a single pixel in comparison to its regional average. Finally, the ERS, the ERS downscaled and the ASAR GM 1km soil moisture products were spatially compared. One date was selected (13th of March, 2006) from the limited available common dates of the ERS and ASAR GM acquisitions.

RESULTS AND DISCUSSION

Soil moisture at 50km (ERS), 1km (ENVISAT ASAR GM) and the 1 km downscaled product covering the study area at 1 km resolution on March 13th, 2006 are demonstrated in Figs 1a-c. The distribution of the very dry areas (0 – 25%), namely Burgenland (Austria) and the north-western part of the Jihomoravsky district (CR) in the ERS data corresponded to the distribution of dry areas (13 – 50%) according to the ASAR GM data. Similarly, the medium wet areas (37 – 63 %) in the west and the southwest of Lower Austria (Niederösterreich) in the ERS data corresponded to medium wet areas in the ASAR GM (approx. 37 – 87 %). In general, while the relative spatial patterns of the ERS and ASAR GM soil moisture data correlated, the soil moisture levels differed.

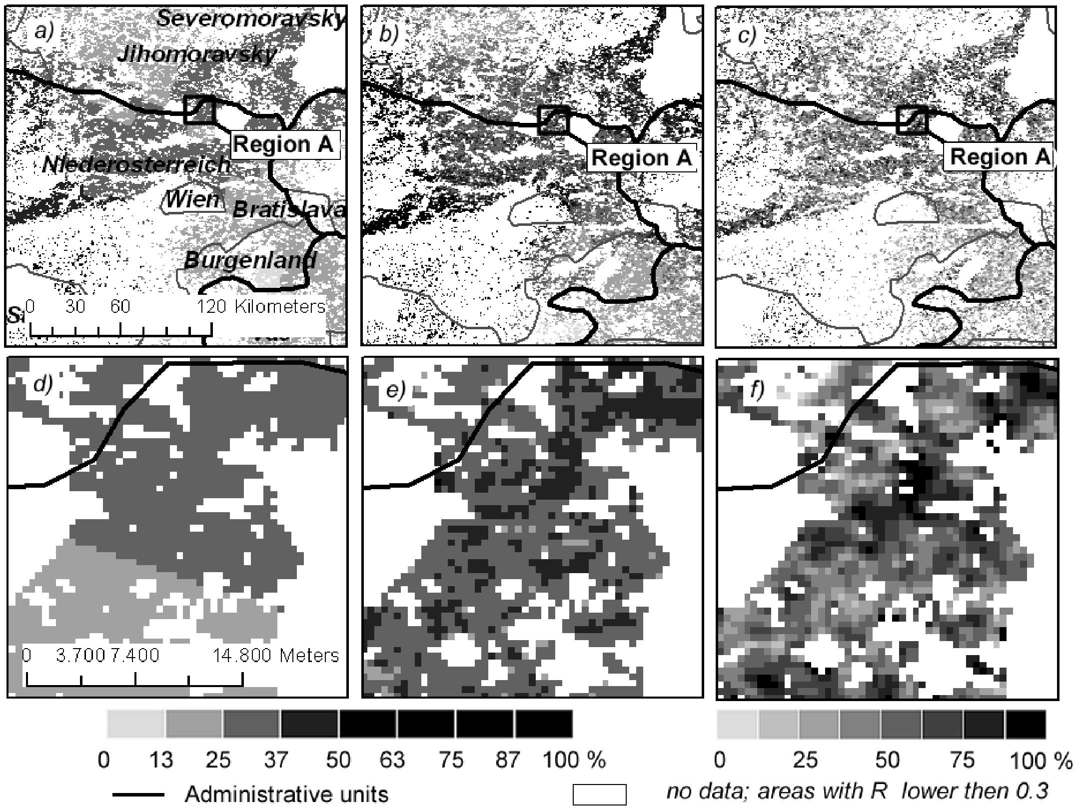

Fig. 1 Soil moisture products over the study area (upper part) and zoomed into the Region A (lower part). Soil moisture products were retrieved from the ERS data (a, d), the ASAR GM data (c, f) and by applying the downscaling techniques on the ERS data (b, e). Data from the downscaling product were masked for areas with R^2 lower than 0.3.

In order to study the additional information gained by the downscaling techniques the soil moisture products were investigated at the scale of single ERS pixels. Two ERS pixels from March 13th, 2006 are displayed in Fig. 1d-f. Agricultural areas dominate the selected area but several forest patches are evident in the east and the southeast (Fig. 2). While narrow range (13 – 37 %) soil moisture values were measured with the ERS data, highly heterogeneous soil moisture patterns were evident in the ASAR GM (13 – 87%). Clearly, large amount of information can not be detected by the ERS coarse measurements.

If a large scale atmospherical forcing dominates over a local forcing (soil type, terrain or land cover), the spatial ASAR GM soil moisture patterns are expected to stay homogenous. Thus, we assumed that the local forcing dominated over the area on 13th of March and gave rise to the fine scale patterns in Fig. 1f. Considering that the fine scale patterns did not correspond to the land cover classes (Figs 1f and 2), we further assumed that the soil types and local terrain conditions functioned as the main local forcings. It's, however, important to mention that the high noise level presented in the ASAR GM product could have increased the uncertainty of these fine scale patterns.

The downscaling linear coefficients *c* and *d* were retrieved by the statistical analyses of the radar backscatter time series at the 1 km scale and are therefore representative of the forcings governing the soil moisture at that scale. Fig. 1 demonstrates the coarse resolution ERS soil moisture (Fig. 1d) and the added spatial information at the 1 km scale via the downscaling coefficients *c* and *d* (Fig. 1e). The patterns in the downscaled product corresponded to the ASAR GM soil moisture patterns (Fig. 1f). While the downscaled product identifies portions of the ERS pixel that are drier or wetter and thus add new information at the 1 km scale, the uncertainties of the downscaled soil moisture levels are still large.

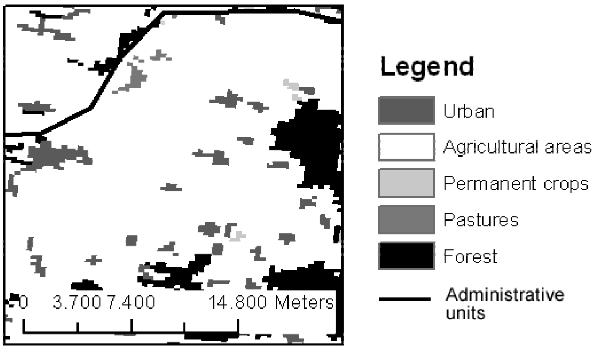

Fig. 2. Land cover classification over the Region A (Fig. 1) from the Corine Land Cover 2000. Classes were simplified.

CONCLUSIONS

The downscaling techniques introduced by Wagner *et al.* (2008) were investigated over northeastern Austria and southeastern Czech Republic.

Despite the high heterogeneity of the landscape, fine resolution spatial patterns were retrieved via the downscaled product. Spatial patterns corresponded well to the ASAR GM 1 km data.

Although these results are preliminary, they present an innovative approach of retrieving 1 km soil moisture information from the coarse resolution products. The downscaling techniques are of high importance for the satellite missions of the coarse resolution microwave sensors (ERS, METOP, AMSR-E).

Acknowledgements The study has been carried out within the framework of EUMETSAT's Satellite Application Facility in Support to Operational Hydrology and Water Management (H-SAF) and further supported by the Austrian Science Fund (L148-N10).

REFERENCES

Bartsch, A.., Scipal, K., Wolski, P., Pathe, C., Sabel, D. & Wagner, W. (2006) Microwave Remote Sensing of hydrology in Southern Africa. *The 2nd Göttingen GIS & Remote Sensing Days: Global Change Issues in Developing and Emerging Countries, Göttingen*, Germany, 4-6 October 2006.

Pathe, C., Wagner, W., Sabel, D., Doubkova, M. & Basara, J. (2008) Using ENVISAT ASAR Global Mode Data for Surface Soil Moisture Retrieval over Oklahoma, USA. *IEEE Transactions on Geoscience and Remote Sensing*, submitted.

Vaschaud, G., Passerat de Silans, A.., Balabanis, P. & Vauclin, M. (1985) Temporal stability of spatially measured soil water probability density function. *Soil Sci. Soc. Am. J.* **49**, 822-828.

Vischel, T., Pegram, G. G. S., Sinclair, S., Wagner, W. & Bartsch, A. (2008) Comparison of soil moisture fields estimated by catchment modelling and remote sensing: a case study in South Africa, *Hydrology and Earth System Sciences* **12**, 751-767.

Wagner, W., Pathe, C., Doubkova, M., Sabel, D., Bartsch, A., Hasenauer, S., Blöschl, G., Scipal, K., Martínez-Fernández, J. & Löw, A. (2008) Temporal stability of soil moisture and radar backscatter observed by the Advanced Synthetic Aperture Radar (ASAR). *Sensors* **8**, 1174-1197.

Wagner, W., Blöschl, G., Pampaloni, P., Calvet, J.-C., Bizzarri, B., Wigneron, J.-P. & Kerr Y. (2007) Operational readiness of microwave remote sensing of soil moisture for hydrologic applications. *Nordic Hydrology* **38**(1), 1–20. DOI 10.2166/nh.2007.029.

Wagner, W., Scipal, K., Pathe, C., Gerten, D., Lucht, W. & Rudolf, B. (2003) Evaluation of the agreement between the first global remotely sensed soil moisture data with model and precipitation data. *Journal of Geophysical Research D: Atmospheres* **108**(19), ACL 9-1 - 9-15.

An integrated subsurface transport modelling approach to assess regional water contamination of Cd by historic smelter emissions: unsaturated zone modelling

INGEBORG JORIS[1], JAN BRONDERS[1], BAS VAN DER GRIFT[2], GIJS JANSSEN[2] & PIET SEUNTJENS[1]
1 *VITO NV, Integral Environmental Studies, Boeretang 200, B-2400 Mol, Belgium*
ingeborg.joris@vito.be

2 *TNO Build Environment and Geosciences – Geological Survey of the Netherlands, Princetonlaan 6, 3584 CB Utrecht, the Netherlands*

Abstract A spatially distributed model for leaching of Cd from the unsaturated zone is developed for the region of the Campine area (SE part The Netherlands and NE Belgium). The model uses as input land-use maps, atmospheric deposition data and soil. The results are then used in an integrated model used to simulate transport of Cd in soil, groundwater and surface water. The integrated model serves as a tool to assist in developing management strategies for the widespread heavy metal contamination in the region. The approach for leaching from the unsaturated zone modelling is discussed.
Keywords integrated modelling; regional contamination; heavy metal leaching; risk based land management

INTRODUCTION

The Campine area, located in the northeastern part of Belgium and the southeastern part of the Netherlands, has a heavy historical load of heavy metals due to the former activities of 4 smelters over the last century. Dust emissions, discharge of wastewater and use of residues (ashes, slacks and muffles) in roadways have resulted in widespread heavy metal pollution in soil, groundwater and surface water. Due to the extent and the diffuse nature of the contamination, remediation and/or management strategies are needed for the entire region. In this study, a spatially distributed model for leaching of cadmium to groundwater is developed predicting dynamic fluxes of cadmium seeping from the unsaturated zone as part of a larger model that simulates transport of cadmium in soil, groundwater and surface water for the entire region. Such an integrated model can assist in developing management strategies for the heavy metal problem in the region.

STUDY AREA

The study area) has a wide-spread diffuse heavy metal pollution in soil, groundwater and surface water that requests a regional transboundary approach. The modelling domain is defined taking into account the area of influence of atmospheric deposition from the 4 smelters and covers part of Belgium and part of the Netherlands. An overview of the study area and the modelling domain is given in Fig. 1.

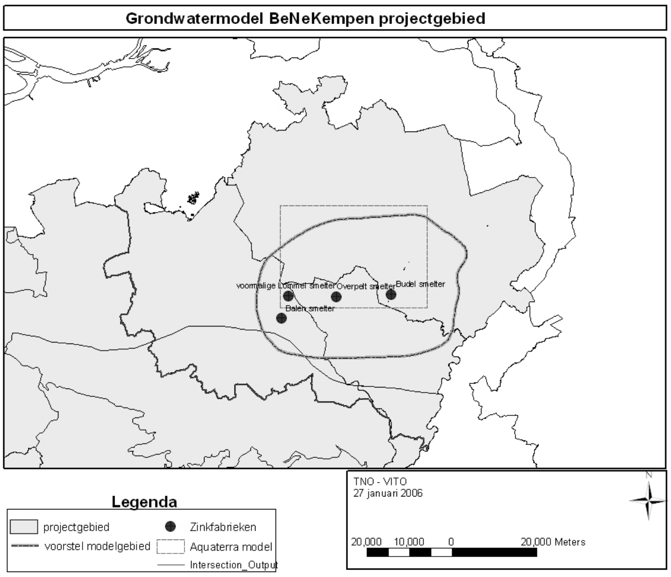

Fig. 1 Overview of the study area with location of the 4 smelter sites.

MODELLING APPROACH

Model concept

The model input consists of land-use maps, heavy metal loads from atmospheric deposition and fertilizer and location of roads constructed with metal containing residues. For different combinations of soil type, land use, net infiltration and inputs of heavy metals, 1D-soil columns were constructed. One-dimensional water flow and metal transport are simulated with the HYDRUS-1D code (Šimůnek *et al.*, 2005). Soil hydraulic properties and Freundlich isotherms are derived from soil properties using the soil map. The top boundary condition is determined by atmospheric deposition at the location and, for agricultural areas, input from fertilizer application. If zinc ashes are present, an additional concentration is added to the leachate concentration at the bottom of the soil column. The model is used for both historic modelling, assuming an initially 'clean' soil and groundwater and calculating the present concentrations in soil and groundwater, as well as forward modelling, forecasting metal leaching fluxes for the next 100 years for different scenarios.

Metal load

Deposition of dust emitted through the factory chimneys was a major diffuse input of Cd to the surroundings of the smelters (Seuntjens *et al.*, 2002; van der Grift and Griffioen, 2008). Deposition maps for different 5-year periods from 1890 to 2010 were reconstructed from (see Fig. 2):

- the production history of the different plants (given for zinc but similar for cadmium)
- the relation between deposition and distance from the factory for 4 different classes of wind direction, as deducted from measured soil concentrations by Mohammadi (1997).

Use of livestock manure and chemical fertilizer comprise an additional diffuse input of heavy metals on agricultural fields. The historical manure application (over the last century) is reconstructed based on historical livestock records. Leaching from the heavily polluted smelter sites (point sources) is not considered in the unsaturated zone model but is incorporated directly in the groundwater model.

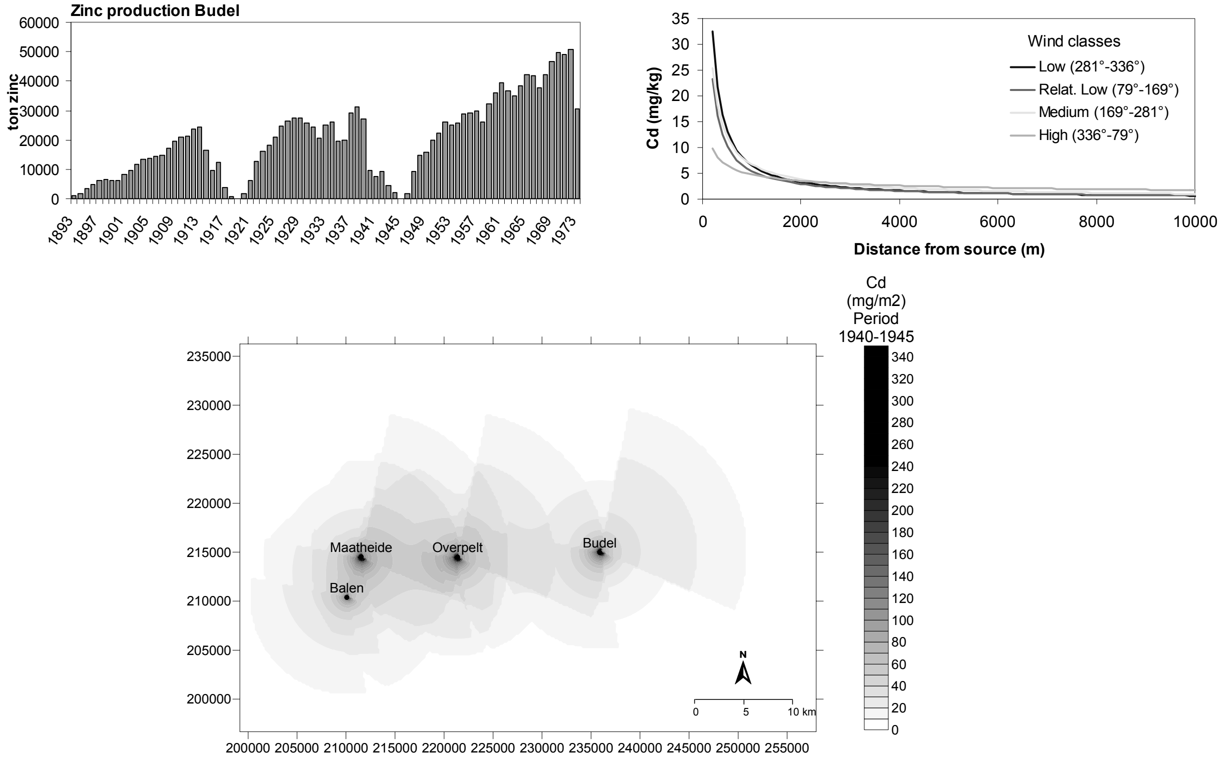

Fig. 2 Production history of the Budel site, relationships between soil concentration and distance from factory and calculated atmospheric deposition map for Cd for 1940-1945.

RESULTS AND DISCUSSION

Validation of historic modelling

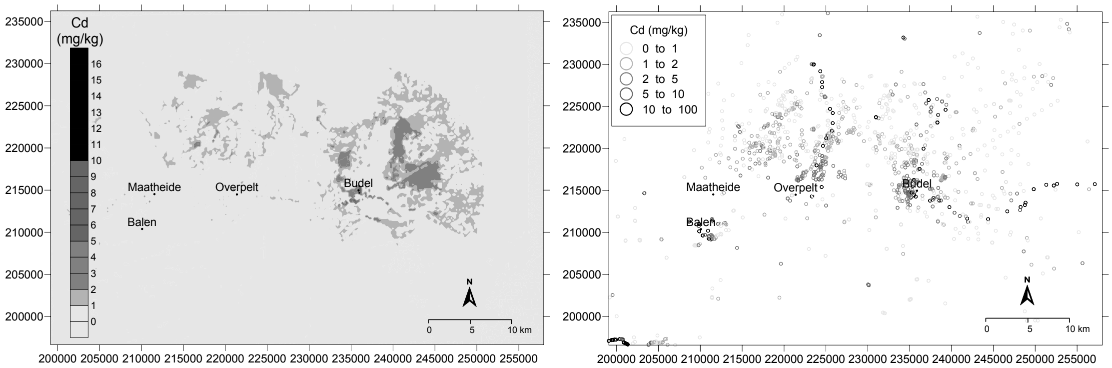

Fig. 3 Calculated and measured soil concentrations of Cd (top 30 cm) in 2010.

Because of the regional scale of the modelling, model validation is focused on whether the model can reproduce spatial patterns of measured concentrations in soil and groundwater rather than on a 1:1 comparison of individual concentration measurements. Fig. 3 shows calculated and measured concentrations of Cd in the top 30 cm of the soil. Colour coding for both graphs is identical. The spatial pattern in measured concentrations is reproduced very well by the model. It can be seen from the figures that leaching from the soil is much more advanced in the SW-part of the region (Belgium) than in the NE-part around Budel.

Metal loads to groundwater

In Fig. 4 loads of Cd to groundwater are shown for the Belgian and the Dutch part of the region. Total deposition of Cd in the period 1890-2010 amounts to 1168.8 tons for the Belgian part and 593.4 tons for the Dutch part. Of this amount, 495.2 tons (or 42.4 % of the deposition in this part of the region) has leached to groundwater during this period in the Belgian part of the area and 70.5 tons (or 11.9 %) in the Netherlands. This indicates a different rate of leaching for the Belgian and the Dutch part, mainly related to differences in soil type. While a significant part of the pollution has already leached to groundwater in Belgium, a rise in groundwater concentrations is still to be expected in the Dutch part of the region.

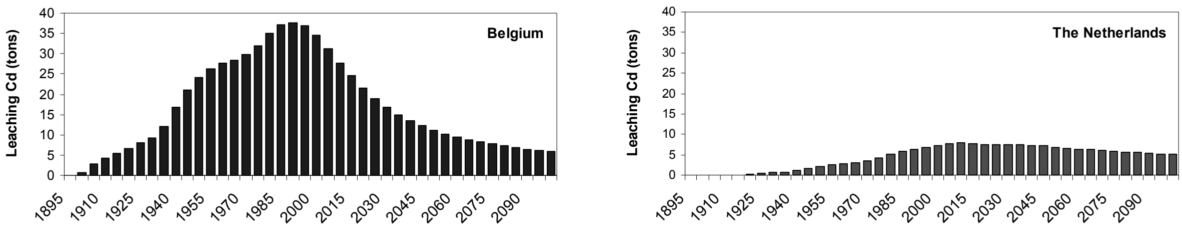

Fig. 4 Loads of Cd to groundwater in the Belgian (left) and Dutch (right) part of the study area.

CONCLUSIONS

In this study, a spatially distributed model for leaching of Cd to groundwater is developed based on land-use maps, soil maps and a reconstruction of atmospheric deposition. The model predicts spatially variable fluxes of Cd seeping from the unsaturated zone and is able to reproduce spatial patterns of concentrations in soil fairly well. Metal loads for the Belgian and Dutch part of the study area show a distinctly different leaching behaviour mainly related to different soil types.

Acknowledgements This study is funded within the Interreg project BeNeKempen (partnership between Campine Active Soil Management (AbdK) and the Public Waste Agency of Flanders (OVAM)).

REFERENCES

Mohammadi, J. (1997) Geostatistical mapping of environmental soil hazards. *PhD dissertation, Faculty of Agricultural and Applied Biological Sciences, University Gent.*

Seuntjens, P., Mallants, D., Šimůnek, J., Patyn, J. & Jacques, D. (2002). Sensitivity analysis of physical and chemical properties affecting field-scale cadmium transport in a heterogeneous soil profile. *Journal of Hydrology* **264,**185-200.

Šimůnek, J., van Genuchten, M. Th. & Šejna M. (2005) The Hydrus-1D software package for simulating the one-dimensional movement of water, heat and multiple solutes in variably saturated media. *Version 3.0, Department of Environmental Sciences, University of California Riverside, Riverside, California*, 240 pp..

Van der Grift, B. & Griffioen, J. (2008) Modelling assessment of regional groundwater contamination due to historic smelter emissions of heavy metals. *J. Cont. Hydrol.* **96**(1-4),48-68.

Modelling summer runoff on small hilly watersheds covered with thin soils over impermeable bedrock

DENIS LÉVESQUE

Sciences du bois et de la forêt, pavillon Abitibi-Price, Université Laval, Québec, Canada, G1V 0A6

mountainhydro@denis-levesque.ca or denis.levesque@sbf.ulaval.ca

Abstract MountainFlow is a 3D grid-based distributed parameters watershed runoff model designed for Canadian Shield. The emphasis is placed on dealing with preferential flow. In the calibration phase, a five week long simulation period had a Nash-Sutcliffe goodness of fit coefficient of 0.95 when compared to observed runoff data. In the validation phase, a second simulation period of same length gave a coefficient of 0.89.

STUDY WATERSHED

The model was parameterized using summer flow data from basin 6 of the Ruisseau des Eaux-Volées Experimental Watershed, located in the Forêt Montmorency Experimental Forest, 80 km north of Quebec City (47°16'20"N, 71°09'40"W) Canada. The terrain is hilly, covered by thin soils of glacial origin, mostly basal till, over impermeable bedrock. Soils are deeper in the U-shaped valleys but usually less than 10 m in depth with bottom sections having low hydraulic conductivity. The study watershed spans a 4 km^2 area with elevations from 729 m to 993 m and a mean slope of 13.8%. Forest cover consists of mature stands of balsam fir (80%), white spruce (10%) and white birch (10%) on thin orthic ferro-humic podzol with mean rooting depth of 30 cm.

MODEL STRUCTURE

MountainFlow is a 3D grid-based distributed parameters watershed runoff model designed for Canadian Shield. The emphasis is placed on dealing with preferential flow because this has been recognized as the dominant hydrological process operating on such watersheds. The model was written in C++ on a Windows/Intel platform and is described at the website http://mountainhydro.denis-levesque.ca/. It divides the watershed into a matrix of uniform- sized cells in the order of 1 ha whose surface elevation and slope are obtained from a vectorial topographic map. Depth, macroporosity, and hydraulic properties of the soil as well as water storage capacity and stomatal conductance of the vegetation are derived from an ecologically-based forestry map showing surficial deposits, tree species, stand height and density.

The vectorial topographic map is rasterized on a 5m x 5m grid and interpolated. From the overlay of the topographic map and the ecological map, a convergence power, which measures the propensity of a cell to generate preferential flow as it approaches saturation, is assigned to each cell surface. This parameter is obtained by performing a local drained area calculation on the cell using the 5m x 5m grid of the elevation interpolation step. The pattern of drained area on the boundary sub-cells is compared to the pattern calculated for a least square plane fitted through the sub-cell elevations. The resulting convergence power will be 0 for a planar cell and 1 for a cell whose flow emerges at a single point. In reality, even an inclined planar cell would exhibit some degree of preferential flow of a magnitude increasing with cell size because of micro topography and soil erodability. These parameters would vary with surfacial deposit and are unknown so we set an arbitrary minimum value for the convergence power. The convergence power map in relation with the perennial streams location is presented in Fig. 1.

A modified drained area calculation leads to a synthetic drainage network for the watershed. This network is formed by the channels running along the edges of the cells. The drained area of a cell is distributed to its lower elevation neighbours pro-rated by the slope but a fraction is diverted to the channels network according to the convergence power of the source cell as depicted in Fig. 2. Channels are interconnected to form a directed ternary tree rooted at the watershed outlet. As

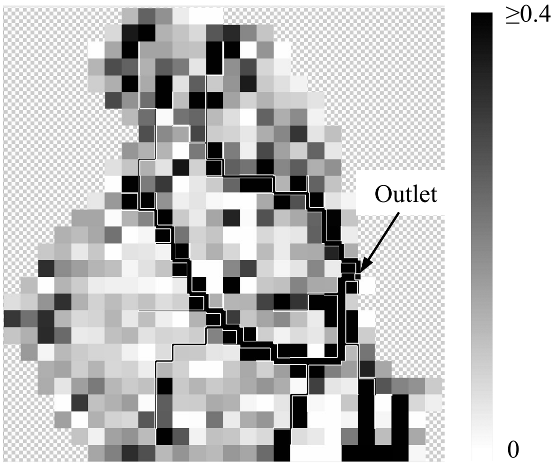

Fig. 1 Convergence power map. The 1 ha cells closest to the perennial streams (black lines with a white contour) have the highest values due to slope inversion there. White cells are either planar or convex. Watershed is delimited by a checker-board pattern.

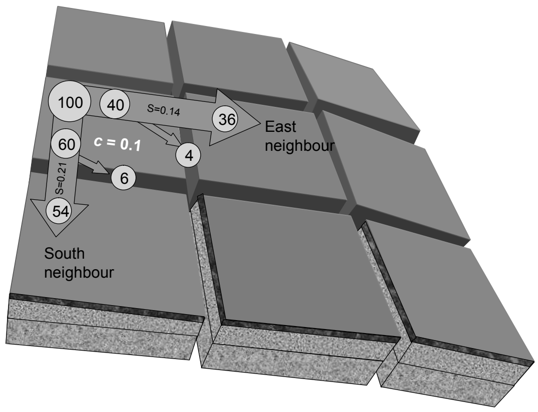

Fig. 2 Channels runs on the edges of the cells. Convergence power c is used to divert a part of the drained area to the channels and channel width is set proportional to this drained area.

drained area is propagated through the network, starting at the highest cell, the interconnections are made in order to get the best fit between the drained area in the synthetic network and the underlying drained area as can been seen in Fig. 3. Base width of the 45° trapezoidal channel section is set to 0.056 $A^{0.44}$ m, where A is the

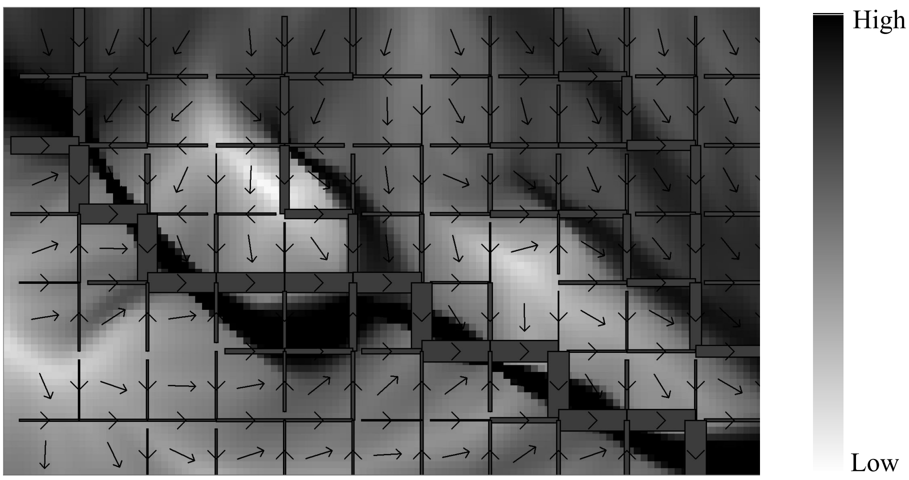

Fig. 3 Synthetic drainage network calculation details over a small part of the watershed. Background is the log(log(drained area)) calculated in the usual way on 5m x 5m sub-cells. Black arrows at cell center point local average flow direction. Fat grey arrows represent the directed synthetic network.

drained area in ha. The slope of a network segment is set equal to the slope of the largest drained area thalweg in the vicinity of the segment. Channel Manning's roughness *n* is is set inversely proportional to channel width *W* by the relation :

$$n(W) = \frac{(2n_{\max} - n_{\min})W_{\min} + n_{\min}W}{W + W_{\min}} \quad \Rightarrow \quad n(W_{\min}) = n_{\max}; \quad n(\infty) = n_{\min} \tag{1}$$

The terms n_{max}, n_{min} and W_{min} become 3 parameters of the model. An example of network for the whole watershed is presented in Fig. 4.

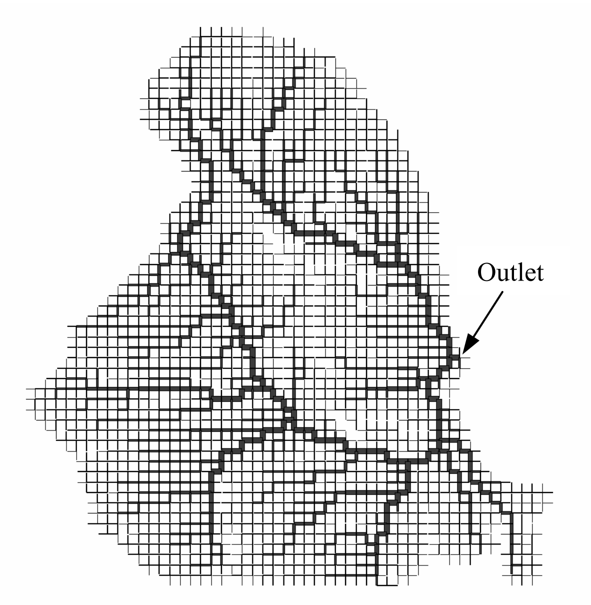

Fig. 4 Synthetic drainage network for the whole watershed when cells are 0.25 ha. Channel width not to scale.

A view of the overall model structure as seen from the south neighbour of the focal cell is shown in Fig. 5. Cells are composed of three layers of soil each containing a conceptual diffuse macropore layer which strives to mimic the behaviour of the network of interconnected individual macropores. Surface and macropore water are concentrated into open channels according to the convergence power and are routed there using the kinematic wave. Flow in the channels is conveyed by a one-dimensional diffusion wave. Vertical unsaturated flow follows Darcy's Law. Pressure potential is neglected when calculating vertical saturated flow. This latter flow is used to fill macropores and will generate lateral flow proportional to the slope so that the omission of pressure potential will have little effect in ponding areas. With high mean slopes, height differentials are such that conditions in lower elevation neighbours may be neglected when calculating lateral flows within cells. Hence, lateral matrix flow is calculated from hydraulic conductivity and slope alone to shorten computation time. The vegetation layer may be composed of up to two sublayers, low and high vegetation, the latter representing forest canopy. Evapotranspiration is estimated on each cell using the Penman-Monteith equation taking into account the cell orientation relative to the sun using auxiliary atmosphere and sun radiation sub-models.

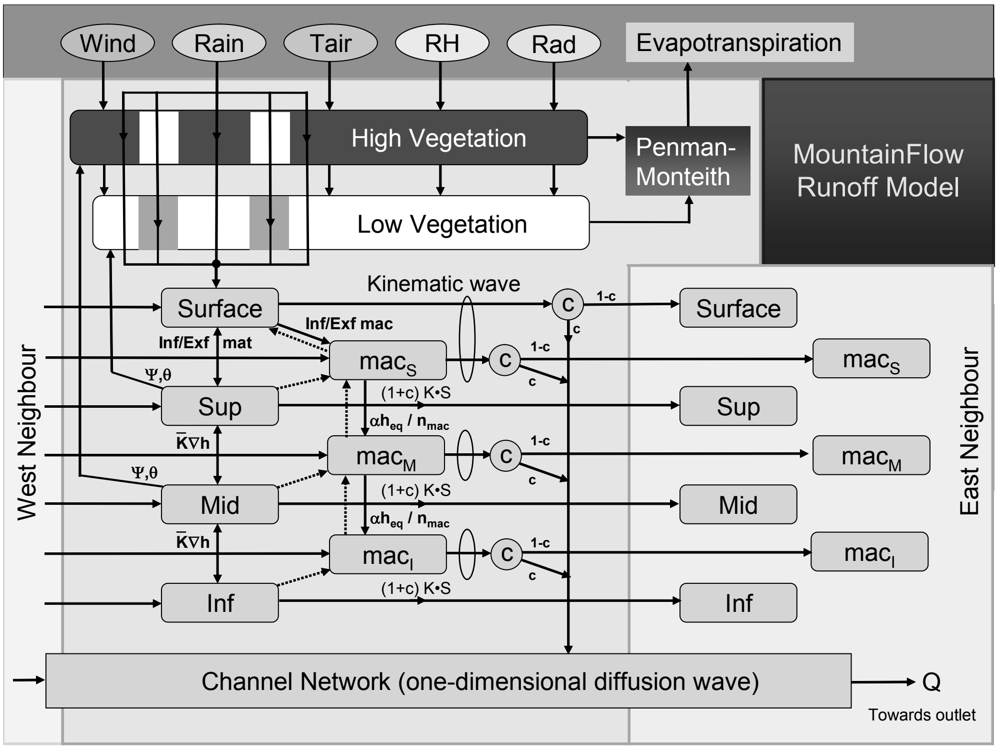

Fig 5 Schematic of the runoff model. Relations identical to those displayed exist along the axis running through the figure for the north and south neighbours. Dotted line flows occur only at matrix saturation. Note that convergence power also controls the lateral matrix flow because a V-shaped cell would yield twice the matrix flow of a \-shaped cell.

DETERMINATION OF INITIAL SOIL WATER CONTENT

We developed an initialisation procedure that depends on a watershed exhibiting a period of relatively dry-weather flow at the beginning of the sequence. Cell water contents are initialized to a constant. We then apply a meteorological time series characteristic of a small rainstorm and run the model until simulated outflow decays to the value observed at the beginning of the target simulation. This procedure is repeated until the model response stabilizes, and the final water content is used as the initial conditions. This produces a realistic and probable state of the watershed before the real simulation is run. The weak capacity of the study watershed to retain water enabled this approach. As simulation length increases, errors in initial conditions become relatively unimportant compared to cumulative error in the evapotranspiration estimates.

PARAMETERS ESTIMATION

The model was calibrated to observed flow rates at the watershed outlet by adjusting manually 18 global multiplying coefficients applied to all cells. An initial soil water content determination was required after each major change. The eleven most sensitive coefficients were hydraulic conductivity at saturation, depth and macroporosity for each of the three soil layers, macropore roughness and evapotranspiration. These coefficients being applied globally, their fitting power will degrade gradually as watershed area increases.

RESULTS

We simulated hydrology of the 4 km^2 watershed over a five week meteorological time series from summer 1976 that included a major storm, a moderate storm, a drought period, a complex of several consecutive small storms and a few individual small storms. Hourly meteorological variables were measured at a station 4.7 km away but precipitations were recorded directly on the watershed. Model cell size was 1 ha and simulation time step was 5 s. Observed and simulated runoff at the outlet compared closely over all meteorological events (Fig. 6). The Nash-Sutcliffe quality of fit coefficient was 0.952 for the period. Observation of internal results during the simulation showed that the preferential flow modeled by the macropore layers was the dominant contribution to the watershed outflow except for the dry-weather periods. We simulated outflow runoff for a similar period the following summer (Fig. 7) using the same coefficients values but with new initial conditions determined as above. The Nash-Sutcliffe coefficient value dropped to 0.891. Each simulation took 14 minutes on a desktop computer (3.4 GHz Pentium IV processor running Windows XP SP2). Use of a 4 ha cell size preserved goodness of fit and reduced computation time to 3 minutes, but at a loss of much realism of the generated image sequence (available at http://mountainhydro.denis-levesque.ca/mountainflow/films/nonmatrixwater4ha.avi).

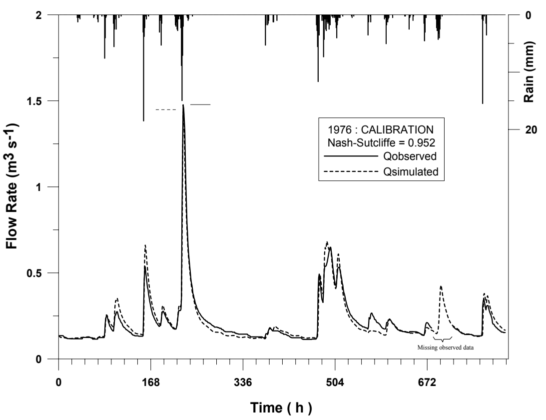

Fig. 6 Five weeks of observed and simulated outflows on basin 6 of the Ruisseau des Eaux-Volées watershed starting June 22nd 1976

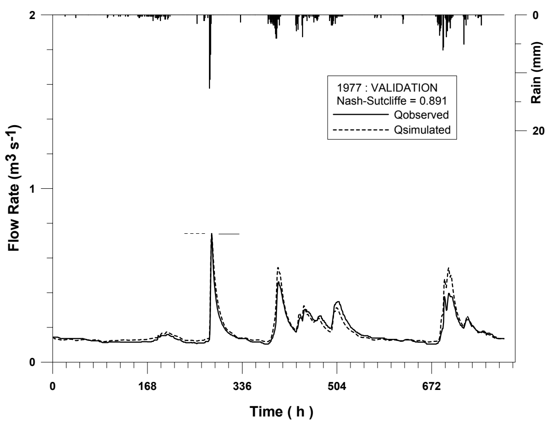

Fig. 7 Five weeks of observed and simulated outflows on basin 6 of the Ruisseau des Eaux-Volées watershed starting June 1st 1977

CONCLUSION

MountainFlow has proved to be effective at simulating the highly dynamic behaviour of a small hilly boreal-shield watershed where peak flows last only for a few hours and where the dominant component is preferential flow. Peak flow response is governed by the macropore conceptual layers and to a lesser extent by the hydraulic properties of the channel network while the presence of soil layers insures that the base flow is simulated adequately during drought periods.

Since the geology, topology, vegetation and especially the surficial deposits of this study watershed are ubiquitous in the Laurentian Mountains, the model should be readily and reliably applied to other watersheds in that area.

Application of SWAT to Kosynthos River basin

K. ZIOGAS & V. HRISSANTHOU

Department of Civil Engineering, Democritus University of Thrace, 67100 Xanthi, Greece

vhrissan@civil.duth.gr

Abstract A continuous rainfall-runoff model based on the hydrologic part of the water quality model SWAT (Soil and Water Assessment Tool) was applied to Kosynthos River basin (Thrace, northeastern Greece), with an area of about 237 km^2. For more precise calculations, the whole basin was divided into ten natural sub-basins. From given daily rainfall depths, the rainfall excess was computed by means of the SCS (Soil Conservation Service) method. The peak discharge was computed by the modified rational method. For the calculation of the baseflow hydrograph, the computation of the subsurface flow and the deep percolation is required. In this study, the contribution only of subsurface flow to baseflow was taken into account. The hydrograph routing from a sub-basin outlet to the outlet of the whole basin was enabled by the variable storage method which is based on the water mass continuity equation. By means of the rainfall-runoff model, a continuous hydrograph at the outlet of Kosynthos River basin for the time period 1996-2006 was computed on the basis of the given hyetogram for the same time period. Individual computed discharge values of the hydrograph for certain days were compared with corresponding measured discharge values.

Keywords SWAT; rainfall – runoff; subsurface flow; hydrograph routing

INTRODUCTION

In this paper, the application of a continuous rainfall – runoff model to the basin of Kosynthos River (district of Xanthi, Thrace, northeastern Greece), as well as the comparison of the computational runoff results with field discharge measurements are presented.

In the 60's, the need of a more realistic simulation of the process of rainfall – runoff, based on physiographic characteristics (i.e. land use, soil cover and slope) in complex larger basins, was urgent. Then, models as Stanford IV and Sacramento River were developed for this purpose. However, the plethora of the data demanded led to no realistic results (Crawford & Linsley, 1966; Burnash *et al.*, 1973). This lack of a one to one relationship between model and reality was the spark of a research attempt in hydraulic and hydrologic institutes [Danish Hydraulic Institute (Denmark), Institute of Hydrology (U.K.) and SOGREAH (France)], which led to the development of a conceptual model. This model included the principal differential equations (continuity and momentum equations) which connect the subprocesses of the model by adjusting boundary conditions. Principal differential equations such as Richards equation for infiltration, Darcy's equation for groundwater flow and Saint Venant equations for routing flood waves were available. The product of this joint effort is the "SHE" model (Système Hydrologique Européen) (Abbot *et al.*, 1986) which is milestone for all these simulation attempts of the rainfall-runoff process.

The rainfall-runoff models are classified into various categories, that depend on the kind of the equations, the time and spatial step etc. The most common categories of the models are the continuous and event models, as well as the lumped and distributed models. The USDA Agricultural Research Service (ARS) delevoped SWAT to predict the impact of land management practices on water, sediment and agricultural chemical yields in large complex watersheds with varying soil, land use and management conditions over long periods of time (Neitsch *et al.*, 2002).

SWAT incorporates features of several ARS models and is a direct outgrowth of the SWRB model (Williams *et al.*, 1985; Arnold *et al.*, 1990). Specific models that contributed significantly to the development of SWAT were CREAMS (Knisel, 1980), GLEAMS (Leonard *et al.*, 1987) and EPIC (Williams *et al.*, 1984).

A BRIEF THEORETICAL MODEL DESCRIPTION

Rainfall excess model

According to Soil Conservation Service (SCS) method, the rainfall excess is computed by:

$$Q_{surf} = \frac{(R_{day} - 0.2S)^2}{R_{day} + 0.8S} \tag{1}$$

where Q_{surf} is rainfall excess (mm), R_{day} is the rainfall depth for the day (mm) and S is the retention parameter (mm). The retention parameter is defined as:

$$S = 25.4\left(\frac{1000}{CN} - 10\right) \tag{2}$$

where CN is the curve number for the day.

Peak flow rate model

The modified rational formula is used to estimate peak flow rate:

$$q_{peak} = \frac{a_{tc} Q_{surf} Area}{3.6 t_{conc}} \tag{3}$$

where q_{peak} is the peak runoff rate (m^3 s^{-1}), a_{tc} is the fraction of daily rainfall that occurs during the time of concentation, Q_{surf} is the surface runoff (mm), $Area$ is the sub-basin area (km^2), t_{conc} is the time of concentration for the sub-basin (hr) and 3.6 is a unit conversion factor.

Subsurface flow (lateral flow) model

SWAT incorporates a kinematic storage model for subsurface flow developed by Sloan *et al.* (1983) and summarized by Sloan & Moore (1984). This model is based on the mass continuity equation, or mass water balance, with the entire hillslope segment used as the control volume.

$$Q_{lat} = 0.024(\frac{2SW_{ly,excess}K_{sat}slp}{\varphi_d L_{hill}}) \tag{4}$$

where Q_{lat} is the water discharge from the hillslope outlet (mm day^{-1}), $SW_{ly,excess}$ is the drainable volume of the water stored in the saturated zone of the hillslope (mm), K_{sat} is the saturated hydraulic conductivity (mm hr^{-1}), $slp = tan(a_{hill})$, a_{hill} is the slope of the hillslope segment, L_{hill} is the hillslope length (m) and φ_d is the drainable porosity of the soil (mm mm^{-1}).

Variable storage routing method

The variable storage routing method was developed by Williams (1969) and is based on the continuity equation:

$$q_{out,2} = (SC)q_{in,ave} + (1 - SC)q_{out,1} \tag{5}$$

where $q_{out,2}$ is the outflow rate at the end of the time step (m^3 s^{-1}), $q_{out,1}$ is the outflow rate at the beginning of the time step (m^3 s^{-1}), $q_{in,ave}$ is the average inflow rate during the time step (m^3 s^{-1}) and SC is the storage coefficient.

APLLICATION TO KOSYNTHOS RIVER BASIN

The above model was applied to Kosynthos River basin (district of Xanthi, Thrace, northeastern Greece) in order to simulate a continuous hydrograph of the years 1996 - 2006. The basin of Kosynthos River has an area of about 237 km^2 consisting of forest (74%), bush (4.5%), urban area (1.5%) and an area with no significant vegetation (20%). The highest altitude of the basin is about 1700 m. The length of the main stream of the basin is about 35 km. For more precise calculations, the basin was divided into ten natural sub-basins (Fig. 1). The structure of the basin, especially for the model operation, is depicted in Fig. 2.

For the estimation of the model parameters, rainfall data, temperature measurements from the meteorological station of Oreo (Fig. 3), as well as topographical, geological, main stream and soil cover maps were used. The meteorological station of Oreo is located in the centre of gravity of the basin. Moreover, the Laboratory of Hydrology and Hydraulic Structures, Civil Engineering Department, Democritus University of Thrace, carried out four field measurements of discharge in October, November, December 2005 and four measurements in June 2006 at the outlet of Kosynthos River basin.

Results

In Fig. 4, the computed discharge hydrograph (direct runoff + baseflow) of October – December 2005 and the measured discharge values at the basin outlet are depicted. In Fig. 5, the computed discharge hydrograph (direct runoff + baseflow) of June 2006 and the measured discharge values at the basin outlet are illustrated.

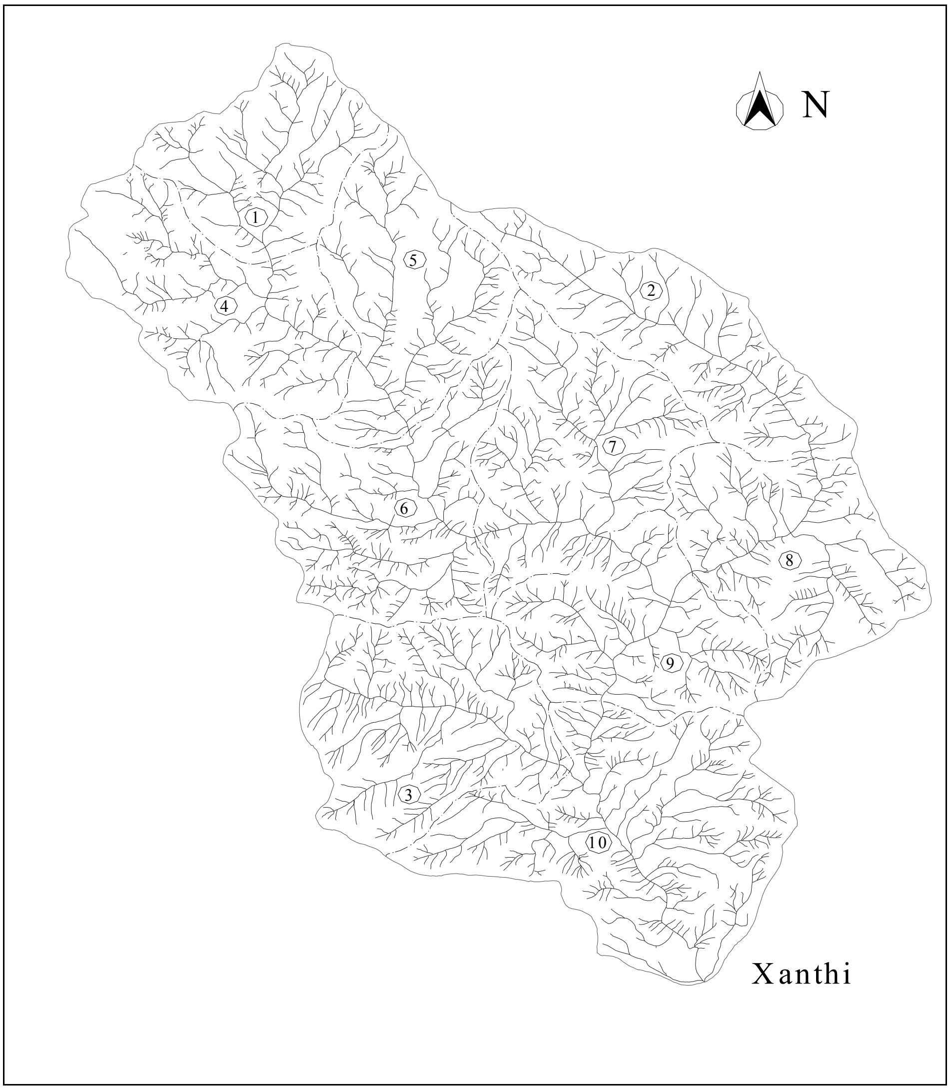

Fig. 1 Kosynthos River basin divided into 10 sub-basins.

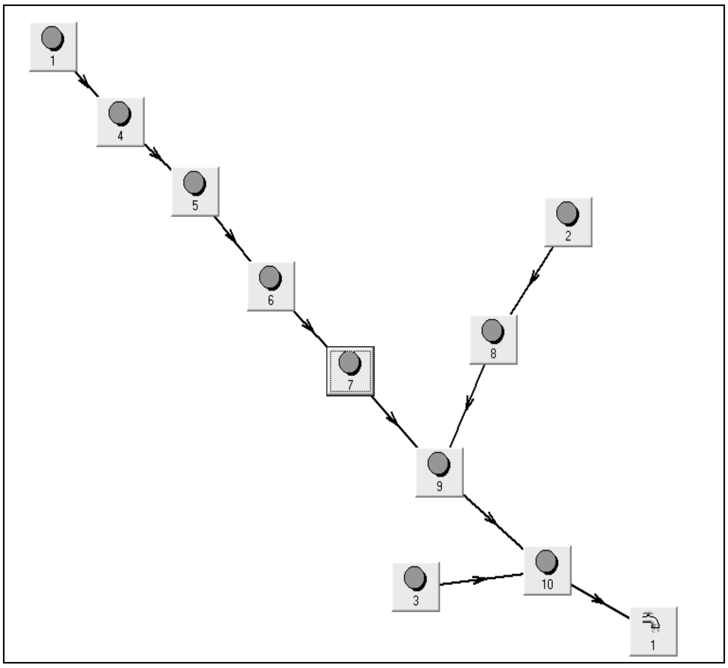

Fig. 2 Structure of the basin for the model operation.

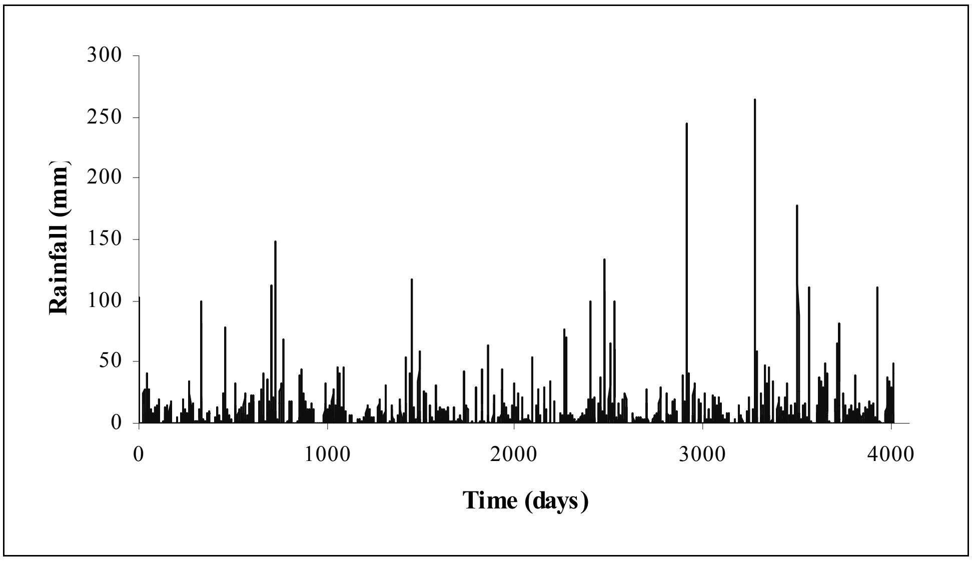

Fig. 3 Rainfall data series from Oreo Station.

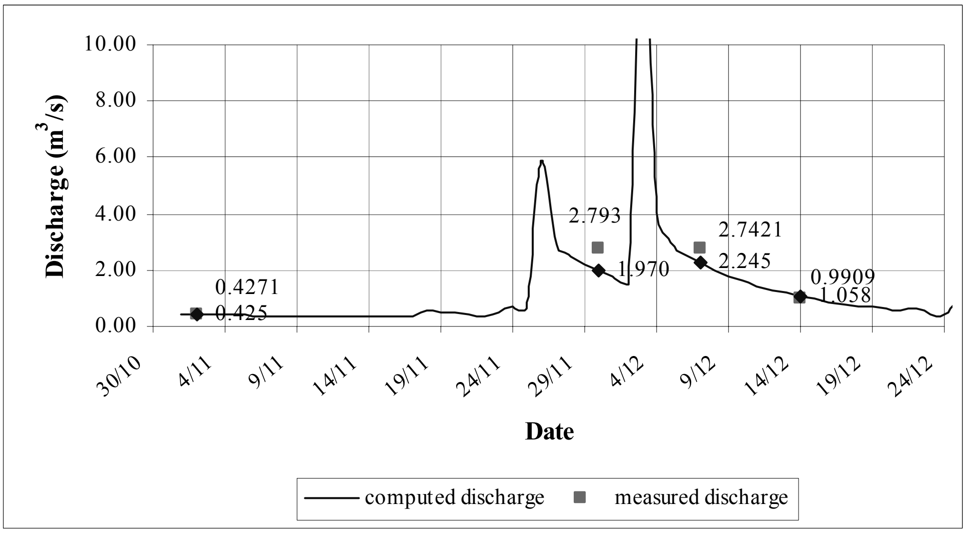

Fig. 4 Discharge hydrograph of November – December 2005.

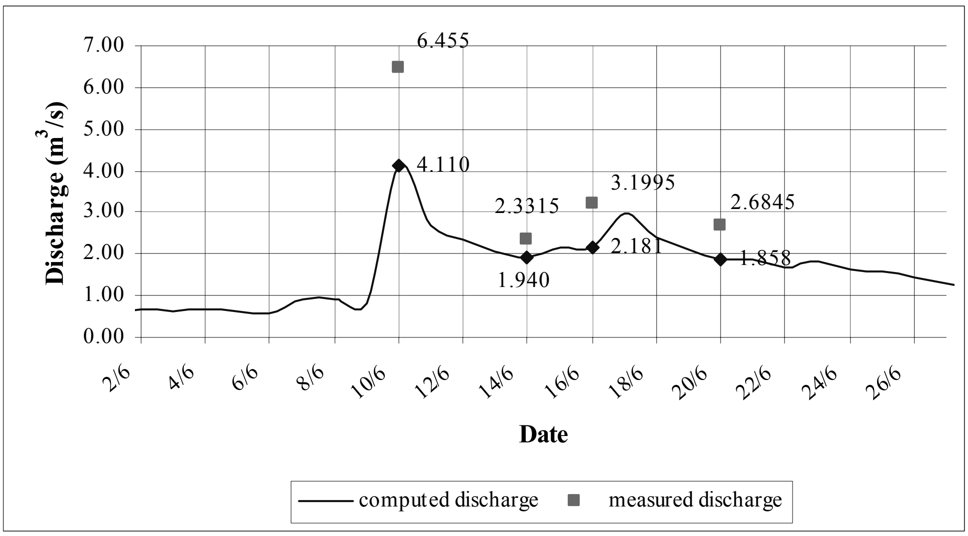

Fig. 5 Discharge hydrograph of June 2006.

The comparison between computed and measured discharge values was performed on the basis of the "root mean square error" (RMSE). The value of RMSE amounts to 1.01 m^3 s^{-1}. The degree of linear dependence between computed and measured discharge values is expressed by the correlation coefficient. This coefficient, as a result of linear regression analysis, is equal to 0.98.

CONCLUSION

From Fig. 4 and 5 as well as from the RMSE-criterion, it is concluded that the deviation between computed and measured discharge values is not considerable. Additionally, the degree of linear dependence between computed and measured discharge values is very high. However, it has to be noted that the number of the measured discharge values is quite small. Therefore, the values of RMSE and correlation coefficient are not widely representative.

REFERENCES

Abbot, M. B., Bathurst, J. C., Cunge, J. A.,. O' Connell, P. E. & Rasmussen, J. (1986) An introduction to the European Hydrological System – SHE, 1: History and philosophy of physically based, distributed modeling system. *Journal of Hydrology* **87,** 45-59.

Arnold, J. G., Williams, J. R., Nicks, A. D. & Sammons, N. B. (1990) SWRB: A basin scale simulation model for soil and water resources management. *Texas A&M Univ. Press*, *College Station, TX.*

Burnash, R. J. C., Ferral, R. L. & McGuire, R. A. (1973) A generalized streamflow simulation system - Conceptual modeling for digital computers. *Report by the Joint Federal State River Forecasts Center*, *Sacramento, Calif.,* USA.

Crawford, N. H. & Linsley, R. K. (1966) Digital simulation in hydrology, Stanford watershed model IV, *Tech. Rep. No 39, Dep. Civ. Eng., Stanford University*, USA.

Knisel, W. G. (1980) CREAMS, a field scale model for chemicals, runoff and erosion from agricultural management systems. *USDA Conservation Research Rept. No. 26*.

Neitsch, S. L., Arnold, J. G., Kinry, J. R., Williams, J. R. & King, K. W. (2002) Soil and Water Assessment Tool - Theoretical Documentation. *Blackland Research Center, Texas Agricultural Experiment Station*, 720 East Blackland Road Temple.

Leonard, R. A., Knisel, W. G. & Still, D. A. (1987) GLEAMS: Groundwater loading effects on agricultural management systems. *Transactions of the ASAE* **30**(5), 1403-1428.

Sloan, P. G. & Moore, I. D. (1984) Modeling subsurface stormflow on steeply sloping forested watersheds. *Water Resources Research* **20**(12), 1815-1822.

Sloan, P. G., Morre, I. D., Coltharp, G. B. & Eigel, J. D. (1983) Modeling surface and subsurface stormflow on steeply sloping forested watersheds. *Water Resources Inst. Report 142, Univ. Kentucky, Lexington*.

Williams, J. R. (1969) Flood routing with variable travel time or variable storage coefficients. *Transactions of the ASAE* **12**(1), 100-103.

Williams, J. R., Jones, C. A. & Dyke, P. T. (1984) A modeling approach to determining the relationship between erosion and soil productivity. *Transactions of the ASAE* **27**(1), 129-144.

Williams, J. R., Nicks, A. D. & Arnold, J. G. (1985) Simulator for water resources in rural basins. *Journal of Hydraulic Engineering, ASCE* **111**(6), 970-986.

The use of modelling in the reduction of flood risk for the town of Dolgellau, Wales

GRAHAM HALL & ROGER CRATCHLEY
School of the Environment and Natural Resources, Bangor University, Ffordd Deiniol, Bangor, Gwynedd, UK
g.hall@meirion-dwyfor.ac.uk

Abstract An integrated meteorological/hydrological model is developed for the Mawddach catchment. This incorporates high resolution rainfall modelling, a hillslope model computing shallow storm throughflow, and a floodplain inundation model. Effects of gravel deposition have been analysed. A flood interception basin scheme with wet woodland is proposed.
Keywords flooding; hillslope hydrology; throughflow; river gravel

INTRODUCTION

Dolgellau lies on the river Wnion which has its source in the Aran mountains of North Wales. The town was subject to regular flooding until the 1960's when flood defence walls were built to protect the historic streets in the town centre. Recent floods have come close to overtopping the river walls, and there is concern that additional defence works will be needed if the town is to continue to be protected. Fieldwork and modelling have been carried out to determine the mechanisms leading to flooding within the catchment, and to produce an improved flood warning system.

Analyses of rainfall patterns from an array of data logging raingauges across the mountains indicate complex rainfall patterns dependent on the approach direction of frontal storms (Fig. 1). Flood models for the catchment are crucially dependant on the accurate forecasting of rainfall patterns up to six hours ahead of storm events. Experimentation has shown that the MM5 meteorological model (Dudhia *et al.*, 2005) running on an Altix minicomputer can successfully predict frontal rainfall to within 20% accuracy on a 1km grid, with convective rainfall predicted to within 40% accuracy. This data has been incorporated into an integrated flood model.

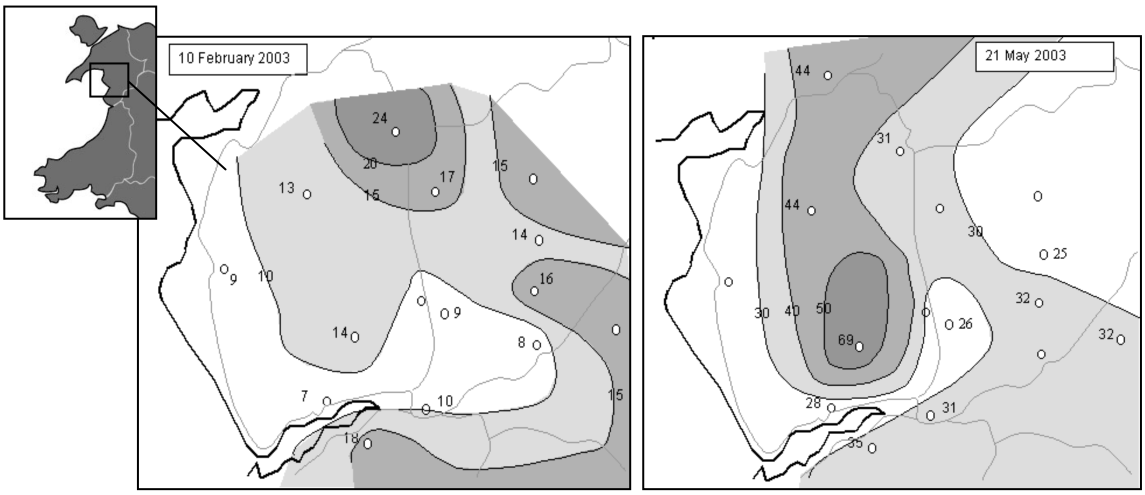

Fig. 1 Examples of total storm rainfall (mm) across the Mawddach catchment. (left) example of Type A pattern with rainfall concentrated along a NW-SE axis, (right) example of Type B pattern with rainfall concentrated on a N-S axis.

The Mawddach catchment is an area of low permeability Lower Palaeozoic sedimentary and igneous bedrock, covered locally by thick deposits of glacial and periglacial clays, sands and gravels. A series of hillslope sites has been instrumented to measure runoff and shallow stormflow for use in calibration of the hydrological model (Fig. 2).

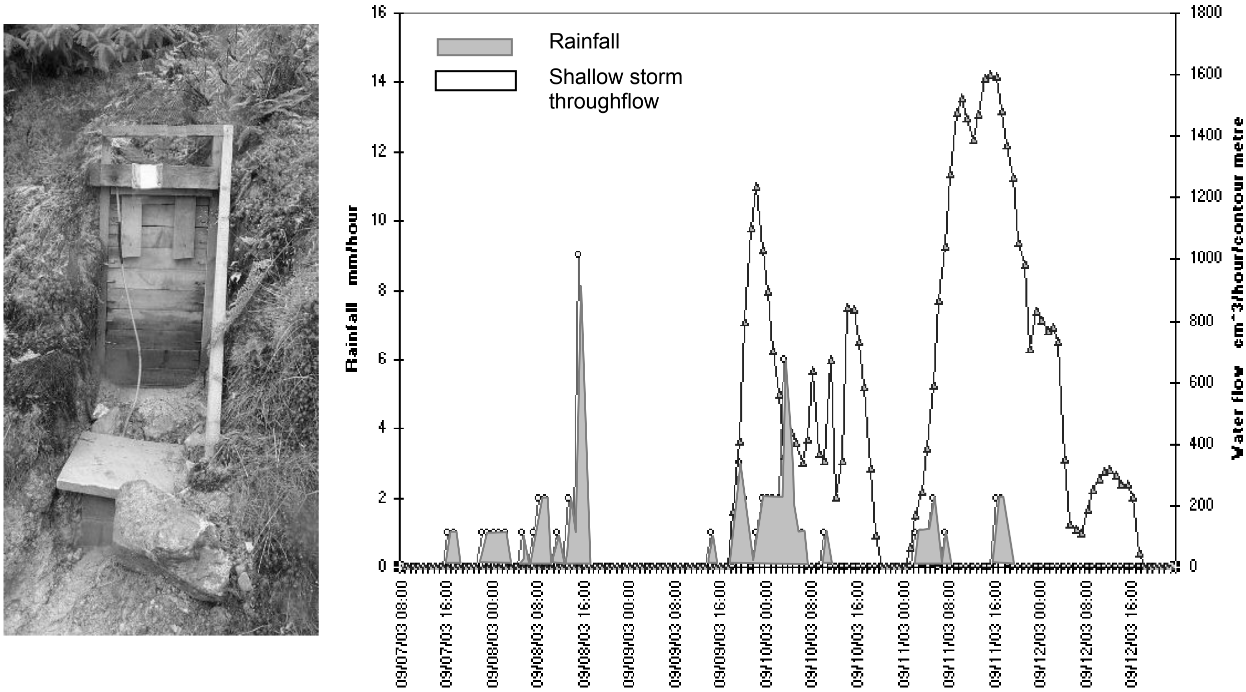

Fig. 2 (left) Hillslope runoff and shallow storm throughflow monitoring site. (right) Progressive increase in shallow storm throughflow as glacial deposits become saturated in response to a sequence of rainfall events.

Shallow storm throughflow was found to be the most important mechanism for generating flood discharges over substantial areas of the catchment, with antecedent rainfall critically important in creating the necessary saturation conditions. Based on this work, a new hillslope model was developed which computes throughflow and runoff in response to soil saturation using the van Genuchten equation (Fig. 3).

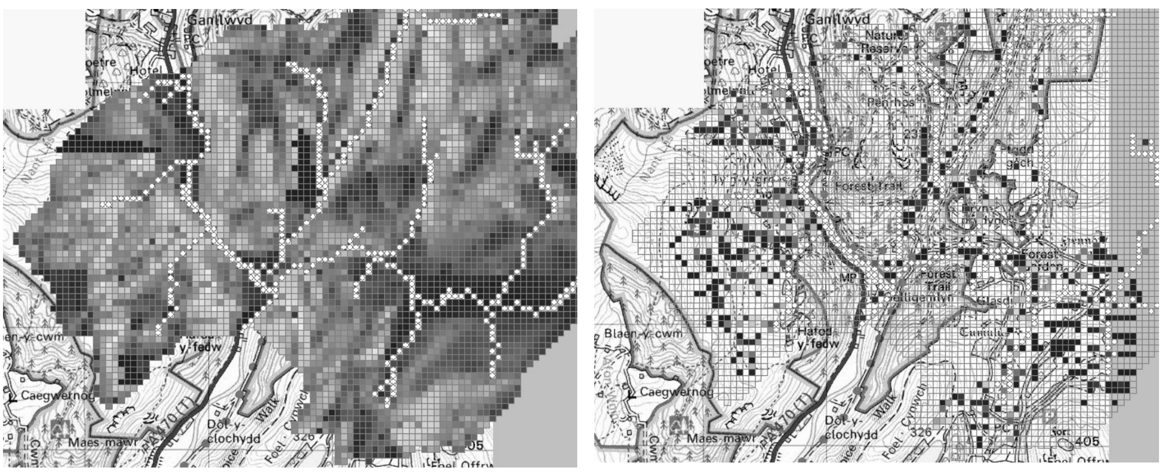

Fig. 3 Example hillslope hydrological plots for the Afon Wen valley. (left) Shallow storm throughflow, showing areas of high flow in (peri)glacial deposits - dark shading. (right) Surface runoff , occurring on lower hillslopes and areas of thin soils on bedrock.

Outflows from a series of sub-catchment hillslope models are routed downstream, with overbank discharge onto floodplains modelled using the River2D software package.

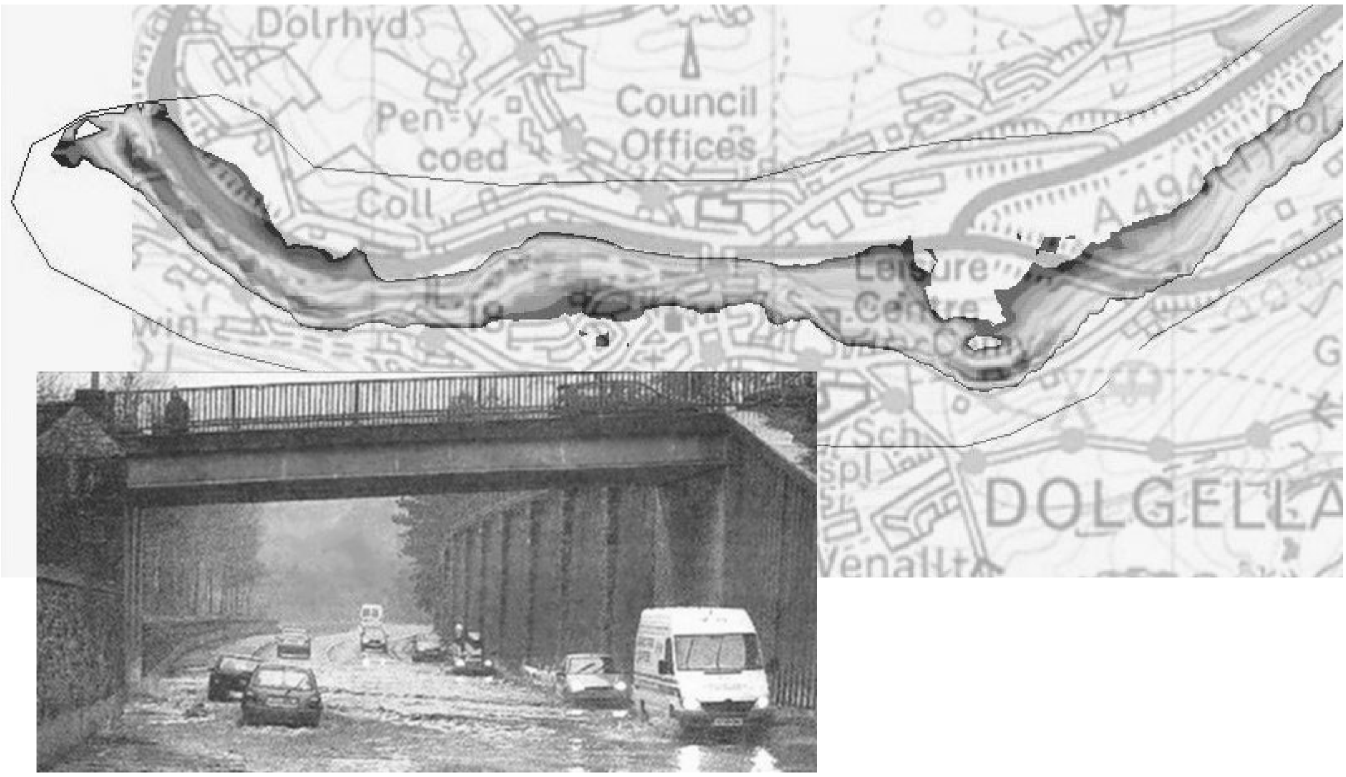

Fig. 4 River2D floodplain model for the Wnion valley around the town of Dolgellau. The extent of flooding at a discharge of $200m^3s^{-1}$ is consistent with observed flood extent.

During fieldwork it became apparent that gravel sediment accumulation in the Dolgellau reach of the River Wnion is raising the channel bed and reducing the effectiveness of flood defence walls (Fig. 5). The extent of gravel movement has been estimated using GSTARS software, with more than 1m depth of gravel accumulation possible during an individual flood event.

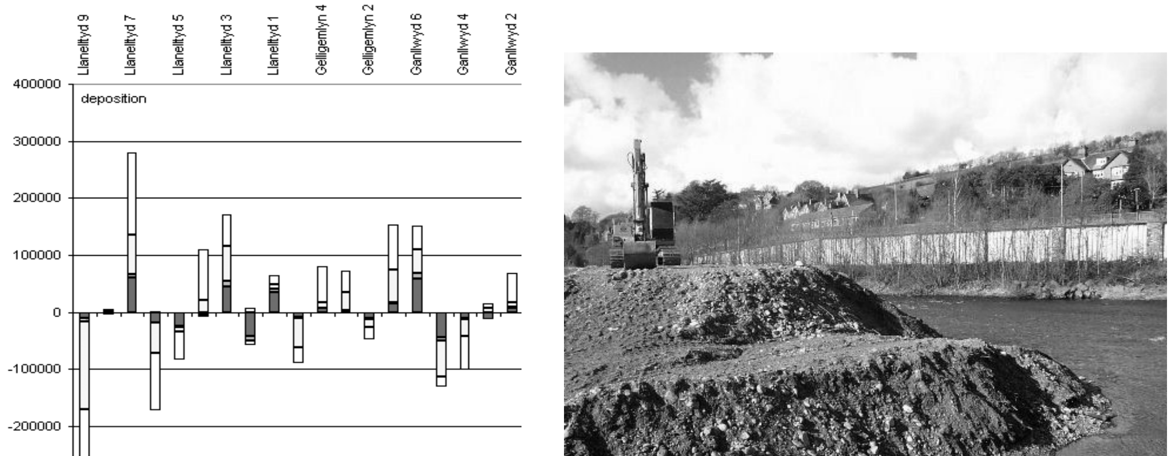

Fig. 5 (left) Example of GSTARS sediment model for a storm event, indicating that erosion and deposition may occur along adjacent reaches of the River Wnion.
(right) Removal of gravel from the River Wnion in Dolgellau.

Modelling has been carried out to determine the effectiveness of possible flood interception basins in the Wnion valley upstream of Dolgellau, and a preferred site identified. Surface roughness and eddy viscosity coefficients for different vegetation categories have been calibrated over a series of historic flood events. The use of floodplain forestry has been modelled, with a view to enhancing temporary overbank storage and reducing flood peak discharge (Fig. 6). Peak discharges would fall from $250 m^3 s^{-1}$ to around $200 m^3 s^{-1}$, representing a reduction in stage height of 40cm through the town. Weirs incorporated into the basin scheme would provide the additional benefit of trapping gravel sediment in locations where it could be safely removed.

Fig. 6 Model for flood interception basin in the lower Wnion valley.
(inset) Wet woodland of willow and alder in the lower Wnion valley, of the type which is proposed for the flood interception basin.

The project has indicated that floodplain land management approaches could be as effective as hard engineering in reducing flood risk, and would have a positive environmental effect in enhancing landscape and species diversity.

REFERENCES

Dudhia, J., Gill, D., Manning, K., Wang, W. & Bruyere, C. (2005) PSU/NCAR mesoscale modelling system. Tutorial class notes and user's guide: MM5 modelling system version 3. *National Center for Atmospheric Research, Boulder, Colorado, USA.*

Hall, G. & Cratchley, R. (2006) Sediment erosion, transport and deposition during the July 2001 Mawddach extreme flood event. *Sediment Dynamics and the Hydromorphology of Fluvial Systems* (ed. J. S. Rowan *et al.*), *International Association of Hydrological Sciences*.

Steffler, P. & Blackburn, J. (2002) River2D – Introduction to Depth Averaged Modelling and User's Manual. *University of Alberta.*

Thomas, H. & Nisbet T. T. (2004) An assessment of the hydraulic impact of floodplain woodland. *Forestry Commission*.

van Genuchten, M. T. (1980) A closed-form equation for predicting the hydraulic conductivity of unsaturated soils. *Soil Science Soc. America Journal* **44**.

Effect of the wastewater treatment levels on the sensitivity of a water-quality model to uncertain model-input parameters

GEMMA MANACHE[1] & CHARLES S. MELCHNG[2]
1 *MWH, North West Business Unit, 240 Cygnet Court, Lakeside Drive, Centre Park, Warrington, WA1 1RN, UK*
gemma.manache@mwhglobal.com

2 *Department of Civil and Environmental Engineering, Marquette University, P. O. Box 1881, Milwaukee, WI 53201-1881, USA*

Abstract Sensitivity analysis is recommended prior to water quality model application to water-pollution control and planning problems. This analysis allows determination of the key sources of uncertainty, i.e. the parameters to which the model prediction is most sensitive. It is important to know whether the key parameters identified under a high pollution load still remain important when the model is applied under reduced pollutant load conditions. In this paper, the effect of implementation of a water-quality management strategy on the identification of the key parameters is investigated through the comparison between sensitivity analysis results obtained for two cases of pollutant loads. The sensitivity analysis is done using Latin Hypercube Sampling in combination with correlation analysis to identify the parameters to which the DUFLOW model developed for the Dender River in Belgium is most sensitive. The results indicate that for a case with limited wastewater treatment, the oxidation rate constant of carbonaceous biochemical oxygen demand (kbod) has the greatest effect on the uncertainty of the simulated dissolved oxygen concentrations in the Dender River. Once the kbod effect is decreased through the reduction of loads, the importance of many other model parameters can be detected.
Keywords sensitivity analysis; water quality modelling; water quality management; uncertainty analysis

INTRODUCTION

Decisions about water pollution control and management in river systems are increasingly based on predictions made with water quality models. Therefore, water-quality models that are used to assess water-pollution plans should be reliable enough to allow successful results. A successful application of a model is strongly related to the quality of model calibration. However, in most cases, the inadequacies of the data in addition to the measurements errors and uncertainties result in weak assumptions regarding model parameters during the calibration process.

In this paper the influence of parameter uncertainty on a water-quality model prediction is investigated through the application of sensitivity analysis. An unbiased sensitivity analysis based on the Latin Hypercube Sampling (LHS) technique in combination with regression and correlation analysis is applied to the DUFLOW model developed for the Dender River in Belgium. This analysis aims to identify the parameters to which model output is most sensitive and to investigate whether the most sensitive parameters identified under a high pollution load still remain important when the model is applied under better water-quality conditions. A comparison with an earlier centralized (i.e. biased toward central values) sensitivity analysis (Manache &Melching, 2004) also is done.

APPLICATION OF THE DUFLOW MODEL TO THE DENDER RIVER

The Dender River is a tributary of the River Scheldt located in the Flemish region of Belgium. Several sources of pollution contribute directly or indirectly to water-quality problems in the Dender River. During dry periods, the high pollutant loads combined with low flow velocity and low discharges result in negative impacts on the water quality in the river. To improve the water quality of the Dender River, a pollution abatement plan (AWP-II) was proposed by the Flemish government (VMM, 1994). This plan considers removal of about 90% of the carbonaceous biochemical oxygen demand (CBOD), 44% of nitrogen, and 75% of phosphorus with reference to pollutant loads during 1994.

The flow and water-quality model DUFLOW (1992) was used to simulate flow and water-quality variables in the Dender River. The DUFLOW model was calibrated to the available measurements of dissolved oxygen (DO), CBOD, ammonium as nitrogen (NH4-N), nitrate (NO3-N), and inorganic phosphorous (PO4-P) concentrations at three places along the Dender River. Taking into account errors in the input data, it is possible that the set of calibrated parameters cannot be considered as unique and conceptually realistic to give good results when the DUFLOW model is applied under conditions different from those of the calibration period.

SENSITIVITY OF THE DUFLOW MODEL TO ITS INPUT PARAMETERS

To identify the parameters to which the model prediction is most sensitive, sensitivity analysis is carried out on the DUFLOW model based on the LHS technique in combination with correlation analysis (McKay *et al*., 1979; McKay, 1988). Within the DUFLOW model, 37 parameters were used for modeling the water quality processes in the Dender River. Twenty nine parameters were considered uncertain, while the other eight parameters are assumed to have a small effect on the model uncertainty (Manache, 2001; Manache & Melching, 2004).

The software package UNCSAM (Janssen *et al*., 1992) was then used to generate the N sets of the random parameter values corresponding to the LHS procedure. The sample size N was taken equal to 4/3 times the number of the uncertain parameters resulting in 40 combinations of 29 parameters. The DUFLOW model was executed successively with the 40 sets of generated parameters to simulate DO, CBOD, NH4-N, NO3-N, and algal biomass concentrations along the Dender River over a period of one year (1990). Sensitivity measures based on correlation analysis (Janssen *et al*., 1992; Janssen, 1994) between the model input parameters and the considered model output were computed. These measures are used to rank the importance of the uncertain DUFLOW parameters. The sensitivity analysis was done on the amount of time that DO concentrations are less than a specified value (2, 3, and 4 mg/l) over a period of one year (1990). Two locations on the Dender River are considered for model analysis: Denderleew and Denderbelle.

EFFECT OF THE WASTEWATER TREATMENT LEVELS ON MODEL SENSITIVITY

In the centralized sensitivity analysis of the DUFLOW model of Manache & Melching (2004) distributions centered around the calibrated model parameters are used to generate the LHS samples. Considering the high level of pollution in the Dender River, it is likely that the effects of the loads overpower the effect of the model parameters for much of the calibration period, and, thus, the calibration might become insensitive to a broad range of the model parameter values.

Taking this hypothesis into account, the effect of the wastewater treatment level on model sensitivity, is investigated without considering any reference values for the parameters so the LHS technique is unbiased. The unbiased sensitivity analysis was done with the LHS sample generated from uniform distributions for all uncertain parameters. Two cases of pollutant load conditions were considered: 1994 conditions where only 12% of the waste flow is treated (case I) and future conditions according to the pollutant reduction scenario (AWP-II) proposed by the Flemish Government (case II). The model is then executed 40 times (for the 40 LHS samples) over a period of one-year (1990) to simulate the DO concentrations in the Dender River.

Correlation-based coefficients the Semi Partial Coefficient (SPC) and the Semi Partial Rank Coefficient (SPRC) are used to identify the parameters to which the DUFLOW model is most sensitive. The SPC and SPRC were identified as the most robust and reliable sensitivity measures by Manache (2001) and Manache & Melching (2008). To study the convergence of LHS results between cases I and II SPC and SPRC values that are different from zero at the 5% significance level are identified as the parameters significantly affecting model-output uncertainty.

In this paper, unbiased sensitivity analysis results are demonstrated on the amount of time during which the DO concentrations are less than 4 mg/l at Denderleew. The comparison of the sensitivity results between cases I and II illustrates whether the identification of key model parameters under a high level of pollution is good enough to allow the model to be reliably used for water-quality planning. The highly ranked parameters determined by the SPC and SPRC for cases I and II are listed in Table 1.

Table 1 Parameters that have a significant effect on the amount of time DO concentrations are less than 4 mg/l at Dendeleeuw as obtained from LHS analysis for cases I and II (only the first 6 ranks are given).

Parameter	**Case I**		**Case II**		Case I		**Case II**	
	SPC	Rank	SPC	Rank	SPRC	Rank	SPRC	Rank
is	0.48	2 *	0.47	1 *	0.28	3	0.33	5 *
e0	0.50	1 *	0.45	2 *	0.32	2 *	0.36	3 *
kdie	0.27	3	0.37	3 *	0.24	4	0.35	4 *
umax	-0.12	11	-0.30	4	-0.19	5	-0.39	2 *
kbod	0.18	5	0.28	5	0.68	1 *	0.45	1 *
kres	0.17	6	0.14	9	0.11	9	0.17	6
kden	-0.19	4	-0.08	13	0.03	23	0.13	11

[* The correlation coefficient is significant at 5% level on the basis of the t-statistic, i.e. coefficient greater than 0.312]

Based on the 5% significance level criterion for the SPC, two sensitive parameters are identified for case I: the optimal light intensity (is) and the background light extinction (e0). For case II three parameters are identified as important parameters: is, e0, and the algal die rate (kdie). Based on the SPRC, more parameters are identified for case II than for case I. Only two important parameters are identified for case I: the oxidation rate constant for CBOD (kbod) and e0 while five sensitive parameters are identified for case II: is, kdie, e0, algal maximum specific growth rate (umax), and kbod. The SPRC results in Table 1 indicate that kbod has a very strong correlation with the selected DO concentration characteristic for the 1994 loading conditions, whereas it has a much weaker but still significant correlation for the AWP-II scenario. This indicates that as the CBOD load is reduced, kbod has less effect on DO concentration characteristics. In particular, once kbod no longer is the dominant parameter, the importance of many other model parameters can be detected. Similar sensitivity analysis results were also obtained for Denderbelle.

CONCLUSIONS

The effect of pollutant load reduction on the identification of the DUFLOW model parameters affecting model output uncertainty has been investigated through the comparison between two scenarios of pollutant loads—the low treatment conditions in 1994 (case I) and future conditions according to the load reduction scenario AWP-II (case II)—via unbiased and centralized sensitivity analyses. For the unbiased sensitivity analysis, uniform distributions are assigned to the uncertain parameters based on the ranges of reasonable values of the parameters obtained from the literature.

According to the 5% significance level criterion of the SPC, the parameters is and e0 were identified to be the most influential in both cases I and II for the model outputs at Denderleeuw and Denderbelle. One additional parameter, kdie, was identified for case II compared to case I. The comparison of results based on the SPRC leads to a different identification of the important parameters for the considered model output. For case I, kbod is identified as the dominant parameter whereas five important parameters were identified for case II: is, kdie, e0, umax, and kbod. This important finding highlights the strong effect of kbod on the model output uncertainty for the untreated conditions in 1994 (i.e. high load of CBOD). When the CBOD load is reduced according to the AWP-II scenario (i.e. removal of about 90% of CBOD), kbod has less effect on the model output. Specifically, once kbod is not dominant, the importance of other model parameters can be detected such as e0, is, kdie, and umax.

The results presented in this paper showed that unbiased and centralized sensitivity analyses may yield similar identifications of key parameters. However, the dominant effect of kbod for the 1994 load conditions in the unbiased sensitivity analysis indicates that this analysis could be useful prior to model calibration to determine parameters for which detailed field data are needed.

REFERENCES

DUFLOW (1992) A micro-computer package for the simulation of one-dimensional unsteady flow and water quality in open channel systems. *Manual for DUFLOW version 2.00, ICIM, Rijswijk.*

Janssen, P. H. M., Heuberger, P. S. C. & Sanders, R. (1992) UNCSAM 1.1: A software package for sensitivity and uncertainty analysis. *Report No. 959101004, National Institute of Public Health and Environmental Protection, Bilthoven, the Netherlands.*

Janssen, P. H. M. (1994) Assessing sensitivities and uncertainties in models: A critical evaluation. In: *Predictability and Nonlinear Modelling in Natural Sciences and Economics*. (ed. J. Grasman & G. Van Straten), Kluwer Academic Publishers, Dordrecht. 344-361, *Proceedings of the 75th Anniversary Conference of WAU, April 5-7, 1993, Wageningen, The Netherlands.*

Manache, G. (2001) Sensitivity of a continuous water-quality simulation model to uncertain model-input parameters. *PhD Thesis. Chair of Hydrology and Hydraulics, Vrije Universiteit Brussel, Brussels, Belgium.*

Manache, G. & Melching, C. S. (2004) Sensitivity analysis of a water-quality model using Latin Hypercube Sampling. *Journal of Water Resources Planning and Management* **130**(3), 232-242.

Manache, G. & Melching, C. S. (2008) Identification of reliable sensitivity analysis measures for importance ranking of water-quality model parameters. *Environmental Modelling and Software* **23**(5)**,** 549-562.

McKay, M. D., Beckman, R. J. & Conover, W. J. (1979) A comparison of three methods for selecting values of input variables in the analysis of output from a computer code. *Technometrics* **21**(2), 239-245.

McKay, M. D. (1988) Sensitivity and uncertainty analysis using a statistical sample of input values. In: *Uncertainty Analysis* (ed. Y. Ronen), *CRC Press, Inc., Boca Raton, Florida*, 145-186.

Vlaamse Milieumaatschappij (VMM) (1994) Ontwerp AWP-II Dender en Mark. VMM-bestuur beleid en planning, Erembodegem. 137 p. (in Dutch).

Tracer measurements and modelling of longitudinal dispersion - a new approach to evaluate renaturation projects and prediction of contaminant transport at river flows

C. NOSS, T. SALZMANN & I. STORCHENEGGER
University of Rostock, Institute for Environmental Engineering, Satower Str. 48, 18051 Rostock, Germany
thomas.salzmann@uni-rostock.de

Abstract Field and flume experiments on dispersion enable to total the integer hydraulic impact of all structural elements between two cross-sections. As a first approximation the gradients between the longitudinal dispersion coefficient and parameters of velocity equations, represented by the ratio of mean velocity and the root of the energy slope, were set constant and could be used to distinguish the investigated streams from each other. Field sides, methods for estimating the dispersion and hence a novel dispersivity factor will be presented.
Keywords longitudinal dispersion; tracer measurements; dispersion model; river flow; stream diversity; field side

INTRODUCTION

River restoration strives to increase flow diversity, however there are no objective result checking so far. Natural channels have little in common with engineered channels. Their roughness, velocity distribution and abrupt change of bed do not meet the basic assumptions of flow equations. Missing a common model to predict velocity distribution (Nikora *et al*., 2007) we experienced a new approach to quantify flow diversity. We focussed on reaches as well as on cross sections and assumed stream diversity to be linearly affected by momentum transfer. Momentum exchange involves exchange of mass which may be observed and quantified as dispersion coefficient. Existing empirical and semi-empirical equations to calculate dispersion coefficients turned out to be poorly comparable (Seo & Cheong, 1998). This study works out a method to characterize low diversity of different rivers by analyzing dispersion coefficients.

TRACER MEASUREMENTS

Tracer Measurements were performed at several reaches of Hellbach- and Nebel-river in north-east Germany. The Hellbach section was returned to a near-natural condition ten years ago. The river bed form and roughness distribution were highly non-uniform with meanders, woody debris and local scours along the section. At the Nebel, three different sections were observed. The bulk of the Nebel measurements were taken in a constructed reach (Nebel 1). Abandoning maintenance reed at the sides and macrophytes in the bed forced the stromstrich to undulate. Additional measurements were taken at two other Nebel sections and at a flume without form resistance. The reach Nebel 2 adjoins the Nebel 1 downstream and is pristine. Nebel 3 is the totally restored reach Nebel 1 with meanders and roughly constructed banks, but without any vegetation or other near-natural components. Table 1 displays the bulk hydraulic characteristics of these five reaches for minimum and maximal discharge. Geometric parameters correlated strongly with discharge at the Hellbach and in addition with the stage of vegetation at the Nebel.

Table 1 Characteristics at the investigated sections for minimum and maximal discharge.

	Q ($m^3\ s^{-1}$)	$A(Q)$ (m^2)	$r_{Hy}(Q)$ (m)	$I_E(Q)$ ($\times10^{-3}$)	$\lambda(Q)$ (1)
Hellbach	0.18 / 1.56	1.69 / 4.22	0.32 /0.63	2.04 / 1.35	2.11 / 0.50
Nebel 1	0.47 / 2.15	4.31 / 6.77	0.55 / 0.66	0.79 / 0.6	2.57 / 0.31
Nebel 2	1.32	-	-	0.64	-
Nebel 3	1.32	-	-	0.48	-
Flume	0.025 / 0.05	0.09 / 0.12	0.10 / 0.12	1.95 / 2.58	0.17 / 0.12

Q = Discharge, minimum / maximum.
A = Mean cross-sectional flow area at minimum / maximum discharge.
r_{Hy} = Hydraulic Radius at minimum / maximum discharge.
I_E = Slope of Energy at minimum /maximum discharge.
λ = Resistance coefficient (Darcy-Weisbach equation) at minimum / maximum discharge.

Uranin ($C_{20}H_{10}O_5Na_2$) was applied as tracer and detected with up to five field fluorometers. The experiments were conducted at night to avoid loss of fluorescence due to sun light. Strong secondary currents lead to intense transverse mixing. That is why total mixing across the entire channel was stated close to the point of injection. Each value of concentration corresponded to the cross-sectional mean and the dispersion could be analysed as longitudinal dispersion.

ESTIMATING DISPERSION COEFFICIENTS

We used the Fickian model of longitudinal dispersion and the Transient-Storage model to determine dispersion coefficients. Rutherford (1994) describes the routing of a tracer cloud with the Fickian model of longitudinal dispersion by

$$c(x_2,t) = \int_{\tau=t_0}^{t} \frac{c(x_1,t)(x_2-x_1)}{(t-\tau)\sqrt{4\pi k_x (t-\tau)}} \exp\left[\frac{\left[x_2-x_1-u_c(t-\tau)\right]^2}{4k_x(t-\tau)}\right] d\tau \tag{1}$$

where $c(x_2,t)$ = concentration (g m^{-3}) at place x_2 (m) and time t (s), k_x = longitudinal dispersion coefficient ($m^2\ s^{-1}$), u_c = mean tracer velocity (m s^{-1}), τ = time lag (s) and t_0 = the time (s) when the tracer cloud $c(x_1,t)$ first arrived the position x_1 (m). Simulated annealing was used to optimize u_c and k_x.

The Transient Storage Model (Eq. 2) is an extension of the Fickian model, taking into account the exchanges with dead zones. We used the software OTIS-P (Runkel, 1998), which solves the dispersion and transient storage equations numerically through the Cranck-Nicolson-Algorithm. A parameter estimation algorithm optimised the dead zone percentage η ($m^3\ m^{-3}$) and the exchange coefficient ε (s^{-1}) in addition to the parameters of the Fickian model for each subsection.

$$\frac{\partial c}{\partial t} + u_c\frac{\partial c}{\partial x} = \frac{1}{A}\frac{\partial}{\partial x}\left(A k_x \frac{\partial c}{\partial x}\right) + \varepsilon\left(c_S - c\right), \qquad \frac{\partial c_S}{\partial t} = \frac{\varepsilon}{\eta}\left(c - c_S\right) \tag{2}$$

where c_S = concentration (g m^{-3}) in the dead zone.

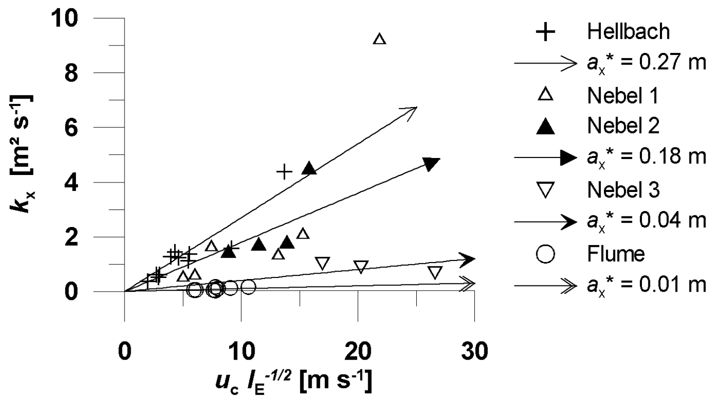

Fig. 1 Dispersivity factors at the investigated sections.

DISPERSIVITY FACTORS

The dispersion coefficient results from velocity shear and turbulent diffusion. Structural elements which increase secondary currents and hence the transverse dispersion homogenize the tracer distribution and reduce the longitudinal dispersion coefficient. Otherwise structural elements which increase the velocity distribution across the flow section increase the velocity shear and thus, the dispersion. It appears impossible to prove stream diversity based only on the dispersion coefficient. Relating dispersion with discharge and characteristics of different rivers or reaches encounters several difficulties. A common geohydrologic parameter to characterize aquifers is the dispersivity, the ratio between dispersion coefficient and the mean transport velocity. With mean tracer velocity approximating the mean transport velocity, the dispersivity could be viewed as a parameter taking into account different discharges and sizes. Multiplying the dispersivity by the square root of the slope of energy, one obtain a factor, below designated as dispersivity factor a_x^*, between the dispersion and the combined influences through flow resistance and river bed geometry.

$$k_x = a_x^* \frac{u_c}{\sqrt{I_E}} = a_x^* \sqrt{\frac{8\, g\, r_{Hy}}{\lambda}} \tag{3}$$

where g = gravity acceleration (m s^{-2}).

Fig. 1 shows pairs of variates k_x and $u_c\ I_E^{-1/2}$ from the routing procedure (Eq. 1). Due to the sample sizes the analysis of correlation coefficients is confined to the experiments at Hellbach and Nebel 1. The highest correlation coefficient was obtained at the Hellbach with r = 0.94 for a dispersivity factor of a_x^* = 0.27 m. Although the Hellbach measurements involved the widest range of discharges and most developed heterogeneity of structural elements, the correlation at Nebel 1 was only r = 0.54. This result could be manifested with the uncontinuous influence of macrophytes onto the dispersion and flow resistance and hence onto the stream diversity. The lowest dispersivity factor occurred, as expected, at the flume with a_x^* = 0.01 m. The measurement at the Nebel 2 showed dispersivity factors in the same range as the Nebel 1 section. Surprisingly Nebel 3 showed dispersivity factors lower than both, which could be interpreted in respect to the lack of near-natural elements along the new river bed. Fig. 2 shows the parameters of the Transient Storage Model (Eq. 2) versus the ratio of transport velocity with root of energy slope at the Hellbach. No functionality was recognized and yielded no advantage for a simple differentiating of river sections in comparison to the routing procedure. In other words, the dispersion coefficient of the simple routing procedure represents all hydraulic impacts of structural elements at the reach of interest.

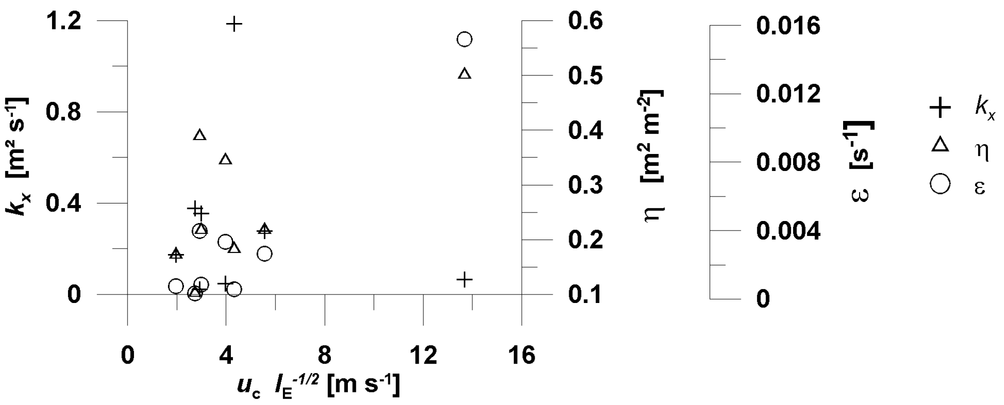

Fig. 2 Parameters of the Transient Storage Model at the Hellbach.

DISCUSSION AND CONCLUSION

The tracer measurements at different open channel flows showed different means of dispersivity factors independent from discharge. As a consequence, the dispersivity factor could be used to estimate stream diversity in river sections or to monitor hydraulically the processes after reconstruction to a near-natural condition. In comparison to analysis based on one-dimensional flow equations or with models for velocity distributions, the dispersion offers the advantage of representing exchange and transport processes integratively within the flow field. Without influences of macrophytes just a small amount of measurements is necessary to calculate the dispersivity factor. Vice versa, knowing the dispersivity factor and the parameters of a one-dimensional flow equation for a river section, it would be possible to predict the dispersion at any discharge. Therefore tracer measurements are a helpful tool for operative protection against gross damages.

REFERENCES

Nikora, V. I., McLean, S. R., Coleman, S., Pokrajac, D., McEwan, I., Campbell, L., Aberle, J., Clunie, D. & Koll, K. (2007) Double-averaging concept for rough-bed open-channel and overland flows: Applications. *Journal of Hydraulic Engineering* **133**(8), 884-895.

Runkel, R. L. (1998) One-dimensional transport with inflow and storage (OTIS): A solute transport model for streams and rivers. U.S. Geologic Survey, *Water Resources Investigation Report* 98-4018.

Rutherford, J. C. (1994) *River Mixing*. John Wiley and Sons, New York, USA.

Seo, I. W. & Cheong, T. S. (1998) Predicting longitudinal dispersion coefficient in natural streams. *Journal of Hydraulic Engineering* **124**(1), 25-32.

Nitrogen leaching forecasting: modelling and measurements

C. SOHIER[1], C. VANDENBERGHE[2], S. DAUTREBANDE, J. M. MARCOEN[2] & A. DEGRÉ[1]

1 *Hydrology and Hydraulic Eng. Gembloux Agricultural University. Passage des Déportés 2, 5030 Gembloux, Belgium*

degre.a@fsagx.ac.be

2 *Geopedology. Gembloux Agricultural University*

grenera@fsagx.ac.be

Abstract European nitrate directive (CEE/91/676) imposes wide monitoring of Nitrogen in farmlands. The Walloon Region (South of Belgium – 750 000 ha of arable land) develops an original combination of methods to reach European objectives in this topic. On the one hand, water and nitrogen flows and balances are modelled, on the other hand, an Agricultural Surface Survey is put into practice to monitor nitrate nitrogen in the soil at the beginning of the leaching period. The Agricultural Surface Survey is constituted by a 30 reference farms network within more than 200 plots are monitored each in order to fix annual standards for nitrate profiles. Each year, about 1% of the Walloon farms are assessed about their good nitrogen management. Thanks to the existence of a useful database of nitrate profiles measured through six years in the whole Walloon Region, validation of the simulations in the vadose zone can be realised. The comparison of the measured data and the simulation shows a good accuracy of the EPICgrid model.

Keywords nitrogen; modelling; leaching; residue measurements

INTRODUCTION

In the Walloon Region of Belgium, winter wheat, sugart beet and silage maize represents more than 70% of the annual crops (Leteinturier *et al.*, 2007). About 80% of the drinking water supply come from groundwater. In the last 15 years, no significant improvement of the water quality has been observed. About 7% of the sites of abstraction show nitrate concentrations higher than 50 mg/l and 61 % are lower than 25 mg/l. In the vulnerable zones, 17% of the sites of abstraction show nitrate concentrations higher than 50 mg/l and only 22 % are lower than 25 mg/l.

Due to the thickness of the loamy unsaturated layer (sometimes higher than 20 meters in the well named loamy region), modelling is necessary to predict the effects of the agricultural practices changes on the groundwater quality.

The European Directive CEE 91/676 was put into practice by the Nitrogen Management Programme in Agriculture ("Programme de Gestion Durable de l'Azote en agriculture", P.G.D.A.). The first Action Programme has limited the application of organic nitrogen to 210 kgN/ha units on grasslands and to 120 kgN/ha on agricultural crop lands (80 kgN/ha in vulnerable zones). Farmers had the possibility to obtain an exemption to apply more organic nitrogen ("Quality Approach"), subject to evidence of good nitrogen management in their farming practice. Such evidence was obtained by means of the nitrate profiles established at the beginning of the leaching period, i.e. from October to December.

In order to determine the annual standards for these nitrate profiles, a network of 30 reference farms is monitored. This network, which is distributed throughout the Walloon region, makes it possible to account for annual meteorological conditions, soil type, cropping systems (Vandenberghe & Marcoen, 2004).

The first aim of this paper is to present how the action program is monitored in Walloon Region using an original combination of local measurements and global and local modelling. The second aim consists in a close-up on the leachable nitrogen present into the soil at the beginning of the leaching period, using measurements and modelling. The combination of these two methods will show how they are complementary to monitor nitrogen management in agriculture.

MATERIAL AND METHODS

Local modelling

Water and nutrient flows and balances are modelled using an EPIC derived software (Williams, 1995): EPICgrid. This model, developed in Gembloux Agricultural University, was adapted to local soil characteristics, particularly concerning soil texture, depth, layering, and hydrodynamic parameters. The “plant-growth” and “nutrient uptake” modules were also reviewed to fit the local crops observations (Cocu *et al*., 1999). The unsaturated soil description was extended down to the groundwater table using geological data (Masereel & Dautrebande, 1995; Hallet & Barbier, 2007).

EPICgrid model allows daily simulation of water and nutrient flows as well as the transformation and degradation processes in the soil (Sohier *et al.*, 2008).

Regional modelling

Once coupled with a geographical information system, and linked with the data bases presented in Table 1, EPICgrid become regional modelling software. It uses one square kilometre grids. Within each cell, it identifies consistent hydrological units. According to the agricultural statistics in the main regions (Borgers *et al*., 2007), EPICgrid represents a soil occupation map statistically representative. Mineral fertilisation, pasture and manure spreading are taken into account, also spatially.

Table 1 Databases used in regional model EPICgrid.

Data	Reference
Soil	Tavernier & Marechal,1972
Geology	Laime & Dautrebande, 1995 and Hallet & Barbier, 2007
Land use	Laime & Dautrebande, 1995
Agricultural practices	Borgers *et al.* 2007
Digital elevation model	Laime & Dautrebande, 1995

In situ measurements

The 30 reference farms constitute the ‘Survey Surface Agricoles” within more than 200 plots are monitored. The fertilisation of the main crops on these fields is calculated to obtain an optimal yield and also to minimise the post-harvest residue. The development of the nitrogen residue is monitored over time by taking three samples on 90 cm depth (3 layers of 30 cm). The average nitrate profiles are then calculated each year for each crop (Table 2), a well as the average per crop for each agricultural region. These averages serve as the reference for evaluating nitrate profiles measured in farms in the scope of the “Quality Approach”. Whenever, for a given culture in a particular region, the nitrate profile of a farm using the “Quality Approach” exceeds the reference value, the farmer must take measures to improve his fertilisation practice as well as the catch crop management.

Table 2 Average nitrate profiles (means of n measures) per crop type (kg N-NO3 / ha) in 2004.

	October Average nitrate profiles	n	November Average nitrate profiles	n	December Average nitrate profiles	n
Cereals	88	40	62	41	47	39
Potatoes	104	7	78	7	63	7
Sugar beet	-	-	34	21	34	18
Maize	-	-	78	20	62	20
Grasslands	55	38	40	42	29	39

About 300 farmers are involved in Quality approach. In 5 of their plots, nitrate profiles are measured each year. So more than 1500 measurements are annually realised and compared with the standards described below.

RESULTS AND DISCUSSION

Modelling's results

EPICgrid allows calculating the water and nutrient flows under actual conditions as well as under different scenarios (climate change, agricultural practices …). As an example, Fig. 1 presents the actual nitrate concentration of leaching water under the root zone (1,5m) at the regional scale (mean value 2001-2005, Sohier *et al*., 2008). This nitrogen, lost for plant uptake, is an important pressure indicator for nitrogen management.

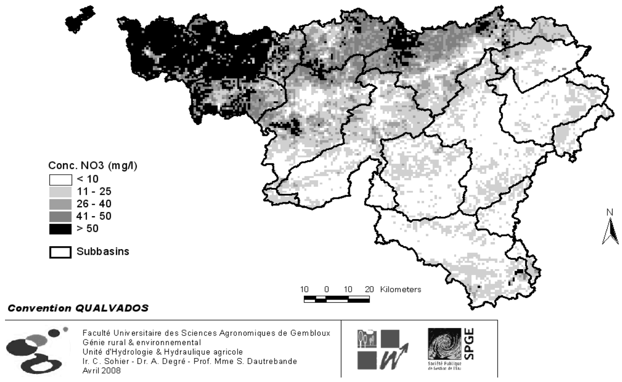

Fig. 1 Nitrate concentration of leaching water under the root zone (1.5m) – years 2001-2005.

One can see that North and particularly North-West of Walloon Region presents the higher pressure level concerning nitrate leaching. This region is mainly dedicated to crop productions.

Measurements results

The measurements made in the 30 reference farms network show, through the four years monitored, differences between years but also the good impact of the catchcrop sowed after the harvest on the nitrate nitrogen residue in the soil (Fig. 2).

The bigger dispersion of the results in the class of winter wheat (without sowing of a catchcrop) is due to the multiplicity of agricultural practices: it could be a bare soil until sowing of sugar beets next spring, a colza or barley sowed in October.

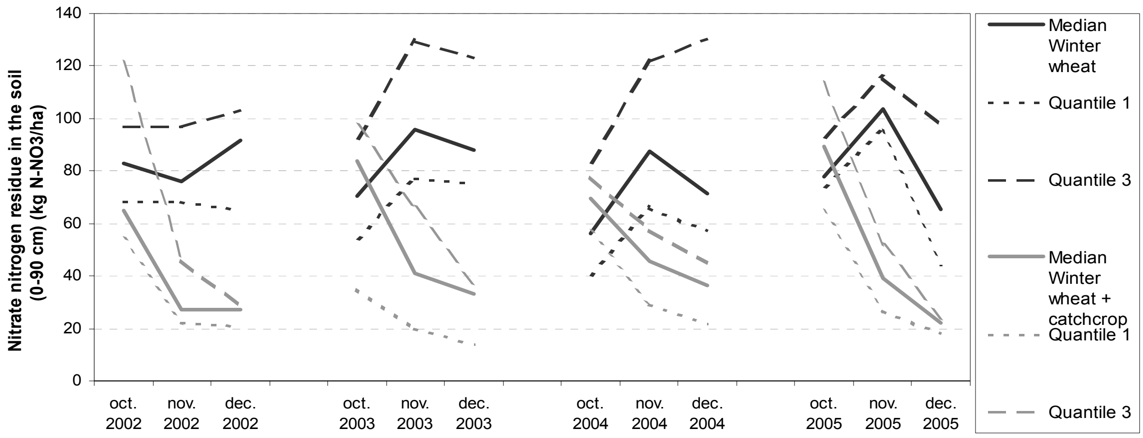

Fig. 2 Nitrate nitrogen residue in the soil during the automn following winter wheat harvest.

Comparison and regional up-scaling

Fig. 3 shows both the modelling's results of nitrate residue in the soil after wheat considering different crop rotations and the results of in situ measurements. One can see that the level of potentially leachable nitrogen in the soil is well evaluated by the model at the beginning of the leaching period and that the degradation and transformation are also well taken into account even if an important variability exists between the rotations.

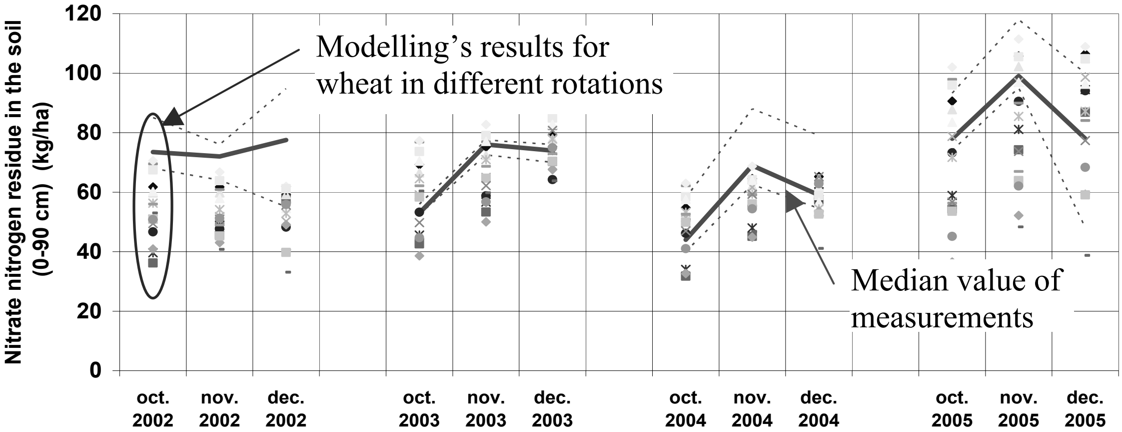

Fig. 3 Potentially leachable nitrogen after wheat: measurements and modelling comparison.

CONCLUSION

Due to the thickness of unsaturated soil in Walloon Region, the Nitrogen management programme will need up to 30 years to impact water recharge quality in the whole Region. To size up its efficiency, a monitoring was put into practice. It includes on the one hand local measurements in 200 fields and, on the other hand local and regional modelling. The local measurements are useful for the evaluation of local agricultural practices and also, we showed that the results of the local modelling are validated by the measurements. As a consequence, the results of regional modelling become useful for regional nitrogen management (e.g. pre-normative modelling).

REFERENCES

Borgers, N., Vandenberghe, C. & Marcoen, J. M. (2007) Des pratiques agricoles aux reliquats en azote nitrique des sols en région wallonne. Collaboration scientifique entre l'Unité d'Hydrologie et d'Hydraulique agricole et le Groupe de Recherche en Environnement et Ressources Azotées dans le cadre de l'Evaluation des mesures prises pour réduire les incidences de la pollution diffuse d'origine agricole et domestique sur la qualité des masses d'eau de surface et souterraines de la région wallonne à l'aide du modèle EPICgrid-PIRENE (Convention RW-SPGE). Gembloux: Faculté Universitaire des Sciences Agronomiques, 76 p. http://www.fsagx.ac.be/gp/grenera/grenera_publications.htm

Cocu, X., Moeremans, B., Frankinet, M. & Dautrebande, S. (1999) Water-soil-crop Model and Radar Interferometry on Fields in Belgium. *Proceedings of the International Conference and Workshop ALPS99*, CNES, Méribel, France, 18-22 January 1999, WK3-P-07-pp 1-5.

Hallet, V. & Barbier, F. (2007) Convention de sous-traitance entre la Faculté Universitaire des Sciences Agronomiques de Gembloux et les Facultés Universitaires Notre-Dame de la Paix dénommée: « Etude bibliographique visant à préciser le cadre géologique et hydrogéologique au droit des mailles du modèle EPICgrid ». Département de Géologie. Faculté des sciences. Faculté Notre-Dame de la Paix. 46p. et annexes.

Masereel, P. & Dautrebande, S. (1995) Modélisation de l'évolution des profils hydriques sous froment en région limoneuse. *Bull. Rech. Agron. Gembloux* **30**(4), 353-372.

Laime, S. & Dautrebande, S. (1995) Projet pilote CARHY. Ministère wallon de l'équipement et des transports. *Service fédéraux des affaires scientifiques techniques et culturelles. Programme de recherche dans le domaine de la télédétection par satellite – phase III*, FUSAGx, 164p+annexes.

Leteinturier, B., Tychon, B. & Oger, R. (2007) Diagnostic agronomique et agro-environnemental des successions culturales en Wallonie (Belgique). *Biotechnologie, Agronomie, Société et Environnement* **11**(1), 27-38.

Sohier, C., Degré, A.. & Dautrebande, S. (2008) Evaluation des mesures prises pour réduire les incidences de la pollution diffuse d'origine agricole et domestique sur la qualité des masses d'eau de surface et souterraines de la Région Wallonne à l'aide du modèle EPICgrid. Convention SPGE-DGRNE-FUSAGx. *Hydrology and Hydraulic Eng., Gembloux agricultural university*. 145p +annexes

Tavernier, R. & Maréchal, R (1972) Carte des Associations des Sols 1:500,000. *Atlas de la Belgique, feuilles IIA et IIB*. Bruxelles, Belgique.

Vandenberghe, C. & Marcoen, J. M. (2004) Transposition de la Directive Nitrate (CE) en Région wallonne: azote potentiellement lessivable de référence pour les sols cultivés en Région wallonne. *Biotechnologie, Agronomie, Société et Environnement* **8**(2), 111-118. http://www.bib.fsagx.ac.be/library/base/text/v8n2/111.pdf

Williams, J. R. (1995) The EPIC model. In: *V.P. Singh, Editor, Computer models of watershed hydrology*, Water Res. Publ., Littleton, CO.

Choosing among costly water quality monitoring schemes: optimal information gathering in the management of surface erosion

DAVID TOMBERLIN
National Marine Fisheries Service, 1315 East-West Highway, Silver Spring, MD 20910 USA
david.tomberlin@noaa.gov

Abstract This paper presents a framework for choosing among protocols for assessing surface water quality when the protocols differ in cost and in the quality of the information they provide. In particular, we consider two protocols for estimating sediment loading from forest roads, one that relies on settling basins only and another that augments the settling basins with laboratory analysis of suspended sediment. Casting the choice among protocols as a partially observable Markov decision process enables us to identify the conditions under which each protocol is preferred, taking into account the expected costs and benefits of available management actions, the cost and quality of information provided by each monitoring protocol, and the ability to adapt as new information becomes available.
Keywords sediment; surface erosion; water quality monitoring; adaptive management; Markov decision process

INTRODUCTION

This paper presents a framework for choosing among water quality monitoring protocols that vary in cost and information quality. In the context of managing sediment loading due to surface erosion, different approaches to monitoring sediment production are possible, with the more expensive protocols generally yielding better information (in the sense of providing more precise estimates of the true rate of sediment loading). Here, the trade-off between the cost and quality of candidate monitoring protocols is treated within a partially observable Markov decision process (POMDP). This approach may be thought of as a particular formalization of adaptive management, in that decisions are made in a dynamic and stochastic environment based on beliefs that change as new information becomes available.

The POMDP is applied in a simplified example based on data from coastal California. Sediment from forest roads is the major water quality issue in the region, but little known about sediment loading rates: simulation models are regarded as untrustworthy by land managers, and field studies require a large commitment of time and money. The analysis here is motivated by an important practical question in water quality management, namely, how much time and money should be put into monitoring sediment loading, when those same resources could be spent instead on remedial measures to reduce sediment production at is source?

MODEL

The POMDP is a collection of sets $\{S, P, A, W, \Theta, R\}$ (Cassandra 1994), where S is the system's state variables, P represents state dynamics as transition probabilities, A is the actions available to an agent, W is the rewards to taking particular actions in particular states, Θ is a set of possible observations on the state variables, and R is a set of observation probabilities. Observations $\theta\in\Theta$ are the only information the agent has on the unobservable true state, S. The observation model R describes the probabilistic relationship between observations θ and the true state S. The problem solver (here, a land manager) uses observations θ and the observation model R to estimate the state S.

The model assumes the manager's goal is to minimize long-run discounted total costs of sediment control, which includes the cost of monitoring sediment production. The actions that achieve this goal are identified with dynamic programming (Bertsekas 2000) through a recursively defined value function V:

$$V_t(\pi) = \max_a \left[\sum_i \pi_i q_i^a + \beta \sum_{i,j,\theta} \pi_i p_{ij}^a r_{j\theta}^a V_{t+1}[T(\pi \mid a, \theta)] \right]$$

where

π_i = subjective probability of being in state $i \in S$ at time t

q_i^a = immediate reward for taking action $a \in A$ in state $i \in S$ at time t

β = discount factor

p_{ij}^a = probability of moving from state $i \in S$ at time t to state $j \in S$ at time $t+1$ after taking action $a \in A$

$r_{j\theta}^a$ = probability of observing $\theta \in \Theta$ after taking action $a \in A$ and moving to state $j \in S$

T = function updating beliefs based on prior beliefs and observed θ

V is the greatest expected net benefit that the agent can achieve over time, taking into account that as conditions change in the future, different actions may be warranted. The solution of V yields an optimal policy, which is a mapping from beliefs about the current state, π, into the optimal action.

In our setting, the state variable S is a forest road segment's potential to deliver sediment to the stream system, which for expository purposes takes only two possible values, *High Erosion* and *Low Erosion.* The action set A consists of *Maintain* (i.e., neither monitor sediment loading nor take remedial measures to reduce loading), *Monitor Low* (i.e., monitor with settling basins only), *Monitor High* (i.e., monitor with settling basins augmented by laboratory analysis of suspended sediment), and *Treat* (i.e., take measures to reduce the potential for sediment production). The observation set consists of the same two possible values as S, *High Erosion* and *Low Erosion*, but an observation of θ = *High Erosion* does not necessarily mean that the true state S =*High Erosion*. Instead, we define an observation model R as follows:

$$R_{j\theta}^1 = \begin{bmatrix} 0.6 & 0.4 \\ 0.4 & 0.6 \end{bmatrix} \quad R_{j\theta}^2 = \begin{bmatrix} 0.63 & 0.37 \\ 0.25 & 0.75 \end{bmatrix} \quad R_{j\theta}^3 = \begin{bmatrix} 0.83 & 0.17 \\ 0.12 & 0.88 \end{bmatrix} \quad R_{j\theta}^4 = \begin{bmatrix} 0.5 & 0.5 \\ 0.5 & 0.5 \end{bmatrix}$$

Each matrix, with the state $j \in S$ defined by row and each observation θ defined by column, defines the probabilistic relationship of observation to true state under a different action. $R_{j\theta}^1$, for example, tells us that after taking action a=1 (*Maintain*) and moving to the unobservable state *j=Low Erosion*, we would observe *θ=Low Erosion* with 60% probability and *θ=High Erosion* with 40% probability. That is, maintaining the *status quo* provides some weak information, presumably through casual observation of the road. $R_{j\theta}^2$, in contrast, tells us that implementing a monitoring plan with settling basins (a=2, *Monitor Low*), yields a stronger basis for inference on S, and $R_{j\theta}^3$ that the more sophisticated scheme *Monitor High* yields still more information.

Finally, $R^4_{j\theta}$ indicates that immediately after treating the road, observations tell us nothing about the true state of erosion, a reflection of how treatments often cause transient changes in erosion rates that tell us little about the true state of the road.

The stochastic dynamics of the erosion level *S* are given by transition probability matrices defined as follows:

$$P^1_{ij} = \begin{bmatrix} 1 & 0 \\ 0 & 1 \end{bmatrix} \quad P^2_{ij} = \begin{bmatrix} 1 & 0 \\ 0 & 1 \end{bmatrix} \quad P^4_{ij} = \begin{bmatrix} 1 & 0 \\ 0 & 1 \end{bmatrix} \quad P^4_{ij} = \begin{bmatrix} 0.95 & 0.05 \\ 0.90 & 0.10 \end{bmatrix}$$

The first two matrices embody the assumption that under *status quo* maintenance or either monitoring program, the state remains unchanged. The final matrix tells us that under a=4 (*Treat*), a *Low Erosion* road stays in that same state with 95% probability, but there is a 5% chance that the treatment will backfire and create a *High Erosion* road. Similarly, treating a *High Erosion* road has an 90% chance of successfully creating a *Low Erosion* road and a 10% chance of failure (meaning the *High Erosion* road stays that way). These values are not derived from field data, but are chosen to reflect a plausible scenario for analysis.

Finally, the reward structure (actually, cost structure) is as follows:

$$W^1_j = \begin{bmatrix} 0 & -15 \end{bmatrix} \quad W^2_j = \begin{bmatrix} -0.5 & -15.5 \end{bmatrix} \quad W^3_j = \begin{bmatrix} -2.5 & -17.5 \end{bmatrix} \quad W^3_j = \begin{bmatrix} -8 & -8 \end{bmatrix}$$

Here the columns of each vector represent the rewards (in USD x 10^3) of taking a particular action in a particular state. W^1 tells us that maintaining the road in *Low Erosion* state will cost nothing, while the cost of maintaining the road in *High Erosion* state is \$15,000 per year, due to the need for cleanup and repair. W^2 and W^3, the payoffs to monitoring, are the same as W^1 less the periodic cost of the monitoring program (\$500 for *Monitor Low* or \$2500 for *Monitor High*, assuming the equipment is already on hand). W^4 tells us that treating the road (by adding rock and mechanically treating likely problems) will cost us the same \$8000 regardless of whether the road is in *Low Erosion* or *High Erosion* state. Comparing all these costs, it's obvious that if the manager knew the true state to be *Low Erosion*, the best choice would be to *Maintain* (a=1), and if the manager knew the true state to be *High Erosion*, the best thing to do would be to *Treat* (a=4). However, the premise of our model, and the reality that managers generally face, is that the true state is unknown.

RESULTS

Fig. 1 shows the value function, *V*, as it evolves over a 5-period decision horizon (the highest solid line is *V* at T-1, the next down is *V* at T-2, etc.). The dashed lines show the division of the state space into policy regions, i.e., the beliefs for which the actions *Treat*, *Monitor Low*, *Monitor High*, or *Maintain* are optimal. The most salient features of the solution are that 1) as the decision horizon lengthens, maintaining the status quo occupies progressively less of the belief space, and 2) *Monitor Low* enters the optimal policy at T-3 and *Monitor High* at T-5, i.e., only after the decision horizon has lengthened sufficiently to merit the increased expenditure on information gathering.

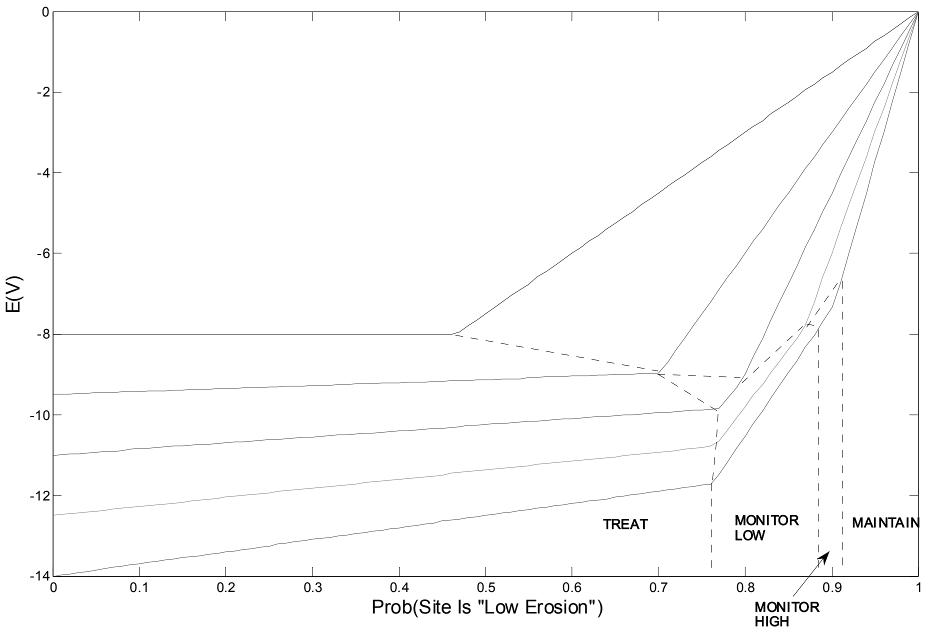

Fig. 1 The value function, V, and optimal policy as a function of beliefs about sediment production, for five different time horizons.

DISCUSSION

The uncertainty inherent in natural resource management requires that we think carefully about allocating scarce resources between monitoring and restoration. The POMDP provides a tool for thinking carefully about this allocation. In the stylized model presented here, we found that for a 5-period decision horizon, both of the monitoring schemes considered (more and less intensive) were part of the optimal policy, but only for 15% of possible beliefs about the true state, while in the other 85% of the belief space the preferred actions were to treat without monitoring or to do nothing. That is, in this example, for most beliefs the costs of monitoring exceed the expected benefit—monitoring was preferred only when the manager had a fairly strong *a priori* belief that the road was a low-erosion site, with monitoring serving essentially to rule out the need for more aggressive and expensive treatment. These beliefs, which we do not have space to explore here, may come from personal experience, field experiments, studies from other areas, or other sources—the POMDP is a Bayesian decision framework that allows beliefs to change with new information.

Our example here has been stylized both for ease of presentation and because POMDPs are known to be computationally intractable. Research on solution techniques is an active field in applied mathematics—more fully developed applications to environmental management will employ recently developed heuristics.

Acknowledgments Thanks to Brian Barrett and Nikos Vlassis for helpful discussions, and to Teresa Ish for work on an earlier application of the model to erosion control.

REFERENCES

Bertsekas, D. (2000) Dynamic Programming and Optimal Control. *Belmont, MA: Athena Scientific*.

Cassandra, A. (1994) Optimal Policies for Partially Observable Markov Decision Processes. *Brown University Department of Computer Science Technical Report* CS-94-14.

Hydro-thermo-mechanical behaviour of the Tournemire compacted shale (SE of France)

J. TREMOSA[1,2], J. GONCALVES[2], J.M. MATRAY[1] & S. VIOLETTE[2]

1 *Institut de Radioprotection et de Sûreté Nucléaire, IRSN/DEI/SARG/LR2S, BP17, F-92262 Fontenay-aux-Roses, France*
joachim.tremosa@irsn.fr

2 *Université Pierre et Marie Curie & CNRS, UMR 7619 Sisyphe, 4 place Jussieu, F-75252 Paris, France*

Abstract A coupled flow process, thermo-osmosis, has been tested in the Tournemire shale, carrying a set of water changes by warmer one in a multi-packers system equipped borehole. Experiments interpretation with a hydrogeological model using coupled flow equations and thermal effects enables to propose a range of thermo-osmotic permeability.

Keywords thermo-osmosis; coupled flow; Tournemire shale

INTRODUCTION

Clay rocks are considered in some countries as a potential host to high-level radioactive waste repositories. The benefits of considering such formations are mainly their containment and insulation natural abilities. Studies on these abilities especially require a full characterisation and quantification of mass transfer processes in these environments. Thermo-osmosis appears to be a process which can significantly affect fluid fluxes in compacted shales (Soler, 2001). However thermo-osmotic coefficients data in the literature are few (Dirsken, 1969; Shrivastava & Avasthi, 1975) and badly constrained as no *in-situ* experiments have been done, so far.

Thermo-osmosis is a coupled transport process which consists in a water flux under a temperature gradient while chemical concentration remains constant. The development of this kind of flux is related to the little pore size of indurate shales and to electrical forces field due to the surface charge of clay minerals. It confers membrane behaviour to the shale, by its ability to partially or fully limit the transport of certain ions and molecules. Thermo-osmosis phenomenon appears because of specific enthalpy differences of water in the boundary layers and pores (Derjaguin *et al.*, 1987).

In the geological context, we can observe temperature gradients at the basin scale due to the regional geothermal gradient or to heat-generating radioactive waste or, during repository galleries excavation (leading to a local modification of the regional geothermal gradient).

THERMO-OSMOSIS EXPERIMENTS

We have carried out *in-situ* thermo-osmosis experiments on the Toarcian shale of Tournemire (SE of France) which presents analogies with rocks likely to host a radioactive waste repository. This formation forms part of the *Grands Causses* Mesozoic basin and is studied at the French Institute for Radiological protection and Nuclear Safety (IRSN) Underground Research Laboratory (URL) located at Tournemire. This URL consists in a century-old tunnel crossing the Toarcian shale and more recent galleries excavated from the tunnel. The shale is characterized by very low porosities (around 9%), hydraulic conductivities (10^{-13} to 10^{-15} $m.s^{-1}$) with a small mean diameter pore size (4-6 nm) and by electrical surface charges (given by a cation exchange capacity about 10 meq.100g^{-1}).

Experiments have consisted in substituting the water in equilibrium with the formation by a warmer one (temperature increments of 2.5, 5 and 9°C) for inducing a potential thermo-osmotic response. Those experiments were performed in a multi-packers system equipped borehole limiting a small test interval (20 cm^3). A special attention was paid for the substitution of the test section water under initial and stabilised pore pressure.

HYDRO-THERMO-MECHANICAL MODELLING OF THE EXPERIMENTS

Pressure evolution in the test interval after the water change shows a rapid decrease, followed by a stabilisation after 1.5 days. Next the pressure tends to increase, very slowly (Fig. 1). We have managed to reproduce the signal by introducing the different expected phenomena in our model.

Experiments were interpreted with a 2D finite differences thermo-hydro-mechanical model based on coupled flux equations combined with mass conservation laws (Gonçalvès *et al.*, 2004), and by adding thermal and thermo-osmotic effects. Thermo-osmotic coupled flow equation can be written:

$$U = -k_T \cdot grad T \qquad (1)$$

where U is the filtration velocity (m.s^{-1}), kT is the thermo-osmotic permeability (m^2.s^{-1}.°C^{-1}) and grad T is the temperature gradient (°C.m^{-1}).

Once the hydraulic properties of the shale were determined, we simulated an aquathermal effect (Luo & Vasseur, 1992) and changes in water properties (viscosity and density) with temperature (Fig. 1). This can account for pressure changes related to water during the temperature dissipation in the shale after the water substitution. In Fig. 1, two curves simulate the thermal effect and limit a range of evolution as a function of the measured system compressibility range. Compressibility appears to be the most sensitive parameter of our model when thermal aspects are introduced.

Next, we identified an additional effect explained as thermo-osmosis by fitting the model prediction to the measured data by using a range of thermo-osmotic coefficients (Fig. 1). However, due to the obtained compressibility range, we are only able to identify a range of thermo-osmotic permeability.

The same methodology was conducted for the three temperature increments (2.5, 5 and 9°C) tested during the different water changes.

Results given by fitting give a range of thermo-osmotic permeability between 4×10^{-11} and 6×10^{-10} m^2.s^{-1}.°C^{-1} as a function of the temperature increment (Fig. 2). These values are in the range of thermo-osmotic permeability obtained in previous experiments (Dirsken, 1969; Shrivastava & Avasthi, 1975). We also observe a decrease of thermo-osmotic permeability inverse to the temperature increment.

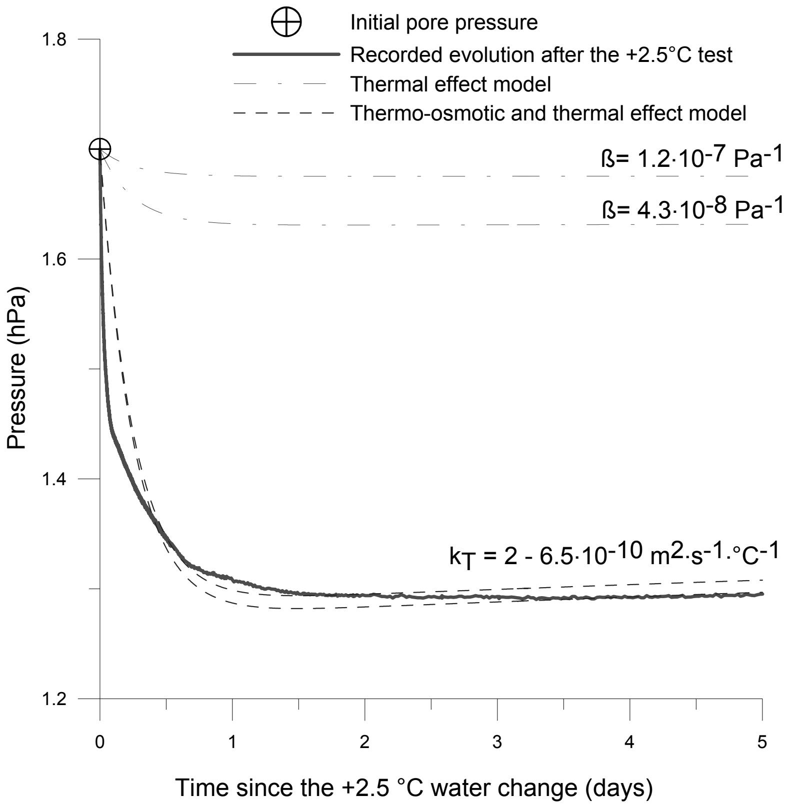

Fig. 1 Measured and modelled pressure evolution after the +2.5°C water change test.

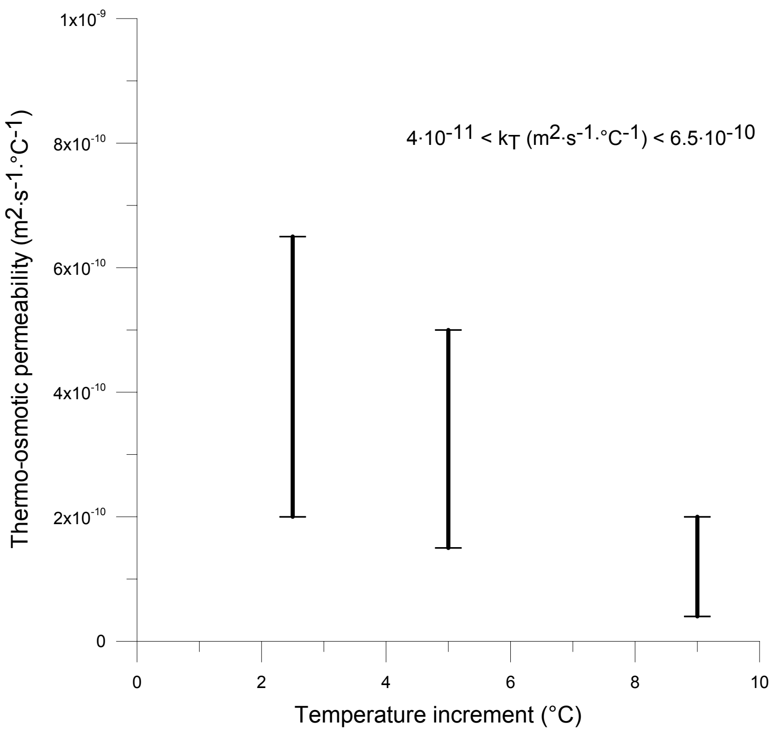

Fig. 2 Thermo-osmotic permeability obtained for different temperature increments applied during the water changes.

CONCLUSIONS AND PERSPECTIVES

In-situ water changes by a warmer one experiments performed in the Tournemire shale and their interpretation with a model integrating coupled flow equations have given rise to a thermo-osmotic effect, which has been quantified. In order to reach a more narrow thermo-osmotic permeability range, we are trying to better constrain sensitive parameters in our modelling.

Thermo-osmotic effect will next be coupled to chemical osmosis, hydraulic advection and other processes, like changes in boundaries hydrodynamic conditions and effect of tectonic compression. The goal of this modelling is to identify the transport phenomena at the origin of overpressures observed in the Tournemire shale and their respective contribution (Matray *et al.*, 2007).

REFERENCES

Derjaguin, B. V., Churaev, N. V. & Muller, V. M. (1987) Surface forces. *Consultants Bureau, New York*.

Dirsken, C. (1969) Thermo-osmosis through compacted saturated clay membranes. *Soil Science Society of America Proceedings* **33**(6), 821-826.

Gonçalvès, J., Violette, S. & Wendling, J. (2004) Analytical and numerical solutions for alternative overpressuring processes: Application to the Callovo-Oxfordian sedimentary sequence in the Paris basin, France. *Journal of Geophysical Research* **109**, B02110, doi:10.1029/2002JB002278.

Luo, X. & Vasseur, G. (1992) Contributions of compaction and aquathermal pressuring to geopressure and the influence on environmental conditions. *American Association of Petroleum Geologists Bulletin* **76**(10), 1550-1559.

Matray, J. M., Gonçalves, J., Savoye, S., Girardin, I., Cabrera, J. & Lecathelinais, P. (2007) PH4: a 250m deep borehole in Tournemire for assessing the contribution of transport phenomena to assumed overpressures in the Toarcian/Domerian semipermeable. *3rd International Meeting on "Clays in Natural & engineered barriers for radioactive waste confinement"*, September 17-18, Lille, France, 409-410.

Shrivastava, R. C. & Avasthi, P. K. (1975) Non-equilibrium thermodynamics of thermo-osmosis of water through kaolinite. *Journal of Hydrology* **24**, 111-120.

Soler, J. M. (2001) The effect of coupled transport phenomena in the Opalinus Clay and implications for radionuclide transport. *Journal of Contaminant Hydrology* **53**, 63-84.

Some exploration of hidden value in tracer experiments for model calibration and validation

S. G. WALLIS
School of the Built Environment, Heriot-Watt University, Riccarton, Edinburgh, EH14 4AS
s.g.wallis@hw.ac.uk

Abstract Tracer experiments are often used to calibrate pollution incident models for rivers. This paper describes a procedure that enables incomplete tracer profiles (that might be considered to be of little value) to make a significant contribution to model calibration. The results suggest that relatively few experiments might be sufficient to calibrate a model over a wide flow range, even in the case where some of the experiments fail to record full profiles.
Keywords advection-dispersion equation; velocity; dispersion coefficient; centroid; routing procedure

INTRODUCTION

The impacts of pollution incidents in rivers are routinely predicted using mathematical models. Any such model needs to take into account that travel times and mixing coefficients vary with flow conditions, and in order to check that a model performs satisfactorily it is usual to calibrate and validate it over a relevant range of flows. This is often accomplished using experiments in which a tracer is released into the watercourse and tracer concentration-time profiles are measured at points of interest.

One frequent question is: "how many tracer experiments are required"? The answer depends on the level of detail involved in model calibration, but clearly the minimum number is that which enables sufficient information to be gleaned on the flow dependence of any required coefficients. Another frequent question is: "how important is it to collect complete concentration-time profiles"? To some extent this depends on the approach being used (e.g. if dispersion coefficients are to be evaluated using the moments of the concentration-time profiles, full profiles are essential) and on the nature of the impact of the pollution incident (e.g. if a downstream water use ceases only when concentrations exceed some allowable limit, the tails may be perceived to be unimportant because they contain low concentrations). The situation may be compounded when having executed the number of experiments deemed necessary, it is subsequently found that some of the profiles are compromised by errors or are incomplete.

In some cases, therefore, the results of one or more tracer experiments may be perceived to be of little use. In this paper, however, the possibility of extracting useful information from apparently unusable data is explored, which might be useful for enhancing the integration of data collection, modelling and river management aims. The work uses an idea that enables travel times to be predicted from the time of the peaks of concentration-time profiles, combined with the application of a routing procedure for applying the advection-dispersion equation model.

DATA ANALYSIS AND RESULTS

Tracer data for the Murray Burn in Edinburgh, comprising concentration-time profiles at two measurement sites 184m apart, were available from previous work (Burke, 2002). In this, tracer experiments were conducted in the stream over a flow range of 0-

3000ls^{-1}. Three calibrations of the advection-dispersion equation model were undertaken. In Case 1 four successful experiments covering a wide flow range were used; in Case 2 the experiments from Case 1with the largest and smallest flows were retained, but the other two experiments were ignored (simulating the situation where two experiments had yielded no data at the downstream site); Case 3 simulated the situation where for the two experiments ignored in Case 2, at the downstream site only information around the peak (five surrounding data points) had been collected. Thus Case 1 contained four reliable data sets; Case 2 contained two reliable data sets; Case 3 contained two reliable and two unreliable data sets. For Cases 1 and 2, the velocity was evaluated from the centroid travel time between the sites (centroids being evaluated using the method of moments). For Case 3, the same method was used for the reliable data sets, but the unreliable data sets needed a different approach (see below) because without the complete concentration-time profiles, the downstream centroids could not be estimated (using profile moments). For all Cases, once the velocity had been found the dispersion coefficient was estimated as the value that gave the best simulation of the downstream data using Fischer's routing procedure (Rutherford, 1994).

The estimation of the missing centroids exploited "hidden value" in the data, namely that, as shown in Wallis (2005), there is a very strong linear correlation between the time of the peak and the time of the centroid of concentration-time profiles collected at the same site under different flow conditions. This is illustrated in Fig. 1 for the downstream site using the four reliable experiments used in Case 1. When estimating the missing centroids for Case 3, of course, only the two reliable experiments were used to establish this relationship (these were the experiments with the largest and smallest flows, see earlier).

The velocities and dispersion coefficients for the three calibrations were then plotted against flow to provide a way of predicting them at other flows, see Figs. 2 and 3. Finally, separate predictions of the downstream concentration-profiles at flows of 500, 1500 and 2500ls^{-1} were made for each Case, by estimating the velocities and dispersion coefficients from the trends shown in Figs. 2 and 3, and by using Fischer's routing procedure. A typical concentration-time profile (taken from the set of tracer data) was used to provide the necessary upstream concentration-time profile. Illustrative results (for the lowest flow) are shown in Fig. 4.

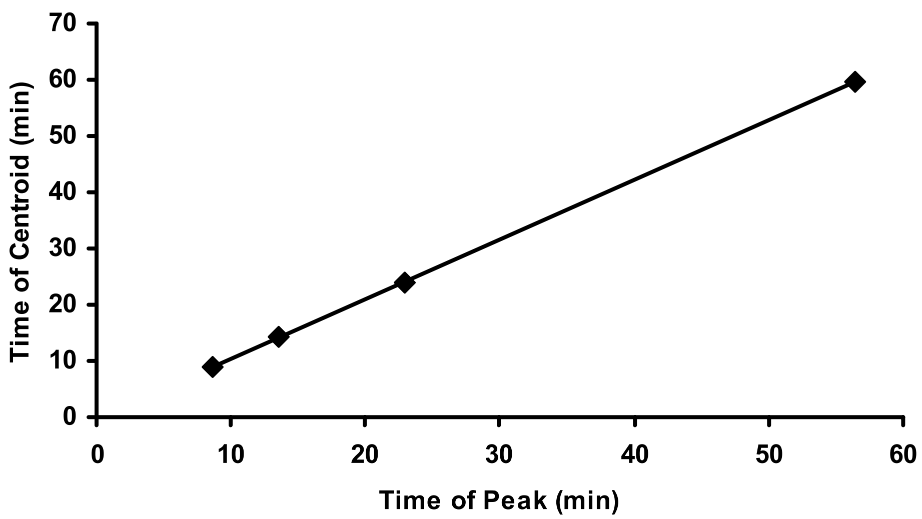

Fig. 1 Correlation between times of centroid and peak.

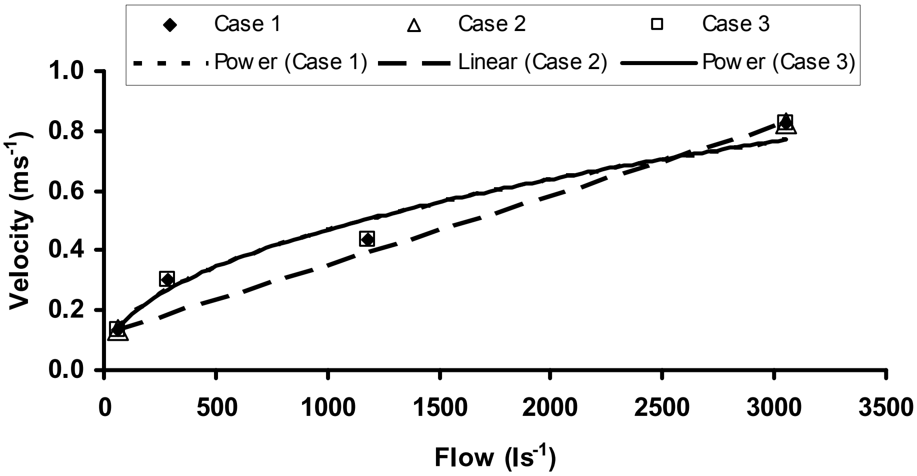

Fig. 2 Velocity – flow relationship.

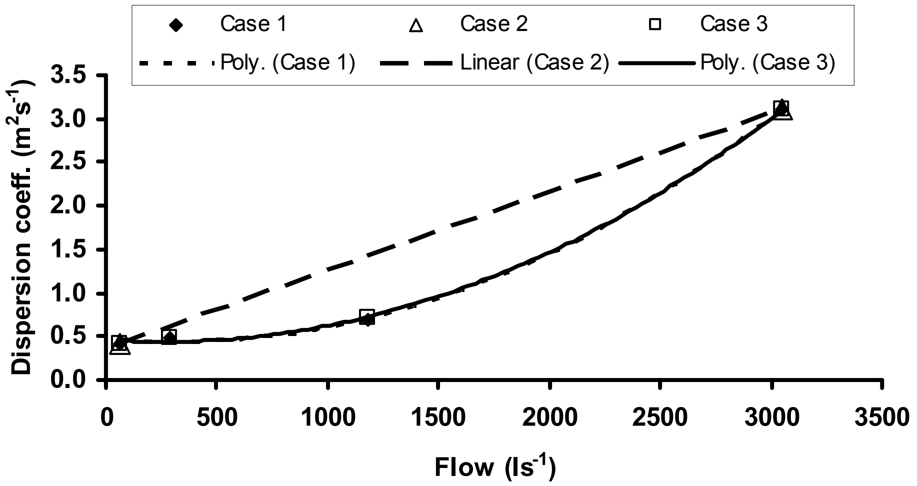

Fig. 3 Dispersion coefficient – flow relationship.

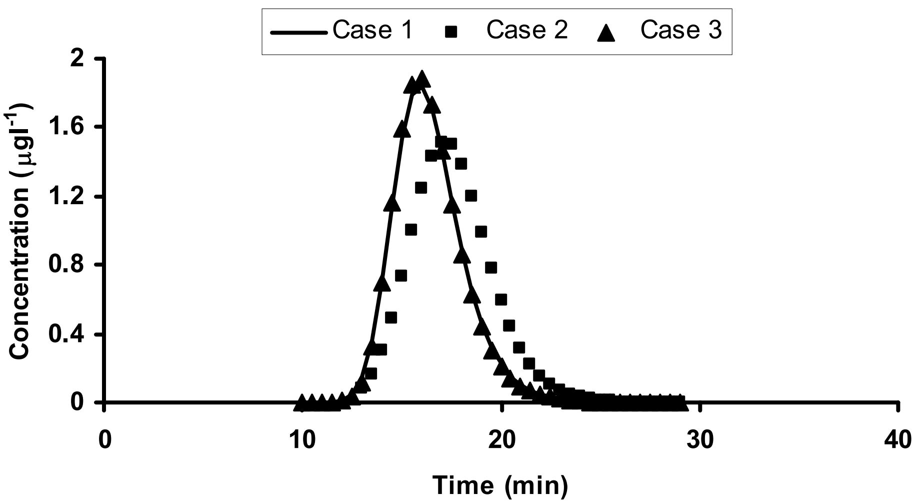

Fig. 4 Predictions at downstream site for flow of 500ls^{-1}.

DISCUSSION

Fig. 4 shows that very similar predictions are obtained using Case 1 and Case 3 calibrations, which illustrates the potential of exploiting hidden value in tracer data. In the absence of knowing that the time of the centroid can be accurately predicted from the time of the peak, incomplete concentration-time profiles would probably be discarded, being thought to be of little use. However, provided that some examples of complete profiles exist, which can be used to establish the peak-centroid relationship, incomplete profiles can still yield reliable reach velocity information. Moreover, since only a few data points close to the peak are required to identify it (in principle only three), even severely truncated profiles remain useful. Indeed, Fig. 2 is particularly striking in that the estimated velocities for Cases 1 and 3 are almost indistinguishable.

In estimating dispersion coefficients using Fischer’s routing procedure it might be thought that better values would be obtained by having as complete a downstream concentration-time profile as possible, so that the whole profile of the routing procedure result can be compared with the whole measured profile. However, Fig. 3 suggests this may not be necessary because the dispersion coefficients for Cases 1 and 3 (comprising complete and incomplete downstream profiles, respectively) are very similar.

Since the velocity- and dispersion coefficient-flow relationships are generally non-linear (see Figs. 2 and 3) at least three tracer experiments are required to establish them. The results above, however, show that it is not necessary that all of them provide complete profiles at the downstream site, so long as they all capture the peak. Of course, to use Fischer's routing procedure complete profiles are required at the upstream site in all experiments. Naturally, the prediction from Case 2 shown in Fig. 4 is rather poor because only two calibration experiments were used, which doesn't permit access to the non-linear behaviour.

CONCLUSIONS

Provided the peak is captured, incomplete downstream concentration-time profiles (combined with complete upstream profiles) can still yield important information for calibrating the advection-dispersion equation model. It is tempting to speculate that the very robust nature of the peak-centroid relationship, in particular, might influence the planning of tracer experiments because one fully successful experiment, together with two less successful ones, might suffice to calibrate the model even over a wide flow range.

REFERENCES

Burke, N. A. (2002) Travel time and flow characteristics of a small stream system. PhD Thesis, Heriot-Watt University, Edinburgh, UK.

Rutherford, J. C. (1994) *River Mixing*, Wiley, Chichester, UK.

Wallis, S. G. (2005) Experimental study of travel times in a small stream. In: *Water Quality Hazards and Dispersion of Pollutants* (ed. by W. Czernuszenko & P. M. Rowinski), Springer, New York, 69-84.

Hydrogeological study in a chloride contaminated site, Romania

IRINA DINU[1], CATALIN ROTAR[2], MARIUS STOICA[1] & TRAIAN MOLDOVEANU[3]

1 *University of Bucharest, Faculty of Geology and Geophysics, 6 Traian Vuia St., 020956 Bucharest 2, Romania*
dinui@gg.unibuc.ro

2 *F & R Worldwide, Bucharest, Romania, 28C G-ral C. Budisteanu St., 010775 Bucharest 1, Romania*

3 *Geotec Consulting, Bucharest, Romania, 1bis Lacul Tei Bd., 020371 Bucharest 2, Romania*

Abstract The Section Cocu, located nearby the city of Pitesti, comprises many injection wells for petroleum exploitation, but only few of them are in function nowadays. Due to damage in the well casings, the saltwater used in the process of injection has determined the increase of chloride concentrations in groundwater. The aquifer system in Section Cocu area is in relationship with the River Cotmeana. Moreover, groundwater is used as drinking water source for the local population. A hydrogeological study in the Section Cocu was commanded, in order to establish a program for monitoring the quality of groundwater and to take appropriate measures for reducing pollution. The aquifer system in this area comprises four aquifers, with different extensions, separated by semi-pervious units. The second aquifer is the most contaminated one. The third and the fourth aquifer are more extended than the first two. The third aquifer is in direct relationship with potential pollution sources, such as oil wells and oil pipelines and it is drained by the River Cotmeana. Several monitoring wells were drilled for the purpose of this study, providing data concerning the lithology and the groundwater heads in the aquifer system. Vertical electric soundings were carried out in order to delineate the zones with different pollution degrees. A numerical flow model synthesizes the available data and provides useful information for establishing a program for monitoring the groundwater quality. Several simulations were made after the calibration of the model, taking into account only advection in estimating the fate of pollutants in the aquifer system. Backward tracking simulations were made in order to identify the zones where particles reaching the monitoring wells come from. Forward tracking simulations were made in order to provide the pathlines of the particles located in the vicinity of potential pollution sources, like pipelines or active oil wells. The travel times of the particles were also estimated. Both backward and forward tracking simulations indicated that the pollutants are more likely to reach certain monitoring wells, screened in the fourth aquifer. Therefore, within the monitoring program, samples from these wells should be taken more often.
Keywords aquifer system; contamination; numerical model; simulation

INTRODUCTION

The Section Cocu, located 16 km west of Piteşti city, is a petroleum exploitation perimeter operated by the National Romanian Petroleum Society PETROM. It comprises many injection wells for oil exploitation, only few of them being in function nowadays. Due to damage in the well casings, the saltwater used in the process of injection has determined the increase of chloride concentrations in groundwater, which is used as drinking water source for the local population. The aquifer system in Section Cocu area is in relationship with the River Cotmeana. The aquifer system comprises four aquifers with different extensions. Based on the data provided by the study wells, a numerical flow model has been built. The results of the model were taken into account in order to establish a program for monitoring the quality of groundwater.

GEOLOGICAL AND HYDROGEOLOGICAL CONDITIONS

The Pleistocene deposits in the Section Cocu area are represented by an alternation of gravel layers and pelitic or sandy intervals. The younger Holocene sediments are represented by top soils, loess, and alluvial deposits in the thalweg of the River Cotmeana and its tributaries.

The aquifer system comprises four aquifers, with different extensions, separated by semi-pervious units. The first and the second aquifers are developed in the eastern part of the study area.

The first aquifer (aquifer I), is unconfined, up to 2 m thick and located in fine sand formations. It is directly supplied from recharge, as well as from the north and it discharges through springs, towards east and west. The main groundwater flow directions are N – S and W – E. Groundwater heads of aquifer I are between 345 m and 360 m.

The second aquifer (aquifer II), is located in 5 to 6 m thick gravels. The consisting gravels are almost dry and there is almost no lateral flow in this aquifer, except for the eastern sector, where water, coming from the aquifer above, is discharged to the east, by springs with salted water. Pollution in these deposits is also indicated by a zone of dry forest (fig.1) and by low apparent resistivity values, between 1 and 8 Ω m.

The third aquifer (aquifer III), is confined in the eastern part of the study area and unconfined in the western part, being directly supplied from precipitation. It is in direct relationship with the River Cotmeana, which also represents its western boundary, and with a segment of its tributary, Măneasa. The aquifer is supplied from the east and north and discharges mostly to the west, being drained by the River Cotmeana, but also towards south and north. The thickness of the aquifer III varies between 1 and 9 m. Groundwater heads range from 297 m, along the River Cotmeana, on the southern boundary, to more than 335 m in the eastern part.

The fourth aquifer (aquifer IV), is extended west of the River Cotmeana. The main groundwater flow direction is NNW – SSE. The thickness of the aquifer IV varies between 2 m and 12 m. The measured groundwater heads range from 293 m (SE) to 310 m (N).

The recharge of the aquifer system was determined using the SCS method (Musy, 1998; Mays, 2001), taking into account the land use and the vegetation cover. The resulted values of effective infiltration are 52 mm year^{-1} for the flood plain of the River Cotmeana and 95 mm year^{-1} for the hill zone.

MODEL OF THE AQUIFER SYSTEM

The model of the aquifer system in the Section Cocu was made using Visual Modflow (Guiguer & Franz, 1996). The model comprises seven layers, corresponding to the four aquifers and the semi-pervious units located between them. Recharge was applied to the highest active cell in each vertical column. Therefore, recharge is 95 mm year^{-1} in the first layer of the model, corresponding to aquifer I and to the hill zone, and 52 mm year^{-1} in the zone of the flood plain, where only aquifers III and IV are present.

The constant-head boundary conditions were prescribed based on the measured groundwater heads in all the layers representing aquifers. In the fifth layer of the model, corresponding to aquifer III (fig.2), the River Cotmeana and its tributary, Măneasa, are represented by constant-head boundary conditions.

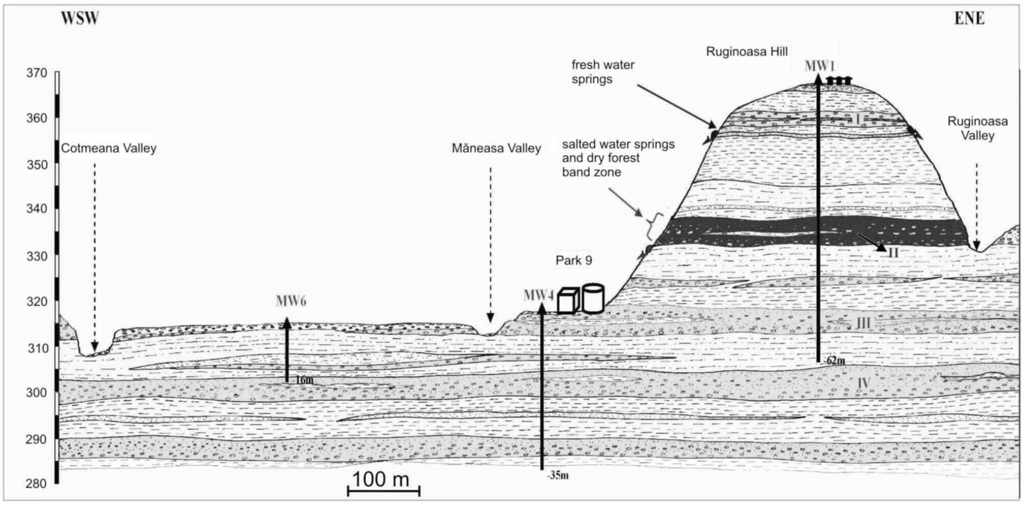

Fig. 1 Cross-section through the Quaternary deposits in the Section Cocu area.

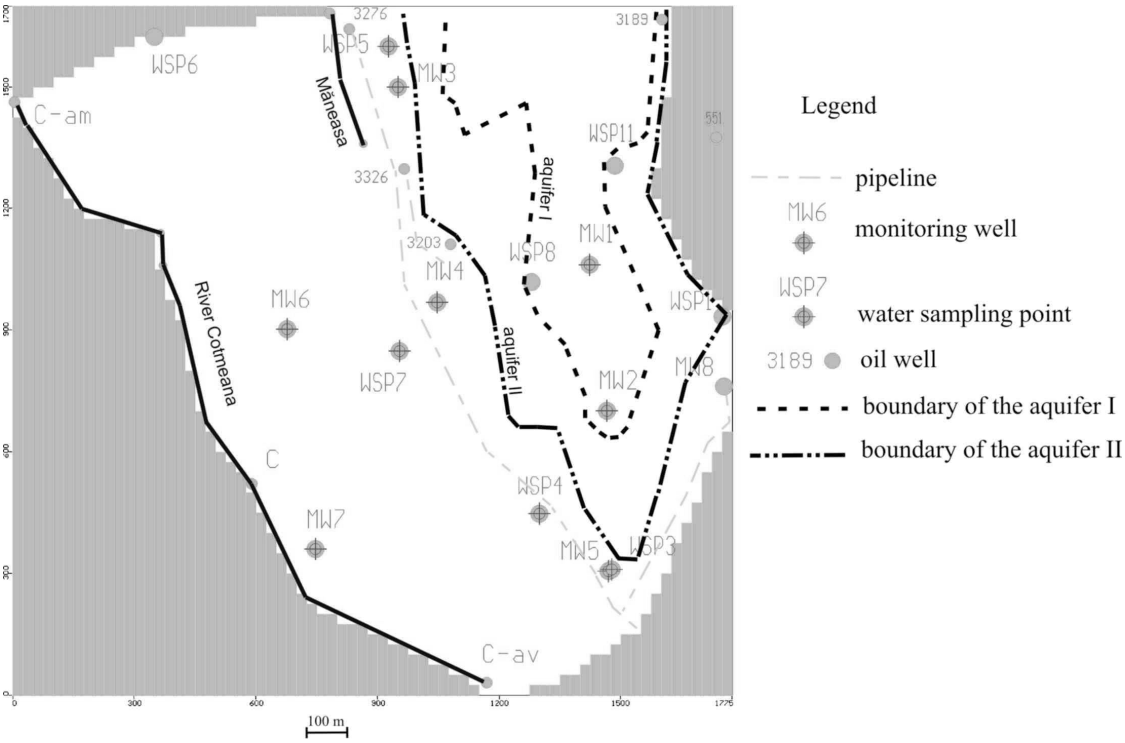

Fig. 2 The fifth layer of the model, representing the aquifer III.

Calibration was reached by the trial-and-error method, by adjusting the values and distribution of the hydraulic conductivity, in order to minimize the differences between the calculated and measured heads at the locations of the wells and sampling points for the aquifers I, III and IV.

SIMULATIONS IN ORDER TO ESTABLISH A MONITORING PROGRAM

Backward tracking and forward tracking simulations were performed after the calibration of the model. Advection was the only mechanism taken into account in estimating the fate of pollutants in the aquifer system. The purpose of the backward tracking simulations was to establish if the particles reaching the monitoring wells come from potential pollution sources, like pipelines or active oil wells. Thus, the particles reaching the monitoring wells MW4 – MW7, screened in aquifer IV, come from the eastern boundary of the aquifer III, crossing the transect of the main pipeline for saltwater transport. The water sampling points along the River Cotmeana are supplied from the northern and eastern boundary and they also cross the transect of the main pipeline.

The purpose of the forward tracking simulations was to determine if particles located in the areas of the potential pollution sources, like oil wells and pipelines for saltwater transport, would reach the monitoring wells. Thus, particles located in the area of the main pipeline, in the aquifer III, reach the aquifer IV and may pass through the monitoring wells MW1 – MW3 and MW5. Particles located in the area of the southern section of the main pipeline may reach the River Cotmeana. Particles located in the area of the pipeline from Park 9, in the aquifer III, reach the aquifer IV and may pass through the monitoring wells MW4 and MW5

These simulations show that there is a risk of further extension of the saltwater pollution.

CONCLUSIONS

This preliminary study in the Section Cocu area provided information concerning the relationship between the four permeable layers that make the aquifer system. The data provided was synthesized by means of a numerical model.

The simulations carried out after the calibration of the model helped in establishing the supply area for every monitoring well. They also provided the pathlines of the particles located in the areas of the potential pollution sources. Pollutants are more likely to reach the monitoring wells MW4 to MW7, therefore these wells should be sampled more often.

REFERENCES

Guiguer, N. & Franz, T. (1996) Visual MODFLOW: the fully integrated, three-dimensional, graphical modelling environment for professional groundwater flow and contaminant transport modelling. *Waterloo Hydrogeologic Software Inc*., Ontario, Canada.

Mays, L. W. (2001) Water Resources Engineering. *John Wiley & Sons*, 761 p., New York – Chicester – Weinheim – Brisbane – Toronto – Singapore.

Musy, A. (1998) Hydrologie appliquée. *Ed. H.G.A*. 366 p., Bucarest, 1998.

Application of geophysical techniques for investigation of geological contaminations due to mine wastes

S. MEHRABIAN & A. AMINI
Institute of Geophysics, University of Tehran, Kargar Shomali Ave. P.O. Box 14155-6466
smehrabi@ut.ac.ir

Abstract The use of various geophysical techniques for investigation of hazardous waste and ground water pollution sites is often a rapid, cost-effective means of preliminary evaluation. In this regard using geophysical methods at hazardous waste and ground water pollution sites is a fairly recent development. In recent years, conducting ground water pollution investigations has coincided with improvements in the resolution, acquisition and interpretation of geophysical data. Therefore, outlines of geophysical techniques and procedures are subject to revision as improvements are made in the instrumentation and interpretation algorithms. Mine wastes or gangues associated with valuable minerals in ores are usually separated before or during mineral processing in different stages of crushing and ore concentration. These waste materials are then dumped in an area close to the mine or mineral processing plant. Leaking solutions from these dumps contain various chemical components and are considered as an important source of soil and groundwater contaminations. Many factors such as precipitation cause more pollutants to percolate underground layers and increase extent of subsurface contaminations in recent years. Accuracy, high speed and significant reduction in expenses are the most dominant advantages of these noninvasive methods. Geoelectrical profiling and sounding surveys will result in the determination of the lateral and vertical extent of contaminations, respectively. This study discusses the advantages of electrical methods in environmental studies of mining activities. After all, we will discuss about methods of resistivity survey (deigning and measuring), that we have used in our study. The obtained results by using these methods on real data, from Geoelectrical survey in a case study are presented.
Keywords mine wastes; mine tailings; resistivity sounding; resistivity profiling

INTRODUCTION AND BACKGROUND INFORMATION

The information obtained from some geophysical investigations can be used to determine the subsurface conditions at, and in the vicinity of, a site. Various geophysical techniques reveal physical properties of subsurface which can be used to determine hydrostratigraphic framework, depth to bedrock, extent of concentrated ground water contaminant plumes, the location of voids, faults or fractures, and the presence of buried materials, such as steel drums or tanks. Geophysical investigations are most effective when used in conjunction with a drilling or boring program, and should not be considered a substitute for such programs. The information gained from a surface geophysical survey can be used to choose optimal locations for the placement of boreholes, monitor wells or test pits, as well as to correlate geology between wells and boreholes. The information derived from a geophysical survey can also be used to reduce the risk of drilling into buried drums or tanks. Recently, measurements of subsurface electric field changes have been conducted by means of borehole antennas. Due to the processes of rocks micro fractures, some mechanisms on the origin of electromagnetic waves, the characteristics and the possible propagation paths of such waves, both underground and over the Earth surface, are considered.

One of the most applicable geophysical methods, called" electrical resistivity method" is used to map the subsurface electrical resistivity structure, which is interpreted by the geophysicist to determine geologic structure and/or physical properties of the geologic materials. The electrical resistivity of a geologic unit or target is a function of porosity, permeability, water saturation and the concentration of dissolved solids in pore fluids within the subsurface. If the purpose of the survey is to map the depths and thickness of stratigraphic units, then the electrical resistivity data should be collected in the sounding mode. Lateral electrical resistivity contrasts, such as lithologic contacts, can best be mapped in the profiling mode. Once the apparent electrical resistivities have been calculated, the next step is to model the data in order geologic structure. Electrical resistivity data acquired in the sounding mode, using either the Wenner or Schlumberger array, can be modeled using master curves or computer modeling algorithms.

THE BASIC APPLIED THEORY

The inversion routine used by the program is based on the smoothness-constrained least-squares method (Keller & Frischknecht, 1966) which is based on the following equation:

$$(\mathbf{J}^{\mathbf{T}}\mathbf{J} + \mathrm{u}\mathbf{F})\ \mathbf{d} = \mathbf{J}^{\mathbf{T}}\mathbf{g}$$

where $\boldsymbol{F} = \boldsymbol{fxfx}^{\boldsymbol{T}} + \boldsymbol{fzfz}^{\boldsymbol{T}}$, $\boldsymbol{fx}$ = horizontal flatness filter, $\boldsymbol{fz}$= vertical flatness filter, $\boldsymbol{J}$= matrix of partial derivatives, u= damping factor, $\boldsymbol{d}$= model perturbation vector, $\boldsymbol{g}$= discrepancy vector. One advantage of this method is that the damping factor and flatness filters can be adjusted to suit different types of data. A detailed description of the different variations of the smoothness-constrained least-squares method can be found in the free tutorial notes by Loke (1999).

RESULTS

In this study, the purpose was discrimination between contaminated sites near an uncontaminated water aquifer. The Trapezoidal grid was used. In Figs 1, 2 and 3, the 3D model obtained from the inversion of the survey data set are shown. The data were plotted as two sets of pseudo depth slices using the two electrode orientation directions, which resulted in markedly different plots. The models are shown in the form of horizontal and vertical slices through the Earth. It should be noted that the Pole-Pole array is used. The completed data set was inverted to the form of a resistivity depth model of the ground using a 3-D least-squares smoothness constrained inversion technique. With respect to the model X and Y grid size are 14m. Number of data points is 1274. Average height is 0.00. Number of iteration is 8, RMS error is 3.60, and average sensitivity value is 1.0128. Units of X and Y electrode spacing are 3.00m. The minimum and maximum X and Y locations are respectively in ohm. m, 0.00 and 39.00, and 0.00 and 40.00. The minimum and maximum resistivity values are respectively, 196.10 and 65.96 ohm. m. Average resistivity value is 96.06.

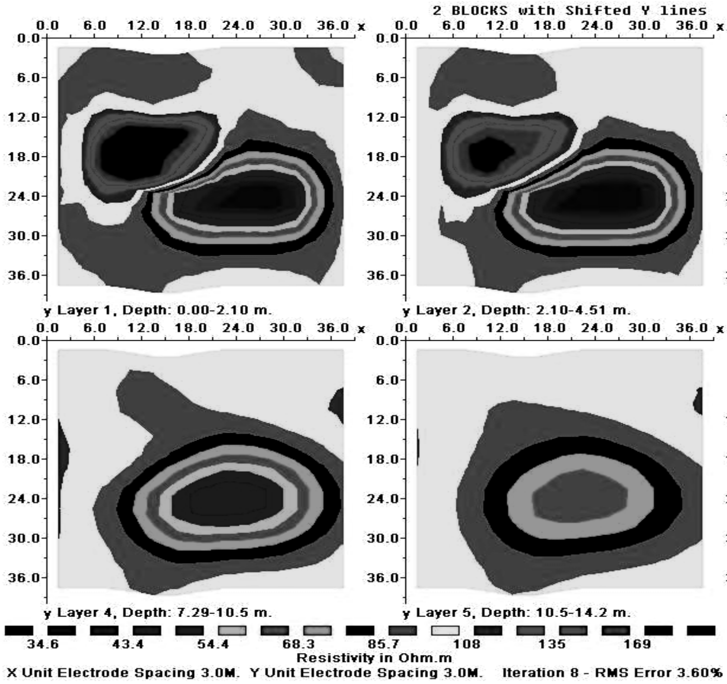

Fig. 1 The 3D model obtained from the inversion of survey data set. The model is shown in the form of horizontal slices through the Earth.

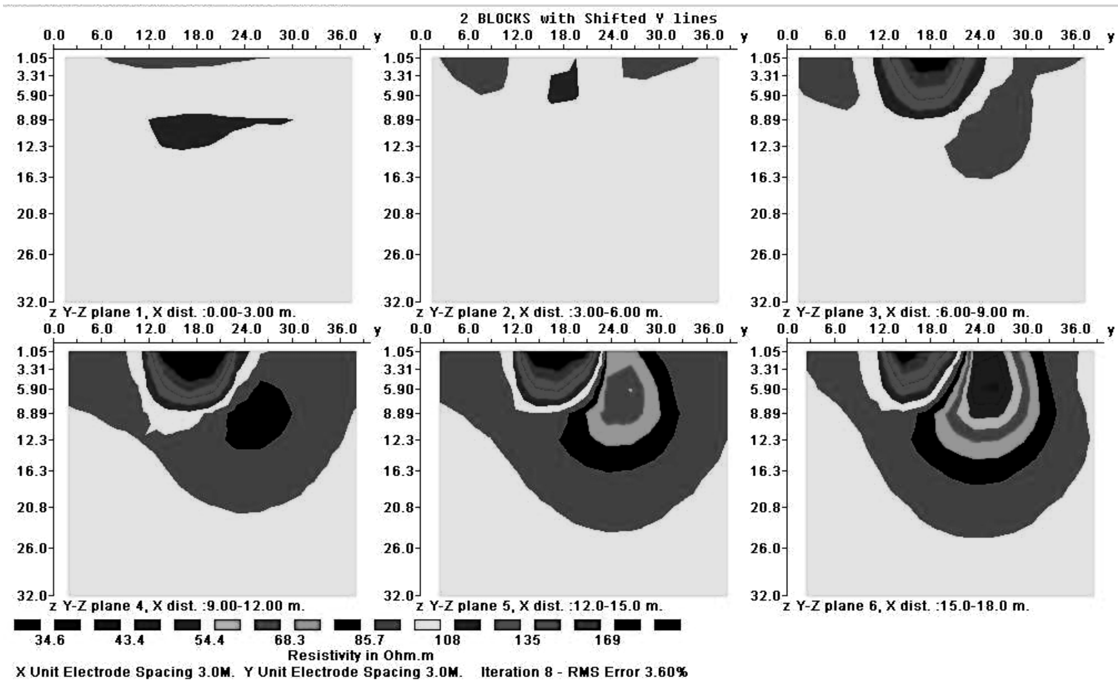

Fig. 2 The 3D model obtained from the inversion of the survey data set. The model is shown in the form of vertical slices through the Earth in Y -Z dimension.

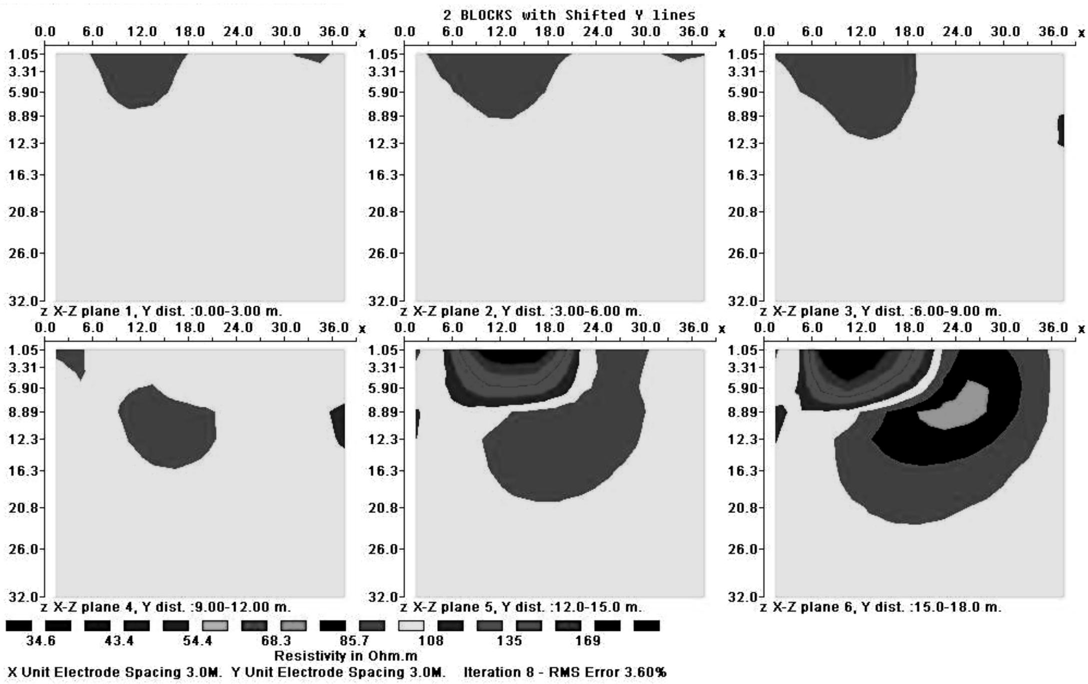

Fig. 3 The 3D model obtained from the inversion of the survey data set. The model is shown in the form of vertical slices through the Earth in X-Z dimension.

Acknowledgements The authors would like to thank the office of research affairs (Vice president in research and technology), University of Tehran for financial support.

REFERENCES

Dahlin, T. (1996) 2D resistivity surveying for environmental and engineering applications. *First Break* **14**, 275-284.

Griffiths, D. H. & Barker, R. D. (1993) Two-dimensional resistivity imaging and modelling in areas of complex geology. *Journal of Applied Geophysics* **29**, 211-226.

Keller, G. V. & Frischknecht, F. C. (1966) Electrical methods in geophysical prospecting. Pergamon Press Inc., Oxford.

Loke, M. H. (2000) Topographic modelling in resistivity imaging inversion. *62nd EAGE Conference & Technical Exhibition Extended Abstracts, D-2.*

Loke, M. H. (2001) Tutorial: 2-D and 3-D electrical imaging surveys. *Geotomo Software, Malaysia.*

Loke, M. H. (1999). Time-lapse resistivity imaging inversion. *5th Meeting of the Environmental and Engineering* Geophysical Society European Section Proceedings. Em1.F

Estimation of the relative age of alluvial sediments using method of changes of chromium and lead concentration: the case of the Obra River valley (western Poland)

M. SŁOWIK

Adam Mickiewicz University, Department of Geographic and Geologic Sciences, ul. Dzięgielowa 27, 61-680 Poznań, Poland

slowikgeo@poczta.onet.pl

Abstract This paper presents the results of laboratory experiment of chromium and lead migration ability in alluvial deposits of the Obra river valley (Western Poland). Main goal of the study was to determine if changes of Cr and Pb concentrations can be used as indicators of relative age of floodplain sediments. The experiment was done in a column of dimensions 40x20x200 cm, which was filled with alluvial deposits. It was observed that very high concentrations occur in the surface layer (chromium: 550 mg kg^{-1}; lead: 380 mg kg^{-1}). In the remaining part of the column, much lower concentrations were noted (3 – 25 mg kg^{-1}). It can be suggested that lead and chromium concentrations in alluvial sediments can be used as indicators of vertical accretion rate of floodplain deposits. The results require confirmation through further research.

Keywords chromium and lead concentration; alluvial deposits; laboratory experiment; weaving industry; the Obra river

INTRODUCTION

Laboratory experiment was done to analyse migration ability of chromium and lead in alluvial sediments of the Obra river valley. Main research problem was to determine the relative age of the deposits using method of changes of lead and chromium concentration. These two chemical elements were chosen because of its low abilities to migrate (Robertson, 1975 in: Ball & Izbicki, 2004; Witczak & Adamczyk, 1995) and because of the fact that centres of weaving industry (Międzyrzecz; Fig.1) were functioning in the lower course of the Obra river (Fig.1) between the XVIth and the XIXth century. One of the main ingredients of paints used at that time were the compounds of chromium in its trivalent form (alum) and lead (lead sulphate) (Mączak, 1955).

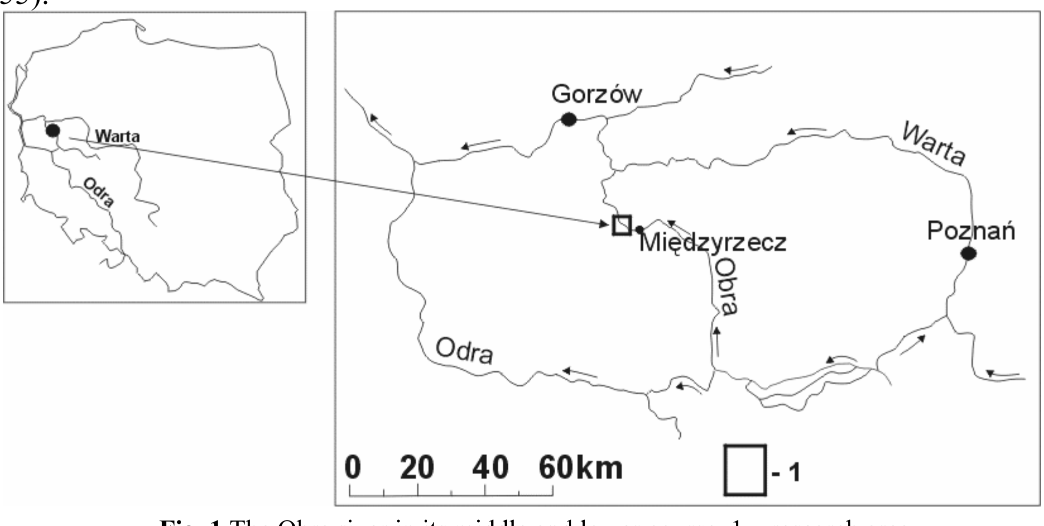

Fig. 1 The Obra river in its middle and lower course. 1 – research area.

During the process of dyeing and rinsing of textures, the chemical compounds were being washed to the Obra river bed and then deposited in alluvial sediments. On the basis of these information, a hypothesis has been proposed that changes in chromium and lead concentration in the Obra valley alluvial fill can reflect changes in the amount of weaving industry production, in the last 300 – 400 years. Earlier studies (Młynarczyk *et al*., Słowik, 2006) has shown that increased concentrations of chromium occur in the deposits much older than the period of development of weaving industry in Międzyrzecz, in the lower course of the Obra river (Fig.1). However, it should be noted that only a fragment of alluvial sediments vertical profile was studied at that time.

THE EXPERIMENT OF CHROMIUM AND LEAD MIGRATION IN ALLUVIAL DEPOSITS

The experiment was done in a column of dimensions 40x20x200 cm, which was filled with alluvial sediments (coarse sands, fine sands and peats; Fig. 2). The deposits in the column reflected the sequence of sediments in one of the vertical profiles, which was investigated in earlier studies (Młynarczyk *et al*., 2006). The column was equipped with piezometers and syringes to observe water level and to collect water samples. In the bottom part of the device, a tap was set to let the water out.

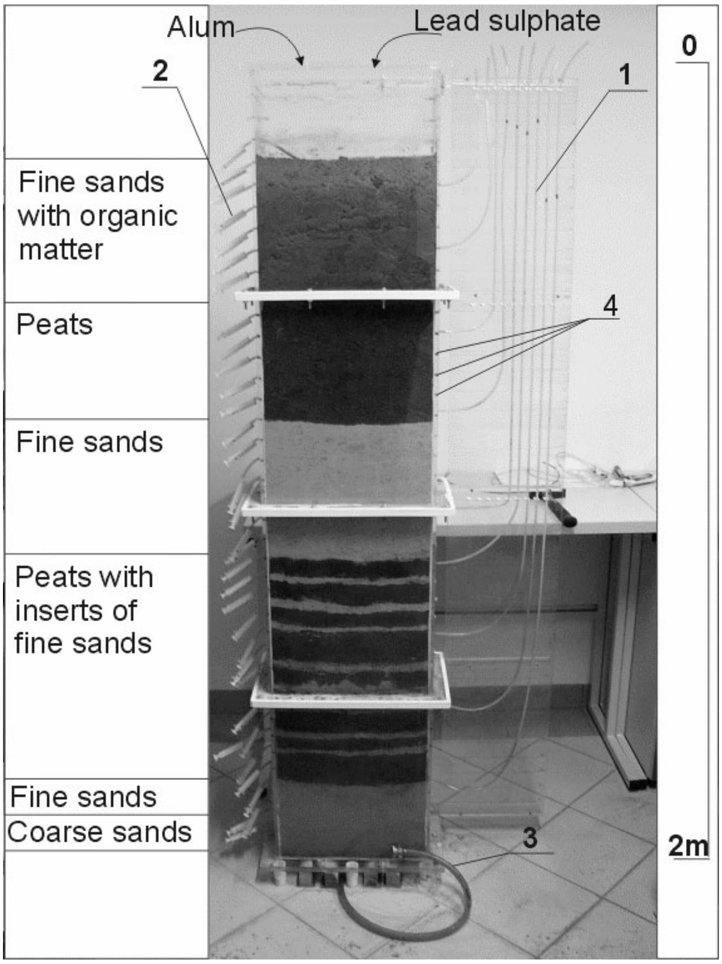

Fig. 2 The column filled with alluvial deposits. 1 – piezometers, 2 – syringes for collecting water samples, 3 – a tap for letting the water out, 4 – holes in the right side of the column for collecting sediment samples.

In the first phase of the experiment, the deposits in the column were soaked with distilled water. Then, after letting the water out, its lower half was filled with water again and the upper part was filled with the compounds of chromium and lead. Next, about 20 dm^3 of the solution was let out to initiate vertical migration of the compounds inside the column. Concentrations of alum (54 mg dm^{-3}) and lead sulphate (130 mg dm^{-}3), which were added to the column, were calculated on the basis of the following data: information about weight proportions of the compounds taken from paint recipes, annual production of textures in the XVI[th] century (Mączak, 1955) and mean annual discharge in the Obra river bed (4 m^3 s^{-1}). Besides, another experiment was done. 1 m^2 of linen texture was "bathed" in 5% solution of chromium and lead. Then it was rinsed in 10 dm^3 of water. Next, concentrations of lead and chromium were determined in the water after rinsing. The concentrations, which were used in the column experiment, generally reflect daily supply of chromium and lead compounds to the Obra river bed during period of texture productions.

RESULTS AND CONCLUSIONS

The analysis of chromium and lead concentrations in the deposits placed in the column has shown that very high concentrations occurred in the surface layer (chromium: 550 mg kg^{-1}; lead: 380 mg kg^{-1}; Fig. 3). In the remaining part of the column, much lower concentrations were noted (3 – 25 mg kg^{-1}; Fig. 3). Besides, it was observed that greater concentrations of investigated chemical elements occur in peats (5 – 25 mg kg^{-1}; Fig. 3). In case of sand deposits, concentration of chromium and lead ranged from 1 mg kg^{-1} to 4 mg kg^{-1} (Fig. 3). Despite observed migration of the chemical elements in the column, its concentrations were dozens of times lower than in the surface layer.

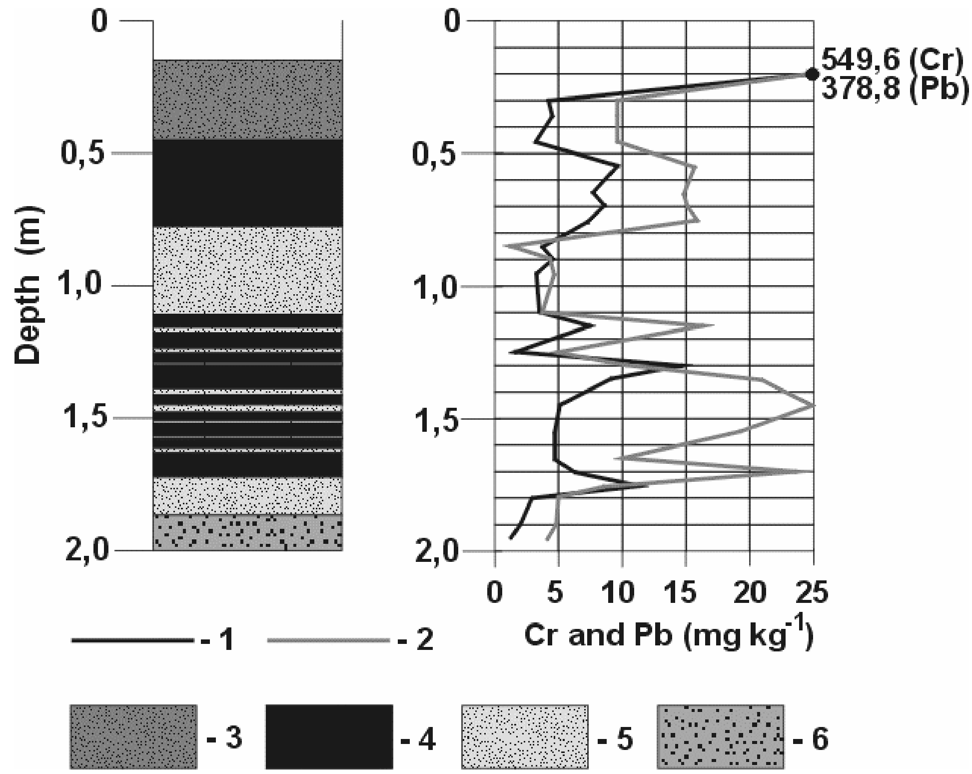

Fig. 3 Chromium and lead concentrations in alluvial sediments in the column after letting out 20 dm^3 of the solution to initiate vertical migration of the compounds inside the column. 1 – Cr concentration, 2 – Pb concentration, 3 – sands with organic matter, 4 – peats, 5 – fine sands, 6 – coarse sands.

On the basis of achieved results, it can be suggested that lead and chromium concentrations in alluvial sediments can be used as indicators of vertical accretion rate of floodplain deposits. Low concentrations (Cr: 0 – 0.6 mg dm^{-3}; Pb: 0 – 2 mg dm^{-3}) in the water samples taken from particular levels of the column (Fig. 2) can also be the result of limited migration ability of studied chemical elements. The results require confirmation through field experiments and the analysis of chromium and lead concentration in vertical profiles of the Obra valley alluvial fill. This research is in progress now.

Acknowledgements This work was supported by State Committee for Scientific Research grant no N 306 052 31/3624. Great help and support of Prof. Zygmunt Młynaczyk, Dr Tadeusz Sobczyński and Eng. Remigiusz Tritt are acknowledged.

REFERENCES

Ball, J. W. & Izbicki, J. A. (2004) Occurrence of hexavalent chromium in ground water in the western Mojave Desert, California. *Applied Geochemistry* **19**, 1123-1135.

Mączak, A. (1955) Sukiennictwo w Wielkopolsce, XIV-XVII wiek. *Weaving industry in Wielkopolska, XIVth-XVIIth century*. PWN, Warszawa.

Młynarczyk, Z., Sobczyński, T. & Słowik, M. (2006) Changes of chromium concentration in alluvial sediments of the Obra river valley. *Environmental Geology* **50**(3), 423-431.

Witczak, S. & Adamczyk, A. (1995) Katalog wybranych fizycznych i chemicznych wskaźników zanieczyszczeń wód podziemnych i metod ich oznaczania, tom II (The catalogue of chosen physical and chemical indicators of groundwater pollution and methods of its analyses*). Biblioteka monitoringu środowiska*, Warszawa.

Efficient prediction of nitrate, sulphate and total hardness concentrations in raw water with a flow path approach

KEES VINK[1], GIJSBERT CIRKEL[2] & MARTIN DE JONGE[3]

1 *Elementair, Ophemert, The Netherlands*
c.vink@elementair.net

2 *Kiwa Water Research, Nieuwegein, The Netherlands*

3 *Vitens drinking water company, Leeuwarden, The Netherlands*

Abstract Developments in land use, spatial planning, risk management and groundwater quality management have evoked the need for efficient modelling techniques that can clarify the relation between land use and groundwater quality. Existing transport modelling codes such as MT3D typically use simulated flux fields that are generated with Modflow or other groundwater models and require substantial input of labour for the setup, calibration and running of the model. As to improve modelling efficiency we developed a new chemical model named RESPOND, that enables efficient analyses of the relation between land use and groundwater quality at locations where endangered objects are located, such as pumping wells or wetlands. Typical elements of the Respond approach are:
-flowpath approach in stead of flux approach;
-standard type curves of historical deposition of chemical parameters per land use class
-automated assessment of geohydrochemical properties per flowpath;
-model calibration by means of a genetic algorithm;
-transport processes sorption and 1st order decay for micro-pollutants and coupled chemical balances for nitrate, sulphate and total hardness.
We applied the model successfully to various case studies in The Netherlands. In this paper we discuss pro's and con's of the modelling approach and present some modelling results.

Keywords groundwater; groundwater quality; groundwater transport modelling; optimisation; parameter estimation; calibration; genetic algorithm

INTRODUCTION

Developments in land use, spatial planning, risk management and groundwater quality management have evoked the need for efficient modelling techniques that can clarify the interaction between land use, groundwater quality and raw water quality at drinking water production sites. The obligations that follow from the implementation of the Groundwater directive of the European Water Framework are currently an important source of groundwater management questions, focussed on the relation between land use and groundwater quality developments.

Since the late nineties of the previous century there exist well known numerical modelling codes such as MT3d (Zheng, 1990, 1999), Rt3d (Clement, 1997) and PHT3d (Prommer, 1999), all coupled to Modflow flux output, and a number of other, less well known codes that enable simulation of groundwater transport and changes in groundwater quality and pumped water quality. These codes typically require substantial labour for the setup of the models. Furthermore, calculation times of these distributed flux-based models often exceed several hours for a single simulation run if the spatial level of detail is high and simulated transport travel times of the groundwater comprise several decades, as is typically the case in groundwater modelling prediction studies for drinking water companies. As a result, both financial costs and computer calculation costs are high.

Therefore we developed a new chemical model that enables efficient analyses of the relation between land use, groundwater quality and finally the chemical composition of raw water in pumping wells or of at locations of interest. Output of the model consists not only of time series of concentrations in pumped groundwater or in seepage water, but also of “gross load” and “net load” maps that clarify relations between infiltration areas and sites where flow paths end, such as drinking water wells, wetlands, rivers and lakes. The maps are meant to be used in risk analyses, land use planning, groundwater management and protection of ecological valuable objects.

METHODS

Generally applied transport modelling codes such as MT3d and Rt3d use cell-by-cell fluxes that are output from Modflow as input for the hydrologic basis of the chemical simulations. The alternative to this “distributed flux approach” is the “flow tube” approach. In stead of simulating transport of chemical species in every model cell, flow tube-based chemical models consider pathlines toward objects of interest. Every pathline represents a flux. This approach implies a reduction of calculation tasks as compared to the distributed flux-based transport models that are typically used to simulate transport in every model cell of the modelled area. The flow paths can be calculated with Modpath and enable an efficient grouping of groundwater fluxes by origin and trajectory. Because of the grouping, calculation time is less than for a distributed flux-based model. Another advantage of the flow-tube approach consists in the explicit relation between origin and destination of groundwater fluxes. The difference in the chemical composition at the start and at the end of a pathline shows directly the influence of the infiltrated load and the subsoil passage on the groundwater quality at the ends of the pathlines.

Results of Respond simulations are:

- maps of gross and net deposition of chemical parameters at the surface
- maps of subsoil properties and concentrations of parameters that are relevant to the groundwater quality
- reconstruction and prediction of concentrations of chemical species that determine pumped raw water quality

Type curves

For facilitation of the modelling process we constructed a large number of ‘standard type curves’ that represent time series of historical loads per chemical parameter per land use class (Fig. 1). During calibration with a genetic algorithm (GA), these standard type curves are modified in a well-prescribed and reproducible manner and thus result in a ‘specific type curve’ where the load in the infiltration zones and the reactivity of the subsoil along the pathlines is calibrated to observed concentrations.

Subsoil reactivity

The reactivity of the subsoil along the particle tracks is characterised by five principal parameters: CEC(cation exchange capacity), OM (organic matter), Redox, presence of $CaCO3$ and pH. Calculation of the parameter values per flowpath segment is carried out by dedicated software procedures that apply interpolation schemes to observations of soil and groundwater properties at specific locations (Fig. 2).

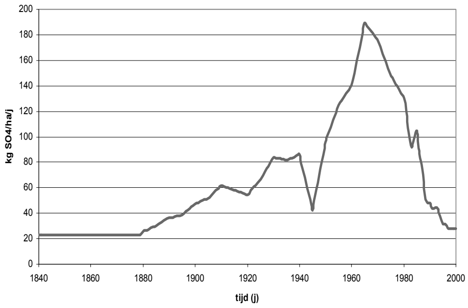

Fig. 1 Standard type curve S deposition

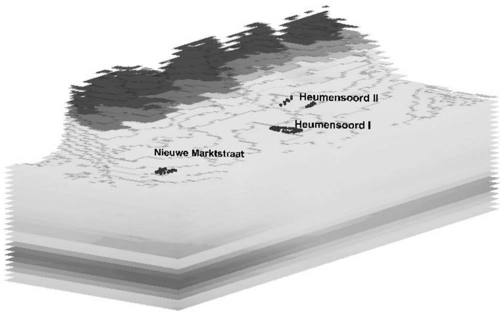

Fig. 2 3-D map of pH in the Nijmegen model area (pH in this example)

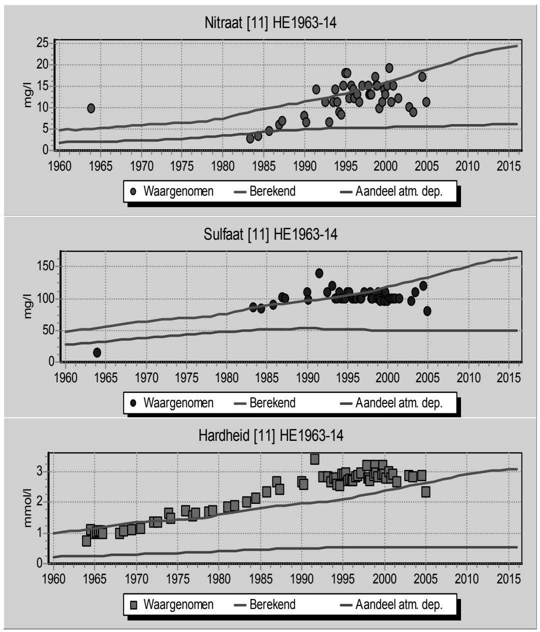

Fig. 3 Observed and simulated concentrations nitrate, sulphate and total hardness

Calibration

The calibration of the model is carried out with a genetic algorithm, where the calibration is defined as a multiple objective optimisation problem. (Vink et al., 2002, 2005). Over the past 20 years, evolutionary algorithms have been applied successfully to multi-objective optimization problems (e.g. Cieniawski et al. 1995). The development of genetic algorithms was inspired by the genetic processes of biological species. The simplified chemical model contains 13 parameters optimised with the GA.

Objectives of the parameter optimisation are: minimum differences between simulated and observed concentrations (1) and minimum differences between initial estimates and finally calibrated parameter values (2).

RESULTS

We applied the modelling instrument to different locations in The Netherlands where regional and local authorities work together with spatial planners, policy makers and technicians from drinking water company Vitens. The consequences of various land use plans were evaluated with respect to risks to the drinking water production, targets with respect the European Water Framework and Groundwater Directive and possibilities for local economic development. Chemical parameters that were modelled consisted of nitrate, sulphate, total hardness and various organic micro pollutants.

An interesting result that came out of the simulations for a well field near Nijmegen is that nitrate loads from urban areas are significantly higher than from areas with agricultural land use (Fig. 4, Fig. 5). Another case study that was carried out near Holten, in the east of the Netherlands showed locally pyrite activity in the subsoil. The activity could be reconstructed from comparison of observed concentrations of nitrate and sulphate in raw water to simulated concentrations with Respond. The most plausible explanation of relatively low nitrate and high sulphate concentrations in some wells assumes significant local activity of pyrite (Fig. 6, Fig. 7).

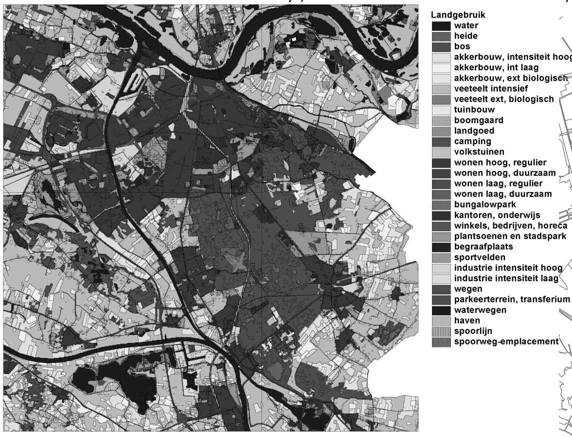

Fig. 4 Land use classes Nijmegen

Fig. 5 Net nitrate loads Nijmegen

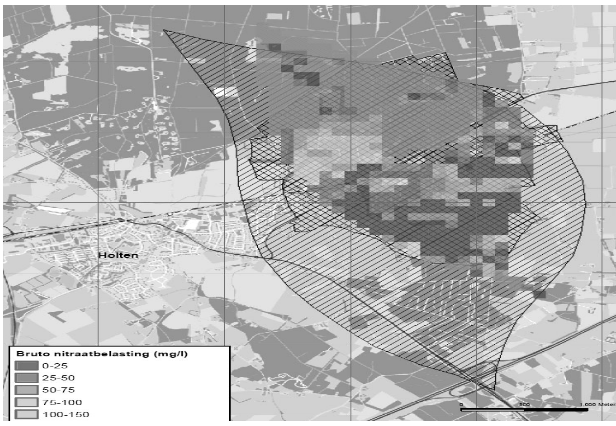

Fig. 6 Gross nitrate loads Holten

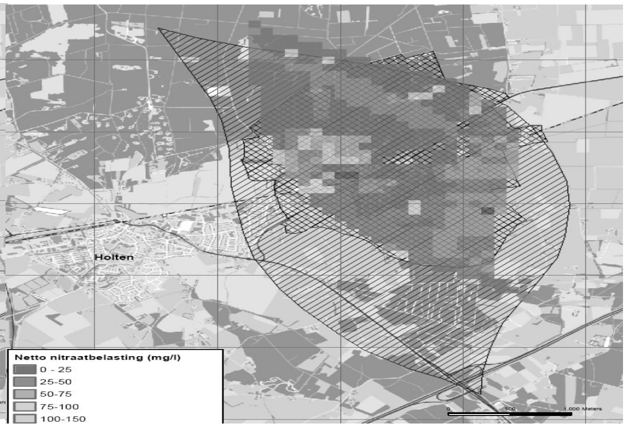

Fig. 7 Net nitrate loads Holten

The use of a relatively simple chemical transport model with a flow path approach enabled very modest calculation times and thus made calibration with GA possible. Use of a flux model such as MT3D is much more expensive with respect to computer time and would not allow the use of GA as a calibration technique. Allocation of stationary discharge rates to flow paths (tubes), as in Respond is probably less accurate than in the distributed flux approach of models such as MT3D, where mixing and nonstationary transport processes can be simulated more adequately. However, we think that in many cases the flowpath approach is justifiable and offers a valuable alternative to the flux approach.

REFERENCES

Appelo, C. A. J. & Postma, D. (2005) Geochemistry; groundwater and pollution. *2nd edition, Balkema publishers*.

Prommer, H., Davis, G. B. & Barry, D. A. (1999) PHT3D-A threedimensional biogeochemical transport model for modelling natural and enhanced remediation. (ed. C. D. Johnston), *Proc. Contaminated site remediation: Challenges posed by urban and industrial contaminants*, Fremantle, Western Australia, 21-25.3.1999, 351-358.

Stuyfzand, P. J. & Luers, F. (1996) Behaviour of environmental pollutants during bank filtration and artificial recharge; effects of aquifer passage as measured along flow paths. *Kiwa-Meded*. **125** ISBN 907474138X

Vink, C. & Schot, P. P. (2002) 'Multiple-Objective Optimization Of Drinking Water Production Strategies Using A Genetic Algorithm'. *Water Resources Research* **38**(9), 1181, Doi:10.1029/2000WR000034, 2002.

Vink, C. (2004) Multiple objective calibration of a groundwater model by means of a genetic algorithm. *Proceedings of the FEM_Modflow 2004 conference in Karlovy Vary, Czech Republic.*

Zheng, C. & Wang, P. P. (1999) MT3DMS: A Modular Three-Dimensional Multispecies Transport Model for Simulation of Advection, Dispersion, and Chemical Reactions of Contaminants in Groundwater Systems. *Documentation and User's Guide.*

Generalised storage-yield-reliability modelling- Independent validation of the Vogel-Stedinger (V-S) storage-yield-reliability model using a Monte Carlo simulation approach

A. J. ADELOYE
School of The Built Environment, Heriot-Watt University, EH14 4AS, UK
a.j.adeloye@hw.ac.uk

Abstract The generalised storage-yield-reliability model by Vogel & Stedinger (V-S) is widely used in the literature but there has never been any validation of the model with measured river runoff data. This project investigated this problem using three different river runoff data records within a Monte Carlo simulation framework. The results showed that the V-S model was most accurate for high demand ratios (i.e. demand/MAR > 0.8, where MAR is the mean annual runoff) and for Cv of annual runoff less than 0.5. These would be essentially over-year systems; hence another model is presented that could be used to adjust the V-S reservoir storage-yield predictions for within-year effects in situations where such effects are significant.
Keywords Vogel & Stedinger; generalised storage-yield model; validation

INTRODUCTION

Sustainable use of surface water resources requires knowledge of how much water is available. Traditionally, the determination of the required storage capacity is done through simulation based on river runoff data, which is infeasible at ungauged catchments. Generalised storage-yield models make such a task feasible by relating the storage capacity to the demand, and river runoff parameters that can reliably be estimated at ungauged sites, e.g. the variability. Generalised storage-yield models are also much quicker and therefore preferable for the preliminary screening of potential reservoir sites. However, to be useful, a generalised model must perform adequately at gauged sites, so as to engender confidence in its capability at ungauged sites.

The generalised model by Vogel & Stedinger (1987), or V-S for short, is one of the widely used in the literature but has never been validated using real runoff data. Additionally, the model only considers over-year systems; it will therefore under-predict when within-year behaviour is significant. Both issues were addressed in this study.

VOGEL-STEDINGER MODEL

Vogel & Stedinger (1987) showed that the distribution of capacity is 3-parameter log-normal, implying that the 100(1-p) % quantile of the scaled storage capacity is:

$$(S_{(1-p)})/\sigma = \vartheta + \exp(\mu_l + z_{(1-p)}\sigma_l) \qquad (1)$$

where ϑ is the lower limit, μ_l is the mean and σ_l is the standard deviation. z(1-p) is the standard normal variate at 100(1-p)% non-exceedance level and σ is the standard deviation of annual runoff, the scaling factor. If ϑ is known, then moment estimates for μ_l, σ_l are (Stedinger, 1980):

$$\mu_l = \ln\left[\frac{\mu_n - \vartheta}{\sqrt{1 + \frac{\sigma_n^2}{(\mu_n - \vartheta)^2}}}\right] \quad ; \quad \sigma_l^2 = \ln\left[1 + \frac{\sigma_n^2}{(\mu_n - \vartheta)^2}\right] \tag{2}$$

where the subscripts *n* and *l* denote normal and log-normal, respectively.

To generalise these parameters, Vogel & Stedinger (1987) used Monte Carlo simulations to generate large replicates of runoff data of different lengths, which were then used to drive the sequent-peak algorithm reservoir capacity estimation method (McMahon & Adeloye, 2005) to derive storage capacity for various yields. The resulting capacity populations were then analysed to determine ϑ, μ_n, σ_n Finally, regression equations for these three parameters were calibrated as (Vogel and Stedinger, 1987):

$$\mu_n' = \exp^{(a+bm)} \alpha^{c} m^{m(d\rho_1 + eN)} N^{(f + g\ln[m])} \left(\frac{1+\rho_1}{1-\rho_1}\right)^{h\ln[N]} \tag{3a}$$

$$\sigma_n'^2 = \exp\left[a + b\alpha + \frac{cN}{m} + \left(\frac{d}{N} + \frac{e}{m}\right)\left(\frac{1+\rho_1}{1-\rho_1}\right)\right] N^{f\ln[m]} \left(\frac{1+\rho_1}{1-\rho_1}\right)^{g\ln[N]} \tag{3b}$$

$$\vartheta' = a\rho_1 + \left(bN + \frac{c(1+\rho_1)}{(1-\rho_1)}\right)\ln[m] + N\left(d + \frac{e}{m} + fm\ln[N] + g\ln\left(\frac{1+\rho_1}{1-\rho_1}\right)\right) \tag{3c}$$

where *a, b, c, d, e, f, g* and *h* are model parameters (see Table 1); *N* is the data record length; α = demand/MAR; ρ_1 is the lag-one serial correlation of annual flow and the superscript $'$ denotes regression estimate. $m = (1-\alpha)/Cv$ is the drift, where $Cv = \sigma$/MAR is the coefficient of variation of annual runoff. The V-S model was developed for $Cv < 0.5$; $m < 1.0$ represents over-year behaviour and $m > 1.0$ represents within-year.

METHODOLOGY

The study used three rivers record as detailed in Table 2; one of these had Cv > 0.5; hence the demand ratio, α, must be carefully selected to ensure that the resulting *m* is less than 1.0. For each river, the capacity quantiles were first determined using the V-S parameters derived with equation (3). Then, 100 replicates of each river runoff data record were generated using a simple non-parametric re-sampling technique. Each of the replicates was then used to drive the SPA and reservoir capacity for each demand ratio α was determined. Repeating this for all the 100 replicates gave 100 estimates of reservoir capacity; this taken as the population from which ϑ, μ_n, σ_n were also determined and thus represent the runoff data-based estimates of these parameters.

RESULTS AND DISCUSSION

Extensive tests were carried out, which ascertained the appropriateness of the 3-p lognormal model for reservoir capacity. Fig. 1 shows the capacity quantile estimates for the various reservoirs. As seen in the Fig, there is a general tendency for the V-S model to under predict the reservoir capacity, particularly when *m* is close to one. Indeed for the Earn, both the V-S and data based capacity quantiles agree perfectly at $\alpha = 0.95$ (i.e. $m = 0.26$). The same observation could be made for Hatchie River at Bolivar but not for the Vis. A possible reason for this is that unlike both the Earn and Hatchie, the Cv of the Vis is 1.29, much higher than the Cv = 0.5 validity threshold for the V-S model. It is therefore not surprising that the error in the V-S estimates is most pronounced for the Vis River. Since the V-S model only considers over-year capacity, its estimates can be adjusted for within-year capacity using the model developed by Adeloye *et al*. (2003) and independently validated by McMahon *et al*. (2007):

$$K/MAR = -0.222 + 0.3222Cv + 0.6\alpha + 1.025S/MAR \qquad ($$

where MAR is the mean annual runoff, K is the total (i.e. within-year + over-year capacity), S is the over-year capacity (obtainable via the V-S model) and all the other variables are as defined previously.

Table 1 Coefficients in Vogel and Stedinger (1987) model.

Coefficients	μ_n'	σ_n'	ϑ'
a	0.237	-5.92	0.467
b	-1.33	4.89	-0.0398
c	1.81	-0.000958	0.189
d	-1.03	10.0	-0.0332
e	0.00621	-0.0342	-0.00407
f	0.369	-0.520	0.00803
g	-0.0562	0.421	-0.00403
h	0.100	0.0	0.0

Table 2 Rivers detail

River	MAR (10^6 m^3)	Cv	Length of record (years)
Earn at Kinkell Bridge Scotland	648	0.19	34
Hatchie at Bolivar USA	2178	0.36	55
Vis at Harderug South Africa	14.1	1.29	33

CONCLUSION

Validation of the V-S model has been carried out using time series runoff data. It was found that in general, the model under-estimates the reservoir capacity, although its performance does improve as the drift *m* becomes much lower than unity, i.e. as over-year behaviour becomes significant. The model is very poor when the Cv of the river is much higher than the 0.5 maximum threshold recommended by Vogel & Stedinger. When the V-S model is appropriately applied, its capacity estimate can be adjusted for within-year contribution using the model developed by Adeloye *et al*. (2003).

REFERENCES

Adeloye, A. J., Lallemand, F. & McMahon, T. A. (2003) Regression models for within-year capacity adjustment in reservoir planning. *Hydrol. Sci. J.* **48**(4), 539-552.

McMahon, T. A. & Adeloye, A. J. (2005) Water resources yield. *Water Resources Publications, CO.,* USA.

McMahon, T. A., Pegram, G. G. S., Vogel, R. M. & Peel, M. C. (2007) Revisting reservoir storage-yield relationships using a global streamflow database. *Adv. Wat. Resour*. **30**, 1858 – 1872.

Stedinger, J. R. (1980) Fitting log-normal distribution to hydrologic data. *Wat. Resour. Res*. **16**(3), 481 – 490.

Vogel, R. M. & Stedinger, J. R. (1987) Generalised storage yield relationships. *J. Hydrol.* **89**, 303 – 327.

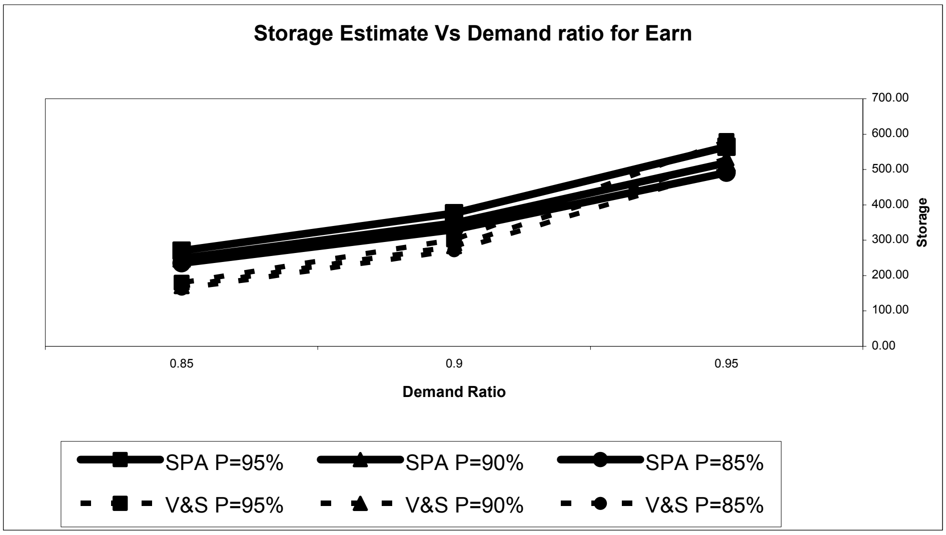

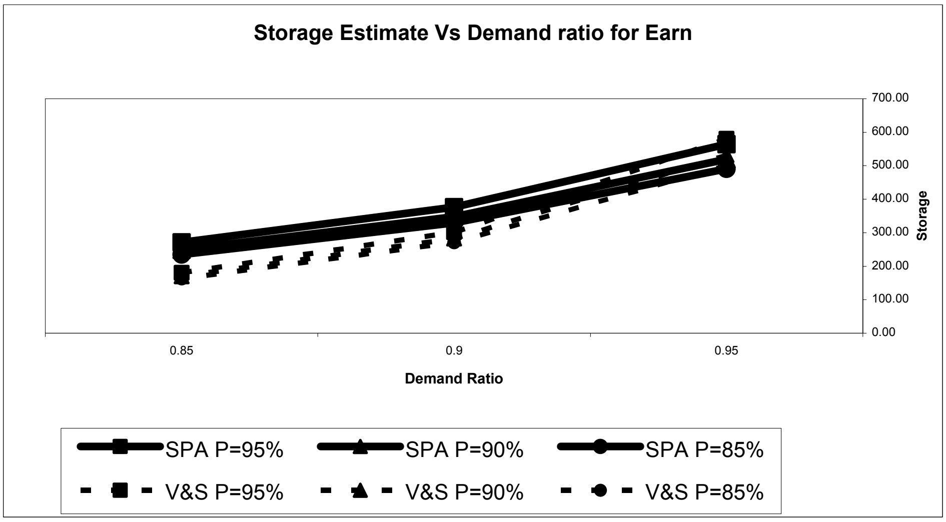

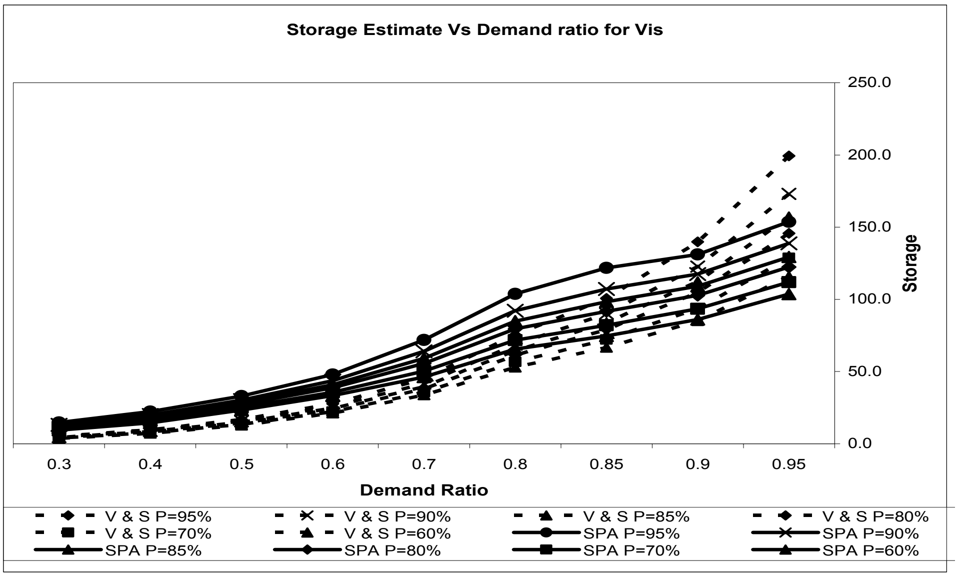

Fig. 1 Performance of the V-S model relative to the SPA for the Earn, Hatchie and Vis Rivers.

Surface water – groundwater interactions in River Murray wetlands and implications for water quality and ecology

R. S. CROSBIE[1], I. D. JOLLY[1], K. L. MCEWAN[1], K. L. HOLLAND[1], S. LAMONTAGNE[1], K. GROTTHING MOE[2] & C. T. SIMMONS[2]

1 *CSIRO Land and Water, PMB 2, Glen Osmond SA 5064, Australia*
russell.crosbie@csiro.au

2 *School of Chemistry, Physics and Earth Sciences, Flinders University, GPO Box 2100, Adelaide SA 5001*

Abstract The wetlands of the lower River Murray in southeastern Australia have been degraded by the damming and regulation of the river for water supply and navigation purposes. This study developed a characterisation scheme to predict the hydrological and salinity regimes of the wetlands based upon some of their physical properties. The framework was used to classify 2000 wetlands in the South Australian section of the river. The framework can also be used to infer wetland ecological health because salinity and hydrological regime are key ecosystem drivers in this environment. A field study was conducted on three wetlands to test the predictions of the characterisation scheme and to understand the processes involved. This study found that the re-introduction of wetting and drying cycles to permanently inundated wetlands in this environment is likely to lead to further salinisation and a decrease in ecological health.

Keywords wetlands; salinisation; Australia

INTRODUCTION

The volume of water stored in arid zone wetlands is as great as that stored in temperate regions but the research effort does not reflect this balance. The arid / semi-arid areas of the world are concentrated in developing countries where resources for research are scarce. Even in Australia, research into wetland ecology has primarily focused on the 30% of the continent that is not within the arid zone (Kingsford, 1997). The water regime of arid / semi-arid wetlands can have some complex groundwater – surface water interactions but they are not always well understood (Jolly *et al.*, 2008). This has resulted in lessons learnt in humid regions being applied to drier regions without knowledge of the consequences.

The River Murray is Australia's largest (10^6 km^2) and most important river system. All the major headwater tributaries have large dams for supplying water to irrigation areas and the lower reaches have weirs and locks installed for navigation. The weirs and locks have permanently inundated many wetlands and the dams have reduced the magnitude, frequency and duration of flooding. The climate of the lower River Murray is semi-arid so potential evapotranspiration is much greater than rainfall. The regional groundwater below the floodplains is saline (~50,000 μS/cm) and much closer to the surface than under natural conditions due to the elevated river stage and additional recharge due to irrigation. This leads to salinisation through groundwater discharge because the reduction in flooding limits the leaching of salt from the soil (Jolly *et al.*, 1993).

There are over 2000 wetlands in the South Australian section of the lower River Murray, and increasing community awareness of their ecological value is driving a need for an active management approach. Many wetlands now have regulation structures at their connection to the river to enable engineered wetting and drying cycles. The engineered wetting and drying cycles aim to mimic the natural variability in hydrological regime which stimulates the life cycles of the biota.

This study aimed to investigate whether the ecological health of a wetland can be predicted from simple physical properties. This was done by developing a characterisation scheme which is capable of predicting the hydrological and salinity regimes of the wetlands (Crosbie *et al.*, 2008) and then testing this characterisation scheme on three wetlands with contrasting surface water regimes (Crosbie *et al.*, 2007).

WETLAND CHARACTERISATION

Previous classifications of the wetlands of the lower River Murray have focused upon the physical and chemical properties as they relate to their ecology. The present study differs from previous work in that it is focused on the hydrology and salinity of the wetlands and uses this to infer the ecological status. The current study has used existing physical data from 70 wetlands (SKM, 2004, 2006) to develop a characterisation scheme (Fig. 1) and existing biological data (SKM, 2004, 2006) to test if wetland ecological status can be reliably predicted.

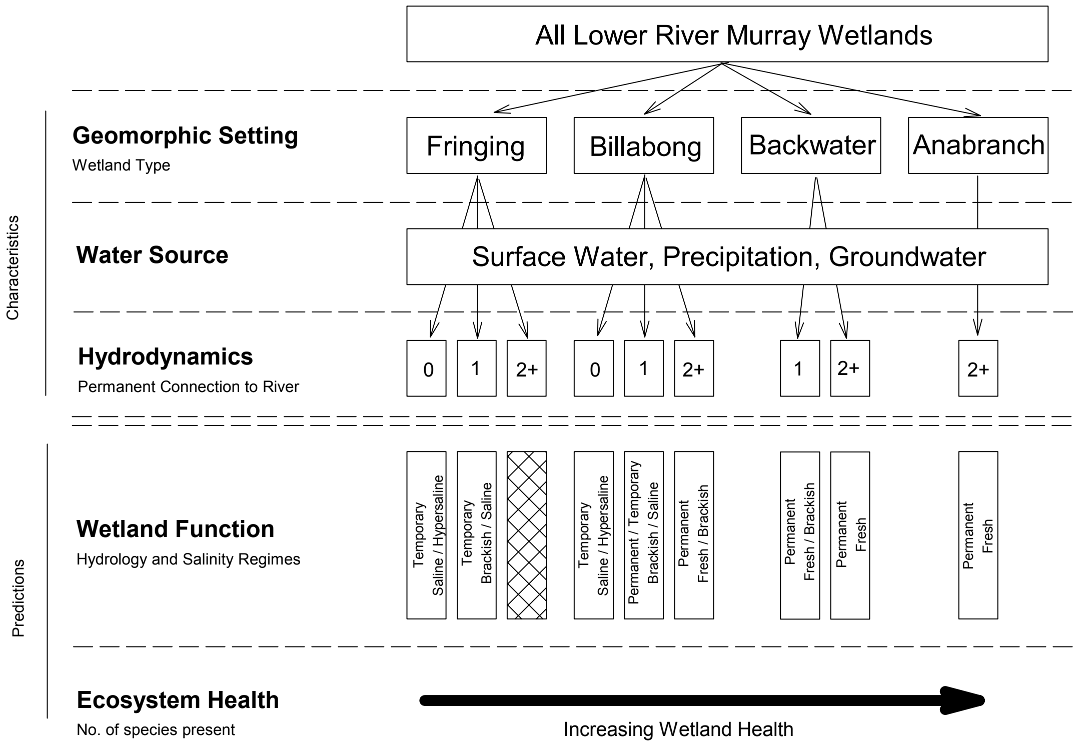

Fig. 1 Characterisation scheme developed for the lower Murray Wetlands.

The use of only eight categories has enabled the characterisation scheme to be kept simple while providing enough explanatory power to predict the hydrological regime and salinity of the wetlands. The eight classes were based on a hierarchical structure (Brinson, 1993) with the wetland type as the first level and the number of permanent connections to the river as the second level. The wetland types were grouped into four classes (anabranches, backwaters, billabongs and fringing wetlands) and the connections to the river grouped into three classes (no connection to the river at weir pool level, one connection at weir pool level and two or more connections at weir pool level).

The ecological health of the wetlands (number of species present) increases with decreasing salinity (Crosbie *et al.*, 2008). The characterisation scheme also predicts that wetlands will have greater species richness with an increasing number of connections to the river at weir pool level for all wetland types. By wetland type, the species richness increased in the order: fringing wetlands, billabongs, backwaters and anabranches.

FIELD STUDY

The field study investigated three wetlands with contrasting surface hydrological regimes during the drying phase of an engineered wetting and drying cycle:

- Lake Littra is a temporary wetland that has no connection to the river except during flood events;
- Hart Lagoon has one connection to the river at weir pool level providing a limited exchange of water and solutes;
- Banrock Station wetland has two connections to the river at weir pool level, one on either side of a weir / lock, providing a substantial flow of surface water through the wetland.

A range of methods were utilised for investigating the surface water – groundwater interactions of these wetlands including EM surveys, analysis of hydrometric observations and the analysis of water samples taken from river water, wetland surface water, and groundwater.

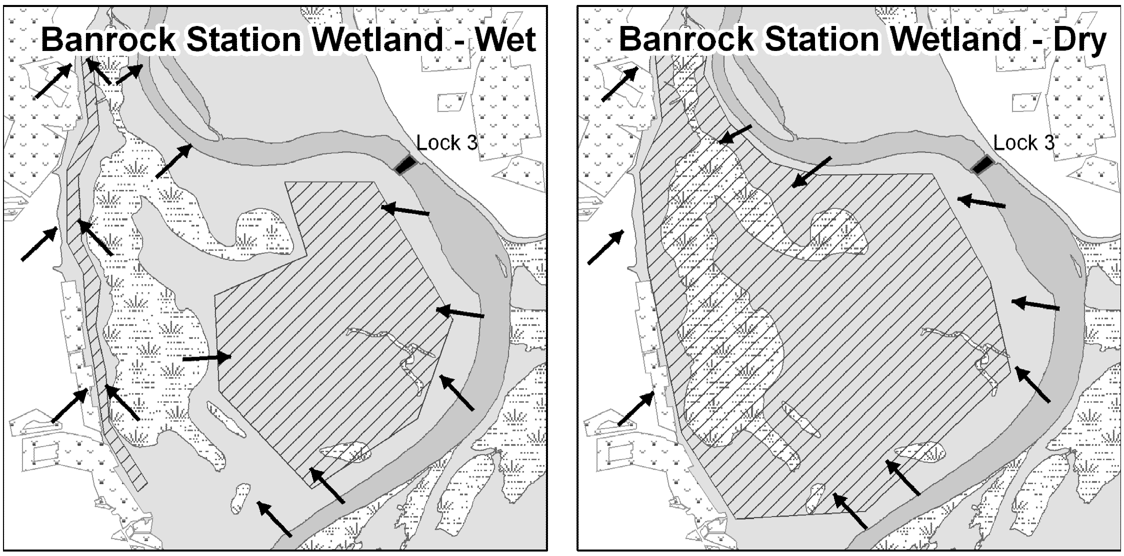

Fig. 2 Conceptual models of groundwater flow and discharge for Banrock Station wetland under conditions of being inundated and dry. Arrows show direction of groundwater flow and hatched areas show groundwater discharge areas. When inundated the wetland acts as a recharge feature and creates a fresh water lens below the wetland, when dry the wetland is a discharge feature and at risk of salinisation.

Each wetland is actively managed meaning the number of connections to the river can be modified. During the drying phase of a wetting and drying cycle, regulation structures are closed severing the link to the river, this shifts the wetland to left in Fig. 1. Lake Littra and Banrock Station wetland (Fig. 2) were found to be groundwater recharge features when inundated, while Hart Lagoon was a groundwater flow through system. After the surface water had been removed, there was a reversal of the hydraulic gradients and all three wetlands became groundwater discharge features (Fig.

2). Groundwater discharge leads to salinisation.

CONCLUSIONS

The results of the field study were consistent with the predictions made using the characterisation framework. The characterisation framework suggested that wetland ecological health (assessed as the number of species present) increases with the number of connections to the river for each wetland type. The field study demonstrated that this occurs because wetlands are more likely to salinise when they have fewer connections to the river. By regulating the wetlands connection to the river wetland managers have the ability to vary the number of connections to the river. When dried lower River Murray wetlands tend to become groundwater discharge features and will accumulate salt. While wetting and drying cycles were ecologically beneficial in the past, they may not be the ideal management option for the South Australian section of the lower River Murray. Both the surface hydrology and the groundwater hydrology of the wetlands have been modified by river regulation. Thus, both surface and groundwater must be considered when designing management strategies for these wetlands.

Acknowledgements The authors wish to acknowledge the financial support given to this project by the *Centre for Natural Resources Management* under Project ID CNRM 054121.

REFERENCES

Brinson, M. M. (1993) A hydrogeomorphic classification for wetlands. *Rep. No. Technical Report WRP-DE-4. U.S. Army Engineer Waterways Experiment Station, Vicksburg, MS.*

Crosbie, R. S., Jolly, I. D., McEwan, K. L. & Holland, K. L. (2008) A framework for the characterisation of the hydrology and salinity regime of wetlands of the lower River Murray. *In 2nd International Salinity Forum, Adelaide*.

Crosbie, R. S., McEwan, K. L., Jolly, I. D., Holland, K. L. & Lamontagne, S. (2007) Surface water – groundwater interactions in three River Murray floodplain wetlands: Results from field studies. *CSIRO Water for a Healthy Country Flagship report, Adelaide.*

Jolly, I. D., McEwan, K. L. & Holland, K. L. (2008) A review of groundwater - surface water interactions in arid / semi-arid wetlands and the consequences of salinity for wetland ecology. *Ecohydrology* **1**, 43-58.

Jolly, I. D., Walker, G. R. & Thorburn, P. J. (1993) Salt accumulation in semi-arid floodplain soils with implications for forest health. *Journal of Hydrology* **150**, 589-614.

Kingsford, R. T. (1997) Wetlands of the world's arid zones. In *A contribution from the Convention on Wetlands (Ramsar, Iran, 1971) to the first Session of the Conference of the Parties to the UN Convention to Combat Desertification*, Rome, 29 September to 10 October 1997.

SKM (2004) River Murray Wetlands Baseline Survey - 2004. *South Australian Murray-Darling Basin Natural Resources Management Board, Berri.*

SKM (2006) River Murray Wetlands Baseline Survey - 2005. *South Australian Murray-Darling Basin Natural Resources Management Board, Berri.*

Non-linear adsorption in a multidimensional and double-porosity model of fractured rock solute transport

JIŘÍ HAVLÍČEK, MILAN HOKR & JIŘÍ KOPAL

Faculty of Mechatronics and Interdisciplinary Engineering Studies, Technical University of Liberec, Hálkova 6, *461 17 Liberec, Czech Republic*

milan.hokr@tul.cz

Abstract We define a model of solute transport in fractured rock as a combination of the standard concepts into a multidimensional double-porosity. As addition to the previous work, we formulate the model with non-linear equilibrium adsorption in each domain. The numerical code uses the finite volume space discretisation and the operator splitting method in time to separate the complex processes. Test problems in 1D and 2D demonstrate the effect of non-linearity to the concentration profile and breakthrough curve shapes.

Keywords discrete fracture network; dual-porosity; immobile zone; non-linear adsorption; solute retention

INTRODUCTION

The paper deals with conceptual models and numerical algorithms for solute transport in the fractured rock. The known difficulties are related to geometric complexity of fracture networks and resulting computational cost and parameter uncertainty. The modelling is based on several approaches; the typical are equivalent continuum, discrete fracture networks, and double-porosity models (Bear *et al*., 1993).

Recently we introduced a concept of combining network of large discrete fractures and double-porosity continuum representation of the remaining fractures – multidimensional double-porosity model. In this paper we introduce the process of adsorption to solid phase, with general non-equilibrium isotherm. Comparing to Gallo *et al*. (2006), we formulate and solve the mobile-immobile model with non-linear adsorption isotherm instead of linear.

There are no special numerical methods derived in literature for combination of the non-equilibrium exchange between mobile and immobile zone and the equilibrium non-linear adsorption. Using the operator-splitting method, known e.g. as a tool for separation of advection and diffusion, we can extract all the additional transport processes to be solved separately with simple analytical formulas (Hokr *et al*., 2003).

In the test problems, we demonstrate the qualitative difference between solute retention and concentration front retardation as consequence of either the transfer from the discrete fracture into the rock matrix, or the transfer from mobile to immobile water in a geometrically same place, or the equilibrium adsorption.

MODEL CONCEPT AND GOVERNING EQUATIONS

We consider a system of 3D continuum, 2D discrete fracture network and a network of 1D fracture intersection. Each part is further composed of a mobile and immobile part (double continuum). We denote the problem domain $\Omega = \Omega_1 \cup \Omega_2 \cup \Omega_3$, $\Omega_i \subset R_3$, $i = 1, 2, 3$, where Ω_3 is polyhedron (3D continuum), Ω_2 is a system of planar polygons (discrete fracture network) and Ω_1 is a systems of lines (intersections of fractures = "pipes"). The governing equations of flow are ($i = 1, 2, 3$)

$$\vec{u}_i = K_i \nabla p_i \quad in\Omega_i \tag{1}$$

$$\kappa_i \frac{\partial p_i}{\partial t} - \nabla \cdot \vec{u}_i = q_i^+ + q_i^- + \sum_{j=1, j\neq i}^{3} \frac{\tilde{q}_{ij}}{\mu_i} \quad in\Omega_i \tag{2}$$

$$\tilde{q}_{ij} = \sigma_{ij}(p_i - p_j) \qquad i \neq j$$

where the unknowns are $u_i(\vec{x},t)$ the velocity and $p_i(\vec{x},t)$ the piezometric head and the parameters are K_i the hydraulic conductivity, κ_i the storativity, q_i sources/sinks, σ_{ij} transmissivity between domains, and the variable $\tilde{q}_{ij}$ (positive from j to i) denotes the flux between domains of different dimensionality. The parameter μ_i is an additional dimension: μ_1 is cross-sectional area of 1D domain, μ_2 is thickness of 2D domain, and $\mu_3 = 1$ (dimensionless). The governing equations of the mass transport are

$$n_i^{(m)} \frac{\partial\left(c_i^{(m)} + f_i^{(m)}(c_i^{(m)})\right)}{\partial t} = -\nabla \cdot (c_i^{(m)}\vec{u}_i) + \nabla \cdot (\mathbf{D}_h^{(i)} \nabla c_i^{(m)}) +$$

$$q^+ c^{(m)*} + q^- c^{(m)} + \sum_{j=1, j\neq i}^{3} \frac{\tilde{q}_{ij}^{(c)}}{\mu_i} + r_i^{(m)} - \alpha_i (c_i^{(m)} - c_i^{(im)}) \tag{3}$$

$$n_i^{(im)} \frac{\partial\left(c_i^{(im)} + f_i^{(im)}(c_i^{(im)})\right)}{\partial t} = r_i^{(im)} + \alpha_i (c_i^{(m)} - c_i^{(im)}) \tag{4}$$

where the unknowns are $c^{(m)}$ the concentration in the mobile zone and $c^{(im)}$ the concentration in the immobile zone, the parameters are D_h the tensor of hydrodynamic dispersion, c^* the injected concentration, $\tilde{q}_{ij}^{(c)}$ the auxiliary solute source/sink from the interaction between domains of different dimension, α is the rate of mobile-immobile exchange, $r_i^{(m)}$, $r_i^{(im)}$ the chemical reaction production terms,. The parameters $n^{(m)}$ and $n^{(im)}$ (porosities) represent the relative volume of mobile and immobile zone of the media, the subscripts i, j denote the part of the domain with respective dimension. The adsorption term $f_i^{(m)}(c_i^{(m)})$ (and corresponding for the immobile zone) is arbitrary continuous non-decreasing function, e.g. the Freundlich isotherm can be written as

$$f_i^{(m)}(c_i^{(m)}) = \rho_i^s K_F c_i^{(m)a_F} \frac{\phi(1 - n_i^{(m)} - n_i^{(im)})}{n_i^{(m)}} \tag{5}$$

$$f_i^{(im)}(c_i^{(im)}) = \rho_i^s K_F c_i^{(im)a_F} \frac{(1-\phi)(1 - n_i^{(m)} - n_i^{(im)})}{n_i^{(im)}} \tag{6}$$

where ϕ is fraction of sorption surface between the mobile zone and the immobile zone and ρ_s is the solid density (in the test problems below included in the K_F value).

NUMERICAL SOLUTION

The model is implemented in our simulation code FLOW123D with batch processing. The discretisation is realized with tetrahedrons in 3D and triangles in 2D. The fluid flow is solved using mixed-hybrid formulation of finite element method with pressure and velocity results, see also Královcová *et al.* (2006). The transport problem is solved with the finite volume method. We use operator splitting method for single transport processes separation (advection and mobile-immobile exchange), whose technical realisation employing an analytical solution of mobile-immobile exchange is described in Hokr *et al.* (2003).

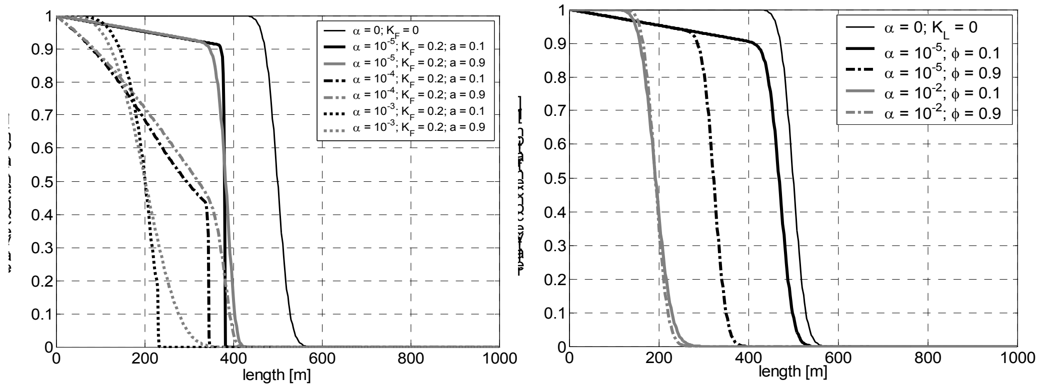

Fig. 1 Profile of the concentration in the final time of simulation for the 1D test problem – effect of mobile-immobile exchange (rate α), Freundlich sorption isotherm (exponent a), and the sorption fractioning ϕ.

MODEL PROBLEMS

One-dimensional test problem

We consider the constant-concentration inflow problem to test the numerical algorithm. The problem is defined as 1000m long line, with constant flow $1\,\mathrm{m\,d^{-1}}$, diffusion coefficient $D=0.5\mathrm{m^2\,d^{-1}}$, zero initial concentration and given inflow concentration $1\,\mathrm{kg\,m^{-3}}$. We consider the mobile-immobile exchange with the rate α (several variants) and linear and Freundlich adsorption isotherm. The volume of the mobile zone and the immobile zone are the same (n_m=0.2, n_{im}=0.2), as well as the sorption fractioning (ϕ=0.5).

The results for selected parameters are displayed in Fig. 1. In the first graph, the case with exponent close to 1 (linear case) is compared to the small exponent (concave sorption curve), leading to larger retardation for smaller concentration and producing steepening of the concentration front. The second graph shows that for small transfer to the immobile zone, only the sorption in the mobile zone contributes to retardation, while for the almost equilibrium case, sorption effect is in both and does not depend on fractioning.

Combination of continuum and fracture network

The problem is defined as a 2D continuum rectangle 12.75 × 8 m, with discrete fracture network composed of lines (section of fractured media). The pressure head is prescribed on the left and right boundaries with gradient 0.001 (steady flow). Prescribed concentration c_{IN}= 1g $\mathrm{l^{-1}}$ is on the inflow boundary (Fig.2).The initial state is zero concentration. The problem is solved in the time interval 1000years. The material parameters for the fracture and the continuum are given in Tab. 1. The three variants of mobile-immobile transfer rate represent the cases of very small mass exchange, medium influence, and almost equilibrium. The three variants of Freundlich exponent represent the effect of non-linearity with respect to the quantitatively similar linear case (a_F=1).

The results are presented by means of concentration contour in the selected time (Fig 2) and breakthrough curves in the outflow point of the fracture (Fig. 3). We can see the front sharpening with decreasing Freundlich exponent in the left and several steps of retardation (rock matrix, immobile zone, adsorbed) in Fig. 3 right. Presence of sorption also changes the breakthrough curve shape besides the retardation (steps).

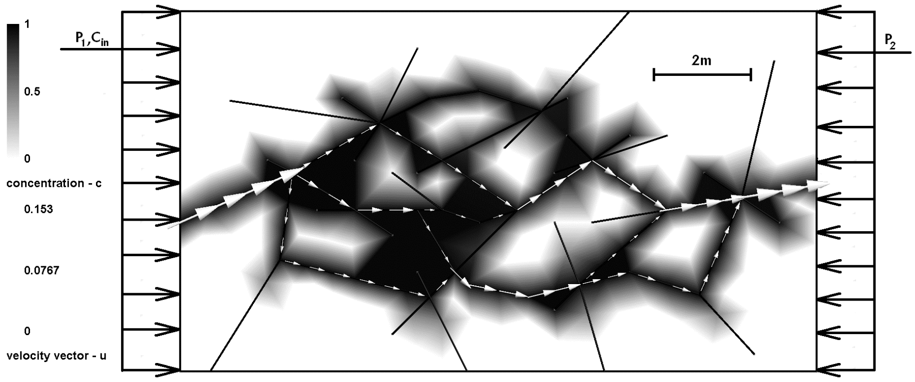

Fig. 2 Illustration of fracture network and boundary condition, together with the results of the scalar field of concentrations in the time t=1000 years for the task with Freundlich sorption (a_{F3}) and no immobile zone. The velocity value is displayed by the arrow size.

Table 1 Material parameters used for the test problem of the multidimensional (fracture-continuum) model, with mobile and immobile parts and non-linear Freundlich adsorption. The coefficients are defined within the equations (3) and (4), the subscript at α and a_F denotes a problem variant.

	K [m s^{-1}]	n_i [1]	n_m [1]	ϕ [1]	μ_1 [m^2]	μ_2 [m]	K_F [m^{3aF} kg^{-aF}]	α_1 [year^{-1}]	α_2 [year^{-1}]	α_3 [year^{-1}]	a_{F1} [1]	a_{F2} [1]	a_{F3} [1]
Rock (2D)	3.2×10^{-10}	0.2	0.4	0.9	-	1	0.002	0.0001	0.01	1	0.1	0.5	1
Fracture (1D)	3.2×10^{-5}	0.2	0.4	0.9	1	-	0.002	0.0001	0.01	1	0.1	0.5	1

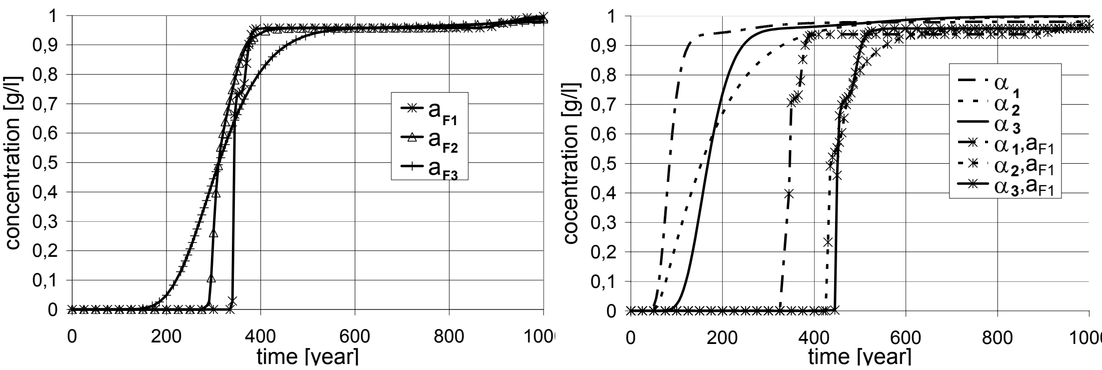

Fig. 3 Breakthrough curves for the various exponents in the Freundlich isotherm (left) and various rates of mobile-immobile exchange (right) with or without sorption.

Acknowledgement

This work has been supported by Ministry of Education of the Czech Republic, under the project "Advanced remedial technologies and processes", code 1M0554.

REFERENCES

Bear, J., Tsang, C. F. & De Marsily, G. (1993) Modelling Flow and Contaminant Transport in Fractured Rocks, *USA: Academic Press, Inc.*

Gallo, C., Paniconi, C. & Gambolati, G. (1996) Comparison of solution approaches for the two-domain model of nonequilibrium transport in porous media. *Adv. Water Resour.* **19**, 241--253.

Hokr, M., Maryška, J. & Šembera, J. (2003) Modelling of transport with non-equilibrium effects in dual-porosity media. *In Current Trends in Scientific Computing (Chen et al, eds), Amer. Math. Soc.,* 175-182.

Královcová, J., Maryška, J., Severýn, O. & Šembera, J. (2006) Formulation of mixed-hybrid FE model of flow in fractured porous medium. *Proceedings of ENUMATH 2005, Springer-Verlag, 2006,* 1184-1191

Predicting the interactions between rivers and groundwater pumping

IAN JOLLY[1], DAVID RASSAM[1], MAT GILFEDDER[1], MATT STENSON[1], TREVOR PICKETT[1], JEFF TURNER[1], ANTHONY BARR[1], GAVIN MUDD[2], MARK SILBURN[3], ADRIAN WERNER[3], GERARD MCMAHON[3], CRAIG JOHANSEN[3], MARK REID[4], XIANG CHENG[4], BRENDAN CHRISTY[4], ANNA WEEKS[4] & MARK LITTLEBOY[5]

1 *eWater Cooperative Research Centre and CSIRO Land and Water, PMB 2, Glen Osmond, SA, 5064, Australia*
ian.jolly@csiro.au

2 *eWater Cooperative Research Centre and Dept of Civil Engineering, Monash University, Australia*

3 *eWater Cooperative Research Centre and Queensland Dept of Natural Resources and Water, Australia*

4 *eWater Cooperative Research Centre and Victorian Dept of Primary Industries, Australia*

5 *eWater Cooperative Research Centre and NSW Dept of Environment and Climate Change, Australia*

Abstract We summarise research that the eWater Cooperative Research Centre is carrying out incorporating groundwater-surface water interaction capabilities into the next generation of river management tools being developed for Australia's large river basins. We describe three simplified modelling approaches that are currently in development: (i) a reach scale 'Groundwater-Surface Water Link' model, which operates as a groundwater link to river models and accounts for interactions at the river-reach scale; (ii) a sub-reach scale 'Floodplain Processes' model, which dynamically models bank storage, evapotranspiration, and floodplain inundation. It enables more refined modelling of groundwater-surface water interactions, and can be linked to ecological response models; and (iii) a catchment scale model that estimates the surface and sub-surface flow components to streams.
Keywords groundwater; surface water; interaction; modelling; water security

INTRODUCTION

The National Water Initiative (NWI; http://www.nwc.gov.au/NWI/index.cfm) is Australia's blueprint for national water reform and has a key aim of more transparent and comprehensive water planning that deals with the interaction between surface and groundwater systems. In many of Australia's river basins extraction of large volumes of groundwater in close proximity to major streams and rivers has the potential to reduce stream flows (and in some instances already has). Basin-scale prediction tools that simulate these complex interactions are needed to assist in providing sustainable allocation of water. One of the core aims of the eWater Cooperative Research Centre is to develop the next generation of river planning, management and operation tools for Australia. The Groundwater Project in eWater is developing modelling tools which will provide the groundwater-surface water (GW-SW) interaction capability for the new RiverManager (http://www.ewatercrc.com.au/downloads/technologies/P2.pdf) and WaterCAST (http://www.ewatercrc.com.au/downloads/technologies/P5.pdf) products.

THE APPROACH TO MODELLING GW-SW INTERACTIONS IN LARGE RIVER BASINS IN AUSTRALIA

In an extensive literature review, Rassam & Werner (2008) found that a key challenge in modelling GW-SW interactions in large river basins (i.e. catchment areas > 20,000 km^2 are typical in Australia) is the spatial and temporal inconsistency of groundwater data that can be used to develop and test the models. They also found that GW-SW interactions are handled poorly in existing surface water models and groundwater models. In river models, these interactions are generally treated simply as a loss term. In groundwater models, the river is generally just modelled simplistically as a boundary condition. More sophisticated models that explicitly account for GW-SW interactions usually require more data, which are not always readily available. They also require a very high degree of modelling expertise and greater computational resources, which are not always available in water management agencies. Identifying the GW-SW interaction processes that are most relevant to the Australian landscape is very critical, as highlighted by the review of Reid *et al.* (2008).

When choosing modelling tools it is important to strike the right balance between surface water processes and groundwater processes. This balance can only be achieved when special-purpose custom-built models are developed to answer specific management questions. With these considerations in mind, the development of simplified modelling approaches is being carried out in this project, specifically: (i) a reach scale 'Groundwater-Surface Water Link' model, which operates as a groundwater link to river models and accounts for interactions at the river-reach scale. This will be a module in RiverManager; (ii) a sub-reach scale 'Floodplain Processes' model, which dynamically models bank storage, evapotranspiration, and floodplain inundation. It enables more refined modelling of groundwater-surface water interactions, and can be linked to ecological response models. This will also be a module in RiverManager; and (iii) at the catchment scale, the groundwater flow and salt transport concepts encapsulated in the existing 2CSalt model will be adapted for inclusion in WaterCAST.

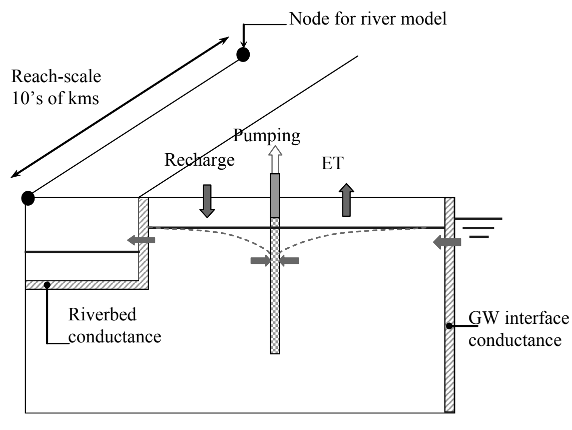

Fig. 1 Groundwater-surface water interactions for a gaining river system to be modelled in the Groundwater-Surface Water Link Model.

REACH-SCALE GROUNDWATER-SURFACE WATER LINK MODEL

This is a bucket-type model, which operates as a groundwater node for RiverManager. The scale at which it will operate is in the order of tens of kilometres and conforms to the node spacing of the RiverManager model to which it is coupled. The groundwater link to the bucket is derived from simple methods such as flow nets or more complex methods such as numerical models. The GW-SW processes are being added in stages to ensure individual processes are modelled correctly. The final model will be applied in the form of multiple spatially distributed buckets along the nodes of a RiverManager model of a river basin. A conceptualisation of this model (for a gaining stream) is shown in Fig. 1.

Based on the best understanding of the GW-SW interaction processes that could take place in a given reach, this model estimates those interactions as an in-out flux to and from the river model links. The various fluxes, such as loss of groundwater via evapotranspiration (ET) and groundwater pumping, are not spatially explicit within a node-to-node bucket, but represented as a total volumetric loss or gain for each time step in the river model.

SUB-REACH SCALE FLOODPLAIN PROCESSES MODEL

Based on the approach of Knight & Rassam (2007) and Rassam *et al.* (2008), this model aims to simulate floodplain processes at a high spatial resolution, in addition to the processes previously outlined in the Groundwater – Surface Water Link Model. A conceptualisation is shown in Fig. 2.

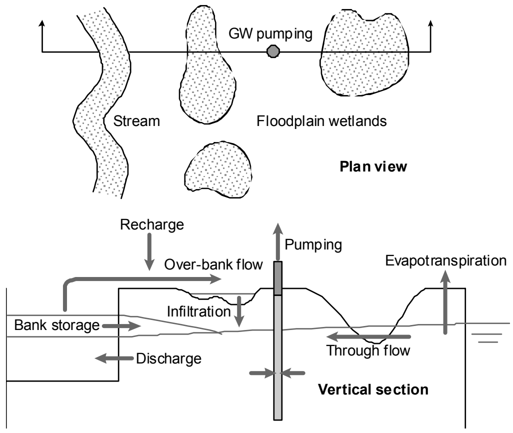

Fig. 2 Conceptualisation of the Floodplain Processes Model.

The groundwater link to the floodplain model is similar to that used in the Groundwater – Surface Water Link Model. Flow of river water into the aquifer can occur via bank storage when flows are within bank, or via flood recharge when infiltration of over-bank flows occur. Groundwater can be lost by pumping, ET (see Rassam *et al.*, 2007) and flow back into the river when river stages drop below the groundwater level. Changes in recharge over time due to land use changes are estimated and applied in the model accordingly. In contrast to the Groundwater – Surface Water Link Model, the temporal modelling of all of these processes in the Floodplain Processes Model is spatially explicit.

CATCHMENT SCALE WATER GENERATION MODEL

This component is adapting and improving the GW-SW interaction concepts from the 2CSalt water and salt generation model (Stenson *et al.*, 2005, 2006; Littleboy, 2006; Gilfedder *et al.*, 2007; Cheng *et al.*, 2007) to WaterCAST. The aim of WaterCAST is to provide daily water and constituent generation to the node-link network of the RiverManager model. Functional Units (FUs) are defined within each sub-catchment to represent areas of similar hydrological behaviour. Water balances for each FU are determined either from lumped catchment rainfall-runoff models or by summing one dimensional water balance models. In order to capture variation across a sub-catchment important for groundwater delays and constituent delivery, each sub-catchment is divided into multiple contour bands based on factors such as elevation or distance from stream. These bands (typically 3-5 in each sub-catchment) are used to lump the water balance outputs from multiple FUs which are situated partially or fully within them. Each band has its own groundwater store which is connected directly to the river by a response function which is related to hydrogeology (groundwater flow systems, topography, distance to stream) and can incorporate groundwater pumping. The water in the river is then routed downstream as part of the node-link network structure of River Manager. Fig. 3 illustrates the structure of the model.

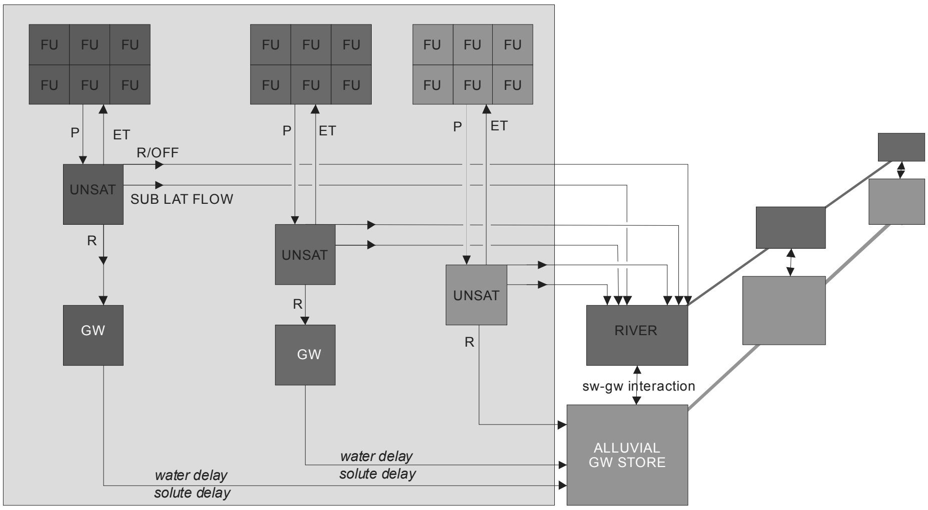

Fig. 3 WaterCAST structure, showing lumped water balance results for each band, contributing to the river and the alluvial groundwater store. It also shows the connection with downstream river links and downstream groundwater links.

Acknowledgements This work is funded by the eWater Cooperative Research Centre (ands its partner agencies) and the National Water Commission Raising National Water Standards Program, under the Project "Australian Hydrological Modelling Initiative - Groundwater Surface Water Interaction Tool".

REFERENCES

Cheng, X., Christy, B., Jarwal, S. & Weeks, A. (2007) Effect of landuse change and climate variation on stream flow and salinity in south-eastern Murray-Darling Basin, Australia. In: *Proceedings of MODSIM07 International Congress on Modelling and Simulation*, December 2007, Christchurch.

Gilfedder, M., Littleboy, M. & Stenson, M. (2007) Two modelling approaches for predicting water and salt generation to upland streams: BC2C & 2CSalt. In: *Proceedings of MODSIM07 International Congress on Modelling and Simulation*, December 2007, Christchurch.

Knight, J. H. & Rassam, D. W. (2007) Groundwater head responses due to random stream stage fluctuations using basis splines. *Water Resources Research* **43**: W06501, doi:10.1029/2006WR005155.

Littleboy, M. (2006) Application of 2CSalt in New South Wales. In*: Proceedings of 2006 MDB Groundwater Workshop*, September 2006, Canberra, [published as CDROM].

Rassam, D. W., Knight, J. H. & Pickett, T. (2007) Modelling ET capture during groundwater pumping. In*: Proceedings of MODSIM07 International Congress on Modelling and Simulation*, December 2007, Christchurch.

Rassam, D. W., Pagendam, D. E. & Hunter, H. M. (2008) Conceptualisation and application of models for groundwater-surface water interactions and nitrate attenuation potential in riparian zones. *Environmental Modelling & Software* **23**(7), 859-875, doi:10.1016/j.envsoft.2007.11.003.

Rassam, D. & Werner A. (2008) Review of groundwater–surface water interaction modelling approaches and their suitability for Australian conditions. *eWater Cooperative Research Centre Technical Report*, Canberra.

Reid, M., Cheng, X., Banks, E.,Jankowski, J., Jolly, I., Kumar, P.,Lovell, D., Mitchell, M., Mudd, G., Richardson, S., Silburn, M. & Werner, A. (2008) Catalogue of conceptual models for groundwater-stream interaction. *eWater Cooperative Research Centre Technical Report*, Canberra.

Stenson, M., Littleboy, M. & Gilfedder, M. (2005) Modelling water and salt export from unregulated upland catchments: the 2CSalt model. In: *Proceedings of International Water Conference*, NZHS, NZSSS, IAH (Aust), Auckland.

Stenson, M., Littleboy, M. Gilfedder, M. & Pickett, T. (2006) The 2CSalt model for reporting salinity impacts of actions in upland areas of the Murray-Darling Basin. In: *Proceedings of 2006 MDB Groundwater Workshop*, September 2006, Canberra, [published as CDROM].

Groundwater recharge estimation in karst by combining soil-moisture and groundwater balance approaches: example of the Jadro Spring, Croatia

DAMIR JUKIĆ, VESNA DENIĆ-JUKIĆ & IVAN TESKERA

Faculty of Civil Engineering and Architecture, University of Split, Matice hrvatske 15, 21000 Split, Croatia
djukic@gradst.hr

Abstract A conceptual approach and the resulting mathematical model for groundwater budget estimation are presented. The karst underground is considered as a lumped system that contains the soil cover, epikarst, phreatic and vadose zones, where the epikarst is divided to the perched and transitory zones. The proposed parameter estimation procedure merges the soil-moisture-balance and the groundwater-balance approaches in order to obtain the complete groundwater budget. The effective rainfall is calculated by using the mathematical model based on soil-moisture balance equations. This model considers separately the soil cover and epikarst perched storage. The groundwater recharge is calculated by applying the mathematical model based on groundwater balance equations. The groundwater recharge model consists of two linear and one nonlinear reservoir representing the vadose seepage, vadose flow and shaft flow. The proposed model is applied to the Jadro Springs located in the Dinaric karst area in Croatia.
Keywords karst hydrology; conceptual model; rainfall-runoff model; groundwater recharge; Jadro Spring

INTRODUCTION

This paper presents the conceptual background and the results of application of a mathematical model for groundwater budget estimation. The proposed model merges the soil-moisture-balance and the groundwater-balance approaches and it requires only meteorological and spring discharge monitoring data. The mathematical background and parameter estimation procedure is based on the theory of linear and nonlinear reservoirs (e.g. Singh, 1988) and composite transfer functions (Denić-Jukić & Jukić 2003). Gauss-Newton and Levenberg-Marquardt optimization algorithms are used for the determination of optimal values of parameters. Series of linear or nonlinear reservoirs are usually applied for the mathematical description of the role of different karst aquifer zones in the karst spring discharge generation (e.g. Fleury *et al.*, 2007; Padilla and Pulido-Bosch, 2007) as well as linear and nonlinear forms of the convolution integral (e.g. Dreiss, 1982, 1983; Labat *et al.*, 1999, 2000; Pinault *et al.*, 2001; Jukić & Denić-Jukić, 2006). The solution of the linear form of the convolution integral is the transfer function that represents the unit response function.

CONCEPTUAL APPROACH AND RESULTS

The karst underground is considered as a lumped system (Fig. 1) that contains the soil cover, epikarst, phreatic and vadose zones. The phreatic zone consists of the perched and transitory zones. The soil-cover receives the mean rainfall in catchment as the input into the system. The infiltration is divided into three basic components: diffuse infiltration entering the aquifer through the soil and fractures and fissures on the karst surface, internal runoff entering the aquifer quickly through the sinkhole drains, and allogenic recharge occurring along sinking or losing streams via infiltration of surface water through porous streambed sediments or through fractures (swallets) in the streambed. It is assumed that allogenic recharge includes also surface and underground streams coming from neighboring catchments. The diffuse infiltration recharges the soil cover and the perched epikarst zone. The allogenic recharge and internal runoff recharge directly the vertical shafts. In addition to the lateral distribution of the effective rainfall between diffuse infiltration and internal runoff, the contribution of the soil cover and epikarst zone is also the lost of moisture in process of evapotranspiration. The perched epikarst zone represents a part of the epikarst zone that traps the infiltrated water. It is assumed that only this part of the epikarst contributes to the lost of moisture in process of evapotranspiration. When the soil is saturated and the epikarst perched zone fulfilled, water left after the evapotranspiration begins to form the diffuse infiltration and internal runoff. The diffuse infiltration recharges the transitory epikarst zone whereas the internal runoff recharges the vertical shafts. The transitory epikarst zone contributes to the retention of percolated water, and the lateral distribution of recharge between fissures and fractures. The total outflow from the fissures, fractures and vertical shafts represents the karst spring discharge.

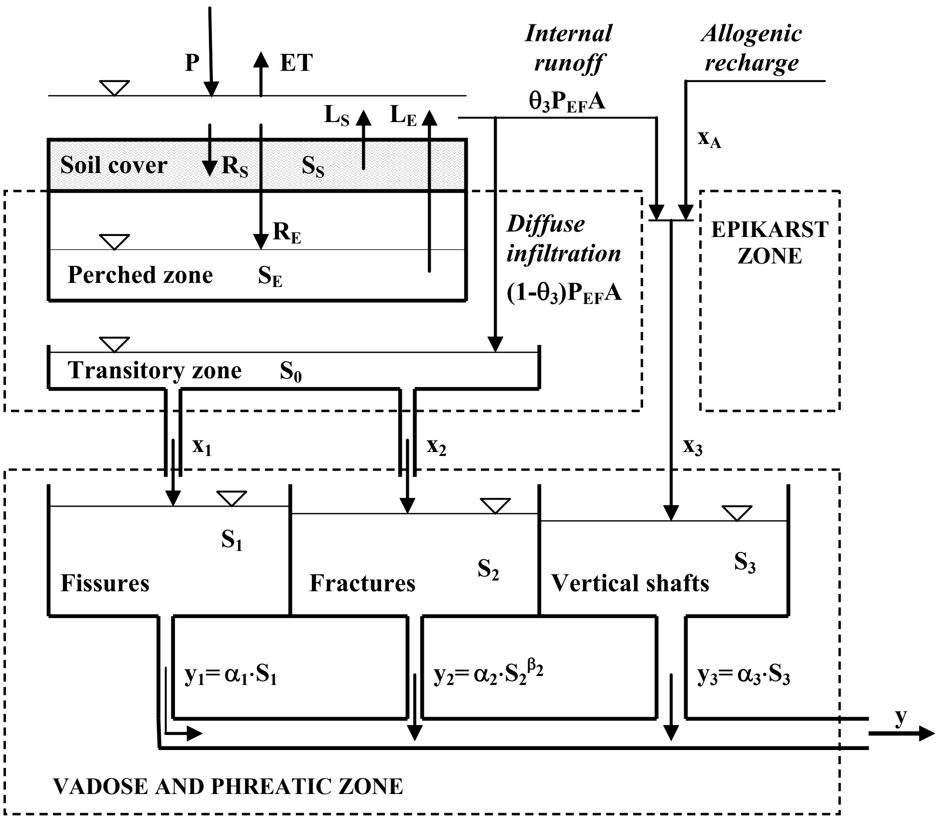

P – rainfall
ET – evapotranspiration
L_S L_E – lost of moisture
R_S R_E – recharge components
S_S S_E – storages
θ_3 – weighted coefficient
P_{EF} – effective rainfall
x_A – allogenic recharge
x_1 x_2 x_3 –groundwater recharge components
α_1 α_2 α_3 – recession coefficients
S_1 S_2 S_3 – groundwater storages
y – spring discharge

Fig. 1 Conceptual model of karst aquifer functioning.

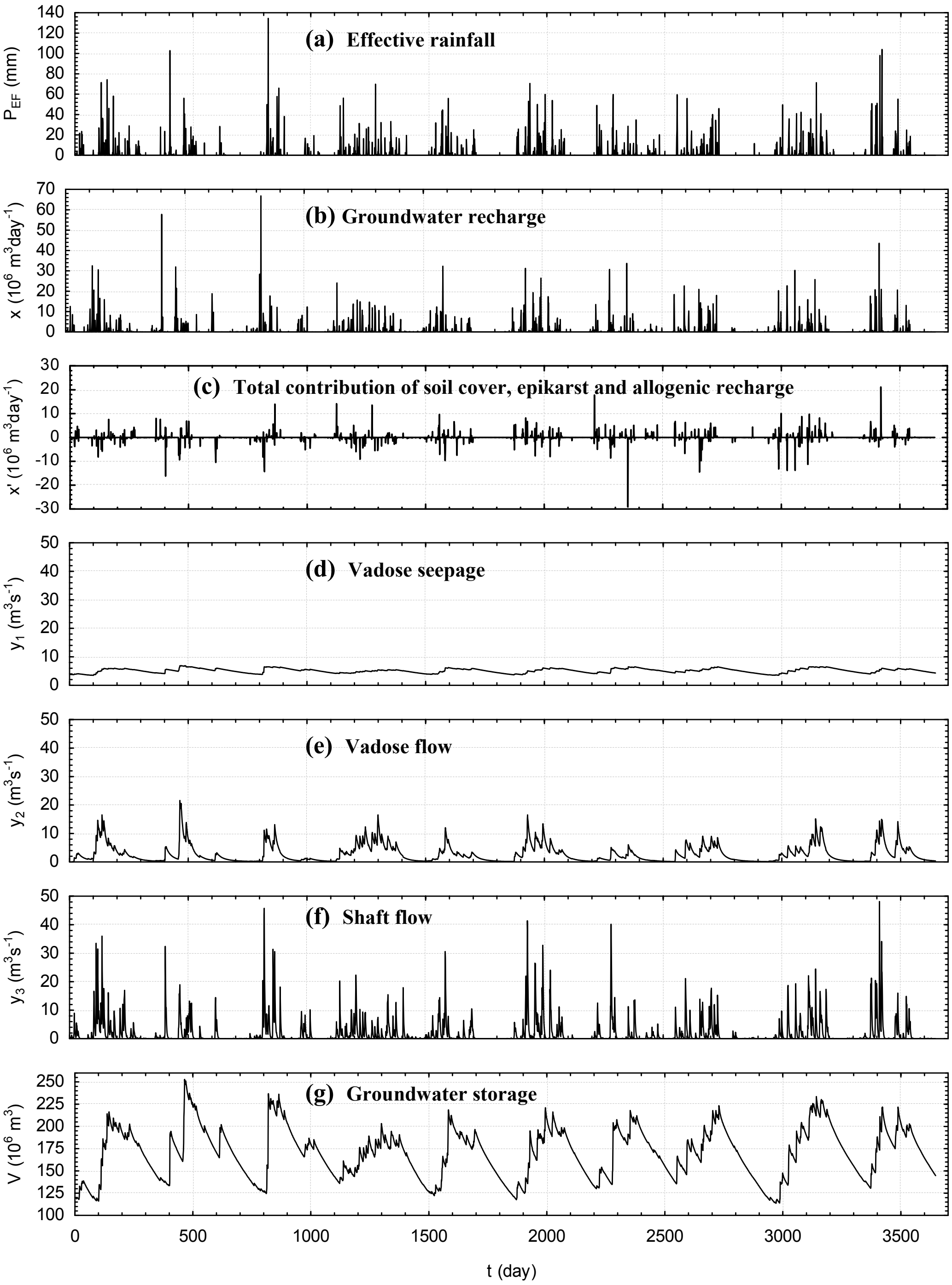

Fig. 2 Results of application: **(a)** effective rainfalls, **(b)** groundwater recharges, **(c)** total contribution of soil cover, epikarst and allogenic recharges, **(d)(e)(f)** outflows from the reservoirs representing vadose seepage, vadose flow and shaft flow, respectively, **(g)** groundwater storage.

The effective rainfall is calculated by using the mathematical model based on soil-moisture balance equations. The proposed model considers separately the soil cover and epikarst perched storage. It assumes that the moisture from the soil cover is lost freely in the processes of evapotranspiration depending on the potential evapotranspiration. The lost of moisture from the perched epikarst zone depends on the saturation of this zone). The groundwater recharge is calculated by applying the mathematical model based on groundwater balance equations. The groundwater recharge model consists of two linear and one nonlinear reservoir representing the vadose seepage, vadose flow and shaft flow. The nonlinear reservoir quantifies and characterizes the nonlinear components in recharge-discharge relation.

The proposed model is applied to the Jadro Springs located in the Dinaric karst area in Croatia. The catchment is located in the Dinaric karst formed mainly of carbonate rocks and partly of impermeable flysch. Except the several small karst fields, the catchment area is practically without soil cover and with poor vegetation. Groundwater system is well developed in limestone and dolomites. The main characteristic of the catchment is the existence of significant underground flows through the karst terrain. The results of application are illustrated in Fig. 2.

CONCLUSION

The groundwater budget calculations show that the Jadro Spring aquifer contains significant groundwater storage capacities. During a year, the aquifer can accumulate up to 140 millions m^3. Usually, the water is accumulated during the autumn months (September, November and December), whereas all other moths are in a balance or the water release prevail. The contribution of the vadose seepage varies between 43% and 62% of total annual discharges, depending on the wetness of hydrological year. The contribution of the shaft flow is between 15% and 25%. Considering the maximal discharges, the contribution of the shaft flow is up to 70% of maximal daily discharges, and it exceeds 48 m^3/s. This investigation confirmed the time variability of the calculated catchment area of the Jadro Spring perceived by the previous investigations. These variations are explained with the time variant allogenic recharges from the catchment of the Cetina River, which depends on groundwater levels. The average catchment area of 396 km^2 for the analyzed period 1995-2000 is estimated by using the average monthly effective rainfall rates and the average monthly groundwater recharge rates.

Acknowledgements This paper is the result of scientific projects (Groundwater and surface water monitoring design in coastal areas & Water balance and modelling of flow in karst) supported by Ministry of science, education and sports of Republic of Croatia.

REFERENCES

Denić-Jukić, V. & Jukić, D. (2003) Composite transfer functions for karst aquifers. *J. Hydrol*. **274**, 80-94.

Dreiss, S. J. (1982) Linear kernels for karst aquifers. *Water Resour. Res*. **18**(4), 865-876.

Dreiss, S. J. (1983) Linear unit-response functions as indicators of recharge areas for large karst springs. *J. Hydrol*. **61**, 31-44.

Labat, D., Ababou, R. & Mangin, A. (1999) Linear and nonlinear input/output models for karstic springflow and flood prediction at different time scales. *Stochastic Environ. Res. Risk Assesment* **13**(5), 337-364.

Labat, D., Ababou, R. & Mangin, A. (2000) Rainfall-runoff relations for karstic springs. Part I: convolution and spectral analyses, *J. Hydrol*. **238**, 123-148.

Jukić, D. & Denić-Jukić, V. (2006) Nonlinear kernel functions for karst aquifers. *J. Hydrol*. **328**, 360-374.

Padilla, A., Pulido-Bosch, A. (2008) Simple procedure to simulate karstic aquifers. *Hydrol. Proc*. **22**(12), 1876-1884.

Pinault, J. L., Plagnes, V., Aquilina, L. & Bakalowicz, M. (2001) Inverse modeling of the hydrological and the hydrochemical behavior of hydrosystems: Characterization of karst system functioning. *Water Resour. Res*. **37**(8), 2191-2204.

Singh, V. P. (1988) *Rainfall-Runoff Modeling, Hydrologic Systems vol. 1, 2*. Prentice-Hall, Englewood Cliffs, NJ.

Fleury, P., Plagnes, V. & Backalowicz, M. (2007) Modelling of the functioning of karst aquifers with a reservoir model: Application to Fontaine de Vaucluse (South of France). *J. Hydrol*. **345**, 38-49.

Trend analysis using nonparametric statistical techniques for detection and evaluation of spatial and temporal chemical changes at a hydrothermal exploitation (Felgueira Spa - Central Portugal)

MANUEL MORAIS
Centre for Geophysics of the University of Coimbra, Portugal
manuelmorais@engenheiros.pt

Abstract Like many thermomineral springs all over Europe, Felgueira Spa (Central Portugal) sulfide alkaline water has been used in therapeutic bathing for centuries. Two periods may now be depicted in the exploitation history of those low enthalpy resources: one characterized by the use of flowing water from springs and a dug well that lasted until the 1990´s when deep drilling wells were promoted to satisfy the increasing demand of medicinal water. After that, a second period of a more active resource extraction begins. Detection of statistical significant monotonic time trends in chemical composition for the period 1991-1998 was done using nonparametric statistical techniques, namely, Spearman rank correlation coefficient and Sen´s slope estimator.
Keywords trend analysis; thermal water; chemical evolution

INTRODUCTION AND GENERAL BACKGROUND

Located at Central Portugal, Felgueira´s low enthalpy hydrothermal system corresponds to a deep circulation of meteoric water in fractured granite. Springs are located along a ENE-WSW trending fault system with water temperatures between 32 and 18 ^{o}C. In the early 1990's, three drilled wells (AC1, AC2 and AC3) intersecting the hydrothermal structure reaching depths of 60 – 300 m, were productive and yielded thermal hybrid waters, with temperatures from 27 to 36 ^{o}C.

The chemical characteristics of these thermal waters can be summarized as low content of dissolved salts (< 350 mg/L), high values of pH (around 8,20), negative redox potential (<-250 mV); Na^+ is the dominant cation and absence of any predominant anion: HCO_3^- (150 mg/L) and Cl^- (50 mg/L). Nitrate is usually below a detection limit of 0,07 mg/L, and nitrogen is present under the species $NH4^+$(0,10 mg/L). Also, presence of F^-, Li^+, low Mg^{2+} contents and sulphur in solution in the forms of SO_4^{2+} and HS^-.

Comparison of the constituents from hot springs and water wells indicates no major differences in chemical composition. This shows that all waters emerge from the same aquifer system and follow identical flow path, submitted to similar physical and chemical processes during its ascent to surface.

This paper presents a study based on sampling results and trend analysis to detect any chemical evolution of the exploited thermal water during the first years of wells production. The interest in detecting chemical trends in groundwater quality is a critical issue in assessing environmental conditions of hydrothermal systems exploitation at a sustainable basis. Considerable amounts of data from monitoring programs will begin to be available to perform such analysis.

DATA AND METHODS

Water quality data presented here come from database of the enterprise, which detains the exploitation concession of the hydrothermal system, and has a monitoring analytical program for these waters. Sampling frequency has varied over time, first on a monthly basis for the first one and half years of monitoring program and after that analyses were done three or four times per year in a more or less regular schedule. Available data covers a period from 1991 to 1998 (for AC1 and AC2 wells) and 1991 to 1996 for AC2 well.

For detection of monotonic trends in time series data a nonparametric rank based statistical test named Spearman´s ranks correlation coefficient can be used (Helsel & Hirsch, 2002). Spearman's correlation coefficient R_{sp} is calculated as:

$$R_{sp} = 1 - \frac{6\sum_{i=1}^{n} d_i^2}{n^3 - n} \tag{1}$$

where d_i is the difference in rank of a pair of variables (x and y), each containing n observations. In time series interpretation the independent variable stands for time.

The null hypothesis H_0: $R_{sp} = 0$ (there is no trend), against the alternate hypothesis H_1: $R_{sp} < \text{or} > 0$ (there is a negative or a positive trend), at a chosen level of significance α, is checked with the test statistic t_t computed by equation (2), and then compared to a table of t distribution with n-2 degrees of freedom:

$$t_t = \frac{R_{sp}\sqrt{n-2}}{\sqrt{(1 - R_{sp}^2)}} \tag{2}$$

Although explicating the statistical significance of the correlation between variables, the above procedure does not provide an estimate of the trend magnitude. This can be approached using a nonparametric slope estimator very robust to outliers and extreme values in the time series like Sen`s slope estimator (Sen, 1968). If a monotonic trend has been detected for a variable over n time periods, if y stands for the variable tested for trend and t stands for the time periods, all the possible slopes for data pairs are defined as:

$$Q = \frac{y_i' - y_i}{t_i' - t_i} \tag{3}$$

Sen’s estimator of slope is the median of all the slopes calculated using the above equation (3). A more detailed description can be found in Gibbons (1995).

DISCUSSION

Hydrochemical data covering ten water quality parameters of sampled water from wells AC1, AC2 and AC3 may give some insights on the chemical evolution of these fluids during a period of more intensive exploitation.

Distribution comparisons between all wells for selected elements concentrations are depicted by the boxplots on Fig. 1. These plots show for AC2 and AC3 wells a stronger departure from a normal distribution for water quality parameters, specially observed in skewness but also by the presence of extreme values. AC3 medians are almost systematically different from the median of the other two wells. Therefore, there are different amplitudes of variations in water chemistry from the wells indicative of some spatial chemical changes. Water from AC1 well discloses a composition with less variance and consequently less dispersion of data. This can be interpreted as being the less hybrid water captured from the hydrothermal system.

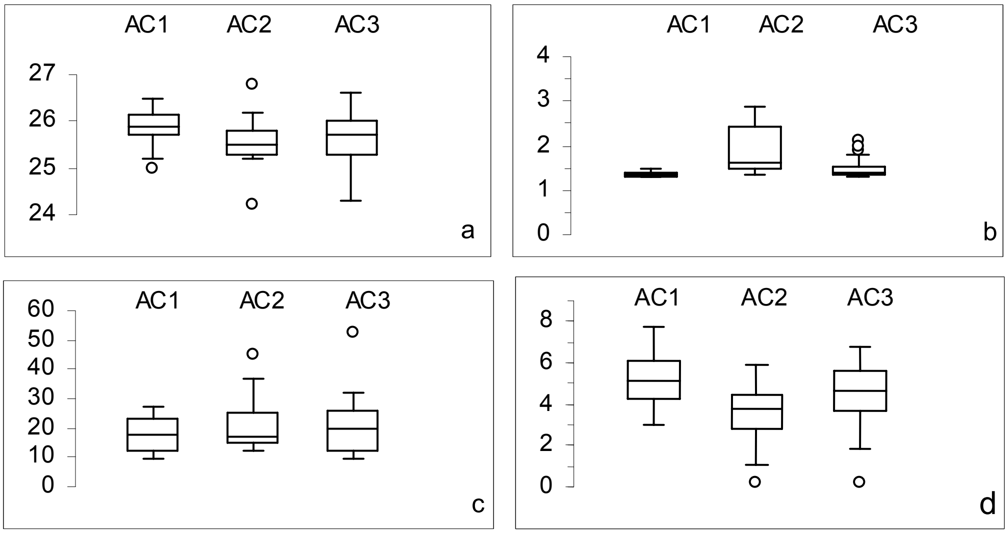

Fig. 1 Boxplots for AC1 water parameters: a) Alkalinity (mL/L HCl 0,1N); b) Hardness (p.p.10^5 $CaCO_3$); c) Sulfate (mg/L); d) Sulfide (mL/L I_2 0,01N).

Fig. 2 displays the time series of measured values of sulphate, chloride, alkalinity, sulfide and hardness at AC1 water well. With the exception of SO_4^{2-} the time series plots are inconclusive in indicating any change over time, i.e., if any trend is developing. In order to detected other possible trends a more detailed statistical analysis is required. The characteristics of data requires a nonparametric statistics as they are irregularly spaced and contain extreme values. The nonparametric technique also has the advantage of being unaffected by the distribution of the population.

Table 1 presents the results of the application of Spearman´s rank correlation coefficient (equation 1). Through this application and the Spearman statistical criterion (equation 2) we detect several monotonous increase and decrease trends in water quality parameters with time.

For AC1 and AC3 wells there is a tendency for increased parameters related to the interaction with a superficial aqueous environment (e.g. hardness, sulfate and nitrate) and a decreasing tendency for pH and constituents associated to a deep thermal environment (sulfide, alkalinity, and F^-). The conservative ions Cl^- and Li^+ remain unaffected. A relatively different pattern is noted for AC2 water well witch is also a sign of the spatial variability of the sampled waters, as already shown by boxplots of water quality parameters.

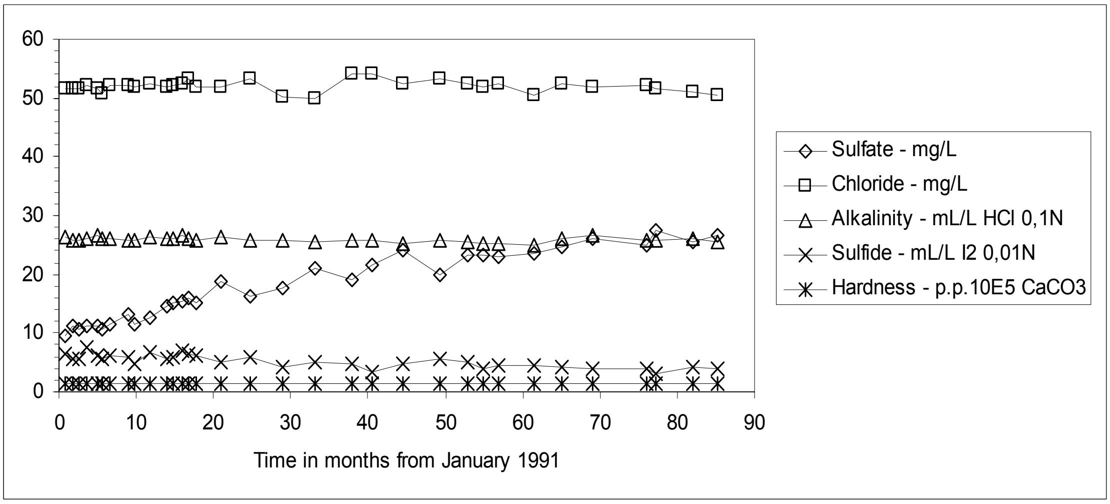

Fig. 2 Time series of water quality parameters of AC1 well.

Table 1 Results of Spearman´s test. The values in bold means that there is a trend considered statistically significant at the 5% level.

	pH	Alkalinity	Sulfide	Hardness	F^-	Cl^-	SO_4^{2-}	NO_3^-	Na^+	Li^+
AC1	**-0,758**	**-0,431**	**-0,789**	**0,808**	**-0,351**	0,050	**0,981**	**0,663**	0,357	-0,151
AC2	**-0,502**	-0,243	-0,317	**0,617**	-0,133	0,130	**0,79**	**0,397**	**0,445**	0,307
AC3	**-0,828**	**-0,627**	**-0,722**	**0,783**	**-0,617**	-0,195	**0,888**	**0,740**	**0,460**	-0,089

The highest slope value for positive trends of water constituents at AC1 was computed for sulfate that presents an increasing rate of 2,10 mg/L year^{-1}. Hardness and nitrate have a slope estimate of 0,02 of their respective measure units per year. Among the decreasing trends Sen´s estimator gives a significant value for sulfide concentration of -0,34 (mL/L I_2 0,01N per year).

CONCLUSIONS

Active exploitation of the hydrothermal system by pumped water has imposed a new dynamic equilibrium in water pressures within the productive geological structure. This amplifies the vulnerability of thermal fluids as they rise to the surface. The observed evolution can be attributable to the impact of acid mine drainage in the area. Although not problematic for the water quality parameters analysed this hybridization will stop when anthropogenic impacts disappears.

REFERENCES

Gibbons, R. D. (1995) Statistical Methods for groundwater monitoring. *John Wiley & Sons, Inc.;* 286 pages.

Helsel, D. R. & Hirsch, R. M. (2002) Statistical Methods in Water Resources -Techniques of Water Resources Investigations. Book 4, chapter A3. *U.S. Geological Survey*. 522 pages.

Sen, P. K. 1968. Estimates of the regression coefficient based on Kendall's tau. *Journal of the American Statistical Association*. **63**,1379-1389.

Indescribable natural flows - differences between field measurements and models of open channel flows

C. NOSS, T. SALZMANN & I. STORCHENEGGER

University of Rostock, Institute for Environmental Engineering, Satower Str. 48, 18051 Rostock, Germany

thomas.salzmann@uni-rostock.de

Abstract Totally 37 three-dimensional ADV measurements were carried out at five cross-sections of two small lowland river sections. One of the sections was returned to a near-natural condition, the second was mainly influenced by vegetation, i.e. flow through submerged vegetation. Velocity distributions as well as distributions of turbulences and shear stresses at these investigated sections indicated, that the stream characteristics did not agree with laws of the theorems of two-dimensional boundary layer and turbulence. Additional analysis of momentum fluxes were carried out and demonstrated the huge amount of secondary currents in comparison to results from flume measurements.

Key words ADV measurements; river flow; turbulence; secondary currents; shear stress; field side

INTRODUCTION

Field measurements are indispensable for verification of physical and numerical models. Most of the models of open channel flows are based on assumptions and cognitions concerning pipe flows, which were adjusted at flumes. E.g. Prandtl's Mixing Length hypotheses for turbulent, i.e. Reynolds shear stress and hence the law of the wall are applicable to open channel flows under the assumptions of stationary uniform flow conditions without secondary currents and a nearly constant stress. According to theory of pipe flow, the shear stress should linearly decrease from maximum at the bottom to zero at surface. Nikora & Goring (2000) as well as Sukhodolov *et al.* (2006) notized certain deviations of the Reynolds shear stress from this linear distribution above fixed and mobile, gravel and alluvial bedforms. Coleman *et al.* (2007) detected, that secondary currents are significant, especially in comparison to the Reynolds shear stress close to and within form-induced sublayers. Several modifications of existing models are necessary to describe the stream under natural conditions, e.g. through vegetation (Stephan & Gutknecht, 2002) or in channel curvature (Falcon & Kennedy, 1983).

Velocity equations deduced from pipe flow fail to fit natural flow conditions. But their coefficients, summarising all influences of surface, form, non-uniformity and in-stationary conditions (Yen, 2002), could be adapted to approach open channel flows. Many investigations focus on the hydraulic impact of individual roughness elements, simple combinations and conditions rather than on the huge complexity of small natural river sections. Our investigation strives to identify the dominant processes in order to verify the suitability of turbulence models in small natural flows while other investigations usually attend to investigate the impact of separated natural elements, velocity distributions or resistance coefficients.

MEASUREMENTS AND DATA PROCESSING

Three-dimensional velocity distributions were measured several times at two small rivers, Hellbach and Nebel, in north-east Germany. The Hellbach has been returned to a near-natural condition ten years ago. The river bed geometry and roughness distribution are far from uniformity. The observed Nebel-section is a straightened channel intercepting the drainage of the riverine grassland. Slightly undulating bars at this section caused by deposition of sediments and organic material in dense reed-vegetations. Macrophytes grew over the entire river section and reached the water surface in summer. Table 1 presents some properties of the investigated cross-sections (Hellbach: No.1 - No.3, Nebel: No.4 & No.5).

The velocities were measured at 25 Hz by a NORTEK and a SONTEK ADV (Lohrmann *et al.*, 1994). The ADV's were mounted on a cable car like construction, spanned over the cross-section. Record lengths about 90 ... 120 s at each measurement point ensured representative turbulence parameters. Point densities of 11.34 ... 48.46m^{-2} were carried out in dependence of the stream heterogeneity. Water surfaces were levelled at the beginning and at the end of each measurement profile to check stationary conditions. Acquired data were filtered by a modified Phase-Space-Threshold method (Goring & Nikora, 2002) using spline-interpolation. Furthermore, the raw data were transformed (rotated) to meet the boundary condition that no mass exchange occurs through the river bed and the water surface. This rotation was necessary to ensure precise primary and secondary currents above the irregular bedforms. Hence the sum of all secondary currents is zero, while the primary velocity tends to maximum.

ANALYSIS AND RESULTS

Table 1 contains hydrometric parameters, i.e. their ranges, at the investigated cross-sections. All flows were turbulent and subcritical. The time-averaged velocities were analysed as primary u (m s^{-1}) in longitudinal and as secondary currents v, w (m s^{-1}) in lateral and vertical direction.

Table 1 Range of hydrometric data at and properties of investigated cross-sections.

X-Sect.	Q (m³ s^{-1})	A (m²)	r_{Hy} (m)	u^* (m s^{-1})	Properties
No. 1	0.06 ... 1.56	0.98 ... 3.77	0.26 ... 0.65	0.04 ... 0.07	backwater, widening, roots
No. 2	0.06 ... 1.56	1.46 ... 4.86	0.24 ... 0.62	0.05 ... 0.09	strong curvature, roots
No. 3	0.06 ... 1.56	0.44 ... 4.44	0.12 ... 0.62	0.08 ... 0.12	straight, higher slope
No. 4	0.50 ... 2.15	4.09 ... 6.98	0.51 ... 0.64	0.07 ... 0.07	straight, macrophytes
No. 5	0.47 ... 2.15	4.44 ... 6.56	0.51 ... 0.69	0.04 ... 0.06	straight, macrophytes

Q = Discharge
A = Mean cross-sectional flow area.
r_{Hy} = Hydraulic Radius, ratio of A to the wetted perimeter.
u^* = Shear velocity, $u^* \approx (g\, r_{\mathrm{Hy}}\, I_{\mathrm{E}})^{1/2}$, g = gravitational acceleration, I_{E} = slope of energy.

Fig. 1 shows examples of time-space-wise averaged velocities $\langle u\rangle(\zeta)$ versus relative flow depth ζ of each cross-section. Like most of all measured velocity distributions, there are no direct linear or logarithmic relationships between wall-normal distances and the presence of stacked wakes generated through form or macro-scale roughness could be assumed (Sukhodolov *et al.*, 2006).

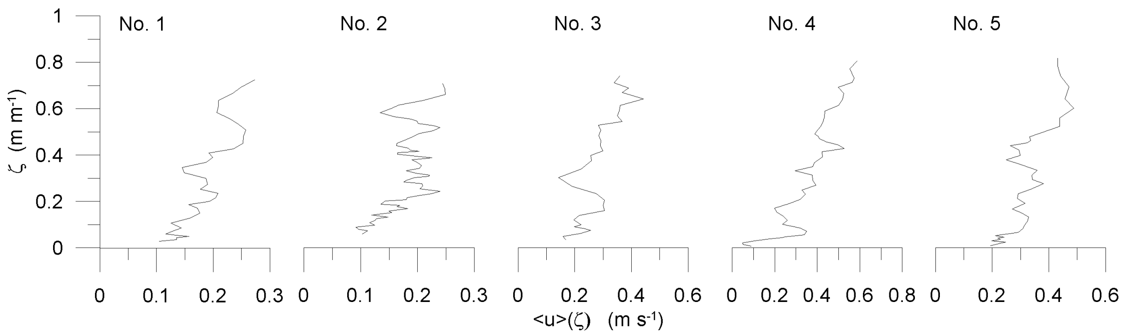

Fig. 1 Examples of averaged velocities vs. relative flow depth at each cross-section.

The logarithmic law of the wall does not fit the measured velocity distributions. The distributions of longitudinal turbulence intensities σ_u arose in the same manner. Neither universal turbulence distributions from Nezu & Nakagawa (1993) nor Nikora & Goring's (2000) approximation were in accordance to the measured turbulence intensities.

Furthermore, two kinds of momentum fluxes through the layers in longitudinal direction were analysed, the mean momentum flux through turbulence, designated as Reynolds shear stresses and the momentum flux arising through secondary currents. Both could be summarised to the total momentum flux. To avoid separated momentum fluxes in lateral and vertical direction, one could use mathematical laws of complex numbers (with $u_r = u$ and $n_r = v$ for the velocities of the real parts and $u_i = 0$ and $n_i = w$ for the velocities of the imaginary parts) to calculate the value $|\tau|$ (N m^{-2}) and the direction of impact φ (°) of the total momentum fluxes directly from measured velocity components. Fig. 2 shows one example. It was obvious, that the momentum fluxes were independent from the distances to the river bed. A summary of all cross-sections is shown in Table 2. Therefore secondary currents always dominated the turbulence influence and prevent the development of two-dimensional shear layers.

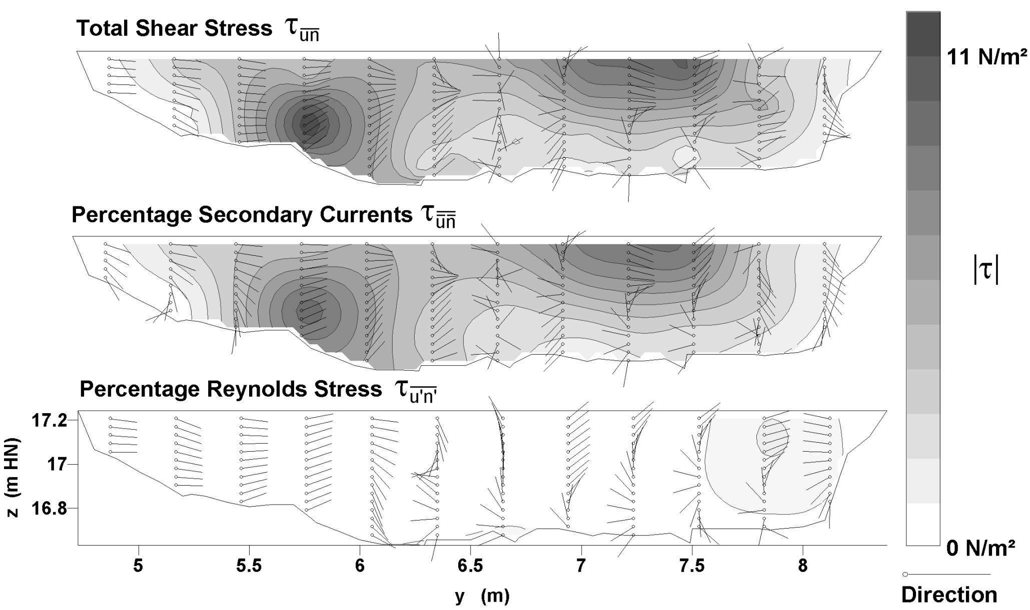

Fig. 2 Example of total and percentages of momentum fluxes at cross-section no.1.

Table 2 Mean momentum fluxes at the cross-sections.

	No. 1	*No. 2*	*No. 3*	*No. 4*	*No. 5*
Total Momentum fluxes (N m^{-2})	4.24	6.38	6.82	6.81	3.96
Percentage Reynolds stress (N m^{-2})	0.56	1.02	1.01	0.69	0.54
Percentage secondary currents (N m^{-2})	3.71	5.74	5.32	6.43	3.49
Ratio Reynolds stress to secondary currents	10%	16%	23%	12%	17%

CONCLUSION

The presented results of velocities, turbulences and distributions of shear stresses point out the differences between hydraulic models, based on two-dimensional shear layer flows and used for pipe and uniform flows in wide flumes, and the characteristics of flow in small natural rivers. Bradshaw (1987) already notes that just a mild three-dimensionality of the stream produces significant changes in turbulence structure parameters. Although many investigations deal with three-dimensional flow structures, the resulting models are mainly limited to boundary conditions, which cannot be stated at natural river sections with non-uniform river beds and non-uniform roughness distributions. Yen (2002) discusses the influence of this non-uniformity on the resistance coefficient and highlights the demand of further investigations, especially if more than one supplementary resistance factors beside the surface resistance are apparent. Unfortunately the investigated transport process at natural river sections neither confirmed to simple turbulence models and hence to usual velocity distributions nor could be recognized systematic structures to modify existing physical descriptions. Continuative field and laboratory measurements are essential to clarify the transport and resistance processes in complex flow fields and to close the gap between existing models and observed stream characteristics at the field side.

REFERENCES

Bradshaw, P. (1987) Turbulent secondary flows. *Annual Review of Fluid Mechanics* **19**, 53-74.

Coleman, S. E., Nikora, V. I., McLean, S. R. & Schlicke, E. (2007) Spatially averaged turbulent flow over square ribs. In: *Journal of Hydraulic Engineering* **133**(2), 194-204.

Falcón, M. A. & Kennedy, J. F. (1983) Flow in alluvial-river curves. *Journal of Fluid Mechanics* **133**, 1-16.

Goring, D. G. & Nikora, V. I. (2002) Despiking acoustic doppler velocimeter data. *Journal of Hydraulic Engineering* **128**(1), 117-126.

Lohrmann, A., Cabera, R., Gelfenbaum, G. & Haines, J. (1995) Direct measurements of Reynolds stress with acoustic Doppler velocimeter. In: *Proceedings of the IEEE Fifth Working Conference on Current Measurement*, 205-210.

Nezu, I. & Nakagawa, H. (1993) *Turbulence in Open-Channel Flows.* A.A. Balkema, Rotterdam, Netherlands.

Nikora, V. I. & Goring, D. (2000) Flow turbulence over fixed and weakly mobile gravel beds. *Journal of Hydraulic Engineering* **126**(9), 679-690.

Stephan, U. & Gutknecht, D. (2002) Hydraulic resistance of submerged flexible vegetation. In: *Journal of Hydrology* **269**(1-2), 27-43.

Sukhodolov, A. N., Fedele, J. J. & Rhoads, B. L. (2006) Structure of flow over alluvial bedforms: an experiment on linking field and laboratory methods. *Earth Surface Processes and Landforms*. **31**, 1292-1310.

Yen, B. (2002) Open channel flow resistance. *Journal of Hydraulic Engineering* **128**(1), 20-39.

Calibration of double porosity parameters using a triple porosity model

JAN ŠEMBERA

Advanced Remedial Technologies and Processes Centre, Technical University of Liberec, Studentská 2, 461 17 Liberec, Czech Republic

jan.sembera@tul.cz

Abstract The contribution briefly reminds the problem of apparent dependence of physical parameters on geometrical dimension of experiment and presents a concept of triple porosity as a tool for explanation of dependence of double porosity parameters on experiment size. The double porosity model and idea of its extension to triple porosity is explained. Then, results of double and triple porosity parameters for specific column experiments are presented a they are interpreted considering their expression in scales of laboratory and pilot experiments.

Keywords double porosity; triple porosity; calibration

INTRODUCTION

Even the laboratory experiments are an important part of technology testing before its pilot application, their results should be used just an orientation information for the practise. Substantial differences between laboratory and pilot experiment results are often observed. This is generally explained by different experiment conditions. Laboratory conditions are always precisely defined and they simulate the reality simplified way and usually with homogeneous physical parameters. The real-world conditions of pilot experiments use to be well surveyed but not precisely defined.

Such a kind of differences between laboratory and pilot experiments is not a substance of our contribution. There can be often observed also difference of directly measured physical parameters of taken medium specimens and their indirect calibration result using pilot experiment results. This can be also in some measure explained by real medium non-homogeneity combined with measurements of small specimen of the medium. But there are some parameters with several-order differences. The most popular example of such a parameter is dispersivity which was examined among many others by Gelhar & Axness (1983) and statistical dependence on geometric dimension of the experiment was enumerated. Such a dependence of locally defined parameters on global geometric dimension of the experiment is, at first sight, unacceptable for a natural scientist or physicist. This phenomenon can be well explained by spatial non-homogeneity of the medium which demonstrates different way at different problem scales. Laboratory results of above mentioned dispersivity measurements is then explained by additional transversal mixing of water in porous medium given by nonzero grain dimension. Observation of its increasing with dimension of pilot experiment is explained by increasing number and size of fractures and cracks in observed specimen which causes more additional mixing and consequent apparent growing of dispersivity maintaining the assumption of medium homogeneity.

We have observed similar behaviour of another physical parameter when indirectly calibrated its value using laboratory column experiments and real site simulations. It was the parameter of separation of total porosity to so called active porosity and blind porosity in double porosity concept. We will focus on explanation of double porosity observations and proposition of difference explanation using triple porosity concept.

Different authors use the term double porosity in different meanings. We use it as it is set in work of Wasserbauer and Hokr (see e.g. Hokr, 2003). The model of porous medium includes system of pores surrounded by grains of impermeable material. The pores can be classified into two classes – active ones realizing communication inside the porous medium and mutually connected into a net, and blind pores which are connected to active pores through a small part of their surface – see Fig. 1a. Blind pores can be understood as water and contaminant reservoirs not present in advective transport but supplying or taking contaminant from active pores. Fig. 1b shows a scheme of such a medium discretizetion using Finite Volume Method. The parameters of such a description are total porosity n_c (ratio of volume of all pores and volume of the rock), active porosity n_a (ratio of volume of active pores and volume of the rock), and exchange half-time $t_{1/2}$ (time needed for reduction of initial concentration difference between active and blind pores to its one half with condition of no flow).

Such an approach to description of porous medium show to be practically sufficient and its parameters can be calibrated for both real-world and laboratory experiments (see e.g. Hokr, 2003).

TRIPLE POROSITY

L. Gombos in Diamo, s. e. performed column flow experiments (Gombos, 2006a and Gombos, 2006b) on bore cores from Stráž pod Ralskem site. M. Slavík at the Technical University of Liberec performed trace experiments (Slavík, 2007) on sandstone blocks from a stonepit. Simulations of column flow experiments from Diamo, s. e. were performed by V. Wasserbauer and shown completely different double porosity parameters than calibration of site observations. In case of laboratory experiment, active porosity was significantly smaller and exchange half-time was much shorter than in real-world observations. This phenomenon could be explained by the idea of Wasserbauer (2006) which extends the double porosity model to triple porosity concept. Such a concept was implemented and tested in Vitouš (2007). We will briefly summarize the triple porosity concept and column experiment calibration results which have been done in Novotná (2007).

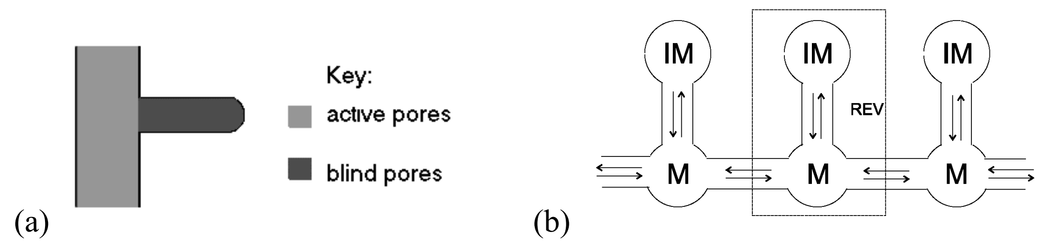

Fig. 1 (a) Schematic picture of active and blind pore idea, (b) Schematic picture of the Representing Elementary Volume (REV) system.

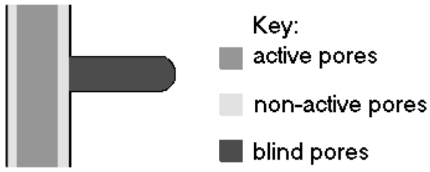

Fig. 2 Schematic picture of triple porosity idea.

The parameters of triple porosity are such as in double porosity total porosity n_c and active porosity n_a and additionally influenced porosity n_o (ratio of active and non-active pore volume and total rock volume). Exchange half-time $t_{1/2}$ is substituted by a pair of exchange half-times $t_{1/2}^{a,n}$ between active and non-active area and $t_{1/2}^{n,s}$ between non-active and blind pores. More details, see in Vitouš (2007) or Novotná (2007).

In Table 1, the typical results of double and triple porosity parameter calibration for column experiments stated in Slavík (2007) is presented. It is result of calibration of trace experiments on stonepit sandstone blocks. During the experiments, tracer NH_4Cl was injected to the clean water saturated sandstone blocks covered in silicon. The concentration of NH_4^+ and Cl^- ions in the column drain was measured. Table 1 summarizes double and triple porosity parameters best fitting the experiment results according to Novotná (2007). The simulation were performed using software based on solution of 1D advective transport with triple porosity using upwind scheme of FVM with space discretization step about 3 mm and time step 20 s. The important result from Table 1 is that active porosity n_a and exchange half-time between active and non-active area $t_{1/2}^{a,n}$ are for both approaches (double and triple porosity) mutually similar. The table includes optimal results when fixed parameter n_c (total porosity) which was independently measured. If we unfixed that parameter, the resulting fit could be better with slightly lower parameter n_c. The table does not include one important parameter – each experiment took about 150 hours. In comparison to optimal value of non-active-blind pore exchange half-time $t_{1/2}^{n,s}$, which is in all cases 200 hours, it comes out that for such a simulation the blind pores were considered as almost isolated from active pores and such a simulation corresponds to double porosity simulation with reduced total porosity parameter. This interpretation of $t_{1/2}^{n,s}$ value corresponds also to the preceding result that better fit can be reached using lower total porosity parameter n_c.

Table 1 Results of calibration of four columns (CD, EF, GH, and LK) using double and triple porosity.

	CD		EF		GH		LK	
	Double poros.	Triple poros.	Double poros.	Triple poros.	Double poros.	Triple poros.	Double poros.	Triple poros.
n_a	4%	3%	4%	3%	6%	3%	2%	2%
$t_{1/2}$ or $t_{1/2}^{a,n}$ [h]	0.15	0.15	0.35	0.4	0.2	0.2	0.08	0.12
n_o		22%		22%		20%		20%
$t_{1/2}^{n,s}$ [h]		200		200		200		200
n_c	26%		26%		26%		26%	

Wasserbauer performed calibration of column experiments realized in Diamo, s. e. (Gombos, 2006a and Gombos, 2006b) and calibration of long-time transport in a large site in Stráž pod Ralskem. Double porosity parameters of sandstone in columns diametrically differed from the ones of the site however the columns were built from sandstone taken from the site. That motivated Wasserbauer to propose the triple porosity concept. Table 1 shows that triple porosity can explain such differences in double porosity parameters in both experiments.

If we hypothetically suppose triple porosity to be well describing model of reality and double porosity to be its reduction, we can see that double porosity can well describe the measurements, if we use slightly reduced total porosity parameter n_c and double porosity parameters n_a and $t_{1/2}$ set to the values of calibrated values n_a and $t_{1/2}^{a,n}$. It can be deduced following way that double porosity can be used also for long-time large problems: The long-time simulation is performed with much longer time step (typically several days to weeks), and much larger space steps (typically ones to tens of meters). In such a simulation the mass exchange between active and non-active areas with $t_{1/2}^{a,n}$ shorter than a half hour appears as an equilibrium phenomenon and distinguishing these areas has no more sense. Long-time double porosity simulation than should be done with active porosity equal to calibrated triple porosity parameter n_o and exchange half-time should correspond to calibrated value of $t_{1/2}^{n,s}$. The resulting double porosity parameters for simulation of column and long-time experiments than differ even though they describe the same rock. We can just wonder if four or more porosity model would not be needed for description of other time scale experiments.

CONCLUSION

An example of system demonstrating different parameters in different scale observations and an example of concept allowing explain this behaviour were presented here. The triple porosity concept is a good approach to explaining different double porosity parameters of the same rock in simulation of column experiment and long-time transport. We also see that double porosity is a description fully adequate for simulation of both small and large scale experiments but calibration using triple porosity is necessary if we want to use the column measurement results for estimation of double porosity parameters in large scale.

REFERENCES

Gelhar, L. W. & Axness, C. L. (1983) Three-Dimensional Stochastic Analysis of Macrodispersion in Aquifers. *Wat. Resour. Res.* **19**, 161–180.

Gombos, L. (2006a) Laboratorní testy imobilizace kontaminantů. Etapa II. Dynamické průtočné testy. Část 1. – injektáž „slivu A“ (Laboratory tests of contaminant immobilisation. Phase II. Dynamic flow tests. Part 1 – injection of “Solution A”). *Technical Report, DIAMO s. p., o. z. TÚU, Stráž p. R.*

Gombos, L. (2006b) Laboratorní testy imobilizace kontaminantů. Etapa II. Dynamické průtočné testy. Část 2. – reinjektáž ložiskové cenomanské vody do směsných alkalických vod (Laboratory tests of contaminant immobilisation. Phase II. Dynamic flow tests. Part 2 – reinjection of field Cenoman water to mixed alkaline water). *Technical Report, DIAMO s. p., o. z. TÚU, Stráž p. R.*

Hokr, M. (2003) Model of flow and solute transport in dual-porosity media. PhD Thesis, *Technical University of Liberec*.

Novotná, Š. (2007) Kalibrace modelu kolonových experimentů (Calibration of column experiment model). Student project, *NTI Technical University of Liberec*.

Slavík, M. (2007) Laboratorní testování transportních charakteristik (Laboratory testing of transport characteristics). *Report of RC ARTEC, Technical University of Liberec*.

Vitouš, M. (2007) Srovnání modelu transportních a chemických procesů v horninovém prostředí s experimentálními daty (Comparison of the model of transport-reaction processes in rock medium with experimental data). Bc Thesis, *Technical University of Liberec*.

Wasserbauer, V. (2006): Testování nového transportně-reakčního modelu (Testing of the new transport-reaction model), *Technical Report, DIAMO s. p., o. z. TÚU, Stráž p. R.*

Importance of conceptual model adaptation during the development of a predictive groundwater flow model of the Deep Basement Aquifer in Flanders (Belgium)

M. VAN CAMP & K. WALRAEVENS
Laboratory for Applied Geology and Hydrogeology, Ghent University, Krijgslaan 281 9000 Gent, Belgium
marcvancqamp@ugent.be

Abstract Predictions produced using groundwater simulation models have often become a critical part in water resources management and are used to plan and conceive groundwater development strategies. Groundwater models are based on a conceptual model that is derived from the data available at the time the model was implemented. But sometimes new data indicate the used conceptual model is erroneous and should be updated, which can mean that also the groundwater model should be revised. This paper illustrates the story of a groundwater model of a deep exploited aquifer in Flanders (Belgium) that had to be revised after extensive monitoring data became available. The story also shows that the reliability of conceptual models can be strongly dependent on available data sets.
Keywords modelling; overexploitation; groundwater management

INTRODUCTION

The Basement Aquifer in Flanders is a fracturated Palaeozoic hard rock aquifer in the Brabant Massif, buried under a few hundred meters of younger porous sediments, which are formed by an alternation of sands and compact clay layers. It has has been exploited since a century now (Walraevens *et al.*, 2001) because the very soft water lend itself to specific industrial applications. In the seventies of last century it became clear that piezometric levels had dropped considerably, but no systematical monitoring of water levels was done, because of the absence of monitoring wells. During the eighties, in 1986 and 1988, two field campaigns were set up during which water levels were measured in abandoned or temporarily interrupted pumping wells. Based on these data two piezometric maps were produced and the dramatic extension of the depression cone was visualised. By that time drawdowns in the centre of the cone were up to more than 150 m. Comparison of the maps showed a decline in levels which was then completely attributed at a steady increase in number of pumping wells and applied pumping rates. As a tool for the further management of the deep aquifer system a groundwater flow model was implemented and the model was calibrated using registered abstraction rates and the measured piezometric levels and maps available from the 1986 and 1988 campaigns.

FIRST GENERATION MODEL (CA 1990)

As the occurrence of the Paleozoic aquifer is not limited to Flanders, model boundaries were located in France and Wallon in the south, in The Netherlands in the north and under the North Sea in the west, the eastern border follows a streamline (Fig. 1). Both the Basement aquifer itself as the overlying covering aquifers and aquitards in Cretaceous, Tertiary and Quaternary deposits were included in the model. The main regional groundwater flow cycle in pre-development condition was from south to north. The aquifer was mainly recharged in the topographical higher regions in the south and as the aquifer dips to the north and north-east, basement water is discharged into the overlying layers in the low lying coastal strip and under the North Sea. Hydraulic parameters for the Basement aquifer were derived from pumping tests in exploitation wells. These revealed the strong heterogeneity of the transmissivity field which is related to the local development of the fracture system. Average transmissivity is about 10 m^2/day, but even on a distance of just a few hundred meters, variations on the order of one magnitude are encoutered. Therefore a spatial homogenisation of indiviual transmissivity values was performed to create the model transmissivity field. Recharge of the whole aquifer is strongly dependent on the hydraulic characteristics of the overlying layers. These were mainly obtained from model calibration. Herefore the measurements of the field campaigns of 1986 and 1988 were used and it was assumed that hydrodynamically the system was in equilibrium and the flow regime could be considered as a steady state. With the obtained parameters calculated drawdowns fitted quite well with observations and deviations were explained mainly by the homogenisation procedure used for creating the transmissivity field. It was thought that with this model further development scenarios could be studied.

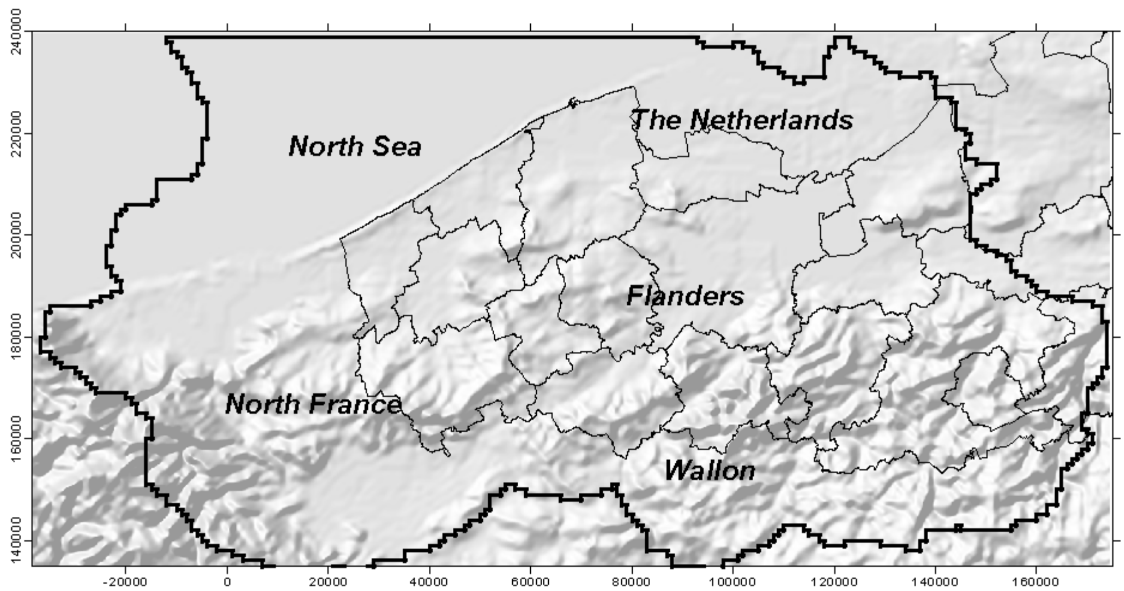

Fig. 1 Location of the study area and groundwater flow model boundaries.

SECOND GENERATION MODEL (CA 2000)

After the first model was completed it was realised that a more restrictive management and permission regulation must be followed. Total exploitation in the Basement aquifer was then around 10 million m^3 $year^{-1}$ (Fig. 2) and this was seen as a maximum for the next future. Also the evolution of levels had to be followed through more intensive monitoring and a special designed network was conceived. During the early nineties a network of around 40 deep observation wells was drilled by the government and since 1992 half-monthly measurements are done. Groundwater licensing had become more restrictive, but by the end of the nineties, the time series (since 1992) showed that, despite the stabilised abstraction rates, levels continued to decline, often in a straigthforward quasi linear way (Fig. 3). This behaviour was not expected and could not be explained with the existing model. It became evident that hydrodynamically the system was not in equilibrium and the situation was strongly transient. Also the quasi linear decline in many places seemed caused by a constant pumping from a very limited recharged system, comparable with a constant discharge from a nearly closed box. Because the first model was calibrated with a steady state assumption, a revision of the model was necessary (Van Camp *et a.l*, 2000) incorporating the data from the - by then - one decade long time series.

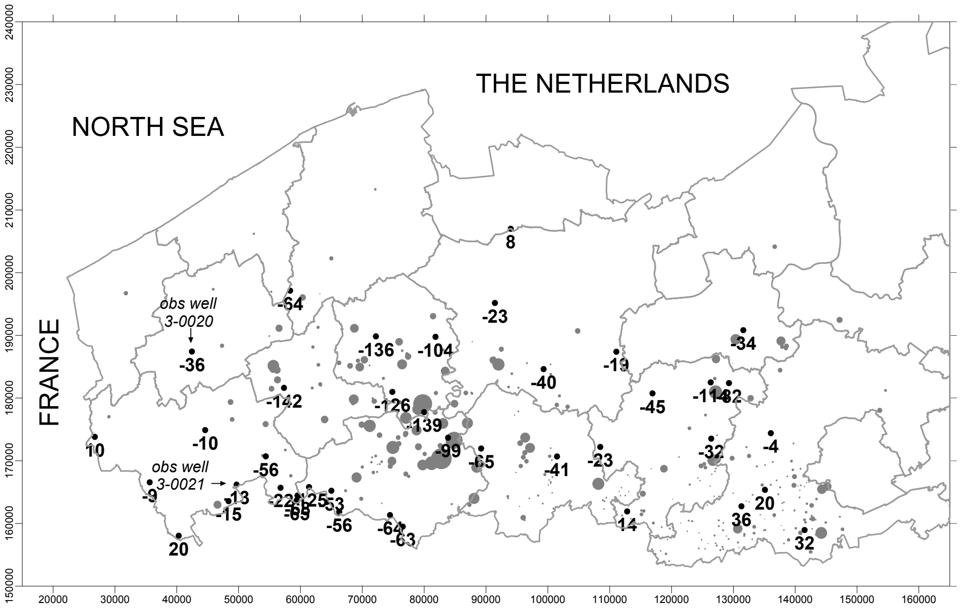

Fig. 2 Measured piezometric levels in 2000, licensed pumping rates (gray cirkels) and location of observation wells 3-0020 and 3-0021 in Basement aquifer**.**

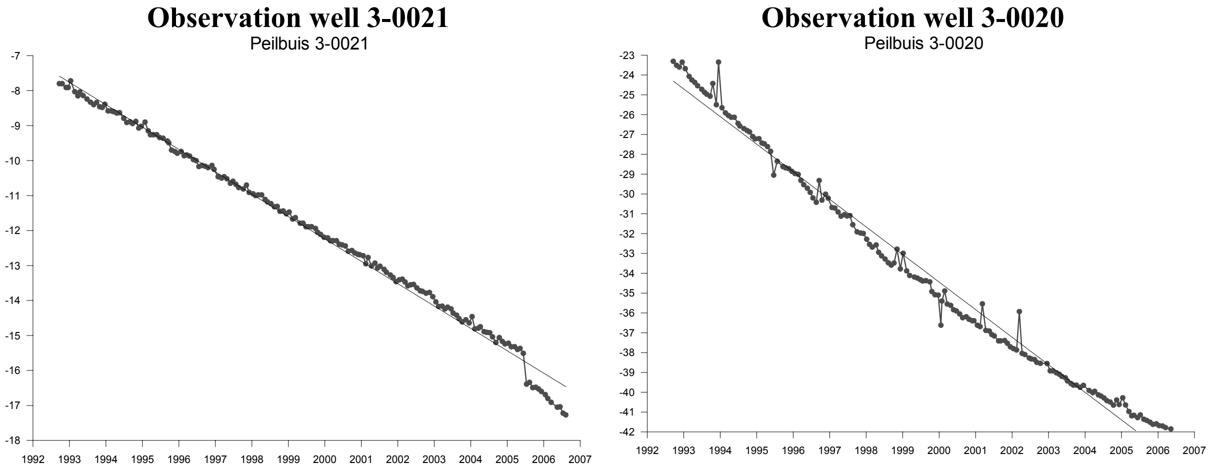

Fig. 3 Time graphs of two representative observation wells (1992-2006).

Using a simple balance model in which the centre of the depression cone is represented as a single cell, upper limits for the hydraulic conductivity of the overlying aquitards could be quantified to allow for nearly linear declining water levels, as observed (Fig 4).

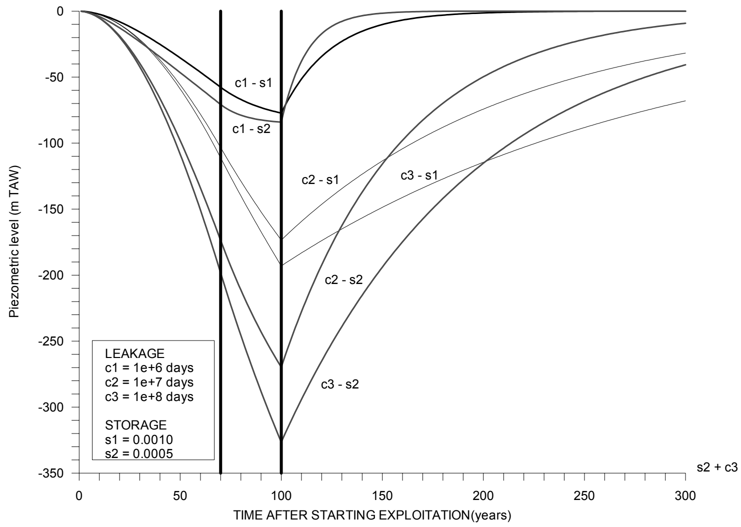

Fig. 4 Results of the single cell balance model calculations.

The model was recalibrated using transient flow simulations of the whole exploitation history and model trends for the period from 1992 and later were compared with observed trends. The piezometric levels in 2000 were not only dependent on the recent pumping rates, but because of the lack of recharge, also on the whole pumping history of the aquifer system (Fig. 5).

1950 **1960**

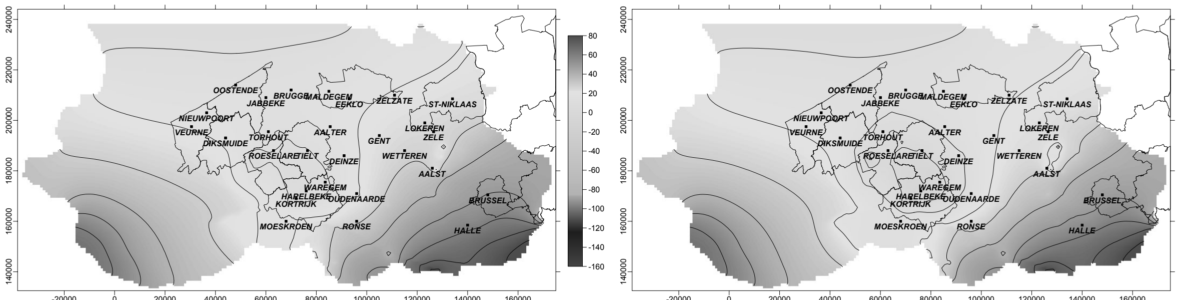

1970 **1980**

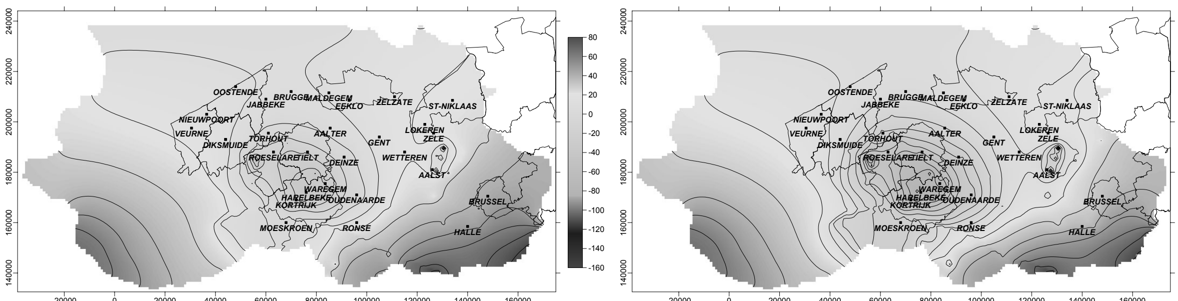

1990 **2000**

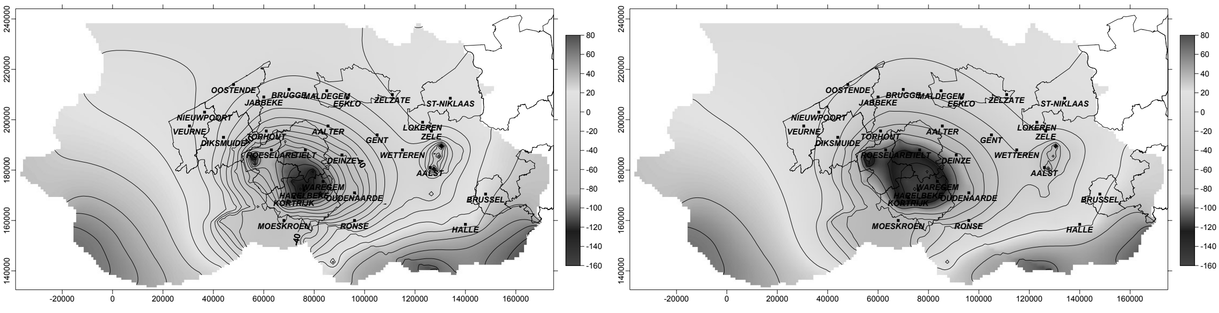

Fig. 5 Calculated evolution of piezometric levels during the last decades.

The new model was used to calculate predictive scenarios for the next 50 years with different exploitation reduction scenarios to estimate recovery times of the overexploited aquifer. Different possible scenarios were evaluated for achieving preset goals within certain time limits. The first goal was to rise piezometric levels above the top of the Basement aquifer

CONCLUSIONS

The deep seated Basement aquifer in Flanders is an example of an aquifer with very limited recharge. Systematic and continued pumping has lead to quasi-linear declining piezometric levels, but this was only recognized after long time series of piezometric levels became available. A first version of a groundwater flow model assuming a hydrodynamical equilibrium situation became obsolete and was replaced by a model simulating and calibrated on transient flow regimes. In this case it was absolutely necessary that transient flow simulations were used and that model calibration was based on time dependent calculations.

REFERENCES

Van Camp, M., Marten,s K. & Walraevens, K. (2000) Grondwatermodellering voor Landeniaan, Krijt en Sokkel: Uitbouwen van beheersinstrument. *Universiteit Gent*. ISBN 90-76878-02-1, 115p. + bijlagen (in Dutch).

Walraevens, K., De Smet, D. & Van Camp, M. (2001) Overexploitation of the Palaeozoic Basement Aquifer in Western Belgium. Future Ground Water Resources at Risk, Lisbon, 2001. *Proceedings. Theme* **10**: Overexploitation and Land Subsidence.

Improved calibration of groundwater models using baseflow estimates for sub-catchments. Case-study: Upper Alzette, Luxembourg

B. VERBEIREN, F. DE SMEDT & O. BATELAAN
Dept. Of Hydrology and Hydraulic Engineering, Faculty of Engineering Sciences, Vrije Universiteit Brussel (VUB), Pleinlaan2, 1050 Brussels, Belgium.
boud.verbeiren@vub.ac.be

Abstract Using MODFLOW the groundwater system of the Upper Alzette catchment was modelled. In general, calibration of groundwater models involves an inverse modelling strategy, using the measured groundwater heads in observation wells. An additional calibration strategy was employed considering the water balances of a number of subcatchments. Baseflow for each of the subcatchments was estimated and used as a criterion for an additional calibration. This analysis clearly showed that considering sub-water balances in the calibration process greatly improves the model results. The uncertainty of the model results was assessed, defining a spatially distributed 'range' for the simulated groundwater levels.
Keywords numerical groundwater model; calibration; baseflow estimation; sub-water balances

INTRODUCTION

A numerical, physically based groundwater model with spatially distributed input data, is often indispensable to describe the global flow dynamics of the groundwater system and gain insight into the valley system dynamics (Verbeiren, 2002; Batelaan, 2000).

Calibration of such a model is an important, time-consuming and often difficult task (Hill & Tideman, 2007, Cao *et al*., 2006). Typically, calibration of a groundwater model involves an inverse modelling strategy (Carrera *et al*., 2006; McLaughlin *et al*., 1996), i.e. optimizing the model parameters as a function of measured groundwater heads in a number of observation wells.

However, in this study an additional calibration strategy was employed considering the water balances of the subcatchments. The main objective is to test this alternative calibration and compare the model output with the original results.

STUDY AREA

The Alzette river basin covers a considerable part of the Grand-Duchy of Luxembourg. The research focuses on the upstream part of the basin (272.6 km²), between Esch-Sur-Alzette and Luxembourg City. The zone between these two urban areas is dominated by pastures and cultivated land. The topography changes from narrow valleys with steep slopes in the southern tip of the basin (450m) to a 2 to 3 km wide alluvial floodplain with gentle slopes (260m) before the Alzette River cuts into the Luxembourg sandstone plateau. The alluvial deposits consist of an alternation of sand, gravel, marls and clay (Matgen, 2006).

METHODOLOGY

Groundwater model

The groundwater system of the Upper Alzette catchment was modelled using the finite-difference groundwater model MODFLOW (Harbaugh *et al*., 2000) in a Groundwater Modelling System environment (GMS developed by Brigham Young University, Utah, USA, 2003).

The model area was discretised in cells of 50 by 50 m. The alternating resisting, permeable and non-resisting, little permeable geological formations were grouped into 4 layers. The Liassic marls form the impermeable base of the groundwater model. A general head boundary was defined to model the contact surface (5 km²) with the Luxembourg sandstone aquifer.

After the set-up of the steady-state groundwater model an extensive sensitivity analysis was performed. The hydraulic conductivities, and especially the horizontal conductivity of layer 3, were identified as 'most sensitive' parameters. The results formed the basis for a trial-and-error calibration process. With an inverse modelling the hydraulic conductivity parameters were optimized as a function of measured groundwater heads in observation wells. As a statistical goodness-to-fit measure, the Root Mean Square Error (1.04 m) was used.

Baseflow estimation

However, due to the limited availability of observation wells on the one hand and reference data on hydraulic conductivities on the other, there was still some uncertainty on the representativeness of the calibration. Therefore an additional calibration strategy was developed and tested in this study. Next to the observed groundwater levels and the total water balance also the water balances of a number of subcatchments was taken into account using river discharge data.

In total 6 stream gauging stations are present in the study area. Next to the total catchment with the outlet near Hesperange the river discharge of 5 subcatchments is monitored. The contributing area for these locations was determined within a GIS environment: Bibeschbach (11.2 km²), Dudelingerbach (37.4 km²), Mierbech-Huncherange (6.3 km²), Livange (312.6 km²) and Schifflange (53.8 km²). For each of these subcatchments the baseflow was estimated based on daily river discharge time series using the Hydrograph Separation tool HYSEP (Sloto & Crouse, 1996), although also other baseflow estimation methods (BFI, WHAT, PART, WETSPRO) were considered. The graphical separation 'sliding interval' method was chosen.

The estimated baseflows were used as additional observations for the calibration of the conductance parameters of the river bed, the general head boundary and the drainage. It is expected that this will result in improved modelled sub-water balances and as such better overall model outputs.

RESULTS AND INTERPRETATION

Initially the groundwater model parameters – hydraulic conductivities and conductance parameters – were calibrated as a function of the measured groundwater heads in 13 observation wells and the total water balance only (= 'original' calibration). Next the conductance parameters only were recalibrated considering also the sub-balances of the different sub-catchments and more specifically the baseflow component. The hydraulic conductivities remain unchanged (= sub-balance' calibration). Table 1 shows both calibration results with regard to the conductance parameters.

Although the baseflow for the complete study area, Hesperange catchment, is comparable (change of 5%) the calibrated conductance parameters differ considerably, which also have a noticeable effect on the water balances of the sub-catchments. In all sub-catchments there still is an under-estimation of the baseflow, but the sub-balance results clearly are a much better approximation of the estimated ("measured") sub-catchment baseflow. Fig. 1 shows for each sub-catchment the estimated and both simulated baseflows. On average the sub-balance results are 33% better. For the respective sub-catchments Bibeschbach, Dudelingerbach, Mierbech-Huncherange, Livange and Schifflange the simulated baseflow improved with 20%, 46%, 33%, 28% and 40%.

The overall under-estimation possibly can be explained by a number of factors: missing smaller watercourses, over-estimation of baseflow with HYSEP, an under-estimation of the total recharge, etc.

Table 1 'Original' and 'sub-balance' calibration results for the conductance parameters.

PARAMETER	DESCRIPTION	ZONE	CALIBRATED C [$m^2\ d^{-1}$] original	sub-balance
RCOND	River bed conductance	River locations	0.05 - 96.7*	0.5 - 9667.6*
GHBCOND	Conductance GHB	Lux. Sandstone (li2)	60	0.60
		Strassen formation (li3)	0.05	0.05
DRN	Drainage conductance	Hesperange catchment	20	0.20

* calculated based on the calibrated hydraulic conductivity of the riverbed (respectively 0.1 m d^{-1} and 10 m d^{-1})

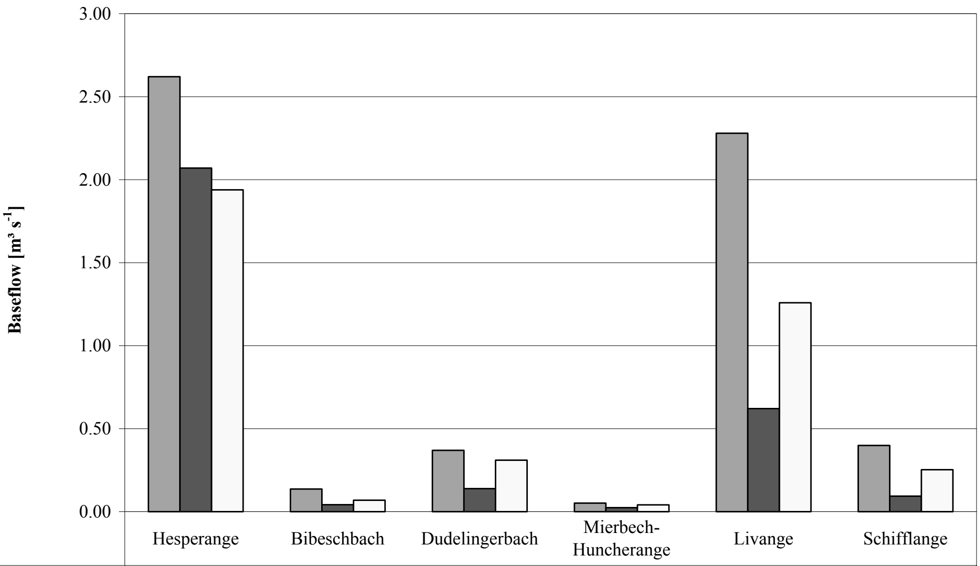

	Hesperange	Bibeschbach	Dudelingerbach	Mierbech-Huncherange	Livange	Schifflange
Estimated baseflow	2.62	0.14	0.37	0.05	2.28	0.40
Original calibration	2.07	0.04	0.14	0.02	0.62	0.09
Sub-balance calibration	1.94	0.07	0.31	0.04	1.26	0.25

After calibration the uncertainty of the model results was assessed. Using the results of the sensitivity analysis a spatially distributed 'range' for the simulated groundwater levels was defined, indicating the deviation at each location. To obtain this 'uncertainty range' the most sensitive parameters were combined.

CONCLUSIONS

While the simulated groundwater heads and the total simulated baseflow remained nearly unchanged, this analysis clearly shows that the sub-balances differ considerably. The simulated baseflows for the sub-catchments are on average 33% more accurate than the original results. This result not only indicates that considering sub-water balances in the calibration process greatly improves the model results, but also considerably increases the understanding of the groundwater dynamics.

Acknowledgements This study was funded by the 'Ministère Luxembourgeois de la Culture, de l'Enseignement Supérieur et de la Recherche'. Many thanks go to Patrick Matgen, Lucien Hoffmann and Laurent Pfister of the 'Centre de Recherche Public Gabriel Lippmann' for their support and providing digital and analogue data. Also the contribution of following persons and institutions is acknowledged: 'Ministère Luxembourgeois de l'Intérieur et de l'Aménagement du Territoire', Mr. Robert Kipgen and the 'Division d'eaux souterraines' at the 'Administration de la Gestion de l'Eau', Mr. Patrick Grivet of the 'Ministère de l'Environnement', Mr. Bernard Reisch of the 'Administration du Cadastre et de la Topographie', Mme Benbrahim and Mr. Robert Maquil of the 'Service Géologique' and Mr. Christian Schroeder of SEBES.

REFERENCES

Batelaan, O., Asefa, T., van Rossum, P. & De Smedt, F. (2000) Groundwater flow modeling of three wetland ecosystems in river valleys in Flanders, Belgium. In: Book of abstracts of European Network of Experimental and Representative Basins (ERB), Conference: Monitoring and Modeling Catchment Water Quantity and Quality, (ed. by N.E.C. Verhoest, Y.J.P. Van Herpe & F.P. De Troch), 65-69, Ghent, Belgium, 27-29 September, 2000.

Carrera, J., Alcolea, A., Medina, A.., Hidalgo, J. & Slooten, L. J. (2005) Inverse problem in hydrogeology. *Hydrogeol J.* **13**, 206 –22.

Cao, W., Bowden, W. B., Davie, T. & Fenemor, A. (2006) Multi-variable and multi-site calibration and validation of SWAT in a large mountainous catchment with high spatial variability. *Hydrol. Process.* **20**, 1057-1073.

Harbaugh, A..W., Banta, E. R., Hill, M. C. & McDonald, M.G. (2000) MODFLOW-2000, the U.S. Geological Survey modular ground-water model – User guide to modularisation concepts and the Ground-Water Flow Process, *U.S. Geological Survey Open-File Report* 00-92, 121 p.

Hill, M. C. & Tideman, C. R. (2007) Effective Groundwater Model Calibration: With Analysis of Data, Sensitivities, Predictions, and Uncertainty. *Wiley-Interscience* (ISBN 978-0-471-77636-9), 455p.

Matgen, P., El Idrissi, A,., Henry, J. B., Tholey, N., Hoffmann, L., de Fraipont, P. & Pfister, L. (2006) Patterns of remotely sensed floodplain saturation and its use in runoff predictions. *Hydrol. Process.* **20**(8), 1805-1826.

McLaughlin, D. & Townley, L. R. (1996) A reassessment of the groundwater inverse problem. *Water Resour Res.* **32**, 1131 –61.

Sloto, R. A. & Crouse, M. Y. (1996) HYSEP: A computer program for streamflow hydrograph separation and analysis. *U.S. Geological Survey, Water Resources Investigation report* 96-4040, 46p.

Verbeiren, B., Batelaan, O. & De Smedt, F. (2002) Development of a Groundwater Model for some Small Sub-Catchments of the Dender Basin. *Proceedings of the first Geologica Belgica International Meeting, Leuven*, 11-15 September 2002. Aardk. Mededel., 2002, 12, 207-210.

Bank filtration induces transient interface conductivity in time and space

B. WIESE[1] **& G. NÜTZMANN**[2]

1 *KompetenzZentrum Wasser Berlin, Cicerostr. 24, D-10709 Berlin, Germany*
bernd.wiese@kompetenz-wasser.de

2 *Institute for Freshwater Ecology and Inland Fisheries, D-12587 Berlin, Germany*

Abstract In order to determine leakage characteristics, a highly transient lake bank filtration site at Lake Tegel, Berlin, Germany has been modelled using MODFLOW and PEST. The model was able to reproduce both, the observed hydraulic head data and measured leakage coefficient, only after incorporating variable leakage coefficients depending on the simulated thickness of the unsaturated zone underlying the clogging zone at the banks. This behaviour is explained by reversible anaerobic clogging. From literature it is known that in contrast to aerobic conditions, clogging is much more pronounced under anaerobic conditions due to enhanced production of extracellular polymeric substances. At high pumping rates the groundwater table declines and air is sucked into the unsaturated zone. Formerly anaerobic regions become aerobic and the extracellular polymeric substances are degraded; the hydraulic conductivity of the clogging zone increase. The behaviour reverses when pumping is reduced and groundwater table increases. Results are consistent with oxygen, nitrate and sulphate concentrations measured below the unsaturated zone.

Keywords lake bank filtration; clogging; Berlin; infiltration; transient leakage coefficient; unsaturated zone; inverse modelling; PEST; MODFLOW

INTRODUCTION AND BACKGROUND INFORMATION

Aim of the study is to determine a formulation that describes adequately the infiltration processes at the study site regarding temporal dynamic, spatial dynamic and geochemical observations. The investigation area is a bank filtration site adjacent to Lake Tegel, Berlin, Germany. The aquifers are about 40 m thick and consist of fine to coarse sand with a hydraulic conductivity of about 3×10^{-4} m s^{-1}. Pumping rates of the site are highly variable, inducing an unsaturated zone below the lake between 2 m and 7 m. The bottom of the lake is impermeable, filled with limnic mud below a water depth of 6.5 m (Fig. 1a). Infiltration is potentially possible in a water depth between 0 m and 6.5 m. An external clogging layer does not exist, due to low concentrations of suspended solids (3 mg l^{-1}), however, an internal clogging layer exists.

METHOD

Hydraulic modelling has been carried out on a well field, consisting of 26 abstraction wells. The model domain is 4 km^2 and the model interval is between 1999 and 2005 with weekly discretisation. Leakage is modelled with the MODFLOW reservoir package, providing alteration between 2nd type (Neumann) and 3rd type (Cauchy) boundary condition for alteration between unsaturated and saturated conditions below the infiltration area. The leakage coefficient is the most sensitive model parameter.

Infiltration was measured under field conditions using seepage meters. Results show a higher leakage coefficient in shallow than in deep water (Fig. 1b). The overall infiltration rate is equal to the abstraction rate at the production wells multiplied by their bank filtration share. Applying this balance, it shows that measured infiltration in shallow water is equal to the total amount of infiltrated water, consequently leakage is very low in deep water.

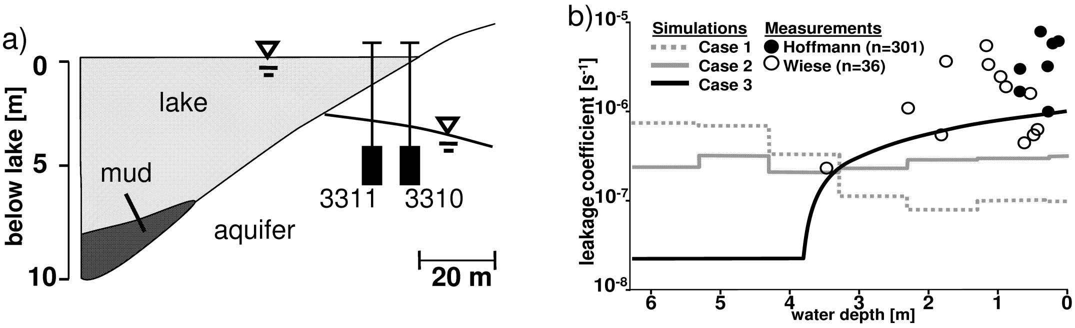

Fig. 1a Cross section of the infiltration zone, **1b:** Measured and simulated depth structure of leakage coefficient. Measurements are carried out by Hoffmann & Gunkel (2006) and Wiese (2006). The infiltration profile of case 3 corresponds to a groundwater table of 3.80 m below lake table.

Three parameterisations of the leakage coefficient (Case 1 to Case 3) have been applied and calibrated with PEST.

- Case 1: The leakage coefficient is temporally invariable. The Infiltration zone is represented with one leakage parameter per metre depths elevation (7 spatial leakage parameters).
- Case 2: Depth parameterisation is identical to Case 1. The temporal leakage L_t [-] is parameterised with a continuous sequence of linear trends of each 2 month length. For each time step L_t is multiplied with the depth distribution. (54 temporal and 7 spatial leakage parameters).
- Case 3: The leakage coefficient *L(f(z,t))* only depends on the presence and the thickness of an unsaturated zone.

$$L(f(z,t)) = L_0 \times \left(1 + p_1 \times h_{usat}{}^{p_2}\right) \tag{1}$$

For saturated conditions the leakage coefficient is L_0, p_1 and p_2 are fitting parameters, h_{usat} is the thickness of the unsaturated zone at each grid cell. Eq. 1 has been introduced into the reservoir package of MODFLOW2000. (3 empirical leakage parameters)

RESULTS - HYDRAULICS

The hydraulic heads of Case 1 (Fig. 2) show a reasonable fit, but are too high for small abstraction and too low for high abstraction. In contradiction to the measurements, the calibrated leakage coefficient is highest in deep water (Case 1, Fig. 1b).

Case 2 provides the best fit, which is not surprising, regarding the high number of 61 free parameters. The important result is the close correlation between the calibrated temporal leakage L_t and the pumping rate (Fig. 3). The calibrated leakage coefficient however, is too low in shallow and too high in deep water (Fig. 1b).

Case 3 provides a good fit of the heads (Fig. 2). Calibrated parameters are: L_0= 2.3×10^{-8} m s^{-1}, p_1=14.8, p_2=0.78. The leakage increases with the thickness of the unsaturated zone (eq. 1) In agreement with the measurements, the leakage coefficient is high in shallow water and low in deep water (Fig. 1b). Applying this leakage depth distribution constant by time, the heads are either too high or the model runs dry.

The authors are aware, that a deficient model set up also might lead to correlation between leakage and pumping rate. Therefore boundary conditions and water balance have been thoroughly revised (Wiese, 2006).

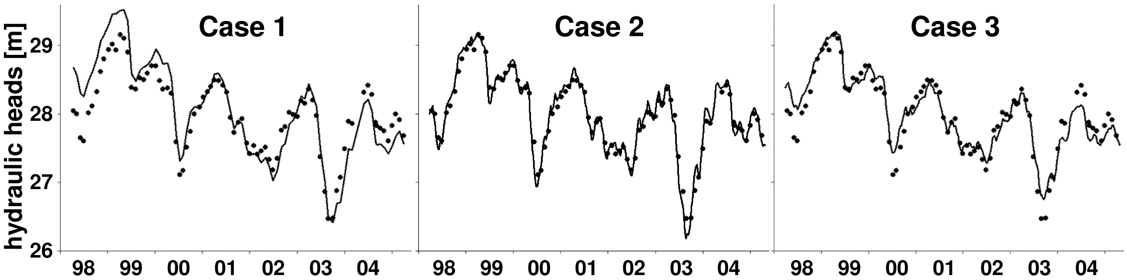

Fig. 2 Observed and simulated hydraulic heads for Case 1 to Case 3. The location of the observation well is close to the well field.

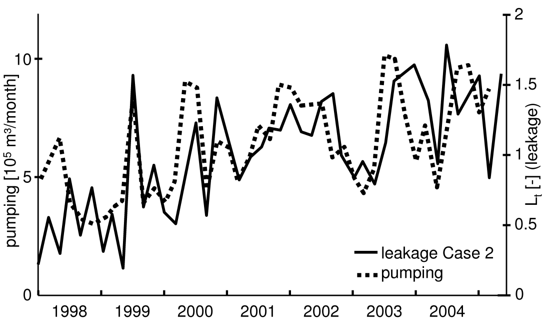

Fig. 3 Monthly average of the pumping rate of the well field and relative temporal leakage calibrated with Case 2.

RESULTS - REDOX

Due to degradation of organic matter electron acceptors are continuously consumed within the clogging layer. Mean nitrate concentration in the lake is 8.4 mg l^{-1} (KWB 2005). In 3311 nitrate is always reduced (mean reduction 6.6 mg l^{-1}). In 3310 at 6 of 13 observation dates nitrate reduction occurs (mean reduction 4.2 mg l^{-1}). When nitrate reduction is observed it is assumed that oxygen becomes entirely depleted within the clogging layer, i.e, before the water reaches the unsaturated zone.

Oxygen concentrations in the aquifer decrease from the bank towards the centre of the lake (Fig. 4). Furthermore, oxygen concentrations strongly depend on the level of the water table: after a long rise of the water table and at high hydraulic heads, concentrations are low (No. 1 to 5, Fig. 4) and vice versa. We conclude that most oxygen in the groundwater derives from lateral inflow of air into the unsaturated zone due to groundwater table decline. Based on the continuous nitrate reduction in 3311, all dissolved oxygen derives from the unsaturated zone at this location. However, at 3310 not necessarily all oxygen derives from the unsaturated zone, as nitrate reduction is not continuously observed.

Measured sulphate concentrations at both observation wells correlate with the water table variations, oxygen and nitrate concentrations. This indicates that redox conditions within the clogging layer become sulphate reducing when the groundwater table is high. During decline of the groundwater table, penetrating atmospheric oxygen reoxidises the previously formed sulfides leading to elevated sulphate concentrations in groundwater. Mn and Fe do not appear in significant concentrations.

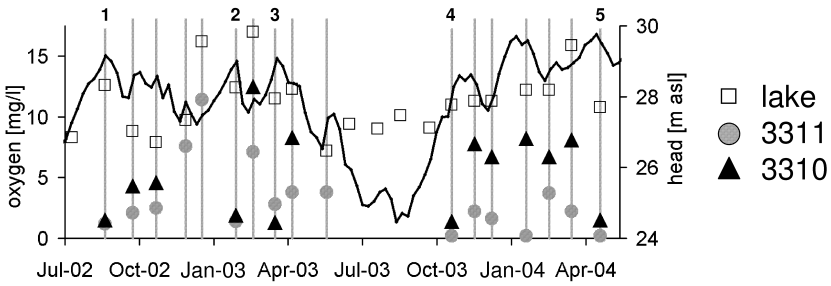

Fig. 4 Left axis: oxygen concentration in observation well 3311, 3310 and in the lake. Right axis: simulated hydraulic heads at observation well 3310. The numbers at the top denote, when oxygen concentrations are low after a continuously rising water table.

CONCLUSIONS

We explain the hydraulic characteristics and geochemical observations by reversible anaerobic clogging controlled by a changing thickness of the unsaturated zone due to transient groundwater abstraction. Clogging is higher under anaerobic than under aerobic conditions (e.g. Okubo & Matsumoto, 1979), especially at sulphate reducing conditions (Wood & Basset, 1975), due to the production of extracellular organic matter (Hoelen *et al.*, 2006). We conclude that at high groundwater table, the available electron acceptors are successively consumed due to degradation of organic matter, leading to the formation of an anaerobic clogging layer. At low water table atmospheric oxygen is sucked into the unsaturated zone and subsequently initiates the degradation of the clogging layer.

This hypothesis can explain, why the leakage coefficient is connected to water table variations and why it is highest close to the bank. It is supported by the observed variations in oxygen, nitrate and sulphate concentrations.

Acknowledgements This work was part of the NASRI project by KompetenzZentrum Wasser Berlin, funded by Berlin Water Works and Veolia Water. Many thanks to Anja Hoffmann (TU-Berlin) for provision of infiltration measurements.

REFERENCES

Hoelen, T. P., Cunningham, J. A.,. Hopkins, G. D., Lebron, C. A. & Reinhard, M. (2006) Bioremediation of cis-DCE at a sulfidogenic site by amendment with propionate. *Ground Water Monitoring and Remediation* **26**(3), 82-91.

Hoffmann, A., & Gunkel, G. (2006) Dynamik und Funktionalität des sandigen Interstitials unter dem Einfluss induzierter Uferfiltration. P*aper presented at DGL, Dresden.*

KWB 2005, NASRI – Natural and Artificial Systems for Recharge and Infiltration. Project database and final project report, KompetentzZentrum Wasser Berlin.

Okubo, T. & Matsumoto, J. (1979) Effect of infiltration rate on biological clogging and water quality changes during artificial recharge. *Water Resources Research* **15**(6), 1536-1542.

Wood, W. W. & Bassett, R. L. (1975) Water quality Changes related to the development of anaerobic conditions during artificial recharge. *Water Resources Research* **11**(4), 553-558.

Wiese, B. (2006) Spatially and temporally scaled inverse hydraulic modelling, multi tracer transport modelling and interaction with geochemical processes at a highly transient bank filtration site, 233 pp, *Humboldt-University Berlin.* full text available: http://edoc.hu-berlin.de/docviews/abstract.php?id=27914

A flood forecasting system based on probabilistic precipitation scenarios: performance evaluation and sensitivity analysis to the re-analysis archive

A. BEN DAOUD[1], E. SAUQUET[1], C. OBLED[2], M. LANG[1] & G. BONTRON[3]

1 *Cemagref, Hydrology - Hydraulics Research Unit, 3 bis quai Chauveau CP220, F-69336 Lyon Cedex 09, France*
aurelien.bendaoud@cemagref.fr

2 *Laboratoire d'Etude des Transferts en Hydrologie et Environnement, Institut National Polytechnique de Grenoble, BP 53, F-38041 Grenoble Cedex 9, France*

3 *Compagnie Nationale du Rhône, Direction de l'Ingénierie – Eau et Environnement, 2 rue André Bonin, 69316 Lyon Cedex 4, France*

Abstract A probabilistic quantitative precipitation forecasting system is applied to the Saone river basin in order to predict ensemble discharge at one station. This method, strictly based on the meteorological analogy concept, depends on the input data. The sensitivity of the precipitation forecasting system to the input database is assessed using two different re-analysis archives. This sensitivity analysis shows in average, weak performance discrepancies.

Keywords PQPF; performance evaluation; ERA-40; NCEP/NCAR; flood forecasting

INTRODUCTION

Flood events may be anticipated by using quantitative precipitation forecasts (QPFs) introduced thereafter in a rainfall-runoff model to simulate discharges. The QPF method considered here is based on the analog sorting technique described by (Bontron & Obled, 2003). A first selection (level 1) of analogous situations is in terms of synoptic circulation is identified, and from this sample a subset of the most similar patterns in terms of hygrometric situation (level 2) is extracted. The predictors involved in the similarity criterion are extracted from a long meteorological archive and results may strongly depend on several choices, such as the meteorological database. The aim of this presentation is to assess the sensitivity of the QPF system to two different re-analysis archives: the first National Centers for Environmental Prediction/National Center for Atmospheric Research re-analysis (NNR) and the 45-Year European Centre for Medium-Range Weather Forecasts Re-Analysis (ERA). The study area covers the Saone river basin in France. The predictand is the daily rainfall amount for three sub-basins. Finally for illustration, a flood forecast is obtained from the GR4J rainfall–runoff model for a river basin within the study area.

SENSITIVITY ANALYSIS OF THE PQPF SYSTEM TO THE RE-ANALYSIS ARCHIVE

This sensitivity analysis to the re-analysis archives is carried out in a context of perfect prognosis, that is the evaluation is based on observations, not forecasted by a model in real time conditions. Numerous appropriate scores to evaluate probabilistic forecast performances can be found in the literature (for a complete list, see Jollife & Stefenson (2003)). Among them, the Continuous Ranked Probability Score (CRPS) (Hersbach, 2000) seems well suited for probabilistic forecast verification. However, methods may lead to very similar CRPS values leading. Thus, the relative skill score (*RSS*) is used instead:

$$RSS(M) = \frac{CRPS(M) - CRPS(M_{ref})}{CRPS_{perf} - CRPS(M_{ref})} \tag{1}$$

where M is the method to evaluate, M_{ref} is a reference forecasting method, which prediction is known whatever the day of prediction, and $CRPS_{perf}$ is the *CRPS* of a perfect forecast (*i.e.* a value of 0). Here, forecasts issued from M_{ref} are given by the climatological distribution of the predictand. The *RSS* score is a function of the numbers of selected situations at level 1 ($N1$) and 2 ($N2$). The performance is evaluated by testing combinations ($N1$, $N2$) with $N1$ between 10 and 100 and $N2$ ranging from 5 to $N1$.

The *RSS* score is plotted against $N2$ with fixed values for $N1$ on Fig. 1 (ERA L2 and NNR L2). Two additional curves are displayed, corresponding to the *RSS* score considering only level 1 as criterion of selection (ERA L1 and NNR L1).

Lastly, the optimum is reached at level 1 for $N1$=70 when using ERA database and $N1$=80 when using NNR, and for $N2$ = 25 with both archives. These values correspond to the maximums of ERA L2 and NNR L2 curves in Fig. 1. The analog method (AM) performs better when using ERA instead of NNR, since ERA provides the highest values for *RSS*. Small deviations between ERA L2 and NNR L2 curves suggest comparable performance around the optimal values. Lastly, the second step of the selection is well justified since the gain in *RSS* of about 5% measured between the maximum of the curves at level 1 and the curves at level 2 is not negligible.

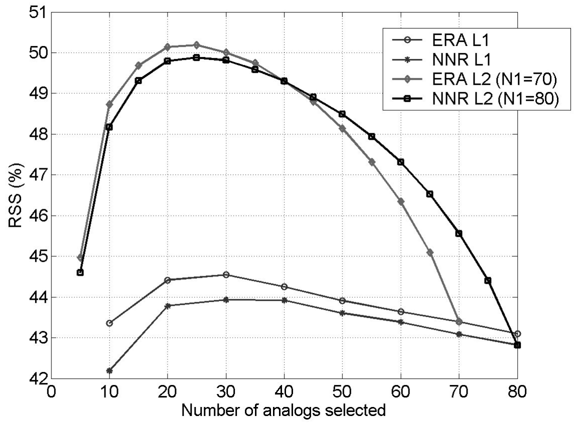

Fig. 1 Evolution of the *RSS* score with the number of analogs selected at level 1 (L1) and level 2 (L2), when ERA and NNR are used as predictors archive. Units are %.

The sensitivity analysis can be carried out using the receiver operating characteristics (ROC), described by Mason (1982) and Stanski *et al.* (1989), which quantifies both the false alarm rate and the hit rate. The ROCs are plotted for different thresholds of daily rainfall amount. Finally, the ROCs are summarised by the area value estimated under the curves (*AROC*). Thus the *AROC* score lies between 0 and 1, a value of 0 corresponding to a worst prediction, a value of 1 to a perfect prediction and a value of 0.5 to a prediction equivalent to the climatological prediction. Five thresholds are considered (Table 1): all precipitation amounts higher than 0 mm, and those higher than the quantiles 50% (P50), 70% (P70), 90% (P90) and 99% (P99) of the marginal rainfall distribution of the catchments.

Table 1 AROC values obtained for each threshold by using ERA and NNR.

	0mm	P50(mm)	P70(mm)	P90(mm)	P99(mm)
ERA	0.9321	0.9358	0.9301	0.9221	0.8948
NNR	0.9297	0.9348	0.9295	0.9223	0.8882

Differences between ERA and NNR in *AROC* scores are rather small. The most important deviation is detected for P99. Nevertheless, most of the highest scores are associated to ERA for all thresholds, except for P90. The AM seems to provide more reliable forecasts for heavy rainfall events when ERA is considered. Furthermore, the best scores for both archives corresponds to medium events, since the maximum of the *AROC* scores are detected for P50.

FLOOD CASE STUDY IN THE SAONE RIVER BASIN

The major event which occurred in January 1995 in the Doubs River sub-basin is one of the examples under study. The QPFs are introduced in the lumped GR4J rainfall-runoff model, running at a daily time step (Perrin *et al.*, 2003). The GR4J model is calibrated using all the data available from 1973 to 2005. The deviation to the observations $err(t)$ is computed for each day, and linear relationships between $err(t)$ and $err(t+j)$, $j \geq 1$ day, are fitted to characterize the persistence of the model error: $err(t+j) = a_j \, err(t) + b_j$. For this study case, at the time of the forecast t_0,

- the AM is applied with data extracted from re-analyses, *i.e.* "perfect" meteorological fields to provide the empirical rainfall distribution for each day t_0+j, $j \geq 1$ day ; ten scenarios of rainfall forecasts are established by selecting randomly one value among the 25 daily rainfall amounts issued from the $N2$= 25 analogous situations;

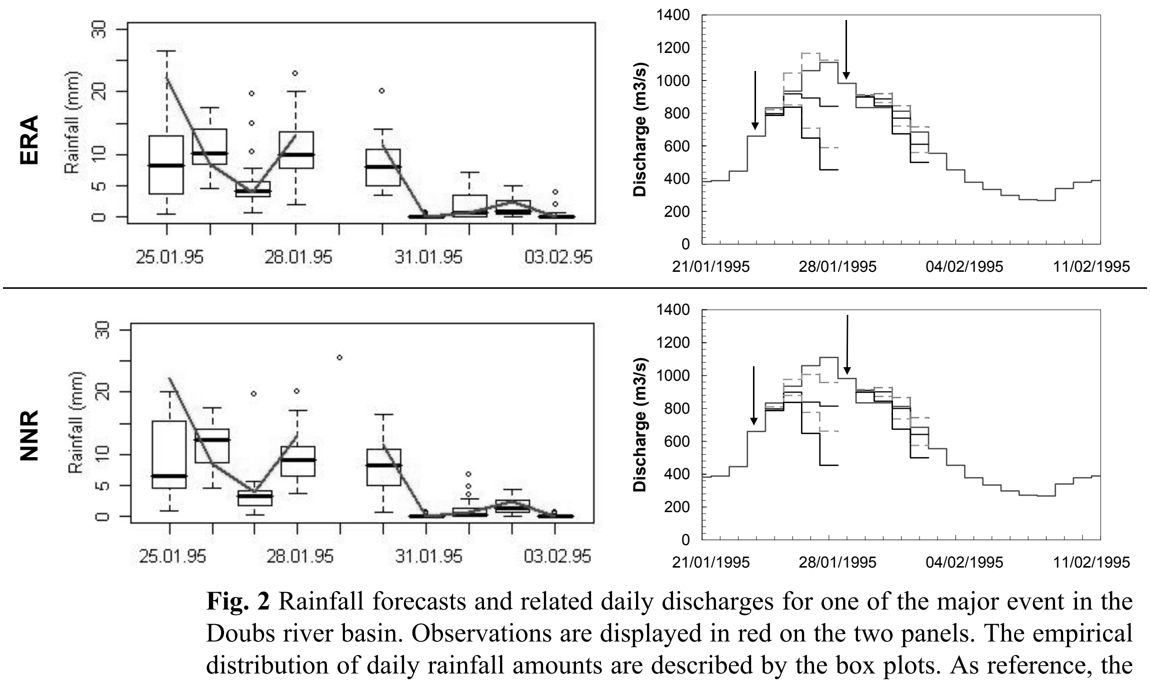

Fig. 2 Rainfall forecasts and related daily discharges for one of the major event in the Doubs river basin. Observations are displayed in red on the two panels. The empirical distribution of daily rainfall amounts are described by the box plots. As reference, the scenario with no rain for time t_0+j, j =1…4 is shown in black. The arrows indicates the day of the forecast t_0. The blue curve corresponds to the median of the discharge forecasts and the grey curves to the extreme values.

- the GR4J model is forced by the ten scenarios;
- a simple adaptive updating procedure to simulate the real-time reduction of forecast error is considered: the forecasted discharge at time t_0+j, $j \geq 1$ day is the sum of the value from GR4J run and the term $err(t_0+j) = a_j\ err(t_0) + b_j$.

Hindcasted discharges are compared with observed values on the right panel of Fig. 2. Here, we consider lead times below 4 days. Forecasts are established at time: t_0 = 24/01/1995 and t_0 = 30/01/1995.

On this specific event the AM fails to predict the major rainfall event of the 24/01/1995 in particular when NNR is used. ERA shows slightly better results since the observed values is within the range of the forecasted rainfall amounts for this day (Fig. 2, left). This behaviour observed on this specific event is of course consistent with results of Table 1 which demonstrate the better accuracy obtained for predicting high quantiles with ERA. On the other hand, both archives provide similar patterns for the recession curves.

CONCLUSIONS

The sensitivity of the AM to the re-analysis archive was examined in a perfect prognosis context with two different scores. Both indicators reveal small discrepancies between the use of ERA and NNR archives. Comparable forecasts are obtained for medium rainfall events but there is a slight increase in forecast skill from using ERA if heavy events are expected. We may suspect that the biases are similar for discharge forecasts. This fact has been observed in this paper on a case study.

Several ways for improving this analog method could be investigated. This approach is already attractive but new predictors and additional analogy criteria could be tested in order to increase more specifically the predictability of extreme events. This study provides preliminary results. It is not possible to conclude about the choice of the meteorological database to be used. To decide between the two re-analysis archives, the reliability of models outputs in an operational context has to be evaluated. This could be achieved applying this framework to re-forecasts.

Acknowledgements The NCEP/NCAR and ECMWF ERA-40 re-analysis data were obtained from the NOAA web site (http://www.cdc.noaa.gov/) and from the ECMWF data server (http://data.ecmwf.int/data/d/era40_daily/), respectively.

REFERENCES

Bontron, G. & Obled, C. (2003) New developments in quantitative precipitation forecasts by analog sorting techniques. *Proceedings of the 5th International EGS Plinius Conference on Mediterranean Storms.* Ajaccio 1-3 Oct.

Hersbach, H. (2000) Decomposition of the continuous ranked probability score for ensemble prediction systems. *Weather Forecasting* **15**, 559-570.

Jolliffe, I. T. & Stephenson D. B. (2003) Forecast verification: a Practitioner's Guide in Atmospheric Science. *Jon Wiley and sons Ed.* 239 p.

Lorenz, E. N. (1969) Atmospheric predictability as revealed by natural occurring analogues. *J. Atmos. Sci.* **26**, 636-646.

Mason, I. B. (1982) A model for assessment of weather forecasts. *Austral. Met Mag.* **30**, 291-303.

Perrin, C., Michel, C. & Andreassian, V. (2003) Improvement of a parsimonious model for streamflow simulation. *J. of Hydrology* **279**, 275-289.

Stanski, H. R., Wilson, L. J. & Burrows, W. R. (1989) Survey of common verification methods in meteorology. *World Weather Watch in Technical Report* **8**, World Meteorological Organisation, Geneva.

A limited-area ensemble prediction system to drive a flood forecasting chain

T. DIOMEDE, C. MARSIGLI, A. MONTANI & T. PACCAGNELLA
ARPA-SIM Servizio IdroMeteorologico dell'Emilia-Romagna, Viale Silvani 6, 40122 Bologna, Italy
tdiomede@arpa.emr.it

Abstract The quantitative precipitation forecast is still a challenging task at the scales of interest for hydrological predictions. Although the use of high resolution limited-area models has improved the short-range prediction of locally intense events, it is sometimes difficult to forecast accurately their space-time evolution, especially for ranges longer than 48 hours. Nowadays, the ensemble prediction techniques are widely used in the meteorological community, allowing to add probabilistic information to the forecasts, especially with respect to risk-related events. Moreover, meteorological ensemble systems have been recently used to provide a probabilistic input to river flow forecasts, in order to improve both their accuracy and the reliability of uncertainty estimates affecting hydrological model predictions. In the present study the usefulness and the skill of a Limited-area Ensemble Prediction System based on the non-hydrostatic limited-area model COSMO (COSMO-LEPS) is evaluated as a tool to provide quantitative precipitation forecasts driving a flood forecasting chain. The river hydrograph simulations are performed by means of the distributed rainfall-runoff model TOPKAPI. The COSMO-LEPS methodology is designed to combine the advantages of a global-ensemble prediction system with the ability typical of limited area models to detail atmospheric phenomena on more local scales, particularly in those regions dominated by the effects of complex orography. The system has been developed for the time range "late-short-range (48h) - early-medium-range (120h)". The ensemble members are differentiated mainly in the initial and boundary conditions by which they are driven: the different model runs are nested on some selected members of the ECMWF Ensemble Prediction System, chosen by means of an ensemble-size reduction technique based on a Cluster Analysis algorithm. The system has repeatedly been updated by increasing the layers in the vertical (from 32 to 40) and the number of members (from 5 to 16). The horizontal resolution is of about 10 km. The performance of the proposed meteo-hydrological coupled system is evaluated for some small/medium-sized catchments located in the Emilia-Romagna Region, northern Italy. In particular, streamflow forecasts are simulated for the autumn and spring seasons of the period 2003-2007. Results are investigated by statistical analyses, especially with respect to the verification of warnings and alarms.

Keywords flood forecasting chain; limited-area ensemble prediction system; COSMO-LEPS; distributed rainfall-runoff model; TOPKAPI

INTRODUCTION

In the field of hydrologic prediction for watersheds with short response times to rainfall events, predicted rainfall is essential for hydrologic models which would increase the lead time up to a minimum critical value, thus allowing for the activation of civil protection plans. Despite the development of more and more sophisticated and resolved numerical weather prediction models, accurate forecasts of locally intense events are still difficult, especially for ranges longer than 48 hours. This limitation is due, among other reasons, to the inherently low degree of predictability typical of the relevant physical phenomena.

The probabilistic approach has been recently more and more explored to try to come to terms with the chaotic behaviour of the atmosphere and to help forecasting phenomena with low deterministic predictability. Global ensemble prediction systems have become extremely important tools to tackle the problem of predictions beyond day 3-to-4. However, the skill of these system in forecasting intense and localised events in the short- and medium-range is currently still limited since they are usually run at a coarser resolution. In order to enhance the present-day prediction capabilities of operational ensemble systems, several approaches have been attempted, as the use of limited area models to perform a dynamical downscaling of the ensemble forecasts produced by a global model (Tibaldi *et al.*, 2006).

In this work, the use of a Limited Ensemble Predictions System (LEPS) is evaluated as a tool to provide quantitative precipitation forecasts driving a flood forecasting chain.

DESCRIPTION OF THE FLOOD FORECASTING CHAIN

The flood forecasting chain proposed herein is based on the following tools:
- COSMO-LEPS, a Limited-area Ensemble Prediction System based on the non-hydrostatic limited-area model COSMO (COnsortium for Small scale MOdeling), daily running (12 UTC) at ECMWF (European Centre for Medium-Range Weather Forecasts) since November 2002;
- TOPKAPI (TOPographic Kinematic APproximation and Integration), a physically-based distributed rainfall-runoff model model (Todini & Ciarapica, 2001).

The LEPS methodology is described in its essential principles in Molteni *et al.* (2001) and Marsigli *et al.* (2001). Currently, COSMO-LEPS is based on 16 runs of the COSMO model. The ensemble is generated as a downscaling of the global ECMWF Ensemble Prediction System (ECMWF EPS). The configuration of the system (whose details are described in Table 1) has been upgraded in time, in particular with respect to the ensemble size (five members up to May 31, 2004; ten members up to February 5, 2006) and the vertical layers. In the present study, all the members have been considered equally likely in the direct coupling with TOPKAPI, without applying any kind of stochastic procedure for rainfall downscaling.

Table 1 Summary of model configurations.

Name	Boundary conditions	Initial conditions	Deep convection parameterisation	Horizontal resolution	Vertical resolution	Forecast range
COSMO-LEPS	EPS forecast	EPS analyses	Tiedtke or Kain-Fritsch (randomly selected)	10 km	40 layers (32 up to 05/02/06)	132 h (120 up to 30/06/05)
COSMO-LAMI	DWD-GME forecast	LAMI mesoscale assimilation (nudging)	Tiedtke	7 km	40 layers (35 up to 25/01/06)	72 h

The performance of the proposed meteo-hydrological coupled system is evaluated for five catchments (whose dimensions range from 500 to 1000 km^2) located in the Emilia-Romagna Region, northern Italy. In particular, hourly streamflow forecasts have been simulated for the Reno, Lamone, Ronco, Montone and Savio rivers, considering the autumn and spring seasons of the period 2003-2007. In addition, the deterministic forecasting chain driven by the meteorological model COSMO operational at ARPA-SIM (COSMO-LAMI, whose configuration details are summarised in Table 1) is used as term of comparison to evaluate the added value of the probabilistic system.

RESULTS

The reliability and accuracy of the streamflow predictions driven by COSMO-LEPS have been evaluated by means of a statistical analysis. Firstly, the study has been carried out in terms of mean error and root mean squared error, in particular with the aim to investigate which quantile confidence interval could be more suitable to represent the ensemble forecast. From the computations, shown in Fig. 1 only for the autumn season of the largest catchment (i.e. the Reno river basin), it derives that, when the season is characterised by high discharge values, the 60%-90% quantile confidence interval performs generally better than the ensemble mean with increasing lead-time. Otherwise, in case of moderate streamflows, the ensemble mean and the percentiles around the median provide the best scores. Furthermore, the performance decay is evident up to the first 48-hour forecast range; for longer lead-times, the decay is partly compensated by the ensemble skill. The spread of the ensemble error is narrow for the first 24 hours, and increases for longer lead-times. The errors are smaller in spring than in autumn.

The performances of the flood forecasting chain obtained for the five selected catchments have been compared in terms of the Nash-Sutcliffe model efficiency coefficient. The results (not shown) reveal that the largest catchment shows a clearly better performance as compared to the smaller ones for the autumn season, whereas there is not a clear evidence of a better performance for the largest catchment during the spring season. For the autumn season, the 75% quantile provides slightly higher scores as compared to the ensemble mean with respect to the largest catchment, whereas the opposite result is obtained for the smaller catchments. The ensemble mean show higher scores as compared to the 75% quantile for all the catchments during the spring season.

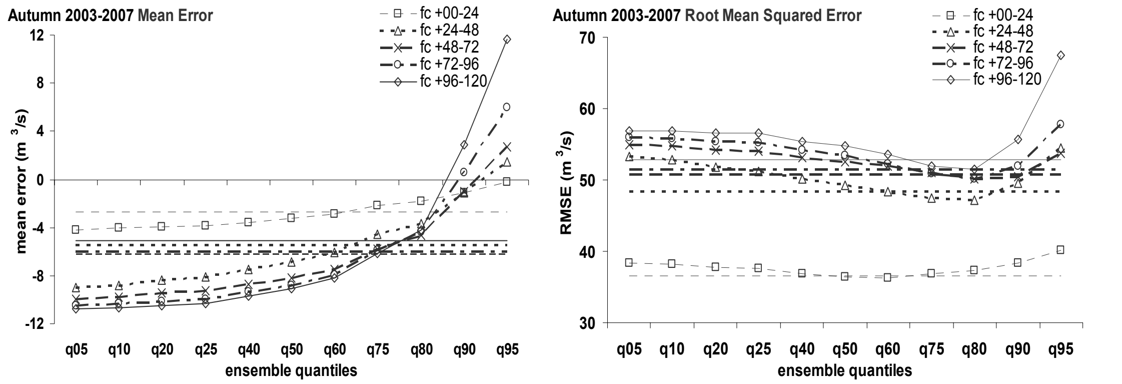

Fig. 1 Mean error and root mean squared error corresponding to different quantiles of the ensemble of hourly discharge forecasts for the autumn season 2003-2007 over the Reno river basin. The statistics are computed over 24-h long forecast ranges, up to +120 h. The statistics of the ensemble mean are displayed as horizontal lines, labelled as the statistics of the different quantiles but without the symbol.

A further analysis (not shown) has been carried out on the verification of warnings and alarms. In practice, three alert thresholds are defined for the aims of civil protection over the largest catchment, and two (those more higher) for the remaining cachtments. For the Reno river basin, in case of the exceeding of the lower threshold, an increase of false alarms and misses results up to the +48-72 h forecast range, afterward this growth is less evident. The false-alarm rate is higher in spring than in autumn, generally for all the forecast ranges. The frequency of misses is quite similar for the two seasons (slightly higher values in spring than in autumn up to +72 h). In case of the exceeding of the medium and the higher alert thresholds, the performance of the probabilistic coupled system cannot be evaluated by means of a statistical analysis, owing to the limited size of the event sample (2-3 events occurred) for all the catchments. Generally, the 75%-90% quantile confidence interval provides a fairly good trade-off in reducing misses without increasing false alarms considerably. However, decision-makers have to evaluate (e.g., on the strength of a cost-loss analysis) which confidence level is more suitable to support their activities.

For the Reno river basin, the performance of the probabilistic coupled system has been compared to that obtained with the deterministic chain driven by COSMO-LAMI. Considering the autumn seasons of the period 2003-2005, the ensemble discharge predictions show performance which are comparable to the single-valued forecast for the first 24-hour forecast range in terms of mean error and root mean squared error. The added value of the probabilistic system comes out with increasing lead-times, especially starting from day three. The verification of warnings and alarms reveals that the deterministic chain provides scores quite similar (or worse) to the ensemble mean.

CONCLUSIONS

COSMO-LEPS turns out to be a promising forecasting tool to drive hydrologic predictions and to assist civil protection authorities for the issues of early warnings on the catchments investigated herein. In case of high streamflows, the 75%-90% quantile confidence interval allows to reduce the missed events while keeping good values of the other statistical scores. Otherwise, in case of moderate streamflows, the ensemble mean and the percentiles around the median perform better. Generally, in case of intense events, a negative bias affects the predictions of the coupled system. This result is due to a typical feature of the COSMO model, which shows the tendency to overestimate the rainfall in upwind areas in presence of a mountain range, with a related underestimation effect in the downwind regions. Since the investigated catchments are located on the north-eastern side of the Apennines barrier, they clearly suffer for this problem when the flow is mainly from south-west. Actually, flood events over these catchments are often associated to south-westerly flows. The COSMO-LEPS methodology is developed to make a dynamical downscaling of different meteorological scenarios provided by the ECMWF EPS, which are related to different possible initial conditions. At present, the system includes only a small perturbation generated to take into account uncertainties associated to the COSMO model errors. The improvements in the model formulation itself, together with a more comprehensive approach which would enable to consider different sources of error, will enhance the performance of the coupling with hydrologic models.

REFERENCES

Marsigli, C., Montani, A., Nerozzi, F., Paccagnella, T., Tibaldi, S., Molteni, F. & Buizza, R. (2001) A strategy for high-resolution ensemble prediction. Part II: Limited-area experiments in four Alpine flood events. *Q. J. R. Meteorol Soc*, **127**, 2095-2115.

Molteni, F., Buizza, R., Marsigli, C., Montani, A., Nerozzi, F. & Paccagnella, T. (2001) A strategy for high-resolution ensemble prediction. Part I: Definition of representative members and global-model experiments. *Q J R Meteorol Soc.* **127**, 2069-2094.

Tibaldi, S., Paccagnella, T., Marsigli, C., Montani, A. & Nerozzi, F. (2006) Limited-area ensemble forecasting: the COSMO-LEPS system. In: *Predictability of weather and climate* (ed. by T. Palmer & R. Hagedorn), 489-513. Cambridge University Press, New York, USA.

Todini, E. & Ciarapica, L. (2001) The TOPKAPI model. In: *Mathematical Models of Large Watershed Hydrology* (ed. by V.P. Singh. *et al.*). Water Resources Publications.

KISTERS Time Series Management system and its integration into flood prediction and flood warning environments

C. GATTKE, R. FUNKE, G. DÖDING & M. NATSCHKE
KISTERS AG, Charlottenburger Allee 5, 52428 Aachen, Germany
christian.gattke@kisters.de

Abstract Due to the frequent occurrence of flood events the implementation of real time flood forecast and management systems came into focus. A typical implementation of such a system based on KISTERS solutions is described. Furthermore, the new KISTERS Time Series Management (TSM) System, which constitutes an excellent basis for the implementation of real time flood forecast and management systems, is introduced. Efficient flood management depends on the response time and predictive quality of the forecast models used. An initial study using neuronal forecast models developed for the power system management, which are relative insensitiv to noisy input data, is presented.
Keywords flood forecast and management; time series management; neuronal network models

INTRODUCTION

For a successful flood management a complete and integrated chain of data acquisition, automatic and operator driven quality control and analysis is necessary. Quick and reliable forecast procedures and alarm and information management are further core requirements. Nowadays hydrological information and time series management systems are widely used to assist the hydrological services in this process.

Since more then 20 years some hundreds of systems were implemented worldwide based on KISTERS Time Series Management and the hydrological workbench WISKI. During the last years real time flood management systems came into focus in addition to the well established information systems optimised for evaluation and distribution of verified hydrological and ecological data sets (Funke *et al*., 2006). The central database and the time series server are building the basis for a system that is able to meet the different requirements of a real time flood forecast and management and long-term information system. A typical implementation of such a system based on KISTERS solutions and the new KISTERS Time Series Management System, designed to meet future requirements, are described here.

The quality of the whole process depends on the response time and predictive quality of the forecast models used. Existing models can be seamless plugged into the system to enhance their reliability by providing them automatically with plausibility checked data sets, thus avoiding to impair the forecast results by propagation of errors in the input data. Currently the liberalized European energy market produces different statistical and neuronal forecast models for optimal adoption of power generation to the power demand. In this context a model faces the requirements of robustness, minimised data and calibration demand and near real time response time. First results utilising this model type for hydrological predictions, including a comparison with a conceptual hydrological model, are shown here.

FLOOD WARNING CENTRE OF SAXONY-ANHALT, GERMANY

As a consequence of the flood disaster in August 2002, the federal state Saxony-Anhalt decided to optimise the activities carried out so far by the Flood Control Centre

(HWMZ) in the State Office for Environmental Protection Halle (LAU Halle) and the State Office for Flood Protection and Water Management (LHW) by combining them to form a modern Flood Warning Centre (HVZ). Within a public European tender the KISTERS AG was awarded as system supplier and general contractor of a group of consulting companies. Flood forecasts (model integration, scenario management), data management (observed data, model scenarios, documents, archive), data publication (Inter-/Intranet, E-Mail, Fax, SMS etc.), redundancy and real-time data exchange with external hydrological databases have been the main requirements of the project. The observed stage, discharge and precipitation measured by the LHW are making the fundamental contribution to the overall information management. Additionally data supplied by the national river authority, the reservoir systems, the neighbouring countries, the groundwater monitoring is integrated into the system, as well as data, forecasts and warnings of the German Weather Service (DWD).

The head office of the new flood control centre is Magdeburg. A redundant emergency control unit is established in Halle as warm stand-by system with an activation period of a few minutes. The Control Unit collects and processes as central communication point any flood-relevant information. It receives flood alarms from the gauging stations as well as storm warnings from the Weather Service and is responsible to alarm the relevant authorities and the Forecast Unit, which creates stage forecasts based on the input data and information received from the Control Unit. Additional data can arrive in the HVZ via email or active/passive FTP-connects. Gauge observers can submit messages by mobile phone and DTMF-entries as well as by telephone answering machine. Core component of the Control Unit is the KISTERS HVZ-monitor, which assists the operation team. It is realised as a web application in the intranet and displays the incoming and outgoing data in real-time. The operation team continuously analyses the flood situation. It is responsible for the coordination of the flood protection measures and prepares the flood bulletins which are published via a public platform. The Information Distribution Unit automatically dispatches the warning messages received by the Control Unit and the flood bulletins created in the Forecast Unit. All flood-relevant information is distributed via the Public Platform. It is implemented as a web portal and divided into three areas: a) the public Internet, b) the Saxony-Anhalt wide Intranet and c) the HVZ internal Intranet. The main difference between these areas is the amount of data presented and the functionality offered.

The functional structure described above is realised through appropriate distribution of services within the network structure in the Flood Warning Centre (HVZ). The electronic data transfer between the authorities inside and outside the country occurs via the TESTA-Network (Trans-European Services for Telematics between Administrations). The Time Series Data Management including the telemetry system for the online collection of hydro-meteorological data, and the complete Control Centre has been implemented by KISTERS.

THE KISTERS TSM (TIME SERIES MANAGEMENT) SYSTEM AS FUTURE TECHNOLOGY

In environmental information systems, it is necessary to acquire, rapidly process and archive mass data in form of time series. For near real time systems rapid processing and quick data access are of utmost importance. This results in a list of special requirements for time series management including mass data capacity, scalability, modular capabilities, flexible operation in various fields, high level of automation, reliability and resilience, security aspects, integration potential and platform independency. These demands call for specific software solutions, which were typically developed independently for each application. The KISTERS Time Series

Management (TSM) System is the new shared system core of all KISTERS products where time series are involved. It represents the central layer of a 3-layer architecture and provides applications built upon it with all services necessary for time series management and calculation (see Fig. 1).

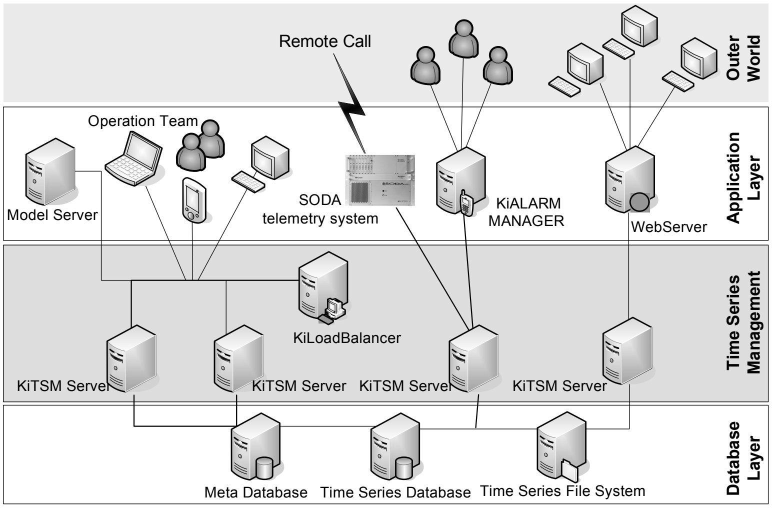

Fig. 1 KISTERS Time Series Management (TSM) System 3-layer architecture exemplified by means of a real time flood forecasting and management system.

The KISTERS TSM System covers all of these requirements and furthermore guarantees that the special requirements of the thematic application are fulfilled exclusively through configuration settings. In order to satisfy these requirements, the KISTERS TSM System has been designed as a multi-layer architecture, which comprises several advantages compared to a classical client-server approach. In client-server architectures, the database server only operates as a data container, and all processing is handled by the client. This leads to the fact, that time series management must be integrated into the client, what makes it difficult or even impossible to meet many of the requirements stated above. A multi-layer architecture, guarantees a high level of flexibility in the design of system solutions. Appropriate definition and implementation of the interfaces yields that any architecture built upon the TSM System is optimized for high-performance management and processing of time series data. As opposed to the client-server model, in which the data provider has a primarily reactive character, the KISTERS TSM System is an active system. The TSM System provides the application layer with all generic functions for time series data management, as well as an optimized automatic calculation server for time series processing and calculation. The architecture of the TSM System is designed to operate as an autonomous server system, so that it may be adjusted to suit all manner of applications.

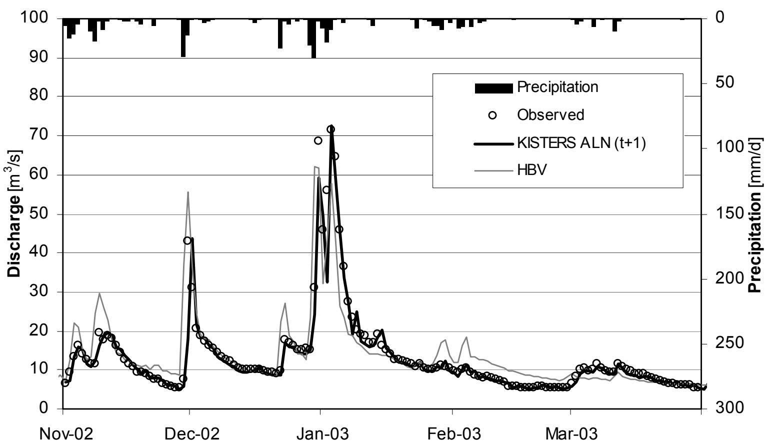

Fig. 2 Comparison of the predicted hydrographs for a section of the validation period.

The TSM System, implemented in state-of-the-art Java technology, is platform independent. The generic interface to the persistence level allows various relational database systems to be used (e.g. Oracle, MS-SQL, PostgreSQL). The broad scalability of the KISTERS TSM System facilitates an adjustment to meet specific requirements regarding computing power and volume of the data flows. Because the TSM System is multi-client capable, i.e. multiple applications with different datasets may be served simultaneously, load balancing of different applications becomes also possible. Thus, the KISTERS TSM System is an excellent basis for a system that is able to meet the different requirements of a real time flood forecast and management system and long-term information system.

MODEL STUDY: COMPARISON OF THE KISTERS ALN AGAINST A CONCEPTUAL HYDROLOGICAL MODEL

First application of a forecast model originally developed for power system (Döding, 1997) to hydrological data has been tested for a mesoscale catchment located at the upper Unstrut river in Mid-East Germany (Möbisburg, 843 km^2). A 23-year period of observed discharge was split into a 18-year and 5-year period for calibration and validation. The simulations were carried out at a daily time-step. An Adaptive Logic Network (ALN) has been used for discharge prediction. An ALN is a type of artificial neural network for supervised learning, whose nodes are grouped in binary trees. ALNs are known for high execution speed, insensitivity to noisy input data and the ability to re-train. The conceptual hydrological model used as benchmark for the model efficiency of the ALN was implemented based on an object-oriented framework designed for adaptive development of hydrological models (Gattke & Pahlow, 2006) following the concept of the HBV model (Lindström *et al*., 1997). The hydrological model has been calibrated by 10,000 Monte Carlo simulations based on parameter sets obtained by randomly generated, uniformly distributed values. The ALN used the observed discharge, temperature and precipitation of the last six days to predict the discharge one day into the future (t+1). The modelling results obtained a Nash-Sutcliffe efficiency (NSE) for the validation period of 0.94 for the KISTERS ALN and of 0.77 for the conceptual model respectively. Fig. 2 compares the predicted hydrographs for a section out of the validation period.

The KISTERS ALN gives better results all over the entire flow regime, except the first peak of the flood event in Dec/Jan. This is due to the sliding window of the past six days, which is used for the prediction of the next day. This time window is too short to consider the hydrologic situation of potential snow accumulation and melt in a sufficient way. Thus, the statistical model still implies a great potential for optimization, which has not considered for in this initially study. However, the KISTERS ALN already exhibits a significant better performance compared to the conceptual model, along with a smaller data demand and less sensitivity to uncertainties in the input data.

REFERENCES

Funke, R., Courtois, B. & Soleilhavoup, S. (2006) Integrated Hydrological Information and Knowledge Management Transfer for Flood Warning Centres in European Countries. (ed. P. Gourbesville, J. Cunge, V. Guinot. & S-Y. Liong), *Proceedings of the 7th International Conference on Hydroinformatics*, Nice.

Döding, G. (1997) Application of artificial neural networks in power system management. *In: 14th International Conference On Electricity Distribution (CIRED), Birmingham.*

Gattke, C. & Pahlow, M. (2006) Using object oriented methods for adaptive hydrological model development and uncertainty estimation. (ed. P. Gourbesville, J. Cunge, V. Guinot & S-Y. Liong), *Proceedings of the 7th International Conference on Hydroinformatics, Nice.*

Lindström, G., Johansson, B., Persson, M., Gardelin, M. & Bergström, S. (1997) Development and test of the distributed HBV-96 model. *Journal of Hydrology*. **201**, 272-288.

Anticipatory water management: decision support for real-time operational and long-term strategic use of new meteorological forecast products in flood control

S. LOOS[1], S. J. VAN ANDEL[2] & A. H. LOBBRECHT[1,2]
1 *HydroLogic BV, www.hydrologic.nl, Amersfoort, Netherlands*

2 *UNESCO-IHE, Institute for Water Education, PO Box 3015, 2601 DA Delft, Netherlands*
s.vanandel@unesco-ihe.org

Abstract Anticipatory Water Management is the operational management of water systems on the basis of forecasts of critical events. Meteorological and hydrological data and tools to support pro-active operational water management become increasingly available. Examples of flood control applications of precipitation radar, ensemble prediction systems, spatially distributed Decision Support Systems and water system control models are being presented.
Keywords ensemble forecasting; early warning; flood control; risk management; decision-making

ANTICIPATORY WATER MANAGEMENT

Anticipatory Water Management (AWM) is the operational management of water systems on the basis of forecasts of critical events. While in real-time control measurements of water levels and precipitation play an important role, in anticipatory water management and early warning decisions have to be made before an event occurs.

DECISION SUPPORT SYSTEMS

AWM relies on the use of real-time operational Decision Support Systems for water management. During crisis situations (extreme precipitation or drought) water managers need reliable and reproducible information, which is communicative and comprehensibly presented. These systems involve hydrometeorological databases for real-time handling vast amounts of actual and predicted information, hydrological and hydrodynamic models and GIS based user interfaces (Fig. 1).

ENSEMBLE PREDICTION SYSTEMS

The availability of Ensemble Prediction System (EPS) weather forecasts permits stochastic analysis with hydrological models (Krzysztofowicz, 2001). DSSs present probability distributions of forecasted excess water, water levels and inundation of land per unit of time (Fig. 1).

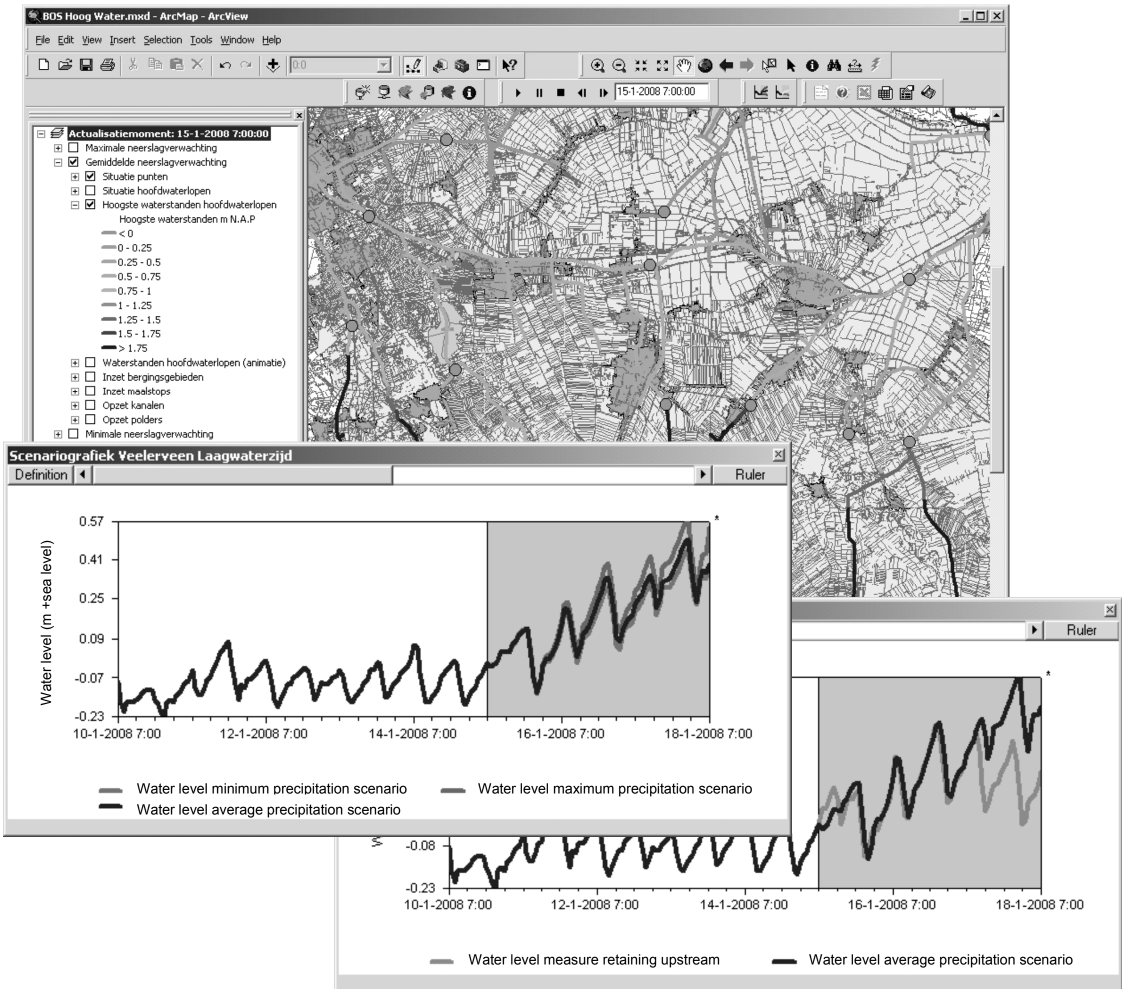

Fig. 1 DSS for flood forecasting "BOS Hoog Water", water board Hunze en Aa's, the Netherlands. GIS based user interface, showing a map of the water board area with all its watercourses. The maps can be animated, showing water levels per time step or water levels with respect to certain threshold levels. Water levels are calculated using several precipitation scenarios based on EPS, and on one or more control strategies to prevent flooding.

PRECIPITATION RADAR

Present precipitation radar information can be of great help in obtaining well performing rainfall-runoff models for use in Decision Support Systems. Such precipitation information can be converted into a hydrological load per sub-catchment of a water system (Fig. 2).

CUSTOMISED HINDCAST VERIFICATION

For every particular water system and for every application, first a customised verification analysis of the ensemble rainfall forecasts must be done to assess the potential of Anticipatory Water Management and identify suitable decision rules. With ensemble rainfall forecasts, often these rules concern thresholds of rainfall (event thresholds) and probability. Also, a wide range of forecast horizons is increasingly available, meaning that a selection has to be made for consideration in daily control decisions (Van Andel *et al.*, 2008a).

WATER SYSTEM CONTROL MODELLING

A second important instrument in the application of AWM is water-system control modelling. In such modelling exercises next to the hydrological and hydrodynamic processes, also the (human-based) control of regulating structures needs to be modelled (Lobbrecht, 1997). This allows preparing water level forecasts on the basis of rainfall forecasts and governing control strategies. If these forecasts indicate flood levels, this can be seen as a warning that additional, anticipatory control actions are needed to reduce water levels. Using water-system control modelling, the operational water management can be simulated (Fig. 3), allowing for new decision rules and control strategies to be verified in hindcast analyses (Van Andel *et al.*, 2008a,b).

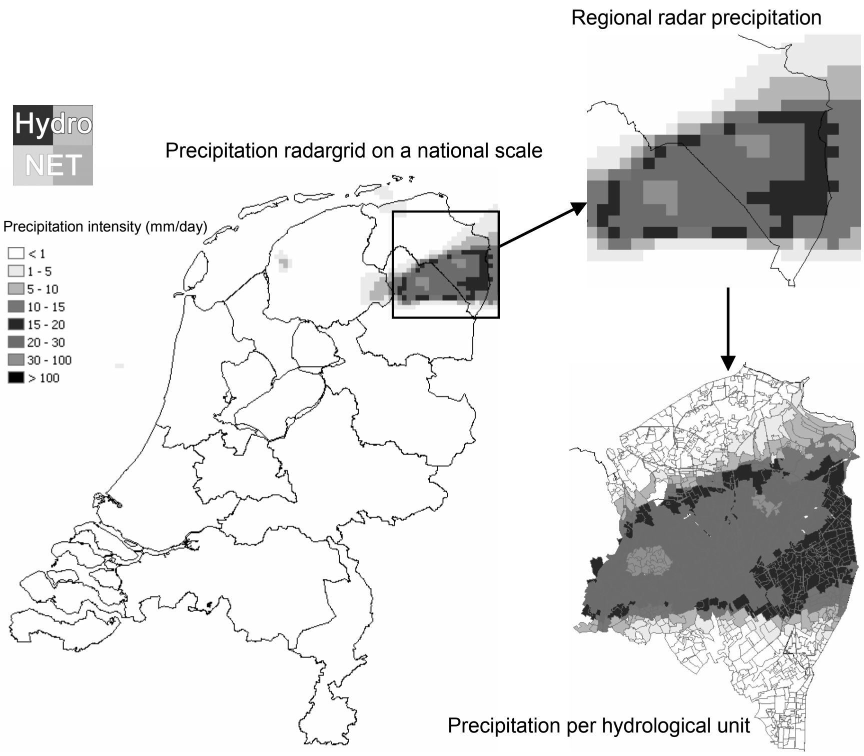

Fig. 2 DSS for flood forecasting "BOS Hoog Water", water board Hunze en Aa's, the Netherlands. High resolution calibrated radar information on precipitation is automatically converted to GIS information on an hourly basis. Then it is automatically recalculated to average precipitation per hydrological unit, resulting in a set of precipitation time series ready for use in the hydrodynamic modelling module within the DSS.

COST-BENEFIT ANALYSIS

In selecting new control strategies and in deciding on policy adoption of anticipatory control, water authorities need cost-benefit information. Benefits of reducing flood damage have to outweigh adverse effects of unnecessary anticipatory control actions as a consequence of false alarms. Adverse effects from unnecessary evacuations, controlled inundation, and low reservoir levels result in direct and indirect costs like damage to crops and loss of confidence in the warning system.

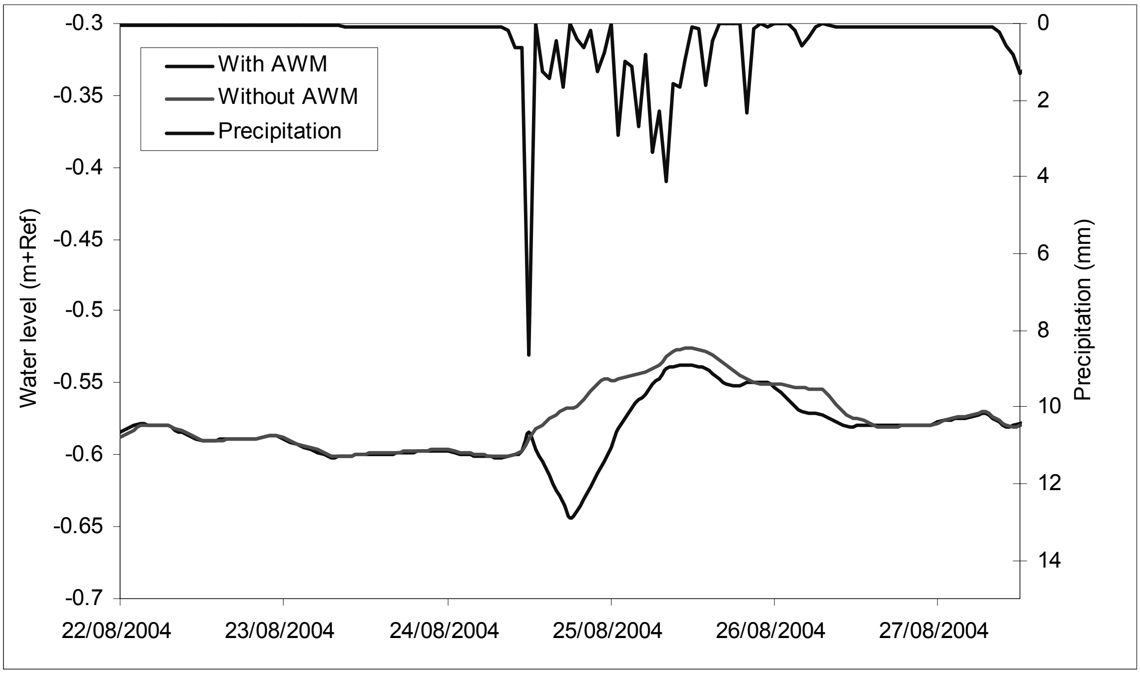

Fig. 3 Modelled anticipatory water management (AWM) in the Rijnland water system, the Netherlands. The modelled peak with AWM is lower than the peak without AWM, because in the model with AWM the water level is lowered before the (second) precipitation event occurs.

CONCLUSION

Anticipatory Water Management allows further optimisation of the use of our water system. Applications of hydrometeorological data and forecasting in decision support systems for anticipatory water management in the Netherlands have been presented.

REFERENCES

Andel, S. J. van, Price, R. K., Lobbrecht, A. H., Kruiningen, F. & Mureau, R. (2008) Ensemble precipitation and water level forecasts for anticipatory water-system control. *Journal of Hydrometeorology* (in press).

Andel, S. J. van, Lobbrecht, A. H. & Price, R. K. (2008) Rijnland case study: hindcast experiment for anticipatory water-system control. Special Issue HEPEX, *Atmospheric Science Letters* (in press).

Lobbrecht, A. H. (1997) Dynamic Water–System Control; Design and Operation of Regional Water–Resources Systems. *A.A. Balkema Publishers Rotterdam, the Netherlands*, 315 pp.

Krzysztofowicz, R. (2001) The case for probabilistic forecasting in hydrology. *J. Hydrol.* **249**, 2–9.

Protection of built and new plan dams against disastrous floods under the climatic change conditions

N. A. NIKOLOV & M. N. MARADJIEVA

University of Architecture, Civil Engineering and Geodesy, Hydraulics and Hydrology department, Christo Smirnenski blvd. 1, Sofia, Bulgaria

m_marajieva@abv.bg

Abstract Climatic changes exert already a great influence on rainfall processes about their extreme fluctuations and as a result disasters are often arising. The major disasters involve loss of live and a destruction of property, built dams and other structures. During the last 20 to 50 years the observations on the maximum water discharges in the rivers are to a great or less degree disturbed depending on the saturated ground water and the depth of the ground. On the other hand the constructed already dams have a smaller water discharge capacity throughout the overflow and other relieving structures as bottom outlets, for example they have 1 to 2 outlets instead their necessary numbers 2 to 25. Based on the experience with the flood in Bulgaria more reliable models are proposed for dam building, protection and river regulation.

Key words: flood; drainage; numerical modelling; correlative dependence; catchments basin; finite strips

INTRODUCTION

The river basin management processes focus our attention to determine a possible maximum of the high wave by observations. The determination of the input data by means of the maximum diurnal rainfall with a normative probability is a very important because the rainfall has not disturbed catchments characteristics. This information needs to provide model parameters for a future real high waves and prediction. The author's algorithm consists of a new numerical method of a finite longitudinal and cross strips shown below (Fig. 1).

First the maximum rainfall of the catchments is determined for the observed period. Then the differential density function and the probability curve are constructed.

Finally an algorithm for the flood and drainage is presented with an appropriate example for a built rock fill Bulgarian dam.

INVESTIGATIONS OF THE RAINFALL DEPENDENCY AND THE CURVES OF THE DENSITY AND PROBABILITY FUNCTIONS

Initially a correlative dependence for an average annual maximum diurnal rainfall is established concerning every selected strip of the catchments. This parameter is calculated for the left and the right river bank respectively - $h_{N\max}^{l(r)}$ and for the catchments basin $\overline{h}_{N\max}^{c.b.}$ as well. The last dependence has the form:

$$\overline{h}_{N\max}^{c.b.} = b\, e^{a\overline{H}\, c.b.} \tag{1}$$

where $\overline{h}_{N\max}^{c.b.}$ is the average annual max diurnal rainfall of the catchments basin (mm), a and b are the correlative dimensionless coefficients, and $\overline{H}_{c.b.}$ is the average elevation of the catchments basin (km).

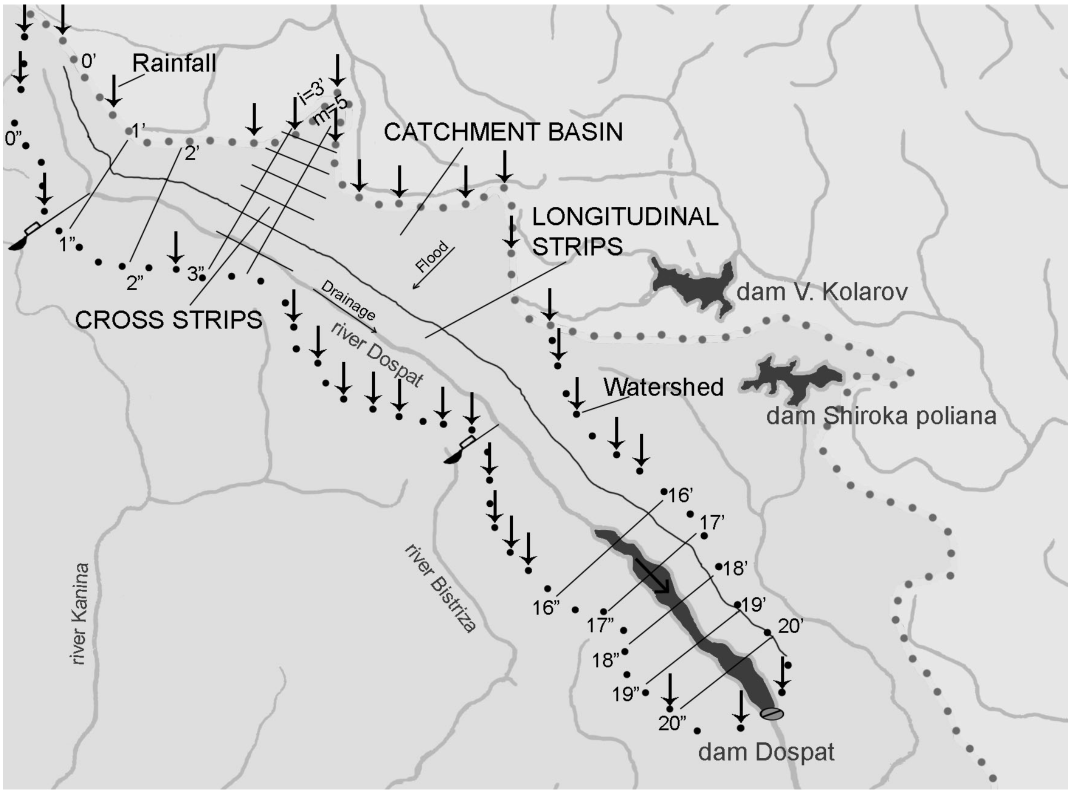

Fig. 1 Design of longitudinal and cross strips in the catchments basin to dam A.

The average elevation $\overline{H}_{c.b.}$ of the catchments basin is calculated from the above sea level altitudes and the quadratures of the accepted cross strips. The cross strips are drawn orthogonally of the horizontals of the basin so that the cross strips and the stream lines coincide. In this instance a first order differential equations is applied for the solution of the unsteady flow in wide beds. The average elevation of the catchments basin $\overline{H}_{c.b.}$ is substituted into equation (1) using the next formula:

$$\overline{H}_{c.b.} = \frac{\sum_i (\overline{H}_i^{/} F_i^{/} + \overline{H}_i^{//} F_i^{//})}{\sum_i (F_i^{/} + F_i^{//})} \tag{2}$$

where i is the current co-ordinate for the cross strip, $\overline{H}_i^{/}$ and $\overline{H}_i^{//}$ are the average absolute elevations in the left and the right banks of the river, $F_i^{/}$ and $F_i^{//}$ are a share due from the catchments basin area i in the left and in the right side respectively (m^2).

In order to define the coefficients a and b in a formula (1) two rainfall gages are chosen. They are situated nearest the elevation $\overline{H}_{c.b.}$ by checking two correlative coefficients – general and true one. In this way the correlative dependence (1) can be evaluated as satisfactory, transferring the entry data of the rainfall gages to the dam A, as well as the annual and maximum diurnal rainfall during the observed years. The observations show that the probability density function and the cumulative probability curve have the more steep character, during the last 15 years, because of the climatic changes. In particular this fact is valid in the branch of the probability curve with normative probability of 1% to 0.01%. Distributions like these could be found by gamma function, maximum likelihood method (Fisher), Weibull distribution, etc. In this study a gamma density function is applied with one additional parameter $\hat{a}$ in the limits $1 \le \hat{a} \le 7.824$. The bigger values have a larger skew ness for the catchments less than 250 km^2 and the smaller ones are valid for the catchments more than 500 to 1200 km^2. In this form the probability density is presented as the formulas (3) and (4):

$$P(X_i) = \frac{\gamma^\gamma}{\Gamma(\gamma)\,\overline{X}_0} e^{-\gamma \frac{X_i}{\overline{X}_0}} \left(\frac{X_i}{\overline{X}_0}\right)^{\gamma-1} \tag{3}$$

$$\gamma = \frac{1}{C^2_{V\lambda_2}}\ ,\quad C_{V\lambda_2} = \sqrt{-\hat{a}\,4.6\,\lambda_2} = \sqrt{-\hat{a}\,4.6\frac{\sum_i \lg K_i}{n-1}} \tag{4}$$

where $\Gamma(\gamma)$ is a generalized gamma function at an argument γ, $C_{V\lambda_2}$ is the standard deviation at the mean value λ_2, λ_2 is the empirical mean value of K_i which is the modulus coefficient and the dimensionless quotient $\frac{X_i}{\overline{X}_0}$ means a modulus coefficient given by the mean record $\overline{X}_0$. For the gamma distribution at the additional parameter $\hat{a} = 7.82$ and with the normative probability 0.1% given in (Norms for Loads and Impact on Hydraulic Structures by Waves, Ice and Navigation, 1988) the average annual maximum diurnal rainfall $\overline{h}^{c.b.}_{N\max}$ is computed as $350.3\ mm\ m^{-2}$. In 1990 approximately the climatic changes were started to influence and they are increasing more and more all over the word. In the course of 2005 and 2007 years the rainfall in Bulgaria reached to 250 mm m^{-2} and many hydro technical structures were destroyed as a result of flood.

ALGORIHTM OF FLOOD, DRAINAGE AND PROTECTION OF DAMS

The flood and drainage flow are taken place during the period of upsurge. Details are given in (Nikolov, 2007). The transient process is described for a wide open bed in the rivers. For the solution of this unsteady motion the following equations are used:

$$i_{c.b.} - \frac{\partial h}{\partial s} = \frac{\partial}{\partial s}\left(\frac{v^2}{2g}\right) + \frac{\partial h_f}{\partial s} + \frac{1}{g}\frac{\partial v}{\partial t} \tag{5}$$

$$\frac{\partial h_f}{\partial s} = \frac{v^2}{C^2 R} \tag{6}$$

$$Q\,t = h_N\ F \tag{7}$$

where $i_{c.b.} - \frac{\partial h}{\partial s} = -\frac{\partial z}{\partial s}$ is the piezometric slope at the first section, $v^2(2g)^{-1}$ is the velocity height (m), h_f is the friction height (m), g is the gravity constant (m s^{-2}), C is the Manning formula, R is the hydraulic radius (m), Q is the water discharge (m^3 s^{-1}), t is the time (h), F is the mean area between two sections (m^2) and h_N is the average rainfall of the catchments (mm) for the time t.

On the bases of the recorded entry information the following data is necessary: the size of longitudinal and cross strips, the slope and the roughness of the terrain and the river, the maximum rainfall for 0.1% probability. After solving the above mentioned system, through the finite strips method, the unknown values are established: the minimum duration of the rainfall passing from the watershed to the river, the maximum water discharge and the shape of the high wave by balance modelling, the values of the maximum 24 hours rainfall and the intensity in mm min^{-1}. The shape of the high wave – upsurge, detention and subsiding is implemented by the balance formulas and empirical data equalizing the rainfall volume and the high wave volume:

$$\text{Upsurge: } Q = Q_0 \left(\frac{t}{t_0}\right)^{1-\left(\frac{t}{t_0}\right)^2} 2^{-\left[1-\left(\frac{t}{t_0}\right)^{\frac{1}{2}}\right]} \tag{8}$$

$$\text{Subsiding: } Q = Q_0\, 2^{-\left[1-\left(\frac{t}{t_0}\right)^2\right]} \tag{9}$$

where the upsurge time is $t = \sum \Delta t$ (h), $t = t_0 + \sum \Delta t$ is the time for subsiding (h) at the upsurge time t_0 corresponding to the initial rainfall flood and Q_0 is the water discharge with a probability of 0.1% (m^{3}s^{-1}). Two built Bulgarian dams are checked up by the new proposed method for the flood in the catchments and the drainage in the river. The both dams are designed in 1952 (Gravity) and in 1965 (Rock fill). They have relieving structures with relatively small discharges 800 m^3 s^{-1} and 500 m^3 s^{-1}. The results for the second dam are given below. The minimum duration for the maximum rainfall is: t_0=2.828 hours and $\bar{h}_{N\max}^{c.b.}$=350.3 mm. The maximum water discharge is given as $Q_{\max}^{0.1\%}$ =8285 m^3 s^{-1}.

The total maximum volume of the catchments basin is assumed to be $W_{N\max}^{c.b.} = 81.98 \times 10^6$ m^3. The overflow head is computed as H=2.75 m and the volume of the side channel spillway is $W_{sp.}$=2.19× 10^6 m^3. The resulting retention height is assumed as $h_{ret.}$=3.71 m and the velocity setup has a value of h'=1.89 m. The final result is given by the comparison between the retention height plus the velocity setup and the overflow head or the sum is: $h_{dest.}$ = 3.71+1.89-2.75=2.85 m.

Where $h_{dest.}$ is the potential risk for destruction (m). The above mentioned result shows the possibility of destruction if the rainfall is bigger than 250-300 mm m^{-2} and if the built dam is constructed before 20 years and more. Concerning the new plan dams an iterative solution has to be done in order to receive optimal numbers and sizes of the relieving structures as overflows, spillways and outlet devices.

CONCLUSIONS

Appropriate local hydrological information is discussed to model the flood rainfall-runoff process in the river on the bases of a new method called finite strips. This method is expected to assess the relieving structures, the reduced high wave with lower section and tributaries along the whole length of the river. By automation and depending on the rainfall intensity the bottom outlets are opening so that when the lake is partial empty the outlets start closing later on and finally the lake is again full. Finally an inverse modeling process closes the system and verify the credibility of this protection.

REFERENCES

Nikolov, N. & Chikalanov, A. (2007) By rainfall and software calculation of high waves generation of a catchments basin and their passing through dams. In: *Waterpower XV – Copyright HCI Publications, Paper N 015*.

Norms for Loads and Impact of Hydraulic Structures by Waves, Ice and Navigation (1988), Sofia (in Bulgarian).

Flood scenario simulation and disaster estimation of Ba-Ma Creek Watershed in Nantou County, Taiwan

SZU-HSIEN PENG[1], CHIH-CHUNG TSAI[2], SU-CHIN CHEN[3] & SHIH-YI FAN[4]

1 *Department of Spatial Design, Chienkuo Technology University, No. 1, Chieh-Sou N. Rd., Changhua City, Taiwan*
shpeng@cc.ctu.edu.tw

2 *Central Region Water Resources Office, Water Resources Agency, Ministry of Economic Affairs, Taiwan*

3 *Department of Soil and Water Conservation, National Chung-Hsing University, Taiwan*

4 *Department of water resources, Changhua County Government, Taiwan*

Abstract The present study proposed several scenario simulations of flood disaster based on the historical flood event and planning requirement in Ba-Ma Creek Watershed located in Nantou County, Taiwan. We employed a 2D numerical model (FLO-2D) which can compute the velocity and depth on the two dimensional actual terrain to simulate floods. Meanwhile, the calculated data are used to estimate the possible damage of flood disaster. The results can be also the reference for the disaster prevention. Besides, the flood disaster loss was estimated by these results of simulations. The estimation method is suggested by Water Resources Agency of Taiwan. Finally, the conclusions and perspectives are presented.

INTRODUCTION

In recent years many hazards caused by typhoons and heavy rainfalls in Taiwan have resulted in large damages or pecuniary loss. The function of local drainage in urban or rural regions usually plays an important role in the task of controlling floods. This is the reason the project called "Outline of Floods Controlling in Potential Flood Districts" is presently executing in Taiwan. The aim of the project is to improve the inundation phenomena from typhoons and torrential rainfalls in the regions near the minor streams or local drainage. In this study, we employed the FLO-2D model to carry out several scenario simulations of flood inundation. Based the computational results, the flood damages of various return periods were estimated and it can be the reference for the planning of flood controlling.

METHODS AND RESULTS

Site description

The main region of Ba-Ma Creek Watershed is in Shui-Li Township, Nantou County, Taiwan and its area is 709.1 ha. The lengths of main stream and two branches are 6.475 km, 1.11 km and 1.878 km long, respectively. A flood frequency of 10-year or 25-year was adopted as the criterion for the peak flow calculation to plan or design the capacity of channels. The design standard is presently considered as 10-year return period including the extra height 0.5 m over the bank, and it will not overflow the levees for a 25-year return period flood at the same time.

Many additional typhoon and storm events occurred during 1957 to 2006 here were used in the hydrological analysis. The peak flow discharges for various return periods at different hydrological stations were also calculated based on the 1-day storms using the rational method, triangle unit hydrograph method and instantaneous unit hydrograph, respectively (Chow *et al*., 1988). Finally, the peak flow discharges estimated by the triangle unit hydrograph method for 2 yr, 5 yr, 10 yr, 25 yr and 50 yr return period are suggested to be the planning discharges.

Numerical model

The hydraulic computations including 1D and 2D modeling were also carried out. In 1D simulation, we used the HEC-RAS model to compute the water level of the flood. The results can assist us to plan the locations and heights of levees and check the stream cross section area of existing structures such as bridges and culverts (US Army Corps of Engineers Hydrologic Engineering Center, 1995). The 2D simulations were also calculated by the FLO-2D model, a two-dimensional flood routing model used by engineers and floodplain managers to predict flood hazards, and the flood damages can be evaluated from the simulation results (O'Brien, 2003; O'Brien *et al*., 1993).

Scenario simulation

To compare the difference of simulation and real flood inundation, we used the rainfall data of Typhoon Toraji occurred in 2001 to compute the flood depths by using the FLO-2D model. Meanwhile, we also visited the locals to realize the flood range caused by Typhoon Toraji and surveyed the flood mark to describe the inundation regions which is approximately 39.2 ha. The maximum depth is around 3 m along the bank of main stream near the National Shui-Li Vocational High School of Industry and Commerce. In this scenario simulation, the numerical result also indicated the main flood area is about 19.2 ha and distributes along the main stream bank near the school of the maximum depth which is approximately about 4 m (see Fig. 1 & Table 1).

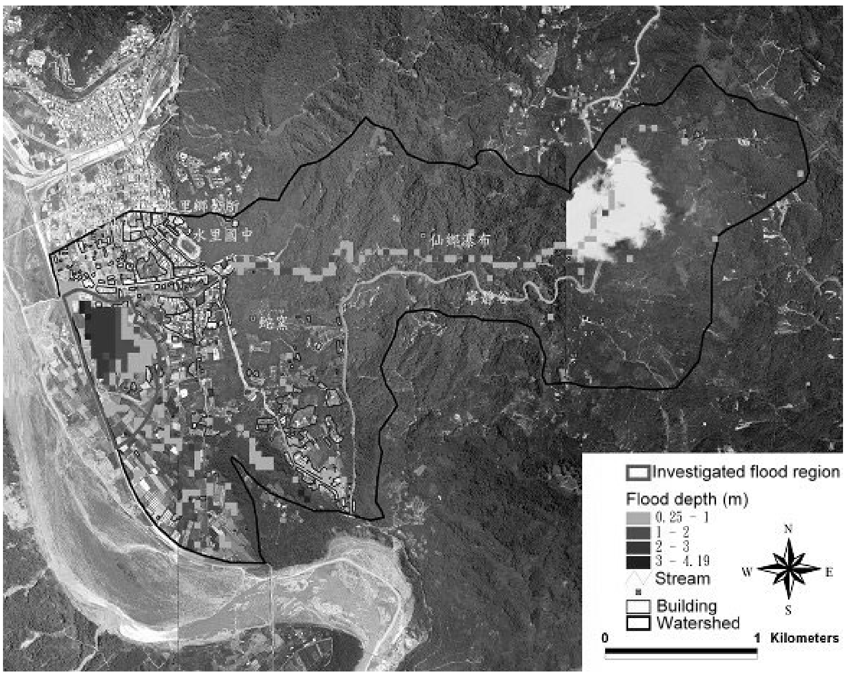

Fig. 1 Comparison of simulation and investigated flood regions.

Table 1 Areas and Depths of scenario simulation of Typhoon Toraji.

Average depth (m)	Maximum depth (m)	Flood area (ha)				Total flood area (ha)
		Depth 0.25~1 m	Depth 1~2 m	Depth 2~3 m	Depth >3 m	
1.092	4.19	31.04	8.8	6.72	0.96	47.52

Damage estimation

In addition to the scenario simulation of Typhoon Toraji, the other simulations of 2 yr, 5 yr, 10 yr, 25 yr and 50 yr return period were also completed, respectively. Based on these simulated flood areas and depths, we can estimate the flood damage. In the first step, the flood areas and depths for the various land use types were extracted from these simulated results by using the GIS software ArcView, and then we can estimate the different damage for farms, buildings and other land use at various depths (Table 2). From this analysis, the each degree of damage can be realized and employed to plan the engineering works of flood control or environmental construction while the designer decide how much he/she should invest in the planning.

Table 2 Flood damage estimations of return period of 2 yr, 5 yr, 10 yr, 25 yr and 50 yr.

Return period (yr)	Depth (m)	Farm land		Building land		Other land		Total damage (NT$ 1,000)
		Flood area (ha)	Damage (NT$ 1,000)	Flood area (ha)	Damage (NT$ 1,000)	Flood area (ha)	Damage (NT$ 1,000)	
2	0.25~1	8.09	469.2	1.35	3,375.0	4.89	283.6	8,599.4
	1~2	5.73	630.3	0.67	3,350.0	0.34	54.4	
	2~3	0.51	76.5	0.00	0.0	0.17	81.6	
	>3	0.17	34.0	0.00	0.0	0.17	244.8	
5	0.25~1	9.77	566.7	1.69	4,225.0	6.07	352.1	10,109.4
	1~2	7.92	871.2	0.67	3,350.0	0.51	81.6	
	2~3	1.35	202.5	0.00	0.0	0.17	81.6	
	>3	0.67	134.0	0.00	0.0	0.17	244.8	
10	0.25~1	11.63	674.5	1.52	3,800.0	6.57	381.1	10,985.9
	1~2	6.40	704.0	0.84	4,200.0	0.84	134.4	
	2~3	4.21	631.5	0.00	0.0	0.17	81.6	
	>3	0.67	134.0	0.00	0.0	0.17	244.8	
25	0.25~1	13.65	791.7	1.69	4,225.0	7.58	439.6	11,999.5
	1~2	5.22	574.2	0.84	4,200.0	0.84	134.4	
	2~3	6.74	1,011.0	0.00	0.0	0.00	0.0	
	>3	0.67	134.0	0.00	0.0	0.34	489.6	
50	0.25~1	14.49	840.4	1.69	4,225.0	7.58	439.6	12,233.6
	1~2	5.39	592.9	0.84	4,200.0	1.35	216.0	
	2~3	7.08	1,062.0	0.00	0.0	0.00	0.0	
	>3	0.84	168.0	0.00	0.0	0.34	489.6	

CONCLUSIONS

In this study, the simulations and damages of flood inundation for various return periods were proposed and estimated based on the method suggested by Water Resources Agency of Taiwan. From this damage analysis, the total cost for the construction and repair of the hydraulic structures is around NT$ 107,480,000 in the preliminary estimation. We expect the implementation of this planning will be helpful for the channel stabilization and the prevention of flood disaster. Furthermore, it is also supposed to be useful for the river restoration or planning of environmental construction if the engineering works are finished.

Acknowledgements This work was partly funded by Nantou County Government, Taiwan. The assistance of Mr. Jian-Da Wu, P.E. of Soil and Water Conservation at Jian-Lei Engineering Co., Ltd. is acknowledged.

REFERENCES

Chow, V. T., Maidment, D. R. & Mays, L. W. (1988) Applied hydrology, McGraw-Hill, Singapore.

O'Brien, J. S. (2003) FLO-2D users manual. *Nutrioso, FLO Engineering Inc. Publishing*.

O'Brien, J. S., Julien, P. Y. & Fullerton, W. T. (1993) Two-dimensional water flood and mudflow simulation. *J. Hydr. Engrg.*, ASCE **119**(2), 244-261.

US Army Corps of Engineers Hydrologic Engineering Center (1995) HEC-RAS river analysis system – hydraulic reference manual. *Davis, USACE Publishing*.

A quantitative precipitation forecast-based real-time operation of a multi-reservoir system for flood management

OLIVER CRISTIAN SAAVEDRA VALERIANO[1], TOSHIO KOIKE[1], KUN[2] YANG & DAWEN YANG[3]

1 *Department of Civil Engineering, University of Tokyo, Bunkyo-ku, Tokyo, 113-8656, Japan*
oliver@hydra.t.u-tokyo.ac.jp

2 *Institute of Tibetan Plateau Research, Chinese Academy of Sciences, Beijing 100085, China*

3 *Department of Hydraulic Engineering, Tsinghua University, Beijing 100084,China*

Abstract To capture the spatial variability of the quantitative precipitation forecast, a distributed hydrological model with an embedded dam network operation was coupled to a heuristic model. The system attempts to control floods downstream taking advantage of the quantitative precipitation forecast. The proposed scheme evaluates different release combination sets automatically based on stochastic seeding considering the dam constraints and the objective function. The error forecast is also introduced into the iteration as a weight to the release of each dam. The developed system was applied to the upper Tone River in Japan using three multipurpose reservoirs. The efficiency of the system's response was evident in reducing the flood peaks and volume downstream comparing the optimized releases against observed release. This approach has shown the feasibility to support dam operators as a real-time reference tool for flood management.

Keywords Tone River; real-time operation; flood management; distributed hydrological model; quantitative precipitation forecast

INTRODUCTION

In South-east Asia region, dam operation during tropical cyclones is crucial to reduce flood peaks down stream and maximize the water level at the reservoirs for different future demands. Ngo *et al*. (2007) reported successful coupling of MIKE 11 and Shuffled Complex Evolution (SCE) by optimizing historical operation rule curves of Hoa Binh dam, Vietnam. However, it was not include forecast data in real-time operation. Hsu & Wei (2007) reported an optimization of the reservoir operation scheme for flood control affected by typhoons in Taiwan. The spatial distribution of rainfall forecast and the error forecast should be also considered. This study attempts to take advantage of quantitative precipitation forecast in real-time dam operation using a coupled physically based distributed hydrological model to an optimization algorithm.

This study employs a physically-based hydrological model, namely Geo-morphological Based Hydrological Model (GBHM) introduced by Yang *et al*. (2002). It is a physically-based hydrological model that simulates hydrological processes using governing equations relying in two modules. First, a hillslope module simulates hydrological processes such as canopy, interception, evapo-transpiration, infiltration, surface flow, and subsurface flow, as well as exchanges between groundwater and surface water. Second, the River network routes water using the kinematic wave approach. This simulation sequence is performed at each sub-basin and linked by the Pfafstetter scheme. Moreover, every sub-basin is divided into a number of flow intervals by considering the flow distance to its outlet. On the other hand, Duan *et al*. (1992) developed a globally based minimization method, namely the Shuffled

Complex Evolution (SCE). Then, the SCE drives the GBHM seeding different combination of dam release until the objective function is fulfilled as seen in Fig. 1.

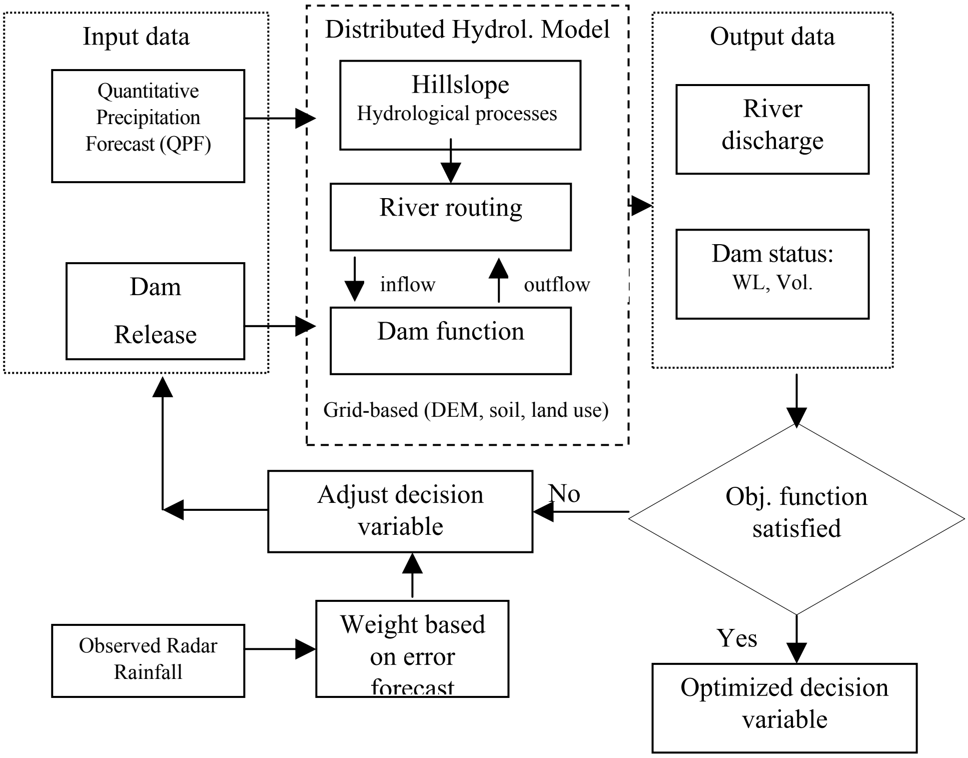

Fig. 1 Overview of proposed system for dam operation using QPF.

This system is expected to release an amount less than or equal to the predicted potential flood volume at the protecting point. So, the flood waters can be stored at the reservoirs. Therefore, the objective function is set at the control point to minimize the Root Mean Square Error (RMSE) between the simulated and a desirable discharge. This is defined as the average of the observed values exceeding the mean annual discharge. It can also be understood as a desirable stream flow expressing Water Resource Management (WRM) and dam purposes for the flood season. Actually, the system is activated when the simulated discharge surpasses the desirable without dam effect. The decisions variables are to release a ratio of the total forecasted flood volume. The weight for each dam is proposed to be a function of the standard deviation obtained from the error forecast averaged over the contributing area to each dam. The error forecast is defined as the difference between a forecast and the actual observed value when it becomes available. In this study the standard deviation was selected to express how spread the error forecast is within the optimization horizon as seen in equation (1):

$$weight_{dam} = 1^{+}_{-} \frac{\sigma_{error\_forecast}}{10} \tag{1}$$

In this fashion, it is expected that lower values of standard deviation (more accurate forecasts) affect the release less and vice versa. Moreover, the over and underestimation of forecast, taken from the average bias, will decide a decrease or increase respectively. In case, a perfect forecast is issue the weight will be one.

Generally, it is expected that the weight reflects the accuracy of last time step's QPF and attempts to compensate at current iteration.

APPLICATION

Tone River basin is a very important water supply and source of power generation for the Tokyo area, and therefore its management is crucial in the region. Yang *et al.* (2004) and Saavedra *et al.* (2006) simulated independently dam release of two sub-basins of upper Tone River using interpretation of observed weather radar products. The present application, besides integrating both areas, focuses on real-time operation using quantitative precipitation forecast in order to forecast optimal dam release schedules.

The Meso-Scale Model (MSM) weather forecast provides, among other weather variables, a quantitative precipitation, namely a Grid Point Value (GPV), at 0.125º spatial resolution issued every 6 hours with hourly records in 18 h lead-time. The data set covers all Japan and it is archived from 1 July 2002. The MSM-GPV data is produced by the Japan Meteorological Agency (JMA) and it is archived at the University of Tokyo' site: http://gpv.tkl.iis.u-tokyo.ac.jp/GPV/. As a reference the latter site also archives global forecast at 1.25º resolution with 24 h lead time issued every 12 hours.

RESULTS

The hydrological model runs at 1-h time step while the optimization horizon is 18-h to match the lead-time forecast. The initial condition of runoff, soil moisture and groundwater is specified over 6 hours using available observed radar products. Three dams arranged in parallel namely Aimata, Sonohara and Fujiwara were selected to control floods at Iwamoto gauge. An example of the system' response is shown in Fig. 2. The left side shows flood peak reduction at the protecting point. The early release from Sonohara dam is evident to increase the flood control capacities as seen at the right side of Fig. 2. During the flood peak, after 13:00, the gates are closed to fulfil the requirement of the objective function.

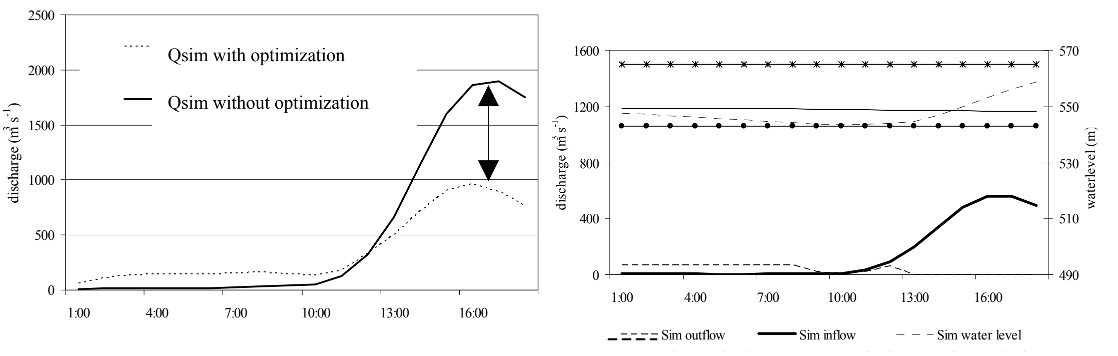

Fig. 2 Flood reduction using 18-h GPV issued at 00:00 on 10 of July 2002 at Iwamoto gauge (left) and Sonohara dam's status (right).

This kind of flushing is typical during typhoon season as a preparedness measure for the following flood event. The objective function using QPF also encourages storing water at reservoirs for future usage by 1) setting the upper boundary of the decision variables to the total flood volume forecasted downstream and 2) the total release can not to exceed the total inflow forecast within the optimization horizon. At the end of each simulation period, the water levels of dams were almost replenished or higher than their initial levels as at the right side of Fig. 2. Accounting the total volume stored at three reservoirs, the present system showed a surplus by comparing to the volume stored using the observed release. This is a clear advantage of choosing the flood volume as a magnitude to solve the allocation problem rather than the flood peak alone.

The standard deviation of the error forecast and the weight introduced in the iteration are summarized in Table 1. The evaluation of different weights for each dam was carried out to highlight the importance to use a distributed hydrological to show the pattern of the QPF. In this application the weight affected conservatively; however, this value can be adjusted according to the accuracy of QPF and scale of the basins to each dam.

Table 1 Summary of optimal release calculation using 18-h GPV issued at 00:00 on 10 of July 2002.

Dam name	Standard deviation	Error forecast Weight	Optimized variable	Flood volume (millions m^3)	optimized release (m3 s^{-1})
Fujiwara	0.0607	1.006	0.0026	4.9733	0.3011
Aimata	0.1117	1.011	0.8197	3.7750	72.4233
Sonohara	0.4156	1.042	0.3075	8.6847	64.4200

The system has shown feasibility to be used by dam operators as a real-time reference tool. The updated initial condition every 6 hours for each 18 hour lead-time forecast can be achieved taking advantage of real-time observed data transmitted through advanced digital network technologies. Moreover, the computation time of less than 6 hours is acceptable for three dams using only one Pentium III 2.3 GHz processor. This type of real-time operation is needed in humid mountain and highly vegetated basins, like in Japan, Taiwan, and Vietnam attacked by typhoons.

REFERENCES

Duan, Q., Sorooshian, S. & Gupta, V. K. (1992) Effective and Efficient Global Optimization for Conceptual Rainfall-Runoff Models. *Wat. Resour. Res*. **28**(4), 1015-1031.

Hsu, N. S. & Wei, C. C. (2007) A multipurpose reservoir real-time operation model for flood control during typhoon invasion. *J. Hydrol.* **336**, 282-293.

Ngo, L. L., Madsen, H. & Rosbjerg, D. (2007) Simulation and optimisation modelling approach for operation of the Hoa Binh reservoir, Vietnam. *J. Hydrol.* **336**, 269-281.

Saavedra, O., Koike, T. & Yang, D. (2006) Application of a distributed hydrological model coupled with dam operation for flood control purposes. *Annual J. Hydraul. Engng*., Japan Society of Civil Engineers JSCE **50**, 61-66.

Yang, D., Herath, S. & Musiake, K. (2002) Hillslope-based hydrological model using catchment area and width functions, *Hydrol. Sci. J.* **47**, 49-65.

Yang, D., Koike, T., & Tanizawa, H. (2004) Application of a distributed hydrological model and weather radar observations for flood management. *Hydrol. Processes*, **18**, 3119-3132.

Ensemble forecasts and Bayesian averaging to consider uncertainties in flood risk management

A. SCHUMANN, J. DIETRICH & Y. WANG
Ruhr-University Bochum, Institute of Hydrology, D-44780 Bochum, Germany
andreas.schumann@rub.de

Abstract Hydrological models are widely accepted tools to predict the spatial and temporal characteristics of floods, resulting from known or assumed meteorological conditions. In many cases future meteorological developments can be forecasted by deterministic models only with high uncertainties. The nonlinearities of hydrological processes, scale problems and an insufficient physical base of hydrological models result in additional uncertainties of flood forecasts. Ensemble forecasts can be used to consider these uncertainties in operational flood management. Here different meteorological ensemble forecasts (physical ensembles, lagged average ensembles and multi-model ensembles) are combined with parameter ensembles of a hydrological model. To provide a single "best guess" forecast, Bayesian inference was used to assimilate data for updated probabilistic assessments of ensemble members and a weighted averaging of them.
Keywords flood forecasts; ensembles; hydrological modelling; Bayesian statistics

INTRODUCTION

Ensembles are tools to communicate uncertainties. Nevertheless a description of uncertainties is not sufficient for operational purposes. Often an assessment of a "most probable" development in future is needed. Probabilistic assessments can be used to provide such information. Measured data can be assimilated to update these probabilities. Today meteorological models for short- and medium-range weather forecasts use data assimilation procedures operationally. As result the uncertainties of meteorological forecasts change within the lead time.

Several ensemble predictions systems exist which differ in their spatial and temporal resolution and in their lead time. To provide a holistic view of future developments they should be used in combination. With regard to flood management, meteorological forecasts have to be transferred into flood forecasts. This can be done with hydrological models. The resulting forecasts depend not only on the uncertainties of input data but also on model and parameter uncertainties. Multi-model ensembles or parameter ensembles can be used to specify them.

METEOROLOGICAL ENSEMBLES

Ensembles can be generated in three different ways:

- As physical ensembles where model parameters, initial or boundary conditions are perturbed. In meteorological models often modifications of precipitation formations by different convection schemes are used.
- Multiple forecasting systems are applied for the same time period and the same data.
- Lagged average ensembles combine forecasts at different time steps with overlapping lead times.

Different meteorological ensemble prediction systems (EPS) are available operationally. For the medium-range (lead times from 3 to 5 days) COSMO-LEPS is provided. It is based on a dynamic downscaling of the global EPS operated by the ECMWF (European Centre for Medium-Range Weather Forecasting) (Molteni *et al.,* 2001). The forecasts are updated once per day. For short-range forecasts the SRNWP-PEPS system can be used. It combines up to 23 deterministic forecasts from 21 national weather services (Denhard & Trepte, 2006). This system has a lead time of 2 d. The forecasts are updated twice per day. The COSMO-DE model provides quantitative precipitation forecasts with a high horizontal resolution (2.8 km). The lead time is 18 hours; the forecasts are updated every 3 hours (Steppeler *et al.,* 2003). Thus the forecasts form a lagged average ensemble.

HYDROLOGICAL FORECASTS

The conceptual hydrological model ArcEGMO (Becker *et al*., 2002) was used to transfer meteorological forecasts into flood forecasts. It was applied in two different ways (Fig. 1). As the uncertainties of medium-range forecasts for a lead time of 3 to 5 days are high, the runoff was simulated with a default parameter set of the model. Compared with the large spread of the meteorological ensemble predictions, the uncertainties of hydrological modelling are low. With reduced lead times the uncertainties of meteorological forecasts becomes smaller, but the hydrological uncertainties become more important. For ensemble forecasts with the SRNWP-PEPS and COSMO-DE systems, parameter ensembles of the hydrological model were used. Here measured data can be used to update the probabilistic assessments of the different ensemble members.

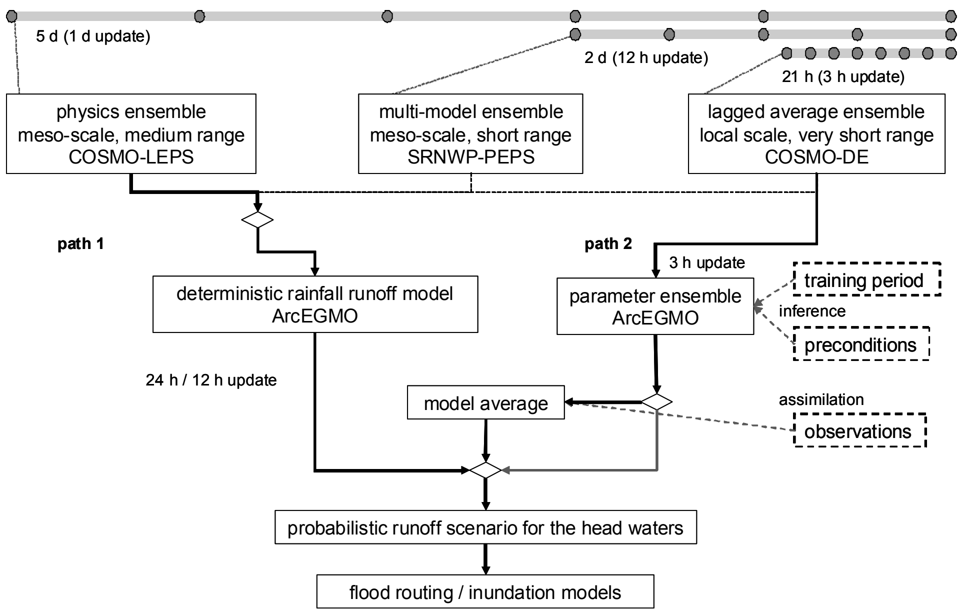

Fig. 1: Flood forecast scheme for combination of meteorological hydrological ensemble forecasts.

It is difficult to differentiate between the uncertainties of the measured input data (here point measurements of precipitation were available only) and the uncertainties of the hydrological model. An overcompensation of the different uncertainties by modifications of model parameters has to be avoided. With regard to the meteorological forecasts the dependencies of the total uncertainties from the weather situation has to considered: in headwaters convective storms may result in higher uncertainties of flood forecasts as spatial extension, location and precipitation intensities are more uncertain than for other weather situations. To reduce this problem the members of the parameter ensembles were evaluate with a Bayesian approach which was based on a pre-selection of parameter sets according to the type of the meteorological event. For this purpose the flood events used for calibration were classified in three groups. For each group different parameter ensembles were provided. As the number of historic events was not sufficient to cover all possible meteorological situations, the measured precipitation data were integrated into the weighting of the four parameter sets (three groups plus default parameters) in model averaging.

RESULTS

Meteorological ensembles were available for the study region, the Mulde river basin in the Ore Mountains in Germany, since 2005 only. The German Weather Service, which was a partner in this research project, provided hindcasts with Cosmo-LEPS and COSMO-DE for the large flood in 2002. Both ensembles forecasts were driven by ECMWF-model runs originated from the time of this flood event. As it is shown in Figure 2 for an example, the COSMO-LEPS ensembles of August 10th, transferred into discharge values with the hydrological model, gave a good forecast of the disastrous flood of 2002 more than two days before the flood peak happened (Dietrich *et al.*, 2008). Unfortunately this excellent result has to be seen more critical as several false alarms became evident when the COSMO-LEPS forecasts were used in a near operational mode for 2005 and 2006.

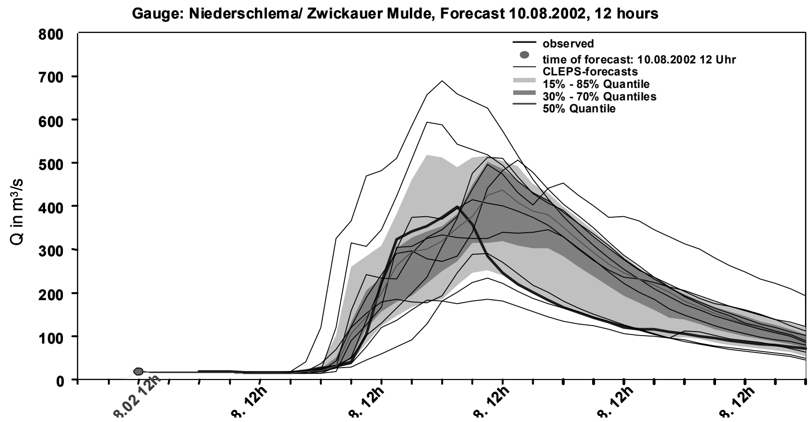

Fig. 2 Discharge forecasts before the disastrous 2002 flood for the catchment of the Zwickauer Mulde at gauge Niederschlema. The COSMO-LEPS hindcasts were initialized at 10/08/2002 at 12:00 UTC and processed by the hydrological model ArcEGMO.

As mentioned above COSMO-DE provides a lagged average forecast ensemble. Here the hydrograph were simulated with measured and forecasted rainfall data. The forecasts can be updated more often and measured discharge and precipitation data can be used for Bayesian inference among hydrological parameter sets. To avoid an overcompensation of meteorological forecast errors, this weighting of parameter ensembles was based on measured data only.

The different sets for the parameter ensemble were estimated with Monte-Carlo-Simulations. Several goodness-of-fit criteria were used. For each event type 5 parameter sets were selected with Compromise Programming. At the beginning of each flood event 20 parallel simulations were used to form an ensemble. The results were combined with weighted averaging. The weighting was modified in a stepwise procedure: among the event groups with measured precipitation data, within the event groups based on a comparison between measured and forecasted discharges. With a Bayesian inference procedure (Box & Tiao, 1992) the number of hydrological scenarios could be reduced if the type of the event becomes evident. An example for the development of the weighting between event types during an event is shown in Fig. 3.

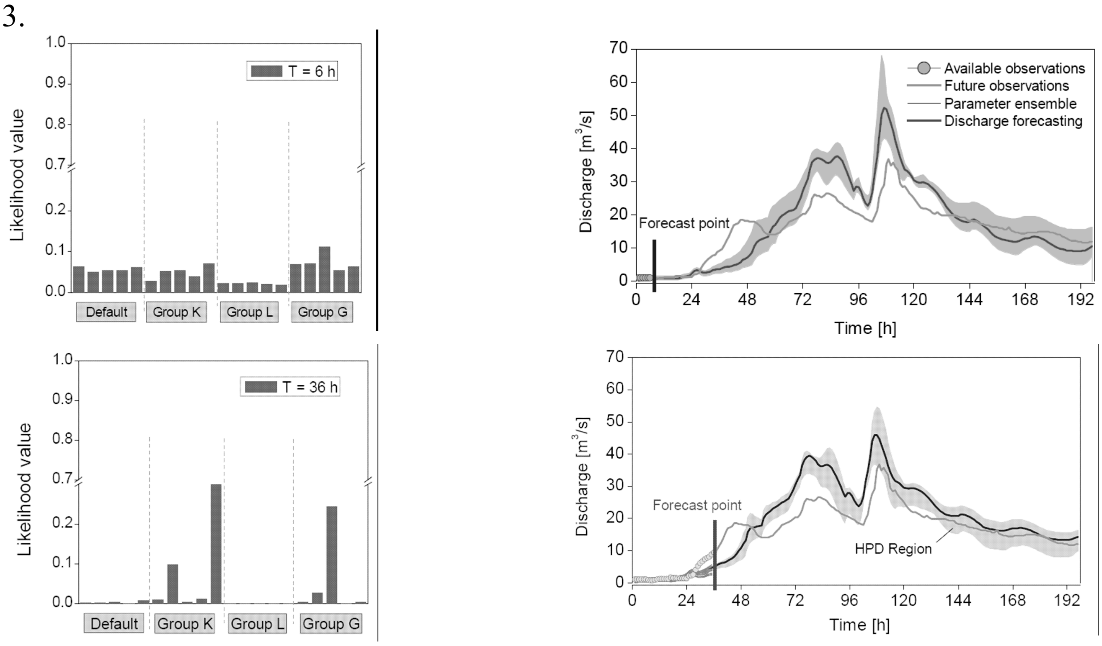

Fig 3. Example for the changes of Likelihood values between event types, used for weighting in model averaging during a flood.

CONCLUSIONS

Ensemble forecasts specify uncertainties. Users are interested in single "most probable" forecast. Tools are needed (e.g. Bayesian averaging of the ensemble members) to provide this information. Data assimilation procedures are helpful for a probabilistic assessment of the different ensemble members. In future the relationships between event types and forecast uncertainties should be considered in greater detail.

REFERENCES

Becker, A.., Klöcking, B., Lahmer, W. & Pfützner, B. (2002) The hydrological modelling system ARC/EGMO, in: Mathematical models of large watershed hydrology (Eds.: V. P. Singh & D.K. Frevert), *Water Resources Publications, Littleton/Colorado.*

Box, G. E. P. & Tiao G. C. (1992) Bayesian inference in statistical analysis. *A Wiley- Interscience Publication*, 176-202.

Denhard, M. & Trepte, S. (2006) Calibration of the European multi-model ensemble SRNWP-PEPS. Second THORPEX international science symposium, WMO/TD No. 1355, WWRP/THORPEX No. 7.

Dietrich, J., Trepte, S., Wang, Y., Schumann, A. H., Voß, F., Hesser, F. B. & Denhard, M. (2008) Combination of different types of ensembles for the adaptive simulation of probabilistic flood forecasts: hindcasts for the Mulde 2002 extreme event. *Nonlin. Processes Geophys*. **15**, 275-286.

Molteni, F., Buizza, R., Marsigli, C., Montani, A., Nerozzi, F. & Paccagnella, T. (2001) A strategy for high-resolution ensemble prediction, part I: definition of representative members and global model experiments. *Quart. J. Roy. Meteor. Soc.* **127**, 2069-2094.

Steppeler, J., Doms, G., Schättler, U., Bitzer, H. W., Gassmann, A., Damrath, U. & Gregoric, G. (2003) Meso-gamma scale forecasts using the nonhydrostatic model LM. *Meteorol. Atmos. Phys*. **82**, 75-96.

Approaches to credible identification of reliable parameters in rainfall - runoff model from long time series

J. BUCHTELE & R. KOŠKOVÁ

Institute of Hydrodynamics, Pod Paťankou 30/5, 166 12 Prague 6 Dejvice, Czech Republic

koskova@ih.cas.cz

Abstract Variability of water regime in the basin is influenced by development of vegetation cover in the annual cycle, but also by its changes in the span of decades. The simulations of rainfall-runoff process have been used with the intention to follow the possible role of this land use The differences between observed and simulated flows in the period 1895 - 2000 can be considered as useful tool for the assessment of changes

Keywords land use; rainfall - runoff simulation; vegetation change

INTRODUCTION

Usually it is assumed that for reliable calibration of rainfall-runoff model the time series 5 -10 years are desirable, in which significant floods and lowflow periods occurred. Simultaneously it is expected that this should be period without important artificial changes in the basin.

Natural, i.e. mostly climatic, oscillations and antropogenic changes induce different tendencies and fluctuations in river flows and in soil- and groundwater storage. The explanations are desirable for implementation of models used for water regime simulations. Natural variability of water regime in a basin is usually influenced by development of vegetation cover in the annual cycle, but climatic conditions create also the conditions for development of this cover in the scale of years. This could cause variation changing and/or tendencies in evapotranspiration demands and consequently of water regime changes. That is significant for reliable identification of parameters of rainfall - runoff process and consequently for successful prediction of future development of water resources.

USED DATA AND TOOLS

For some simulation of rainfall-runoff process the input data file relatively long have been available:

- for the Czech Labe River a bit longer than 100 years, with most results (Fig. 1)
- for two experimental basins in Beskydy Mts. approx. 50 years

That are series, in which it has been expected that some tendencies in runoff course could appear and some uncertainties with parameters identification then might exist.

These expectations are supported by the development of vegetation cover in the Labe River basin during the past century presented in Fig. 2, while the areas were relatively stable. Moreover, suspicion of higher variability of evapotranspiration demands could be supported by some recent explanations concerning variability of solar radiation, (Beer, 2005). The calibration of the conceptual model SAC-SMA, (Burnash, 1995) has been carried out for both basins and for the mentioned experimental basins also the BROOK model, prepared in U.S. Forest Service, has been used. The models provide similar course of differences between observed and simulated flows.

In the calibrations procedure two alternatives of starting file length have been applied, i.e. firstly identification of parameters based on the whole period of observation, secondly from initial period approx.10 years long and subsequently for several other 10 years long intervals. This has been motivated by the intention to identify the occurring changes of runoff. Values of parameters are mostly stable, but evapotraspiration demands are not well-balanced for distinct periods.

In the Labe River basin it corresponds probably with vegetation development, Fig.1. In this basin is the problem complex, namely in the period years 1955 - 70. Considerable volumes of water were needed for the filling of built water reservoirs. This is visible in the lower part of Fig. 1 in the deviations between observed and simulated flows, what means the ´losses´ in observed flows.

Fig. 3 presents temporary increased runoff in the forested experimental basin located in Beskydy Mts. as the consequence of relatively extensive cutting and reforestation at some parts of basin.

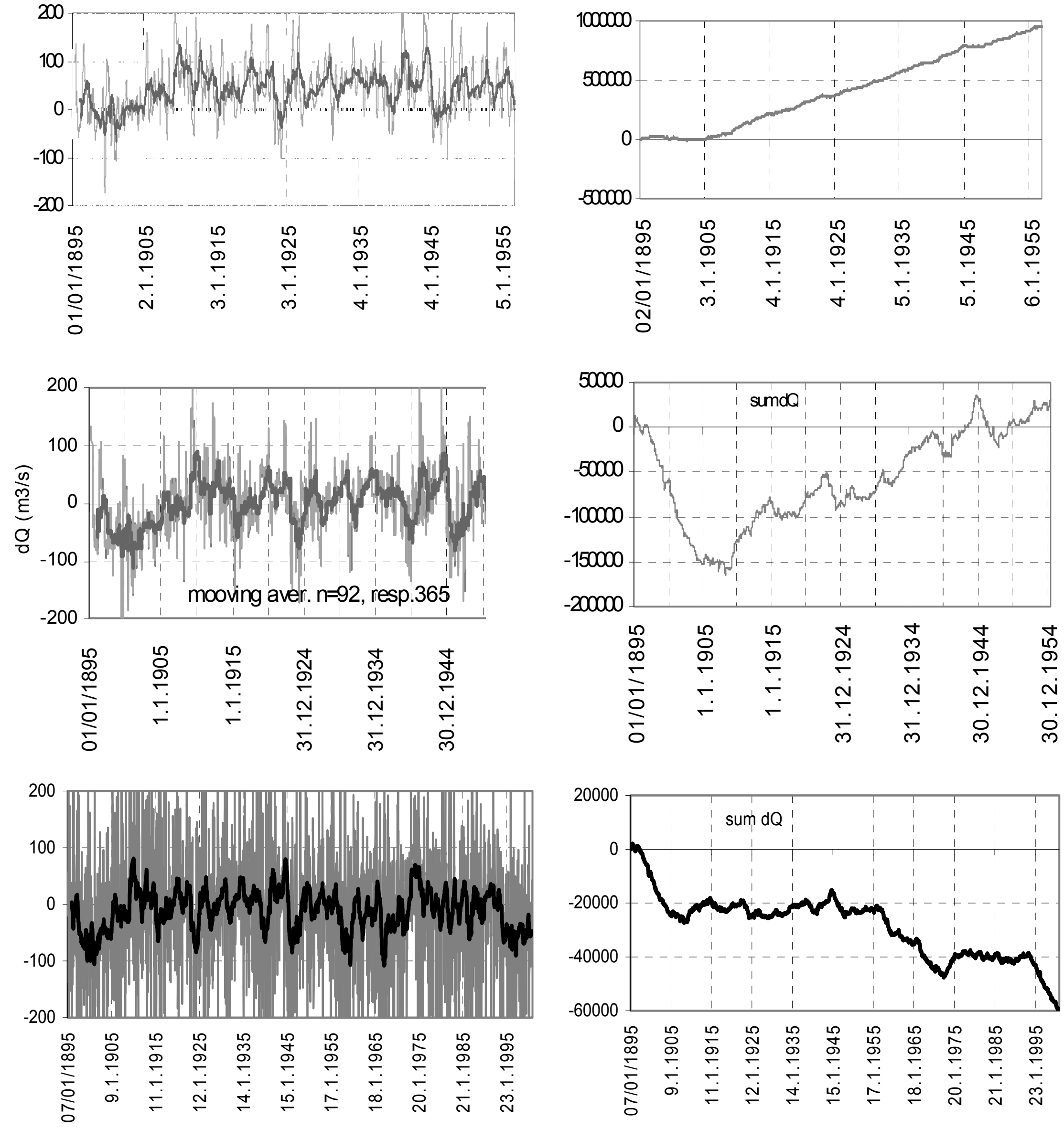

Fig. 1 Differences dQ = Qobs - Qsim and sum dQ obtained using for calibration of rainfall-runoff model the periods: years 1895 - 1905 (upper part), 1895 - 1954 (central part) and 1915 - 1954 (lower part).

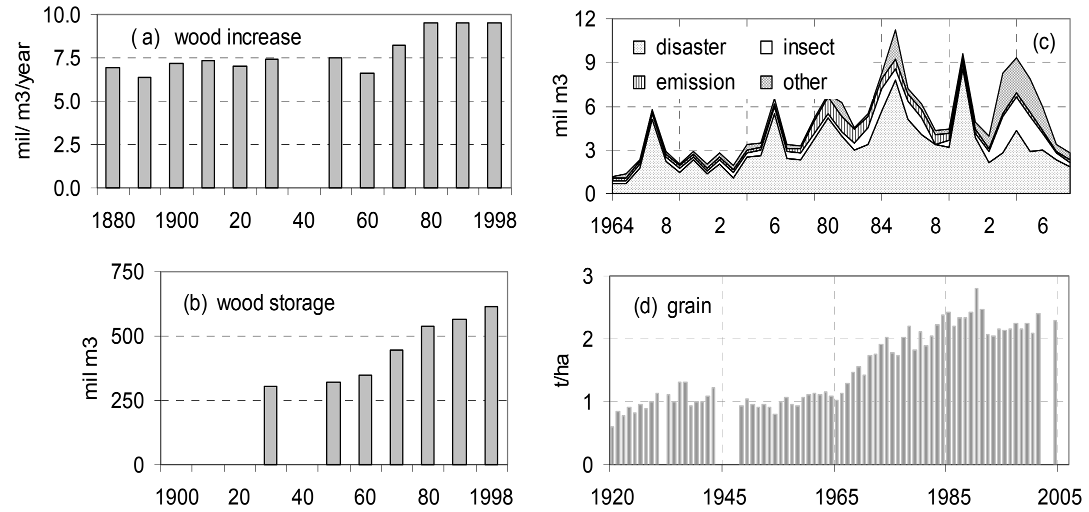

Fig. 2 Variability of forest cover, its disasters and grain production tendency in the country.

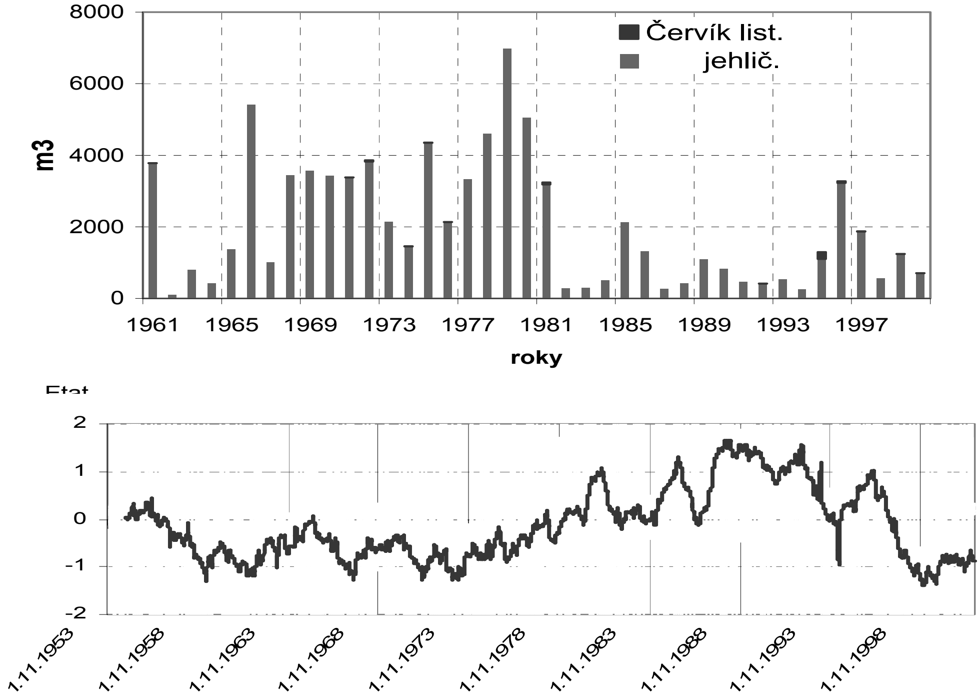

Fig. 3 Volumes of wood cutting and differences of discharge dQ = Qobs – Qsim smoothed with m= 365 days .

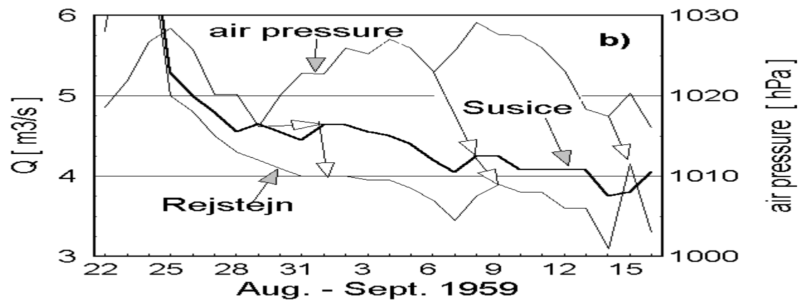

Fig. 4 Interrupted recession process of discharge in rainless period.

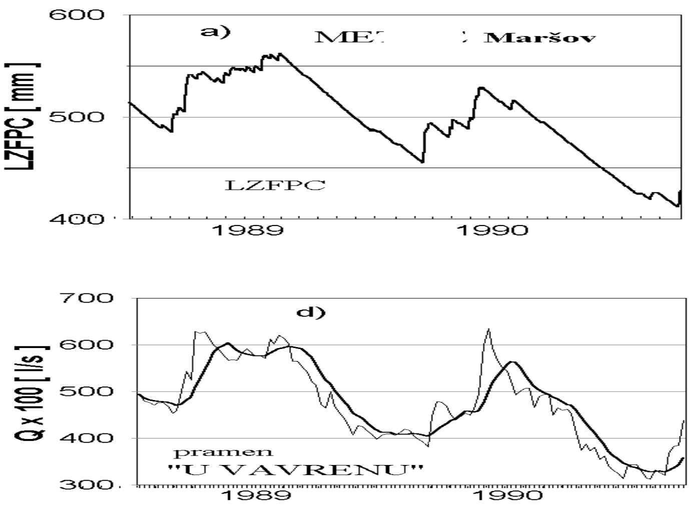

Fig. 5 Simulated groundwater storage and observed bore holes and spring.

FURTHER CHANGES IN WATER REGIME

For Labe River basin the years 1895 - 1910 expressive in Fig. 1 is the period of building the system of weirs at the Elbe River and Vltava River for the ship transport. Moreover, it is the time of newly growing forests at large areas in the upper part of the Vltava River basin after great disasters between years 1865 and 1875.

After the year 1989 the decrease of differences dQ can be influenced by the converting the parts of arable fields again into meadows and by newly reforestation of forest areas damaged by acid rains.

For the identification of model parameters could be meaningful other circumstances:

Rainless long periods provide the data which show some runoff increase can appear due to decreased air pressure as the consequence of dominating baseflow, Fig. 4. This phenomenon appeared in the Otava River which is sub-basin of the Labe River.

Useful for assessment of groundwater storage variability the outputs of rainfall-runoff modelling in Metuje River have been, Fig. 5. The spring outflow and the bore holes water level could be sometimes compared with simulated content of water in LZFPC (Lower Zone Free Primary Content) of the SAC-SMA model. The larger differences could be due to role of preferential routes, which probably contribute to content in LZFSC (Lower Zone Supplemental Content). This could be assumed taking into account the course of runoff components

Acknowledgements This research has been supported by EU Integrated Project NeWater - Contract No.511179.

REFERENCES

Burnash, R. J. C. (1995) The NWS River Forecast System - Catchment modelling. *In*: Singh,V.P. (ed.) *Computer Models of Watershed Hydrology*. Water Resources Publications, ISBN No. 0-918334-91-8.

Beer, J. (2005¨) Solar variability and climate change. *Global Change NewsLetter* **63**, 2005

Application of streamflow forecasting models in the Brazilian electric system operation planning

F. S. COSTA[1,2], M. E. P. MACEIRA[1,2] & J. M. DAMÁZIO[1,2]

1 *Electric Power Research Center – CEPEL, Av. Horácio Macedo, Cidade Universitárioa, Ilha do Fundão, P.O.Box 68007-Zip Code 21944-970, Rio de Janeiro, RJ, Brazil.*
fernanda@cepel.br

2 *Rio de Janeiro State University – UERJ, Statistics Department, Rio de Janeiro, Brazil.*

Abstract The paper presents three streamflow forecast models, PREVIVAZM, PREVIVAZ and PREVIVAZH, that belongs to the chain of models used in the operation planning of the Brazilian interconnect hydrothermal system, providing respectively monthly, weekly and daily forecasts and discusses its insertions in the system operation chain of models, model formulations, parameter estimations and model validation procedures.
Keywords streamflow forecast; national interconnected system; operation planning numerical simulation; stochastic

INTRODUCTION

Differently from the majority of other countries, in Brazil hydropower is the main primary energy source for electric energy generation, more than 80% of the electricity is hydro generated. One the drawbacks of hydro-based electric generation system are the time fluctuations of natural streamflows. In order to provide protection against streamflow fluctuations, the Brazilian electric energy generation system counts with complementary thermal plants, which operation implicates in fuel expenses, and with a set of accumulation reservoirs, which large available retention capacity permits seasonal and multi-year streamflow regulation, protecting the system against the occurrence of sequences of dry years.

The coordination of the operation of the reservoirs together with the operation of the complementary thermal plants permits the best use of the natural streamflow, avoiding waste of water and excessive fuel expenditures. This coordination is done in the framework of the Interconnected System Operation Planning Studies performed at the Brazilian Electrical System National Operator – ONS. In general, the quality of the streamflow forecasts affects the performance of the generation system, increasing benefits and reliability, and reducing operating costs. Potentially, the Brazilian electric energy generation system can largely benefit from continuing improvement of hydrological forecast models.

Due to its complexity, the operation planning of the Brazilian interconnect hydrothermal system is done by steps using a chain of models (Maceira *et al.*, 2002), with different planning horizons, time discretizations, and levels of detail in system representation, in particular with respect to the uncertainty about the future inflows. Table 1 presents the main energetic and hydrological modelling characteristics in the chain of models. At the hierarchy top, the medium term operation planning model (NEWAVE) builds the operation policy to be used at the beginning of each month to decide the shares of the next month total energy demand which will be supplied by the thermal plants and by each sub-set of hydro-plants grouped in sub-regions. At this step, the hydrological uncertainty is considered using a set of synthetic generated sequences of natural energy inflows to each sub-region for the next five years. These sequences are generated by the GEVAZP model (Maceira & Mercio, 1997) using a linear autoregressive approach, taking as initial conditions the energy inflows occurred in the last at most eleven months. The actually used number of lagged occurred inflows varies with the month and sub-region.

In the short term planning, the hydro and thermal generation portions defined by the medium term operation policy for the first month ahead are disaggregated in weekly targets for each plant of the system using DECOMP model. The hydrological modelling is mixed, in part deterministic, in part stochastic. For each week of the first month, the natural streamflows are considered known, using the forecasts obtained with the models PREVIVAZ (Maceira *et al.*, 1994). For the other months in the planning horizon, it is considered a set of synthetically streamflow sequences generated by GEVAZP. At present, the adopted planning horizon is just two months. In the daily programming (DESSEM model), the hydrology is considered deterministically, using the daily streamflow forecasts for the planning horizon (7 to 13 days).

Table 1 Modelling Characteristics.

Step	Medium term	Short term	Daily Programming
Hydrological Model	GEVAZP	PREVIVAZ / GEVAZP	PREVIVAZH
Optimization Model	NEWAVE	DECOMP	DESSEM
Planning Horizon	10 years at most	1 year at most	14 days at most
Time Discretization	Monthly	Weekly/ Monthly	hourly / levels
Streamflow modelling	Stochastic	Deterministic/Stochastic	Deterministic

PREVIVAZ AND PREVIVAZM MODELS

The PREVIVAZM model (Costa *et al.*, 2003) provides monthly streamflow forecast for the Brazilian hydroelectric system hydro-plants until 12 months ahead. The PREVIVAZM is a toll for special studies that aim to verify the energy demand supply conditions in the annual horizon. On the other hand, the PREVIVAZ model provides the weekly streamflow forecasts until six weeks ahead that are used in the first month of the short term planning (Monthly Operation Program (PMO) and its weekly revisions). So, this model is used at the end of each month for the PMO, and every week for its revisions.

The two models adopt the common approach of obtaining streamflow forecasts from time series modelling expected values. This forecast approach takes advantage of the seasonal pattern of the precipitation and of the important hydrological phenomenon known as hydrological persistency. In the time series terminology, the hydrological persistency is known as time dependency structure, being quantified by the autocorrelation function estimated from the streamflow historical data. Essentially, any type of seasonal time dependency structure can be reproduced by using a linear time series model in the PARMA(p,q) family. This family of models is a very flexible modelling approach, and is very popular in the streamflow stochastic modelling (Hipel & McLeod, 1994). The models, in order to obtain respectively weekly and monthly streamflow forecasts, use models in the PARMA(p,q) family, considering different pre-transformation of the historical data (Box-Cox (Box & Cox, 1964)) and different model parameter estimation procedures. So the forecasting algorithms are defined by the combination of the model, the estimation method and the pre-transformation of the historical data. The split sample approach is used to choose the algorithm with minimum mean squared forecast error. The PREVIVAZ and PREVIVAZM models adopt for each week and month respectively, the algorithms which present the minimum mean squared forecast error. Table 2 presents the mean absolute percentage errors for weekly inflow forecasting one to six weeks ahead for three hydro plants located in the Brazil South region, Foz do Areia, Salto Osório and Itaipu, in the period 1992-2001.

Table 2 Mean absolute percentage forecast errors for weekly inflow forecasting (1992-2001).

Hydro plant	Week 1	Week 2	Week 3	Week 4	Week 5	Week 6
Foz do Areia	35,9 %	48,9 %	56,2 %	60,8 %	63,0 %	63,3 %
Salto Osório	33,9%	45,9%	52,0%	56,9%	59,3%	60,6%
Itaipu	26,2%	32,9%	33,2%	34,4%	34,5%	35,1%

PREVIVAZH MODEL

The PREVIVAZH model (Costa *et al.*, 2000) adopts both physical conceptions and non-parametric statistical approach to formulate a daily streamflow time series from which a synthetic sequence set is generated. The sequence of daily streamflow forecasts is obtained by choosing the sequence in the generated set that best agree with the PREVIVAZ week streamflow forecast. The daily streamflow sequences are generated by DIANA model (Kelman *et al.*, 1983) modified to consider the last two observed daily streamflow. In DIANA model, the daily streamflow, Q(t), is modelled as a sum of two parcel, one, U(t), represents the action of external factors (for example: precipitation) and the other, O(t), representing the continuing draft of the basin (recession basin). The U(t) is modelled by its empirical marginal distribution and the dependence between U(t-1) and U(t) is represented by a censured normal autoregressive lag-1 process. O(t) is defined as k(t) times Q(t-1), where k(t) is the recession rate modelled by its empirical probability distribution.

Sometimes the last two observed daily streamflows show that the PREVIVAZ weekly streamflow forecast is very unrealistic, so the model has an algorithm to identify the discrepancy degree and actualize the weekly forecast. Table 3 presents the mean absolute percentage errors for daily streamflow forecast one to seven days ahead, for the same three hydro plants located in the Brazil South region, in the period 1992-2001.

Table 3 Mean absolute percentage errors for daily streamflow forecasting (1992-2001).

Hydro plant	Day 1	Day 2	Day 3	Day 4	Day 5	Day 6	Day 7
Foz do Areia	5,6 %	10,9 %	16,2 %	21,6 %	26,7 %	31,6 %	37,2 %
Salto Osório	6,4 %	13,2 %	19,6 %	25,4 %	29,7 %	33,9 %	38,5 %
Itaipu	7,5 %	13,6 %	18,7 %	23,9 %	27,6 %	29,9 %	33,5 %

MODELS IMPROVEMENT

It is natural to imagine that including precipitation information in the streamflow forecasting models will increase its accuracy, and that this effect will be greater in daily and weekly forecasting. Table 4 shows the results obtained by the first version of PREVIVAZH that considers precipitation information (Costa *et al.*, 2004). In this study we consider the "perfect" daily precipitation forecasting, using the observed average daily precipitation on the basin. It is possible to see the influence of the precipitation from the third day onward.

Table 4 Mean absolute percentage errors for daily streamflow forecasting considering precipitation information in the PREVIVAZH model (1992-2001).

Hydro plant	Day 1	Day 2	Day 3	Day 4	Day 5	Day 6	Day 7
Foz do Areia	5,9 %	10,4 %	14,8 %	17,9 %	21,8 %	25,3 %	28,8 %
Salto Osório	7,8 %	13,2 %	17,5 %	21,1 %	22,9 %	25,9 %	29,3 %
Itaipu	7,8 %	13,2 %	17,5 %	21,1 %	22,9 %	25,9 %	29,3 %

The Table 5 shows the effect of considering the observed average daily precipitation on the basin and the last two daily observed streamflow in the mean absolute percentage errors for weekly streamflow forecasting one week ahead for the period 1992-2001. It is important to highlight that the improvement obtained with the consideration of the precipitation in the forecasting models depends on the precipitation forecasting quality.

Table 5 Mean absolute percentage errors for weekly inflow forecasting one week ahead considering precipitation information in the PREVIVAZH model (1992-2001).

Hydro plant	PREVIVAZ	PREVIVAZH with precipitation	Reduction
Foz do Areia	35,9 %	16,7 %	53 %
Salto Osório	33,8 %	15,1 %	55 %
Itaipu	26,2 %	16,8 %	36 %

CONCLUSION

Due to its hydro dominant characteristic, the operation planning of the Brazilian electric power generation system can largely benefit from continuing improvement of hydrological models. The actual chain of models used in the operation planning activities uses a set a of forecast/simulation hydrological models which formulation and estimation of parameters were described in the paper. In general, they adopt the time series formulation approach adapted for streamflow modelling. The general building strategy aims to minimize squared or percentage forecast errors. Recent development includes the consideration of precipitation information.

REFERENCES

Box, G. E. P. & Cox, D. R. (1964) An Analysis of Transformations. *Journal of the Royal Statistical Society* A127, 211-252.

Costa, F. S., Damázio, J. M., Maceira, M. E. P., Souza, M. D. S., Guilhon, L. G. & Silva, S. B. (2003) Modelagem Estocástica de Previsão de Vazões Mensais, PREVIVAZM. *Proceedings of the XV Simpósio Brasileiro de Recursos Hídricos*, Curitiba, PR, Brasil.

Costa, F. S., Damázio J. M., Livino de Carvalho, A. R. & Dantas, H. M. (2000) PREVIVAZH – Modelo Estocástico de Previsão de Vazões Diárias. *Proceedings of the Seminário Internacional sobre Hidrologia Operativa*, CIER.

Costa F. S., Damázio J. M. & Souza M. D. S. (2004) Uso de Informação Quantitativa de Precipitação na Previsão de Vazões Diárias Através de uma Abordagem Estocástica. *Proceedings of the XXI Congresso Latino Americano de Hidráulica São Pedro*, São Paulo, Brasil.

Hipel, K. W. A. & McLeod, I. (1994) Time Series Modelling of Water Resources and Environmental Systems, *Elsevier*.

Kelman J., Damázio J. M. & Costa J. P. (1983) Geração de Séries Sintéticas de Vazões Diárias – Modelo Diana. *Revista Brasileira de Engenharia – Caderno Recursos Hídricos* **1**(2), Brasil.

Maceira, M. E. P. & Mercio, C. M. V. B. (1997) Stochastic Streamflow Model for Hydroelectric Systems, *Anais do V International Conference PMAPS - Probabilistic Methods Applied to Power Systems*, Vancouver, Canada.

Maceira M. E. P., Damázio J. M., Ghirardi A. O. & Dantas H. M. (1999) Periodic ARMA Models Applied to Weekly Streamflow Forecasts. *Proceedings of the 1999 IEEE Powertech*, Budapest.

Maceira, M. E. P., Terry, L. A., Costa, F. S., Damázio, J. M. & Melo, A.. C. G. (2002) Chain of Optimization Models for Setting the Energy Dispatch and Spot Price in the Brazilian System. *Anais do XIV Power Systems Computation Conference*, session 43, paper 1, Sevilla, Spain.

Regionalization of parameters of a rainfall-runoff model using artificial neural networks and data mining techniques

L. S. DINIZ & A. M. B. PASSERAT DE SILANS

Agência Executiva de Gestão das Águas do Estado da Paraíba – AESA. Av. Epitácio Pessoa n° 1457 – 2nd Andar. 58000-000 João Pessoa Brazil.

laudizio@terra.com.br

Abstract To use a conceptual or semi-conceptual hydrological rainfall–runoff model on a drainage basin without flow records, it must first have been calibrated at one or more sites where flow data are available and in a drainage basin having characteristics similar to those of the basin of interest. The transformation of rainfall into runoff needs some assumptions in both calibration and application sites that cannot be verified, leading to uncertainties. Moreover, the limited availability of hydrological data imposes some restriction on the application of rainfall-runoff models, particularly when the goal is to generate daily or monthly flow series. This paper describes the development and validation of a parameter regionalization technique based on the use of genetic algorithms and artificial neural networks. The rainfall–runoff model used is the monthly version of the SMAP model. Data from 41 drainage basins in the Paraíba State of the semi-arid north-east of Brazil are used, 14 of which have a streamflow gauge station whilst 27 contain a dam at which reservoir levels are recorded. In each drainage basin, 32 physical and climatic attributes are calculated. Six of these describe linear dimensions of the basin, three are shape parameters, nine characterize the drainage network, seven describes the relief, two the run-off capacity, three the soil class and two the climatic conditions. The analysis of the available data is made in two phases. The first consists of evaluating the importance of each basin in the whole ensemble, by means of a non-supervised hierarchical learning procedure, and the second consists of selecting attributes using a supervised learning procedure which eliminates redundancies and less important data that diminish the precision and understanding of the assumptions used when relationships between parameters and basin characteristics are formulated.

Keywords regionalization of parameters; SMAP model; artificial neural networks; data mining

INTRODUCTION

Hydrologic regionalization is a tool whose main aim is to transfer information from gauged basins to other ungauged basins (Mosley, 1981). The regionalization of parameters of a rainfall-runoff model is difficult because of errors associated with the calibration process and with the input data, and also because of the interdependencies of the parameters and the non-linearity of the physical process. According to Abdulla & Lettenmaier (1997), there are also difficulties to meet some regional relationships for the model parameters. However Heuvelmans *et al*. (2006) assert that the main requirement for successful regionalization of hydrologic model parameters is to associate them with physical attributes of the basin. According to Seibert (1999) the number and the type of the attributes are geographically feature dependent.

The purpose of this paper is to illustrate a successful method for regionalizing rainfall-runoff model parameters developed and used in the semi-arid region of Brazil.

METHODOLOGY

The methodology developed is a combination of data mining and artificial intelligence techniques. The rainfall–runoff model used is the monthly version of the SMAP model. Data from 41 drainage basins in the Paraíba State of the semi-arid north-east of Brazil are used, 14 of which have a streamflow gauge station whilst 27 contain a dam at which reservoir levels are recorded.

In each drainage basin, 32 physical and climatic attributes are calculated. Six of these describe linear dimensions of the basin, three are shape parameters, nine characterize the drainage network, seven describes the relief, two the runoff capacity, three the soil class and two the climatic conditions.

The analysis of the available data is made in two phases. The first consists of evaluating the importance of each basin in the whole ensemble, by means of a non-supervised hierarchical learning procedure, and the second consists of selecting attributes using a supervised learning procedure which eliminates redundancies and less important data that diminish the precision and understanding of the assumptions used when relationships between parameters and basin characteristics are formulated. These are formulated with artificial neural networks.

Location of each drainage basin into the whole ensemble - similarity

The evaluation of the importance of each drainage basin in the whole ensemble is made with a non-supervised hierarchical learning procedure. To do this, the attributes of the 41 selected basins were submitted to the Single Link (SL), Complete Link (CL), Average Link(AL) and Ward hierarchical grouping algorithms. A similarity distance is used to group the basins. In this work, the Euclidian distance was used. Then hierarchical clusters are drawn by a dendrograph which can be used as a similitude criterion for ungauged basins.

SMAP Model and calibration procedure

The SMAP – Soil Moisture Accounting Procedure Model (Lopes *et al*., 1981) has a simple structure and has been used successfully in the semi-arid north-east of Brazil. It is composed of two linear reservoirs which represent soil moisture and groundwater storage. The monthly version of SMAP runs with monthly rainfall and potential evapotranspiration. In the semi-arid north-east of Brazil, groundwater is non-existent because of the crystalline geological base, so with this condition, only four parameters are needed to run the model. They are E2 and STR which are mainly runoff-related, and E1 and CINF which determine the soil moisture budget. An automatic calibration procedure has been used to determine the optimum parameters for all the drainage basins selected in the first step. It is based on the SCE-UA (shuffled Complex Evolution) algorithm (Diniz, 1994) with the Nash & Sutcliffe (1970) efficiency criterion as the objective function.

Selection of the attributes

For each parameter of the model, a sub-ensemble of attributes is searched. The chosen technique is able to eliminate redundancies and unimportant attributes to explain the variance of the parameters. To do this, the Correlation-based Feature Selection – CFS algorithm due to Hall (1999) is used in the WEKA (Waikato Environment for Knowledge Analysis) environment (Witten & Frank, 2000).

Formulation of relationships between parameters and selected attributes

According to Maier & Dandy (2001), artificial neural networks (ANN) are ever more widely used in hydrology to represent the transformation of rainfall into runoff. They argue that it is due to the facility of considering the non-linearities of the physical processes and the interdependencies of the parameters of the models by the learning procedure of the ANN. In this work, the software QNET for Windows was used. The methodology used is drawn in Fig. 1. From the N basins available, each one is omitted sequentially and is used for validation. From the N-1 remaining basins, one is also sequentially drawn. It is used to test the learning procedure and is termed the Meta basin. At the end of the process, one has N-1 ANN able to best reproduce the parameter for the Meta basin. In the validation phase of the proposed methodology, each parameter of the sampled out basin is calculated by the ANN whose Meta basin is most similar to itself.

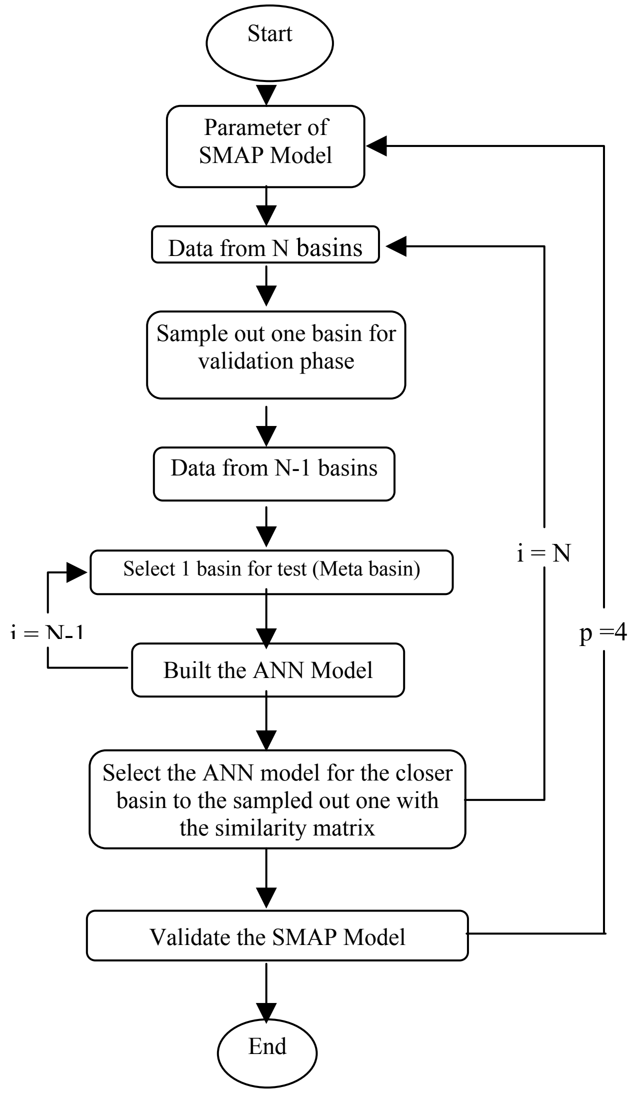

Fig. 1 Diagram of the regionalization Model

RESULTS

The 41 selected basins have drainage area varying from 9.5 to 17,220 km². From the four dendrographs drawn to locate each basin in the ensemble, five basins were systematically out of the clusters. They are the two largest drainage basins (BA10 e BF11) and three of the four smallest drainage basins (BA1, BA13 e BF13). So, from the 41 selected basins, only 36 were considered in this study. The best dendrograph for the 36 basins was given by the AL algorithm. It shows the existence of three similar groups of drainage basins.

The SMAP model was calibrated on the 36 drainage basins, and then the attributes which best explain the variance of the parameters were determined by the CFS algorithm. Results are indicated in Table 1, which shows that for each parameter of the SMAP model, there exists one sub-ensemble of attributes. Some attributes appear for more than one parameter.

Table 1 Selected attributes for each parameter of the SMAP model.

SMAP Parameters	Selected attributes	Deserving criteria
E2	Pr, Lt, Kf, Rb, Rl, Ra, Ct, SIN, Cmed, Ip, DS, P	0,629
STR	Rb, Ra, Ct, solo1, solo2, PAE	0,643
E1	Rb, Ct, Cmed, Solo1, PAE	0,506
CINF	Ld, Ra, Ct, Cmed, solo1, PAE	0,373

Multiples regressions between the parameters and the attributes have been explored but without success. So the ANN technique was used.

For each parameter the best ANN structure and transfer functions between the layers are shown in Table 2.

Table 2 ANN structure and transfer functions for the SMAP parameters

Layer	Number of Neurones				Transfer Function			
	E2	STR	E1	CINF	E2	STR	E1	CINF
Input	12	7	5	7	-	-	-	-
Hidden 1	5	3	3	4	Gaussian	Gaussian	Hyperbolic secant	Gaussian
Hidden 2	-	2	2	-	-	Gaussian	Hyperbolic secant	-
Output	1	1	1	1	Gaussian	Sigmoid	Sigmoid	Gaussian

For the STR parameter, a good fit for the output was found when introducing the E2 parameter as an input neurone. The same occurs with CINF parameter for which one of the input neurone is the value of E1. These results show the high non-linear dependence of the parameters between each other.

The validation procedure treated the omitted basins as ungauged. Then for each parameter the most similar Meta basin is looked for, using the AL algorithm with the selected attributes for the considered parameter. Note that by this methodology, the Meta basin of an ungauged basin can differ for each parameter of the model. Then using the ANN, the model parameters are calculated from the ANN associated with the Meta basin and the results are compared with the calibrated parameters. Comparisons were very good except for five basins. More investigation is required to understand the reason.

CONCLUSION

Combining data mining techniques with artificial neural networks modelling, it has been possible to regionalize the parameters of the SMAP model from several sets of physical and climatic attributes. The proposed model has been successfully validated.

Acknowledgments

We thanked Dr. R. T. Clarke for constructive comments and revision of the text.

REFERENCES

Abdulla, F. A. & Lettenmaier, D. P. (1997) Development of regional parameter estimation equations for a macroscale hydrologic model. *Journal of Hydrology* **197**, 230-257.

Diniz, L. S. (1994) Calibração automática de modelos chuva-vazão usando um algoritmo genético. *Dissertação de mestrado. Universidade Federal da Paraíba, Campina Grande-PB,* 130p.

Hall, M. (1999) Correlation-based feature subset selection for machine learning. *PhD thesis,* Department of computer science. http://www.cs.waikato.ac.nz/~mhall/thesis.pdf.

Heuvelmans, G., Muys, B. & Feyen, J. (2006) Regionalization of the parameters of a hydrological model: comparison of linear regression models with artificial neural nets. *Journal of Hydrology* **319**, 245-265.

Lopes, J. E. G., Braga, B. P. F., & Conejo, J. G. L. (1981) Simulação hidrológica: aplicações de um modelo simplificado. *IV Simpósio brasileiro de hidrologia e recursos hídricos* **1**, 42-62.

Maier, H. R. & Dandy, G. C. (2001) Neural network based modelling of environmente variables: a systematic approach. *Math. Comput. Model* **33**, 669-682.

Mosley, M. P. (1981) Delimitation of New Zealand hydrological regions. *Journal of Hydrology* **49**, 173-192.

Witten, I. H. & Frank, E. (2000) Data Mining: Pratical Machine Learning Tools and Techniques with Java Implementations. *Morgan Kaufmann*, California.

Flow numerical modelling: an alternative approach to define peat hydraulic properties and direct recharge of an Alpine mire

A. GARGINI & A. PONTIN
Earth Sciences Department, University of Ferrara, Via Saragat 1, B block - 44100, Ferrara, Italy
gga@unife.it, pntlsn@unife.it

Abstract. In the Alpine environment peatlands are a minor component of landscape also if their ecological value is very high for the maintainance of biodiversity and also as possible recharge or discharge zones of local groundwater flow systems. This is the case of one mire, called CS (Coltrondo South), located in the Eastern Alps (Veneto Region, Northern Italy), near the border with Austria at the northern edge of the Piave river watershed (Coltrondo site, 1800 m a.s.l.). GPS surveying in RTK modality was performed in August 2005; water table data and piezometric gradients continuous monitoring are collected during 2006 growing season. A transient state numerical flow model was implemented, adopting finite differences code Modflow 2000, relatively to actual 2006 conditions with a total 170 number of stress periods. For calibration in transient conditions, the simulated water-table has been compared with the actual 2006 monitoring period and piezometric surveys. Mass balance is in the calibration range of 0.2%. Mire water budget was performed by ZoneBudget tool, relatively to the three active layers of the flow domain, adding a powerful tool for the best investigations in the intrinsic complexity of mire's hydrologic budgeting.
Keywords groundwater; wetlands; Alps; ecosystem; monitoring; hydraulic head; piezometers; numerical modelling

LOCATION AND HYDROGEOLOGICAL OUTLINE

The research deals with one mires located near the border with Austria (Fig.1) at the northern edge of the Piave river watershed (Coltrondo site), 46°39' N Lat., 12°26' E Long.,1800 m a.s.l.

Climatic Köppen classification is Dfb boreal type. Average annual, coldest (January) and warmest (July) month temperature is about 4°C, –5°C and 12,5°C. Annual rainfall (rainy days per year are in 100-120 range) attains 1000 mm (continental climatic regime, maximum in summer); snow-fall is relevant with 376 cm mean annual snow height with 152 days of snow permanence (1975-2000).

From a geologic stand-point Coltrondo site is located in the easternmost sector of subalpine basement of Eastern Alps; the mires are located over a phylladic bedrock with surrounding scattered outcrops of red Val Gardena Sandstones (Lower Permian).

Groundwater circulation is active in the bedrock and glacial deposits: in Coltrondo site*, Val Gardena sandstones* and *Permian phyllites* shallow aquifers feed Valentino creek base-flow and some minor spring.

CS mire is substantially hydraulically isolated by the occurrence of lacustrine fine-grained sediments (clays and sandy silts) deposited in small lakes originated by structurally controlled glacial erosion. For this reason active groundwater flow systems in bedrock or morraines poorly affect mire hydrology; in that sense we can consider the base of the peat mass as a zero-flux plane from an hydrogeologic point of view (Fraser *et al*., 2001; McKenzie, 2002; McNamara *et al.,* 1992).

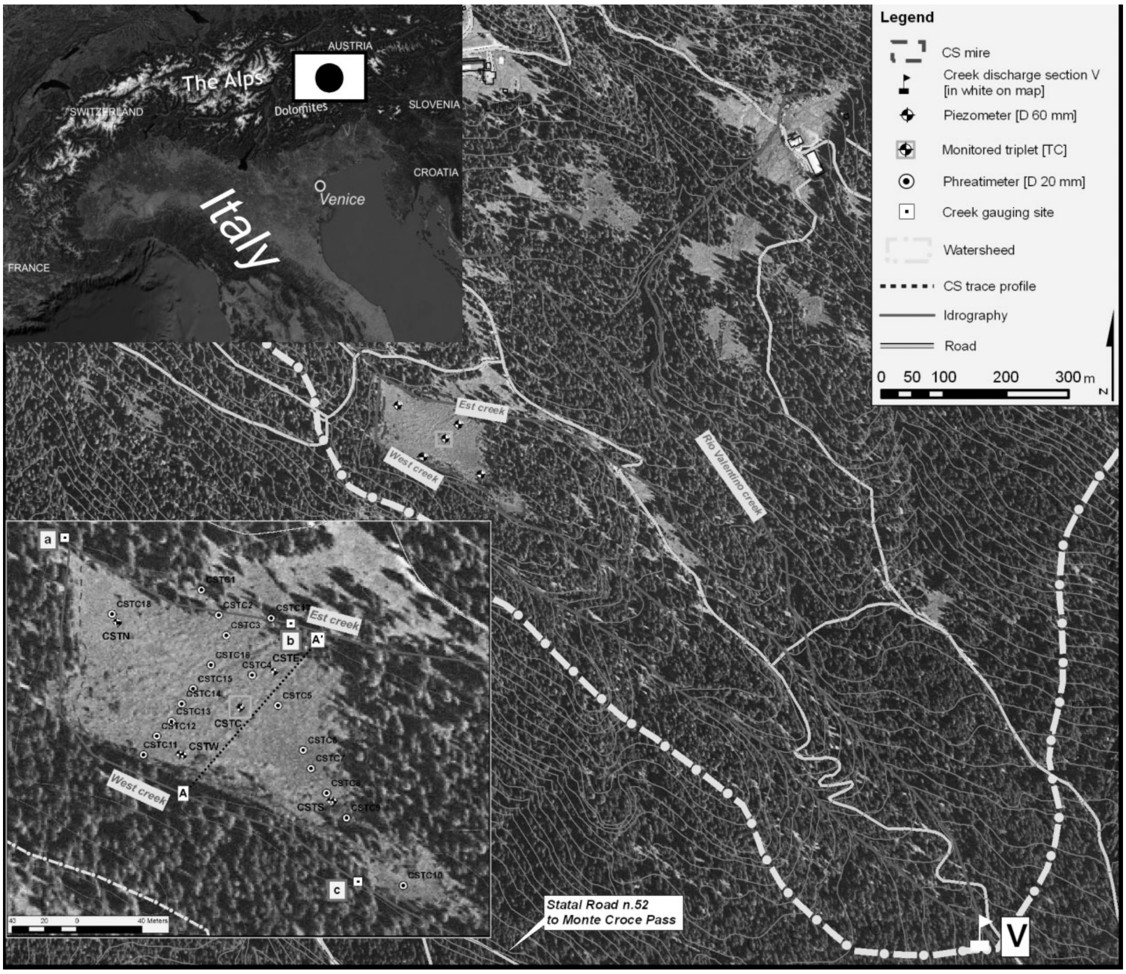

Fig. 1 Location of the site, piezometers, phreatimeters and lateral creeks gauging stations.

MATERIALS & METHODS

17 PVC open stand-pipes (length 0.8 m; I.D. ∅20 mm; fully slotted with 5 mm holes), called phreatimeters, were hand-driven into the ground at the beginning of 2005 growing season. Moreover, during the first half of October 2005 15 HDPE or PVC open-stand pipe piezometers (O.D. ∅60 mm, I.D. ∅51.6 mm), 0.5-1 m long screened (0.4 mm slotted), have been hand-drilled, in 5 triplets (Fig.1). The triplets permit to measure hydraulic head at the following distinct depth intervals (according piezometer ID number): “1”: shallowest meter below ground level (more permeable *acrotelm*); “2”: upper part of *catotelm* (interval range between 1 and 2.5 m b.g.l.); “3”: lower part of *catotelm*, immediately above the substratum (interval range between 1.5 and 4.5 m b.g.l.). All piezometers were hand-drilled by an *Eijkelkamp* probe; no filter-pack or bentonite seal was used but single end-threaded columns of piezometric tube were simply hand driven into the peat mass down to the hole bottom and the following collapse of the peat mass around the tubes avoided hydraulic short circuiting along the annulus. CS topography and well heads coordinates were determined by GPS surveys (Hofmann *et al.*, 2001) in August 2005. Two *Leica SR 530* double frequency receivers working in RTK (*Real Time Kinematics*) modality were used. This procedure allowed to measure a great number of points in few hours obtaining a good accuracy (<0.5 cm). Reference benchmarks for RTK surveys were previously determined with high

accuracy by static relative positioning, post-processing the observations acquired (during a 3,5 hour period) with the data collected by the permanent station of Bolzano (BZRG), Northern Italy. Since May 27th 2006 one piezometers triplet has been instrumented for hydraulic head and water temperature continuous monitoring (acquisition frequency: 1 hour) during 2006 growing season (until 7th October 2006). *DIVER* type probes (*Eijkelkamp -Van Essen Instruments/Schlumberger*) have been employed. Each probe (stainless steel stuff; 0.125 m length, ∅22 mm, 160 g weight) is a mini pressure transducers with an encapsulated data-logger and records absolute fluid pressure (water+atmospheric pressure); raw-data were barometrically compensated through one *BaroDIVER* atmospheric pressure probes (installed in the neighbourhoods). For hydrodynamic parameterization 5 slug or bail tests have been performed in two piezometers triplets. The slug effect was obtained by pouring semi-instantaneously a volume of water into the hole up to the upper rim; the bail effect was obtained by purging completely 1 volume of water from the entire piezometer column (Chason & Siegel, 1986). In both cases, the respective lowering and rising of water level have been recorded by Diver probe (time acquisition variable from 0.5 to 30 s); K value was derived by application of Bouwer & Rice (1976) method.

DATA ANALYSIS AND NUMERICAL FLOW MODELLING

Water-table morphology relative to 2006 median value, expressed either as absolute hydraulic head or depth-to-water table, has been performed by *Surfer 8* (*©Golden Software Inc.*) with interpolation by *kriging* with default linear variogram. Groundwater flow pattern reflects local morphology of the substratum: CS mire has a well structured groundwater flow field with steep hydraulic gradient from NW to SE due to more pronounced regional topographic gradient and to the bordering creeks (Fig.1). Water-level discontinuous weekly monitoring on piezometers triplets during 2006 has permitted to define vertical distribution of hydraulic head, assigned to the half of the screen length (see also Fraser *et al.*, 2001; Kellner *et al.*, 2004): flow vertical inversions (negative hydraulic gradient, upward directed) occur frequently in CS *acrotelm*. The continuous water level (heads) monitoring during 2006 growing season put in evidence the “reactivity to rainfall signal” of mire water-table; head hydrograph is a series of peaks, connected to rainfall events, followed by recession periods, with the absence of any particular seasonal trend; resulting hydrograph show the practically instantaneous water table recovery, even after a long recession period (July); infiltration in the unsaturated upper peat mass is very rapid, suggesting the importance of saturation – excess overland flow (Holden *et al.*, 2003). A groundwater (peatwater) numerical flow model has been implemented adopting finite differences code Modflow 2000 (Harbaugh *et al.*, 2000), updated version of first release of Modflow (McDonald & Harbaugh, 1988), with Visual Modflow 4.1 interface (©Waterloo Hydrogeologic, Inc.). CS mire offers good conditions for modelling: regularity of water-table morphology, well defined boundary conditions (discharge into border creeks) with a monitoring activity of the creek itself for output calibration. A good knowledge of boundary conditions is one of the main requisite preconditioning the modelling reliability (Bear & Verruijt, 1987; Anderson & Woessner, 1992). Flow domain has a rectangular shape (300x450 m), 40° clockwise rotated respect to the local meridian to accomplish main groundwater flow direction. The mesh is composed by 137 columns, 282 rows, 4 layers and a cell size variable between 10x1m e 1x1m. Active cell size is always equal to 1x1 m, specifically fitted to the micro variability of peat topography. The four layers have been defined on the basis of GPS survey and stratigraphic logs obtained by piezometers hand-boring (Fig. 2). Layer 1 (*acrotelm*): located between the upper surface of the model domain (digital terrain model, in *grd Surfer* format, derived from the GPS survey integrated with topographic map) and the base of the *acrotelm*, defined simply with a 1 m downward off-set from upper ground surface; Layer 2 (*catotelm*): located between Layer 1 and the bottom surface, defined with a 1 m upward off-set respect to bedrock upper surface, interpreted from soil coring stratigraphic logs and interpolated by *Surfer 8* (*©Golden Software Inc.*) with minimum curvature algorithm; Layer 3 (lacustrine clays and sandy silts): thickness considered equal to 1 m; Layer 4 (bedrock): considered hydraulically inactive (inactive cells). For the simulation *PCG2* solver has been chosen (*Preconditioned Conjugate-Gradient Package*; Hill, 1997) with the application of a $1x10^{-2}$ convergence criterion. For calibration in transient conditions, the simulated water-table has been compared with the actual 2006 monitoring period piezometric surveys.

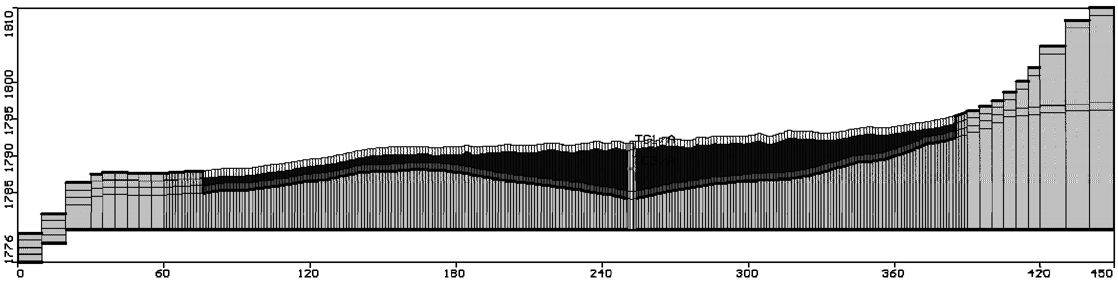

Fig. 2 MODFLOW cross section at column n° 70: in white, blue and green are represented the three active layers; gray colour define inactive cells (inactive flow condition). The monitored piezometers (TC1 and TC3) is also visible in the centre (x – axis: progressive in m; y – axis: height in m a.s.l.).

At the beginning, through a *trial & error* procedure (Zheng & Bennett, 1995), an acceptable set of parameters (K, storage, *RIVER* conductance) has been defined to simulate adequately hydrological processes, leaving constant the initial guess of recharge. Afterward automatic calibration tool *PEST* (*non-linear Parameter ESTimation*; Doherty, 2001) has been applied in two steps: at first to better estimate new recharge values (leaving all other parameters constant) and, at second, to better adjust K and storage parameters (with recharge left constant). At the end of the calibration phase, direct recharge values for each month have been calculated by the model. Modelled recharge follows the same pattern that soil water budget surplus evaluated approach according Thornthwaite method. Whole mire water budget was performed, by *ZoneBudget* tool, relatively to the three active layers of the flow domain so the total amount of exchanged water between the three different layers is quantified (in mm). Water exchange between *acrotelm* and *catotelm* is about 1 order higher respect to what happens between *catotelm* and the mire-bed lacustrine deposits. Upward flux from the *catotelm* is about twice respect to the opposite (downward flux from the *acrotelm*) and suddenly activates when the whole system is subjected to strongest recessions. So it seems that direct recharge coming from rainfall remains substantially in the *acrotelm* and does not go deeper inside the mire body. Only during the strongest recessions water upward flux from the lacustrine bottom ("vertical hydrologic reversal"; McNamara *et al.*, 1992) is appreciable. In CS mire the more active layer, from an hydrogeological standpoint, is *acrotelm*, that receives direct recharge from rainfall above and not secondary contributions from *catotelm* below; so in the *acrotelm* mainly horizontal saturated flow prevail and excess water discharges to edge creeks, main output term of the budget.

CONCLUSIONS

The paper demonstrates the importance of continuously monitoring recharge-discharge hydrologic processes in order to obtain a clear rationale of horizontal as well as vertical component of peat-water heads and fluxes. In addition, using in parallel numerical modelling of peat-water flow is a main tool for a proper hydrologic budgeting of a mire to overcome intrinsic difficulties related to high hydraulic properties heterogeneities (K occurrence and anisotropy) and complexities of water exchanges with local surface and groundwaters.

Acknowledgements This work was granted by R.I.T.A project (Vicenza municipality-CARIVERONA Foundation).

REFERENCES

Anderson, M. P. & Woessner, W. W. (1992) Applied Groundwater Modeling: Simulation of Flow and Advective Transport. *Academic Press, San Diego (USA).*

Bear, J. & Verruijt, A. (1987) Modeling Groundwater Flow and Pollution. *D.Reidel, Dordrecht (NED).*

Chason, D. B. & Siegel, D. I. (1986) Hydraulic conductivity and related properties of peat, Lost River Peatland, northern Minnesota. *Soil Science* **142**, 91-99.

Fraser, C. J. D., Roulet, N. T. & Lafleur, M. (2001) Groundwater flow patterns in large peatlands. *Journal of Hydrology* **246**, 142-154.

Hill, M. C. (1997) Preconditioned Conjugate-Gradient 2 (PCG2). A computer program for solving Groundwater Flow equations. *USGS Water-Resources Investigations Report 90-4048*.

Hofmann-Wellenhof, B., Lichtenegger, H. & Collins, J. (2001) GPS Theory and practice. *Fifth revised edition, Springer Verlag, Wien (AUT).*

Holden, J. & Burt, T. P. (2003) Hydrological studies on blanket peat: the significance of the acrotelm-catotelm model. *Journal of Ecology* **91**, 86-102.

Kellner, E., Price, J. S. & Waddington, J. M. (2004) Pressure variations in peat as a result of gas bubble dynamics. *Hydrological Processes* **18**, 2599-2605.

McKenzie, J. M., Siegel, D. I., Shtyk, W., Steinmann, P. & Pfunder, G. (2002) Heuristic numerical and analytical models of the hydrologic controls over vertical solute transport in a domed peat bog, Jura Mountains, Switzerland. *Hydrol. Process.* **16**, 1047-1064.

McNamara, J. P., Siegel, D. I., Glaser, P. H. & Beck, R.M. (1992) Hydrologic controls on peatland development in the Malloryville wetland, New York (USA). *Journal of Hydrology* **140,** 279–296.

Zheng, C. & Bennett, G. D. (1995) Applied Contaminant Transport Modeling, Theory and Practice. *John Wiley & Sons, New York (USA).*

Hydrological modelling of aquifers by using improved IP data

S. MEHRABIAN & A. AMINI

Institute of Geophysics, University of Tehran, Kargar Shomali Ave. P.O. Box 14155-6466, Iran

smehrabi@ut.ac.ir

Abstract Electrical resistivity is one of the most popular geophysical methods used for ground-water exploration. It is sometimes used with the induced polarization method (IP) to have a better interpretation. The IP method is an electrical geophysical technique, which measures the slow decay of voltage in the subsurface following the cessation of an excitation current pulse. Water in subsurface geologic material (within pores and fissures) allows for certain geologic material to show an effect called IP when an electrical current is applied. During the application of the electrical current, electrochemical reactions within the subsurface material take place and electrical energy is stored. After the electrical current is turned off the stored electrical energy is discharged which results in a current flow within the subsurface material. The IP instruments then measure the current flow. Thus, in a sense, subsurface material acts as a large electrical capacitor. The induced polarization method measures the bulk electrical characteristics of geologic units; these characteristics are related to mineralogy, geochemistry and grain size of the subsurface materials through which electrical current passes. Induced polarization measurements are taken together with electrical resistivity measurements using specialized IP instruments. Although the IP method historically has been used in mining exploration to detect disseminated sulfide deposits, it has also been used successfully in ground water studies to map clay and silt layers which serve as confining units separating unconsolidated sediment aquifers. Induced polarization data can be collected during an electrical resistivity survey, providing the proper equipment is used. The addition of IP data to a resistivity investigation improves the resolution of the analysis of resistivity data in three ways: 1) some of the ambiguities encountered in resolving thin stratigraphic layers while modeling electrical resistivity data can be reduced by analysis of IP data; 2) IP data can be used to distinguish geologic layers which do not respond well to an electrical resistivity survey; and 3) the measurement of another physical property (electrical chargeability) can be used to enhance a hydrogeologic interpretation, such as discriminating equally electrically conductive targets such as saline, electrolytic or metallic-ion contaminant plumes from clay layers. The main objective of this study is to show how the results of the numerical modelling of the geophysical data can serve as useful tools to prepare a hydrogeological model of the aquifer for the purpose of the prosperous drilling. To achieve the goal, the acquired geophysical data of a relatively vast plain, located in a city of Iran, are first verified and corrected and then fed to the computer programs for the one and two-dimensional (1D and 2D) inverse modelling. The obtained results by these models were then used to provide a hydrogeological model of the plain in the form of contour map of ground-water surface. This map helped us to find the suitable area within the studied zone for the future drilling.

Keywords induced polarization; stratigraphic layers; hydrogeological model; inverse modelling

INTRODUCTION AND BACKGROUND INFORMATION

The use of geophysical methods at hazardous waste and ground water pollution sites is a fairly recent development. In the past, many of these techniques were used in mineral, geothermal and petroleum exploration industries. In recent years, the need to conduct ground water pollution investigations has coincided with improvements in the resolution, acquisition and interpretation of geophysical data. The induced polarization (IP) method is an electrical geophysical technique, which measures the slow decay of voltage in the subsurface following the cessation of an excitation current pulse. Water in the subsurface geologic material (within pores and fissures) allows for certain geologic material to show an effect called “induced polarization” when an electrical current is applied. The induced polarization method measures the bulk electrical characteristics of geologic units; these characteristics are related to the mineralogy, geochemistry and grain size of the subsurface materials through which electrical current passes.

Induced polarization measurements are taken together with electrical resistivity measurements using specialized IP instruments. The IP method is used successfully in ground water studies to map clay and silt layers which serve as confining units separating unconsolidated sediment aquifers. The addition of IP data to a resistivity investigation improves the resolution of the analysis of resistivity data in three ways: 1) some of the ambiguities encountered in resolving thin stratigraphic layers while modeling electrical resistivity data can be reduced by analysis of IP data; 2) IP data can be used to distinguish geologic layers which do not respond well to an electrical resistivity survey; and 3) the measurement of another physical property (electrical chargeability) can be used to enhance a hydrogeologic interpretation, such as discriminating equally electrically conductive targets such as saline, electrolytic or metallic-ion contaminant plumes from clay layers.

Induced polarization fieldwork tends to be labor intensive and often requires two to three crew members. Like electrical resistivity surveys, induced polarization surveys require a fairly large area, far removed from power lines and grounded metallic structures such as metal fences, pipelines and railroad tracks.

Induced polarization instruments are similar to electrical resistivity instruments. There are two different types of induced polarization systems. Probably the most common type of IP instrument is the “time-domain” system. This instrument transmits a constant electrical current pulse during which time the received voltage is sampled for an electrical resistivity measurement, acting like a conventional electrical resistivity system. The electrical current is then shut off abruptly by the system, and after a specified time delay (several milliseconds) the decaying voltage in the subsurface is sampled at the IP receiver, averaging over one or more time windows or “time gates.” The second type of IP instrument is the “frequency-domain” system. In this type of system, transmitted current is sinusoidal at a specified frequency. Since the system is always on, only an electrical resistivity measurement can be collected at a particular frequency. Survey Design, Procedure and Quality Assurance: Induced polarization survey design depends on the specific characteristics of the site and the objective of the survey.

METHODOLOGY

The data collected from IP surveys consists of two sets, the normal apparent resistivity measurements and an apparent IP data set. One possible method to invert such a joint data set is to treat the two data sets as completely separated data sets. The inversion of the resistivity data is completed before starting on the inversion of the IP data set. In this case, the resistivity model obtained at the last iteration of the inversion of the resistivity data set (which usually has the lowest RMS error) is used in the inversion of the IP data set. This is probably the most efficient method if the resistivity model is a good representation of the true subsurface resistivity. However, it has been found that even in the inversion of computer generated data sets, the model obtained can contain distortions particularly if a large number (more than 5) of iterations is used in the inversion of the resistivity data set. This is because of the inversion is based on a finite number of datum points. The distortion becomes worse when the data contains noise. Many users tend to use a large number of iterations together with relatively low damping factors in an effort to reduce the RMS error to the lowest possible value. If a resistivity model with distortions is used in the inversion of the IP data, then the distortions will affect the IP models for all iterations of the IP inversion. The inversion method used in this program is a step-wise refinement of IP inversion model. The inversion of the resistivity and IP data sets are still carried out separately. However, immediately after an iteration of the inversion of the resistivity data, an iteration of the IP inversion is carried out. The resistivity model obtained at the particular iteration of the resistivity data is used for the inversion of the IP data at the same iteration. Since the resistivity models at the earlier iterations are less distorted by noise in the data, the corresponding IP models are also less influenced by the distortions in the resistivity models.

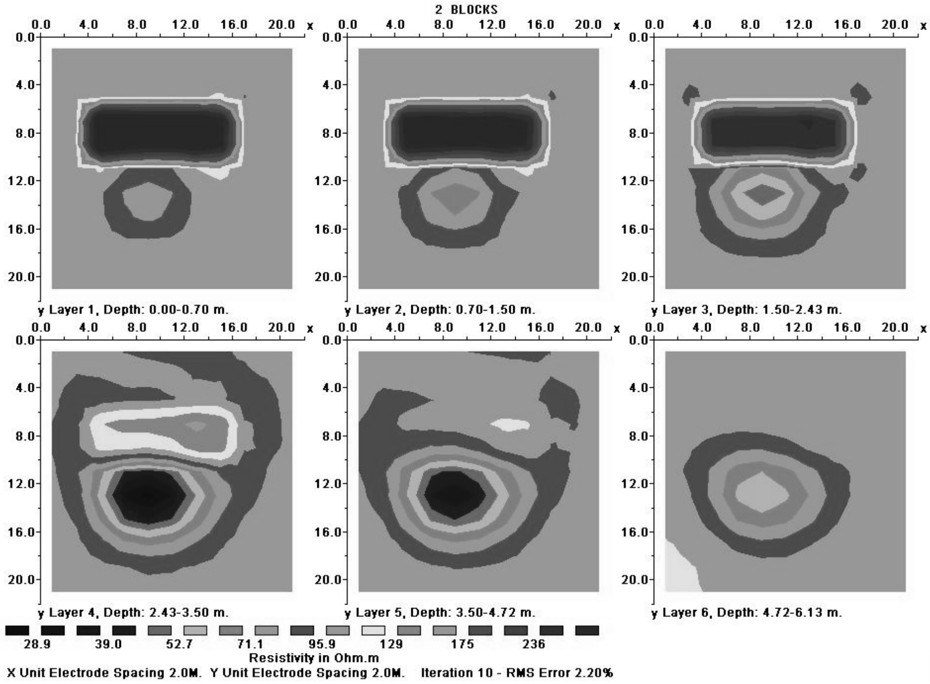

Fig. 1 The 3D model obtained from the inversion of the survey data set. The model is shown in the form of horizontal slices through the Earth.

RESULTS

In this study, discrimination between a contaminated site near an uncontaminated water aquifer by IP and Resistivity methods was the main purpose. The models obtained from the inversion of this data set are shown in Figs 1, 2 and 3. The models are shown in the form of horizontal and vertical slices through the Earth. It is used of IP and Dipole-Dipole array; X and Y grid size are 12m. Number of data points is 1440. Average height is 0.00. Number of iteration is10; RMS error is 3.60, average sensitivity value is 1.0128. The minimum and maximum in both X and Y locations are, 0.00 and 22.00 in ohm. m. Unit x and y spacing are respectively 2m. Average height is 0.57. Number of iteration is10; RMS error 3.60, average sensitivity value is 103.66. The results obtained were compared to other geophysical and background data, and a good agreement was found.

In this study, the purpose was discrimination between a contaminated site near an uncontaminated water aquifer by IP and Resistivity methods. The models obtained from the inversion of this data set are shown in Figs 1, 2 and 3. The models are shown in the form of horizontal and vertical slices through the earth. It is used of IP and Dipole-dipole array; X and Y grid size are 12m. Number of data points is 1440. Average height is 0.00. Number of iteration is 10; RMS error 3.60, average sensitivity value is 1.0128. Minimum and maximum in both x and y locations are, 0.00 and 22.00

ohm. m. Unit X and Y spacing are respectively 2m. Average height is 0.57. Number of iteration is 8; RMS error 3.60, average sensitivity value is 103.66. The results obtained were compared to other geophysical and background data, and a good agreement was found.

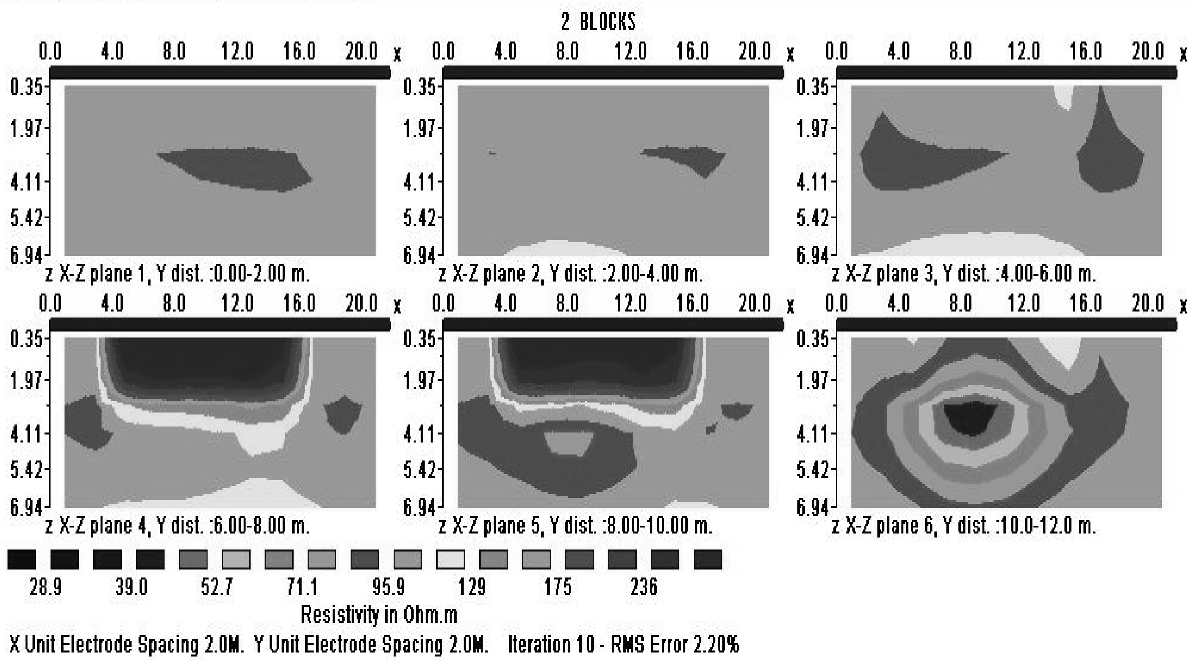

Fig. 2 The 3D model obtained from the inversion of the survey data set. The model is shown in the form of vertical slices through the earth in x-z dimension.

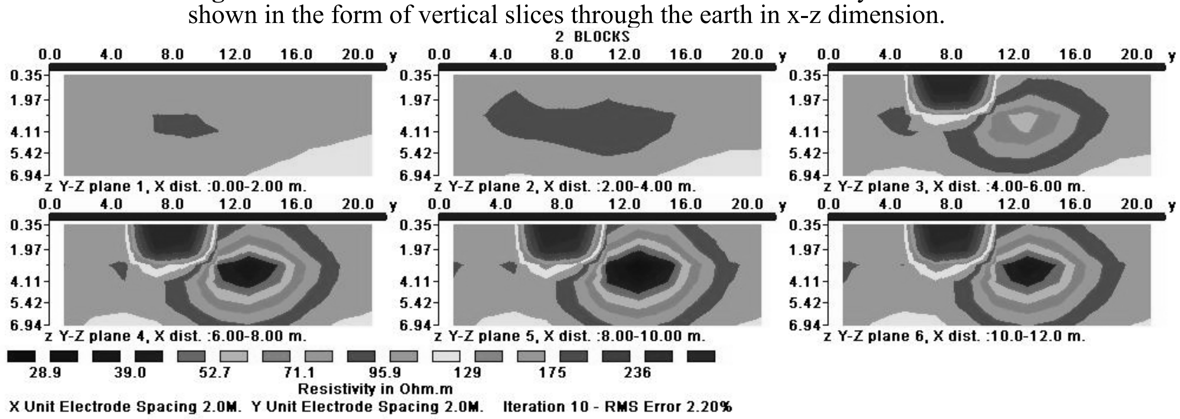

Fig. 3 The 3D model obtained from the inversion of the survey data set. The model is shown in the form of vertical slices through the earth in Y-Z dimension.

Acknowledgements The authors would like to thank the office of research affairs (Vice president in research and technology), University of Tehran for financial support.

REFERENCES

Christensen, N. B. & Sorensen, K. I. (1994) Integrated use of electromagnetic methods for hydrogeological investigations. *Proceedings of the Symposium on the Application of Geophysics to Engineering and Environmental Problems*, March 1994, Boston, Massachusetts, 163-176.

Griffiths, D. H., Turnbull, J. & Olayinka, A. I. (1990) Two-dimensional Resistivity mapping with a computer-controlled array. *First Break* **8**,121-129.

Keller, G. V. & Frischknecht, F. C. (1966) Electrical methods in geophysical prospecting. *Pergamon Press Inc., Oxford*.

Loke, M. H. (1999) Time-lapse resistivity imaging inversion. *5th Meeting of the Environmental and Engineering Geophysical Society European Section Proceedings*. Em1.

Summer, J. S. (1976) Principles of induced polarization for geophysical exploration. *Elsevier Scientific Publishing Company*.

Runoff forecasting in hydropower industry: a holistic approach through modular assembly

R. SPOLWIND, F. FRÖSCHL & K. HEBENSTREIT

Resource Optimization Hydro Power, Verbund / Österreichische Elektrizitätswirtschafts-AG, Am Hof 6A, 1010 Wien, Austria

robert.spolwind@verbund.at

Abstract VERBUND is Austria's leading electricity company in generation and wholesale. Run-of-river power plants, pondage power plants and alpine storage power plants as well as procurement rights from different hydropower plants represent the hydropower asset park of VERBUND. The deregulated energy market and VERBUND's trading activities in central Europe demand high market flexibility, causing the application of accurate forecasting and optimisation tools. The strategic Energy Economic Decision Support System (EEDSS) of VERBUND integrates modules of short term runoff and capacity forecasting, long term planning, short term and long term energy price forecasting and modules of strategy-optimisation in power plant management. The hydropower-dominated asset structure of VERBUND implies the dependency of production and planning quality to meteorological situations, corresponding runoff responses and its accurate forecasting. Short term and seasonal variation in runoff and resulting variance in hydro power production turns forecast quality into a remarkable economic factor.

Keywords hydropower; forecasting; flood; optimisation

INTRODUCTION

The asset park of VERBUND is characterised by an integrative concurrence of run-of-river power plants, pondage plants, storage power plants and, on a smaller scale, thermal power plants. VERBUND is Austria's leading electricity company, operating more than 100 hydro power plants all over the country with an annual generation capacity of about 25 TWh.

Run-of-river power stations use the natural flow of river water to drive turbines. Run-of-river power stations operate continuously, the amount of electricity produced depends on the river's flow. The reservoirs of pondage power plants have limited magnitudes that provide weekly regulation of streamflow. More than 70 % of VERBUND's annual generation capacity originate from run-of-river and pondage power production, therefore the relevance of not or short term disposable energy becomes obvious. Variance in runoff correlates significantly with variance in energy production., accurate forecasting of runoff is crucial for economic success.

A bottom up model pyramid provides strong fundamental soil and snow model results based on temperature and precipitation forecasts as well as global radiation, exact topological simulation of the catchment and albedo simulation. Responses of the snowmelt and soil moisture modules are used as a fundamental basis for a hierarchical series of attached models: A forecast package called HYSIM (Hydrological Simulation) provides forecasts up to 36 hours in hourly discretisation. A precipitation to runoff model (P2R) with an hourly grid generates hydrological impulses at the Alpine head gauges, reacts on the basis of the fundamental snowmelt / soil moisture model and is an essential input for HYSIM. A combined regression model provides daily mean values with a forecast horizon of 96 hours, ridge regression equations with post processed multilayer perceptions show highest model performance. Neural networks, in combination with regression approaches or Mutual Information Selection complete the modular assembly for nowcasting questions. The variety of models and modules, ranging from the soil moisture / snowmelt basis to the specific nowcasting equation have to be handled by the operational user. A self learning optimisation algorithm provides one single, optimized forecast and its respective uncertainty by weighting the accuracy of the different models in the past. Case studies confirm the importance of inflow forecasting and, stressed in our examples, flood forecasting.

Model Co-Operation: A Holistic Approach

The hydropower-dominated asset structure of VERBUND implies the dependency of production and planning quality to meteorological situations, corresponding runoff responses and its accurate forecasting. A crucial condition for successful online – forecasting is the modular based, holistic framework of the forecast models, based on various methods.

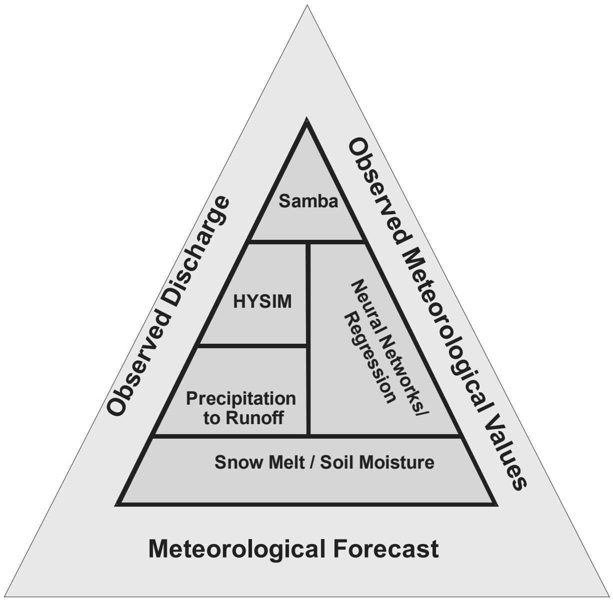

Fig. 1 Hydrological Forecasting at VERBUND: an intergrated, holistic approach under permanent maintenance.

Fig. 1 shows the forecast-system of VERBUND, stressing model cooperation and result consolidation in the module “SAMBA”.

A cooperation with ZAMG, the Austrian meteorological service, ensures the supply of accurate meteorological forecasts. ZAMG provides weighted results of the ECMWF and ALADIN-Vienna forecasts as well as INCA - forecasts (Integrated Nowcasting through Comprehensive Analysis). Each runoff forecast model is supplied by an oracle database including:

- Discharge values at gauging stations from Austrian and German hydrological services.
- Discharge values from Austrian and German hydro power plants.
- Precipitation: Readings from several gauges are combined to areal precipitation in order to reduce the amount of data.
- Areal temperature values at four altitudes, also defined for areas relevant for the VERBUND system (Andrade-Leal *et al*., 2002).
- Precipitation forecasts for selected regions up to 216 hours ahead are provided by ZAMG.

- Temperature forecasts at four altitudes for selected regions up to 216 hours ahead are also provided by ZAMG.

The bottom-up pyramid of hydrological forecasting as part of EEDSS provides:

- A model competition independent from the methodological background
- An integration of soil moisture model memory due to separate model implementation
- The coexistence of hydrological and statistical approaches within one model landscape
- The independence of model outliers due to an integrated, multilayer approach

The **Snowmelt** and **Soil Moisture Model** uses temperature data at different altitudes results based on temperature and precipitation forecasts as well as global radiation, exact topological simulation of the catchment and albedo simulation (Holzmann & Nachtnebel, 2002).

The **Rainfall-Runoff Model P2R** (Precipitation to Runoff) operates at the same layer as the snowmelt / soil moisture model. It is a conceptual model based on the physical basics characterizing the catchment (Hebenstreit, 2000). The result of the snowmelt model – the output discharge - is an essential input for P2R.

The **HYSIM** runoff forecast system is a river basin model consisting of integrated modules. The different modules are calibrated and adjusted to the conditions of the different catchments. For each module the parameters of the hydrological model are estimated online from runoff observations by a recursive Bayes-Kalman-Filter algorithm (Schnatter *et al.*, 1987). Rainfall-runoff modules and flood routing modules are realised (Drabek *et al.*, 2002). Overflowing in inundation areas during floods are described by an additional flood routing ‘inundation’ module, confluence of rivers is described by a superposition model.

Neural Network - Regression - Mutual Information Approach: Forecasting lead time in rainfall runoff and flood routing modules is limited to 36 hours. Operational planning and trading activities often demand longer foresights. We solved this requirement by operating a ridge regression approach and, in many catchments, using a postprocessed multilayer perceptron. Runoff upstream gauging stations, past and observed areal precipitation and temperature of defined regions, meteorological forecasts of rainfall and temperature as well as the results of the snow/soil moisture models were selected by pre - processing regression algorithms, the post – processing multilayer perceptrons with variable net architectures provide online equations. Neural networks, in combination with regression approaches or Mutual Information Selection complete the modular assembly for nowcasting questions, forecasting the next 6 to 12 hours. Especially for intraday trading activities and other operational decisions forecast results with highest accuracy are essential.

SAMBA and the Disposable Energy: The described forecast modules with different lead times and discretisations are combined to a single optimised forecast by an algorithm called SAMBA (Andrade-Leal *et al.*, 2002). SAMBA calculates a probability weighted linear combination of all available forecasts, SAMBA is calibrated permanently, results of calibration indicate directly model accuracy in the forecast lead time. SAMBA calibration allows hourly model evaluation: In the first hours - the nowcasting period up to six hours – Neural Networks in combination with Mutual information show highest performance. The second block - a forecast period up to 20 hours – is characterised by a model dominance of hydrologically based models (HYSIM with P2R) in the SAMBA result. The third block is defined by the best performance of Regression / Neural Network algorithms. The forecast system at gauge

Ybbs has a lead time of 96 hours, beginning with hour 37 only the module Regression / Neural Network is available and can contribute to SAMBA.

Flood Forecasting in Hydropower Industry

The inflow forecast system of VERBUND as a part of an optimisation system has to perform its demand – an accurate forecast of runoff and resulting disposable energy – independently from water levels or meteorological situations. Nevertheless flood events with a significant exceedance of rated power plant discharges provide good examples for the accuracy of our forecast tools and their performance in hydrological risk situations. A current flood event, happened in September 2007 was caused by heavy precipitation in the Danube catchment associated with a stationary low north of the Alps. Danube tributaries in lower Austria faced flood peaks of high intensity, resulting in a statistical 15-years flood event at the Danube. Online-results of the forecast modules provide the basis for the operational decision making process from individual model interpretation to energy stock market activity. The flood-caused exceedance of rated power at the Danube system require optimised decision making. Run –of- river production decrease due to flood situations have to be substituted well timed at the energy market.

CONCLUSIONS

VERBUND, Austria's leading electricity company, generated approximately 85 % of its electricity from renewable hydropower in 2006. It is therefore one of the most environmentally friendly electricity producers in Europe. Optimisation of hydropower energy within the liberalised market targets at optimisation of revenue and the sustainable use of the resource hydropower. A modular forecast system within an Energy Economic Decision Support System (EEDSS) helps to meet these targets. The credit of hydropower as a renewable resource is remarkable, the dependence on physical input parameters as precipitation and snow melt is self evident. In our approach different forecast models compete permanently, a method called SAMBA allows the combination of divergent results, weighing the accuracy in the past. Optimisation and accurate forecasting in different hydrological situations legitimates the permanent operational use with high maintenance costs. Meteorological stress situations as flood events provide evident examples for model accuracy, a flood situation occurring in 2007 is discussed.

REFERENCES

Andrade-Leal, R. N., Drabek, U. & Kirnbauer, R. (2002) SAMBA: Ein selbstkalibrierendes Fehler-System für die Ermittlung einer optimierten Prognoseganglinie und ihres Streubereiches. In: *Proceedings of the XXI. Conference of the Danubian Countries on Hydrological Forecasting and Hydrological Bases of Water Management*. CD-Rom, Bucharest, Romania.

Drabek, U., Kirnbauer, R., Gutknecht, D. & Andrade-Leal, R. N. (2002) Das Durchflussprognosesystem HYSIM als Teil des EPV - Energiewirtschaftliches Planungssystem VERBUND. *VAW Mitteilungen* **174,** 301 – 310. ETH, Zürich, Switzerland.

Hebenstreit, K. (2000) Auswirkungen von Klimaänderungen auf die Hydrologie alpiner Einzugsgebiete. *Wiener Mitteilungen* **160**(5), 19-56, IWHW, Vienna, Austria.

Holzmann, H. & Nachtnebel, H. P. (2002) Abflussprognose für mittelgroße Einzugsgebiete - Methodik und Anwendungen. *Österreichische Wasser- und Abfallwirtschaft* **54**(9-10), 142-153. Springer, Vienna, Austria.

Schnatter, S., Gutknecht, D. & Kirnbauer, R. (1987) A Bayesian Approach to Estimating the Parameters of a Hydrological Forecasting System. In: *Probability and Bayesian Statistics*, 415-422, Plenum Press, London, UK.

Spolwind, R., Hebenstreit, K., Bachhiesl M. & Precht J. (2005) Experience with a combined runoff forecast system in the Austrian Danube Area. Floods, from Defence to Management. In: *Proceedings of the 3rd International Symposium on Flood Defence*. CD-Rom, Taylor & Francis, Leiden, The Netherlands.

Stochastic downscaling for regional precipitation projections

S. P. CHARLES & G. FU
CSIRO Land and Water, Private Bag 5, Wembley, Western Australia 6913, Australia
steve.charles@csiro.au

Abstract The 1.5 million hectares of irrigated agriculture in the Murray-Darling Basin (MDB), southeastern Australia, consume 70% of all water used for irrigated agriculture in Australia. A recent decade of low precipitation, runoff and storage inflows has intensified interest in assessing the impacts of projected climate change. As coarse spatial resolution GCM precipitation is not suitable for direct hydrological prediction, statistical downscaling techniques have been developed to link large-scale atmospheric processes with regional to local scale precipitation. Here we show that the nonhomogeneous hidden Markov model can relate southern MDB multi-site daily precipitation to large-scale atmospheric forcing, informing our understanding of observed precipitation variability and trends. However, when used to produce GCM downscaled projections of future precipitation, concerns are raised due to inadequacies in the GCM's reproduction of atmospheric predictors for the current climate. Future research needs and implications for climate change hydrological prediction and MDB water resource management are discussed.
Keywords climate change; statistical downscaling; GCM; precipitation; uncertainty; regional scale; stochastic; Murray Darling Basin

INTRODUCTION

The highly utilised water resources of the Murray-Darling Basin (MDB), in south eastern Australia, are particularly vulnerable to climate change. This is highlighted by a current decade long drought where low precipitation, decreased year to year precipitation variability, and increasing temperatures have led to significant economic, social and environmental impacts. Van Dijk *et al.* (2006) identified climate change as the major risk to future water availability in the MDB, and the majority of Intergovernmental Panel on Climate Change Fourth Assessment Report (IPCC–4AR) climate models project a decrease in winter precipitation due to modelled enhanced greenhouse forcing (Shi *et al*., 2008). This provides the impetus for developing tools for understanding and quantifying climate change impacts at the catchment scale. This study applies stochastic downscaling, aiming to provide precipitation projections suitable for probabilistic hydrological prediction, and presents an initial assessment of some limitations and uncertainties.

Statistical downscaling (SD) aims to bridge the gap between the coarse scales simulated by global and regional climate models (GCMs and RCMs, respectively) and finer scales required by hydrological models. Useful SD techniques: (1) transfer GCM or RCM climate change scenarios to local or regional scales (often multiple 'points', e.g. rain-gauges) to provide probabilistic projections; (2) aid diagnosis and understanding of observed trends in the inter-relationship between climate and regional precipitation patterns; and (3) allow assessment of climate model performance in terms of the key drivers (predictors) of regional precipitation variability and change. Experience using SD to assess the regional hydrological impacts of projected climate change has been limited (Fowler *et al.*, 2007). Wilby *et al.* (2004) provide guidance in the use of SD for impacts assessment, highlighting important issues concerning the choice of technique, predictor selection and GCM performance. SD techniques need to reproduce observed trends to be used with any confidence for climate change projection and, correspondingly, a GCM or RCM has to adequately reproduce observed predictor characteristics if it is to be used with confidence to drive a SD model.

DATA AND MODELS

Thirty high-quality precipitation stations were selected across the southern MDB (Fig. 1) and modelled using the nonhomogeneous hidden Markov model (NHMM) which relates multi-site daily precipitation occurrence patterns to atmospheric predictors through a small number of discrete "hidden" weather states. A first-order Markov process defines the daily sequence of weather states, with transition probabilities conditional on atmospheric predictors. Calibrated NHMMs are evaluated in terms of weather state physical realism and distinctness, statistical testing to select a parsimonious model, and reproduction of key properties of at-site and inter-site precipitation (Hughes *et al*., 1999). Conditional on the weather states of the NHMM, daily precipitation amounts are modelled as regressions of transformed amounts at a given site on precipitation occurrence at neighbouring sites. This approach captures the mean, variability and inter-site correlations of daily precipitation amounts (Charles *et al*. 1999, 2004).

NHMM calibration was undertaken using 1986–2005 data for April-October 'winter' and November-March 'summer' seasons, with 1958–1985 data reserved for validation (results not shown). Predictors, selected from NCEP/NCAR reanalysis data, for winter were north–south mean sea level pressure (MSLP) gradient, 700 hPa and 850 hPa dewpoint temperature depression (DTD, a measure of relative humidity) and north–south 700 hPa geopotential height (GPH) gradient, and for summer they were MSLP, 700 hPa DTD, and east–west 500 hPa GPH gradient.

For climate change projection, these predictors were extracted from four GCMs for IPCC 20th century runs (1961-2000) and the A2 scenario for 2046-2065 and 2081-2099. The A2 scenario is characterised by continued high level emissions growth and so is at the high end of IPCC scenarios. The four GCMs (CSIRO Mk3.5 and CCAM, GFDL-2.0, and MRI-2.3.2a) were selected from those available based on their ability to reproduce the distributions and seasonal characteristics of the required daily predictors (report available from authors).

EVALUATION AND PROJECTIONS

Extensive evaluation of the NHMM's ability to reproduce multi-site daily precipitation characteristics from 1958 to 2005 confirmed adequate simulation of observed wet-day frequencies, run-length distributions, daily amount distributions, spatial occurrence and amount correlations, and interannual variability (not presented). One benefit of the NHMM is the ability to investigate how observed precipitation trends relate to synoptic-scale atmospheric forcing. Fig. 1 highlights observed changes in the frequencies of dry and wet precipitation occurrence patterns (weather states) for May and June. The corresponding atmospheric predictor time-series (also Fig. 1) show that the May drying trend is associated with a decreasing trend for both north–south MSLP and 700 hPa GPH gradient; whereas the wetting trend in June has the opposite trend for these predictors. Both months show consistency in trends of reducing middle and lower atmosphere relative moisture (increasing 700 and 850 hPa DTD).

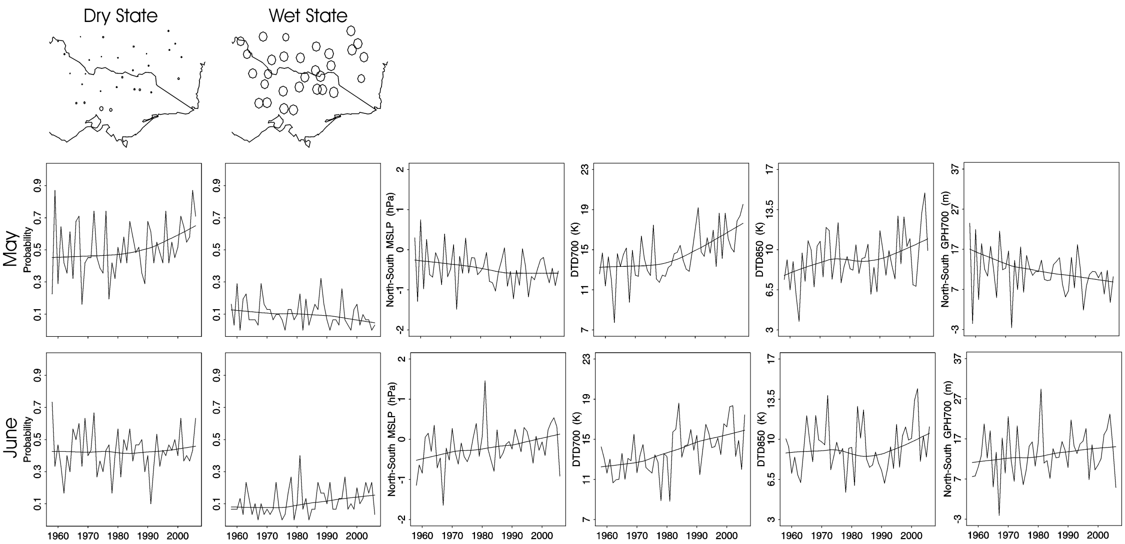

Fig. 1 Probability of precipitation occurrence at the 30 stations for dry and wet weather states (top row, probability is proportional to the size of circle) and time-series for corresponding weather state probabilities, and four atmospheric predictors, for May (middle row) and June (bottom row). Smoothed line is a loess fit. Note that the winter NHMM has 5 weather states with only the driest and wettest presented.

For multi-model downscaling from the four selected GCMs, the projected annual precipitation for the A2 scenario is summarised in Fig. 2. For the observed record there is obviously just one realisation whereas for the downscaled simulations 50 realisations were generated stochastically by the NHMM, conditional on the single predictor series extracted from the NCEP/NCAR reanalysis and the four GCMs.

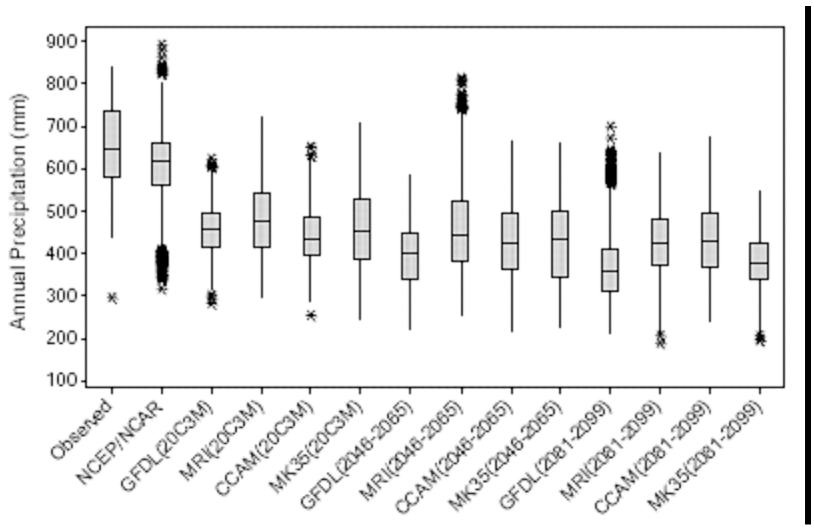

Fig. 2 Observed and downscaled annual precipitation for 30 southern MDB stations for the SRES A2 scenario. Observed, downscaled reanalysis (NCEP/NCAR) and downscaled 20th century GCM runs (20C3M) use 1981-2000. The boxes represent the interquartile range and the stars are outliers.

The underestimation bias for the 20th century GCM downscaled results are of significant concern, a result of less frequent simulation of the wet weather state. Given that GCM selection was based on reasonable reproduction of the probability density functions and seasonal cycles of the required predictors, this highlights the importance of continued assessment of GCM predictor quality at each step of a SD investigation.

Analysis is on-going to determine which GCM predictor properties are responsible for this wet state frequency underestimation. This bias obviously limits confidence in the use of GCMs to drive the NHMM for this region. Other studies, e.g. for southwestern Australia, have highlighted a seasonal bias in GCM current climate predictors and resultant downscaled precipitation (Charles *et al.*, 2007).

Overall the uncertainty between the A2 scenario and A1B and B1 (not shown) is less than the uncertainty between the different GCMs. This is a similar result to other recent studies, see e.g. Fowler *et al.* (2007) and references therein. Research is on-going to assess sub-annual and subregional variation and the relationship between SD uncertainty and resultant hydrological prediction uncertainty.

CONCLUSIONS

The NHMM can produce stochastic realisations of precipitation reproducing observed multi-site daily precipitation characteristics and thus is potentially of use in hydrological modelling. However provision of hydrologically relevant precipitation projections is compromised by GCM predictor biases, causing the underestimation of precipitation when downscaling from multiple GCMs for current climate.

Thus this initial assessment is limited to comparing *relative* trends of downscaled precipitation projections, highlighting a consistent drying trend that will have significant implications for water management in the MDB, which is the subject of on-going research. Future SD development needs to focus on predictor selection, GCM validation, and quantification of uncertainty. Collaboration between the climate, SD, and hydrological modelling communities should aim to provide probabilistic hydrological projections with better quantification of uncertainty.

Acknowledgements This research was part funded by the South Eastern Australia Climate Initiative and the eWater Cooperative Research Centre, Australia. Thanks are due to Neil Viney and Freddie Mpelasoka for reviewing the manuscript.

REFERENCES

Charles, S. P., Bates, B. C. & Hughes,. J. P. (1999) A spatio-temporal model for downscaling precipitation occurrence and amounts. *Journal of Geophysical Research* **104,** 31657 – 31669.

Charles, S. P., Bates, B. C., Smith, I. N. & Hughes, J. P. (2004) Statistical downscaling of daily precipitation from observed and modelled atmospheric fields. *Hydrological Processes* **18,** 1373 – 1394.

Charles, S. P., Bari, M. A., Kitsios, A. & Bates, B. C. (2007) Effect of GCM bias on downscaled precipitation and runoff projections for the Serpentine catchment, Western Australia. *International Journal of Climatology* **27,** 1673-1690.

Fowler, H. J., Blenkinsop, S. & Tebaldi, C. (2007) Linking climate change modelling to impacts studies: recent advances in downscaling techniques for hydrological modelling. *International Journal of Climatology* **27,** 1547-1578.

Hughes, J. P., Guttorp, P. & Charles, S. P. (1999) A non-homogeneous hidden Markov model for precipitation occurrence. *Journal of the Royal Statistical Society: Series C (Applied Statistics)* **48,** 15-30.

Shi, G., Ribbe, J., Cai, W. & Cowan, T. (2008) An interpretation of Australian rainfall projections. *Geophys. Res. Lett.*, **35,** L02702,doi:10.1029/2007GL032436.

Van Dijk, A., Evans, R., Hairsine, P., Khan, S., Nathan, R., Paydar, Z., Viney, N. & Zhang, L. (2006) Risks to the Shared Water Resources of the Murray-Darling Basin, Murray-Darling Basin Commission, Canberra.

Wilby, R. L., Charles, S. P., Zorita, E., Timbal, B., Whetton, P. & Mearns, L. O. (2004) Guidelines for Use of Climate Scenarios Developed from Statistical Downscaling Methods. http://www.ipcc-data.org/guidelines/dgm_no2_v1_09_2004.pdf. *Supporting material to the Intergovernmental Panel on Climate Change*, 27pp.

Modelling water availability from a snow influenced basin in central Chile under past scenarios of climate change

A. OSSES & X. VARGAS

División Recursos Hídricos y Medio Ambiente, Departamento de Ingeniería Civil, Facultad de Ciencias Físicas y Matemáticas, Universidad de Chile. Casilla 228/3, Santiago, Chile

xvargas@ing.uchile.cl

Abstract The aim of this study is to compare water availability obtained using a hydrological simulation model considering averaged and individual meteorological input series of SRES A2 and B2 downscaled scenarios from years 1980 to 2005, generated from HadCM3 general circulation model for a mountainous catchment located in central Chile. If averaged series of mean daily temperature and daily evaporation are used as inputs of the hydrologic model, results are not statistically different from those obtained with individual series of these variables. By other hand, if the average precipitation series is used as input of the hydrological model, the resulting flows are significantly different from those obtained with individual series. In conclusion, the flow generated with the averaged series of the generated weather variables show an overestimation of the discharge and a poor statistical relationship with the observed values (1980-2005), being a poor approach to assess the water availability. Better results can be obtained using individual series of downscaled precipitation. Neither A2 nor B2 scenarios of climate change seem to have occurred during the censored period.

Keywords climate change; water availability; modelling

INTRODUCTION

Assessing water availability at a local scale in a reliable way is nowadays challenge, especially when different future scenarios of climate change are possible. Possible scenarios of climate change can be obtained from simulations made in centres especially dedicated to the study of these changes, being one of these the Hadley Centre for Climate Prediction and Research from UK. In this study we use climate predictions for two scenarios generated by the Hadley Centre through the HadCM3 atmosphere-ocean global circulation model (GCM) to obtain forcing meteorological variables for hydrological models. To transfer this data to the local scale is possible to use different techniques. This study explores a statistical downscaling technique and intends to verify the occurrence of these scenarios during the censored period. Also results of modelled discharge using average or individual downscaled series of precipitation are analyzed for the snow influenced basin, El Yeso.

"El Yeso" reservoir is located in the Andes Mountains (2450 amsl) at "Piuquenes" valley 100 km from Santiago, Chile's capital; The reservoir was built all through 1953 and 1967 as one of the sources of drinking water supply for the city. The climate in this region is characterized by relative warm summers (14.4ºC, mean) and cold winters (2.9ºC mean), with temperature under 0°C low as -9ºC. The precipitation is concentrated in winter and falls mostly as snow.

The water availability assessment is achieved through downscaling of the weather-impacted variables that are used subsequently as inputs of the hydrological model to simulate the basin discharge. The hydrological model selected for the study was Sacramento model coupled with a snow model based in degree-day approach. This model was calibrated and validated using observed available daily data from years 1980 up to 2005. We assessed the climate change scenarios performance in the registration period by comparing observed data (1980-2005) and simulated flows using climate change scenarios with averaged and single downscaled series

MODEL CALIBRATION AND VALIDATION

The implemented hydrological Sacramento-Snow17 model was calibrated using the available daily data of temperature, evaporation and precipitation, from year 1980 to 1986 and validated from year 1986 to 1989 and 2000 to 2005. It is important to note that, because the basin area has only one weather station, the model considers the uncertainty of the observed lapse rate to represent the spatial and temporal variability of the weather input variables (Muñoz & Vargas, 2006).

As it is seen in Fig. 1, simulated monthly values are close to observed values in the calibration period (Nash-Sutcliffe coefficient, NS, is 0.83) but during validation period there is a low adjustment especially at the end of the period (NS ranges from 0.86 to 0.25). This was attributed to a change in the measurement procedure of meteorological variables and a new calibration of the parameters associated to those input variables was performed; the final result is also presented in Fig. 1 and shows a better representation of data with an increase of efficiency criteria (NS=0,59).

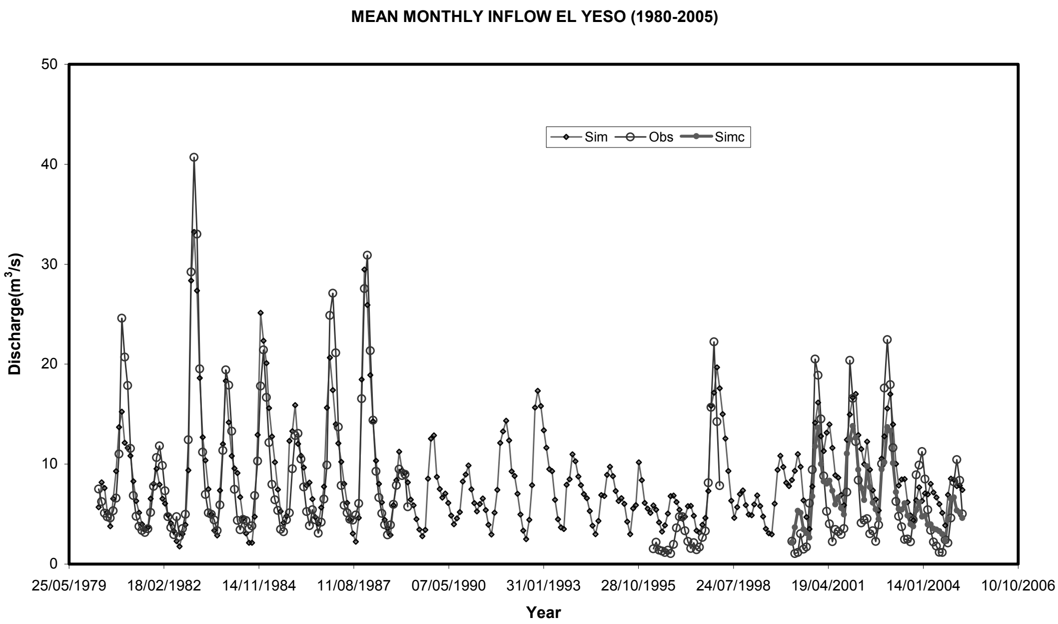

Fig. 1 Observed (Obs) mean monthly inflow to El Yeso reservoir and modelled mean monthly flow calibrated in period 1980-1986 (Sim) and recalibrated in period 2000-2005 (Simc).

CALCULATION OF DISCHARGE FOR RECENT CLIMATE CHANGE SCENARIOS A2 AND B2

Through statistical downscaling, using the software SDSM 3.1 (Wilby *et al.*, 2004), we evaluated the effect of regional changes in three climate variables (temperature, precipitation and evaporation). The downscaling was done using the results from HadCm3 global circulation model and the historical data series of the climate variables from 1980 to 2000. The analysis of downscaled weather variables for the censored period (Osses & Vargas, 2007) showed good agreement for the monthly mean temperature and evaporation values observed at the weather gage station; however, monthly precipitation, especially high values, are not detected. For scenarios A2 and

B2, Osses & Vargas (2007) propose the use of any set of the single series of daily precipitation, evaporation or mean temperature generated by the program SDSM 3.1 but they also show that the average series of mean daily temperature or daily evaporation are statistically indistinguishable with the single series; therefore these average series can also be used in modelling. Finally, they indicate that if there is a climate change scenario, B2 scenario is more similar to observed meteorological variables.

The comparison between basin discharge observed data (1980-2005) and simulated discharge under climate change scenarios using average and single series of precipitation were used to assess the climate change scenarios performance in the censored period. Figs 2 and 3 illustrate the results for SRES A2 and B2, respectively.

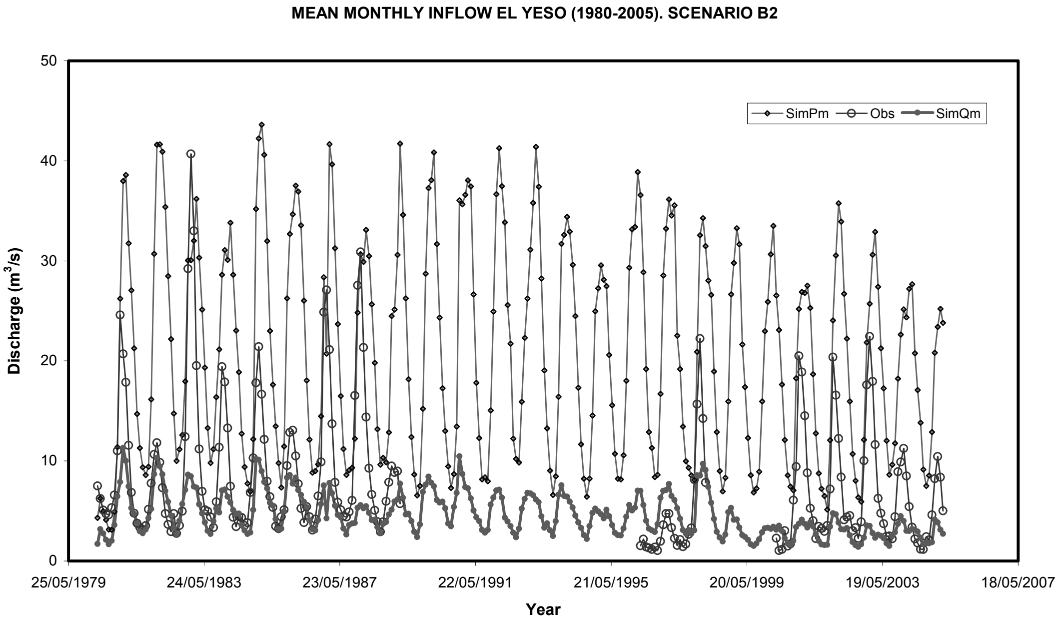

Fig. 2 Observed (Obs) mean monthly inflow to El Yeso reservoir and modelled under B2 scenario using average (SimPm) precipitation series and average (SimQm) of modelled mean monthly flow using single precipitation series as inputs.

These figures indicate that for scenarios A2 and B2 the discharge is greater than observed values if the averaged precipitation series are used as input but lower if the single precipitation series are used. For the first cases the probability of storm events in the basin is near 55 percent, much greater than the 12 percent observed value. The probability of snowfall is near 10 percent, value that is close to the observed value of 6.3 percent. By other hand, when single series of precipitation are used, the probability of storm events is close to 7.5 percent and the probability of snowfall is near to 1.5 percent, being both values a little higher for A2 scenario.

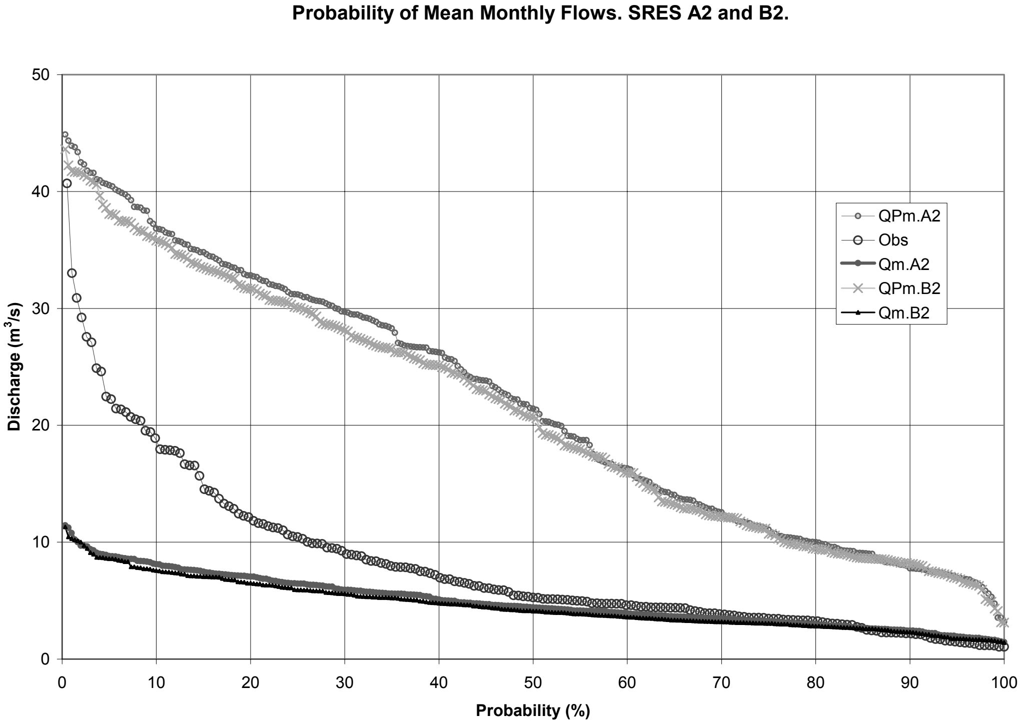

Fig. 3 Probability of Observed (Obs) mean monthly inflow to El Yeso reservoir and modelled under B2 and A2 scenarios using mean (QPm) precipitation series and average (Qm) of modelled mean monthly flows using single precipitation series as inputs.

CONCLUSIONS

As expected, results obtained indicated that when the average precipitation series is used as input of the hydrological model, the resulting flows are significantly different from those obtained with the single series.

Results obtained for both, SRES A2 and B2, scenarios are comparable and significantly different from the observed discharge. Consequently, neither of these two scenarios has been occurring in this basin.

To state the former conclusion, regional atmospheric models should be used as an alternative procedure for obtaining downscaled meteorological variables.

Acknowledgements The assistance and support of Rodrigo Herrera, civil engineering student and the data support by Aguas Andinas are acknowledged.

REFERENCES

Osses, A.. & Vargas, X. (2007) Análisis de Escenarios de Cambio Climático en el Período 1980-2005 en la Cuenca del Embalse El Yeso. In: *Analysis of Climate Change Scenarios during 1980-2005 for El Yeso Reservoir Basin*, XVII Chilean Congress of Hydraulics, Santiago, Chile.

Muñoz, R. & Vargas, X. (2006) Escalamiento Espacial con error aleatorio en variables de entrada al modelo de simulación hidrológica Sacramento. In: *Spatial distribution with random error of Sacramento hydrological model input variables*, XXII Latin-American Congress of Hydraulics, IAHR, Venezuela.

Wilby, R. L. & Dawson, C. W. (2004) Using SDSM Version 3.1: A Decision Support Tool for the Assessment of Regional Climate Change Impacts, User Manual. Available at https://co-public.lboro.ac.uk/cocwd/SDSM/

Predictions for snow cover, glaciers and runoff in a changing climate

ALBERT RANGO[1] & JAROSLAV MARTINEC[2]
1 *USDA-ARS Jornada Experimental Range, 2995 Knox St., Las Cruces, New Mexico 88003, U.S.A.*
alrango@nmsu.edu

2 *CH-7270 Davos-Platz, Switzerland*

Abstract The problem of evaluating the hydrological effects of climate change has opened a new field of applications for snowmelt runoff models. The Snowmelt Runoff Model (SRM) has been used to evaluate climate change effects on basins in North America, the Swiss Alps, and the Himalayas. Snow covered area depletes about one month earlier in response to warmer temperatures (+4°C) with runoff peaks shifted accordingly. Runoff will be higher in winter at the expense of summer runoff. In glacerized basins, runoff is not only redistributed, but increased due to glacier melting. This improved knowledge facilitates long-term decisions concerning hydropower, flooding, water allocations, and water management in general.
Keywords climate change; snowmelt runoff modelling; runoff shifts; water management

NEW TASKS FOR SNOWMELT RUNOFF MODELS

The growing awareness of the problem of climate change opened a new field of applications for snowmelt runoff models. Originally designed to simulate and forecast the seasonal runoff, they should now be capable to predict snow cover and runoff in a distant future. Thanks to its deterministic approach, the SRM model has been easily adapted to this new task. In the present climate, it is run with the real seasonal snow cover monitored by satellites as one of the input variables. In a future climate, this snow cover is transformed by changed temperatures and precipitation according to any given climate scenario, so that the future runoff can be computed. The necessary amendments to the computer program were facilitated by the transparent structure of the model which had been made possible by taking into account the role of the subsurface runoff (Martinec & Rango, 1999). As has been pointed out by other investigators (e.g. Klemeš, 1985) hydrological models which depend on calibration of their parameters are not suitable for evaluations of the climate change effect. In the meantime, such studies have been carried out by the non-calibrated SRM model in different climate zones of North America, the Swiss Alps, and the Himalayas.

HYDROLOGICAL EFFECTS OF CLIMATE CHANGE

The effects of global warming, combined in some cases with changed precipitation, were evaluated in a wide range of basin size and altitude, as illustrated in Table 1. Various climate types are represented so that the runoff coefficient (runoff/ precipitation ratio in a hydrological year) varies from 0.25 in Rio Grande, 0.57 in Kings River and to 0.78 in Illecillewaet. With the exception of the Himalayan basins, runoff is dominated by snowmelt so that it occurs mostly in the summer half of the hydrological year (April-September).

Table 1 Characteristics of basins.

Country	Mountain Range	Basin	Size km^2	Elevation Range
U.S.A., Colorado	Rocky Mountains	Rio Grande	3419	2432-4215 m a.s.l.
U.S.A., California	Sierra Nevada	Kings River	4000	171-4341 m a.s.l.
Canada, British Columbia	Rocky Mountains	Illecillewaet	1155	509-3150 m a.s.l.
Switzerland	Alps	Upper Rhine	3249	562-3425 m a.s.l.
India, Bangladesh	Himalayas	Brahmaputra	547346	0-8848 m a.s.l.
India, Bangladesh	Himalayas	Ganges	917444	0-8848 m a.s.l.

Consequently, the hydroelectric plants, for example, in the European Alps and in Scandinavia, accumulate water in the summer and release it in the winter in order to meet the electricity demands. The situation is different in the U.S.A. with regard to the extensive use of air conditioning in summer. In any event, it is important for future reservoir operations to predict how the present runoff regime will be affected by the climate change, and in particular by global warming.

The present and climate-affected runoff volumes are compared in Table 2. The runoff computed with the present temperatures "T" agrees well with the measured runoff corrected for reservoir operation or water diversion (Rango & Martinec, 2000).

Table 2 Redistribution of runoff in a warmer climate.

Basin	October-March		April-September		Hydrological Year	
	10^6 m^3	%	10^6 m^3	%	10^6 m^3	%
Rio Grande 1979						
Computed T	91.87	7.6	1120.15	92.4	1212.02	100
Computed T+4°	146.76	12.3	1046.16	87.7	1192.92	100
Rio Grande 1976						
Computed T	93.22	13.1	616.52	86.9	709.74	100
Computed T+4°	192.95	28.1	494.80	71.9	687.75	100
Rio Grande 1977						
Computed T	63.56	24.3	198.17	75.7	261.71	100
Computed T+4°	77.34	29.2	187.42	7.8	264.76	100
Illecillewaet 1984						
Computed T	169.29	10.2	1495.56	89.8	1664.85	100
Computed T+4°	341.63	18.9	1465.32	81.1	1806.95	100
T+4°. P + 20%	383.55	18.3	1717.06	81.7	2100.59	100
T, P + 20%	185.91	9.5	1769.01	90.5	1954.92	100
Kings River 1973						
Computed T	428.78	17.1	2080.53	82.9	2509.33	100
Computed T+4°	973.66	37.2	1642.67	62.8	2616.33	100
Upper Rhine T, P, adapted for 1961-1990						
Winter: T + 2.1°, P+5%	872	22.5	3010	77.5	3882	100
Summer: T + 2.4°, P-10%	970	28.0	2491	72.0	3461	100

In a warmer climate, the winter runoff will be increased at the expense of the summer runoff. The magnitude of this effect varies from basin to basin and, as data for Rio Grande show, also from year to year (Rango & Martinec, 2000). In the Illecillewaet basin, a comparison of three hypothetical climate scenarios reveals that the annual runoff will increase in a warmer climate due to glacier melt (as long as glaciers last) and increase further should precipitation (P) become higher. The effect of P + 20% is greater than that of T+4°. In the Rhine basin, temperature and precipitation have been adapted for the period 1961-1990 in order to represent today's climate better than a single year (Ehrler, 1998).

In the Himalayan basins (Seidel & Martinec, 2002), the major concern is summer floods. In a warmer climate, for example T+4° C, an increase of peak flows by 20-30% is indicated.

EVALUATION OF CLIMATE EFFECTS BASED ON A NORMALIZED YEAR

As data for Rio Grande in Table 2 show, results for these selected years point in the same direction (more runoff in winter), but are also influenced by specific conditions (snow covered areas, temperatures, precipitation) in each year. The present climate is better characterized by a "normalized" year, in which temperatures and precipitation correspond to long term averages (1957-1994), but their daily variations are taken over from a real year by the updated SRM computer program (Martinec *et al*., 2008). When the year 1979 in the Rio Grande basin is normalized (designated as 9979) the effect of a temperature increase T+4° C is greater than with the year 1979 (see Tables 2 and 3):

Table 3 Redistribution of runoff with the use of a normalized year.

Basin	October – March		April – September		Hydrological year	
	10^6 m^3	%	10^6 m^3	%	10^6 m^3	%
Rio Grande 9979						
Computed T	74.66	11.7	561.66	88.3	636.32	100
Computed T+4°	153.06	24.2	479.58	75.8	632.64	100

As a prediction of runoff conditions in a future year, these data are more realistic because the original year 1979 was unusual in two respects:

1. Extremely cold winter reducing the effect of a warmer climate.
2. Very high precipitation and snow accumulation resulting in a high runoff.

Runoff volumes in Tables 2 and 3 are totals of daily computed flows. The runoff peak is shifted from May to April. Each evaluation also predicts the future water equivalent of the seasonal snow cover on 1 April and the depletion curves of the snow covered areas in the subsequent months.

CLIMATE EFFECTS IN GLACIERIZED BASINS

The runoff increase in the Illecillewaet basin due to glacier melt with T+4° (Table 2) was computed with the present glacier area. However, this area will gradually decrease before the climate scenario will take place. Therefore the effect of a changed climate cannot be evaluated in one step. Glaciers must be modelled year by year using a stochastic series of temperatures and precipitation which reach the value of a climate scenario in the year in question. In the starting year, the depletion curves of the snow coverage and the glacier area must be known as well as temperatures and precipitation. From the computed glacier melt volume, the reduced glacier area for the next year is estimated by statistically derived relations between the volume and area of glaciers (Bahr *et al*., 1997). With this new glacier area, plus temperature and precipitation data, the glacier melt volume and the reduced glacier area for the next year are calculated. In a cold year, which can occur even in a warming climate, unmelted snow may prevent glacier melt and is carried over to the subsequent hydrological year. Sooner or later, the glacier melt will start again and the computation of the glacier decline can continue until the target year of the climate scenario or until he disappearance of glaciers, whichever comes first.

TEST OF PREDICTION RELIABILITY

Unlike weather or runoff forecasts, predictions of the hydrological effects of climate change, referring for example to the year 2100, cannot be compared with reality within a reasonable time. Therefore, the method was tested by "predicting" snow conditions and runoff not for a distant future year, but for an actual year with measured data.

Table 4 Runoff volumes in the Rio Grande basin.

Runoff	October-March	April-September	Hydrological Year
	10^6 m^3	10^6 m^3	10^6 m^3
Computed 1979	91.87	1120.15	1212.02
1977 Predicted by changed climate	49.92	244.05	293.07
1977 Measured	76.26	190.37	266.63

Daily temperatures and precipitation in 1977 were used as a changed climate for 1979 to "predict" the snow conditions and runoff in 1977. Data in Table 4 are a comparison between prediction and reality.

CONCLUSION

Modelling and prediction of the future climate-affected snow cover, of the decline of glaciers and of changed runoff regimes provide essential information for hydropower production, flood control, winter sport resorts, water allocation, and generally for water management.

REFERENCES

Bahr, D. B., Meier, M. F. & Peckham, S. D. (1977) The physical basis of glacier volume / area scaling. *Journal of Geophysical Research* **102**(B9), 20355-20367.

Ehrler, C. (1998) Climate change and alpine snow cover. *NFP 31*, ETH Zurich, Switzerland.

Klemeš, V. (1985) Sensitivity of water resources systems to climate variations. *WCP Report No. 98*, WMO Geneva.

Martinec, J. & Rango, A. (1999) Snowmelt runoff conceptualization based on tracer and satellite data. *IAHS Publ. No. 258*. 47-55.

Martinec, J., Rango, A. & Roberts, R. (2008) Snowmelt Runoff Model (SRM) User's Manual (7th Edition). *New Mexico State University, Agricultural Experiment Station, Special Report* 100, Las Cruces, NM. USA

Rango, A. & Martinec, J. (2000) Hydrological effects of a changed climate in humid and arid mountain regions. *World Resources Review*. **12**(3) 493-508.

Seidel, K. & Martinec, J. (2002) NOAA/AVHRR monitoring of snow cover for modeling climate-affected runoff in Ganges and Brahmaputra rivers. EARSeL Workshop Bern, Switzerland, *EARSeL eProceedings* **2**.

The role of ENSO in the characterization of drought in Australia

GERALDINE WONG[1], ANDREW V. METCALFE[1] & MARTIN F. LAMBERT[2]

1 *School of Mathematical Sciences, The University of Adelaide, SA 5005, Australia*
geraldine.wong@adelaide.edu.au

2 *School of Civil and Environmental Engineering, The University of Adelaide, SA 5005, Australia*

Abstract Drought is a common feature of Australia's climate and the effects are damaging to the economy. The El-Niño Southern Oscillation (ENSO) is a global climatic phenomenon that is related to the climatic index, the Southern Oscillation Index (SOI) and is often associated with extreme weather conditions in Australia. This phenomenon is known to have an impact on rainfall over the eastern coast of Australia. This paper looks at incorporating the SOI in April and May to improve the prediction of June to October rainfall in neighbouring districts in Australia. Appropriate marginal distributions are fitted to district rainfall and the multivariate dependence structure between these variables is modelled through a copula. Copulas are multivariate uniform distributions, which allow for the dependence structure to be modelled independently of the marginal distributions. Separate copulas are fitted to historical data, segregated according to their SOI states, and their parameters are estimated by the Maximum Likelihood Estimation (MLE) method. Statistical tests demonstrate there is statistical significant difference between the fitted copulas in the different SOI state. The method is general and can be applied with other climatic indices, such as the Interdecadal Pacific Oscillation (IPO), which may affect the occurrence of drought.
Keywords drought; copulas; Southern Oscillation Index; marginal distributions

INTRODUCTION

Over the past century, drought has been prevalent in Australia and has caused economic loss and social hardship. Many studies explored the relationship between climatic indicators and rainfall and drought in Australia (Chiew, 1998; Stone, 1996), so that adequate water resource infrastructure and management can be planned well in advance to reduce their effects.

Due to its location, Australia's variable rainfall is largely connected to the Southern Oscillation Index (SOI). The SOI is a commonly used indicator for the El-Niño Southern Oscillation (ENSO), and persistently negative values of the SOI often occur during El-Niño episodes. The Troup SOI is defined as the difference in atmospheric pressure anomalies between Tahiti and Darwin, divided by the standard deviation of the difference and multiplied by 10.

The winter cropping season in eastern Australia is from June to October. The aim of this study is to predict June to October rainfall in two neighbouring districts in the New South Wales (NSW) state by modelling the association between them and the SOI with a trivariate Gumbel copula. The concept of copulas will be introduced and fitted to historical data. Separate copulas are fitted according to the SOI state in the preceding month and simulations obtained from the respective copulas are analysed. The copula is conditioned on the April SOI and the aim is to predict drought risk from the April and May SOI, before crops are sown.

STUDY AREA AND DATA

The Australian Bureau of Meteorology (BOM) divides the country into 99 relatively homogeneous rainfall districts. In this paper, June to October rainfall from District 62 (Central Tablelands north) and District 64 in NSW, from 1913 to 2002 are used. The monthly SOI data used here is obtained from the Queensland Government Long

Paddock website.

COPULAS

A n-dimensional copula is a multivariate distribution function defined on the unit cube $[0,1]^n$, with uniform marginals. There exists an n-copula, C, with univariate marginal distributions $F_1,\ldots,F_n$ and joint distribution function, F, such that

$$\begin{aligned} F(x_1,\ldots,x_n) &= P(X_1 \le x_1,\ldots,X_n \le x_n) \\ &= C(F_1(x_1),\ldots,F_n(x_n)) \\ &= C(u_1,\ldots,u_n) \end{aligned} \tag{1}$$

where $F_k(x_k) = u_k$ for $k = 1,\ldots,n$ and U_k follows the uniform distribution $U(0,1)$. The copula allows for the correlation structure of the n-dimensional multivariate distribution to be modelled separately from its univariate marginal distributions.

Different copula families exist, of which the Archimedean copulas are typically used in hydrology due to their versatility in modelling dependence structure and have the following form for the bivariate case

$$C(u_1,u_2) = \varphi^{-1}\left[\varphi(u_1) + \varphi(u_2)\right] \tag{2}$$

where φ is the generator of the copula. Most drought studies, of which we are aware have concentrated on using the symmetric Archimedean copulas to model the dependence structure between 2 variables (Shiau, 2006). However, when there are more than 2 variables, this form of copula is unrealistic, because the correlations between any pairs of variables are identical as a result of symmetry from the construction of the copula. The asymmetric copula is thus introduced to overcome this constraint.

Within the Archimedean copula family, the Gumbel copula is chosen for this drought analysis due to its ability to model upper tail dependence (Wong, 2007). The Gumbel copula is defined by its generator $\varphi(t) = (-\ln t)^{\theta}$, where $\theta \ge 1$ is the dependence parameter between variables. In this study, the trivariate Gumbel asymmetric copula will be fitted to the sum of June to October rainfall in both Districts 62 (u_1) and 64 (u_2) and the SOI in May (u_3) and is given as

$$\begin{aligned} C(u_1,u_2,u_3) &= \varphi_1^{-1}\left(\varphi_1\left\{\varphi_2^{-1}\left[\varphi_2(u_1) + \varphi_2(u_2)\right] + \varphi_1(u_3)\right\}\right) \\ &= \exp\left[-\left\{\left[(-\ln u_1)^{\theta_2} + (-\ln u_2)^{\theta_2}\right]^{\theta_1/\theta_2} + (-\ln u_3)^{\theta_1}\right\}^{1/\theta_1}\right] \qquad \theta_1 \le \theta_2 \end{aligned} \tag{3}$$

Parameters θ_1 and θ_2 are estimated by Maximum Likelihood Estimates (MLE) (Joe, 1997). θ_2 measures the highest correlation between any pair of variables. θ_1 measures the dependence between the rainfall sum in District 62 and SOI May, and similarly the dependence between rainfall sum in District 64 and SOI May. θ_2 measures the dependence between the rainfall sum between District 62 and 64. The correlations between u_1 and u_3 and u_2 and u_3 are equal as a consequence of the construction of the asymmetric copula, which attempts to average out the weaker correlations.

APPLICATION

Negative values of SOI are linked to El-Niño events in Australia, which often result in droughts. This SOI relationship can be used to effectively predict drought risk.

Trivariate Gumbel copulas fitted with different dependence parameters, conditioned on the SOI in April are obtained. Data triplets are segregated into 2 groups; given the value of SOI April is positive (+ve) or negative (-ve). Table 2 provides the basic statistics of the variables in the 2 groups and Table 3 shows the correlations between variables in the 2 groups.

There is a general decrease in mean June to October rainfall when SOI April is negative in both Districts 62 and 64. The mean of SOI May is also positive, when SOI April is positive. The correlations between all variables in SOI April negative state is overall higher compared to in the positive state.

Marginal distributions are fitted to each of the variables, for both SOI April states, and transformed to uniform variables. Let the uniform variables of District 62 rainfall, District 64 rainfall and SOI May be u_1, u_2 and u_3 respectively in Equation (3). The parameters for the trivariate copula for each SOI state and their standard errors given in brackets are shown in Table 4. The dependence parameters in the SOI April negative state are noticeably higher than during the positive state. This can be attributed to the higher correlations observed in Table 3 in SOI April negative state.

In order to assess whether the trivariate copula fitted in the SOI April positive state is significantly different from the negative state, statistical significance tests at the 5% level are performed on the estimates of the dependence parameter θ. The test statistics for testing the hypotheses of the equality of parameters in the two SOI states are 1.38 for θ_1 and 1.96 for θ_2, which corresponds to p-values of 0.18 and 0.05 respectively. Results indicate that there is very strong evidence that θ_2 is higher during the SOI April negative state than positive state. There is also weak evidence that θ_1 is higher in SOI April negative than positive state. These results justify allowing for different dependence parameters during different climatic conditions.

Table 2 Means and standard deviations of copula variables.

	District 62 June-Oct rainfall sum		District 64 June-Oct rainfall sum		SOI May	
	SOI April -ve	SOI April +ve	SOI April -ve	SOI April +ve	SOI April -ve	SOI April +ve
Number of droughts	50	40	50	40	50	40
Mean	237.4	262.6	226.2	239.1	-2.7	3.5
Standard deviation	110.8	83.7	120.6	70.5	10.1	7.1

Table 3 Correlations between variables given SOI April state.

Correlations	SOI April +ve	SOI April -ve
District 62 rainfall, District 64 rainfall	0.91	0.93
District 62 rainfall, SOI May	0.11	0.37
District 64 rainfall, SOI May	0.10	0.31

Simulations of length 100,000 are generated for the three variables from the appropriate trivariate Gumbel copula given SOI April state. Table 5 displays the correlations between pairs of simulated variables. The correlations obtained from the simulations are almost similar to the correlations of the historical data. This suggests that the fitted trivariate copulas in both SOI states are adequate in modelling the dependence structure of the historical data. Simulations from these copulas are used to generate the distribution of June to October rainfall in District 62 and 64 given the SOI in April and May and this is shown in Fig. 1.

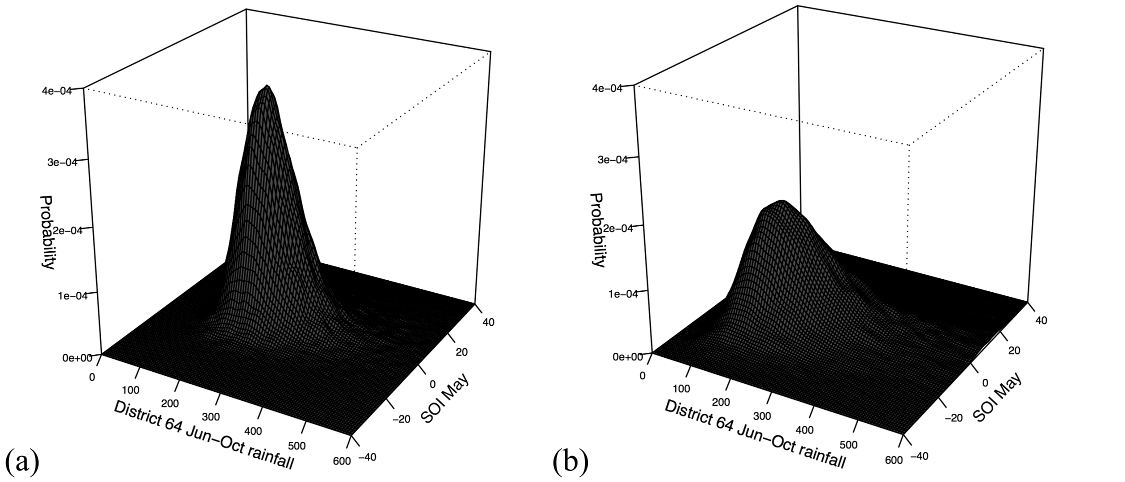

Fig 1. Probability plots of June to October rainfall in District 64 and SOI May during (a) SOI April +ve state; and (b) SOI April –ve state.

The distribution plots here can be used to derive the probability of obtaining a certain amount of rainfall in this district given the SOI state in preceding months. Consequently, the Standardized Precipitation Index (SPI) equivalent of this amount of rainfall can be calculated and used to assess whether this district is in drought, if the SPI value falls below the threshold of -1.

CONCLUSIONS

Results from this study show that copulas can provide a description of rainfall in neighbouring rainfall districts in terms of the preceding SOI. Furthermore, June to October rainfall in neighbouring districts can be explained using the SOI May. These predictions improved when the SOI April is incorporated in the construction of the copula. Hence, to improve drought modelling through the use of rainfall predictions from copulas, global climatic indices such as the SOI should be considered.

Table 4 Dependence parameters of trivariate Gumbel copula given SOI April state.

Parameter	SOI April +ve	SOI April -ve
$\hat{\theta}_1$	1.04 (0.09)	1.26 (0.13)
$\hat{\theta}_2$	3.21 (0.41)	4.52 (0.52)

Table 5 Correlations between simulated variables given SOI April state.

Correlations	SOI April +ve	SOI April -ve
u_1, u_2	0.87	0.93
u_1, u_3	0.057	0.31
u_2, u_3	0.057	0.31

REFERENCES

Chiew, F. H. S, Piechota, T. C., Dracup, J. A. & McMahon, T. A. (1998) El Niño/ Southern Oscillation and Australian rainfall, streamflow and drought: Links and potential for forecasting. *Journal of Hydrology* **204**(1), 138-149.

Joe, H. (1997) Multivariate models and dependence concepts. *New York: Chapman & Hall*

Longpaddock website (http://www.longpaddock.qld.gov.au/SeasonalClimateOutlook/SouthernOscillationIndex/SOIDataFiles/index.html)

Accessed on September 2007.

Shiau, J. T. (2006) Fitting Drought Duration and Severity with Two-Dimensional Copulas. *Water Resources Management* **20**, 795-815.

Stone, R. C., Hammer, G. L. & Marcussen, T. (1996) Prediction of global rainfall probabilities using phases of the Southern Oscillation Index. *Nature*. **384**, 252-255.

Wong, G., Metcalfe, A. V., Lambert, M. F. (2007) Trivariate copulas for characterisation of droughts. *ANZIAM Journal.* **49**, C289-C306.

Hydrological impact of climate change on a complex basin: from data collection to conceptual model formulation

MAURICIO ZAMBRANO & ALBERTO BELLIN
Department of Civil and Environmental Engineering, Università di Trento, Via Mesiano #77, Trento, I-38100, Italy
mauricio.zambrano@ing.unitn.it

Abstract This ongoing work examines the formulation process of the conceptual model for a large basin, with multiple and competing water uses, in order to assess the hydrological impact of climate change. In order to achieve an in-depth understanding of the overall system, long-term series of different kinds of data were gathered from the local water authority. Spatial information about river networks, hydrogeological units, land use, basin elevations, water transfers and withdrawals has been acquired as shapefile and raster maps. Temporal data series about the main anthropogenic water uses has been also collected. Observed data are used for selecting theories and temporal/spatial scales that best suit to this kind of problem. Preliminary results include: a) main trends in the local climate; b) variables that will be used as a link between the downscaled climate and the hydrological model; c) selection of the variables that will be used to determine the agreement between the measurements and the results; and d) conceptual model.
Keywords climate change; hydrological impact; Ebro River; data collection; conceptual model

BACKGROUND INFORMATION

This ongoing work examines the formulation process of the conceptual model for a large basin, with multiple and competing water uses, in order to assess the long-term hydrological impact of climate change. The Ebro River basin (NE of Spain, 85362 km^2) is drained by the Ebro River, through a roughly plain central valley, from the Cantabrian Mountains to its delta in the Mediterranean Sea. Significant influence of snow retention is observed in the Pyrenees. Precipitation, besides its scarcity, presents a strong inter-monthly and inter-annual irregularity. Three large groundwater areas are distinguished: pyrenean, alluvial and iberian, with different regulation capacity (Oficina de Planificación Hidrológica, 2005).

Within the Ebro basin exists more than 350 reservoirs, ponds and natural lagoons. Reservoirs make the hydrological modelling difficult, because their regulation perturbs the natural flow regime. Although most of the analysed reservoirs have a good data record, their effect on the hydrological regime is hard to predict, because their behaviour changes according to variations in the relationship between water availability and demand. More than 380 hydropower plants give rise to attenuation of high streamflows, while low flows are increased. Irrigation systems roughly cover a 10% of the total area of the basin, and the agricultural use reduces streamflows downstream the withdrawal point, whereas irrigation returns increase the expected flows during the irrigation period (May to September). The impact of more than 90 fish farms on flow regime is expected to be small in comparison with the effect of reservoirs and irrigation uses (Oficina de Planificación Hidrológica, 2000).

DATA

Spatial information about river networks, hydrogeological units, land use, basin elevations, water transfers and withdrawals has been acquired as shapefile and raster maps. Hydrological time series has been mainly downloaded from the Confederación Hidrográfica del Ebro (CHE) web site: www.chebro.es, and they include: daily water flows for 445 stations, daily and monthly precipitations in 1557 stations, daily and monthly minimum and maximum temperature for 848 stations, monthly mean computed evapotranspiration for 402 stations, snow density and depth for 112 poles 2-3 times a year, and monthly/quarterly piezometric heads for 263 points. The temporal extension and reliability of collected data varies between stations (1900-2007), and from one kind of measurement to another.

OBSERVED TRENDS

As a first approach for detecting long-term trends in the precipitation and temperature time series, the nonparametric Mann-Kendall technique (Burn, 1994; Wesmacott & Burn, 1997) was applied to gauge stations, located in different subcatchments and with different elevations, with a 5% of significance level, to total and mean monthly values of precipitation and temperature, respectively. Additionally, a 3 years moving average were computed for each one of the previous series, as a way of "visually" observe possible trends.

Table 1 Results of Mann-Kendal test on precipitation and temperature stations, with a 5% of significance level.

Variable	Station	Mann Kendall at 95%	MK Zc
Precipitation	9971	Accepted Ho	-1.41
Precipitation	9492	Accepted Ho	0.08
Precipitation	9491	Accepted Ho	-1.54
Precipitation	9269	Accepted Ho	-0.20
Precipitation	9037	Accepted Ho	0.10
Precipitation	9041	Accepted Ho	-0.72
Precipitation	9562	Accepted Ho	0.71
Precipitation	9136	Accepted Ho	1.16
Precipitation	9451	Accepted Ho	-0.52
Temperature	9971	Accepted Ho	-0.05
Temperature	9492	Accepted Ho	1.23
Temperature	9491	Accepted Ho	1.63
Temperature	9269	Accepted Ho	0.13
Temperature	9037	Accepted Ho	-0.38
Temperature	9041	Accepted Ho	0.04
Temperature	9562	Accepted Ho	0.83
Temperature	9136	Accepted Ho	-0.36
Temperature	9451	Accepted Ho	-1.38

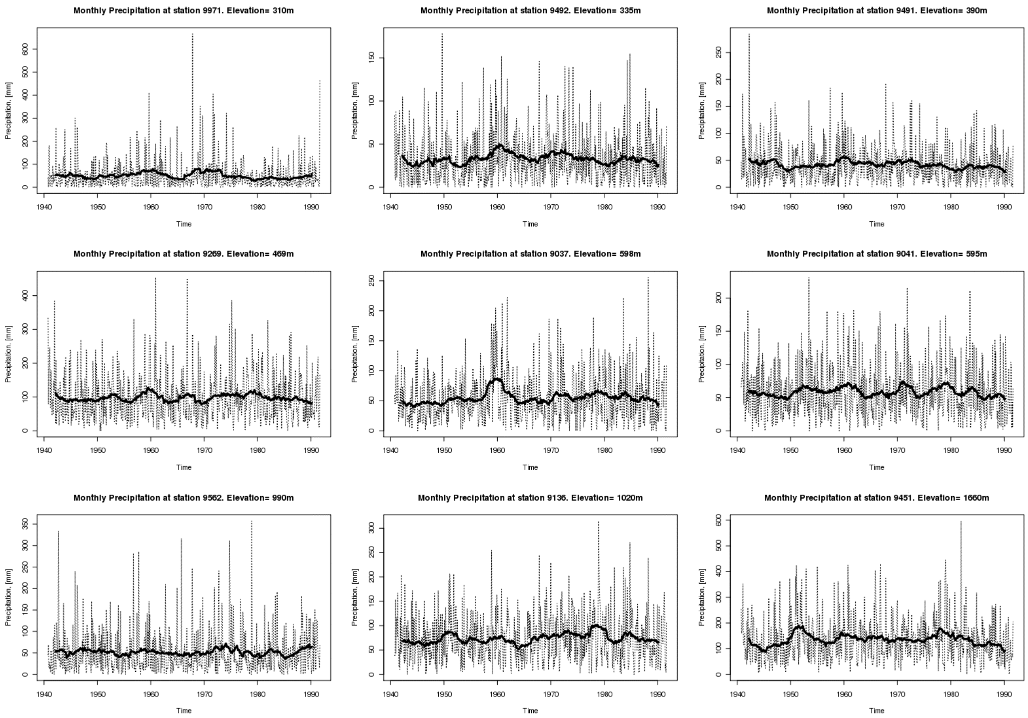

Fig. 1 Monthly precipitation series (dotted line), with a 3 years moving average (black solid line).

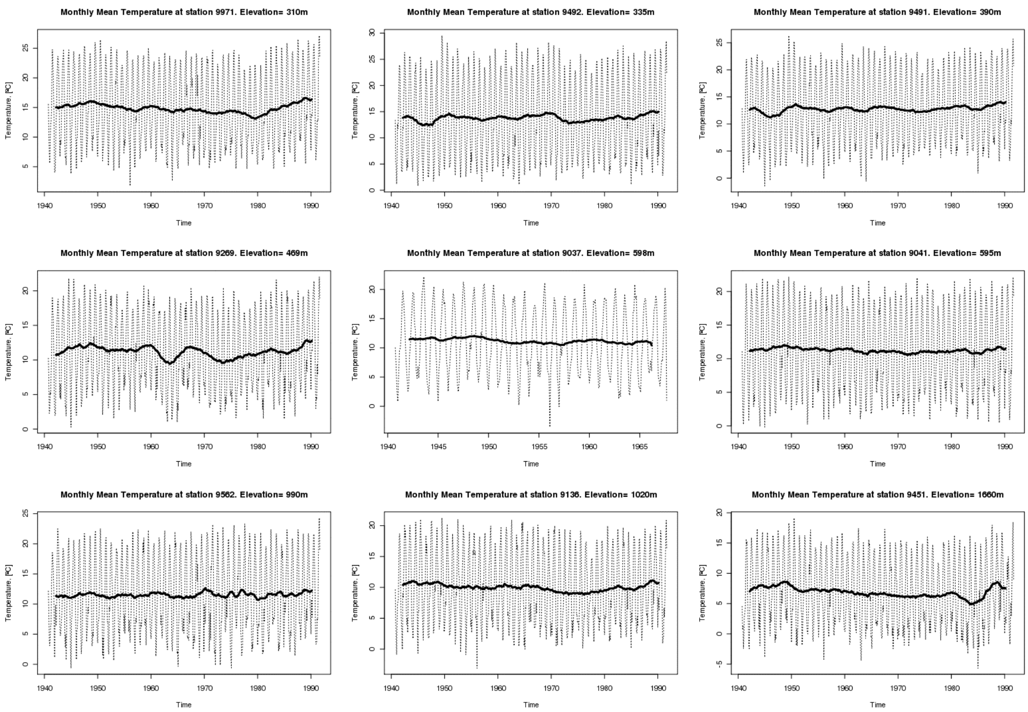

Fig. 2 Monthly mean temperature series (dotted line), with a 3 years moving average (black solid line).

CONCEPTUAL MODEL FORMULATION

The presence of different climatological regimes and different types of groundwater regulation has lead to the formulation of a conceptual model with two (at the moment) different model structures (as a way to deal with the model structure uncertainty), because the performance of a model structure might vary according to the response mode of the of the modelled system (Shamseldin *et al*., 1997). The approach that will be used for combining the output obtained with different model structures into a single prediction will be decided in the short term. The size of the basin, and the intense anthropogenic impact have lead to the selection of a semi-distributed modelling approach (so far, Majone *et al*., 2006), where the main basin is divided into homogenous morphological units, and their behaviour is represented through a limited number of parameters, with daily time steps for simulations but a monthly scale for calibrations. So far, only stream flows will be used for the calibration of the hydrological model, but the inclusion of piezometric heads and delivery of the reservoirs will be decided during the computational implementation.

Once the hydrological model be calibrated for the historical scenario (1961-1990), the impact of climate change will be assessed using downscaled climate scenarios, with daily point precipitations and temperature (2030-2100), provided by the University of Newcastle, for being used as driving forcings for the hydrological model.

CONCLUSIONS

No trend could be proved according the Mann-Kendall test neither for total monthly precipitation nor mean monthly temperature. Significant difficulties found are: a) the high anthropogenic impact on this basin, which turns into a real challenge the development of a conceptual model that could represent all the interactions on the basin; b) the large amount of available information, which converts the data analysis and management into a laborious and complex task; c) file format and organisation of original data are designed mainly for storing and performing analysis of individual stations, making difficult and time-consuming to use them with a global perspective or managing it as a whole.

Aknowledgments: This work is carried out within the context of the European Union FP6 Integrated Project "AquaTerra" under the thematic priority "Sustainable development, global change and ecosystems". The assistance and support of people from the Confederación Hidrológica del Ebro are acknowledged.

REFERENCES

Burn, D. (1994) Hydrologic Effects of Climate Change in West-Central Canada. *J. Hydrol*. **160,**53-70.

Majone B., Alberici D., Bertagnoli A. & Bellin A. (2006) Structural uncertainty assessment of hydrological models: the semidistributed model GEOTRANSF. In: Eos Trans. AGU **87**(52), Fall Meet. Suppl., Abstract H44D-04: 2006 AGU Fall Meeting", San Francisco (USA), 11-15 December, 2006. URL: http://www.agu.org/meetings/fm06/waisfm06.html.

Oficina de Planificación Hidrológica. Confederación Hidrográfica del Ebro. (2005) Implantación de la Directiva Marco del Agua: caracterización de la demarcación y registro de zonas protegidas (Introduction of the Water Framework Directive: characterization of the demarcation and register of the protected areas).

Oficina de Planificación Hidrológica. Confederación Hidrográfica del Ebro. (2000) Los Aprovechamientos en la Cuenca del Ebro: Afección en el Régimen Hidrológico Fluvial. (Withdrawals in the Ebro River Basin: Impact on the Hydrological Fluvial Regime). 2000-PH-24.I.

Shamseldin, A. Y., O'Connor, K. M. & Liang, G. C. (1997) Methods for combining the outputs of different rainfall runoff models. *J. Hydrol*. **197**, 203.229.

Westmacott, J. R. & Burn, D. H. (1997) Climate Change Effects on the Hydrologic Regime within the Churchill-Nelson River Basin. *J. Hydrol.*. **202**, 263-279.

http://www.chebro.es/.

Modern climate changes and channel network formation in Terek delta

IGOR ZEMLIANOV[1], OLGA GORELITS[1] & VLADIMIR KRYJOV[2]

1 *State Oceanographic Institute (SOI), 6, Kropotkinsky per., Moscow, 119034, Russia.*
isys_lab@geocentre.ru

2 *State hydrometeorological centre of Russia (HMC), 11-13, B.Predtechensky per., Moscow, 123242, Russia.*
kryjov@yahoo.co.uk

Abstract Modern changes of hydrological conditions in Terek delta occur on a background of global climate changes. The climate warming and increase of humidity cause the activization of erosion processes in Terek watershed, the essential increase of the water runoff and sediment load. The observational data in the Terek drainage basin over the recent 50 years has shown that against the background of the general tendency of increasing in the mean annual air temperatures, the annual sums of precipitation also increase. The main factors of Terek delta channel network formation are considered. The results of complex monitoring of the delta are presented, including the land-based observations at the gauge stations, prompt analysis of the remote sensing data, and the field inspections of the present state of the main delta branch and its seasonal dynamics

Keywords river delta formation; hydrological regime; flooding; runoff distribution; remote sensing

INTRODUCTION

According to experts WMO the steady tendency of increase of material losses and vulnerability of a society because of increasing influence of the dangerous natural phenomena now is marked. Flooding are one of most frequently repeating natural acts, they quite often surpass all other extreme situations in the area of inundated territories and damage for population. In 2002 and 2005, catastrophic floods, largest for last 50 years occurred in the River Terek basin (Gorelits *et al*., 2005, 2006). They caused flooding of vast areas in the river delta and inflicted a huge damage to the environment and economy of the region. In high waters vast areas were flooded; dwelling houses, bridges, and other constructions were destroyed; several-kilometer segments of protective levees and dams were washed away; ten thousand hectares of agricultural grounds were inundated, the settlements located in zones of flooding have suffered.

The Terek delta is one of the most dynamic deltas on the marine coast of the South of Russia, it was forming cyclically, the duration of each full cycle of delta formation averaging 50-70 years. That high intensity of delta formation, which persists at present time as well, is due to a unique combination of natural and anthropogenic factors that govern the hydrologic-and-morphologic processes in the Terek delta (Zemlianov *et al*., 2007).

Researches which SOI spend together with HMC since 2002 in Terek delta, testify, that the reason of these catastrophic flooding are modern features of development of hydro-morphological processes in delta of Terek and the tendency of climatic changes in the extensive territory including Terek drainage basin. At the present stage in Terek delta there were conditions for existence of constant threat of flooding during high waters period.

RESULTS

Modern changes of hydrological conditions in Terek delta occur against the background of global climatic changes. The general warming and wetting leads recent years to increase water runoff and activization of erosion and washout on the Terek drainage basin located on northern slopes of the Great Caucasus, causing thereby essential increase in water discharges and sediment load arriving to the Terek delta top.

For research of tendencies of climatic parameters changes (air temperature and precipitations) at the Terek drainage basin data of meteorological supervision on stations of Federal Hydrometereology and Environmental Monitoring Service and net data CMAP (CPC Merged Analysis of Precipitation), Xie &. Arkin (1996, 1997), are used. The analysis of change of annual mean air temperatures during 1960-2006 is spent according to meteorological stations (MS), located at the Terek basin at different elevation (Fig.1).

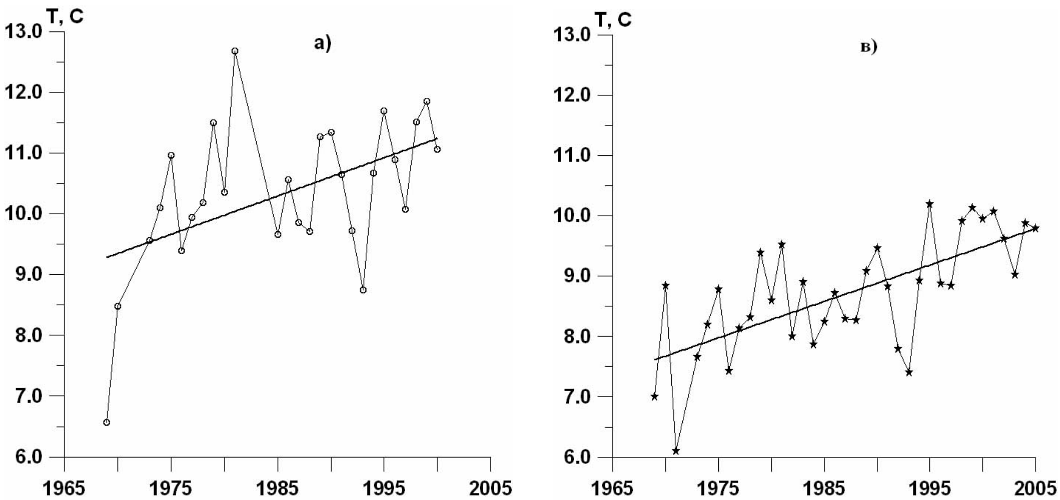

Fig. 1 Annual mean air temperatures at the Terek drainage basin.
a – lowland (MS Mozdok), в – hills (MS Vladikavkaz).

For the analysis of tendencies of wetting changes at the Terek basin are used average pentad precipitation data CMAP during the 1979-2006 received by merging seven kinds of individual input data sources, Xie & Arkin (1996, 1997). These input data sets include the gauge data (the GPCC gauge-based analyses over land and the atoll gauge data over ocean), 5 sets of different satellite estimates. Precipitation fields generated by the NCEP/NCAR reanalysis are also utilized as an additional source. These data allow not only to reveal interannual and seasonal changes of precipitations in the Terek basin, but also to allocate the short-term heavy shower caused by passage of storm fronts. The analysis of average pentad precipitation data at the Terek basin has allowed indicating the periods of sharp increases of Terek water runoff, connected with increase of repeatability and duration of heavy showers (Fig. 2).

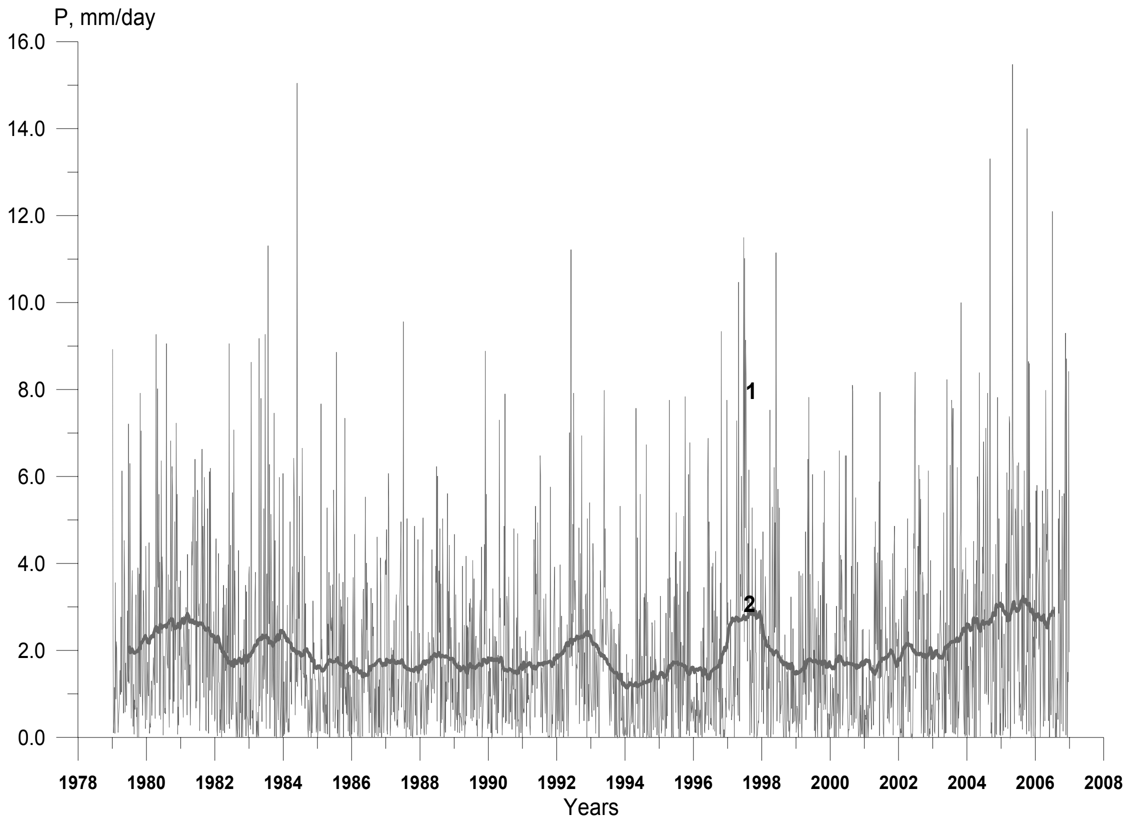

Fig. 2 Average pentad precipitation data at the Terek basin (1) and annual running average (2).

Since 2002, the State Oceanographic Institute has been performing a program of complex monitoring the Terek mouth area (Gorelits *et al*., 2004). In 2002-2007, fourteen specialized seasonal field studies were carried out in order to assess the present-state of the Terek delta. Parallel to hydrologic studies, specialized ground-truth reconnaissance surveys are carried out for deciphering the data of remote sensing of the Earth from space, the data having various spatial-temporal resolutions. Remote sensing data received by Terra, Landsat-7, IRS, Radarsat satellites were used in complex monitoring program. The estimation of inundated areas dynamics during floods of 2002 and 2005 were received by daily remote sensing data of middle resolution (Terra/Modis).

The results of complex monitoring have shown that by the beginning of the XXI century, the conditions in the Terek delta were ripe for the start of a new cycle of delta formation (Gorelits *et al.*, 2004, 2005, 2006; Zemlianov *et al.,* 2007). The catastrophic floods of 2002 and 2005 could have triggered a new stage of the delta evolution. However, because of the anthropogenic interference, instead of the natural start of the successive cycle of delta formation, at present we observe the continuation of the current Kargalinsky cycle that began in 1914.

Due to the hydrologic-and-morphologic conditions developed in the lower part of the Terek delta, the stage of a few-branch superimposed-attached delta, which generally completes the cycle of delta formation, did not terminate by its dying off. After the floods in 2002 and 2005, a new stage of the revival and development of a multi-branch superimposed delta began on the territory of the former delta, which had existed till the cut-off Prorez was constructed.

A unique feature of this process in the Terek delta is the simultaneous processes of regenerating the old channel network, which was separated and died off after the

Prorez had been constructed, and forming the new network of diversion water courses, permanent and temporal. When the high floods of 2002 and 2005 were passing, the temporal channel network was intensely involved into the process of runoff distribution and reduced the flood loading on the main branch channel. During 2-3 high-water seasons, the largest temporal water streams become permanent. The reserve capacity of Southern Agrakhan Bay and the runoff through Northern Agrakhan Bay into the Caspian Sea provide the natural regulation in the lower part of the delta. After the catastrophic floods in 2002 and 2005, specialists of SOI and HMC recorded (for the first time after the Prorez had been opened) the regeneration of the mechanism of natural runoff distribution which was similar in terms of its nature to the runoff distribution in the multi-branch deltas (Gorelits *et al*., 2006).

CONCLUSIONS

The investigations in 2002-2006 have shown that one of the most efficient solutions of the problem of the flood water conveyance in the lower part of the Terek delta is the reduction of the load on the main branch channel by way of construction of new artificial tracts for water flow, along with the use of the natural network of delta water courses. In the short- and medium-term prospect, the hazard of breakthroughs and inundations in the Terek delta can be reduced by way of operative runoff redistribution over the entire delta area, in order to decrease the water discharges and sediment load through the main branch. The use of regulating capacities of the Northern and Southern Agrakhan Bay makes it possible to cut off the flood peaks; also, these conveyance capacities are very important for the Terek delta ecological state.

Acknowledgements This study was supported by Russian Foundation for Basic Research (projects №06–05–65205 and №07-05-00533).

REFERENCES

Gorelits, O. V., Zemlyanov, I. V. & Pavlovsky, A. E. (2004) Satellite Monitoring of Seasonal Processes in Marine River Mouths. A New Line of Investigations. *Tr. Gos. Okeanogr. Inst.* **209**, 374–405.

Gorelits, O. V., Zemlyanov, I. V., Pavlovsky, A. E., Artemov A. K & Yagotintsev V. N. (2005) Catastrophic Flood in Terek Delta in June–July 2002. *Meteorol. Gidrol.* **5**, 62–71. (in Russian).

Gorelits, O. V., Zemlyanov, I. V., Pavlovsky, A. E. & Illaev T. S. (2006) Channel deformations and runoff redistribution within the Terek river mouth area after the catastrophic flood of 2002. *Vodn. Resur.* **33**(6), 654-662 [*Water Resour.* (Engl. Transl.) **33**(6), 677-685]. (in Russian).

Zemlianov, I. V., Gorelits, O. V.,.Postavik, P. V, Pavlovsky, A. E. & Sapozhnikova A. A. (2007) Modern tendencies in Terek delta formation. In: *"Research of oceans and the seas ",* Moscow. *Proc.SOI* **210**, 253-264. (in Russian)

Xie, P. & Arkin, P. A.. (1996) Analyses of global monthly precipitation using gauge observations, satellite estimates, and numerical model precipitations*. J. Clim.* **9**, 840 – 858.

Xie, P. & Arkin, P. A. (1997) Global Precipitation: A17-year monthly analysis based on gauge observations, satellite estimates and numerical model outputs*. Bull. Amer. Meteor. Soc*..**78**, 2539 – 2558.

Simulation of water resource and its relation to urban activity in Dalian City, northern China

T. NAKAYAMA, T. FUJITA, Y. GENG & S. HASHIMOTO
Asian Environment Research Group, National Institute for Environmental Studies (NIES), 16-2 Onogawa, Tsukuba, Ibaraki 305-8506, Japan
nakat@nies.go.jp

Abstract The NIES Integrated Catchment-based Eco-hydrology (NICE) model was applied to the Biliu River Catchment, Northern China, in order to estimate the water resources there. The model reproduced well the water/heat budget after the construction of reservoir in the middle reach of the river. The model also backcasted the degradation of water resources such as river discharge and groundwater after the completement of Biliu reservoir in the middle of the catchment. The simulated results are very effective for evaluating the linkage between the innovative urban development in the Dalian City and the sustainable water resource management.
Keywords water stress; urban; ecosystem degradation; reservoir; NICE model

INTRODUCTION AND BACKGROUND INFORMATION

Water stress in northern China has intensified water use conflicts between upstream and downstream areas and also between agriculture and municipal/industrial sectors (Nakayama *et al*., 2006). Biliu River Catchment (2814 km^2) is located in the south part of Liaoning province, a heavy industrial base in northeast China. This river is one of the largest rivers in the south part of this province, with a total length of 156 km, and the primary water source for Dalian City with over six million population and thousands of industries. Most of the necessary water in this city is transferred from the Biliu Reservoir at the middle of this river by some water pipelines because this area is one of the most water-scarce areas in China. This region has changed from water-rich in the past to water-poor area after the completement of the dam, which indicates various ecosystem degradations such as dry-out of the river, groundwater degradation, seawater intrusion, and various ecosystem degradations. Therefore, how to meet the water demands of its swelling urban and industrial sectors without undermining both its own agriculture and the local ecosystem is the biggest challenge for the local government. The objective is to evaluate the linkage between the innovative urban development in the Dalian City and the sustainable water resource management in the Biliu River Catchment.

DEVELOPMENT OF NICE MODEL

The authors have so far developed the process-based model, called NIES Integrated Catchment-based Eco-hydrology (NICE) model (Nakayama, 2008a, 2008b; Nakayama & Watanabe, 2004, 2006a, 2006b, 2008a, 2008b; Nakayama *et al*., 2006, 2007), in various catchments of East Asia (Fig. 1). The NICE includes surface-unsaturated-saturated water processes and assimilates land-surface processes describing variations of *LAI* (leaf area index) and *FPAR* (fraction of photosynthetically active radiation) derived from MODIS satellite data. The NCE connects several sub-models from the ground to the surface by considering water/heat fluxes, for example, (i) the gradient of hydraulic potential between the deepest layer of unsaturated flow and the groundwater level, (ii) effective precipitation calculated from the precipitation rate, infiltration of precipitation into the upper soil moisture store, and evapotranspiration rates, and (iii) seepage between river and groundwater. Details have been described in Nakayama & Watanabe (2004, 2006b).

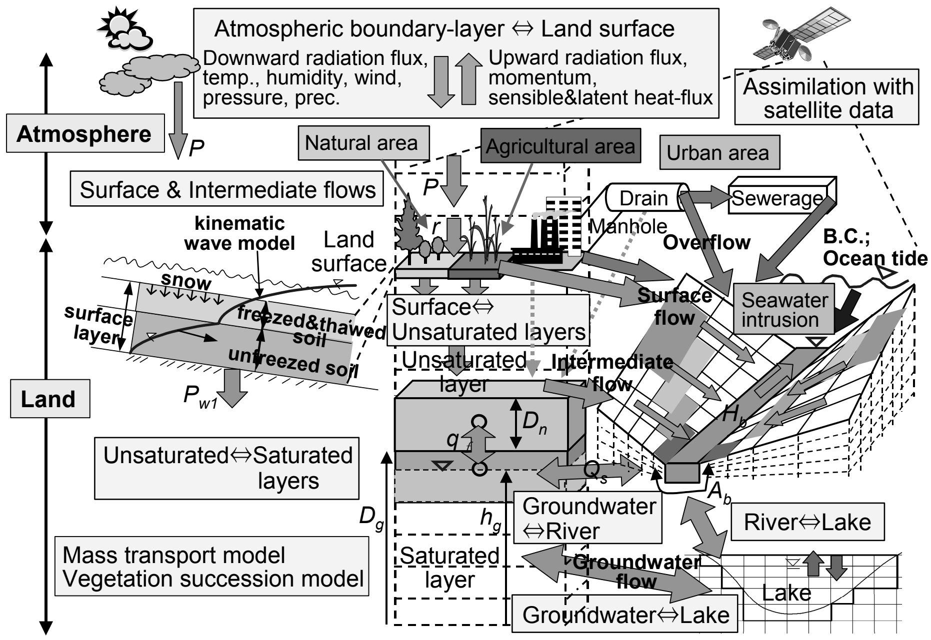

Fig. 1 NIES Integrated Catchment-based Eco-hydrology (NICE) model.

SIMULATION OF HYDROLOGIC BUDGET IN BILIU RIVER CATCHMENT

The mean elevation of each 1-km grid cell was calculated by using the spatial average of a global digital elevation model (DEM; GTOPO30) with a horizontal grid spacing of 30 arc-seconds (approximately 1-km mesh) (U.S. Geological Survey, 1996) throughout the Biliu River Catchment. Vegetation class and soil texture were categorized and digitized into 1-km mesh data by using the Vegetation and Soil Maps of China (1:4,000,000) (Chinese Academy of Sciences, 1988). These finer-resolution data were more accurate than the ISLSCP data with a resolution of 1° ´ 1° (Sellers *et al.*, 1996). Digital landcover data produced by the Institute of Remote Sensing Applications (IRSA) at the Chinese Academy of Sciences (CAS) based on Landsat TM data from the early 1990s (Liu, 1996) were categorized into 1-km mesh data for the simulation (Fig. 2). Details were written in Nakayama & Watanabe (2008b). Forests, grasses, and bushes cover the mountainous and hilly areas in the upper region of the catchment. Cultivated field is widely distributed in the valley and the lower regions. The construction of Biliu Reservoir at the middle of the river was completed in the 1980s, where most of the water resources have been transferred to the Dalian City by the pipeline. The drying of the downstream river has occurred the environmental degradation, such as groundwater decrease and seawater intrusion, *et al*. there.

The NICE model was applied to the catchment (60 km wide by 110 km long) with a resolution of 1 km for two years during 2005-2006 (Fig. 3). The simulated river discharges reproduce excellently the observed values in the catchment. In particular, the discharge at the downstream of Biliu Reservoir is greatly affected by the water transfer there to the Dalian City. Because there were no available observation data at the downstream of the reservoir, the authors analytically evaluated the outflow discharge from the reservoir by using the simple method of the hydrologic budget (Nakayama & Watanabe, 2008a). This budget-derived value underestimates the simulated value, which is mainly by ignoring surface runoff and groundwater seepage to the reservoir. These results indicate that the simulation is very effective for evaluating the linkage between the innovative urban development in the Dalian City and the sustainable water resource management.

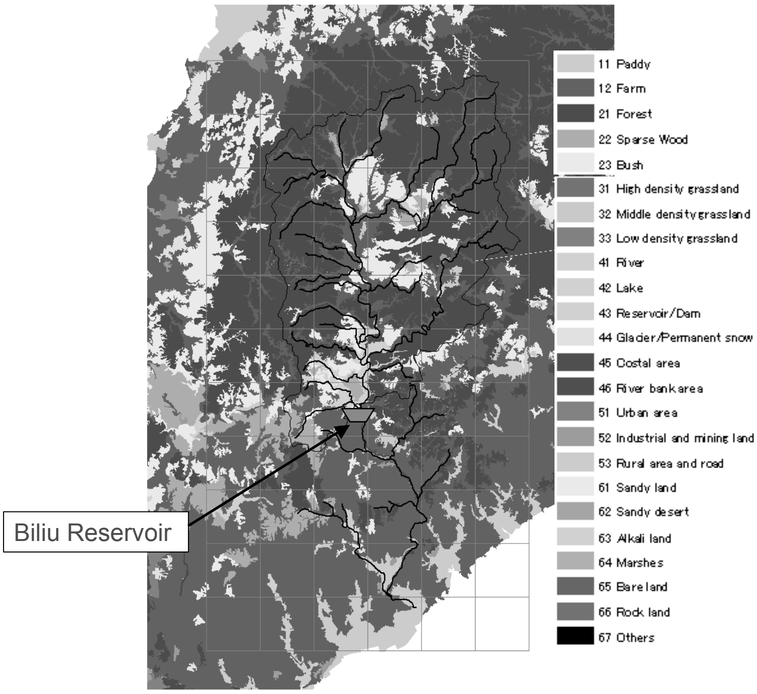

Fig. 2 Landcover in the Biliu River Catchment.

CONCLUSIONS

The authors analytically evaluated the hydrologic budget in the reservoir in order to estimate the relation between the water transfer and the outflow from the dam. The NIES Integrated Catchment-based Eco-hydrology (NICE) model reproduced well river discharge, groundwater level, evapotranspiration, and crop productivity, *et al*. Furthermore, the model backcasted the groundwater degradation after the completement of Biliu reservoir in the middle of the catchment. The simulation also clarified that this water shortage is related to little flow discharge to the Yellow Sea. Finally, the authors conducted forecast simulation in order to clarify whether the dilemmas between water stress and ecosystem degradation would diminish more or less in the future.

Acknowledgements This work was partly funded by the Ministry of the Environment (MOE) of Japan. Some of the simulations in this study were run on an NEC SX-6 supercomputer at the Center for Global Environment Research (CGER), NIES.

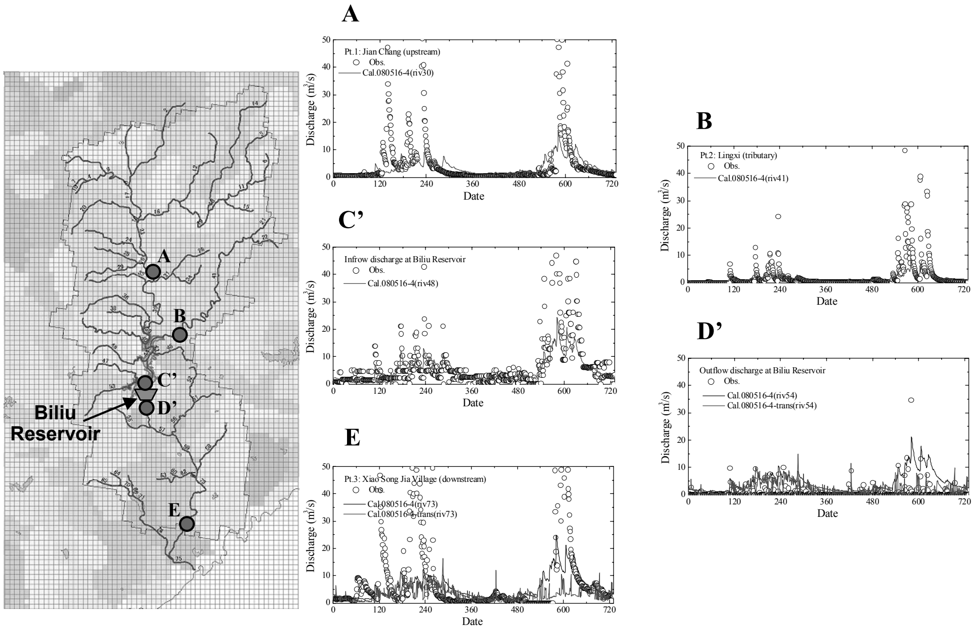

Fig. 3 Simulated results of river discharge in the catchment (2005-2006).

REFERENCES

Chinese Academy of Sciences (1988) Administrative division coding system of the People's Republic of China. *Beijing*.

Liu, J. Y. (1996) Macro-scale survey and dynamic study of natural resources and environment of China by remote sensing. *Chinese Science and Technology Publisher*, Beijing, China (in Chinese).

Nakayama, T. (2008a) Factors controlling vegetation succession in Kushiro Mire. *Ecol. Model.*, doi: 10.1016/j.ecolmodel.2008.02.017.

Nakayama, T. (2008b) Simulation of Ecosystem Degradation and its Application for Effective Policy-Making in Regional Scale. In: *River Pollution Research Progress* (ed. by Mattia N. Gallo & Marco H. Ferrari), Nova Science Publishers, Inc., New York (in press).

Nakayama, T., & Watanabe, M. (2004) Simulation of drying phenomena associated with vegetation change caused by invasion of alder (Alnus japonica) in Kushiro Mire. *Water Resour. Res.* **40**, W08402, doi: 10.1029/2004WR003174.

Nakayama, T., & Watanabe, M. (2006a) Simulation of spring snowmelt runoff by considering micro-topography and phase changes in soil layer. *Hydrol. Earth Syst. Sci. Discuss.* **3**, 2101–2144.

Nakayama, T., & Watanabe, M. (2006b) Development of process-based NICE model and simulation of ecosystem dynamics in the catchment of East Asia (Part I). *CGER's Supercomputer Monograph Report 11*, NIES, 100 pp., http://www-cger.nies.go.jp/publication/I063/I063.html.

Nakayama, T., & Watanabe, M. (2008a) Missing role of groundwater in water and nutrient cycles in the shallow eutrophic Lake Kasumigaura, Japan. *Hydrol. Process.* **22**, 1150-1172, doi: 10.1002/hyp.6684.

Nakayama, T., & Watanabe, M. (2008b) Role of flood storage ability of lakes in the Changjiang River catchment. *Global Planet. Change*, doi: 10.1016/j.gloplacha.2008.04.002.

Nakayama, T., Yang, Y., Watanabe, M., & Zhang, X. (2006) Simulation of groundwater dynamics in North China Plain by coupled hydrology and agricultural models. *Hydrol. Process.* **20**(16), 3441–3466, doi: 10.1002/hyp.6142.

Nakayama, T., Watanabe, M., Tanji, K., & Morioka, T. (2007) Effect of underground urban structures on eutrophic coastal environment. *Sci. Total Environ.* **373**(1), 270–288, doi: 10.1016/j.scitotenv.2006.11.033.

Sellers, P.J., Randall, D.A., Collatz, G.J., Berry, J.A., Field, C.B., Dazlich, D.A., Zhang, C., Collelo, G.D., & Bounoua, L. (1996) A revised land surface prameterization (SiB2) for atomospheric GCMs. Part I : Model formulation. *J. Climate*, **9**, 676-705.

U.S. Geological Survey (1996) GTOPO30 Global 30 Arc Second Elevation Data Set. USGS, http://www1.gsi.go.jp/geowww/globalmap-gsi/gtopo30/gtopo30.html.

Model based impact analyses of global change and agro-political developments with regard to the implementation of the Water Framework Directive in the Elbe Basin

A. RICHMANN, H. GÖMANN & P. KREINS

Institute of Rural Studies, Johann Heinrich von Thünen-Institute (formerly FAL), Bundesallee 50, D-38116 Braunschweig, Germany

agnes.richmann@vti.bund.de

Abstract Since agriculture uses more than half of the total area in the Elbe basin diffuse nutrient emissions have a major influence on water quality. Hence, future development of land use and nutrient surpluses is of great interest within the context of the implementation of the Water Framework Directive. Increasing prices on world food markets and the promotion of Renewable Resources are substantially changing the framework conditions which will lead to an intensification of land use. Projecting future land use, nutrient balance surpluses and impacts on water quality under various developments of Global Change is tackled in the GLOWA-Elbe project using an interdisciplinary model network. Analyses with the regionalised agricultural sector model RAUMIS suggest an overall decrease of nutrient surplus of about 10 % in the German Elbe basin until the year 2020, which is primarily due to a reduction of cattle production. This effect outweighs the negative impacts of an increasing intensity of land use e.g. an expansion of the biomass crop area of about 250,000 hectares mostly on former set-aside area.

Keywords Global Change; agro-economic modelling; biomass crops; agricultural nitrogen balance surpluses; Water Framework Directive

INTRODUCTION

According to a survey of the status of water bodies the aim of the Water Framework Directive i. e. good ecological conditions in water bodies by 2015 cannot be achieved in more than half of the surface and ground water bodies in Germany. A main reason for this are diffuse nutrient emissions by agriculture. In the Elbe basin more than 50 % of the total area is used by agriculture. An increasing intensification of agricultural production due to rising prices on world food markets and a strong support of Renewable Resources may aggravate the situation. Against this background analyses of the impacts of Global Change, the further development of Common Agricultural Policy and a growing production of Renewable Resources on adjustments in agricultural land use and the consequences for water management and quality in the Elbe Basin are carried out in the GLOWA-Elbe project.

AGRO-ECONOMIC MODELLING WITHIN AN INTERDISZIPLINARY FRAMEWORK

The GLOWA Elbe project, funded by the BMBF, investigates the global and regional interactions of agro-environmental measures, land use changes, nutrient surpluses and income in the Elbe basin under different scenarios of Global Change up to the year 2020. The interdisciplinary network that consists of the eco-hydrological model SWIM (Soil And Water Integrated Model, Krysanova *et al.*, 1998), MONERIS (Modelling Nutrient Emissions in River Systems, Behrendt *et al.*, 2003) and the agro-economic model RAUMIS (Regional Agricultural and Environmental Information System, Henrichsmeyer *et al.*, 1996) is applied to analyze complex interactions of diffuse nutrient input from cropland up to water quality.

RAUMIS is a mathematical programming model which represents the German agricultural sector on a regional scale and has been developed for medium and long-term agricultural and environmental policy impact analyses. In order to take the emerging production of Renewable Resources and the impacts of the German nutrient management regulation (DüV) into account a new activity “energy maize” as well the nutrient balancing methodology of the DüV were implemented into RAUMIS. Hence, the agricultural contributions achieving the aims of the Water Framework Directive and their consequences for agricultural production and income can be quantified as well as calculating regionally differentiated measure costs arising from water pollution control.

Within the project, the agro-political development is investigated for two contrasting storylines, Globalisation and Differentiation, each with two versions: environmental aspect status quo and a pronounced consideration of environmental aspects. The following results always refer to more likely version, the increased environmental orientations. In the case of Globalisation, the intensification of agricultural land use, resulting from an assumed sustained agricultural price increase, and the promotion of bioenergy stands at the forefront. In the Differentiation scenario a product restriction on local markets by achieving 100 percent self-sufficiency, as well as a 20 percent reduction in the use of animal products is aspired.

RESULTS

Support of renewable resources

Within the last years a considerable development has influenced agricultural production: Due to the amendment of the German Renewable Energy Sources Act (EEG) of 2004 an attractive support of using Renewable Resources for sustainable energy production has been established. Since then, this has caused a rapid expansion of biomass crop, particularly energy maize for biogas production, and thus an intensification of cultivation affecting water quality.

Energy maize proved to be the most competitive among the various renewable energy crops and its cultivation competes directly with traditional crops for scarce land resources.

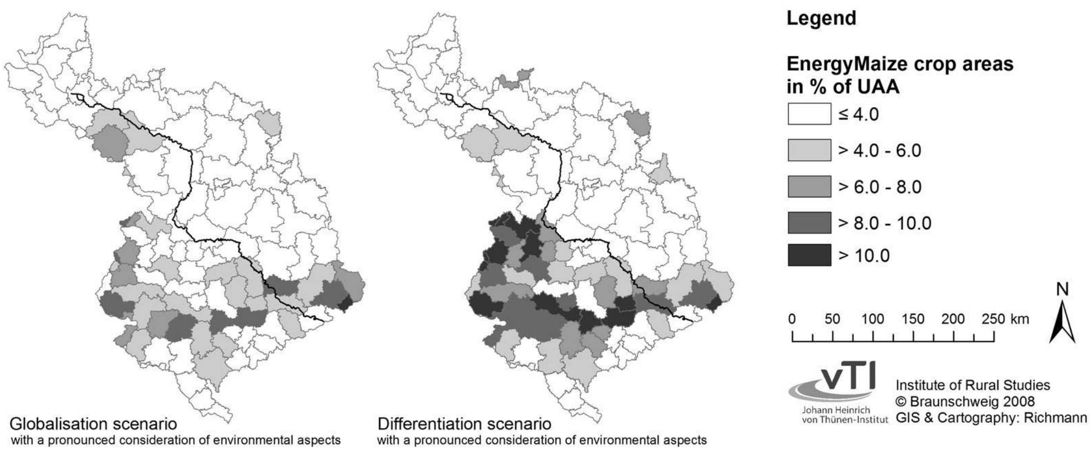

Fig. 1 Energy Maize crop areas in the German Elbe Region 2020 with the two baselines: Globalisation and Differentiation in percent of UAA (see Gömann *et al.*, 2008).

According to RAUMIS, in the Globalisation scenario the cultivation of energy maize will increase to a total of 250,000 ha in the German Elbe Basin by 2020, assuming a price increase of cereals of about 50 % (see Gömann *et al*., 2008). In the Differentiation scenario there will be even a stronger expansion of energy maize planting. Above all in the arable crop areas of Saxony Anhalt, Thuringia und Saxony, the land portion could in part exceed 10 % of the utilised agricultural area (UAA) (see Fig. 1).

Consequences for water management and water quality

The expansion of the energy maize crops takes place mostly on fallow land, although the extent of set-aside land is regionally very limited and thus the capacity of evapo-transpiration and the water regime are visibly influenced. If this development is continued, an increase in the existing competitive use for limited land areas will occur. Due to the high water requirements for energy crops in comparison to traditional crops, an expansion of the biomass crops depends on sufficient water availability and thus leads to an aggravation of the existing water conflicts.

It must be particularly noted that through the increase in temperature and observed drop in summer precipitation in the Elbe region during the vegetation period, there is already an increased pressure on the water resources. In the interest of sustainable use of water reserves, it is thus recommended to crop energy maize at different levels of intensity for each region. To document the sensitive areas, regionally specific estimations are needed that can be provided with the model system described above.

In consideration of accompanying intensification of the agricultural land use, the increase planting of energy maize presents also a challenge for water quality, and thus for the implementation of the Water Framework Directive. Since energy maize crops require the return of large quantities of fermentation substrates from the biogas facilities to the agricultural areas. The redistribution of the fermentation substrates, as well as the plant availability of the nutrients contained (nitrogen and phosphorous), have decisive consequences for nutrient leaching into water bodies.

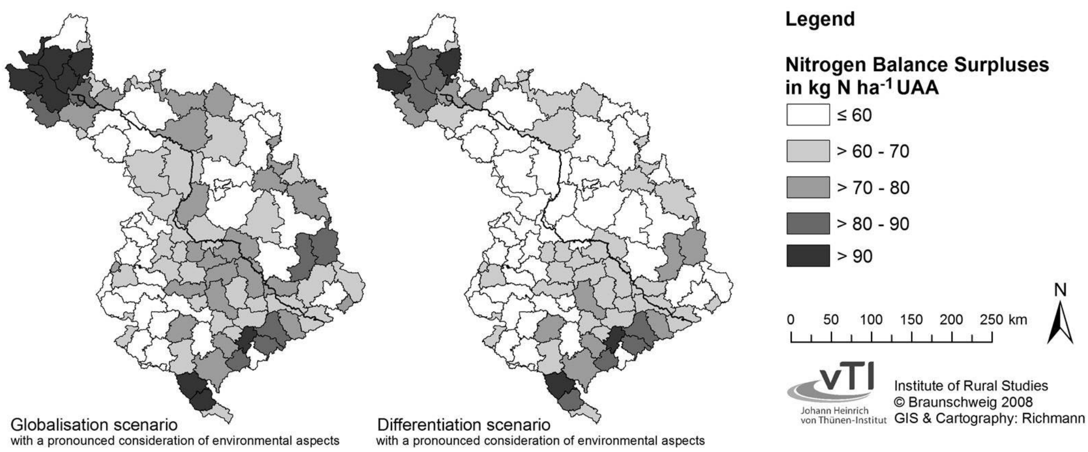

Fig. 2 Regional Nitrogen Balance Surpluses in the German Elbe Basis 2020 with the two baselines: Globalisation and Differentiation in kg N ha^{-1} UAA (see Gömann *et al*., 2008).

For the Globalisation scenario, the RAUMIS simulations by Gömann *et al.* (2008) showed a reduction in nitrogen surpluses in the German Elbe region of a total of 23,000 tons, or an average of 8 kg ha^{-1} UAA in comparison to 1999, which can be explained primarily by the reduction in cattle herd size due to the increase in milk yield. Fig. 2 shows the regional distribution for the nitrogen balance surpluses predicted for 2020 in the German Elbe Basin area. It is clearly evident that in the Differentiation scenario, the maximum nitrogen balance surplus limits of 60 kg ha^{-1} UAA set by the Water Framework Directive can be met in most counties. The nitrogen surpluses drop as a consequence of an assumed reduction in the consumption of animal products by 20 %, which leads to a decrease in the average nitrogen balance surplus of about 13 kg N to about 61 kg ha^{-1} UAA (Gömann *et al*., 2008).

CONCLUSIONS

The analysis provides important information about the scope of adjustments in the agricultural sector in the Elbe region, for example in regard to the implementation of the Water Framework Directive, and serves as the basis for the development of regionally specific measures.

On the one hand, agricultural production is very sensitive to vulnerable climate and water supply conditions. On the other hand, changes in agricultural production might alleviate or aggravate emerging water supply conflicts in Central Europe.

However, the impacts vary within the regions reflecting heterogenic soil conditions and regional characteristics of climate change. In this context, an important step is to disaggregate RAUMIS results from NUTS III to homogenous response units below the NUTS III level. Therefore information from NUTS IV level and geo-referenced high-resolution natural site conditions, like soil and climate information, will be considered to estimate crop yields. In the first step, the yield estimations will be carried out on the basis of yield information for Lower Saxony and showed promising results.

REFERENCES

Behrendt, H., Bach, M., Kunkel, R., Opitz, D., Pagenkopf, W.-G., Schloz, G. & Wendland, F. (2003) Quantifizierung der Nährstoffeinträge in die Oberflächengewässer Deutschlands auf der Grundlage eines harmonisierten Vorgehens. *Umweltbundesamt* (Hrsg.): UBA-Texte 82/03. Berlin.

Bundesministerium für Umwelt, Naturschutz und Reaktorsicherheit (BMU) und Bundesumweltamt (UBA) (2005) Die Wasserrahmenrichtlinie – Ergebnisse der Bestandsaufnahme 2004 in Deutschland. Berlin.

Gömann, H., Kreins, P. & Breuer, Th. (2007) Deutschland – Energie-Corn-Belt Europas? *Agrarwirtschaft Band* **56**, 263-271.

Gömann, H., Kreins, P. & Richmann, A. (2008) Projektionen zur Änderung der regionalen landwirtschaftlichen Landnutzung, Produktion und Stickstoffüberschüsse bis 2020 im Elbeeinzugsgebiet vor dem Hintergrund sich wandelnder Rahmenbedingungen. Regionalisierung der Szenarioanalyse (der Antriebskräfte und des Nutzungsdruckes) des Globalen Wandels für die Wasserwirtschaft. In: Wirkungen des Globalen Wandels auf den Wasserkreislauf im Elbegebiet - Risiken und Optionen. Schlussbericht zum BMBF-Vorhaben GLOWA-Elbe II (forthcoming)

Henrichsmeyer, W., Cypris, C., Löhe, W., Meudt, M., Sander, R., von Sothen, F., Isermeyer, F., Schefski, A., Schlef, K.-H., Neander, E., Fasterding, F., HElmcke, B., Neumann, M., Nieberg, H., Manegold, D. & Meier, T. (1996) Entwicklung eines gesamtdeutschen Agrarsektormodells RAUMIS 96. *Endbericht zum Kooperationsprojekt. Forschungsbericht für das BML (94 HS 021), vervielfältigtes Manuskript*. Bonn/Braunschweig.

Krysanova, V., Müller-Wohlfeil, D.-I. & Becker, A. (1998) Development and test of a spatially distributed hydrological/water quality model for mesoscale watersheds. *Ecol. Model.* **106**(1/2), 261-289.

Richmann, A., Gömann, H., Kreins, P. & Hattermann, F. (2007) Auswirkungen der Förderung des Biomasseanbaus auf Landnutzung und Wasserhaushalt im Elbe-Einzugsgebiet - Zwischenergebnis des GLOWA-Elbe Modellverbundes. *Forum für Hydrologie und Wasserbewirtschaftung* **20**, 139-142.

Future developments of nitrogen balances and suitable combinations of measures to reduce diffuse nitrogen leaching in agriculture in the Weser River basin

A. RICHMANN[1], H. GÖMANN[1], P. KREINS[1], K. SEIDEL[1,] U. HIRT[2], B. TETZLAFF[3] & F. WENDLAND[3]

1 *Institute of Rural Studies, Johann Heinrich von Thünen-Institute (formerly FAL), Bundesallee 50, D-38116 Braunschweig, Germany*
agnes.richmann@vti.bund.de

2 *Department of Lowland Rivers and Shallow Lakes, Institute of Freshwater Ecology and Inland Fisheries (IGB)*
3 *Institute of Chemistry and Dynamics of the Geosphere (ICG), Institute 4: Agrosphere, Research Centre Jülich*

INTRODUCTION

Experts are unanimous in the opinion that the status of water bodies has improved clearly over the past decades. But despite all previous successes in water protection, now as then, large parts of the water bodies are still more or less strongly polluted. Here, agriculture plays a large role in terms of nutrient load and water pollution. For this reason, the water management is demanding that agriculture take appropriate measures to help reduce the nutrient pollution of ground and surface water bodies.

Analyses from a network of existing and proven models were used in the framework of the AGRUM Weser (Analyses of Agricultural and Environmental measure in the field of agricultural water protection in terms of the EU Water Framework Directive in the Weser River basin http://www.arge-weser.de/pilotprojekte_fge.html) pilot study (Kreins *et al*., 2008) to create a program of measures to prevent diffuse nutrient leaching from agriculture in the Weser River Basin. The model network consists of the regionalised agricultural and environmental system RAUMIS (Heinrichsmeyer *et al*., 1996), the hydro(geo)logical model GROWA/WEKU (Wendland *et al*., 2002, 2004), and the MONERIS model (Modelling Nutrient Emissions in River Systems, Behrendt *et al*., 1999; 2003). To further develop the coupling of models, data from various sources was updated, harmonised, and combined into a consistent data base. With the model network, a uniform method as well as a uniform evaluation and analysis approach has been developed and made available to carry out differentiated status, monitoring and measure analyses.

METHODS

To illustrate the entire Agriculture-Groundwater-Surface Water System and pollution loads in coastal waters, the model network described above were applied within the AGRUM Weser project. The range of application by the individual models are as follows: With the agricultural sector model RAUMIS, regionally differentiated status and impact analyses of agricultural and agri-environmental measures are undertaken and nutrient balances calculated as indicators relevant for water bodies. The GROWA/WEKU model provides high resolution spatial results (i.e., in 100 m x100 m grids) for the nutrient leaching in surface water. It considers the nutrient breakdown and the nutrient retention in soil and ground water and thus alleviates concerns about the uncertainties surrounding the determination of diffuse nutrient leaching. The MONERIS model describes all relevant paths of leaching (point sources and diffuse leaching sources) and presents a consistency framework for the entire range of nutrient leaching. The spatial resolution is related to the river basin area, the size of which can vary between about 10 and 1,000 km².

INVESTIGATED REGION

The availability of a large range of diverse hydrological and agricultural structures in the river basin played an important role in the selection of the investigation area Weser. Thus it could be ensured that the analysis approach is transferable beyond the Weser basin to other river basin areas. Also, the Weser river basin is a large multi-state river basin (see Fig. 1), making measurement analysis for the complete river basin district possible.

Fig. 1 The Weser River Basin.

The river basin extends over various landscape types (i.e. Rhenish Slate Mountains, Weser Mountain Areas, North German Plain). These regions must be evaluated very differently, both in terms of soil science and hydrological conditions as well as with regard to the agricultural structures and types of farming as well as the population density.

RESULTS FOR THE WESER RIVER BASIN

The current development in agricultural and agri-environmental policy are expected to cause an overall drop in the diffuse nutrient leaching, whereas the regional characteristics and levels of impact may vary greatly. While an increase in production intensity through the predicted agricultural price increases, a drop in set-aside areas and increases in the planting of energy maize could lead to an increase in the nutrient balance losses, this could be offset by the decoupling of animal premiums due to a reduction in beef cattle herds and the expected increase in efficiency in the use of natural fertilisers. Overall, by the year 2015, a drop in nutrient surpluses can be expected of between 10-15 kg N ha^{-1} UAA. For major animal regions, marked by above average nutrient balance surpluses from the start, a relatively strong decrease in nitrogen balance surpluses will be shown. At the same time these regions will also show the highest nutrient balance surpluses in the future.

According to the model analyses, 22 ground water bodies (about 20% of the total area of the river basin) which did not meet the objectives of the WRRL at the start can achieve them in the long term simply through the expected reduction in N-balance surpluses within the framework of the basic measures of the Common Agricultural Policy.

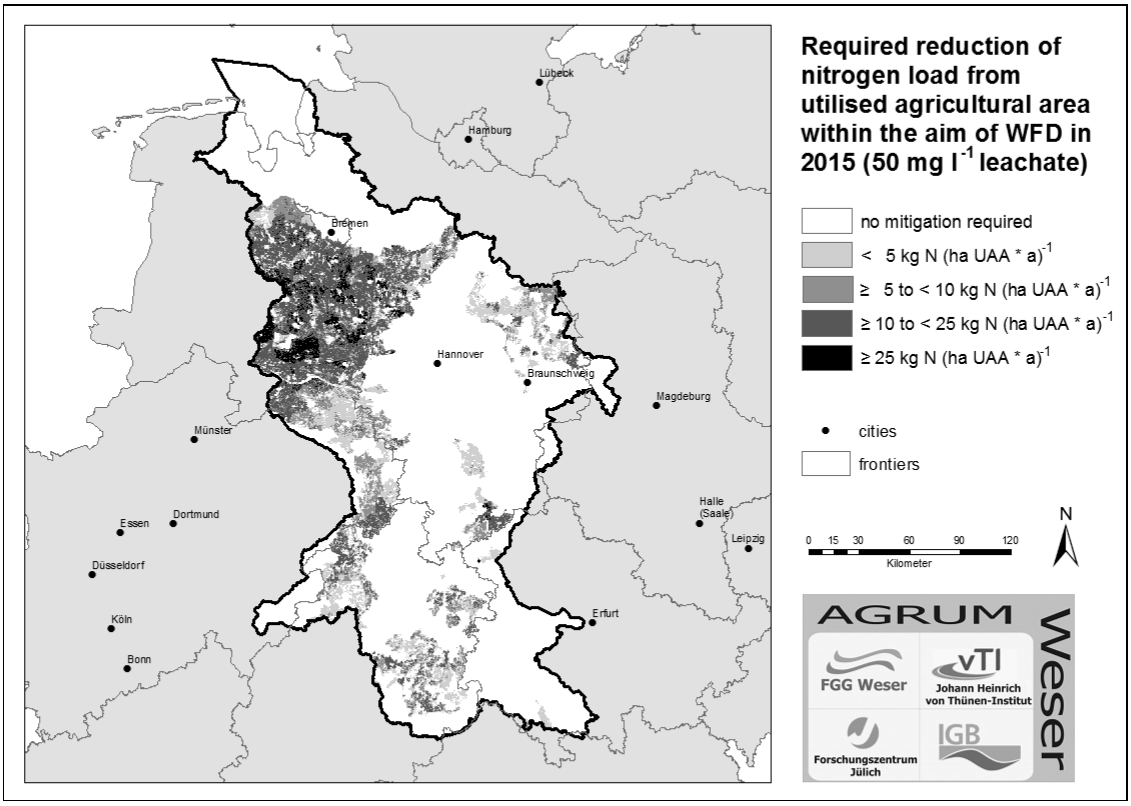

Fig. 2 Necessary Reductions in Nitrogen Leaching to Reach the Goals of the Water Framework Directive.

Although a reduction of the leached nitrate concentrations is expected almost all parts of the Weser River Basin, it can be assumed that in the “hot spot” regions additional measures will be required to reach the environmental quality targets of 50 mg l^{-1} by the year 2015 (See Fig. 2).

The reduction of nitrogen balances causes the nitrogen loads in the Weser River Basin area drop by 11%. Under mean hydrological conditions, they would then reach 78,497 t a^{-1} for the year 2015, while the nitrogen leaching calculated for 2003 was still 88,168 t a^{-1}.

REFERENCES

Behrendt, H., Bach, M., Kunkel, R., Opitz, D., Pagenkopf, W.-G., Scholz, G. & Wendland, F. (2003) Quantifizierung der Nährstoffeinträge der Flussgebiete Deutschlands auf der Grundlage eines harmonisierten Vorgehens. *UBA-Texte* 82/03, 201 S.

Behrendt, H., Huber, P., Ley, M., Opitz, D., Schmoll, O., Scholz, G. & Uebe, R. (1999) Nährstoffbilanzierung der Flußgebiete Deutschlands. *UBA-Texte* 79/99. Berlin.

Henrichsmeyer, W., Cypris, C., Löhe, W., Meudt, M., Sander, R., von Sothen, F., Isermeyer, F., Schefski, A., Schleef, K.-H., Neander, E., Fasterding, F., Helmcke, B., Neumann, M., Nieberg, H., Manegold, D. & Meier, T. (1996) Entwicklung eines gesamtdeutschen Agrarsektormodells RAUMIS96. *Endbericht zum Kooperationsprojekt. Forschungsbericht für das BML* (94 HS 021), vervielfältigtes Manuskript Bonn/Braunschweig.

Kreins, P., Gömann, H., Seidel, K., Behrendt, H., Hirt, U., Herrmann, S., Kuhn, U., Kunkel, R., Tetzlaff, B. & Wendland, F. (2008) Analysis of Agricultural and Environmental Measures in Agricultural Water Protection against the Background of the EU Water Framework Directive – Implementation of an integrative model network in the Weser river basin. *Springer Verlag (in Begutachtung)*.

Wendland, F., Kunkel, R., Grimvall, A., Kronvang, B. & Müller-Wohlfeil, D.I. (2002) The SOIL-N/WEKU model system - a GIS-supported tool for the assessment and management of diffuse nitrogen leaching at the scale of river basins. *Water Science and Technology* **45**(9), 285-292.

Wendland, F., Kunkel, R. & Voigt, H.-J. (2004) Assessment of groundwater residence times in the pore aquifers of the River Elbe Basin. *Environmental Geology* **46**, 1-9.

The challenges and uncertainties of modelling the impacts of land management changes on flooding: a case study in north-east England

ZDENKA ROSOLOVA
JBA Consulting Ltd., South Barn, Broughton Hall, Skipton, BD23 3AE, North Yorkshire, United Kingdom
zdenka.rosolova@jbaconsulting.co.uk

Abstract The effect of land management practices and their changes on flood generation was investigated using a series of conceptual rainfall-runoff models known as Probability Distributed Moisture (PDM) models. PDM models enabled the development of scenarios to represent plausible changes to the land management in parts or all of the study area, the River Skell catchment draining through the town of Ripon in north east England. Two main constricting factors had to be accounted for and addressed within the methodology, namely: (a) limited sources of observed data for model calibration, and (b) assumptions related to the quantification of the impact of changes to land use, land management or soil properties on runoff generation. The modelled results showed that the worst case plausible land management degradation scenario increased peak flows by up to 20% and advanced the timing of the peak flow by up to 1.5 hours in the town of Ripon when compared to the baseline (current) case.
Keywords land management; runoff generation; PDM models; PDM model parameters; soil properties

INTRODUCTION AND METHODOLOGY

The hydrological characteristics of catchments in rural landscapes, such as runoff generation potential or the retention capacity of the soils, are influenced by land management practices. To date, research has not been able to quantify how changes at the field or farm scale will affect the dynamics of flood generation at the catchment scale. To help address this gap in knowledge, a short modelling project was undertaken using sensitivity testing as a means of indicating the potential impact that such changes may have on the generation of floods. The project aimed to show how much and what distribution of land management change would be needed to generate significant changes to flood hydrographs downstream. The study area chosen for this project was the catchment of the River Skell and its tributaries, 120km^2 in size, in north east England.
In order to represent the potential impact of land management changes on runoff generation, we used the results of an earlier research project comissioned by Defra1 (Department for Environment, Food and Rural Affairs, the UK, http://www.defra.gov.uk)on how physical catchment descriptors, including soil hydrological properties, relate to the parameters of a particular rainfall-runoff model, the Probability Distributed Moisture (PDM) model (Calver *et al*., 2005). This study developed empirical formulae which we used to provide a link between changes in catchment properties and the predictive parameters of the individual PDM models developed for a number of sub-catchments within the study area. With this in mind, seven land management change scenarios were set up and their impact on runoff generation was investigated. These scenarios included: soil structural degradation on 50% and 100% of the degradable soils area in all PDM models, conversion of grassland to maize, combination of soil structural degradation (i.e. drainage ditch maintenance) and moorland degradation, moorland degradation and moorland restoration (i.e. ditch blocking) and conversion of moorland to deciduous woodland.

In order to model the above scenarios and to target the land use changes spatially, ten sub-catchments were indentified across the entire study area, each representing similar physical characteristics such as topography, rainfall, soils and current land use.

These were represented by ten individual PDM models, which were then linked together via a hydraulic model (an ISIS Routing model) in order to propagate the runnoff from each PDM model downstream to the town of Ripon.

The PDM model is a conceptual rainfall-runoff model, which uses rainfall and potential evapotranspiration as inputs and transforms these into a flow (i.e. the discharge from a catchment). The version of the PDM used in this study specifies a surface store, through which direct runoff is routed, a soil store and a ground water store (Fig. 1).

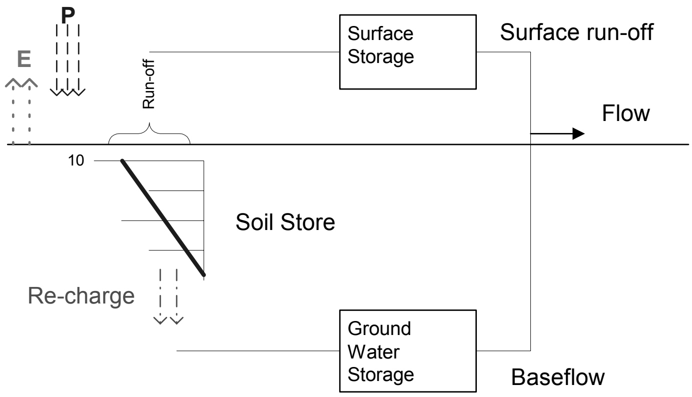

$$Q_s = \left[1 - \left(1 - \frac{C_i}{C_{\max}}\right)^b \times Rain\right]$$

$$Q_{SOUT} = \left(\frac{1}{K_s}\right) \times S_s$$

$$Q_g = \left(\frac{1}{K_b}\right) \times GW_i^m$$

Fig. 1 Schematic of PDM rainfall-runoff model and the core relationship between specific PDM parameters and surface/groundwater flow (after Moore, 2007).

The important distinction of the PDM model compared to other conceptual rainfall-runoff models is the way it apportions rainfall into that which enters the soil store and that which runs off the surface directly. The concept of the probability distributed element represents the effect of the runoff production. During a rainfall event, the soil becomes more saturated forcing the watertable to intersect with the ground higher up the slope, hence increasing the area of catchment that can contribute directly to runoff. Within the PDM model, this is simulated by apportioning rainfall according to the content of the soil store. The amount of rainfall routed as quick flow is therefore a function of how full the soil store is and two model parameters (b, Cmax) that may be adjusted to give a good calibration. Direct runoff is routed through a series of two linear reservoirs which are modelled using the transfer function equations, as described in Moore (2007). This runoff is a function of the content of the surface store and the (calibrated) parameters K1 and K2. These constants control the 'peakiness' of the runoff routed through the surface stores, i.e. increasing the value of K1/K2 decreases the peak flow whereas decreasing the value of K1/K2 exaggerates the response. These features of the PDM model principle were at the core of the modelling approach adopted to represent the changes in soil properties as a result of changes to land management practices in the catchment.

The modelling approach consisted of setting up the baseline PDM models for all the ten sub-catchments. In order to realistically represent runoff from a catchment, the PDM model parameters need to be calibrated using observed flow records. Unfortunately, the only flow record applicable to this modelling were the flow series recorded at the outflow point from the catchment. Therefore, the initial set of PDM model parameters was calibrated on the entire study catchment. Two series were calibrated, one for the winter part of the water year and one for the summer part. This is advisable as the two seasons can differ considerably in terms of the soil moisture status and the rainfall characteristics (especially intensity and duration). The initial winter and summer PDM parameters were then used to set up parameters for the ten individual PDM models, representing the ten sub-catchments. This was based on the mixture of judgement and experience with the PDM modelling but particularly on a thorough understanding of the soils in the catchment and their hydrological characteristics, which were reflected by the PDM model parameters. This, of course, introduces some uncertainties into the modelling and will be, among other limitations, discussed later. The set of calibrated PDM models was regarded as the baseline condition, i.e. the existing conditions of the soil and land management in the catchment. In terms of the overall land management effect, the baseline condition could be described as being degraded to a certain extent as a result of the general intensification of the agricultural systems that has taken place over the last 50 years, primarily as a result of UK and EC agricultural policies.

All of the subsequent scenario testing made adjustments to specific PDM parameters which control the pathways of water flow (i.e. Cmax, kb) and the speed of runoff response (K1/K2) to represent a set of specified land management changes. The runoff response parameter (K1/K2) was used specifically to accomodate the effect of ditch blocking/maintenance on the flood peaks. Table 1 summarizes the type of changes addressed by the scenarios and their representation within the PDM model structure.

Table 1 Suggested land management scenarios.

Catchment zone	Scenario	Management change	PDM Model parameter change	PDM Model parameters affected
Moorland	Current condition	No change	No change	-
	Improved	Grips blocked	Increased residence time	Increase Ks (i.e. K1/K2)
		Conversion of moorland to deciduous woodland	Decrease SPR (Standard Percentage Runoff) Increased residence time	Increase Cmax, Ks (i.e. K1/K2)
	Degraded	Maintenance of grips, loss of peat	Decreased residence time	Decrease Ks (i.e. K1/K2), Kb
Improved grassland	Current condition	No change	No change	-
	Degraded	Increased stocking density, more compaction or capping	Increase SPR Decreased residence time	Decrease Cmax, Ks (i.e. K1/K2)
		Conversion to intensive arable (possibly maize production)	Increase SPR Decreased residence time	Decrease Cmax, Ks (i.e. K1/K2)
Arable	Current condition	No change	No change	-
	Degraded	More intensive, inappropriate land management, more compaction or capping	Increase SPR Decreased residence time	Decrease Cmax, Ks (i.e. K1/K2)

RESULTS

The empirical formulae presented by Calver *et al.* (2005) were used to link changes to soil properties (associated with land management changes) to the specific PDM model parameters. This way it was possible to investigate the likely impact of a change in land management on the generation of runoff and the magnitude and timing of the resulting flood peak downstream in the town of Ripon.

A series of 10 year, 50 year and 100 year return period design events were generated and run through the baseline PDM models as well as the scenario PDM models. The resulting hydrographs, and specifically changes to the magnitude of the flood peaks and their timing were compared for each scenario against the baseline. Overall, the soil degradation scenarios advanced the timing of the flood peak, with the combined soil structural degradation and moorland degradation scenario causing the largest change to the peak flow. The percentage increase in the downstream peak flow as a consequence of degradation scenarios was greater for the smaller design event (10 year) than for the large design event (100 year), with the 50 year event in between. The scenario representing the combined soil structural degradation and moorland degradation increased the magnitude of the flood peaks by about 10 – 20% and advanced the timing of the peak by up to 1.5hr. All the other degradation scenarios had smaller impact on the magnitude and timing of the peak. The moorland restoration scenario (drainage ditch blocking) had little effect on the magnitude of the 10 year peak, but reduced the peak of the 50 year and 100 year events by 5-7%. It should be noted that the magnitude of changes to flood peaks due to the land management changes was also influenced by the routing effect in the river network. For example, it was observed throughout the routing model that in some cases the increase in flood peak due to the land management changes was subsequently attenuated by flood storage areas downstream.

CHALLENGES AND UNCERTAINTIES

The sensitivity testing carried out in this project showed that floods can be made worse by inappropriate land management practices. However, it should be recognised that the results obtained here are subject to a degree of uncertainty. The results should be considered in light of the inevitable uncertainties stemming from the modelling (i.e. errors in the input rainfall and calibration flow data) as well as for example the assessment of degradability of soils and other changes in the catchment, which lie at the core of the scenarios.

Within this study, the greatest challenge and uncertainty is seen to be attached to the specification of the land management scenarios. Firstly, the assessment of the current state of the soils in different parts of the catchment and subsequently estimation of the degree to which these should be regarded as degraded, had to be based on thorough knowledge of the soils and the catchment. This introduces uncertainty in terms of setting up the baseline conditions of the soils, from which the magnitude of plausible changes to the soil properties was designed. Further, highly generalised parameters had to be applied to represent the changes to soil properties, based on a very generalised set of regression equations. This was then ‚translated‘ to the PDM model parameters in order to reflect the magnitude of a specific change to the soil properties in terms of the simulated flood flow. The results, therefore, are seen as an indication of a possible change, i.e. a prediction ‘envelope‘ rather than a precise prediction of the catchment response. More research in this subject is desirable, as other hydrological models might give different results. However, currently there are few studies of this type and these all indicate how difficult it is to represent runoff production dynamics as a function of land management change.

This short project has hopefully contributed to widening the current limited knowledge of how rural land management changes might affect the generation of floods and adopted a modelling approach that can be used to simulate impact of such changes. Further investigation of other possible interventions in the catchment (e.g. the effect of on-farm flood storage ponds, cascading weirs or floodplain woodland) would help further inform the development of flood risk management policy regarding more practical measures that could be taken on a farm scale to contribute to flood mitigation downstream where people and property are at risk.

REFERENCES

Moore, R. J. (2007) The PDM rainfall-runoff model. *Hydrology & Earth System Sciences* **11**(1), 483-499.

Calver, A., Crooks, S., Jones, D., Kay, A., Kjeldsen, T. & Reynard, N. (2005) National river catchment flood frequency method using continuous simulation. *Defra/Environment Agency R&D Technical Report FD2106/*TR. Centre for Ecology and Hydrology, Wallingford.

Hindcast of water availability in regional aquifer systems using MODFLOW's Farm Process

W. SCHMID[1], R.T. HANSON[2], C.C. FAUNT[2] & S. P. PHILLIPS[3]

1 *Dept. Hydrology & Water Resources, University of Arizona, Tucson, Arizona, USA*
w_schmid@hwr.arizona.edu

2 *U.S. Geological Survey, California Water Science Center, San Diego, USA*

3 *U.S. Geological Survey, California Water Science Center, Sacramento, USA*

Abstract Coupled groundwater and surface-water components of the hydrologic cycle can be simulated by the Farm Process for MODFLOW (MF-FMP) in both irrigated and non-irrigated areas and aquifer-storage and recovery systems. MF-FMP is being applied to three productive agricultural regions of different scale in the State of California, USA, to assess the availability of water and the impacts of alternative management decisions. Hindcast simulations are conducted for similar periods from the 1960s to near recent times. Historical groundwater pumpage is mostly unknown in one region (Central Valley) and is estimated by MF-FMP. In another region (Pajaro Valley), recorded pumpage is used to calibrate model-estimated pumpage. Multiple types of observations are used to estimate uncertain parameters, such as hydraulic, land-use, and farm properties. MF-FMP simulates how climate variability and water-import availability affect water demand and supply. MF-FMP can be used to predict water availability based on anticipated changes in anthropogenic or natural water demands.
Keywords groundwater; surface-water; irrigation; water availability; response to climate variability/change

INTRODUCTION

The Farm Process (FMP) of the U.S. Geological Survey's hydrologic model, MODFLOW (MF) can simulate land-use processes affecting the movement and use of surface and groundwater (Harbaugh *et al*., 2000; Schmid *et al*., 2006). MF-FMP can assess water availability for developed and undeveloped land use. Because FMP fully couples simulations of surface-water and groundwater flow, and of water demand and supply, it can be used to evaluate how management decisions impact water availability in complex water-resource systems. The FMP has been applied to regions in the State of California, USA, at spatial scales ranging from the 50,000-km^2 Central Valley (Faunt *et al*., 2008) to the 400-km^2 Pajaro Valley, a coastal watershed of Monterey Bay (Hanson *et al*., 2008). An ongoing medium scale application is the 2,700-km^2 Stanislaus-Tuolumne River Groundwater Basin (STRGB) within the Central Valley. The FMP is particularly useful in areas where historical groundwater pumpage is unknown, or where future pumpage to meet anticipated anthropogenic or natural demands needs to be estimated. Where pumpage is known, the pumpage can be used with other observations to constrain estimates of uncertain parameters, such as the transpiratory and evaporative fractions of evapotranspiration, fractions of inefficient losses to either surface-water runoff or deep percolation, crop-coefficients, rooting depths, and on-farm irrigation efficiencies.

OBJECTIVES

In each of the three productive agricultural regions in California, where FMP is being applied, expanding irrigated agriculture and urban growth have increased the competition for water resources. The MF-FMP is used to simulate the conjunctive use of surface-water deliveries and historical groundwater pumpage for water-budget regions. These regions are simulated as single virtual model farms at different model discretizations (Central Valley Hydrologic Model, CVHM: 1.61x1.61 km; STRGB Model: 400x400 m; Pajaro Valley Hydrologic Model, PVHM: 250x250 m).

Primary objectives of the models are to help evaluate the effects of development on conjunctive use, water levels, groundwater storage, and groundwater discharge to streams. The CVHM can be used to evaluate proposed water allocations, such as water exportation from the Sacramento Valley to Southern California. The PVHM is being used to assess basin-management strategies for mitigating overdraft and seawater intrusion. These strategies include implementing aquifer-storage-and-recovery systems (ASRs) and improving irrigation efficiencies. The STRGB model can be used to assess a proposed ASR in the upper part of the basin, drainage in the lower part of the basin, and migration of poor-quality groundwater.

The program UCODE-2005 (Poeter *et al.*, 2005) is used to estimate uncertain hydraulic properties and land-use/farm properties, assess sensitivities of predictions, and determine the goodness of fit of predictions to observations. Observations include heads, surface-water flows, groundwater pumpage, and land subsidence.

MODEL RESULTS

In the CVHM, simulated water demand and supply indicate that, during non-drought periods, surface water typically satisfies most of the demand augmented with groundwater later in the season (Fig. 1a). During drought periods, groundwater is used earlier in the season, owing to insufficient surface-water supplies (Fig. 1b).

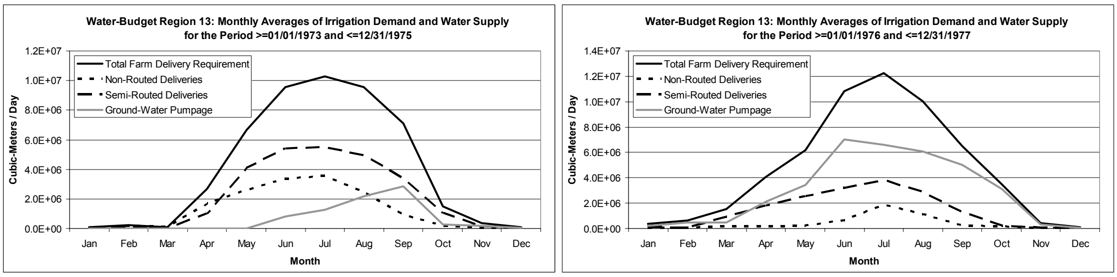

Fig. 1 Monthly averages of irrigation demand and supply during a (a) non-drought (left) and (b) drought period (right) for water-budget region 13 (non-routed = routing not simulated; semi-routed = routing simulated to point of diversion).

In the 1960s, irrigation demand peaked, groundwater pumpage exceeded surface-water deliveries, and water levels declined to historical lows causing land subsidence. Generally since the 1970s, overall groundwater pumping has decreased due to increased surface-water deliveries, particularly during peak demand periods. Surface-water deliveries often exceeded groundwater pumpage, water levels recovered, and subsidence slowed or ceased. Throughout the CVHM simulation, irrigation demand and dominant water source (non-routed water transfers, semi-routed surface water, or groundwater) respond to climate variability and water-import availability. During droughts (e.g., 1976–77 and 1987–92), the long-term trend of recovering water levels is disrupted, water levels decline, and subsidence resumes. The CVHM shows that, during wet years, water generally goes into aquifer storage, and during typical and dry years, water is removed from storage. However, even during dry years some recharge is simulated during heavy spring precipitation and through irrigation return flow.

In contrast to the CVHM, in the PVHM, precipitation provides most of the crop water supply early in the growing season, which is augmented later in the season by irrigation with groundwater, and, in recent years, by supplemental supplies through ASRs (Hanson *et al*., 2008).

SENSITIVITY ANALYSIS AND MODEL CALIBRATION

Parameter estimation and sensitivity analysis are useful for identifying and quantifying uncertainties in the FMP parameters, such as transpiratory and evaporative fractions (FTE), fractions of inefficient losses to surface-water runoff (IESW) and on-farm irrigation efficiency (OFE). Estimates of crop coefficients and reference evapotranspiration may be weakly constrained for specific model areas or times of the year, such as the non-growing season. Initial estimates of the FTE were approximated using ratios between a basal transpiration crop coefficient and the evapotranspiration crop coefficient, and the complementary fraction for evaporation. The latter was reduced if the exposed area was not fully wetted. Initial estimates of fractions of IESW were based on known irrigation methods and farming practices. Initial estimates of OFE fractions were based on surveyed records for farms and crop types. The groundwater demand estimated by the FMP is sensitive to the OFE. Small changes in the OFE can cause large changes in the irrigation requirement and associated residual between the irrigation requirement and deliveries. Vertical hydraulic gradients and seasonal fluctuations within the production zone of the aquifer system are, in turn, sensitive to groundwater demand. The parameter estimation process can incorporate these vertical gradients. For the CVHM and the PVHM, select parameters were estimated using UCODE-2005 by fitting head- or flow-dependent simulated values to observations. Even though the STRGB model is not yet calibrated, the parameters and observations to be used in the parameter estimation procedure have been defined (Table 1). Though the models share common parameters and observations, the procedure differs, in terms of both estimated parameters and calibration observations (Table 1).

Table 1 Estimated Parameters of Hydraulic and Farm-Process Properties and Observations to be used; (Estimated parameters and observations are shaded if common to all three models and unshaded if specific for individual models; MODFLOW Packages/Processes in parentheses).

<table>
<tr><th></th><th>CVHM</th><th>PVHM</th><th>STRGB - planned</th></tr>
<tr><td colspan="4">Estimated Parameters</td></tr>
<tr><td rowspan="4">Hydraulic Properties</td><td colspan="3">Aquifer Hydraulic Conductivity and Aquifer Storage Coefficient (LPF)</td></tr>
<tr><td colspan="2">Streambed Hydraulic Conductivity (SFR)</td><td></td></tr>
<tr><td colspan="2">Multi-Node Well Skin Factor (MNW)</td><td></td></tr>
<tr><td>Aquitard Storage (SUB)</td><td>General-Head Boundary Conductance (GHB)</td><td></td></tr>
<tr><td rowspan="10">Land-use and Farm Properties</td><td colspan="3">Fractions of transpiration and evaporation (FMP</td></tr>
<tr><td colspan="3">Fractions of inefficient losses to runoff (FMP)</td></tr>
<tr><td colspan="2">related to precipitation in areas of native vegetation, truck crops, orchards and related to irrigation in areas of truck crops and orchards.</td><td></td></tr>
<tr><td colspan="3">On-farm efficiency (FMP)</td></tr>
<tr><td>related to rice</td><td>scale factors for wet and dry seasons</td><td></td></tr>
<tr><td colspan="2">related to native vegetation, truck crops, and orchards, to unknown efficiencies, and to scale factors for wet and dry seasons</td><td></td></tr>
<tr><td colspan="2">Crop coefficients (FMP)</td><td></td></tr>
<tr><td>various crop types, including native vegetation</td><td>scale factors for wet and dry seasons</td><td></td></tr>
<tr><td>Capillary fringe (FMP)</td><td></td><td></td></tr>
<tr><td>Root-zone depth (FMP)</td><td></td><td></td></tr>
<tr><td colspan="4">Observations</td></tr>
<tr><td rowspan="3">Hydraulic Observations</td><td colspan="3">Heads and Head Differences</td></tr>
<tr><td colspan="2">Streamflows</td><td></td></tr>
<tr><td colspan="2">Streamflow Losses/Gains</td><td></td></tr>
<tr><td>Water Supply</td><td></td><td>Diversions: Public Supply and ASR</td><td></td></tr>
</table>

		Reported cumulative pumpage for Virtual Farms for seasonal/semiannual periods	
Storage Depletion	Land Subsidence (SUB)		

When fitting predictions to observations, the estimated FMP parameters become head and flow-dependent. Therefore, these parameters are estimated collectively with parameters of other MF-packages that also are head and flow-dependent, such as streambed hydraulic conductivities, well skin factors, and aquifer hydraulic properties. Certain FMP parameters are sensitive to farm-related flow rates. For example, if more farm deliveries were observed then simulated (e.g., surface-water diversions or cumulative pumpage) then crop coefficients are increased or irrigation efficiencies decreased to increase the crop water demand and irrigation requirement. Aside from standard observations, such as heads and streamflows, non-standard observations, such as metered pumpage (PVHM) or land subsidence (CVHM) also were used during parameter estimation.

OUTLOOK AND MANAGEMENT IMPLICATIONS

These models are predesigned to allow coupling with output derived from Global or Regional Climate Models (GCMs/RCMs), such as precipitation and potential crop evapotranspiration. This coupling utilizes GIS interfaces, which also facilitate the use and efficient update of remotely sensed spatial and temporal FMP climate input data. In addition to the direct linkage of MF-FMP and GCMs/RCMs, the models also can be indirectly linked through streamflow and infiltration simulated by Precipitation-Runoff models, such as PRMS in GSFLOW (USGS, 2008). PRMS can link with FMP through MF's Streamflow Routing, Lake, and Unsaturated Flow Packages (USGS, 2008). In addition, the application of optimization and adaptation analysis can be used systematically to assess vulnerability to changes and potential responses to changes in land use, water availability, storage, markets and transfers, surface-water rights constraints, efficiencies of conveyance systems, and ecological requirements.

Estimating uncertain parameters for MF-FMP models and preprocessing other data input parameters by GCMs/RCMs or by Precipitation-Runoff models can enable stakeholders to transition the three discussed MF-FMP hindcast models into forecast models. These models can predict water demand and supply of surface and groundwater and changes in groundwater storage for the Central Valley (CVHM) or a subregion of the Central Valley (STRGB) and for the Pajaro Valley (PVHM). Sub-regional scale processes and water management strategies (e.g., water exportation, ASR-storage), also could also be incorporated into regional models using MF's local grid refinement package (USGS, 2008).

REFERENCES

Faunt, C. C., Hanson, R. T., Schmid, W. & Belitz, K. (2008) Application of MODFLOW's Farm Process to California's Central Valley. *Modflow & More – Ground Water and Public Policy, Golden, CO*, May 18-21, 2008, 496 – 500.

Hanson, R. T., Schmid, W., Lear, J. & Faunt, C. C. (2008) Simulation of an Aquifer-Storage-and-Recovery (ASR) System using the Farm Process in MODFLOW for the Pajaro Valley, Monterey Bay, California. *Modflow and More – Ground Water and Public Policy, Golden, CO*, May 18-21, 2008, 501 – 505.

Harbaugh, A. W., Banta, E. R., Hill, M. C. & McDonald, M. G. (2000) MODFLOW-2000. U.S. Geological Survey Modular Ground-Water Model—User Guide to Modularization Concepts and the Ground-Water Flow Process, *U.S. Geological Survey Open-File Report 00-92*, 121 p.

Poeter, E. P., Hill, M. C., Banta, E. R., Mehl, S. & Christensen, S. (2005) UCODE_2005 and six other computer codes for universal sensitivity analysis, inverse modeling, and uncertainty evaluation. *US Geological Survey Techniques and Methods Report* TM 6-A11, 283pp.

Schmid, W., Hanson, R. T., Maddock III, T. M. & Leake, S. A. (2006) User's guide for the Farm Process (FMP1) for the U.S. Geological Survey's modular three-dimensional finite-difference ground-water flow model, MODFLOW-2000. *U.S. Geological Survey Techniques and Methods* 6-A17, 127 p.

USGS (2008) References of MODFLOW packages available under: http://water.usgs.gov/nrp/gwsoftware/modflow.html

Hydrological scaling for predicting catchment response to land management changes

OLGA VIGIAK[1], LACHLAN NEWHAM[2], DAN RATTRAY[3], ALICE MELLAND[4], ANNA RIDLEY[1], JANE WHITFORD[1] & BARRY CROKE[2]

1 *Department of Primary Industries, Future Farming Systems Research Division, Rutherglen Centre, RMB 1145 Chiltern Valley Road, Rutherglen, VIC 3685, Australia.*
olga.vigiak@dpi.vic.gov.au

2 *Integrated Catchment Assessment and Management Centre, The Fenner School of Environment and Society, the Australian National University, Canberra, ACT 0200, Australia*

3 *Natural Solutions Environmental Consultants, PO Box 1185, Toowoomba, QLD 4350, Australia*

4 *Department of Primary Industries, Future Farming Systems Research Division, Ellinbank Centre, 1301 Hazeldean Rd, Ellinbank, VIC 3821, Australia*

Abstract A methodology is proposed to link rainfall-runoff relationships at the field scale, to rainfall-streamflow responses at the catchment scale in order to assess the impact of land management practice changes on streamflow. Field-scale predictions of runoff and percolation from unique combinations of climate, soil and land management types (hydrologic response units) were calculated with a one dimensional soil column hydrology model (HowLeaky?). Rainfall-streamflow data at three gauging stations for different land management decades were analysed with a parametrically parsimonious rainfall-runoff catchment model (IHACRES). Multiple regression analysis showed that two IHACRES parameters (soil storage capacity and catchment moisture threshold) were strongly linearly correlated with spatially aggregated runoff and percolation predicted by the HowLeaky? model. Streamflow estimated by IHACRES using the parameters obtained by applying the regression equations were good or acceptable in twelve out of the eighteen catchment calibration datasets. The methodology has the potential to predict catchment streamflow responses to broad-scale changes of land management practices.

Keywords upscaling; regionalisation; IHACRES; HowLeaky?; catchment modelling

INTRODUCTION

In this study we propose a methodology to link field-scale rainfall-runoff to catchment-scale rainfall-streamflow relationships to assess the impact of broad-scale adoption of land management practices on streamflow responses. The methodology is adapted from regionalisation studies. If hydrological similarity between catchments can be assumed, a rainfall-streamflow relationship defined for gauged catchments can be transferred to ungauged ones by inferring model parameters from the spatial extent of hydrologic response units and their contribution to surface runoff or percolation (Post & Jakeman, 1999). Rather than applying the methodology to geographically different catchments (regionalisation *sensu strictu*), we applied it to different historical periods of land management in the Avon Richardson catchment, a 3300 km^2 catchment of the Wimmera landscape (North Central Victoria, Australia). The aim of this work was to explore the potential and the limits of predicting streamflow responses from field-scale water balance estimations.

FIELD-SCALE WATER BALANCE ESTIMATION

Hydrologic response units were defined as unique combinations of climatic zones, soil groups, and historical farming systems of the Avon Richardson catchment. Agro-climatic zones varied from grazed uplands in the south (average rainfall = 504 mm a^{-1}), mixed farming (i.e. combination of grazing and cropping) in the mid-catchment (average rainfall = 446 mm a^{-1}), and flat croplands in the north (average rainfall = 393 mm a^{-1}). Soils are mainly deep and clayey, with uniform or duplex soil profile.

Historical changes in the farming systems (crop rotation, pasture management, and tillage operations) from the 1960s until today were assessed from interviews with local farmers and historical records. Few changes occurred in grazing management from the 60s to the 90s, i.e. set stocking on annual pastures. In the mixed farming areas, cropping land expanded from 20% in the 70s to around 40% in recent times. Meanwhile, cultivation intensified. In the 70s cultivation systems consisted of wheat-fallow rotation in the mixed farming and wheat-barley-pasture-fallow in the flat croplands. Starting from the 80s, rotations changed to wheat-barley-fallow in the mixed farming, and canola-wheat-barley-legumes in the flat croplands.

Daily and annual water balance of the hydrologic response units (252 in total) were estimated with a one-dimensional soil column hydrology model (HowLeaky?; Rattray *et al.*, 2004). HowLeaky? predicts runoff using the SCS-USDA curve number method modified to account for changes in soil cover. Evapotranspiration occurs from the soil's top layer down to the depth explored by roots. The model uses a storage routine technique to predict vertical flow through each soil layers. Percolation occurs when field capacity of the lowest soil layer is exceeded. HowLeaky? estimates of annual average runoff and percolation from the 70s to the 90s are shown in Table 1.

Table 1 Annual average runoff (R) and percolation (P) from grazing and cropping land in the Avon Richardson estimated with HowLeaky? model.

	1970-1979		1980-1989		1990-1999	
	R	P	R	P	R	P
	(mm a^{-1})	(mm a^{1})	(mm a^{-1})	(mm a^{-1})	(mm a^{-1})	(mm a^{-1})
Grazing land	11	58	5	48	5	47
Cropping land	18	31	12	22	11	23

CATCHMENT-SCALE RAINFALL-STREAMFLOW ANALYSIS

Daily streamflow data of three gauging stations were used to analyse rainfall-streamflow responses at catchment scale (Table 2). From the 60s to the 90s grazed land extension declined from 92% to 68% in the Carrs Plains (CP), from 97% to 87% in Beazley's Bridge (BB), and from 91% to 63% in the Wimmera Highway (WH). As

Table 2 Characteristics of the gauged catchments of the Avon Richardson selected for this study.

	Streamflow data period	Area	Drainage density	Farming system		
				Grazed upland	Mixed farming	Flat croplands
		(km^2)	(km km^{-2})	(%)	(%)	(%)
Carrs Plains (CP)	1971-1999	121	195	23	77	
Beazleys' Bridge (BB)	1969-87; 1993-95	255	176	68	32	
Wimmera Highway (WH)	1963-1999	550	167	37	60	3

farm management entails remarkable differences in surplus water (i.e. runoff plus percolation, Table 1), changes in land use might have had an impact on streamflows, especially in the CP and WH catchments where grazing land decline has been stronger.

Fig. 1 shows the comparison between annual streamflow measured at WH and the aggregated annual runoff and percolation estimated with HowLeaky? for the hydrologic response units that contribute to the WH catchment. HowLeaky? runoff and percolation estimations follow the annual variations in streamflow closely. The surplus water estimated at the field scale is larger than total streamflow, however it is likely that part of the field surplus water percolates and recharge deep aquifers rather than reaching the stream.

A catchment-lumped model (IHACRES; Croke *et al.*, 2006) was applied to analyse rainfall-streamflow relationships at the three gauging stations for time periods between 1964 and 2001. IHACRES uses a nonlinear loss module to transform rainfall into effective precipitation and a linear module to partition effective precipitation into streamflow pathways (or stores, e.g. quick and slow flow). The upper reaches of the Avon and the Richardson rivers are ephemeral. Ye *et al.* (1997) introduced a catchment moisture threshold parameter (l) to account for the lack of response to rainfall of ephemeral streams under dry conditions. In the linear partition module, common structures that apply for ephemeral catchments are a single exponential store, or an instantaneous store in parallel with an exponential store. The model gave comparable results when using either of these structures, so the simpler single exponential store model was selected for further analysis.

Some IHACRES parameters were considered constant across the Avon Richardson catchment: the drying rate at reference temperature (τw = 16˚C), the temperature dependence of drying rate (f = 3.5), and the streamflow decay coefficient (α = -0.355). Model parameters set for calibration were the conceptual storage maximum volume (c) and the catchment moisture threshold (l). Eighteen calibration periods were selected to cover different farm management and rainfall periods (Table 3).

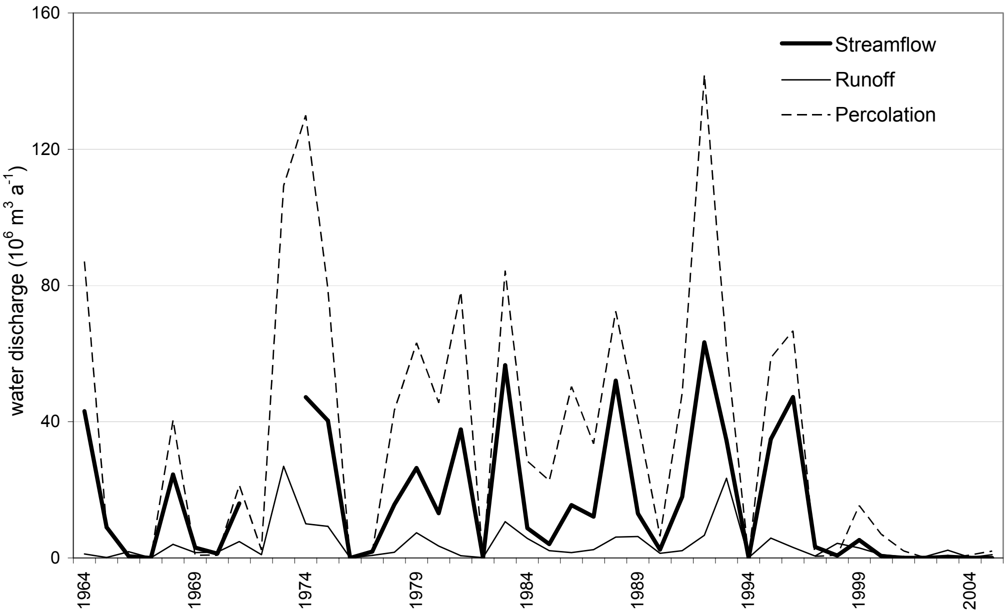

Fig. 1 Comparison of annual streamflow (thick line; in 10^6 m^3 a^{-1}) measured at Wimmera Highway gauging station, with the aggregated runoff (continuous thin line) and percolation (dotted line) estimated with HowLeaky?.

Calibration set CP8687 yielded low efficiency (< 0.5) during the calibration and was therefore excluded from the multiple regression dataset.

Multiple linear regression analysis between IHACRES calibrated parameters, HowLeaky? estimates and catchment characteristics yielded the following best fitting equations:

$$c = -0.018 - 0.000017(R + P) + 0.00014DD \qquad R^2=0.75,\ n = 17 \qquad (1)$$

$$l = 98 - 0.25(R + P) \qquad R^2=0.67,\ n = 17 \qquad (2)$$

where R (mm a^{-1}) and P (mm a^{-1}) are the catchment aggregated average annual runoff and percolation estimated with HowLeaky?, and DD is the catchment drainage density (km km^{-2}, Table 2). The bias in streamflow estimated by IHACRES using c and l

calculated with equations (1) and (2) increased, but efficiency remained acceptable for 12 of the 18 calibration sets. In six cases, however, streamflow predictions were poor and resulted in large absolute bias (> 20 mm) or low efficiency (< 0.5, Table 3).

Table 3 IHACRES calibration periods and results. WH = Wimmera Highway, BB = Beazleys' Bridge; CP = Carrs Plains; numbers indicate first and final year of the calibration period. *c* and *l* are IHACRES calibrated parameters. Bias = model bias and Eff = Nash and Sutcliffe efficiency of streamflow estimation. Post-regression bias and Eff refers to IHACRES streamflow estimation when using *c* and *l* estimated with equations (1) and (2).

Calibration set	Average Rainfall	Average Streamflow	IHACRES				Post-regression	
			c	*l*	Bias	Eff	Bias	Eff
	(mm a^{-1})	(mm a^{-1})		(mm)				
WH6465	533	52	0.0031	65	-1.3	0.626	-4.9	0.610
WH7073	475	2	0.0048	70	0.1	0.766	9.5	0.403
WH7475	646	43	0.0030	40	0.7	0.738	35.7	0.597
WH8689	535	22	0.0040	55	3.4	0.710	25.3	0.582
WH95	597	79	0.0027	55	-2.9	0.636	-5.1	0.625
WH9701	442	1	0.0072	90	0.4	0.694	2.5	0.711
BB7072	592	55	0.0056	115	-1.8	0.663	-37.4	0.649
BB7374	795	108	0.0026	30	-10.7	0.672	15.2	0.608
BB7778	444	27	0.0057	95	-0.9	0.753	-9.8	0.688
BB8384	625	87	0.0044	75	-1.9	0.718	-15.5	0.723
BB95	691	129	0.0034	75	0.4	0.751	-13.3	0.785
CP7374	740	143	0.0063	50	-7.2	0.690	-0.0	0.681
CP7778	472	17	0.0099	85	2.4	0.687	15.1	0.646
CP8384	586	73	0.0052	70	0.6	0.745	-14.8	0.690
CP8687	473	21	0.0033	65	1.7	0.422	0.0	0.272
CP91	496	76	0.0103	100	-2.1	0.592	-35.4	0.258
CP9293	648	79	0.0072	70	-0.5	0.585	-17.6	0.583
CP9500	433	23	0.0081	95	-1.4	0.521	-6.8	0.552

CONCLUSIONS

A single column water balance model that estimated field-scale water balance was successfully linked to catchment rainfall-streamflow responses. The spatially aggregated surplus water of the hydrologic response units captured the effects of climate and farm management changes across several decades, and closely related to annual streamflow measurements. A strong linear correlation was found between aggregated field-scale estimates of surplus water and catchment streamflow via two important conceptual parameters that describe rainfall-streamflow response of ephemeral rivers, i.e. the catchment storage maximum capacity and the catchment moisture threshold.

The poor results yielded in six of the 18 calibration sets of the catchment-scale model, however, indicates that further work is required to improve the methodology, such as the incorporation of other factors not considered thus far (e.g. rainfall intensity), and extension of the analysis to other areas or historical farming periods.

REFERENCES

Croke B. F. W., Andrews F., Jakeman A. J., Cuddy S. M. & Luddy A. (2006) IHACRES Classic Plus: a redesign of the IHACRES rainfall-runoff model. *Environmental Modelling and Software* **21**, 426-427.

Post D. A. & Jakeman A. J. (1999) Predicting the daily streamflow of ungauged catchments in S.E. Australia by regionalising the parameters of a lumped conceptual rainfall-runoff model. *Ecological Modelling* **123**, 91-104.

Rattray D. J., Freebairn D. M., McClymont D., Silburn D. M., Owens J. & Robinson J. B. (2004) HowLeaky? the journey to demystifying simple technology. In: *Conserving soil and Water Society: sharing solutions ISCO 2004, 13th International Soil Conservation Organization Conference*, Brisbane, July 2004.

Ye W., Bates B. C., Viney N. R., Sivapalan, M. & Jakeman, A. J. (1997) Performance of conceptual rainfall-runoff models in low-yielding ephemeral catchments. *Water Resources Research* **33**(1), 153-166.

Prediction of agro-hydrological effects of a large brackish lake at Wieringen, the Netherlands, with integrated modelling of water and solute transport in variably saturated soils

T.H. VAN WEE & A. BIESHEUVEL
Witteveen+Bos engineering, P.O. Box 10095, NL-1301 AB Almere, The Netherlands
t.vwee@witteveenbos.nl, a.biesheuvel@witteveenbos.nl

Abstract The Wieringerrandmeer project comprises the construction of a lake with an area of roughly 700 hectares in the north of the Netherlands. The project area is an important agricultural region. An increase in exfiltration rates and salinisation of groundwater is expected in the surroundings of this lake, which could cause effects on the crop yield. In order to predict possible agricultural effects of the lake an extensive modelling was carried out. This modelling, which takes into account the unsaturated zone, was necessary for communication with the stakeholders. By integrating SWAP in the existing models MODFLOW/MT3D/SEAWAT time dependent predictions till the year 2030 of the crop growth and the development of fresh water lenses were made. This paper describes the methods used and discusses the results.
Keywords agro-hydrological effects; ground water salinisation; modelling water and solutes in the unsaturated zone; modelling crop growth; water (resources) managament; communication stakeholders

INTRODUCTION

The Lake Wieringen project comprises the establishment of a brackish lake with an area of roughly 700 hectares, located on the fringe of the former island of Wieringen and the Wie-ringermeerpolder in the north of the Netherlands (see Fig. 1). This is mainly an agricultural area.

Fig. 1 Project location Lake Wieringen (Wieringerrandmeer).

The surface water level of the proposed Wieringerrandmeer will be around 4 meters above the polder surface water level. For this reason, the establishment of the lake is expected to impact both on groundwater flow and salinity patterns. The impact of the lake on the regional groundwater system was calculated (Bonte & Biesheuvel, 2006) with the variable density code SEAWAT, including the effects of expected climate change (Biesheuvel & Bonte, 2006). It appeared that in the surroundings of the lake an increase in upward seepage and salinisation of groundwater is expected. This could cause effects on the crop yield and is therefore of great concern to the farmers in this area.

EFFECT ON FRESHWATER LENSES AND CROP GROWTH

The low-lying polder area of the Wieringermeer is reclaimed from the sea some 75 years ago. Brackish/saline groundwater seeps upward through the covering layer. Shallow freshwater lenses are formed, fed by recharge from precipitation. In winter these lenses are formed and in summer they diminish. Due to capillary rise fresh water reaches the root zone and makes crop growth possible. Increased upward seepage and salinsation, as is expected after establishing Lake Wieringen, can reduce crop growth through salt stress (see Fig. 2).

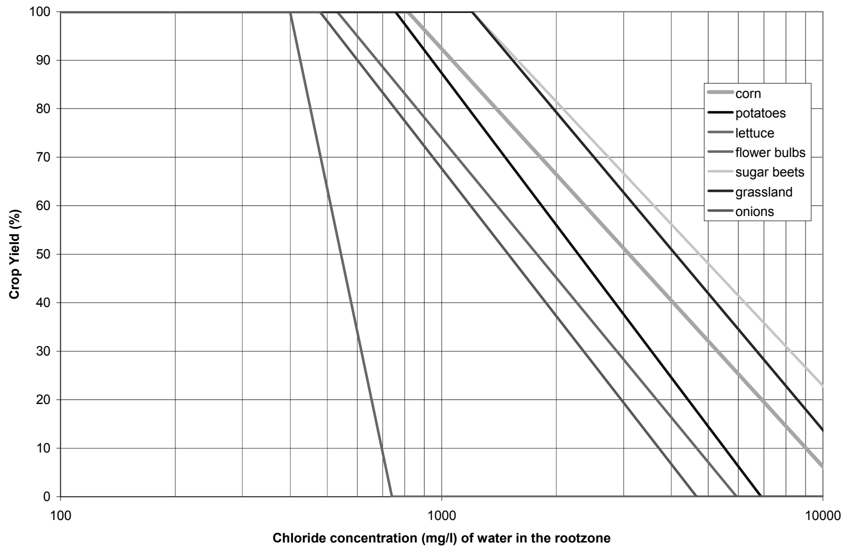

Fig. 2 Reduction of crop growth due to saltstress in the rootzone.

SWAP CALCULATIONS

In order to predict possible agricultural effects of the lake an extensive modelling was carried out with the SWAP-code. SWAP (Soil-Water-Atmosphere-Plant system) simulates vertical transport of water, solutes and heat in variably saturated, cultivated soils. It can calculate crop growth under influence of drought- and salt stress. By integrating the SWAP-model with the regional SEAWAT-model it was possible to carry out time dependent predictions till the year 2030 of the development of the fresh water lens and the agricultural yield in the surroundings of the lake under different climate conditions. In the affected area several representative locations were chosen, considering soil-conditions, crops and effects of the Lake. For these locations SWAP-calculations were carried out on a daily basis for a twenty year period with a large variety of climate conditions (including extremely dry conditions, as appeared in 1976). The model was calibrated on groundwater levels. Due to a lack of data, no calibration on the thickness of the fresh water lens was possible.

RESULTS

Calculations were carried out and for several scenario's and for different crops, including expected developments such as sea level rise. The calculations gave insight in the crop yield under different conditions, the influence of irrigation, the amount of water needed for irrigation and the influence of salt stress for different crops (potatoes, grassland, flower bulbs) for years with average climate conditions and for years with extreme conditions.

For a representative location in the Wieringermeer, an exfiltration rate (upward seepage) of 1 mm/d was calculated, with a chloride-concentration of 2000 mg/l. Fig. 3 shows that the thickness of the fresh water lens in winter exceeds 100 cm and in summer it reduces to a few decimetre. The thickness of the unsaturated zone in summer is about 200 cm. In dry years irrigation takes place to reduce effects of drought stress. Irrigation water has an chloride concentration of 600 mg/l.

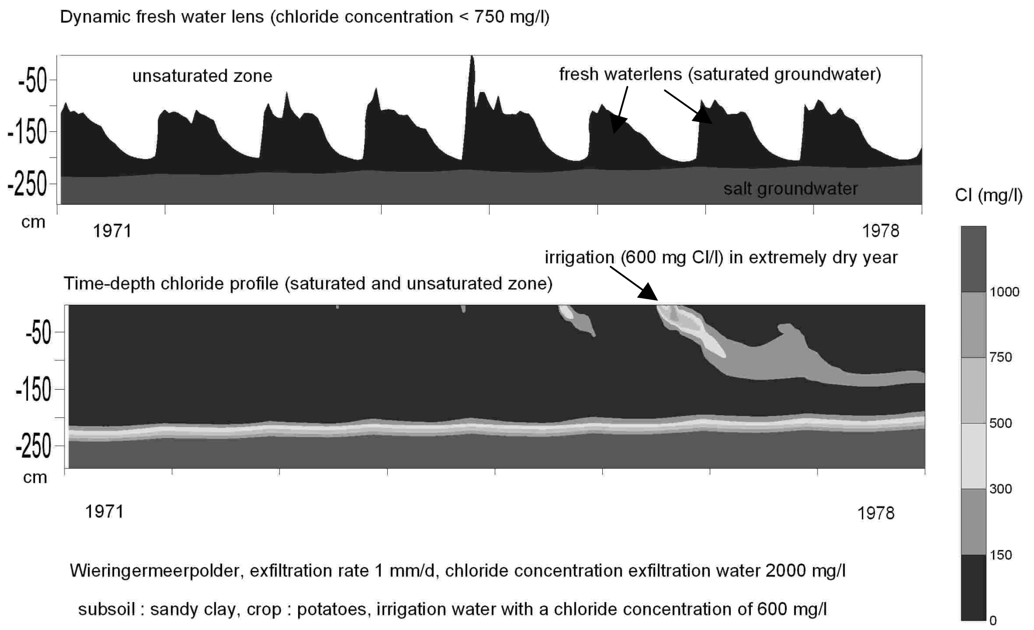

Fig. 3 Current fresh water lens and time-depth chloride profile.

Due to the establishing of Lake Wieringen, it is expected that the exfiltration rate will increase to 1.5 mm/d at the representative location, with a chloride-concentration of 2500 mg/l. Higher groundwater levels are calculated and the thickness of the fresh water lens is reduced (Fig. 4) in the surroundings of Lake Wieringen. However, this will not lead to a (significant) decrease of the crop yield (potatoes) in this area, because the salt-concentration in the root zone will not increase significantly and potatoes are not very sensible to salt stress at lower chloride-levels. Flower bulbs are more sensitive to salt stress; since water in the root zone has a low chloride content, the chloride content of irrigation water (600 mg/l) is the most critical factor.

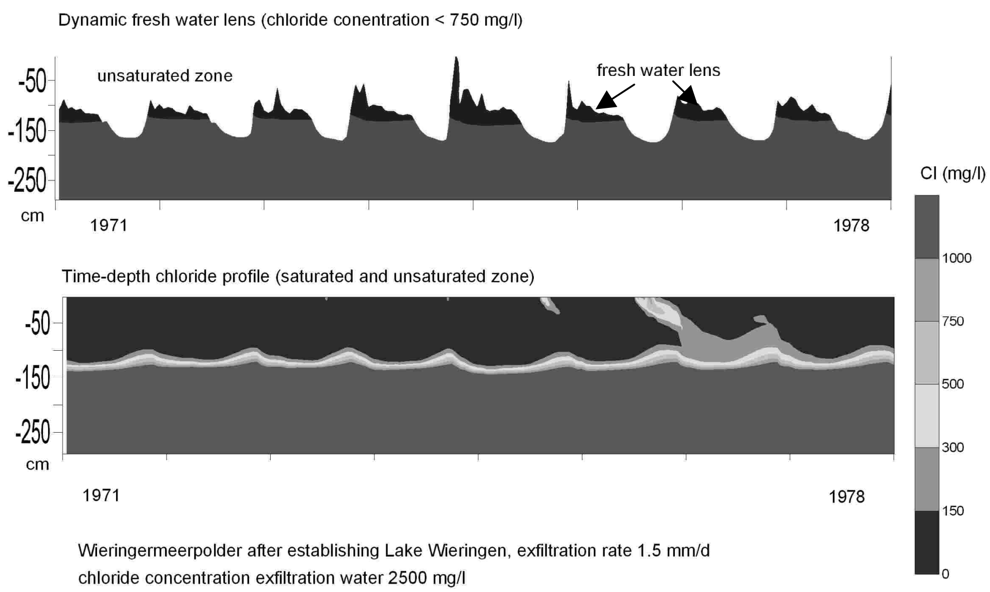

Fig. 4 Fresh water lens and time-depth chloride profile, after establishing Lake Wieringen.

Due to irrigation a reduction of crop yield through salt stress is expected of 20–35%. However, this reduction will not be influenced by establishing Lake Wieringen. To maximise the crop yield of flower bulbs additional fresh water (chloride concentration < 200 mg/l) is necessary, both in the present situation and after establishing Lake Wieringen. Reducing negative effects is possible by means of hydrological measures; an interception ditch between the lake an the agricultural area and additional drainage in this area will have a positive effect on the thickness of the saltwater lens (see Fig. 5).

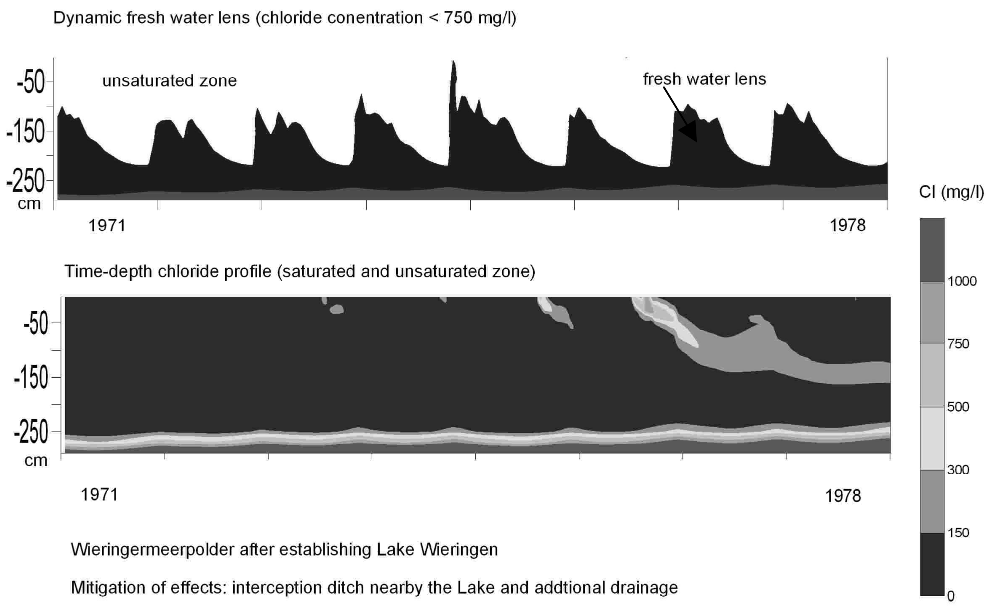

Fig. 5 Fresh water lens and time-depth chloride profile, with Lake and mitigation measures.

COMMUNICATION

The results are regular discussed with the land owners, farmers and the residents in the Wieringerrmeer. A special ‘area committee’ (with regulary meetings) takes into account all interests, so everybody could recognise the agro-hydrogical research and the results of it. Due to this communication the stakeholders have confidence that the construction of the lake has no negative effects on agricultural production.

CONCLUSIONS

Establishing Lake Wieringen will reduce the thickness of the fresh water lenses in the agricultural area surrounding the lake. However, this will not lead to a significant decrease of crop yield in this area. Through hydrological measures as interception ditches and additional drainage, the decreasing thickness of the fresh water lens can be diminished and possible negative effects can be reduced. Growing flower bulbs in this area demands additional fresh water, both in the present situation as well as after establishing Lake Wieringen. Communication with stakeholders leads to confidence en trust that there will be no negative effects of the lake.

REFERENCES

Biesheuvel, A. & Bonte, M. (2006) Effects of climate change, Lake Wieringen, The Netherlands. *Proceedings Aquatech Conference on “Innovations in coping with water and climate risks”*, Amsterdam.

Bonte, M. & Biesheuvel, A. (2006) The Application Of The Seawat 2000 Variable Density Model For The Wieringerrandmeer Project. *Proceedings 1st SWIM-SWICA meeting*, Italy.

Witteveen+Bos (2008) Geohydrologisch vervolgonderzoek Wieringerrandmeer - verzilting en watervoorziening. *Report WRW5-37* (in Dutch).

Modelling and optimisation of the Murzuq Basin aquifer system in Libya for effective water resources management

A. J. ADELOYE[1] & A. SHAKI[2]

1 *School of the Built Environment, Heriot-Watt University, Edinburgh, EH14 4AS, UK*
a.j.adeloye@hw.ac.uk

2 *Soil and Water Department, Faculty of Agriculture, Sebha University, P. O. Box 19332, Sebha, Libya*

Abstract The Murzuq basin in southwest Libya currently provides water for a number of large scale irrigation schemes, including the Irawan project. In order to evaluate the possible impacts of the large scale abstractions on the hydraulic conditions in the aquifer, a MODFLOW model was developed and calibrated with satisfactory results. The simulation model was then linked with a linear programming optimisation model to develop optimal pumping strategies for the field.
Keywords Murzuq basin; Irawan project; Libya; arid; groundwater; mathematical modeling; optimization

INTRODUCTION

The low rainfall and high temperature situations characterising Libya mean that naturally occurring surface water resources are almost non-existent, implying that groundwater resources are exclusively relied upon for meeting the huge irrigation demands which account for over 80% of total water withdrawals (Al-Ghariani, 2002). The Murzuq basin in south-west Libya contains one of the country's major water bearing aquifers; its water is extensively abstracted for irrigating the Irawan irrigation project. Currently, there are 27 wells which are pumped continuously for irrigating the fields but there are concerns about the low efficiency of utilization of the water caused by too much water wastage.

Despite the above, however, there has been no systematic study of the potential effects of such abstractions on the hydraulic situation of the aquifer systems (Shaki & Adeloye, 2006). The aim of the current study is to provide this information by developing a mathematical model of the aquifer system. The hydraulic model was then coupled with a linear programming optimisation model to develop an optimal pumping strategy for the Irawan irrigation project.

DESCRIPTION OF THE MURZUQ BASIN & IRAWAN PROJECT

Located in the southwest of Libya (see Fig. 1), the Murzuq basin is usually hot (average max temperature = 39 ^{o}C) and dry (annual rainfall < 30 mm); consequently natural recharge is considered non-existent. Its geology is dominated by a thick deposit of continental sandstones overlain by Lower Cretaceous sands and sandstones with alternating clays. These formations delineate two aquifer groups- the upper one which is essentially phreatic and the lower one which is semi-confined (Shaki, 2006). The upper aquifer is saline, particularly at shallow depths; however, the TDS concentration of the lower aquifer is low, 100-200 mg/l. Consequently, abstraction for irrigation is limited to the lower aquifer groups.

The Irawan agricultural project is located close to the northern border of the Basin and derives its water exclusively from the Murzuq. Established in 1987, it covers 13.5 km^2 of land devoted to growing wheat in the winter (October – March) and maize in the summer (May – September). This total area is divided into 27 (× 0.05 km^2) circular planting sub-areas, with each sub-area having its own well as shown in Fig. 2.

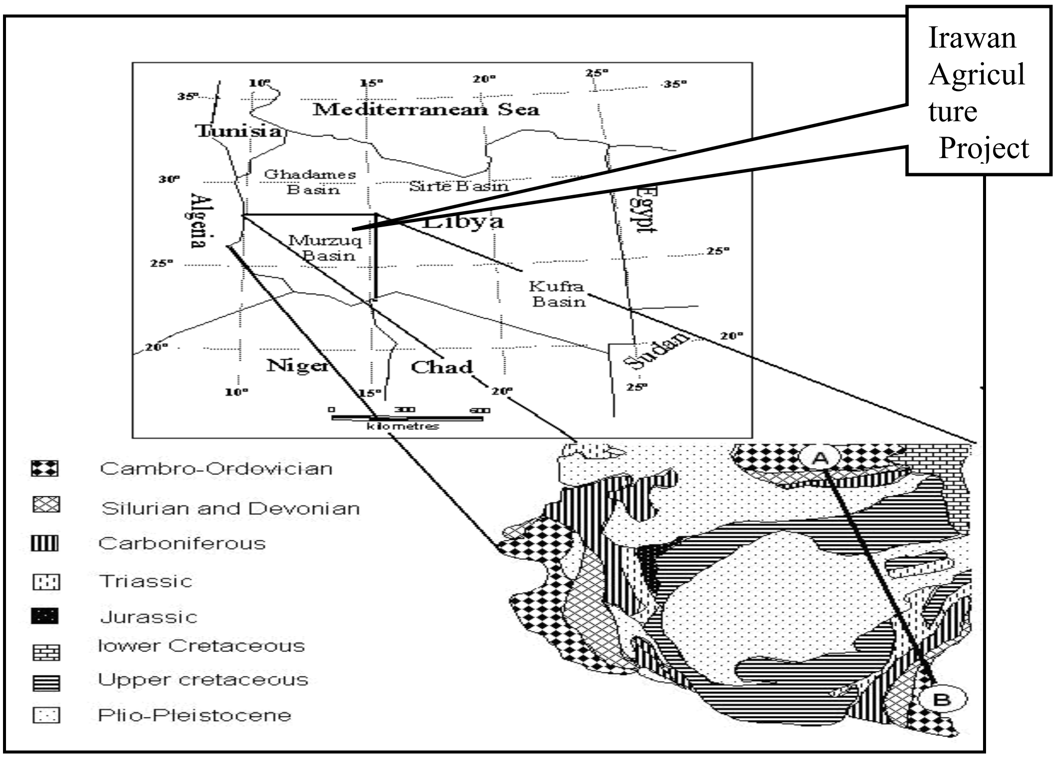

Fig. 1 Location of the Murzuq Basin and Irawan irrigation project, southwest Libya (Cross-section detail A-A not shown).

GROUNDWATER FLOW SIMULATION AND OPTIMISATION

A simulation model of the Murzuq aquifer was developed using MODFLOW (McDonald & Harbaugh, 1988), which implements a finite difference solution of the 3-D groundwater flow equation:

$$\frac{\partial}{\partial x}\left(K_{xx}\frac{\partial h}{\partial x}\right)+\frac{\partial}{\partial y}\left(K_{yy}\frac{\partial h}{\partial y}\right)+\frac{\partial}{\partial z}\left(K_{zz}\frac{\partial h}{\partial z}\right)-W=S_S\frac{\partial h}{\partial t} \tag{1}$$

where K_{xx}, K_{yy} and K_{zz} are values of hydraulic conductivity along the x, y and z coordinate axes, which are assumed to be parallel to the major axes of hydraulic conductivity (Lt^{-1}); h is the potentiometer head (L); W is volumetric flux per unit volume and represents sources and/or sinks of water (t^{-1}); S_S is the specific storage of the porous material (L^{-1}); and t is time (t). The modelling was concentrated on the lower group aquifer because its water was used for irrigating Irawan.

The objective function for the optimisation of the pumping strategy was the minimisation of the total withdrawal while meeting a number of constraints including the consumptive use of the crops, allowable piezometric drawdown at specified locations and pump rates among others, as described by Shaki (2006).

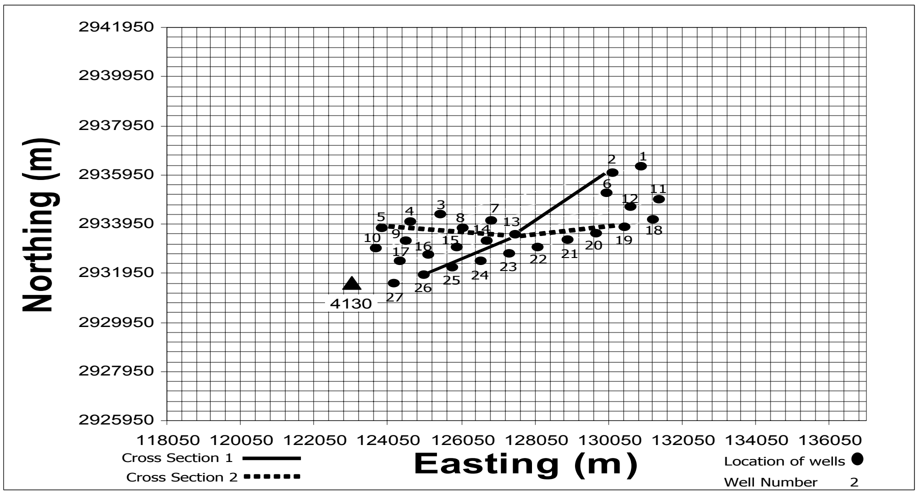

Fig. 2 Well locations at Irawan irrigation project.

RESULTS

Simulation

Time-drawdown data were available for wells 3, 19, 20, 22, 25 and 27 based on 7 days of pumping in well 24 at a constant rate of 4750 m^3 day^{-1}. The data for well 25 (radial distance = 800m from pumped well 24) were used to obtain initial estimates of the hydraulic characteristics of the aquifer based on the Walton curve fitting method (Kruseman & de Ridder, 1994); the results are shown in Table 1. These estimates were used as initial parameters values for the calibration of the MODFLOW model. Additionally, drawdown data were available for various times between 1988 and 2003 (16 years) at well number 4130 located slightly west of the Irawan project area, based on simultaneous pumping of some of the 27 wells, and were used for the unsteady state calibration of the model. Fig. 3 compares the observed and predicted piezometric head at well 4130, which is quite satisfactory.

Table 1 Initial estimates of aquifer parameters based on a weakly leaky system.

Parameter	Value
Transmissivity (m^2 day^{-1})	2807.6
Aquifer storage coefficient	1.09×10^{-5}
Hydraulic Resistance	91181
Hydraulic conductivity of the aquitard (m/day	0.000329

Once calibrated satisfactorily, the model was used to assess the long-term effects of the current pumping regime at the Murzuq, post- 2003. The maximum post-2003 depression in well 4130 was 7m in year 2033, representing a maximum drawdown of 30 m. Thus, the piezometric level will stabilize at 446 m, unless inflow from outside the boundary changes or agricultural water withdrawal changes drastically.

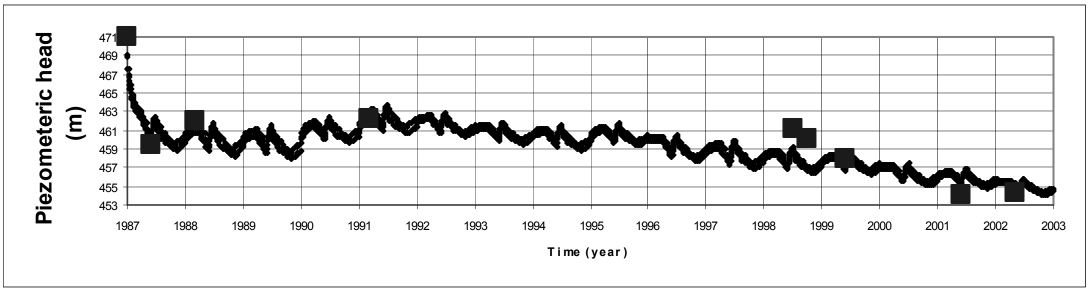

Fig. 3 Comparing measured and simulated heads in well 4130 during calibration.

Optimisation

There are two planting seasons per year, each with different water needs; consequently, water applications were optimised differently for the two seasons. The optimised value of the objective function obtained for the wheat optimization was 11,034,000m^3, representing the total amount of water pumped over the entire growing season and field. However, only 23 of the wells are active, with each pumping at the maximum pumping rate 4750 m^3 day^{-1}. The optimised value of the objective function was 6,507,500 m^3, achieved with just 10 active wells, each pumping at 4750 m^3 day^{-1}.

CONCLUSIONS

The development of a hybrid simulation-optimisation model for the Murzuq basin in southwest Libya has been successfully carried out. From the overall study, it is clear that, based on the current cropping pattern, the drawdown will stabilize at a maximum of 30m in the long term. However, based on the results of the optimisation, it is certainly not necessary to continuously pump all the wells, since a subset of the wells will meet the demand, particularly during the summer planting season. If this optimal pumping arrangement is implemented, much of the drawdown currently being experienced could be significantly reduced.

REFERENCES

Al-Ghariani, S.A. (2002) Future perspectives of irrigation in southern Mediterranean region: Policies and management issues. *Proceedings of the international conference on water resources management in arid regions*, March 23-27, 2002, Kuwait.

Kruseman, G. P. & de Ridder, N. A. (1994) Analysis and evaluation of pumping test data. Second edition. *International Institute for Land Reclamation and Improvement, Wageningen, the Netherlands.*

McDonald, M.G. & Harbaugh, A. W. (1988) A modular three-dimensional finite-difference groundwater flow model: U.S. *Geological Survey, Techniques of Water Resources Investigations*, Book 6.

Shaki, A. A. & Adeloye, A, J. (2006) Evaluation of quantity and quality of irrigation water at Gadowa irrigation project in Murzuq basin, southwest Libya. *Agricultural water management* **84**, 193-201

Shaki, A. A. (2006) Simulation and Optimization Studies for Better Groundwater Management in the Murzuq Basin, Libya. *Unpublished Ph.D thesis, School of the Built Environment, Heriot*-Watt University, Edinburgh, UK.

A decision support system and the water resource management in the Tiber River Basin

S. CASADEI, M. BELLEZZA & A. PIERLEONI

Dept. of Civil and Environmental Engineering, University of Perugia, Borgo XX Giugno 74, 06121 Perugia, Italy
casadei@unipg.it

Abstract In the present work, two software tools are presented; they combine the scientific aspect of the issues with a feasible and widely accessible application of the mathematical modelling in techno-operative fields within a sustainable management policy of the water resource at the basin scale. The first evaluation model of the available superficial water resource bases its algorithms upon regionalization procedures of flow parameters deduced from the geomorphologic features of the soil of the basin (BFI, Area) and presents, as output, a set of hydrological information for each section of the river network. The second software tool is a simulation model of a managed water resource for multipurpose uses. The algorithm is based on a topological sketch of the river network in terms of "Nodes" and "Links" combined with computation procedures for managing the water resource of big reservoirs.

Keywords model; water resource; multipurpose management; decision support system; WEB-based

INTRODUCTION AND BACKGROUND INFORMATION

The management of surface water at the basin scale can be divided into two fundamental steps: the first one is the evaluation of the water available while the second is the integrated management of the resource itself, with particular regard to the hypothesis of development of the demand and the occurrence of more and more severe critical periods (Arnell & Delaney, 2002).

All the problems that arise in this process, if faced from a theoretic point of view and in a rigorous way, are extremely complex because of the many technical, economic and political issues involved. Anyway, the development of the technology for data collection and analysis allows to study these problems from different angles and achieve different conclusions offering a wide range of possible interpretations that are very useful both from a scientific (Simonovic, 2000) and decisional (Sechi & Zuddas, 2002; Georgiou *et al.*, 2006) point of view.

This research faces the two phases of evaluation and management of the water resource dividing the global issue in three steps.

The first step is based on the organization and validation of the hydrological data and the information about the exploitation of the resource. For this purpose it has been decided to build a WEB-GIS software environment in order to create a shared database for all the institutions concerned, so that the differences and uncertainties of the raw data could be highly reduced before any model analysis.

The second one concerns the evaluation of the water resource naturally available and calculates various hydrologic indexes that are needed in the next managing step. In fact using time series of instream flows taken from measures may lead to wrong evaluations in the management of the water resource at the basin scale, especially when all the active upstream withdrawals are not taken into the proper consideration and this is even more evident for semi-permanent or low flows. In this step the model is strongly centered on three algorithms: the first one evaluates the historic natural time series starting from measured flows and the information on the demand and the withdrawal licenses; the second is a mathematical fit of the duration curves with a three-parameters Log-Normal frequency distribution; the third is a regionalization of the duration curves with parameters that can be obtained from the geomorphologic features of the basin. In general, these three procedures allow an estimation of the available surface water resource representing the instream flows by means of duration curves.

Finally the third step analyses the hypothesis of water resource management with simulation models of the hydraulic network in the natural and human-modified conditions, with particular regard to scenarios where multipurpose reservoirs serving large demands are present. This step obviously takes advantage of all the evaluations and calculations made in the previous steps. Particularly, the hydraulic input used is represented by the natural instream flows time series calculated on the base of the procedure mentioned in the previous step, while the constrains on the minimal instream flows may be well approximated with the Q_{355} value extracted from the duration curve of the section of the network of concern.

CASE STUDY: TIBER RIVER BASIN

The methodology illustrated previously was applied to the Tiber River basin, where a widespread situation of water withdrawals for multiple uses makes it particularly interesting for developing this study.

All hydrologic data regarding the water withdrawals, the hydro-geological features of the basin and its sub-basins have been archived in an open source WEB-GIS system. This system has been built on the base of expandability and flexibility criteria so that it can contain all the information that may become useful in order to feature the basin. The database is accessible with a user friendly interface and different access levels depending on the type of user (http://wrme.hydrogate.unipg.it/). Therefore this system is based on the goal of sharing the data and minimizing the variability of results that derives from the use of databases and information that are not validated and aligned.

The application of the model for the evaluation of the available water resources in the entire Tiber River basin showed how the methodological approach can be practically developed; however, there is considerable indetermination in the input data regarding water withdrawals, anyway, this problem could be solved applying the previous approach to the entire basin.

In Fig. 1, natural and measured duration curves are compared with the estimated curve at the Ponte Felcino hydrometric station. In particular, one can observe the weight of water withdrawals on low flows, made evident by the different trend of the two corresponding curves for durations of over 270 days, and how the trends of the estimated curve and natural curve coincide at the values normally used as low flow indicators (Q_{347}, Q_{355}).

In the next step, the simulation model, takes into account two very important considerations:

- the model input must necessarily derive from the time series of natural flows;
- the minimum flow thresholds for ungauged sections must take into account the low flow indicators, which can be obtained by the estimated duration curves of any section of interest of the network.

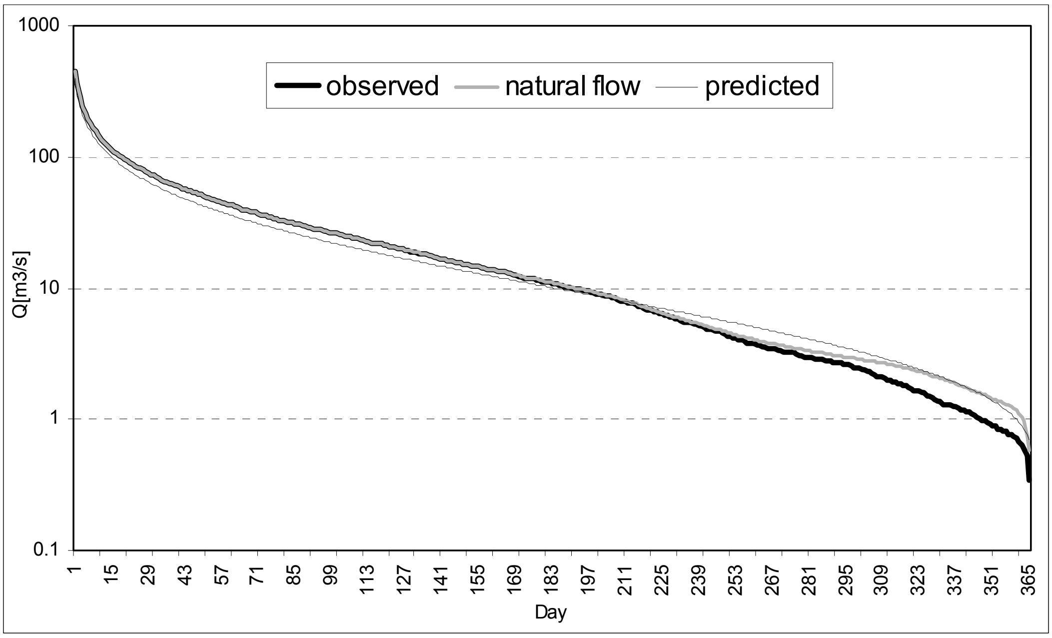

Fig. 1 Ponte Felcino hydrometric station, comparison between measured, natural and predicted duration curves.

The practical application regarded only the upper basin of the Tiber River, where there are two large artificial reservoirs (Montedoglio, Vmax=153 Mm^3; Casanova, Vmax=200 Mm^3) for multipurpose use (Casadei *et al., 2005*). The management of these structures involves various administrative and socioeconomic spheres, with considerable planning difficulties as to the allocation of the available water resources among the various users and among users in different territorial areas.

In this context, the simulation model makes it possible to hypothesize numerous simulation scenarios on the basis of the different combinations of water requirements for different uses, indicating the results both in terms of artificial reservoir management (Fig. 2) and in terms of satisfying the requests of the various users (Fig. 3), including those of an environmental nature.

Over one hundred simulations were run on a time series of 33 years, attempting to evaluate various scenarios in a perspective of the evolving of requirements over time and of different sensitivities to the environmental usage of the water, with the latter being understood as the increase of the minimum releases in the river downstream from the artificial dams.

CONCLUSIONS

The final aim of this project is to be able to share these scientific tools and hydrological data among many institutional uses. For this purpose, a WEB-based system, under the control of an administrator, provides on the one hand the possibility to easily keep the database up-to-date and on the other, the possibility to share data and retrieve the results of the procedures optimized for managing superficial water resources at the basin scale.

Lastly, from a methodological viewpoint, simulation modeling can be integrated with optimization criteria, which make it possible, in a controlled manner, to highlight the economic aspects in the choosing of water resource management hypothesis.

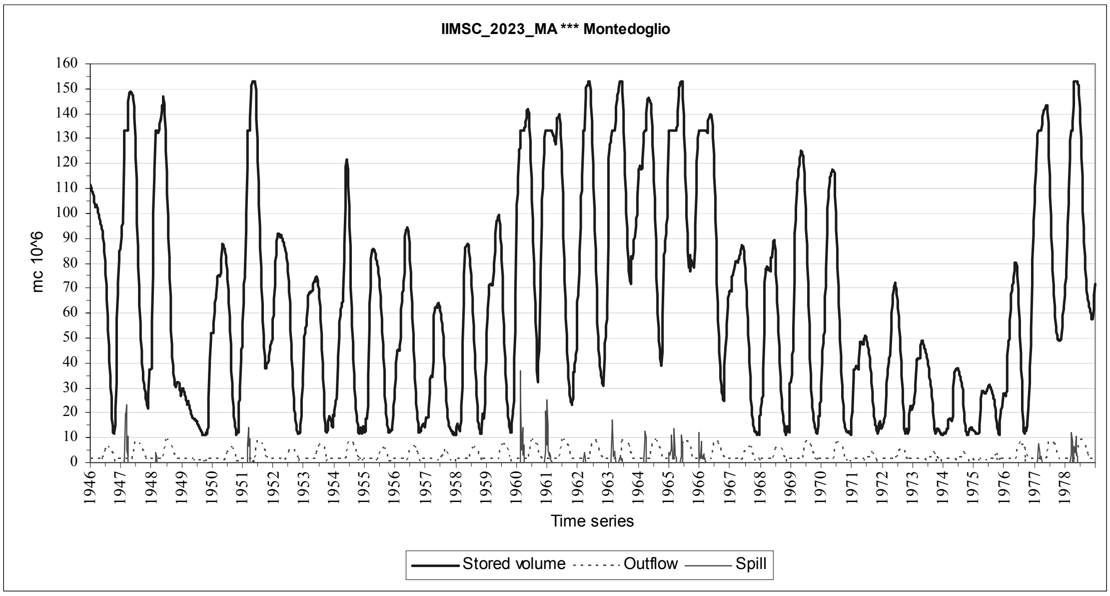

Fig. 2 Montedoglio reservoir: stored volume, releases for the demand (outflow) and spill.

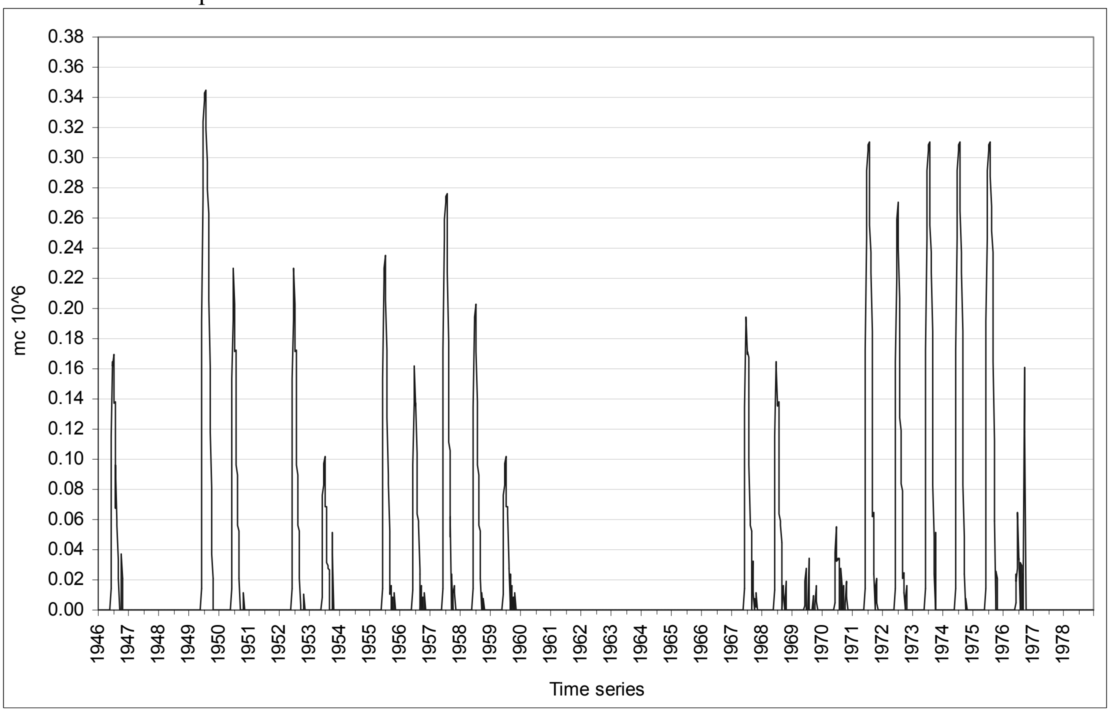

Fig. 3 Deficit time series for an irrigation area.

REFERENCES

Arnell, N. W. & Delaney E. K. (2002) Adapting to climate change: public water supply in England and Wales. In: *Climate Change*, **78,** 227–255.

Casadei, S., Manciola, P. & Bellezza M. (2005) Sulla gestione di un grande invaso a scala di bacino. Un caso di studio, Collana degli atti dei Convegni Lincei, Giornata mondiale dell'acqua 2005, Lagune, Laghi e Invasi Artificiali Italiani (Bardi Editore), 147–157.

Georgiou, P. E., Papamichail D. M. & Vougioukas S. G. (2006) Optimal irrigation reservoir operation and simultaneous multi-crop cultivation area selection using simulated annealing, *Irrigation and Drainage*, **55,** 129–144.

Sechi, G.. M. & Zuddas P. (2002) The optimization package WARGI: water resource systems optimization aided by graphical interface, *28° Convegno di Idraulica e Costruzioni Idrauliche*, Potenza-Italy, 71–80.

Simonovic, S. P. (2000) Tools for water management – One view of the future, *I.W.R.A., Water International* **25,** 76–88.

Increasing the yield of the joint water supply system of Dachia and Daan rivers through management

FREDERICK N.-F. CHOU, HAO-CHIH LEE & CHIA-WEN WU
Department of Hydraulic and Ocean Engineering, National Cheng Kung University, 1 University Road, Tainan 701, Taiwan
n8893101@ncku.edu.tw

Abstract The water demand is increasing continuously, on the other hand, construction of large water resources projects are prohibited due to environmental concern. In this situation, both development and management alternatives are considered to increase the reliable water yield in Taiwan. The joint water supply system of Dachia and Daan Rivers was selected as case study in this paper to analyze the potential contribution of system yield through joint utilization of water resources of these two rivers. Two alternatives were simulated to compare the capabilities of supplying water to meet the demand of Taichung metropolitan at year 2021: (1) adjusting the pattern of peak hydrogenation of Derchi Reservoir, and (2) transferring raw water form Dachia River to Daan River. Three situations were encountered in the simulation: (1) high turbid raw water might prohibit the water to be transferred or restrict the quantity of water can be processed in the treatment plant after heavy storm, (2) peak hydrogenation carried out in a few hours might reduce the available amount of water withdrawn for a certain purpose, and (3) water should be supplied directly to Taichung instead of passing through the transbasin waterway. Special algorithms were provided in the Generalized Water Allocation Simulation Model (GWASIM) to correctly simulate the water utilization of this complex system. The analyzed results showed that the first alternative could increase the water supply capability of the joint water supply system, but it could reduce part of hydrogenation as trade-off. The second alternative could increase the utilization rate of the water released from the hydropower plant and the unregulated flow to the downstream. It also could improve the complementary ability of supplying water between the two rivers system.
Keywords transbasin water transfer; peak hydrogenation; network flow programming

FOREWORD

Under the presumption of not building any large scale water facilities, this paper discusses the possibility of increasing the yield capability of this water supply system by establishing small scale water facilities or by implementing the operation strategy i.e., increasing the respensible yield from the reservoir to the public water demand in the downstream. This paper assesses the following proposed measures could fulfill the water demand in 2021:

1. Amending the operating purposes of the Dachia Reservoir.

   By subsidizing the Taiwan Power Corporation, it could increase the water resources use and water supply capability in the system by giving in some efficiency of hydrogeneration.

2. Constructing the Divert

   By diverting the excess water of the Dachia River to the Liyutan Water Treatment Plant, it could reduce the release from the Liyutan Reservoir and maintain its storage water level to use in the drought seasons.

SYSTEM SUMMARY AND ANALYSIS CONDITIONS

The joint operating system of the Dachia River and the Daan River

This research analyzes the joint operating system of the Dachia River and the Daan River as a case study of the impact on water supply and peak hydroelectricity imposed by different environmental flow levels. This system supplies water to both the Taichung public and industrial water use demand as well as supporting parts of the Jhanghua and Miaoli public water use demand, the system is shown in the Fig. 1.

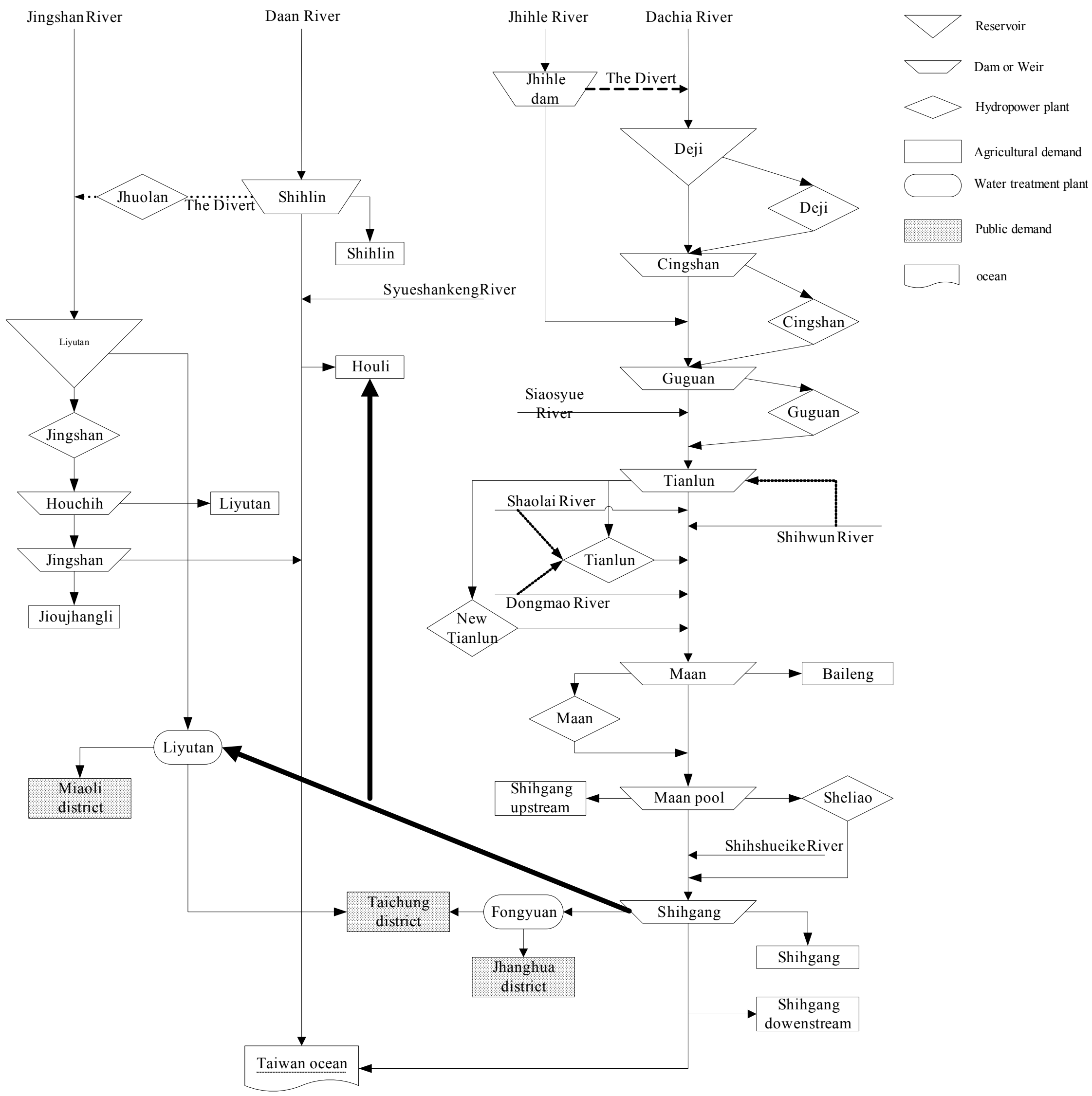

Fig. 1 The water resources system in the Dachia River and the Daan River.

METHODOLOGY

Simulation Model

In this study, the dynamic module of the General Water Allocation Simulation Model (GWASIM) was used to analyze the water allocation strategy of a very large scale water supply system. The GWASIM Model has two modules such as: water supply simulation module and water allocation optimization module. This model was developed based on the theory of MCNFP and the OKA (Out-of-Kilter) method, specifically for Taiwan's water resources system.

During the analysis of the model, day was used as its unit. Because most of the Taiwan's water resources system had developed using joint operation system including the reservoirs, the tributaries at the downstream, and the other systems in the neighborhood water basin and day is used as unit for all of the systems. The GWASIM Model has the ability to simulate: (i) the special operation rules of the reservoirs of Taiwan, (ii) the through demand i.e., the minimum environmental flow or the power generation demand, (iii) the losses in the water supply system, (iv) the restricted yield of the water treatment plant due to high turbid water, (v) the unsteady flow due to the peak hydrogeneration is routed through the river channel within a day to the downstream.

The limited withdrawal ability due to high turbidity

The limited withdrawal ability due to high turbidity includes (i) stop diverting water from other basin to the reservoir, and (ii) decrease the water supply capability of the water treatment plant. The operator decides stop diverting water based on the amount of the flow, and decrease the water supply capability of the water treatment plant based on the turbidity of the raw water. The relationship would be considered in the simulation.

The method of simulation of the releasing water process of the Deji Reservoir during the peak hydrogeneration period

In traditional water resources analysis, the flow includes (i) the river, (ii) the releasing water from reservoir, (iii) the demand would be assumed that it would be distributed uniformly during the simulation. But during the peak hydrogeneration in the power plants of this system, the water is usually released for six hours in a day from the reservoir, and it is expected that the unsteady flow is routed through the river channel within a day. If the withdrawal of water capability of the facilities in the downstream is still assumed uniform, the actual amount of water which could be withdrawn will be limited. Unless there existed high capacity reserve water facilities or divert facility in the downstream, when the process of flow distributed uniformly is used as an assumption in water resources analysis, the amount of water withdrawn in the downstream would be evaluated highly.

In order to simulate the water releasing process during the peak hydrogeneration correctly, the special operation procedure which could calculate the withdrawal amount of water individually was designed in GWASIM model. But the model didn't consider that the unsteady flow would be routed through the river channel within a day. This model assumed that the water is releasing uniformly during the peak hydrogeneration, and the pattern of the water flow from the power plants to the facilities in the downstream would be the same in the analysis. The results of the simplified simulation appeared that this method is conservative due to the amount of water withdrawal would be less than that of the real amount but also would be close to the real phenomenon.

CONCLUSIONS AND RECOMMENDATIONS

The results of this research are summarized as follows:

1. The amount of the responsible water supply of the Deji reservoir for Taiching district is higher and the water supply capability within the condition of shortage index equal to one is also higher, but there exists a trade-off relationship between the increment of the water supply capability and the lack of hydrogeneration. It is feasible to shift the operation strategy of hydropower facilities to increase the water supply capability under the prohibition of constructing large water resources projects. The results of this study showed that the public and the industrial demand of Taichung district in 2021 would be fulfilled under the acceptable shortage by means of increasing the amount of the responsible water supply of the Deji reservoir for Taichung district.
2. The Divert in this system could be used to (i) utilize the surplus water in the Dachia River efficiently, (ii) increase the storage of the Liyutan reservoir indirectly, (iii) increase the water supply capability approximately 50,000 or 60,000 CMD under the condition of the shortage index equal to one, and the increment would be varied with the amount of the responsible water supply of the Deji reservoir for Taiching district. Furthermore, the analytical results showed that there would not be any lack of the hydrogeneration due to the Divert only could withdraw the surplus water in the Dachia River.
3. The public and the industrial demand of Taichung district in 2021 would be fulfilled under the acceptable shortage by means of shifting the operation strategy of the Deji reservoir. The shifting of the operation strategy of the Deji reservoir would reduce the hydrogeneration efficiency, thus it is necessary to compensate the Taiwan Power Corporation for the reasonable indemnification.

Acknowledgments
The authors gratefully acknowledge the research support from the Liming Engineering Consultants Corporation and the help from the Central Region Water Resources Office, Water Resources Agency, Taiwan.

REFERENCES

Water Resources Agency (2004) Planning Study of Control Mechanism for Total Water Resources in Taiwan, *Technical Report.*

Water Resources Planning Institute, Water Resources Agency, MOEA (2000) The Possible Project of Utilizing the Water Resources in Dachia River Review and Planning Study. *Technical Report*.

Central Region Water Resources Office, Water Resources Agency, MOEA (2004) The Reconnaissance Planning Study of the Joint System of the Dachia River and the Daan River, *Technical Report*.

Central Region Water Resources Office, Water Resources Agency, MOEA (2000) The Utilization Review of the Water Resources of the Liyutan Reservoir and the Shihgang Dam. *Technical Report*.

Water Resources Planning Institute, Water Resources Agency, MOEA (2002) The Feasibility Planning Study of the Dajiasi Weir. *Technical Report*.

Water Resources Planning Institute, Water Resources Agency, MOEA (2004) Development of Generalized Priority-Based Allocation Models for Regional Water Resources Management and Transfer. *Technical Report*.

Fulkerson, D. R. (1961) An Out-of-Kilter Method for Minimal-Cost Flow Problems. *Journal of the Society for Industrial and Applied Mathematics*.**9**(1), 18-27.

Barr, R. S., Glover, F. R& Klingman, D. (1974) An Improved Version of the Out-of-kilter Method and a Comparative Study of Computer Codes. *Mathematical Programming* **7**(1), 60-85.

Central Region Water Resources Office, Water Resources Agency, MOEA (2001) The Evaluation Report of the Damage and Restoration of the Shihgang Dam due to the Chih-Chih Earthquake. *Technical Report*.

Hydrogeology and groundwater resource management of the Friuli Venezia Giulia Plain alluvial aquifers, northeastern Italy

F. CUCCHI, G. FRANCESCHINI, F. TREU, L. ZINI, O. FLORA, A. LUTMANN & B. STENNI

Department of Geological, Environmental and Marine Sciences, University of Trieste, Italy
giuliana.franceschini@units.it

Abstract The constantly increasing water demand for human consumptions has necessitated a reconstruction of the hydrogeologic properties and isotopic features of the alluvial aquifers of the Friuli Venezia Giulia Plain. These aquifers are composed of an unconfined aquifer, and deeper aquifers containing both shallow (up to 120-130 m) and deep confined groundwater. The pattern of geochemical and stable isotope variations suggests that the unconfined and shallow confined groundwaters are recharged mostly by rainfall and local river (mainly Tagliamento) infiltrations. This fast recharge process makes these groundwaters susceptible to contamination. Four hydrogeological provinces have been recognised for these subsurface groundwaters. Radiocarbon dating indicates that there is very little continuity between the subsurface groundwaters and the deeper aquifers that have complex groundwater circulations and have substantially changed during the varying temperature regimes of the Holocene-Pleistocene. Comparison with deep confined aquifers in other regions of the Padain Plain indicates that the recharge rates of these deep confined aquifers are low and that, consequently, the deep groundwaters are very sensible to overexploitation.

Keywords hydrochemistry; groundwater maps; aquifers; water management; Italy

INTRODUCTION AND BACKGROUND INFORMATION

The Friuli Plain is bordered to the north by the Carnic Alps, to the east by the Julian Alps and the Classical Karst and the south border is formed by the Adriatic Sea (Fig. 1). Towards the west the Livenza River marks the border between the Friuli Plain and the Venetian Plain. The Friuli area is characterized by sedimentary rocks ranging from Paleozoic to Quaternary (Bosellini, 2004; Carulli, 2006). The Paleozoic rocks that outcrop in the northern part of the area are mainly composed of terrigenous rocks, limestones, frequent evaporites and minor volcanic deposits. The geologic units of the central part of the area are mainly made up of limestones and carbonatic rocks (Triassic–Cretaceous), belonging to the thick shelf complex of the Friuli Platform. This Mesozoic platform is in average 750 to 1000 m deep and it is overlain by flysch and molasses that represent the Cenozoic deposits. Pliocene-Quaternary alluvial deposits are found above the flysch and molasses (Cati *et al*., 1987; Carulli, 2006). The main surface drainage of the Friuli Plain is the Tagliamento River that is 180 km long and is the 6th longer Italian river. The average discharge of the Tagliamento River, 30 km inland from the Adriatic Sea, is 90-100 m^3/sec (Fontana & Bondesan, 2006), with a maximum discharge of 3,000 to 4,500 m^3/sec and over 6,000 m^3/sec over a return period of 500 years (Spalviero, 2003). The Isonzo River is the second largest river and it has an averaged discharge of 180 m^3/sec. Other perennial rivers are the Torre River (average discharge of 17 m^3/sec), the Natisone River (7 m^3/sec), the Cellina River (average discharge of 16 m^3/sec) and the Meduna River (average discharge of 11 m^3/sec). The Livenza River (average discharge of 85 m^3/sec) is fed by three perennial karst springs called Molinetto, Santissima and Gorgazzo (Fontana, 2006). The Friuli Plain has several climatic cells due to it extend from the Alps to the Adriatic Sea. In the plain the average rainfall is 1200 mm/yr lowering down to 1000 mm/yr in the coastal areas, whereas in the mountain area the average rainfall is 1800 mm/yr.

Geomorphologically the Friuli Plain is divided into two units, the Upper Friulian and the Lower Friulian, which are separated by the resurgence belt (Fig. 1). The Upper Friulian Plain includes calcareous and dolomitic gravels with a well developed phreatic

(P) aquifer, with an aquifer transmissivity of approximately 10^{-2} m^2s^{-1} to 10^{-4} m^2s^{-1} in a southerly direction (Mosetti, 1983). This aquifer has an average thickness of 60 to 80 m, reaching depths of 200 m close to the border between the plain and the Alps and surfacing in the resurgence belt. The resurgence belt is positioned in the zone of slope change between mean slope of 5‰ for the Upper Friulian Plain and 3‰ in the Lower Friulian Plain. The Lower Friulian Plain is characterized by alternating gravels and sand interbedded by clay and silty layers that become thicker in a southerly direction. In the Lower Friulian Plain the groundwater is confined to a multilayer aquifer. This aquifer system is hydrogeologically divided at approximately 100 to 120 m depth, into shallow (SC) and deep confined (DC) groundwaters by a 10-15 m thick impermeable layer of silty material, dated back to the Late Pleistocene (Cucchi *et al.*, 2007). Thermal aquifers with water temperatures reaching 40 degrees have been found at depths of 550-600 m during drilling explorations and are presently partly used by local industries. These deep geothermal aquifers have not been samples in this study.

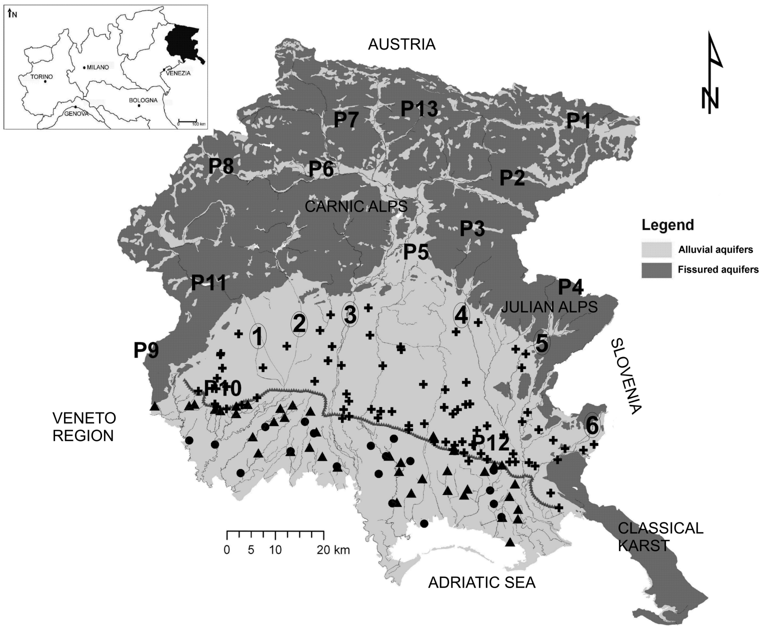

Fig. 1 Location of the study area (dotted line= Resurgence belt, P = Pluviometer, crosses = phreatic well samples, triangles = shallow confined well samples and circles = deep confined well samples; 1 = Cellina River, 2 = Livenza River, 3 = Tagliamento River, 4 = Torre River, 5 = Natisone River and 6 = Isonzo River).

GEOCHEMICAL CHARACTERISTICS OF THE GROUNDWATER

The dominant ion in the groundwater samples from the unconfined and confined aquifer is HCO_3 and five hydrochemical facies have been found: Facies 1: Ca-HCO_3; Facies 2: Ca-Mg-HCO_3; Facies 3: Ca-Mg-HCO_3-SO_4; Facies 4: Ca-Mg-SO_4-HCO_3 and Facies 5: Na-Ca-Mg-HCO_3. Na-Ca-Mg-HCO_3-type waters are located only in confined aquifers beneath clay and silt layers, likely reflecting exchange reactions by water-rock and microbial interactions. Groundwater generally shows a conductivity and mineralisation decrease with increasing depth. Mean concentrations of major ions is shown in Fig. 2. The $\delta^{18}O$ of groundwater ranges from -6.25‰ to -8.90‰ (mean value of -7.59‰) in the phreatic groundwater samples, from -6.83‰ to -9.14‰ (mean value of -8.05‰) and -7.01‰ to -10.35‰ (mean value of -8.74‰) in the shallow and deep confined groundwater samples, respectively (Fig. 3). The most depleted groundwater samples (-10.32‰ and -10.35‰) are collected from the southwest of the Friuli Venezia Giulia Plain amongst the deep confined groundwater samples.

Percent modern carbon (pmc) values range from 36 to 48 in the shallow confined groundwater to 0.8 to 0.9 in the deep confined groundwater indicating a good correlation between pmc and depth. The presence of organic source of *dead* carbon affects the ^{14}C activity correlation, thus precluding precise dating. However, residence times have been calculated using the model described by Ingerson & Pearson (1964) which is the most suitable model for terrigenous aquifers and has been applied in similar groundwater conditions in the neighboring region of Veneto as well as in Lombardy (Zuppi & Sacchi 2004; Pilla *et al*., 2006;). The following values have been used in age calculation: the activity of soil CO_2, which is equal to 100 pmc, -25‰ as $\delta^{13}C$; the activity of inorganic carbonates within the aquifer matrix, which are equal to 0 pmc and $\delta^{13}C=0$‰. Using this calculation the variation in pmc was interpreted as reflecting differences in groundwater residence time rather than relative dissolution with old radioactively dead radiocarbon. Several shallow groundwater samples have negative ages that almost certainly represent groundwater recharged since atmospheric nuclear testing in the 1960s, which produced atmospheric CO_2 with pmc contents of up to 200. The shallow confined groundwater residence time is ~100 years, whereas the deep confined groundwater is ~8 to 27 ka. The occurrence of relatively old groundwater in the deep confined waters is consistent with its high clay contents as a consequence of its low hydraulic conductivities (Mosetti, 1983). Accordingly to the radiocarbon data presented in this work, the shallow groundwater moves at a speed of 1 km/yr, whereas the deep confined groundwater only 3 m/yr.

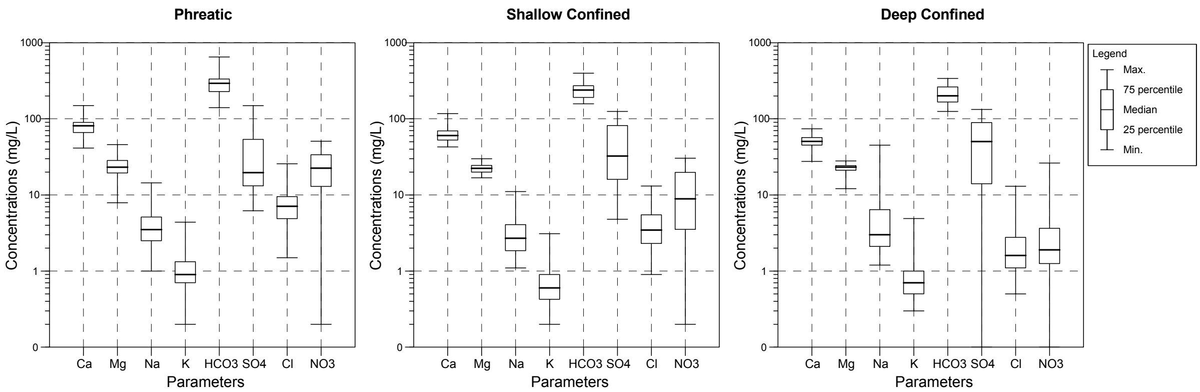

Fig. 2 Box and Whisker plots for the major ion concentrations.

CONCLUSIONS

Groundwater in the Friuli Plain is commonly used for stock watering, irrigation and increasingly for domestic supply. Escalating population and economic activities in the region are intensifying groundwater usage. The combination of major ions, stable isotopes and radiocarbon dating has enabled several aspects of the hydrogeology and hydrochemistry of the sampled aquifer systems to be constrained. Results from this study (Fig. 4) indicate that the isotopic content of unconfined and shallow confined groundwaters display fast recharge that makes these groundwaters susceptible to contamination by pesticides and fertilizers as well as by discharge from industries and urban areas. The unconfined and shallow confined groundwaters have been subdivided into four different hydrological zones (Cellina-Meduna Plain, Tagliamento River Plain, Plain between Torre and Natisone rivers and the Isonzo River Plain) based on chemical ion distributions and geohydrological factors. A distinct and complex hydrogeological circulation occurs within the deep confined groundwater. Lower isotopic values of these groundwaters, compared to rainfall water, as well as lower radiocarbon content show that these waters are not being recharged by local rainfall in a relatively short time-scale. The deep confined waters in the Friuli Plain have passive hydrodynamic conditions, with almost no cross-transfer with polluted shallower groundwaters. To date, agricultural contaminations such as nitrate, have not impacted the deeper groundwater. Since groundwater contributes to surface water, over pumping and or contamination of shallow and deep aquifers may results in increased risk to water resources throughout the entire region catchments. The integration of all stratigraphic data in a GIS database as well as radiocarbon dating on selected deep confined groundwater are presently underway and will provide additional and useful information for groundwater recharge periods, exploitation and rock-water interactions making this research vital for water management strategies.

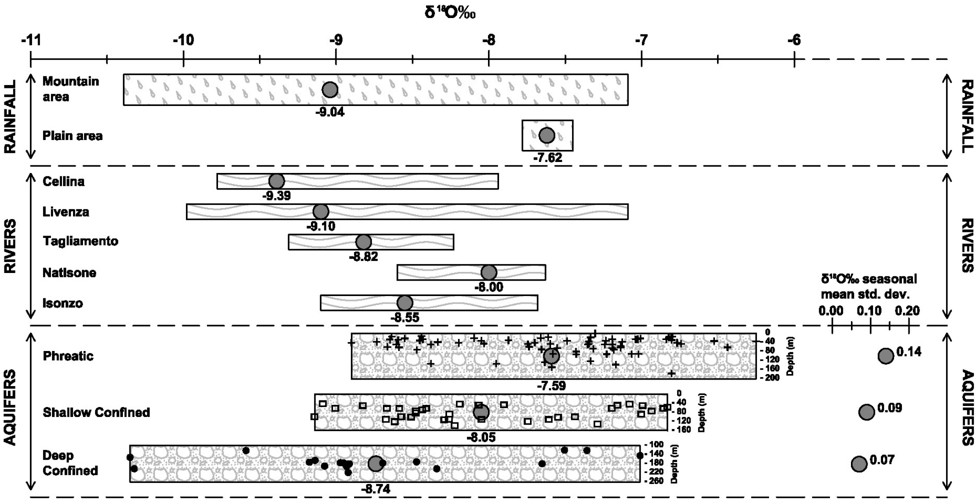

Fig. 3 δ^{18}O mean values for the Friuli Venezia Giulia rainfall, river and ground waters.

Acknowledgements The authors thank the stable isotope laboratory of the University of Trieste for stable oxygen analyses, and ARPA FVG for the geochemical data of groundwater samples.

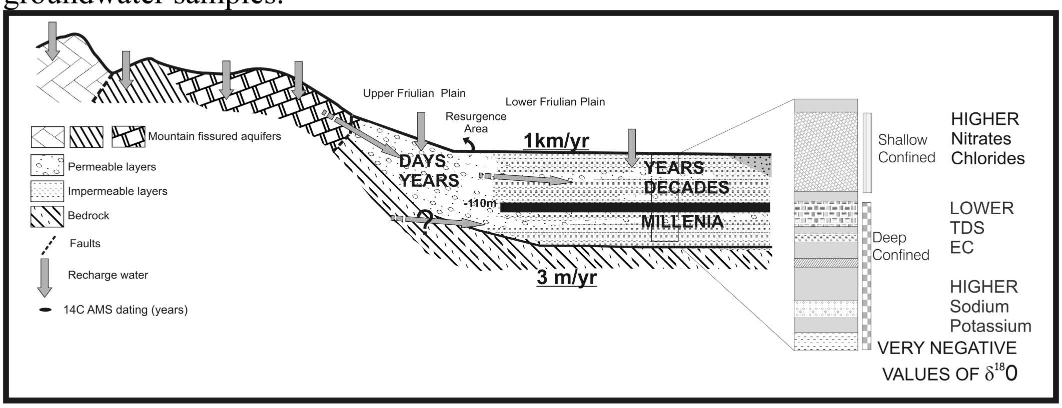

Fig. 4 Schematic reconstruction of groundwater characteristics and recharge periods for the Friuli Venezia Giulia Plain.

REFERENCES

Carulli, G. B. (2006) Carta geologica del Friuli Venezia Giulia [Geological Map of Friuli Venezia Giulia [Scala 1: 150000 Ed. S.E.L.C.A., Firenze.

Cati, A., Fichera, R. & Capelli, V. (1987) Italia nordorientale. Interpretazione integrata dei dati geofisici e geologici [Geophysical and geological data interpretation of north-western Italy]. *AGIP San Donato Milanese*, 154 pp.

Cucchi, F., Franceschini, G., Zini, L. & Treu, F. (2007) Hydrogeochemical and oxygen isotope investigations in multilayer aquifers of the Friuli Venezia Giulia Plain, north-eastern Italy. *Special publication of the XXXV Congress of the International Association of Hydrogeologists (IAH) Lisbon 2007*.

Fontana, A. (2006) Evoluzione geomorfologica della bassa pianura friulana [Geomorphological evolution of the lower Friulian Plain]. *Ed. museo friulano di storia naturale* **47**, Udine, 287 pp.

Fontana, A. & Bondesan, A. (2006) Il Tagliamento nella bassa pianura, tra dossi e incisioni fluviali [The Tagliamento River in the lower Friulian Plain]. *Ed. Circolo Menocchio*, 127-145.

Ingerson, E. & Pearson, F. J. (1964) Estimation of age and rate of motion of groundwater by the 14C-method. *Recent Researches in the Fields of Atmosphere, Hydrosphere, and Nuclear Geochemistry.*

Mosetti, F. (1983) Sintesi sull'idrologia del Friuli Venezia Giulia [Summary of the Friuli Venezia Giulia hydrology]. *Quad Ente Tutela Pesca* **6,** 1-296.

Pilla, G., Sacchi, E., Zuppi, G., Braga, G. & Ciancetti, G. (2006) Hydrochemistry and isotope geochemistry as tools for groundwater hydrodynamic investigation in multilayer aquifers: a case study from Lomellina, Po plain, South-Western Lombardy, Italy. *Hydrogeol J.* **14**, 795-808.

Zuppi, G. M. & Sacchi, E. (2004a) Hydrogeology as a climate recorder: Sahara-Sahel (North Africa) and the Po Plain (Northern Italy). *Glob Plan Change* **40**, 79-91.

Paper relating to expressing economic value of groundwater reserves

H. ČERMÁKOVÁ, J. NOVÁK & J. ŠVIHOVSKÝ

Technical Univerzity of Liberec, Faculty of Mechatronics and Interdisciplinary Engineering Studies, Institute of Systems Control and Reliability Management, *Studentská 2, 461 17 Liberec, Czech Republic*

hana.cermakova@tul.cz; jan.novak@tul.cz; jaromir.svihovsky@tul.cz

Abstract Present-day practice of evaluating of ecological risks is mostly focused on qualitative expressing of their acceptability. Aggregated methodology of quantitative evaluation of direct and indirect impacts on environment has not been elaborated so far. Remedial action is mainly oriented on achieving acceptable level of critical contamination without economical effectiveness of these processes being taken into account. Our purpose is to contribute to create general methodology of environmental risks evaluation which allows theirs expression in comparable values, financial if possible. Consequently environmental damages and contributions could be confronted with the costs on preventative or remedial actions. Such comparison could serve as a basis for choosing optimal procedures of reducing risks within the scope of water resources management.

Keywords remedial costs; groundwater reserve; economic value

INTRODUCTION

Nowadays practice which is dealing with evaluation of ecological risks is focused mostly only on qualitative formulation of their acceptability. Aggregated methodology of quantitative evaluation of direct and indirect impacts on environment has not been elaborated so far. Our intention is to contribute to establish general methodology of evaluation of groundwater reserve which will enable confrontation environmental claims and benefits with preventative costs or remedial procuration costs and make decisions about efficient procedures and actions. There are three possible approaches concerning the evaluation suggested in the paper.

WATER PRICE STRUCTURE

In regions of the Czech Republic the water price has been controlled and approved by state authorities according to the documented costs from water supply organizations. One part of water tariff price is state charge for water withdrawal (currently 3,- CZK m^{-3}, i. e. 0,12 EUR m^{-3}), see table 1. The charge reverberates a price of water as a raw material. Evaluation of groundwater reserve is focused on determining those components of water value into which costs of investor – groundwater reserve protection (government in Czech Republic) should be put on. Externalities which protection is also the interest of the society are not included in this way of expressing water value.

CHARACTERISTICS OF PARTICULAR METHODS

Objective method of evaluation – Expended costs method

Expended costs method comes out from evaluation of natural sources by costs for its revitalization. When using this method it is necessary that information about remedial costs and quantity of endangered waters in concrete localities is available. A difficulty is presented by quantification of endangered waters. Range of contamination changes with time and so evaluated time horizon is very important. It is possible to evaluate statical or dynamical reserves. When looking at large remedial projects which persistence exceeds 10 years, it is possible to speculate about conversion of remedial costs to present value by the help of discount rate factor.

Table 1 Structure of consumer`s water price.

Element	Rough	Water purification	Water distribution	Drainage	Wastewater treatment
	Water tariff			Wastewater tariff	

Objective method of evaluation – Investment in water protection method

This method comes out from determining anticipated future value of water and from corresponding state charge, which could be involved. Determining the discount rate could be found out as disputable.

Subjective method of evaluation – Willingness to pay method

Subjective evaluation is mostly investigated by the help of questionnaires. In our case they come out from actual water price from water supply network for consumers and from consumption of packaged water. Willingness to pay is then derived from real data and reverberates a price which is in reality paid by public. Difficulty of this method is lack of basis for determining future demand and corresponding price progression. It is possible to presume that willingness to pay is higher than presently accepted price.

EXAMPLES OF DETERMINATION OF WATER VALUE

Expended costs method

In connection with chemical mining of uranium extensive contamination of groundwater in chalk collectors arised in bearing of Straz pod Ralskem. Remediation is planned to take about 50 years and anticipated costs (www.diamo.cz) are estimated on 45 bil. CZK (1,8 billions EUR). Remediation is financed mainly from state funds. Determining of endangered water dimension is not unique. Possible scenarios of development of water pollution which illustrate considerable signification of uncertainties especially in the conditions which will be stabilized after finished remedial activities are known from modeling simulations. In the period of 200–500 years it is possible to suppose that 500–1500 m^3 of statical reserve will be depreciated. It corresponds with value of groundwater reserves of about 30–90 CZK m^{-3} (1,2–3,6 Euros m^{-3}). More suitable is evaluation of dynamical reserves. Endangered area with potential sources lies in the area of regionally significant accumulation of high-quality groundwater. Contamination would afflict particular collectors in the area of 30-75 km^2 during another 500 years. The remediation would speed up its development towards the place of withdrawal if there is more remarkable water withdrawal. Therefore it is necessary to take into account blocking reserves on the area of 60 km^2 at least and eventually as far as 100 km^2. At average fruitfulness 3–4 l km^{-2} s^{-1} it means dynamical reserves of 180–400 l s^{-1} which (in the case of failure of remediation) could not be used as a fresh water supply. When thinking about longer time horizon, contamination dissemination would cause another need of blocking groundwater reserves. In table 2 there is mentioned total quantity of nonutilisable water when blocked fruitfulness of 180 – 400 l s^{-1} in time interval of 50–500 years.

If we consider that spending for remediation should assure groundwater source for next generation, we can esteem time dimension of 100–200 years as real values. Value of groundwater reserves then vary between 18–79 CZK m^{-3}, i.e. 0,72–0,16 EUR m^{-3}. Investment into revitalization of locality Straz will not be single shot expenditure in reality, but it presents step-by-step financing of the remediation with higher expenditures in the beginning and lower expenditures during final stages of remediation. For discount rate at the level of 1% net present value of remedial costs amounts to 38 billions CZK and value of groundwater is then 15–69 CZK m^{-3}. For higher discount rate (2%) it is 32 billions CZK with values 13–56 CZK m^{-3}.

Table 2 Estimations of values of groundwater reserves for variant quantity of blocked reserves and duration of evaluated time interval.

Fruitfulness of source	180 l s^{-1}		400 l s^{-1}	
Number of years	Blocked water reserve [mil. m^3]	Water value [CZK m^{-3}]	Blocked water reserve [mil. m^3]	Water value [CZK m^{-3}]
50	284	158	631	72
100	568	79	1261	36
200	1135	40	2523	18
300	1703	26	3784	12
500	2838	16	6307	7

Investment in water protection method

This method comes out from determining anticipated future value of water as raw material and from corresponding charge for investor (government in the Czech Republic), which could be put on in it. We suppose that water value will not decline. Value of groundwater reserves which are less predisposed to weather changes (expected in relation with global warming), will more likely go up. Therefore low discount rate 1–2 % has been chosen. In table 4 there are mentioned single shot expenditures which would be covered by charge to investor (government), withdrawal of 1 m^3 with the price of 25–100 CZK (i.e. 1–4 EUR) for water source fruitfulness of 400 l s^{-1}, used for period of 50–200 years. It is perceptible from table 3 that remedial costs in the location of Straz would be covered by state charge in the amount of 40 CZK m^{-3} at discount rate 1% and about 75 CZK m^{-3} at discount rate 2%.

Table 3 Single shot expenditures in billions CZK which would be covered by charge to government.

Years of usage	Charge CZK m^{-3} / discount rate 1%				Charge CZK m^{-3} / discount rate 2%			
	25	50	75	100	25	50	75	100
50	12,5	24,9	37,4	49,8	10,0	20,1	30,1	40,1
100	20,0	40,0	60,0	80,0	13,7	27,4	41,0	54,7
200	27,3	54,6	81,9	109,2	15,5	31,0	46,5	62,0
1000	31,5	63,1	94,6	126,1	15,8	31,5	47,3	63,1

Willingness to pay method – consumer approach

In 2008 actual water price tariff varies according to regions in the range of 47–63 CZK (1,88–2,52 EUR) m^{-3}. The price consists of direct costs for gaining water from the source, costs for water purification, costs for distribution, reparations, investments, overhead costs etc. which are related to water service authority organization and to the water distribution to final consumer. Government charges 3 CZK (0,12 EUR) m^{-3} for groundwater. Willingness to pay for fresh water could be reverberated by purchase of packaged water which price is many times higher than from water supply network. Current packaged water consumption is 87 litres $person^{-1}$ $year^{-1}$. It means 0,24 l per person a day from average fresh water consumption 120 l $person^{-1}$ day^{-1}. Price for packaged water is currently about 7–8 CZK l^{-1}. Consumption of packaged water is increasing every year also in countries with distribution of fresh water in water supply network of high quality and reliability, like in the Czech Republic. It is possible to presume an increase of 0,4 l $person^{-1}$ day^{-1}.

Table 4 Source data for estimation of willingness to pay for fresh water.

Indicator	Unit of measure	Quality	
		min	max
Estimated water consumption in CR	l $person^{-1}$	120	120
Average water price (water tariff)	CZK m^{-3}	47	63
Water consumption from water supply	l $person^{-1}$	119.76	119.6
Average consumption of packaged water	l $person^{-1}$	0.24	0.4
Average price of packaged water	CZK l^{-1}	7	8
Water price accepted by consumer	CZK m^{-3}	61.5	89.5

If we take off lowest regional water price from nowadays tolerated values, charge for water as a raw material could be increased from present 3 CZK m^{-3} to 18–46 CZK m^{-3} (0,72–1,84 EUR). The estimation comes out from current consumption of packaged water and its price and from current water tariffs. It represents lower limit of willingness to pay by the consumer.

CONCLUSION

Water value as a raw material is evaluated by state charge for its withdrawal from natural source. It is possible to imply possible costs for groundwater protection into the state charge. The paper is focused on finding out its tolerated level. The groundwater value is higher by externalities which are not initiated but they deserve protection. Three methods for determining the water value are compared. First method comes out from costs for revitalization. It requires knowledge about remedial costs and endangered water dimension at particular localities. The method is applicated at the locality of Straz pod Ralskem where chalk collectors of regional importance are contaminated. Determining risk extent in relation with time horizon is disputable. Protection of 1 m^{-3} in dynamical reserves works out 13–79 CZK (0,52–3,16 EUR) in a period of 100–200 years. Second approach is based on determining groundwater price and finding out relevant costs which could be effectively used for protection of certain groundwater reserves. This method uses discounting a water price that means water price is decreasing into the future. Difficulty of this method is determining discount rate which should be low when thinking of natural source protection. The example in the paper shows how high remedial costs on different condition (value of 1 m^{-3} of groundwater, discount rate) correspond with regional groundwater protection, comparable with locality of Straz. Source data are determined with regard to outputs of first two methods. Third approach comes out from actual water price from water supply network and from consumption and price of packaged water. Current tolerated water price as a raw material covered up to price for final consumer is 18–46 CZK (0,72–1,84 EUR). The advantage of last method is easy availability of data; disadvantage is non-acquaintance of real willingness to pay which could be higher then current reality.

Acknowledgements This research was supported by the Environmental Ministry of Czech Republic, project code SPII1a10 45/07 – Complex Interaction between Major Processes and Industry with Regards to Major Accident Prevention.

Validation of streamflow scenarios for scheduling in the Brazilian hydrothermal electric generation system

JORGE MACHADO DAMÁZIO[1,3], MARIA ELVIRA PIÑEIRO MACEIRA[2,3], DÉBORA DIAS JARDIM PENNA[2] & WELINGTON LUIS DE OLIVEIRA[2]

1 *Electric Power Research Center – CEPEL, CP 68007 Rio de Janeiro, Brazil*
damazio@cepel.br

2 *Electric Power Research Center – CEPEL, CP 68007 Rio de Janeiro, Brazil*

3 *Rio de Janeiro State University, São Francisco Xavier 525, Rio de Janerio, Brazil*

Abstract Validation statistical tests that measure the goodness of first and second theoretical moments reproduction in synthetic generated streamflow sequences are derived and implemented. The tests were needed to validate synthetic monthly multivariate two-step ahead streamflow scenarios to be used in the definition of the generation schedule for the next month in the Brazilian hydrothermal electrical energy generation system. An application with a system configuration formed by thirty-nine hydro plants showed the goodness of reproduction.
Keywords streamflow; synthetic streamflow sequence generation; statistical validation test

INTRODUCTION

The definition of the next month generation schedule in the Brazilian hydrothermal electrical energy generation system is done aiming the supply of the forecasted load with minimum expected operating costs for the adopted planning period, considering an expected cost-to-go function for the end of the planning period obtained in the long term operation planning studies. In terms of streamflow representation, the adopted optimization model takes into account weekly forecasts for the first month, whereas for the following months in the planning a period, a set of monthly streamflow scenarios are generated by a multivariate time series generator. The scenario generator model uses the same periodic autoregressive modelling approach (Maceira *et al.*, 1997 and Maceira *et al.*, 2005), referred as PAR(p) model, used in the long term operation planning studies to represent the uncertainty about future flows. This modelling is chosen to ensure resemblance between historical and synthetic streamflow sequences and reproducibility of droughts as severe as those observed in the historical records. In this way, the streamflow time dependency structure necessary to represent the drought regime adopted in the long term operation planning studies is also adopted in the generation schedule studies, guaranteeing coherence in these two steps of the chain of studies that form the operation planning of the complex Brazilian electrical generation system (Maceira *et al.*, 2002). On the other hand, strictly considering the definition of the next month generation schedule, the generated scenarios should reflect the multivariate probability distribution of the monthly streamflows from the second month ahead in the planning period conditioned on the recent recorded and forecasted streamflows. The following sections present the development of validation statistical tests implemented that measure the goodness of the reproduction in the generated scenarios of first and second theoretical conditioned moments and an application with a system configuration formed by thirty-nine hydro plants displayed along several cascades.

METHODOLOGY

In the following, we use letter t to indicate the first time step in the planning horizon; the letter *z* to represent the streamflow (historical or synthetically generated by the PAR(p) model). The Greek letters μ, σ and ϕ represent respectively the mean, standard deviation and the autoregressive coefficient. We use the notation |t_ to indicated conditioning to the past. Consider a set of synthetic sequences (scenarios) generated in a tree structure, as illustrated in Fig. 1. The number of openings in each time period is N_t.

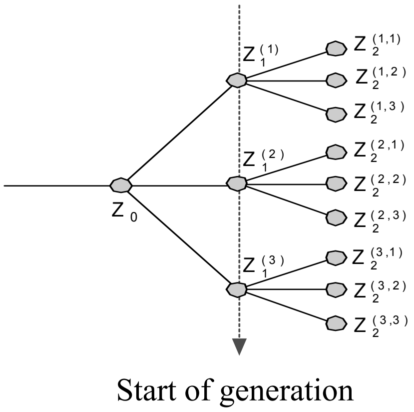

Fig. 1 Tree Structure of Generated Scenarios.

The PAR(p) model describes the standardized flow correspondent to a certain hydroelectric plant at time period t, as a linear combination of the standardized streamflows in periods t-1, t-2, …, t-p_t summed to a random noise.

$$\frac{z_t-\mu_t}{\sigma_t}=\phi_1^t\left(\frac{z_{t-1}-\mu_{t-1}}{\sigma_{t-1}}\right)+\ldots+\phi_{p_t}^t\left(\frac{z_{t-p_t}-\mu_{t-p_t}}{\sigma_{t-p_t}}\right)+a_t\,, \tag{1}$$

In (1), a_t is the random noise with zero mean and standard deviation σ_{at} and p_t is the order of the autoregressive model at the time period t. If the flows at periods t-1, t-2, …, t-p_t are known, the conditional expectation, variance and serial correlation lag one of the one-step and two-step ahead streamflows are given by:

$$E[Z_t|t\_]=\mu_t+\sigma_t\left[\phi_1^t\left(\frac{z_{t-1}-\mu_{t-1}}{\sigma_{t-1}}\right)+\ldots+\phi_{p_t}^t\left(\frac{z_{t-p_t}-\mu_{t-p_t}}{\sigma_{t-p_t}}\right)\right], \tag{2}$$

$$VAR[Z_t|t\_]=\sigma_t^2\sigma_{a_t}^2\,, \tag{3}$$

$$E[Z_{t+1}\,|\,t\_]=\mu_{t+1}+\sigma_{t+1}\left[\phi_1^{t+1}\left(\frac{E[Z_t\,|\,t\_]-\mu_t}{\sigma_t}\right)+\ldots+\phi_{p_{t+1}}^{t+1}\left(\frac{Z_{t-p_{t+1}+1}-\mu_{t-p_{t+1}+1}}{\sigma_{t-p_{t+1}+1}}\right)\right], \tag{4}$$

$$\mathrm{VAR}[Z_{t+1} \mid t\_] = \sigma^2_{t+1}\left[(\Phi_1^{t+1})^2 \frac{\mathrm{VAR}[Z_t \mid t\_]}{\sigma_t^2} + \sigma^2_{a_{t+1}}\right], \tag{5}$$

$$\mathrm{CORR}\left[Z_{t+1}, Z_t \mid t\_\right] = \frac{\sigma_{t+1}\sigma_t \phi_1^{t+1} \sigma^2_{a_t}}{\sqrt{\mathrm{VAR}\left[Z_t \mid t\right]\mathrm{VAR}\left[Z_{t+1} \mid t\right]}}, \tag{6}$$

The comparison between the sample moments obtained in the generated scenarios at each time period with tolerance intervals built around their theoretical counterparts in (2) to (6) permits to verify the goodness of the generation scheme. The building of 95% tolerance intervals is done using the expectation plus and minus 1.96 times the square root of the variance of the sample moments. The expectations are equal to the theoretical values and the variances are given by:

$$\mathrm{VAR}\left[\overline{Z}_{t|t-}\right] = \frac{\sigma_t^2\ \sigma^2_{a_t}}{N_t} \tag{7}$$

$$\mathrm{VAR}\left[S^2_{t|t\_}\right] = \frac{1}{N_t}\sigma_t^4\ \mathrm{VAR}\left[(a_t)^2 \mid t\_\right] \tag{8}$$

$$\mathrm{VAR}(\overline{Z}_{t+1|t\_}) = \sigma^2{}_{t+1}\left(\frac{1}{N_t}\left(\phi_1^{t+1}\right)^2 \frac{1}{\sigma_t^2}\mathrm{VAR}\left(Z_t \mid t\_\right) + \frac{\sigma^2_{a_{t+1}}}{N_t N_{t+1}}\right). \tag{9}$$

$$\begin{aligned}\mathrm{VAR}[S^2_{t+1|t\_}] = {} & \frac{\sigma^4_{t+1}\left(\phi_1^{t+1}\right)^4}{\sigma_t^4}\mathrm{VAR}\left[S^2_{t|t\_}\right] + \left(\frac{\sigma^2_{t+1}}{N_t N_{t+1}}\right)^2 \sum_{i,j}\mathrm{VAR}\left[\left(a_{t+1}^{(i,j)}\right)^2 \mid t\_\right] + \\ & \frac{4\sigma^4_{t+1}\left(\phi_1^{t+1}\right)^2}{N_t N_{t+1}}\sigma^2_{a_t}\sigma^2_{a_{t+1}}\end{aligned} \tag{10}$$

$$\begin{aligned}\mathrm{VAR}(r_{t+1,t|t\_}) = {} & \left(\frac{\sigma_t\sigma_{t+1}\phi_1^{t+1}}{\sqrt{\mathrm{VAR}(Z_t \mid t\_)\mathrm{VAR}(Z_{t+1} \mid t\_)}}\right)^2 \frac{1}{N_t}\mathrm{VAR}[(a_t)^2 \mid t\_] + \\ & \left(\frac{\sigma_t\sigma_{t+1}}{\sqrt{\mathrm{VAR}(Z_t \mid t\_)\mathrm{VAR}(Z_{t+1} \mid t\_)}}\right)^2 \frac{\sigma^2{}_{a_t}\sigma^2{}_{a_{t+1}}}{N_t N_{t+1}}.\end{aligned} \tag{11}$$

$$\mathrm{VAR}\left[a_t^2 \mid t\_\right] = \mu_{4_{a_t}} - \sigma^4_{a_t} \tag{12}$$

RESULTS

The application considered a system configuration formed by thirty-nine hydro plants displayed in several cascades, as showed in Fig. 2, and the generation of two-step ahead monthly flows starting in January adopting 100 openings in the first month and in the second month. The historical goes from 1931 until 1998. As recent observations it was used the year of 1959. For each moment it was obtained a t-value calculated as difference between the sample moment and the theoretical moment divided by the standard deviation of the sample moment. Whenever the t-value is inside the (–1.96, +1.96) interval, the sample moment is inside its confidence interval. Fig. 3 shows that almost all generated sample moments are inside their 95% confidence interval.

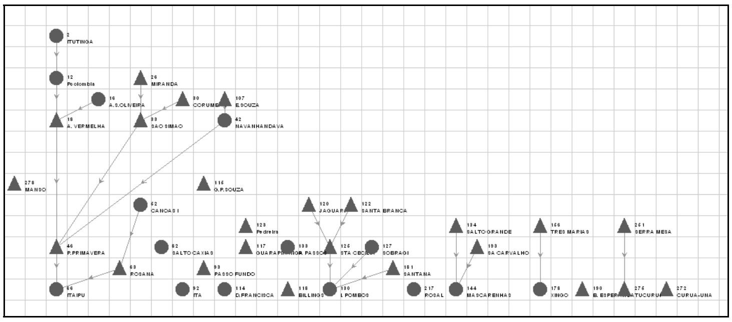

Fig. 2 Thirty-Nine Plants Displayed in Several Cascades.

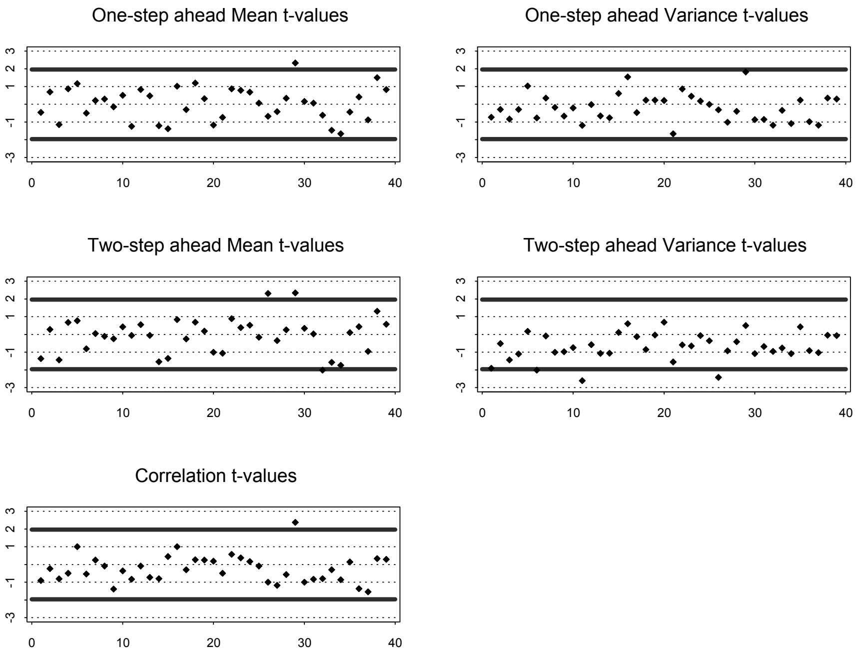

Fig. 3 Validation of the Generated Scenarios.

CONCLUSIONS

The uncertainty about future streamflow possible sequences is modelled in the short-term operation studies of the Brazilian hydrothermal system using synthetically generated realizations conditioned to recent streamflows. The quality of the generation can be assessed comparing the sample moments of order 1 and 2 of the one-step and two-step ahead generated flows with confidence intervals built around their theoretical values. These confidence intervals can be written in terms of the expectation and variance of the sample moments using the results derived in the paper. An application showed the goodness of the reproduction of the conditioned first two order moments in a case of thirty-nine hydro plants displayed in several cascades.

REFERENCES

Maceira M. E. P. & Bezzera, C. V. (1997) Stochastic Streamflow model for Hydroelectric Systems. In: *Proceedings of 5th International Conference on Probabilistic Methods Applied to Power Systems*, 305-310, Vancouver, Canada

Maceira, M. E. P., Penna, D. D. J. & Damázio, J.M. (2005) Geração de Cenários Sintéticos de Energia e Vazão para o Planejamento da Operação Energética. In: *XVI Water Resources Brazilian Conference*, João Pessoa, Paraíba, Brazil

Maceira, M. E. P., Terry, L. A., Damázio, J. M., Costa, F. S. & Melo, A. C. G. (2002) Chain of Models for Setting the Energy Dispatch and Spot Price in the Brazilian System. *Power System Computation Conference* – PSCC'02, Sevilla, Spain

UISGE: an unstructured information system for GeoGRAPHICAL Environments

J. R. MANSON

School of Natural Sciences and Mathematics, Richard Stockton College of New Jersey, PO Box 195, Pomona, New Jersey, 08240, USA
Russell.Manson@stockton.edu

Abstract This paper describes a computational model for natural earth systems and its application to modelling seiches in lakes. The model utilises a computational grid that is spatially unstructured and constructed from connected arbitrarily placed triangles and rectangles. This makes the grid particularly flexible and adaptable to complex geometries and spatially non-uniform system properties. The computational grid and domain specific equations (hydrodynamics) are described and the numerical solution technique is outlined. Finally the model is applied to a simple test case which consists of an idealised water filled rhombic basin with the water surface subject to some initial slope. The model produces plausible results and further analysis is recommended.
Keywords unstructured grid; finite volume; seiche; loch; hydrodynamics; numerical testing

INTRODUCTION

Developing spatially explicit models of natural earth systems (geophysical, ecological, hydrological, etc) is often made difficult by the irregular, non-uniform and non-linear spatial variations in their system properties. When combined with the, often non-linear, differential equations that describe the systems recourse to a numerical or computational solution is unavoidable. Traditional computational grids, which tend to be structured and regular (e.g. Cartesian grids), do not always delineate the underlying system efficiently or adequately. Unstructured grids allow for an arbitrary placement of computational nodes which means that complex boundary shapes and irregular patches of internal system properties can be properly represented. Irregular grids can therefore be a useful basis for natural system computational models. The model described in this paper utilises an unstructured grid as its computational foundation. The model, which is called UISGE (**u**nstructured **i**nformation **s**ystem for **g**eographical **e**nvironments), consists of a set of domain specific equations which are solved on the unstructured grid for the geographical region of interest. The domain equations utilised in this particular application of UISGE are the hydrodynamic equations which describe water circulation patterns however other domain equations could be employed to describe other types of systems such as ecological or socio-economic systems.

The application of hydrodynamic and water quality models to glacial lakes and fjords is a useful tool in paleoclimate studies (Austin & Inall, 2002). These systems (typified by the western coast of Scotland and Norway) reveal complex geometries and are therefore prime candidates for this unstructured grid approach.

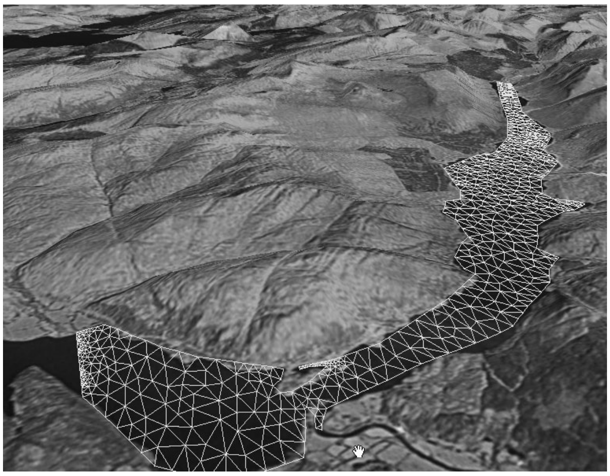

Fig. 1 Unstructured grid applied to Loch Etive, Scotland. Image modified from Google Earth.

In this research we are developing the unstructured grid approach to model seiche hydrodynamics in glaciated lakes. In this paper we apply the model to a simplified geometry to allow us to test the model.

COMPUTATIONAL GRID

In order to solve the domain equations the grid first must be designed and specified mathematically. The grid for UISGE is an orthogonal unstructured grid similar to the one used by Casulli & Walters (2000) and may be composed of triangles and rectangles. Ideally all equilateral triangles would be used since this provides for the highest accuracy (Casulli & Walters, 2000). For practical application this will usually be difficult to achieve but it remains the ideal. As the triangles move further away from this ideal the accuracy degrades. If any triangles are non-orthogonal (i.e. obtuse) the solution technique can have difficulty converging and so we try to avoid these types of triangles at all cost.

We utilise a tool called Triangle (Shewchuck, 2002) for generating our initial computational grid but we usually refine the initial grid by smoothing techniques in order to produce a more orthogonal grid. Once a suitable computational grid is designed we move to task of discretising the domain equations on this grid. This involves replacing any differential expressions with finite difference expressions based upon locally discrete points in the grid.

PRESENT MODEL EQUATIONS – THEORY AND DISCRETISATION

The system is completely described by velocity (in three coordinate directions) and pressure throughout the domain and throughout time, i.e. u(x,y,z,t), v(,x,y,z,t), w(x,y,z,t) and p(x,y,z,t). In practice, because we assume a hydrostatic pressure variation in the vertical we can use water level, η(x,y,t), as a surrogate for pressure. So there are four unknown quantities and we require four equations to solve for them.

$$\frac{\partial u}{\partial t}+\frac{\partial u^2}{\partial x}+\frac{\partial uv}{\partial y}+\frac{\partial uw}{\partial y}+g\frac{\partial \eta}{\partial x}+g\frac{\partial}{\partial x}\left[\int_z^{\eta}\frac{\Delta\rho}{\rho_0}dz\right]=\frac{\partial}{\partial z}\left[\nu_t\frac{\partial u}{\partial z}\right]-fv \quad (1)$$

$$\frac{\partial v}{\partial t}+\frac{\partial vu}{\partial x}+\frac{\partial v^2}{\partial y}+\frac{\partial vw}{\partial y}+g\frac{\partial \eta}{\partial y}+g\frac{\partial}{\partial y}\left[\int_z^{\eta}\frac{\Delta\rho}{\rho_0}dz\right]=\frac{\partial}{\partial z}\left[\nu_t\frac{\partial v}{\partial z}\right]+fu \quad (2)$$

$$\frac{\partial \eta}{\partial \mathrm{t}}+\frac{\partial}{\partial \mathrm{x}}\left[\int_{-\mathrm{h}}^{\eta}\mathrm{udz}\right]+\frac{\partial}{\partial \mathrm{y}}\left[\int_{-\mathrm{h}}^{\eta}\mathrm{vdz}\right]=0 \quad (3)$$

$$\frac{\partial \mathrm{u}}{\partial \mathrm{x}}+\frac{\partial \mathrm{v}}{\partial \mathrm{y}}+\frac{\partial \mathrm{w}}{\partial \mathrm{z}}=0 \quad (4)$$

Equations (1) and (2) describe the conservation of momentum in the two horizontal directions. Equation (3) is a statement of the global conservation of mass while equation (4) is a statement of local continuity. In these equations the variables used are: x,y,z - principal coordinate directions; u - velocity in primary horizontal direction (x); v - velocity in secondary horizontal direction (y); w - velocity in vertical direction (z); η – water level measured above some datum; h - the depth to the bed below the same datum; g - gravitational acceleration; ρ_o - ambient fluid density; $\Delta\rho$ - deviation from ambient fluid density; ν_t - eddy viscosity (turbulent diffusion); f – the Coriolis constant. Note we have omitted the horizontal eddy viscosity terms in the equations (1) and (2); they are easily included but are much less important than the vertical eddy viscosity terms for our application here.

Equations (1)-(3) are solved simultaneously with a semi-implicit finite difference scheme in time and with all spatial derivatives approximated using the unstructured grid. The barotropic terms in equations (1) and (2) are treated implicitly while the baroclinic terms are treated explicitly. Because of the implicit treatment of the barotropic terms equations (1)-(3) must be solved simultaneously as a linear system. We achieve this using a preconditioned conjugate gradient technique. Once u, v and n are computed at the future time, w may be recovered by solving equation (4).

Pressure may now be calculated at any depth by using equation (5) although note that pressure is usually not required.

$$p=\rho_0 g(\eta-z)+\rho_0 g\int_z^{\eta}\frac{\Delta\rho}{\rho_0}dz \quad (5)$$

The transport and fate of scalar quantities (e.g. salinity, temperature) may be calculate by solving the advection-diffusion-reaction equation below utilising the velocity field computed with the hydrodynamic computation.

$$\frac{\partial c}{\partial t}+\frac{\partial uc}{\partial x}+\frac{\partial vc}{\partial y}+\frac{\partial wc}{\partial y}=\frac{\partial}{\partial x}\left[\frac{\nu_t}{\sigma_c}\frac{\partial c}{\partial x}\right]+\frac{\partial}{\partial y}\left[\frac{\nu_t}{\sigma_c}\frac{\partial c}{\partial y}\right]+\frac{\partial}{\partial z}\left[\frac{\nu_t}{\sigma_c}\frac{\partial c}{\partial z}\right]\pm reaction \quad (6)$$

where c is the concentration of the scalar quantity; σ_c – Schmidt number. The model is developed in Visual Studio.NET with Visual Basic.

APPLICATION TO SEICHES IN IDEALISED BASIN

The application of the model in this paper is to an idealised regular parallelogram of side 90m. We utilise a grid composed of equilateral triangles. The basin contains water to a uniform depth of 2 m. We give the water an initial profile along a north-south axis. The initial profile ranged from +0.001m. to -0.001m. in a sinusoidal fashion. The water is allowed to slosh back and forth within the basin for 800s. The water level throughout time at point D is shown in Fig. 2(b). The model predicts a seiche with period 32.6 s. This compares favourably with the theoretical seiche period (first mode) for a rectangular basin of length L and depth h which is given by ($\frac{2L}{\sqrt{gh}}$) and here would be 35.21 s given a basin length of 77.94 m.

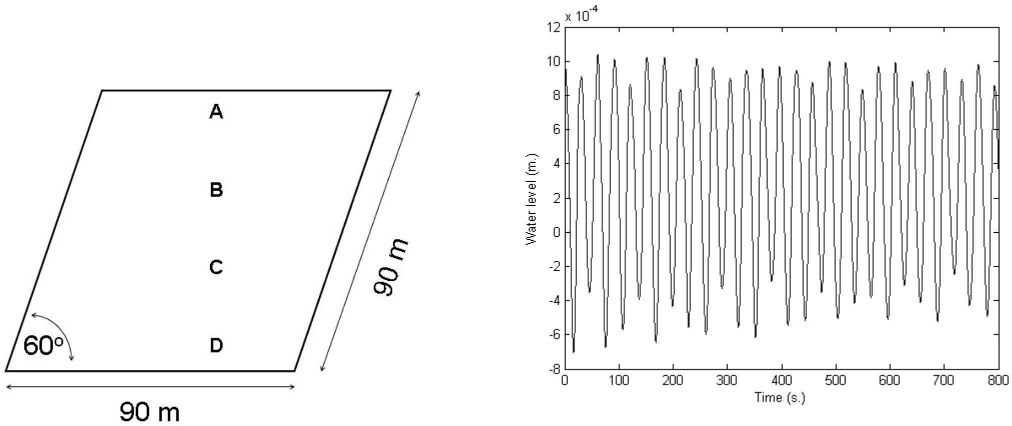

Fig. 2 (a) The test geometry (b) Water level variation predicted by model at D.

CONCLUSIONS

This paper describes the development and first application of a new model for modelling geographic systems, in this case a hydrological system. The model utilises an unstructured grid in space and a semi-implicit numerical discretisation in time. The model is applied here to an idealised rhombic basin and correctly predicts the seiche period. Further testing and application of the model is recommended.

REFERENCES

Casulli, V. & Walters, R. A. (2000) An unstructured grid, three-dimensional model based on the shallow water equations. *International Journal for Numerical Methods in Fluids* **32**(3), 331-348 DOI: 10.1002/(SICI)1097-0363(20000215)32:3<331::AID-FLD941>3.0.CO;2-C

Casulli, V., Cheng, R. T. (1992) Semi-implicit finite difference methods for three-dimensional shallow water flow. International Journal for Numerical Methods in Fluids **15**(6), 629-648. DOI: 10.1002/fld.1650150602

Shewchuk, J. R. (2002) Delaunay Refinement Algorithms for Triangular Mesh Generation, Computational Geometry. *Theory and Applications* **22**(1-3), 21-74.

Austin W. E. N. & Inall, M. E. (2002) Deep-water renewal in a Scottish fjord: temperature, salinity and oxygen isotopes. *Polar Research* **21**(2), 251–257 doi:10.1111/j.1751-8369.2002.tb00078.x

An automated MATLAB procedure for computing river mixing coefficients from tracer data

J. R. MANSON[1], S. G. WALLIS[2] & V. A. DZHUSSOEVA[1]

1 *School of Natural Sciences and Mathematics, Richard Stockton College of New Jersey, PO Box 195, Pomona, New Jersey, 08240, USA*
russell.manson@stockton.edu

2 *School of the Built Environment, Heriot-Watt University, Riccarton, Edinburgh, EH14 4AS, UK*

Abstract This paper is concerned with a sophisticated computational solver for the advection-dispersion equation with the option to include transient storage. The algorithm employed is based on the DISCUS method (Manson & Wallis, 2000) and has been implemented here as a callable function for the popular computational tool, MATLAB. Although the algorithm itself is complicated the user of the function does not need to know any of its intricacies. The callable function may be used as part of an optimisation approach for model parameter fitting. Herein it was used with MATLAB's genetic algorithm toolbox and with stream tracer data obtained from a local study. The model fitted the data well, and the resulting parameter values were consistent with the observable stream characteristics.
Keywords tracer studies; rivers; MATLAB; numerical method; advection; model fitting

INTRODUCTION

The advection-dispersion equation (ADE) is used widely to model solute transport in rivers. This two-parameter model is characterized by the velocity, u, and the dispersion coefficient, D, that represent advective and dispersive transport, respectively. A potentially serious deficiency with the ADE is that it cannot adequately represent long tails found in observed tracer data caused by transient storage. Transient storage zones include recirculation areas, streambed irregularities and bed sediment interstices. They are thought to be important for nutrient cycling and stream metabolism (DeAngelis *et al.*, 1995), and have long been recognised as playing an important role in the transport of dissolved or suspended materials in rivers (Sabol & Nordin, 1978; Valentine & Wood, 1979; Worman *et al.*, 2002). The storage zones are characterized by their size (cross-sectional area), A_s, and the rate at which solute mass is transferred to and from them, α. So this enhanced ADE model has four characterizing parameters.

The parameters for both the standard and enhanced ADE models may be found by fitting the model to observed solute concentration data, and identifying the parameter values that minimise an appropriate objective function. When casting the model via a numerical solution it is important to use a numerical method that is known to be free of problems such as numerical diffusion and grid scale oscillations. The authors' semi-Lagrangian method DISCUS (Domain of Influence Search for Convective Unconditional Stability) is one such approach that has been successfully applied to a wide range of fluvial scenarios (Wallis *et al.*, 1998; Manson & Wallis, 1999; Neelz & Wallis, 2007). As well as being accurate, numerically robust and computationally efficient the semi-Lagrangian approach is also particularly attractive for optimisation problems because it caters well for the use of large time steps. Unfortunately the method's complexity and its various computational nuances can be a barrier to its use.

The aim of the work reported here, therefore, was to create an easy-to-use approach for enhanced ADE modelling that anyone familiar with MATLAB could use. The paper describes a MATLAB function created for this purpose and illustrates its application with a set of tracer data.

MODEL DESCRIPTION

The enhanced ADE model, which describes one-dimensional solute transport in steady, non-uniform flows in rivers with transient storage is described by:

$$\frac{\partial m}{\partial t} + \frac{\partial um}{\partial x} = \frac{\partial}{\partial x}\left(DA \frac{\partial c}{\partial x} \right) + \alpha A(s - c) \tag{1}$$

$$\frac{\partial s A_s}{\partial t} = -\alpha A(s - c) \tag{2}$$

where m(x,t) is the solute mass per unit length in the main channel (= cA), c(x,t) is the concentration of solute in the main channel, s(x,t) is the concentration of solute in the transient storage zone, A(x) is the main channel cross-sectional area, x is the longitudinal spatial co-ordinate and t is time (u(x), D(x), α(x) and A_s(x) are as previously defined). The following boundary conditions are frequently used with these equations. At the upstream boundary, $c(0,t) = c_i(t)$, which specifies the solute mass entering the computational domain; at the downstream boundary a zero diffusive flux is assumed which implies that solute is carried out of the domain unhindered.

Equations (1) and (2) were solved using a finite volume approach in space (with space step, Δx), evaluating the advection term explicitly in time and evaluating the dispersion and transient storage terms (fully) implicitly in time. The DISCUS method was used for equation (1) (Wallis *et al.*, 1998; Manson & Wallis, 1999; Manson & Wallis, 2000; Manson *et al.*, 2001). The backward implicit method used for the dispersion term and the transient storage terms is unconditionally stable and robust. It is deficient in the sense that it assumes that conditions at the future time prevail over the entire time step (Δt): however, it does not suffer from the grid-scale oscillations of the formally more accurate Crank-Nicolson method. Tests have shown that for the range of parameters investigated here the method is satisfactory [Manson *et al.*, 2001].

When equations (1) and (2) are solved the solution consists of estimates for c and s over some discretised spatial and temporal domain, i.e. (c_i^n, s_i^n) for i=1 to N and n=1 to T where N is the number of cells in the spatial domain and T is the number of points in the temporal domain. When the model is fitted to observed data that has been collected at a downstream station then a fitting parameter may be defined as,

$$R = 1 - \sqrt{\frac{1}{T}\sum_{n=1}^{T}\left(Observed_N^n - Model_N^n\right)^2} \tag{3}$$

so that an R value of 1 indicates a perfect fit. Only in-stream concentration is usually used for the fitting, because concentrations in the storage zones are rarely measured.

IMPLEMENTATION AND RESULTS

The current implementation of the model used an existing FORTRAN code which solves equations (1) and (2) using the techniques described earlier. The FORTRAN code consisted of a subroutine that takes the concentration-time curve at an upstream station and predicts the concentration-time curve at a downstream station subject to given parameters (u, D, α, A_s, N, T, Δt and Δx). The FORTRAN subroutine (discus.f) was combined with the code required by MATLAB and then compiled using the GNU FORTRAN compiler (g77) to create object code (discus.o) and then linked with the "fmexlib*" object libraries to create the final MATLAB callable function (discus.dll), see Fig.1. The MATLAB function is available from the first author by email.

```
>> cdn =discus(cup,u,D,N,T,dx,dt,alpha,storage_area)

where

cdn: one dimensional array of size T containing predicted downstream concentration profile
cup: one dimensional array of size T containing upstream concentration profile
u: real variable representing velocity
D: real variable representing dispersion
N: integer variable representing number of cells in space
T: integer variable representing number of time steps
dx: real variable representing space step
dt: real variable representing time step
alpha: real variable representing α
storage_area: real variable representing As
```

Fig. 1 Usage of the MATLAB function.

The new function was tested using MATLAB's genetic algorithm toolbox to find the best set of parameter values [u, D, α, A_s] which would fit the model equations (1) and (2) to data from a tracer study from a local freshwater stream in May, 2008. The stream was relatively small having a width of 5.5 m and a depth of 0.45 m; there was a large macrophytic population present which added to the transient storage. In the tracer study 8 L of water containing 2kg of NaCl was released at a point well upstream of two monitoring sites that were 100m apart. Temporal profiles of conductivity were measured at the monitoring sites using PASCO Xplorer GLX dataloggers with conductivity probes. The measured conductivities are shown in Fig. 2 and serve as a surrogate for concentration. The model was fitted to this data suggesting values for the parameters of: $u = 0.04\ ms^{-1}$; $D= 0.05\ m^2s^{-1}$; $\alpha = 0.005\ s^{-1}$; $A_s = 0.4\ m^2$. The model prediction is also shown in Fig.2, and indicates a reasonably good fit. The stream was modelled as a uniform reach. The estimated parameter values are commensurate with the size and nature of the stream.

CONCLUSIONS

A useful new function for MATLAB has been developed. The function allows the user to predict the downstream concentration-time profile for a river tracer experiment given an upstream profile and knowledge of the river's flow and mixing characteristics. Alternatively the function may be used as part of an optimisation approach for parameter estimation. Although the algorithm itself is complicated the user of the function does not need to know any of its intricacies. Herein it was used with MATLAB's genetic algorithm toolbox and used to estimate the mixing characteristics of a small stream for which tracer data were available. The model fitted the data well, and the estimated parameters were consistent with the size and nature of the stream.

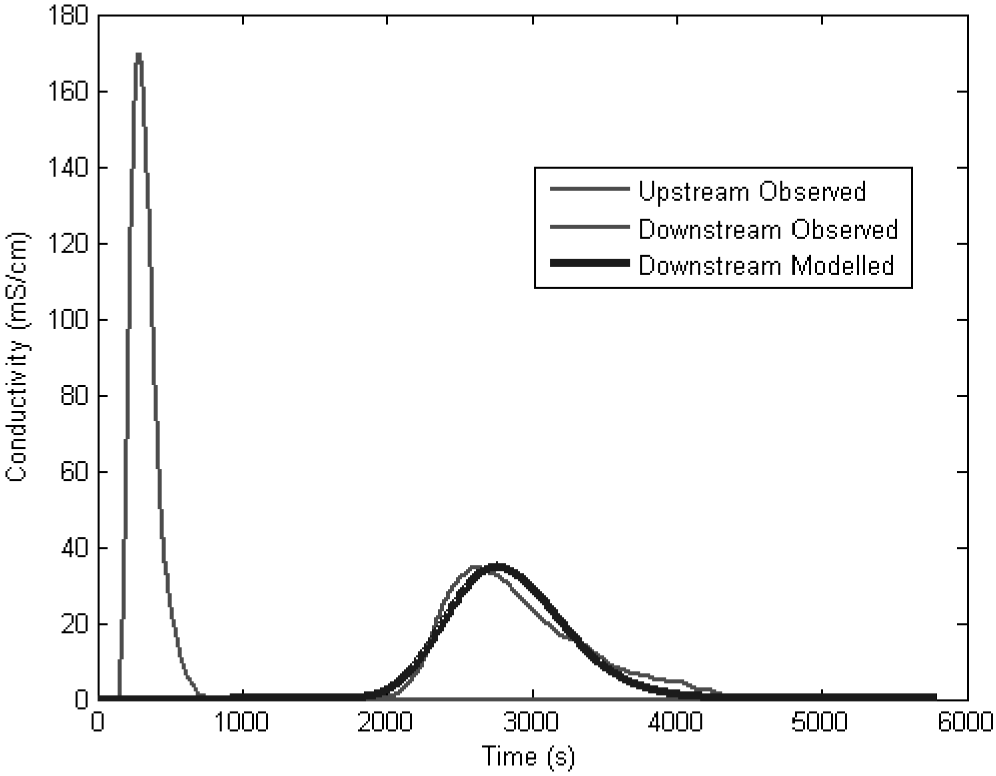

Fig. 2 Observed and modelled conductivity versus time.

REFERENCES

DeAngelis, D. L., Loreau, M. & Marzolf, E. R. (1995) Modelling nutrient - periphyton dynamics in streams: the importance of transient storage zones. *Ecological modelling* **80**, 149-160.

Manson, J. R., Wallis, S. G. & Hope, D. (2001) A Conservative Semi-Lagrangian Transport Model For Rivers with Transient Storage Zones. *Water Resources Research* **34**(15).

Manson, J. R. & Wallis, S. G. (2000) A conservative, semi-Lagrangian fate and transport model for fluvial systems: Part 1 - Theoretical Development. *Water Research* **34**(15).

Manson, J. R. & Wallis, S. G. (1999) Conservative Semi-Lagrangian Algorithm for Pollutant Transport in Rivers. *Journal of Environmental Engineering*, *ASCE* **125**(5).

Neelz, S. P. F. & Wallis, S. G. (2007) Tracking accuracy of a semi-Lagrangian method for advection-dispersion modelling in rivers. *International Journal for Numerical Methods on Fluids* 53, 1-21.

Sabol, G. V. & Nordin, C. F. (1978) Dispersion in rivers as related to storage zones. *Journal of the Hydraulics Division*, ASCE **104**, 695-708.

Valentine, E. M. & Wood, I. R (1979) Experiments in longitudinal dispersion with dead zones. *Journal of the Hydraulics Division*, ASCE **105**, 999-1016.

Wallis, S. G., Manson, J. R. & Fillippi, L. (1998) A Semi-Lagrangian Algorithm for One-Dimensional Advection-Diffusion. *Communications in Numerical Methods for Engineering* **14**, 671-679.

Wallis, S. G. & Manson, J. R. (1997) Accurate numerical simulation of advection using large time steps. *International Journal of Numerical Methods in Fluids* **24**, 127-139.

Worman, A., Packman, A. I., Johansson, H. & Jonsson, K. (2002) Effect of flow-induced exchange in hyporheic zones on longitudinal transport of solutes in streams and rivers. *Water Resources Research* **38**(1), 1-15, 1001, doi:10.1029/2001WR000769.

Coupling monitoring networks and regional scale flow models for the management of groundwater resources: the Almádena-Odeáxere Aquifer case study (Algarve-Portugal)

J. MARTINS & J. P. MONTEIRO

Algarve University Geo-Systems Centre UALG/CVRM, Marine and Environmental Sciences Faculty, Campus de Gambelas 8005-139 Faro, Portugal

joaoambiente@gmail.com

Abstract Automatic monitoring networks were settled to provide datasets for the calibration and validation of regional flow models, as a strategy to complement data available in official monitoring networks for the main regional aquifers in Algarve (Portugal). The Almádena-Odeáxere aquifer system is presented as an example, where the comparative analysis of variables representing "reality", consisting of data obtained in these networks, was made against values simulated with a finite element numeric model. This methodology contributed for a better calibration and validation of the model, together with the design of effective groundwater monitoring networks, at the regional scale.

Keywords inverse calibration; use of models to guide data collection; use of data to calibrate models; Algarve

INTRODUCTION

The 17 aquifer systems presently identified in the Algarve region (South Portugal) are currently being monitored by the Coordinating Commission of the Algarve - CCDR (official entity) through a set of monitoring networks, comprising 138 observation points, which control several state variables, relevant for water management. However, the density of these networks and the respective frequency of data collection cannot provide datasets detailed enough to characterise the spatial distribution and temporal evolution of these variables in order to allow the calibration and validation of quantitative regional flow models.

In order to overcome these difficulties on the Almádena-Odeáxere aquifer system (AO), the work undertaken consisted in coupling: (1) a regional finite element flow model, developed to investigate the hydraulic behaviour of the AO; (2) the setting up of an automatic monitoring network of 10 additional in-situ environmental sensors for real-time monitoring, custom-designed in a complementary way the official monitoring network already existing at AO (11 observation points). Subsequent adjustments on the position of the settled observation points were made by continuously retrieving and analysing available head data. These adjustments were performed alongside with the purpose of calibrating the finite element flow model through inverse methods, thus providing the necessary model input data to fulfil this objective.

MONITORING NETWORKS AND CONCEPTUAL FLOW MODEL

The AO (Fig. 1) has an area of 63,5 km^2 spanning from Odeáxere (East) to Almádena (West). It develops in carbonate Lias-Dogger lithologies (limestones, dolomitic limestones and dolostones), which show, in some places, a well developed karst with a thickness in the order of 750 m (Reis, 1993; Almeida *et al.*, 2000).

According to the conceptual model, regional water is expected to flow predominantly from NE to SW (towards the effluent reach of "ribeira de Vale do Barão" creek) and N to S (towards the effluent reach of "ribeira de Bensafrim" creek).

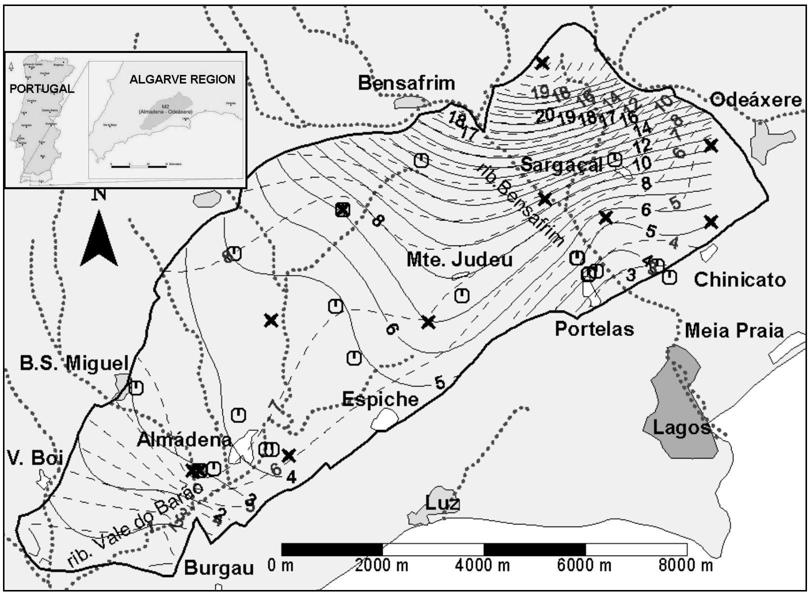

Fig. 1 Hydraulic head contours, interpolated from the official monitoring network ("x" marks) data (dashed lines) and interpolated from the joint use of the implemented automatic monitoring network (circle symbols), represented as solid lines.

An analysis of the piezometric surface of AO (contoured using data obtained at the official monitoring network, from March 1978 to February 2007) showed that the available data was insufficient to provide a consistent estimate of the hydraulic behaviour of the aquifer. According to this data, flow predominantly occurred NW to SE, which should not happen in reality due to the existence of an impermeable geologic boundary at the SE limit of AO. The existent monitoring network lacked the necessary coverage, on important sectors of the aquifer, for an efficient calibration of the aquifer's finite-element model. In order to complete the existing data, an additional automatic monitoring network was implemented at AO, in articulation with the process of calibrating the regional groundwater flow model, built for this aquifer.

The elaboration of potentiometric surface maps based on the blending of data from these two monitoring sources has contributed considerably for the subsequent definition of 16 constant transmissivity, *T*, zones inside AO (Fig. 2, right). The subdivision of these zones took place on the basis of the character of the piezometric contours because there is little obvious variation in geology throughout the study area. This assumption follows the methodology carried out by Doherty (1998) which has already led to good calibration results. A similar procedure has also been used by Monteiro *et al.* (2006), Monteiro *et al.* (2007) to study Algarve aquifer systems.

In order to overcome the lack of information on hydraulic head values at the defined zones, which were necessary for a successful calibration, 22 auxiliary "fictional" data points were distributed throughout the aquifer area. Hydraulic head values assigned to these points were based on the interpolation results of real head data at each of the corresponding coordinates. The introduction of these points did not result on a change on the flow pattern revealed by piezometry data obtained on the monitoring networks (as can be observed on Fig. 2, left).

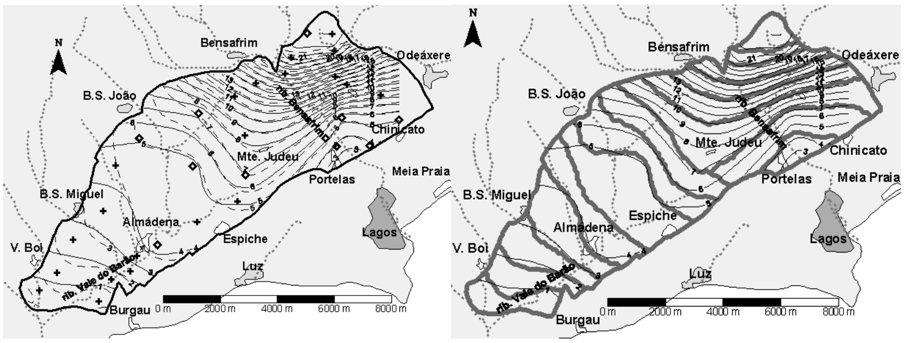

Fig. 2 On the left, contours of hydraulic heads based on two datasets: the dashed lines represent data from the official network ("x" marks on Fig. 1) blended with data extracted from the automatic monitoring network (lozenges), the solid lines were created by adding auxiliary fictional hydraulic head values (crosses) to this data. On the right, 16 constant *T* zones (limited by grey thick lines) were defined according to the character of the obtained potentiometric surface (solid lines, on the left and right).

INVERSE CALIBRATION OF THE MODEL

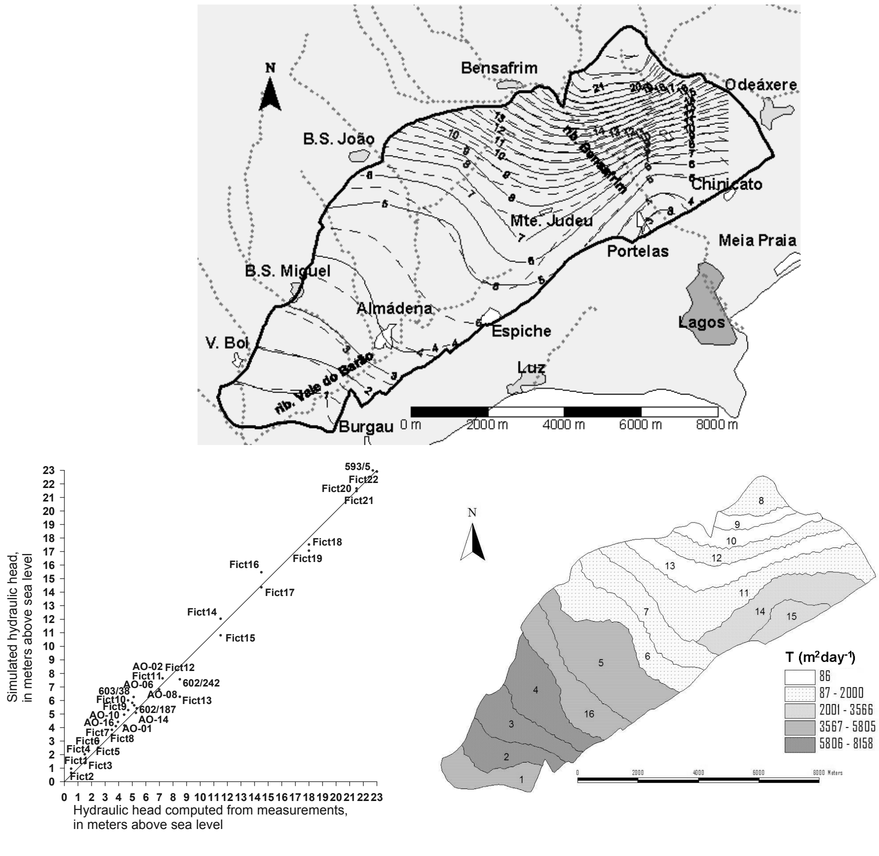

Fig. 3 Simulated (dashed line) and measured (solid line) hydraulic head contours (above). Scatter plot of simulated vs. measured hydraulic heads (left and below). Spatial distribution of *T* values along the 16 predefined zones, obtained using inverse calibration (right and below).

In the last two decades, hydraulic parameters were obtained for AO from pumping tests on individual boreholes. These values ranged from 25 to 8784 m^2 day^{-1} (Reis, 1993; Almeida *et al.*, 2000). However these methods cannot provide the necessary data to carry out realistic representations of aquifers at the regional scale.

The performed calibration consisted consequently on the first attempt to obtain regionally distributed values of *T* using a synthetic bi-dimensional numerical representation of the AO (Martins, 2007). This hydraulic parameter was estimated by inverse modelling, using the Gauss-Marquardt-Levenberg method, implemented in the nonlinear parameter estimation software PEST (Doherty, 2002).

The calibration results (Fig. 3), obtained using the inverse method, ranged from 86 m^2 day^{-1} to 8158 m^2 day^{-1} on 16 predefined zones of equal transmissivity. The calibration revealed a good fit between simulated and measured head values (Fig. 4), the correlation coefficient, *R*, value was higher than 0,9 (0,9967) and the sum-of-squared weighted residuals between model outcomes and corresponding field data (i.e. the objective function, Φ) was 4,56 m.

CONCLUSIONS

Networks which automatically monitor hydraulic data in AO were designed in conjunction with the process of calibrating a numerical model through inverse methods. This model consists of a "synthetic representation" of the current knowledge regarding the hydrogeology of this aquifer. The Gauss-Marquardt-Levenberg method, implemented in the nonlinear parameter estimation software PEST, was used.

Calibration results provided the first estimate on the aquifer's regional transmissivity values distribution, which ranged from 86 m^2 day^{-1} to 8158 m^2 day^{-1}. A good fit between simulated and measured head values was obtained, since the correlation coefficient, R, value was 0,9967 and the objective function, Φ, was 4,56 m.

This work has contributed for improving the reliability of future simulations of spatial distribution and temporal evolution of state variables (hydraulic head and natural outflows), on natural conditions and also for different scenarios of water use.

Acknowledgements The authors gratefully acknowledge the Portuguese Science and Technology Foundation (FCT) for the financial support of the POCTI/AMB/57432/2004 Project "Groundwater flow modelling and optimisation of groundwater monitoring networks at the regional scale in coastal aquifers – The Algarve case study" (CVRM Geo-Systems Centre, Algarve University).

REFERENCES

Almeida, C., Mendonça, J. L., Jesus, M. R. & Gomes, A. J. (2000) Sistemas Aquíferos de Portugal Continental. [Aquifer Systems of Mainland Portugal]. INAG. *Relatório Técnico* [Technical Report], CD-ROM, 661pp.

Doherty, J. (1998) Use of MODFLOW in Groundwater Management in an Area of High Seasonal Rainfall. In: *Proceedings of MODFLOW'98*. Golden CO. U.S.A., 8pp.

Doherty, J. (2002) PEST, Model-Independent Parameter Estimation. 4th Edition, *Watermark Numerical Computing*, Australia, 279 pp.

Martins, J. (2007) Inverse Calibration of a Groundwater Flow Model for the Almádena-Odeáxere Aquifer System (Algarve – Portugal). *MSc. Thesis, Faculdade de Ciências do Mar e do Ambiente*, Universidade do Algarve.

Monteiro, J. P., Vieira, J., Nunes, L. & Younes, F. (2006) Inverse Calibration of a Regional Flow Model for the Querença-Silves Aquifer System (Algarve-Portugal). In: *Integrated Water Resources Management and Challenges of the Sustainable Development*. Marrakech. Morocco, CD-ROM, 6pp.

Monteiro, J. P.; Oliveira, M. M. & Costa, J. P. (2007) Impact of the Replacement of Groundwater by Dam Waters in the Albufeira-Ribeira de Quarteira and Quarteira Coastal Aquifers. In: XXXV IAH Congress. *Groundwater and Ecosystems. Lisbon*. Portugal, pp 489-480, CD-ROM, 10pp.

Reis, E. (1993) Estudo Hidrogeológico das Formações do Lias-Dogger situadas a ocidente do Rio Arade (Algarve), [Hydrogeologic Study of the Lias-Dogger Formations West of River Arade (Algarve)]. *MSc. Thesis*, FCUL.

The importance of understanding the functioning of prevailing groundwater flow systems for an adequate water and environmental management, the south of the Mexico Basin

L. A. PEÑUELA-ARÉVALO[1] & J. J. CARRILLO RIVERA[2]

1 *Earth Sciences Postgraduate Programme, Geophysical Institute, UNAM, Av. Universidad No.3000, México, D.F. 04510*
lilianapenuela@gmail.com

2 *Institute of Geography, UNAM, Av. Universidad No.3000, México, D.F. 04510*
joeljcr@igg.unam.mx

Abstract The Mexican Federal Government began in 2003 the first Environmental Hydrological Services Payment Programme (EHSPP), to preserve its forest areas, specifically to keep their groundwater recharge potential. However, the application of this programme was not supported by hydrogeological studies of the physical media that would have identified recharge areas and possible flow paths as well as probable impacts to groundwater or to other components of the environment. This study intents to highlight the importance of including groundwater flow systems investigations as a base to environmental projects or this kind of programme (EHSPP) to obtain a clear understanding of the functioning of groundwater in relation to the zone receiving the payment and finally to have a basic tool to make an adequate water and environment management.

Key words environmental hydrological services; groundwater; flow paths; recharge areas; water management

INTRODUCTION

Nowadays, demographic growing is a significant problem related with environmental damage considering the excessive use of the natural elements by the increasing population, specially water and forest. This situation has created an alert in different communities of the world and governments are now interested in formulating new strategies that might help to reach a sustainable development. Thus, the Mexican Federal Government initiated an Environmental Hydrological Services Payment Programme in 2003, based on the Costa Rica experience in 1996-2002, to preserve its forest areas, specifically to keep their groundwater recharge potential.

The aim of the programme is to stimulate the communities in the mountains through an annual payment to the communities (owners of land forest) who preserve their forest areas during the payment period. The hypothesis of the programme is that a forest cover contributes to regulate the hydrologic cycle and also provides other environmental services. However, this theory is still waiting to be scientifically proved.

The present study results from a series of investigations and analysis (Carrillo-Rivera *et al.,* 2004; Peñuela, 2007) with which it is proposed to demonstrate the importance to include groundwater flow systems investigations through an interdisciplinary approach that acquires the knowledge of groundwater flow and its interaction with other components of the environment that might permit to obtain an adequate environmental management.

The study zones

This work is focused on the environmental hydrological services payment (EHSP) at the south of the Mexico Basin. It includes the analysis of twenty *ejidos* (communal properties) that are grouped in two areas (Fig. 1). Area 1 is located in the southwest part of the *Distrito Federal,* and Area 2 is in the limit between Puebla, Tlaxcala and Mexico states. There is a particular interest to protect the recharge areas of this basin because Mexico City is included in its perimeter and about 70% of its total water supplies is obtained from groundwater (Edmunds, *et al.*, 2002).

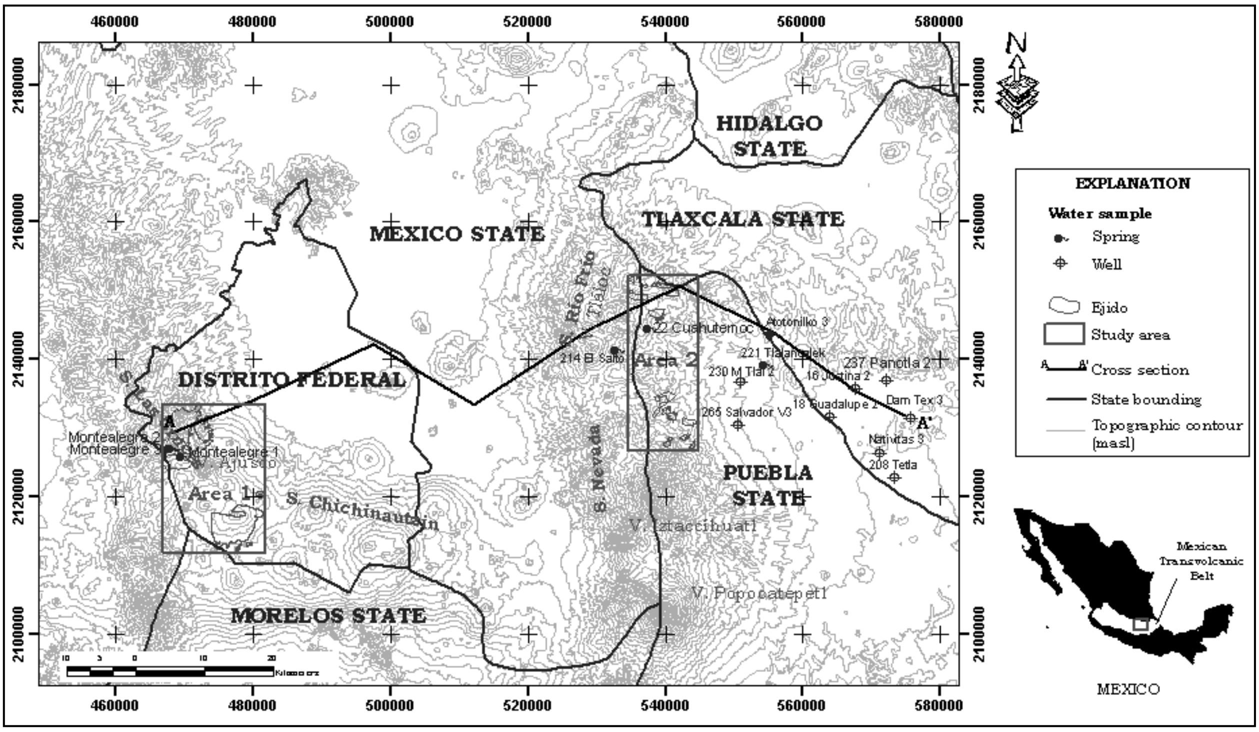

Fig. 1 Location of study areas for hydrological services evaluation.

The Mexico Basin is a closed basin located in the Mexican Transvolcanic Belt. For this reason, the geological units outcropping in the basin have a regional extension, a continuous distribution, more than 2,000 m thick, which are composed mainly by fractured volcanic rocks of Tertiary and Quaternary age (Fig. 1). From the groundwater flow systems perspective, there is an underground hydraulic continuity among surface watersheds which, is enhanced by the thickness (depth to basement) of more than 3,000 m.

METHODS

The methodology used in this study consisted in three phases: 1) analysis and integration of accessible information (climatology, hydrogeology, geomorphology, edaphology, vegetation, land use, urban growth and people migration), 2) fieldwork (sampling of groundwater in discharge zones -15 samples, Fig. 1- for physicochemical and isotopic analysis, as well as checking of soil use and vegetation), and 3) analysis and interdisciplinary interpretation of the information acquired according to the groundwater systems flow theory (Tóth, 1999). The defined procedure included a hydrogeochemical analysis to define minimum depth reached by water flow using chalcedony geothermometer; stable isotopes (δ^2H and $\delta^{18}O$) provided the possible recharge rainfall elevation for water not affected by evaporation; geomorphology, soil and vegetation were used to define recharge/discharge characteristics.

RESULTS

Hydrogeochemical analysis

Three major groundwater quality groups were identified in the region, according to the analytical results (Table 1) and their interpretation (Fig. 2).

Table 1 Main chemical and physical parameters of water samples.

GROUP	T (ºC)	Na (mg l^{-1})	HCO_3 (mg l^{-1})	SO_4 (mg l^{-1})	Cl(mg l^{-1})	Li (mg l^{-1})
1. Local	9.5-17	3.0-11.2	9.8-92.7	1.0-7.2	0.5-1.9	<0.001-0.002
2. Mix	17.7-19.1	16.1-29.2	136.6-402.6	4.0-54.2	4.9-12.4	0.004-0.027
3. Intermediate	19.9-23.7	42.2-120.0	305-610	2.8-25.9	4.8-37.9	0.015-0.089

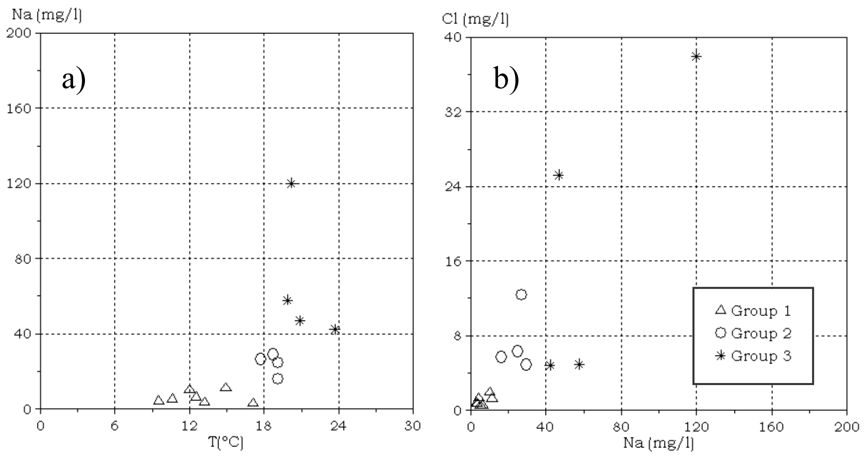

Fig. 2 Relation among: a) temperature and sodium; b) sodium and chloride.

Stable isotopes analysis

Fig. 3 shows $\delta^{18}O$ and δ^2H values of the sampled water in relation to the global meteoric water line (GMWL, $\delta^2H = 8\ \delta^{18}O + 10$) and to the local meteoric water line (LMWL, $\delta^2H = 7.95\ \delta^{18}O + 11.77$; Cortés & Farvolden, 1989). Some samples are located in a narrow field close to the GMWL and LMWL; others are situated defining two evaporation lines (EVL 1, $\delta^2H = 5.102\ \delta^{18}O – 21.12$ and EVL 2, $\delta^2H = 5.014\ \delta^{18}O – 23.95$) suggesting that those samples were influenced by this process (Fig. 3).

The altitude of the precipitation was calculated with the equation established by Cortés & Durazo (2001): $\delta^{18}O^*(X,Y)= -2.13\ Z(X,Y) – 3.2$, where: $\delta^{18}O^*$ is ^{18}O isotopic concentration of the precipitation (‰ versus Vienna-SMOW); Z is topographic elevation and (X,Y) are spatial referring. In this way, it was possible to obtain the altitude of the area receiving precipitation and the potential recharge area altitude for each spring, for samples not affected by evaporation.

Fig. 4 shows a great deal of possibilities for recharge areas, the system must be considered in 3D where the Sierra Nevada and mountains of the eastern part of the region need to be included. In this regard, the payment for preserving the established zones of interest is considered to be misleading the objective of the ESHPP because there is not a direct definition that these highlands are recharge area of the prevailing flow systems discharge that are used by rural and city dwellers on the plain.

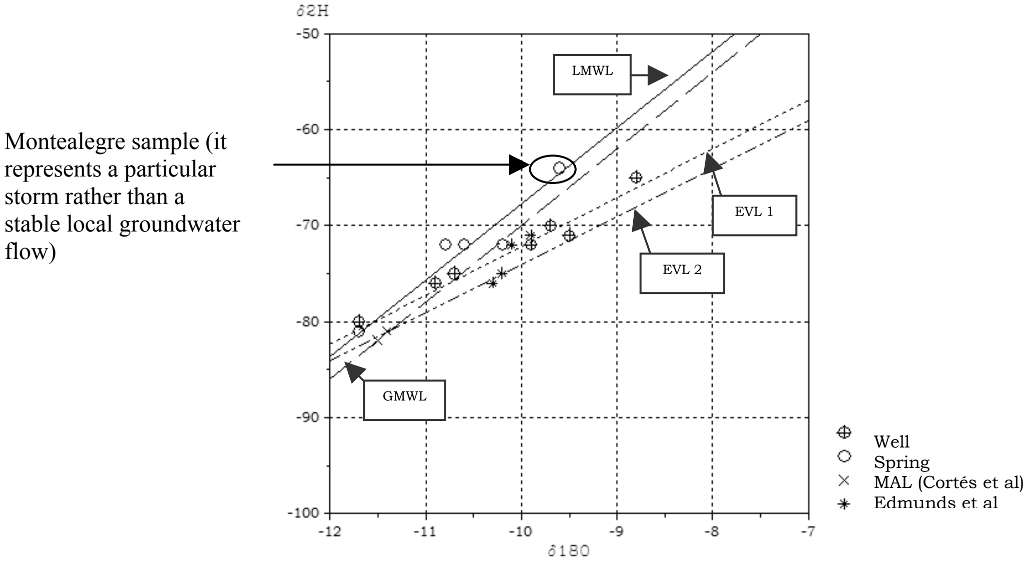

Fig. 3 Distribution of $\delta^{18}O$ and $\delta^{2}H$ in the south portion of Mexico Basin.

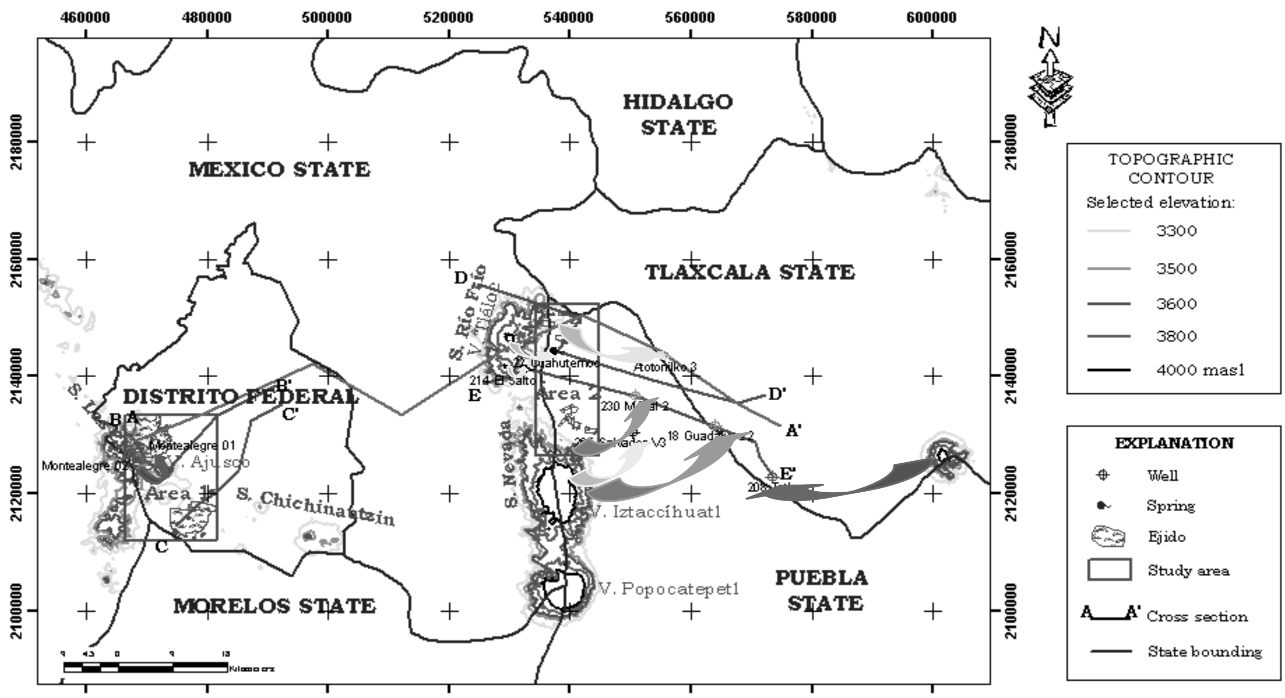

Fig. 4 Altitudes of precipitation and possible recharge areas with their flow path (samples not affected by evaporation).

DISCUSSION

Hydrogeological sections of the sites were elaborated to gain an initial understanding of the water flow mechanism that may provide an environmental service in the study sites. Therefore, the functioning of groundwater was proposed through direct and indirect data. According to the previous estimates of the altitude of precipitation, the possible altitude for recharge for each of the defined water group in this study is presented in Table 2.

Table 2 Possible altitude for recharge for each group of water.

GROUP	Possible altitude for recharge (km asl)
1. Local	3.5 – 4.0
2. Mix	3.4 – 3.8
3. Intermediate	3.3 – 3.7

It is important to indicate that the number of *ejidos* and other communities involved in the EHSP in Mexico is increasing. However, there is a lack in knowledge on groundwater functioning and its interaction with different elements of the landscape. It is clear that the application of the EHSP was not supported by the required studies of the physical media (specifically hydrological and hydrogeological) that would have identified recharge areas to groundwater (aim of EHSP) and potential impacts to water or to other elements of the environment. Therefore, this study recommends ecological and hydrogeological studies to define groundwater functioning previous to the start of any environmental programme such studies should focus in defining the presence of flow systems and their hierarchy.

CONCLUSIONS

Results of this study (flow paths, groundwater flow systems, definition of the possible recharge and its associated groundwater discharge area) are an initial contribution to the knowledge of groundwater dynamics in the south of the Mexico Basin. The evaluation of the groundwater flow systems allows the identification of problems related with the implementation of the EHSP because the selected areas for payment need to be satisfactorily defined in terms of their location. Obtained results are considered to highlight the importance of understanding the groundwater flow systems functioning before any application of EHSP or other environmental programme; their definition is also an adequate tool for water and environmental management. A similar analysis may assist in formulating new strategies towards sustainable development, to protect and preserve ecosystems located in a discharge area taking in mind that these areas are as important as the recharge areas. It is essential to create an environmental consciousness in people willing to protect nature, and on the importance of incorporating all the components involved because the environment works as a system.

Acknowledgements The authors gratefully acknowledge all of the support provided by the institutes of Geophysics and Geography of the UNAM, which was invaluable in each activity related to the present study.

REFERENCES

Carrillo-Rivera, J. J., Perevochtchikova, M., Táutiva, M., Godoy, A., Peñuela, L. & Herat, T. (2004) Definición de indicadores de impacto al recurso hídrico en zonas receptoras de pago por servicios ambientales hidrológicos 2003-2004. *Convenio Instituto Nacional de Ecología-Instituto de Geografía UNAM. Informe final*, 91 p.

Cortés, A. & Farvolden, R. N. (1989) Isotope studies of precipitation and groundwater in the Sierra de las Cruces, Mexico. *J. Hydrol*. **107**, 147-153.

Cortés, A. & Durazo, J. (2001) Tendencia del oxígeno-18 en la precipitación del centro de México. *Ingeniería Hidráulica en México* **16**(2), 93-102.

Edmunds, W. M., Carrillo-Rivera, J. J. & Cardona, A. (2002) Geochemical evolution of groundwater beneath Mexico city. *J. Hydrol*. **258**, 1-24.

Peñuela-Arévalo, L. A. (2007) Proceso de recarga-descarga de agua subterránea en zonas receptoras de pago por servicio ambiental hidrológico, Sierras Nevada y Las Cruces - México. *MSc thesis in Earth Sciences, Instituto de Geofísica. Universidad Nacional Autónoma de México UNAM.*

Tóth, J. (1999) Groundwater as a geologic agent: An overview of the causes, processes, and manifestations. *Hydrogeol. J.* **7**(1)1-14.

Simulation for solving management problems of combined surface-ground system

E. PROSHKINA
Geology department, Lomonosov Moscow State University, GSP-2, Leninskie Gory, Moscow, 119992, Russian Federation
alenaproshkina@yandex.ru

Abstract It is offered to apply combined use water resources for small river basin. Numerical simulation definite required distance between compensating well and riverbank to maintain stream and estimates influence hydrodynamic parameters on it. Researching analyzed applicability analytic equations to evaluate this distance. Numerical models estimate error, caused by using the equation.
Keywords water resources; conjunctive use; combined use; numerical simulation; stream depletion; small river basin

INTRODUCTION

The problem of water resources shortage becomes global. Rational use of water supplies requires "conjunctive use water resources", implying groundwater and surface water are utilized jointly. Conjunctive use water resources have been designated by a variety of titles. These include conjunctive use (Downing, 1993), economic aspects (Sahuquillo, 1989) and integrated management (Hall, 1997). The term «conjunctive use» is widespread, including artificial recharge; groundwater, pumped from aquifer to river; supplemental water available from reclaimed wastewater; surface reservoir and supplemental groundwater pumping. It is offered to apply the combine use sources of water, which is proved, allow to increase quantity of available water resources. The combine system compounds of basic and compensating pumping well. Field of basic wells exploits surface flow, compensating well periodically in the seasonal limiting periods of year - ground waters. Influence hydrodynamic parameters and prediction changes in water budget were investigated by numerical simulating.

RESULTS

Combined water system

Available water resources (AWR) are less than total water resources because they are estimated as minimal river flow according to normative requirements. However, there is 60-80 % of surface flow related to a flood in main climatic zones of Russian Federation and therefore large quantity is excluded from consideration. The water resources lack is especially strong for the small river basins, where the water demand is much more than low-water flow. Combined use of groundwater and surface water increases AWR.

Combined system represents a technological complex of basic and compensating production wells. Basic well operates during high recharge period, when there is no danger lowering river flow or its level (depth) over permissible limits. In limited periods when the basic system can not provide for the water demand, compensating well is engaged. Discharge is determined by a difference between calculated demand and allowable withdrawal of the basic well. The compensating well operates short-term and exploits specific storage of aquifer.

The main hydrogeologic problem is a determination of compensating production well position. There are following requirements to compensating well work:

maintaining river flow during pumping,

enough recovery due to natural processes or artificial recharge,

basic and compensating production wells pump inside one river basin.

There are formulated three schemes of location compensating well:

1. Well is sited in valley, where aquifer is intimately associated with streams and represents single hydraulic system. The minimization of stream depletion is achieved by removing well from the river.

2. Well uses aquifer, which is badly hydraulically connected with river due to watertight river beds. In this case wells can be sited close to the river.

3. Well exploits confined aquifer. The stream reduction is minimized by low permeability of impermeable bed.

The paper researches the first scheme (Fig. 1). Influence hydrodynamic parameters and prediction changes in water budget were investigated by modelling.

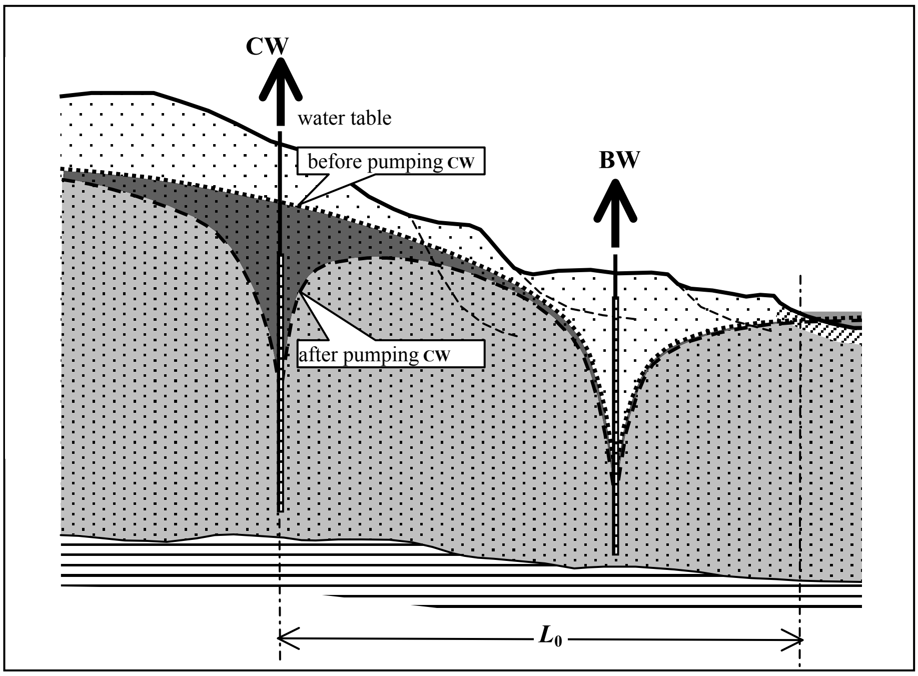

Fig. 1 The first scheme of location compensating well.

Numerical simulating

Basic parameters, determining value and time of lowering river flow, are transmissivity and specific yield of aquifer and permeability of river bed. The first task of the model experiments was to determine favourable conditions for combined system of water resources. The second task was comparison between analytic and model distance of compensating well from riverbank.

A two-dimensional numerical model was constructed using ModTECH 2.3. Aquifer was simulated as horizontal, unrestricted, unconfined, underlying impermeable bed. Transmissivity is ranged from 100 to 1000 m^2/d, specific yield is ranged from 0.054 to 0.54 and leakage coefficient of river bed is 0.5 1/d. A constant river width of 10 m was used.

The overall dimensions of the model domain are 25 m depth, 1000 m width, and 1000 m length. Size of column and row is 10 m. The pumping rate of compensating well is 5184 m^3/d.

Is was realized, that high specific yield (more than 0,1) and low transmissivity (less than 1000 m^2/d) are appropriate conditions for effective use combined systems.

Table 1 Hydrodynamic input parameters for numerical simulations.

Transmissivity, m^2/d	100	300	500	800	1000
Specific yield	0,054	0,0675	0,108	0,18	0,54

The second task was to analyze influence riverbed permeability on difference in analytic and model distance compensating well from riverbank. Distance between compensating well and riverbank can be estimated by following equation:

$$L^* \approx 2\sqrt{\frac{T}{S}t_{\mathrm{k}}} \inf erfc(\varepsilon \frac{Q}{Q_{\mathrm{k}}}) \tag{1}$$

T – transmissivity, S – storage coefficient, t_k time – length of calculated period, ε - normative error of the hydrometric measurements, Q – minimal river flow, Q_k – production rate of compensating well.

However, the equation (1) was written for condition with constant head in river. L^* is real distance between compensating well and riverbank. In case of watertight river beds, impermeable sediments decrease hydraulic conductance riverbed and create additional virtual space between compensating well and riverbank. Existent equations for river with impermeable bed are onerous and unsuitable for decision inverse problems.

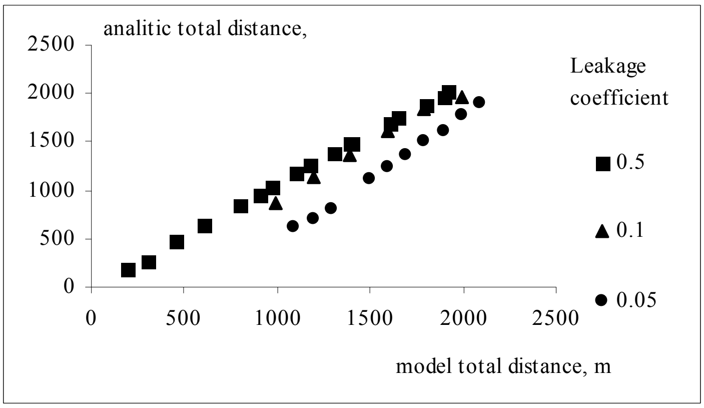

Fig. 2 Distance scatter diagram.

Numerical models can estimate error, caused by using the equation (1), in which total distance between compensating well and riverbank calculates as sum real and virtual distance (Fig. 2).

Model results show, the equation (1) is suitable if riverbed leakage coefficient is more than 0.05 1/d. In other case (leakage coefficient is less than 0.05 1/d) this equation is seldom applicable especially if distance between compensating well and riverbank is 100-200 m.

Equation (1) can be used also for calculation possible compensating well rate if L^* is determined:

$$Q_К = \frac{\varepsilon P_{ОСТ}}{\operatorname{erfc}\left(\frac{L^*}{2\sqrt{at}_К}\right)} \tag{2}$$

CONCLUSIONS

Appling the combined use sources of water allow to increase quantity of available water resources. It is especially necessary for the small rivers basins. There are three schemes of location compensating well. The favourable conditions for effective applying the first scheme are low transmissivity (less than 1000 m^2/d) and high storage property (specific yield more than 0.1). It is possible analytically estimate distance between compensating well and riverbank, if riverbed leakage coefficient is more than 0.05 1/d, in other case there is applicable only numerical simulation.

Acknowledgements The assistance and support of R. S. Shtengelov, A. A. Maslov and others in the Hydrogeology Laboratory are acknowledged.

REFERENCES

Downing, R. A. (1993) Groundwater resources, their development and management in the UK an historical perspective. *Quarterly Journal of Engineering Geology* **26**, 335-358.

Hall, W. A. & Dracup J. A. (1970) Water resources systems engineering. 372.

Kovalevskii, V. S. (2001) Combined use surface and groundwater resources. 332.

Sahuquillo, A. (1989) Economic aspects of conjunctive use of ground and surface water. *Ground water economics* **39,** 347-359.

Optimal operation of a reservoir system using predicted inflow

A. SHARMA[1], C. HUEBNER[2], A. JAIN[1] & M. W. OSTROWSKI[2]
1 *Hydraulics & Water Resources, IIT Kanpur, 208016, India*
ajaysharma483@gmail.com

2 *Darmstadt University of Technology, Petersenstrasse 13, D-64287, Germany*

Abstract During floods, for an efficient management of a water resources system, flow forecasting often play a vital role. The benefit of the reservoirs operation can also be improved by obtaining accurate forecast of reservoir inflow during floods. Main objective during high peak flow is to have the reservoir water level as low as possible to reduce flooding and the dangers resulting from high discharge. On the other hand, to have the reservoir water level as high as possible to increase the efficiency of the hydropower generation and to full fill other demands like irrigation, industrial etc. This paper investigates the development of a model for the reservoir Urftalsperre (Germany) where the inflow of the reservoir during flood periods was predicted and also to be able to give optimized values of reservoir releases and storages by fulfilling multiobjective tasks during floods. Inflow prediction is done by Artificial Neural Networks (ANNs). Optimal operation of reservoir system is performed by NSGAII (Non Dominated Sorting Genetic Algorithms) and PAES (Pareto Archived Evolution Strategy). It was found that ANN model gives accurate values of Reservoir inflow. NSGAII outperformed PAES in terms of computation time consumption to get Pareto optimal fronts, but gave similar results for objective function and decision variables.
Keywords neural networks; NSGAII; PAES; Pareto fronts

INTRODUCTION

The work was divided into two phases. First phase describes the development of ANN model which was used to predict 3 consecutive day's of reservoir inflow values and their results were compared on the basis of various performance evolution statistics. ANNs are supposed to posses the capability to reproduce the unknown relationship between a set of input variables of the system and one or more output variables (e.g., runoff) (Chakraborty *et al*., 1992).

Feed forward back propagation training algorithms were used to train the Neural Network. Input selection for Neural Network was based upon auto and cross correlation analysis. The data set covered the values of rainfall and inflow to the reservoir for the period of the flood years 1960 to 2002. The whole data set was then divided into training and testing part. After selection of input parameters for the neuron model, hidden neurons have been varied from 1 to 15, and then on the basis of various performance statistics the best model structure was selected.

Second phase describes the optimal operation part of reservoir system using 3 days of predicted inflow to the reservoir using NSGAII and their performance compared with PAES. Deb (2001) described several, Elitism and Non Elitism based Optimization techniques, and we used two of Elitism based techniques to solve the problem. Keeping the fix mutation and crossover parameters in different trials, results were evaluated by varying the population size and number of generation. The objective functions which were used to perform the flood mitigation and hydropower generation are described in equations 1 and 2.

To fulfill the first objective function, outflow is trying to reduce during the flood time. Objective function formulated as follows

OBJECTIVE FUNCTIONS

$$\text{Maximize } f_1 = [I_t - R_t] - [S_t - S_{t+1}] \tag{1}$$

Where
I_t is the per day predicted reservoir inflow; values taken from best ANN prediction model, R_t is the per day reservoir release, S_t is the initial reservoir storage, S_{t+1} is the final reservoir storage

To achieve the second goal of maximizing the hydropower generation, a 2nd objective function was formulated. The hydroelectric power generation is proportional to the product of the total release and the operating head of reservoir. The objective function was formulated as follows

$$\text{Maximize } f_2 = [c.\eta.\gamma.R_t.H_t] \tag{2}$$

Where c is the Constant to convert release m^3sec^{-1} to m^3, η is the efficiency of turbine taken as .85, γ is the weight density of water taken as 9.81 KNm^{-3}, H_t is the per day operating head of reservoir, R_t is the per day reservoir release.

CONSTRAINTS

Various constraints are used to control the reservoir release and storage capacity of reservoir as follows:

Mass balance or continuity equation

$$S_{t+1} = S_t + I_t - R_t - E_r \tag{3}$$

Where S_{t+1} is the final storage at the end of one day and herewith the initial storage of day 2, S_t is the initial storage at day 1, I_t is the per day reservoir inflow, R_t is the per day reservoir release, E_r is the per day evaporation losses, we have neglected this loss.

Storage and release bound

The decision variable S_t can vary only between the maximum storage and the dead storage of the Urft reservoir, in this case the value of S_{min} and S_{max} for 1 day are 470424 m^3 and 48407547 m^3 respectively.

$$S_{min} < S_t > S_{max}$$

The decision variable R_t can vary only between the maximum and minimum release of the Urft reservoir, in this case the value of R_{min} and R_{max} for 1 day are 648000 m^3 and 2592000 m^3 respectively.

$$R_{min} < R_t > R_{max}$$

RESULTS

The various performance statistics for the selection of best model structure for 3 days forecast to reservoir inflow are taken as: AARE (Average Absolute Relative Error), SSE (Sum Square Error), TS (Threshold Statistics), R (Correlation Coefficient) and E (Nash-Sutcliffe Efficiency).

Table 1 Comparison of NSGAII and PAES in terms of front solution and time require.

Method	Population Size	Generation	Evaluations	Non dominated solution	Time require(second)
NSGAII	**750**	**100**	**75000**	**750**	**31**
PAES	**150**	**500**	**75000**	**750**	**480**

The best model structure obtained by Neural Network model for the 3 consecutive days taken as input for the reservoir operation. The overall comparison of NSGAII and PAES in terms of front solution and time require calculating non dominated solutions have shown in Table 1.

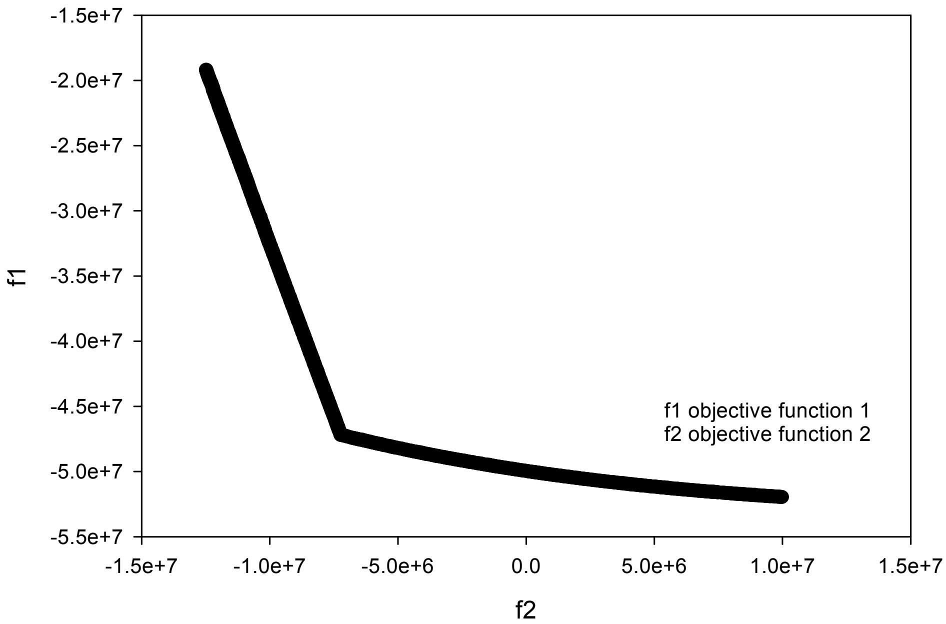

Fig. 1 Pareto optimal front for Population size 750 and Generation 100 by NSGAII.

Pareto optimal fronts between the objective function f1 and f2 have shown in Fig. 1 and 2 by NSGAII and PAES respectively.

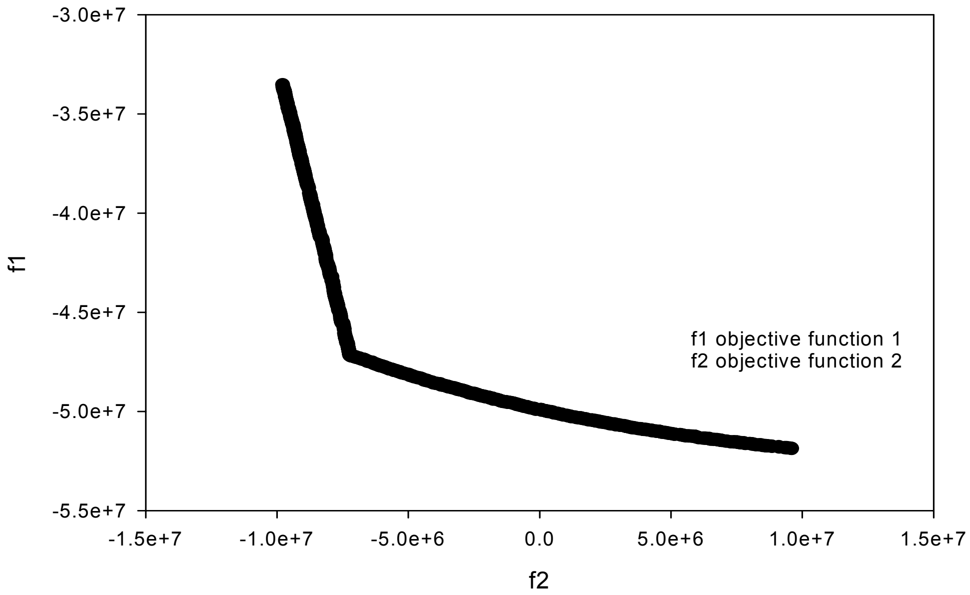

Fig. 2 Pareto optimal front for Population size 100 and Generation 750 by PAES.

CONCLUSION

This work explains the importance of inflow forecasting in optimal operation of reservoirs. Perfectly forecasted inflow values if available, would result in maximum possible benefits of operation during floods, by satisfying the conflicting objectives. Using the results obtained by ANN, optimization of reservoir performed with the help of NSGAII. With different trials of population size and generation, Pareto optimal fronts have been computed and the best results using NSGAII were obtained by using a population size of 750 and a generation size of 100. Again for the same reservoir problem of reservoir to fulfill multi-objective tasks, PAES method have been used, and it is found that PAES model is good enough to delivers the same results in terms of decision variables and objective function values but needs more time as compare to NSGAII.

REFERENCES

Chakraborty, K., Mehrotra, K., Mohan, C. K. & Ranka, S. (1992) Forecasting the behaviour of the multivariate time series using neural networks. *Neural Networks* **5**, 961–970.

Deb, K. (2001) Multi-Objective Optimization using Evolutionary Algorithms. *John Wiley & Sons, Chichester, UK.*

Groundwater modelling for improving groundwater-surface water regime in Slovak part of the Medzibodrožie region

A. ŠOLTÉSZ & D. BAROKOVÁ
Slovak University of Technology in Bratislava, Faculty of Civil Engineering, Department of Hydraulic Engineering
andrej.soltesz@stuba.sk
dana.barokova@stuba.sk

Abstract Presented contribution deals with impact issues of proposed water management arrangements in the upper part of the Medzibodrožie region on groundwater level regime. One of the alternatives for solution of the Tice River watering involves the weir construction on the Latorica River near the Leles bridge with consequential surface water level increase on the whole Slovak reach of the Latorica River up to the Ukrainian border. Our task was by means of FEM numerical modelling to determine the impact of such an intervention on groundwater level regime. For groundwater level simulation the TRIWACO software package has been used
Keywords groundwater level regime; finite element modelling, steady-state; field site; Medzibodrožie; water management

INTRODUCTION AND BACKGROUND INFORMATION

The project had more very important goals to be solved, but the most important can be characterised shortly as follows:

- water management - ecological (with appropriate technical solution),
- landscape (depending on water management solution),
- socio-economic (close connected with previous two).

The concentration was given on the first – for us the main and most important goal – the solution of water management control – from quantitative as well as from qualitative point of view.

The first task for the working team was to analyse the recent hydrological state of surface-, ground- as well as soil water in the given area and to find the water source for the water management solution for revitalisation of the old river bed and branches of the Tice River (Fig. 1). The inter-regional and "the joint" point, as well, was the water source which is located mostly on the Slovak side. The next specific point of the project is already working water management measures on both sides of the Medzibodrožie region. They are completely other and do not coincide but utilising the proposed water management obtained in the project it could be possible to achieve the symbiosis in water management on both sides. (Šoltész *et al*. 2006, 2007 2008).

The project itself was divided into seven phases of solution, which involved in the water management part of the project a detailed analysis of hydrological conditions of the whole Medzibodrožie region, hydraulic and morphological conditions of surface flows (last passports have been elaborated almost 40 years ago), hydro-geological conditions as well as hydro-pedological conditions of the Medzibodrožie region. It has to be considered that the "inter-regional" means that the water knows no political or regional constructions and it is flowing with no respect to state border. Several research institutions on Slovak and Hungarian side have been involved into the solution of the project.

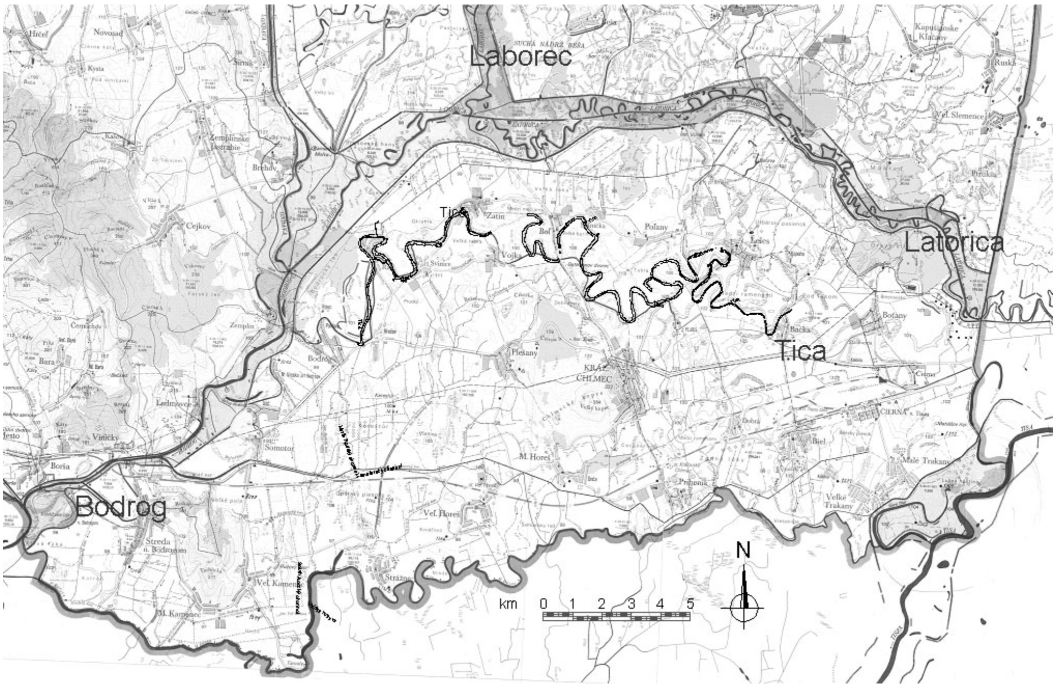

Fig. 1 Situation of the solved region on the Slovak and Hungarian border.

MEASURING, MODELLING PROCEDURES AND RESULTS

The technical solution for the revitalisation of the Tice River is assumed to be realised through outlets in the left hand-side protection dyke of the Latorica River. The problem is that the overflowing can be realised at the discharge Q= 55 $m^3.s^{-1}$ in the Latorica river, which is appearing approximately 30 days per year. It would not be so unfavourable but the problem is that it appears mostly in such period when the watering of the Tice River is not necessary or unreasonable from water quality in the Latorica river point of view (flood situation).

To obtain more information about the Latorica river bed in planned realisation of technical measures detailed geodetic measurements in the floodplain have been performed in 2006 and 2007 with recent discharge measurements in the Latorica River, as well. Results of the measurements have been compared with the river passport information from 1969 and been used when modelling the water level regime in the Latorica river for different discharges to recommend an optimum water level regime in the river. Mathematical model of the Latorica River has been elaborated using input data based on longitudinal and cross-section profiles as well as on new geodetical measurements and airborne DTM. For surface water modelling purposes the HEC-RAS computational program as well as MIKE-11 program (in GIS environment) for flood-mapping have been used. (Kamenský & Hašková, 2007, 2008), (Květon 2008)

These calculations were followed by analyses and prognoses of groundwater level regime in the Slovak part of the Medzibodrožie region (Šoltész & Baroková, 2006 - 2007). Several results of groundwater level regime have been achieved for different discharges in the Latorica River as well as for proposed surface water level regime after introducing the bag weir construction in the Latorica river bed and connecting channels (Fig. 2). Numerical modelling of the groundwater flow was realised by means of TRIWACO (Royal Haskoning Software, 2002) using finite element method. The basic finite element mesh is illustrated in the Fig. 3. There were different modifications undertaken to achieve a most proper computation finite element mesh with most important surface flows – rivers, drainage channels as well as proposed surface flows which connect the natural flows with artificial channels to supply the Tice river on Slovak side using the outlets in the left hand-side protection dyke of the Latorica river.

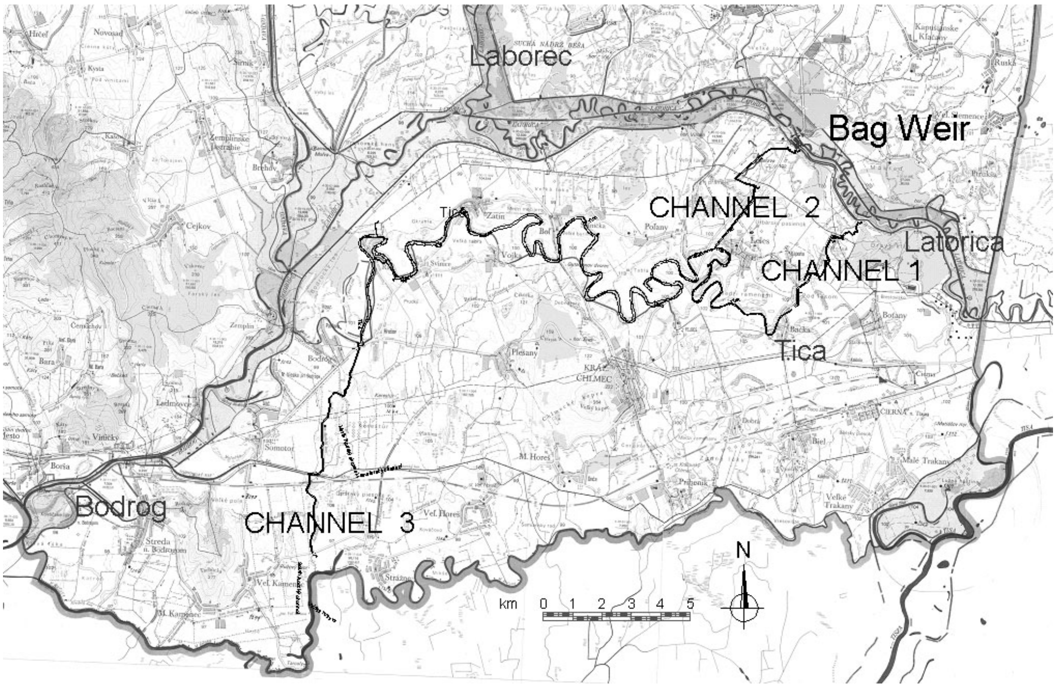

Fig. 2 Proposal of technical measures for Tice river revitalisation.

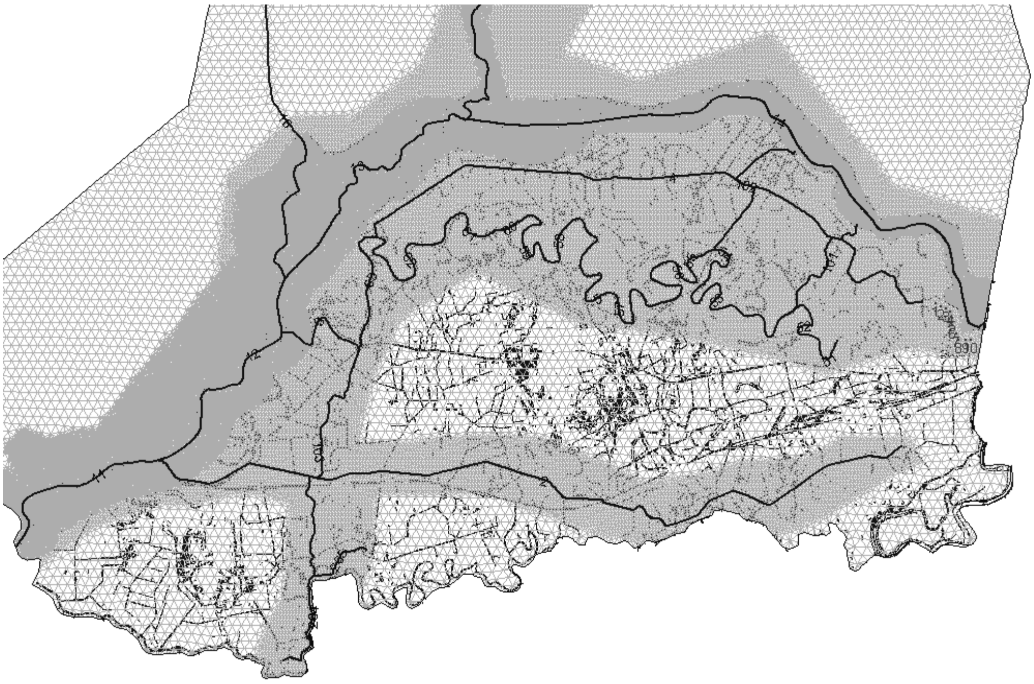

Fig. 3 2-D FEM computational mesh for groundwater flow modelling after introducing technical measures

All other activities as calibration, verification and sensitivity analysis have been realised and groundwater level prognosis after realising technical measures in the Latorica river bed and watering the Tice river bed is shown in the Fig. 4 and Fig. 5. (Baroková & Šoltész, 2008)

These modelling calculations of surface and groundwater level regime have been accomplished by soil moisture measurements in the Medzibodrožie region and modelling in the unsaturated zone realised by Institute of Hydrology, Slovak Academy of Sciences in Bratislava. (Šútor *et al*., 2008), (Gomboš & Šútor, 2008), (Pavelková *et al*., 2006).

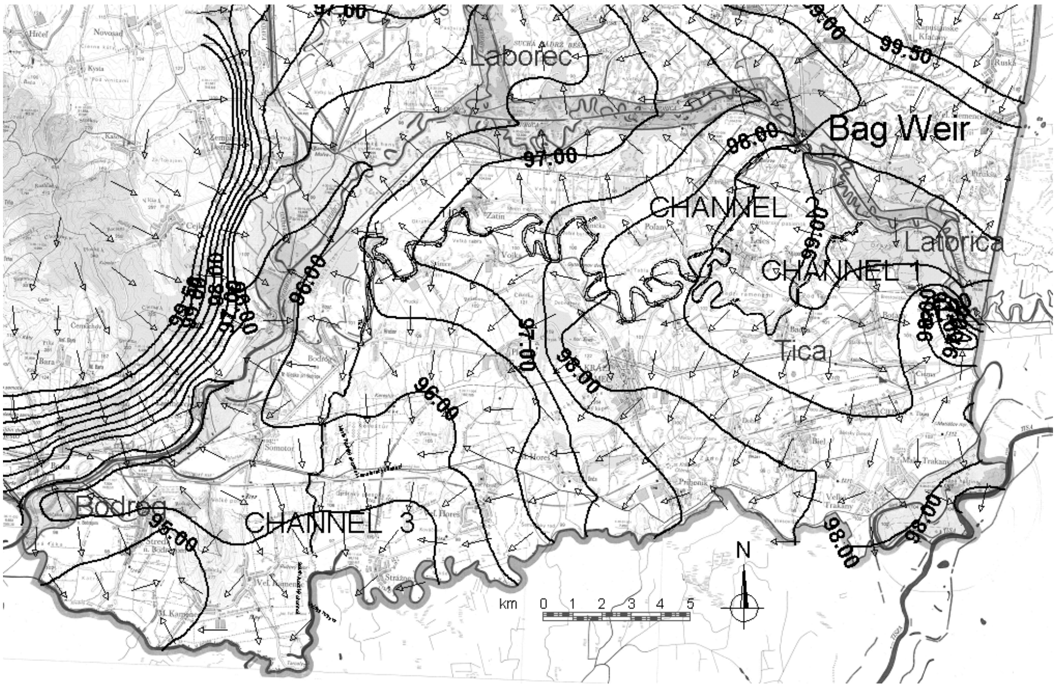

Fig. 4 Groundwater level course in the Medzibodrožie region after realisation of technical measures.

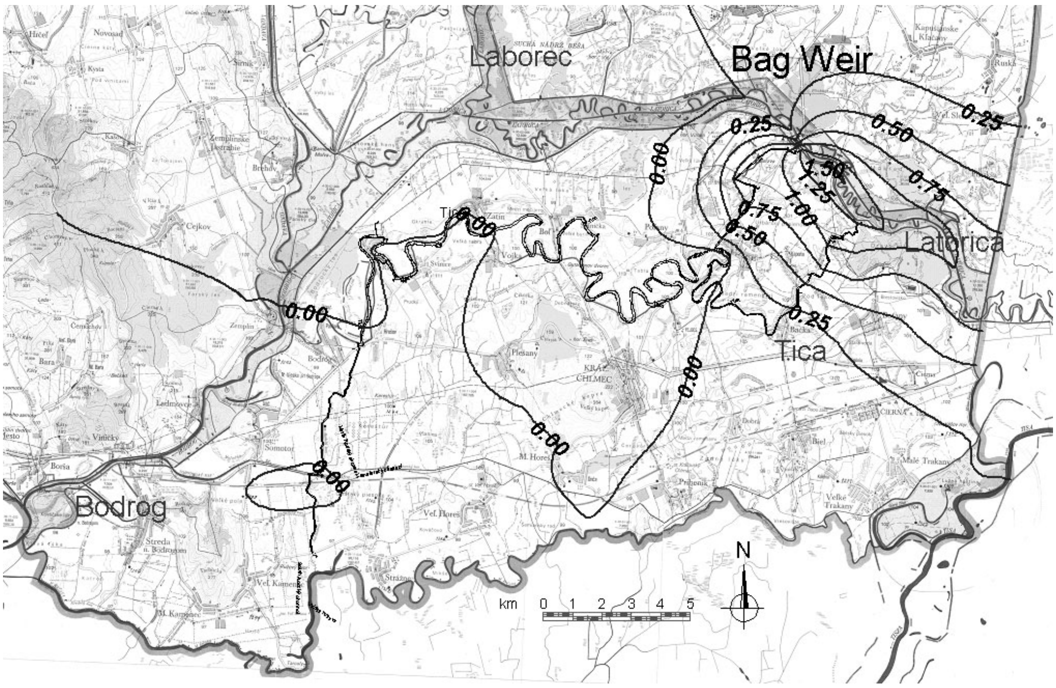

Fig. 5 Groundwater level differences before and after introducing technical measures.

The results of the numerical modelling have shown that mainly the northern part of the Medzibodrožie region which is directly affected by the weir construction (Šulek, 2007) is positively influenced by introduced technical measures. The most important issue is that the total area of the water level in revitalised 44,4 km long Tice River is approximately 2,8 mil. m^2 and the whole water volume in the Tice River at maximum operation levels in individual reaches of the river is 2,95 mil. m^3.

CONCLUSIONS

The presented inter-regional project deals with inter-disciplinary and inter-regional problems of water and land-use management in the Medzibodrožie region is not the first research project solving the water management principles in this region. But certainly is it the first project which in wide spectrum and cross-bordered absorbs water management problems of the Medzibodrožie region on both sides of the border between the Slovakia and Hungary. The Tokayer wine region is one part of the solved region, as well.

REFERENCES

Baroková, D, & Šoltész, A., (2008) Prognóza vývoja hladinového režimu podzemných vôd v oblasti Slovenskej časti Medzibodrožia - numerický model. *Čiastková správa k projektu Interreg IIIA - Vypracovanie spoločnej koncepcie krajinného a vodného hospodárstva, posúdenie možností jej realizáciea projektovanie jednotlivých prvkov koncepcie v Medziboroží, Bratislava.*

Baroková, D. (2007) GroundwaterLevel Regime in the Medzibodrožie Region – Analysis and Prognosis. *International Symposium on Interreg III.A Programme, Budapest.t*

Gomboš, M. & Šútor, J. (2008) Vplyv navrhovaných vodohospodárskych úprav Medzibodrožia na zásoby vody v pôde, VII. vedecká konferencia s medzinárodnou účasťou Vplyv antropogénnej činnosti na vodný režim nížinného územia. *CD, ISBN 978-80-89139-15-6, Michalovce, Vinianske jazero.*

Kamenský, J. & Hašková, L. (2007) Hydrologic and Hydraulic Evaulation of the Water level and Discharge Regime of the Latorica River. *International Symposium on Interreg III.A Programme, Budapest.*

Kamenský, J. & Hašková L. (2008) Sprietočnenie Tice, Popis systému, hydraulika povrchových vôd. *Čiastková správa k projektu Interreg IIIA - Vypracovanie spoločnej koncepcie krajinného a vodného hospodárstva, posúdenie možností jej realizáciea projektovanie jednotlivých prvkov koncepcie v Medziboroží. Bratislava.*

Květon, R. (2008) Vodohospodársko - prevádzkový model rieky Tice. *VII. Vedecká konferencia s medzinárodnou účasťou, Vplyv antropogénnej činnosti na vodný režim nížinného územia, Vinianske jazero.*

Pavelková, D., Invančo, J. & Burger, F. (2006) Hladinový režim podzemných vôd v Medzibodroži a jeho trendy za obdobie 1963-2005. *Acta Hydrologica Slovaca* **7**(2), 210-219.

Royal Haskoning (2002) TRIWACO - a Simulation Package for Groundwater, Version 3.0. *Rotterdam, Royal Haskoning, Nederland B.V.*

Šoltész, A. *et al.* (2006) Vypracovanie spoločnej koncepcie krajinného a vodného hospodárstva, posúdenie možnosti jej realizácie a projektovanie jednotlivých prvkov koncepcie na Medzibodroží, (súčasný stav riešenia). *Projekt INTERREG HU-SK-UA, Vplyv antropogénnej činnosti na vodný režim nížinného územia, VI. vedecká konferencia s medzinarodnou činnosťou, Sarospatak.*

Šoltész, A. & Baroková, D. (2007) Hydrogeology of the Medzibodrožie Region – Slovak Part. *International Symposium on INTERREG IIIA Programme, Budapest.*

Šoltész, A. (2007) Vypracovanie spoločnej koncepcie krajinného a vodného hospodárstva na Medzibodroží. *(Projekt INTERREG IIIA, Program susedstva Maďarsko-Slovensko-Ukrajina), Dni vody, Michalovce.*

Šoltész, A. (2008) Koncepcia vodohospodárskeho riešenia revitalizácie riek na Medzibodroží, VII. *Vedecká konferencia s medzinárodnou účasťou, Vplyv antropogénnej činnosti na vodný režim nížinného územia, Vinianske jazero.*

Šoltész A., Baroková,D. & Hašková, L. (2007) Optimalizácia vodného režimu na Medzibodroží (in Slovak). *Acta Hydrologica Slovaca* **8**(2), 173-181.

Šoltész, A. & Baroková, D. (2007) Hydrogeology of the Medzibodrožie Region – Slovak Part. *International Symposium on INTERREG IIIA Programme, Budapest.*

Šoltész, A. *et al.* (2007) Water Management in the Medzibodrožie (Bodrogköz) Cross-Border River Basin Region – Case study. *Proc. of the IX. Intern. Symposium on Water Management and Hydraulic Engineering, Šibenik, 1-7.*

Šoltész, A & Baroková, D. (2006 – 2007): Hladinový režim podzemných vôd v oblasti Slovenskej časti Medzibodrožia Numerický model – analýza podkladových materiálov 35 p. and súčasný stav, 46 p. *Čiastkové správy k projektu Interreg IIIA (in Slovak), Bratislava.*

Šútor, J., Gomboš, M., Tall, A. & Kandra, B. (2008) Potenciálne a monitorované zásoby vody v zóne aerácie pôd v Medzibodroží. *VII. vedecká konferencia s medzinárodnou účasťou Vplyv antropogénnej činnosti na vodný režim nížinného územia, CD, ISBN 978-80-89139-15-6, Michalovce, Vinianske jazero.*

Šulek, P. (2007) Pohyblivá hať v toku Latorica v rkm 21,950. *Návrh k projektu Interreg IIIA.*

Author Index

Name of author – page